

THE EFFECTS OF LONG-DURATION EARTHQUAKES ON CONCRETE
BRIDGES WITH POORLY CONFINED COLUMNS

By

THERON JAMES THOMPSON

A thesis submitted in partial fulfillment of
the requirement for the degree of

MASTERS OF SCIENCE IN CIVIL ENGINEERING

WASHINGTON STATE UNIVERSITY
Department of Civil and Environmental Engineering

DECEMBER 2004

To the Faculty of Washington State University:

The members of the Committee appointed to examine the thesis of
THERON JAMES THOMPSON find it satisfactory and recommend that it be accepted.

Chair

Acknowledgements

Funding for this project has been provided by the Federal Highway Administration. Information, earthquake records, and drawings of bridges in Western Washington State were supplied by the Washington State Department of Transportation.

Special thanks goes to Dr. Cofer for his invaluable help and guidance throughout this project. I would like to thank Dr. McDaniel and Dr. McLean for their assistance during the project. Special thanks goes to Seth Stapleton for all of the work he did in the laboratory testing. I would especially like to thank my mother and father for their continual support and encouragement.

THE EFFECTS OF LONG-DURATION EARTHQUAKES ON CONCRETE
BRIDGES WITH POORLY CONFINED COLUMNS

Abstract

By
Theron James Thompson, M.S.
Washington State University
December 2004

Chair: William F. Cofer

The main goals of this research were to implement a mathematical damage model for older, poorly confined, concrete bridge columns into the computer program WSU-NEABS and then evaluate bridge response to long-duration earthquakes. Two actual highway bridges were modeled with finite element spine models and analyzed with this modified version of the nonlinear analysis program. The analyses were done in two stages, the first of which included analyzing the bridges subjected to a suite of ten earthquakes. The suite of earthquakes incorporated short and long-duration events. Results from the analyses were used to predict the response of the bridges and determine if long-duration earthquakes significantly change their response.

The second stage of the analyses involved a parametric study in which the soil stiffness at the column bases and abutments was varied. In each case, the response of the bridge was then compared to that of the original model in the first stage. The results were also evaluated to determine if long-duration earthquakes were more damaging with these variations. A simplified bent model was also constructed to represent the center pier of

the bridge with the most critical response. This model was then analyzed to determine if a bent model can accurately model the response of the bridge, or if the entire bridge model is necessary.

The results from the analyses show that neither the short or long-duration events will cause major damage in the bridge columns for the bridges considered. However, the analyses do show that the bridges are predicted to have issues with pounding and possible failure of the bearing pads. The second stage of the analyses shows that the current modeling techniques used by the Washington Department of Transportation, in which rollers are applied at the abutments and the column bases are fixed, predicts more damage to the bridge columns compared to results from more refined foundation models. Thus, the present techniques are a conservative practice for the bridge columns. However, models based on these techniques under predict the pounding at the expansion joints and possible failure of the bearing pads, thus representing an unconservative approach these elements in the bridge.

Table of Contents

ACKNOWLEDGEMENTS	III
ABSTRACT	IV
TABLE OF CONTENTS	VI
LIST OF TABLES.....	XIV
LIST OF FIGURES	XXI
CHAPTER 1	1
INTRODUCTION	1
1.1 Pre-1970 Bridge Column Design	1
1.2 Research Objectives.....	2
1.3 Seismicity of Western Washington State	3
1.4 Program Modification	5
1.5 Bridge Modeling.....	5
1.6 Bridge Analysis.....	6
CHAPTER TWO	7

LITERATURE REVIEW	7
2.1 Introduction.....	7
2.2 Current Damage Analysis Methods	7
2.2.1 Damage Models Based on Strength and Stiffness Degradation	8
2.2.2 Damage Models Based on Measures of Deformation and/or Ductility.....	16
2.2.3 Damage Models Based on Energy Dissipation	20
2.2.4 Damage Models Based on Hybrid Formulations	23
2.2.5 Damage Models Based on More Complex Fatigue Models.....	26
2.3 Additional Topics	30
 CHAPTER 3	 32
 WSU-NEABS COMPUTER PROGRAM.....	 32
 3.1 The History of the Computer Program WSU-NEABS.....	 32
 3.2 Review of the Previous Beam-Column Element	 34
3.2.1 Previous Damage Coefficient.....	34
3.2.2 Yield Function	35
 3.3 Modification of WSU-NEABS	 39
3.3.1 Modification of the Damage Model	39
3.3.2 Modification of the Hysteresis Model for the Beam-Column Element.....	42
 3.4 Examples.....	 47

3.4.1 Example 1	47
3.4.2 Example 2	50
3.4.3 Example 3	52
3.4.4 Damage Level Comparison	54
CHAPTER 4	56
SEISMIC ANALYSIS OF BRIDGES UNDER LONG-DURATION LOADING	56
4.1 WSDOT Bridge 5/518	56
4.1.1 Introduction	56
4.1.2 Description of the Bridge	57
4.1.3 Structural Model	63
4.1.4 Seismic Excitation	71
4.2 WSDOT Bridge 5/826	79
4.2.1 Introduction	79
4.2.2 Description of the Bridge	80
4.2.3 Structural Model	86
4.2.4 Seismic Excitation	88
CHAPTER 5	89
ANALYTICAL RESULTS AND INTERPRETATION	89
5.1 Introduction	89

5.2 Bridge 5/518.....	89
5.2.1 Modified Peru Earthquake.....	89
5.2.2 Modified Chile Earthquake	100
5.3 Bridge 5/826.....	110
5.3.1 Modified Peru Earthquake.....	110
5.3.2 Modified Chile Earthquake	118
5.4 Summary of all other Earthquakes	126
5.4.1 Bridge 5/518	126
5.4.2 Bridge 5/826	135
 CHAPTER 6	 143
 SOIL-STRUCTURE PARAMETRIC STUDY AND BENT MODEL COMPARISON	
	 143
6.1 Introduction.....	143
6.2 Soil-Structure Parametric Study Protocol.....	143
6.3 Results and Interpretation	145
6.3.1 Run No. 1.....	145
6.2.2 Run No. 2.....	154
6.3.3 Run No. 3.....	156
6.3.4 Run No. 4.....	158
6.3.5 Run No. 5.....	160

6.3.6 Run No. 6.....	162
6.3.7 Run No. 7.....	164
6.3.8 Run No. 8.....	166
6.3.9 Run No. 9.....	168
6.3.10 Run No. 10.....	170
6.3.11 Run No. 11.....	172
6.3.12 Run No. 12.....	174
6.3.13 Run No. 13.....	176
6.4 Bent Model Comparison.....	178
CHAPTER 7	186
SUMMARY AND CONCLUSIONS	186
7.1 Summary.....	186
7.2 Analyses with Constant Soil Stiffness	187
7.3 Analyses with Varying Soil Stiffness.....	190
7.4 Bent Model Comparison.....	193
7.5 Recommendations for Future Work	194
REFERENCES	196
APPENDIX A.....	203

ADDITIONAL TIME HISTORIES USED IN STUDY	203
APPENDIX B	212
APPENDIX C	246
ADDITIONAL OUTPUT FROM STUDY	246
C.1 Introduction.....	246
C.2 Bridge 5/518; Unmodified Peru	246
C.3 Bridge 5/518; Unmodified Chile Earthquake.....	251
C.4 Bridge 5/518; Mexico City 475-Year Earthquake.....	256
C.5 Bridge 5/518; Mexico City 950-Year Earthquake.....	260
C.6 Bridge 5/518; Olympia 475-Year Earthquake.....	265
C.7 Bridge 5/518; Olympia 950-Year Earthquake.....	269
C.8 Bridge 5/518; Kobe 475-Year Earthquake	274
C.9 Bridge 5/518; Kobe 950-Year Earthquake	279
C.10 Bridge 5/826; Unmodified Peru Earthquake.....	284
C.11 Bridge 5/826; Unmodified Chile Earthquake.....	288
C.12 Bridge 5/826; Mexico City 475-Year Earthquake.....	292

C.13 Bridge 5/826; Mexico City 950-Year Earthquake.....	296
C.14 Bridge 5/826; Olympia 475-Year Earthquake.....	300
C.15 Bridge 5/826; Olympia 950-Year Earthquake.....	304
C.16 Bridge 5/826; Kobe 475-Year Earthquake	308
C.17 Bridge 5/826; Kobe 950-Year Earthquake	312
APPENDIX D	316
ADDITIONAL OUTPUT FROM SOIL-STRUCTURE STUDY	316
D.1 Introduction.....	316
D.2 Run No. 1	316
D.3 Run No. 2	318
D.4 Run No. 3	324
D.5 Run No. 4	329
D.6 Run No. 5	335
D.7 Run No. 6	340
D.8 Run No. 7	346
D.9 Run No. 8	352

D.10 Run No. 9	357
D.11 Run No. 10	362
D.12 Run No. 11	368
D.13 Run No. 12	374
D.14 Run No. 13	379

List of Tables

Table 3.4-1 Structural Properties of Column.....	48
Table 3.4-2 Summary of Standard Cyclic Protocol (Stapleton 2004)	51
Table 3.4-3 Structural Properties of Column.....	52
Table 4.1-1 Structural Properties for Columns, Crossbeams, and Deck Beams	65
Table 4.1-2 Yield Function Constants for the Columns	66
Table 4.1-3 Stiffness Properties for Soil Springs (k/in)	67
Table 4.1-4 Input Parameters for Expansion Joints.....	70
Table 4.2-1 Structural Properties for Columns and Crossbeams	87
Table 4.2-2 Yield Function Constants for the Columns	87
Table 4.2-3 Stiffness Properties for Soil Springs (k/in)	87
Table 4.2-4 Input Parameters for Expansion Joints.....	88
Table 5.2-1 Maximum Moment (kip-in) at the Top and Bottoms of Columns,	93
Table 5.2-2 Maximum Shear (kips) in the Columns, Modified Peru Earthquake....	97
Table 5.2-3 Maximum Shear (kips) at the Abutments, Modified Peru Earthquake	98
Table 5.2-4 Maximum Moment (kip-in) at the Top and Bottoms of Columns,	103
Table 5.2-5 Maximum Shear (kips) in the Columns, Modified Chile Earthquake.	108
Table 5.2-6 Maximum Shear (kips) at the Abutments, Modified Chile Earthquake	109
Table 5.3-1 Maximum Moment (kip-in) at the Top and Bottoms of Columns,	113
Table 5.3-2 Maximum Shear (kips) in the Columns, Modified Peru Earthquake..	115
Table 5.3-3 Maximum Shear (kips) at the Abutments, Modified Peru Earthquake	116

Table 5.3-4 Maximum Moment (kip-in) at the Top and Bottoms of Columns,	121
Table 5.3-5 Maximum Shear (kips) in the Columns, Modified Chile Earthquake.	123
Table 5.3-6 Maximum Shear (kips) at the Abutments, Modified Chile Earthquake	
.....	124
Table 5.4-1 Results from the Unmodified Peru Earthquake	127
Table 5.4-2 Results from the Unmodified Chile Earthquake	128
Table 5.4-3 Results from the Mexico City 475-Year Earthquake	129
Table 5.4-4 Results from the Mexico City 950-Year Earthquake	130
Table 5.4-5 Results from the Olympia 475-Year Earthquake	131
Table 5.4-6 Results from the Olympia 950-Year Earthquake	132
Table 5.4-7 Results from the Kobe 475-Year Earthquake.....	133
Table 5.4-8 Results from the Kobe 950-Year Earthquake.....	134
Table 5.4-9 Results from the Unmodified Peru Earthquake	135
Table 5.4-10 Results from the Unmodified Chile Earthquake	136
Table 5.4-11 Results from the Mexico City 475-Year Earthquake	137
Table 5.4-12 Results from the Mexico City 950-Year Earthquake	138
Table 5.4-13 Results from the Olympia 475-Year Earthquake	139
Table 5.4-14 Results from the Olympia 950-Year Earthquake	140
Table 5.4-15 Results from the Kobe 475-Year Earthquake.....	141
Table 5.4-16 Results from the Kobe 950-Year Earthquake.....	142
Table 6.2-1 Analysis Protocol.....	144
Table 6.3-1 Maximum Moment (kip-in) at the Top and Bottoms of Columns,	148
Table 6.3-2 Maximum Shear (kips) in the Columns, Modified Peru Earthquake,.	153

Table 6.3-3 Results from the Modified Peru Earthquake, Bridge 5/518, Run No. 2	155
.....	
Table 6.3-4 Results from the Modified Peru Earthquake, Bridge 5/518, Run No. 3	157
.....	
Table 6.3-5 Results from the Modified Peru Earthquake, Bridge 5/518, Run No. 4	159
.....	
Table 6.3-6 Results from the Modified Peru Earthquake, Bridge 5/518, Run No. 5	161
.....	
Table 6.3-7 Results from the Modified Peru Earthquake, Bridge 5/518, Run No. 6	163
.....	
Table 6.3-8 Results from the Modified Chile Earthquake, Bridge 5/518, Run No. 7	165
.....	
Table 6.3-9 Results from the Modified Peru Earthquake, Bridge 5/826, Run No. 8	167
.....	
Table 6.3-10 Results from the Modified Peru Earthquake, Bridge 5/826, Run No. 9	169
.....	
Table 6.3-11 Results from the Olympia 950-Year EQ, Bridge 5/518, Run No. 10..	171
Table 6.3-12 Results from the Kobe 950-Year EQ, Bridge 5/518, Run No. 11.....	173
Table 6.3-13 Results from the Olympia 950-Year EQ, Bridge 5/826, Run No. 12..	175
Table 6.3-14 Results from the Kobe 950-Year EQ, Bridge 5/826, Run No. 13.....	177
Table 6.4-1 Maximum Moment (kip-in) at the Top and Bottoms of Columns	181
Table 6.4-2 Maximum Shear (kips) at the Top and Bottoms of Columns	185
Table 7.2-1 Summary of Results for Bridge 5/518.....	187

Table 7.2-2 Summary of Results for Bridge 5/826.....	190
Table 7.3-1 Analysis Protocol.....	191
Table 7.3-2 Summary of Results for Bridge 5/518.....	192
Table 7.3-3 Summary of Results for Bridge 5/826.....	192
Table C.2-1 Maximum Moment (kip-in) at the Top and Bottoms of Columns.....	249
Table C.2-2 Maximum Shear (kips) in the Columns.....	249
Table C.2-3 Maximum Shear (kips) at the Abutments	249
Table C.3-1 Maximum Moment (kip-in) at the Top and Bottoms of Columns.....	254
Table C.3-2 Maximum Shear (kips) in the Columns.....	254
Table C.3-3 Maximum Shear (kips) at the Abutments	254
Table C.4-1 Maximum Moment (kip-in) at the Top and Bottoms of Columns.....	258
Table C.4-2 Maximum Shear (kips) in the Columns.....	258
Table C.4-3 Maximum Shear (kips) at the Abutments	258
Table C.5-1 Maximum Moment (kip-in) at the Top and Bottoms of Columns.....	263
Table C.5-2 Maximum Shear (kips) in the Columns.....	263
Table C.5-3 Maximum Shear (kips) at the Abutments	263
Table C.6-1 Maximum Moment (kip-in) at the Top and Bottoms of Columns.....	267
Table C.6-2 Maximum Shear (kips) in the Columns.....	267
Table C.6-3 Maximum Shear (kips) at the Abutments	267
Table C.7-1 Maximum Moment (kip-in) at the Top and Bottoms of Columns.....	272
Table C.7-2 Maximum Shear (kips) in the Columns.....	272
Table C.7-3 Maximum Shear (kips) at the Abutments	272
Table C.8-1 Maximum Moment (kip-in) at the Top and Bottoms of Columns.....	277

Table C.8-2 Maximum Shear (kips) in the Columns	277
Table C.8-3 Maximum Shear (kips) at the Abutments	277
Table C.9-1 Maximum Moment (kip-in) at the Top and Bottoms of Columns.....	282
Table C.9-2 Maximum Shear (kips) in the Columns.....	282
Table C.9-3 Maximum Shear (kips) at the Abutments	282
Table C.10-1 Maximum Moment (kip-in) at the Top and Bottoms of Columns	286
Table C.10-2 Maximum Shear (kips) in the Columns.....	286
Table C.10-3 Maximum Shear (kips) at the Abutments	286
Table C.11-1 Maximum Moment (kip-in) at the Top and Bottoms of Columns	290
Table C.11-2 Maximum Shear (kips) in the Columns.....	290
Table C.11-3 Maximum Shear (kips) at the Abutments	290
Table C.12-1 Maximum Moment (kip-in) at the Top and Bottoms of Columns	294
Table C.12-2 Maximum Shear (kips) in the Columns.....	294
Table C.12-3 Maximum Shear (kips) at the Abutments	294
Table C.13-1 Maximum Moment (kip-in) at the Top and Bottoms of Columns	298
Table C.13-2 Maximum Shear (kips) in the Columns.....	298
Table C.13-3 Maximum Shear (kips) at the Abutments	298
Table C.14-1 Maximum Moment (kip-in) at the Top and Bottoms of Columns	302
Table C.14-2 Maximum Shear (kips) in the Columns.....	302
Table C.14-3 Maximum Shear (kips) at the Abutments	302
Table C.15-1 Maximum Moment (kip-in) at the Top and Bottoms of Columns	306
Table C.15-2 Maximum Shear (kips) in the Columns.....	306
Table C.15-3 Maximum Shear (kips) at the Abutments	306

Table C.16-1 Maximum Moment (kip-in) at the Top and Bottoms of Columns	310
Table C.16-2 Maximum Shear (kips) in the Columns	310
Table C.16-3 Maximum Shear (kips) at the Abutments	310
Table C.17-1 Maximum Moment (kip-in) at the Top and Bottoms of Columns	314
Table C.17-2 Maximum Shear (kips) in the Columns	314
Table C.17-3 Maximum Shear (kips) at the Abutments	314
Table D.3-1 Maximum Moment (kip-in) at the Top and Bottoms of Columns.....	322
Table D.3-2 Maximum Shear (kips) in the Columns	322
Table D.4-1 Maximum Moment (kip-in) at the Top and Bottoms of Columns.....	327
Table D.4-2 Maximum Shear (kips) in the Columns	327
Table D.4-3 Maximum Shear (kips) at the Abutments	327
Table D.5-1 Maximum Moment (kip-in) at the Top and Bottoms of Columns.....	333
Table D.5-2 Maximum Shear (kips) in the Columns	333
Table D.6-1 Maximum Moment (kip-in) at the Top and Bottoms of Columns.....	338
Table D.6-2 Maximum Shear (kips) in the Columns	338
Table D.6-3 Maximum Shear (kips) at the Abutments	338
Table D.7-1 Maximum Moment (kip-in) at the Top and Bottoms of Columns.....	344
Table D.7-2 Maximum Shear (kips) in the Columns	344
Table D.7-3 Maximum Shear (kips) at the Abutments	344
Table D.8-1 Maximum Moment (kip-in) at the Top and Bottoms of Columns.....	350
Table D.8-2 Maximum Shear (kips) in the Columns	350
Table D.9-1 Maximum Moment (kip-in) at the Top and Bottoms of Columns.....	356
Table D.9-2 Maximum Shear (kips) in the Columns	356

Table D.10-1 Maximum Moment (kip-in) at the Top and Bottoms of Columns	361
Table D.10-2 Maximum Shear (kips) in the Columns	361
Table D.11-1 Maximum Moment (kip-in) at the Top and Bottoms of Columns	366
Table D.11-2 Maximum Shear (kips) in the Columns	366
Table D.12-1 Maximum Moment (kip-in) at the Top and Bottoms of Columns	372
Table D.12-2 Maximum Shear (kips) in the Columns	372
Table D.13-1 Maximum Moment (kip-in) at the Top and Bottoms of Columns	378
Table D.13-2 Maximum Shear (kips) in the Columns	378
Table D.14-1 Maximum Moment (kip-in) at the Top and Bottoms of Columns	383
Table D.14-2 Maximum Shear (kips) in the Columns	383

List of Figures

Figure 1.2-1 The Cascadia Subduction Zone Boundary (NRCan, 2004).....	4
Figure 1.2-2 The Cascadia Subduction Zone (NRCan, 2004).....	4
Figure 2.2-1 Hysteresis Behavior of Concrete as Modeled in IDARC	10
(Williams and Sexsmith 1997).....	10
Figure 2.2-2. Moment and Rotation Relation: (a) Backbone Curve; (b) Hysteretic	
Laws (Pincheria et al 1999)	11
Figure 2.2-3. Shear Force and Displacement Relation: (a) Backbone Curve; (b)	
Hysteretic Laws (Pincheria et al 1999).....	12
Figure 2.2-4. Stiffness and Strength Degradation (Sivaselvan et al 2000).....	16
Figure 2.2-5 Plastic Displacement Increments (Stephens and Yao 1987).....	17
Figure 2.2-6. Physical Meaning of Wang and Shah (1987) Damage Index	18
Figure 2.2-7 Primary (PHC) and Follower (FHC) Half-cycles (Kratzig et al 1989). 	21
Figure 2.2-8. Moment – Curvature Characteristics for Damage Index.....	25
(Bracci et al 1989).....	25
Figure 2.2-9 Definitions of Failure Under (a) Monotonic and (b) Cyclic Loading	
(Chung et al 1987)	27
Figure 3.2-1 Moment vs. Curvature Relationship (Zhang 1996).....	34
Figure 3.2-2 Generalized Yield Surface (Zhang 1996)	37
Figure 3.2-3 Yield Curve of Isotropic Strain Softening Material at a Constant Level	
of Axial Force(Zhang 1996).....	38
Figure 3.2-4 Hysteresis Model for the Previous Beam-Column Element	39
(Zhang 1996).....	39

Figure 3.3-1 Results of Constant Amplitude Testing (Stapleton 2004).....	41
Figure 3.3-2 Hysteresis Model for the Beam-Column	43
Figure 3.3-3 Effect on the Unloading Stiffness with the Variation of D^*_1 and D^*_2....	46
Figure 3.3-4 Effect on the Reloading Stiffness with the Variation of D^*_1 and D^*_2	46
Figure3.4-1 Structural Model of Single Column.....	48
Figure 3.4-2 Constant Amplitude Comparison from Experiment (Stapleton, 2004) and WSU-NEABS.....	50
Figure 3.4-3 Changing Amplitude Comparison from experiment	51
(Stapleton, 2004) and WSU-NEABS	51
Figure 3.4-4 Kunnath’s Test Results (Kunnath 1997).....	52
Figure 3.4-5 WSU-NEABS Simulation of Kunnath’s Test	53
Figure 3.4-6 Final State of Damage for Column	55
Figure 4.1-1 Bridge 5/518	56
Figure 4.1-2 Plan and Profile Views of Bridge 5/518.....	57
Figure 4.1-3 Bearing of I-Girders.....	58
Figure 4.1-4 Intermediate Bent Cross Section	59
Figure 4.1-5 Cross Section of Cross Beam.....	60
Figure 4.1-6 Girder Stop Details.....	61
Figure 4.1-7 Structural Model of Bridge 5/518	63
Figure 4.1-8 Bent from Structural Model.....	64
Figure 4.1-9 Bilinear Representation of Moment-Curvature	65
Figure 4.1-10 Effective Stiffness of Circular Bridge Columns (Priestley, 2003).....	66
Figure 4.1-11 Idealized Expansion Joint.....	68

Figure 4.1-12 Expansion Joint Coordinate System.....	69
Figure 4.1-13 Idealized Expansion Joints at Intermediate Piers.....	70
Figure 4.1-14 Acceleration Spectra Developed from Attenuation Relationships (Stapleton 2004).....	72
Figure 4.1-15 E-W Peru Spectral Acceleration (Stapleton 2004).....	73
Figure 4.1-16 Modified Peru Earthquake, E-W Time History (Stapleton 2004).....	73
Figure 4.1-17 N-S Peru Spectral Acceleration (Stapleton 2004).....	74
Figure 4.1-18 Modified Peru Earthquake, N-S Time History (Stapleton 2004).....	74
Figure 4.1-19 E-W Chile Spectral Acceleration adapted from Stapleton (2004).....	75
Figure 4.1-20 Modified Chile Earthquake, E-W Time History (Stapleton 2004).....	75
Figure 4.1-21 N-S Chile Spectral Acceleration (Stapleton 2004).....	76
Figure 4.1-22 Modified Chile Earthquake, N-S Time History (Stapleton 2004).....	76
Figure 4.1-23 5% Damped Spectral Accelerations for Seattle, WA.....	77
(Frankel, 1996)	77
Figure 4.1-24 5% Damped Spectral Accelerations for Olympia, WA	78
(Frankel, 1996)	78
Figure 4.1-25 5% Damped Spectral Accelerations for Grey’s Harbor, WA (Frankel, 1996)	78
Figure 4.2-1 Bridge 5/826	80
Figure 4.2-2 Plan View of Bridge 5/826	81
Figure 4.2-3 Elevation View of Bridge 5/826.....	81
Figure 4.2-4 Cross Section of Cross Beam of Bridge 5/826.....	82
Figure 4.2-5 Column Cross Section of Bridge 5/826.....	83

Figure 4.2-6 Column Footing Plans for Bridge 5/826.....	84
Figure 4.2-7 Abutment Footing Plan for Bridge 5/826.....	85
Figure 4.2-8 Structural Model of Bridge 5/826	86
Figure 5.2-1 Total Relative Displacement at Pier 1, Modified Peru Earthquake.....	90
Figure 5.2-2 Total Relative Displacement at Pier 2, Modified Peru Earthquake.....	91
Figure 5.2-3 Total Relative Displacement at Intermediate Pier 3, Modified Peru Earthquake	91
Figure 5.2-4 Transverse Displacement Envelope of Bridge Deck, Modified Peru Earthquake	92
Figure 5.2-5 Plastic Rotations at the Top of the Columns, Modified Peru Earthquake	93
Figure 5.2-6 Damage at the Top of the Columns, Modified Peru Earthquake	94
Figure 5.2-7 Longitudinal Hysteresis Plot for the Center Column of Pier 2, Modified Peru Earthquake	95
Figure 5.2-8 Transverse Hysteresis Plot for the Center Column of Pier 2, Modified Peru Earthquake	96
Figure 5.2-9 Relative Longitudinal Displacement at the West Abutment, Modified Peru Earthquake	99
Figure 5.2-10 Total Relative Displacement at Pier 1, Modified Chile Earthquake	101
Figure 5.2-11 Total Relative Displacement at Pier 2, Modified Chile Earthquake	101
Figure 5.2-12 Total Relative Displacement at Pier 3, Modified Chile Earthquake	102
Figure 5.2-13 Transverse Relative Displacement Envelope of Bridge Deck, Modified Chile Earthquake	102

Figure 5.2-14 Plastic Rotations at the Top of the Columns, Modified Chile	
Earthquake	104
Figure 5.2-15 Damage at the Top of the Columns, Modified Chile Earthquake	105
Figure 5.2-16 Final State of Damage in Column.....	106
Figure 5.2-17 Longitudinal Hysteresis Plot for the Center Column of Pier 2,	
Modified Chile Earthquake.....	107
Figure 5.2-18 Transverse Hysteresis Plot for the Center Column of Pier 2, Modified	
Chile Earthquake	107
Figure 5.2-19 Relative Longitudinal Displacement at the West Abutment, Modified	
Chile Earthquake	109
Figure 5.3-1 Total Relative Displacement at Pier 1, Modified Peru Earthquake... 111	
Figure 5.3-2 Total Relative Displacement at Pier 2, Modified Peru Earthquake... 111	
Figure 5.3-3 Total Relative Displacement at Pier 3, Modified Peru Earthquake... 112	
Figure 5.3-4 Transverse Relative Displacement Envelope of Bridge Deck, Modified	
Peru Earthquake	112
Figure 5.3-5 Longitudinal Hysteresis Plot for the Center Column of Pier 2, Modified	
Peru Earthquake	114
Figure 5.3-6 Transverse Hysteresis plot for the Center Column of Pier 2, Modified	
Peru Earthquake	114
Figure 5.3-7 Relative Longitudinal Displacement at the West Abutment, Modified	
Peru Earthquake	117
Figure 5.3-8 Relative Longitudinal Displacement at the East Abutment, Modified	
Peru Earthquake	117

Figure 5.3-9 Total Relative Displacement at Pier 1, Modified Chile Earthquake ..	119
Figure 5.3-10 Total Relative Displacement at Pier 2, Modified Chile Earthquake	119
Figure 5.3-11 Total Relative Displacement at Pier 3, Modified Chile Earthquake	120
Figure 5.3-12 Transverse Displacement Envelope of Bridge Deck, Modified Chile Earthquake	120
Figure 5.3-13 Longitudinal Hysteresis Plot for the Center Column of Pier 2, Modified Chile Earthquake.....	122
Figure 5.3-14 Transverse Hysteresis Plot for the Center Column of Pier 2, Modified Chile Earthquake	122
Figure 5.3-15 Relative Longitudinal Displacement at the West Abutment, Modified Chile Earthquake	124
Figure 5.3-16 Relative Longitudinal Displacement at the East Abutment, Modified Chile Earthquake	125
Figure 6.3-1 Total Displacement at Pier 1, Modified Peru Earthquake, Bridge 5/518	146
Figure 6.3-2 Total Displacement at Pier 2, Modified Peru Earthquake, Bridge 5/518	146
Figure 6.3-3 Total Displacement at Pier 3, Modified Peru Earthquake, Bridge 5/518	147
Figure 6.3-4 Transverse Displacement Envelope of Bridge Deck, Modified Peru Earthquake, Bridge 5/518.....	147
Figure 6.3-5 Plastic Rotations at the Bottom of the Columns, Modified Peru Earthquake, Bridge 5/518.....	149

Figure 6.3-6 Plastic Rotations at the Top of the Columns, Modified Peru Earthquake, Bridge 5/518.....	149
Figure 6.3-7 Damage at the Bottom of the Columns, Modified Peru Earthquake, Bridge 5/518	150
Figure 6.3-8 Damage at the Top of the Columns, Modified Peru Earthquake, Bridge 5/518.....	150
Figure 6.3-9 Longitudinal Hysteresis Plot for the Center Column of Pier 2, Modified Peru Earthquake, Bridge 5/518	151
Figure 6.3-10 Transverse Hysteresis plot for the Center Column of Pier 2, Modified Peru Earthquake, Bridge 5/518	152
Figure 6.3-11 Relative Longitudinal Displacement at Pier 1, Modified Peru Earthquake, Bridge 5/518.....	154
Figure 6.4-1 Relative Transverse Displacement of Bridge Pier.....	179
Figure 6.4-2 Relative Transverse Displacement of Bent Model	180
Figure 6.4-3 Plastic Rotations at the Top of the Columns for the Bridge Pier	181
Figure 6.4-4 Plastic Rotations at the Bottom of the Columns for the Bridge Pier..	182
Figure 6.4-5 Plastic Rotations at the Top of the Columns for the Bent Model	182
Figure 6.4-6 Plastic Rotations at the Bottom of the Columns for the Bent Model .	183
Figure 6.4-7 Damage at the Top of the Columns for the Bridge Pier	183
Figure 6.4-8 Damage at the Top of the Columns for the Bent Model.....	184
Figure 6.4-9 Damage at the Bottom of the Columns for the Bent Model	184
Figure A-1: Original Peru Earthquake, E-W Time History.....	203
Figure A-2: Original Peru Earthquake, N-S Time History	204

Figure A-3: Original Chile Earthquake, E-W Time History	204
Figure A-4: Original Chile Earthquake, N-S Time History	205
Figure A-5: 475 Year Mexico City Earthquake, E-W Time History	206
Figure A-6: 475 Year Mexico City Earthquake, N-S Time History	206
Figure A-7: 950 Year Mexico City Earthquake, E-W Time History	207
Figure A-8: 950 Year Mexico City Earthquake, N-S Time History	207
Figure A-9: 475 Year Kobe Earthquake, E-W Time History	208
Figure A-10: 475 Year Kobe Earthquake, N-S Time History	208
Figure A-11: 950 Year Kobe Earthquake, E-W Time History	209
Figure A-12: 950 Year Kobe Earthquake, N-S Time History	209
Figure A-13: 475 Year Olympia Earthquake. E-W Time History	210
Figure A-14: 475 Year Olympia Earthquake, N-S Time History	210
Figure A-15: 950 Year Olympia Earthquake, E-W Time History	211
Figure A-16: 950 Year Olympia Earthquake, N-S Time History	211
Figure C.2-1 Total Displacement at Piers.....	246
Figure C.2-2 Transverse Displacement Envelope of Bridge Deck	247
Figure C.2-3 Plastic Rotations at the Top of the Columns.....	247
Figure C.2-4 Damage at the Top of the Columns	248
Figure C.2-5 Hysteresis Plots for the Center Column of Pier 2.....	248
Figure C.2-6 Longitudinal Displacement of Expansion Joints	250
Figure C.3-1 Total Displacement at Piers.....	251
Figure C.3-2 Transverse Displacement Envelope of Bridge Deck	252
Figure C.3-3 Plastic Rotations at the Top of the Columns.....	252

Figure C.3-4 Damage at the Top of the Columns	253
Figure C.3-5 Hysteresis Plots for the Center Column of Pier 2.....	253
Figure C.3-6 Longitudinal displacement of Expansion Joints.....	255
Figure C.4-1 Total Displacement at Piers.....	256
Figure C.4-2 Transverse Displacement Envelope of Bridge Deck	257
Figure C.4-3 Hysteresis Plots for the Center Column of Pier 2.....	257
Figure C.4-4 Longitudinal Displacement of Expansion Joints	259
Figure C.5-1 Total Displacement at Piers.....	260
Figure C.5-2 Transverse Displacement Envelope of the Bridge Deck.....	261
Figure C.5-3 Plastic Rotation at the Top of the Columns	261
Figure C.5-4 Damage at the Top of the Columns	262
Figure C.5-5 Hysteresis Plots for the Center Column of Pier 2.....	262
Figure C.5-6 Longitudinal Displacement of Expansion Joints	264
Figure C.6-1 Total Displacement at Piers.....	265
Figure C.6-2 Transverse Displacement Envelope of Bridge Deck	266
Figure C.6-3 Hysteresis Plots for the Center Column of Pier 2.....	266
Figure C.6-4 Longitudinal Displacement of Expansion Joints	268
Figure C.7-1 Total Displacement at Piers.....	269
Figure C.7-2 Transverse Displacement Envelope of Bridge Deck	270
Figure C.7-3 Plastic Rotations at the Top of the Columns.....	270
Figure C.7-4 Damage at the Top of the Columns	271
Figure C.7-5 Hysteresis Plots for the Center Column of Pier 2.....	271
Figure C.7-6 Longitudinal Displacement of Expansion Joints	273

Figure C.8-1 Total Displacement at Piers.....	274
Figure C.8-2 Transverse Displacement Envelope of Bridge Deck	275
Figure C.8-3 Plastic Rotation at the Top of the Columns	275
Figure C.8-4 Hysteresis Plots for the Center Column of Pier 2.....	276
Figure C.8-5 Longitudinal Displacement of Expansion Joints	278
Figure C.9-1 Total Displacement at Piers.....	279
Figure C.9-2 Transverse Displacement Envelope of Bridge Deck	280
Figure C.9-3 Plastic Rotations at the Top of the Columns.....	280
Figure C.9-4 Damage at the Top of the Columns	281
Figure C.9-5 Hysteresis Plots for the Center Column of Pier 2.....	281
Figure C.9-6 Longitudinal Displacement of the Expansion joints	283
Figure C.10-1 Total Displacement at Piers.....	284
Figure C.10-2 Transverse Displacement Envelope of the Bridge Deck	285
Figure C.10-3 Hysteresis Plots for the Center Column of Pier 2.....	285
Figure C.10-4 Longitudinal Displacement of the Expansion Joints.....	287
Figure C.11-1 Total Displacement at Piers.....	288
Figure C.11-2 Transverse Displacement Envelope of the Bridge Deck	289
Figure C.11-3 Hysteresis Plots for the Center Column of Pier 2.....	289
Figure C.11-4 Longitudinal Displacement of Expansion Joints	291
Figure C.12-1 Total Displacement at Piers.....	292
Figure C.12-2 Transverse Displacement Envelope of the Bridge Deck	293
Figure C.12-3 Hysteresis Plots for the Center Column of Pier 2.....	293
Figure C.12-4 Longitudinal Displacement of Expansion Joints	295

Figure C.13-1 Total Displacement at Piers.....	296
Figure C.13-2 Transverse Displacement Envelope of the Bridge Deck	297
Figure C.13-3 Hysteresis Plots for the Center Column of Pier 2.....	297
Figure C.13-4 Longitudinal Displacement of Expansion Joints	299
Figure C.14-1 Total Displacement at Piers.....	300
Figure C.14-2 Transverse Displacement Envelope of Bridge Deck	301
Figure C.14-3 Hysteresis Plots for the Center Column of Pier 2.....	301
Figure C.14-4 Longitudinal Displacement of Expansion Joints	303
Figure C.15-1 Total Displacement at Piers.....	304
Figure C.15-2 Transverse Displacement Envelope of Bridge Deck	305
Figure C.15-3 Hysteresis Plots for the Center Column of Pier 2.....	305
Figure C.15-4 Longitudinal Displacement of Expansion Joints	307
Figure C.16-1 Total Displacement at Piers.....	308
Figure C.16-2 Transverse Displacement Envelope of Bridge Deck	309
Figure C.16-3 Hysteresis Plots for the Center Column of Pier 2.....	309
Figure C.16-4 Longitudinal Displacement of Expansion Joints	311
Figure C.17-1 Total Displacement at Piers.....	312
Figure C.17-2 Transverse Displacement Envelope of Bridge Deck	313
Figure C.17-3 Hysteresis Plots for the Center Column of Pier 2.....	313
Figure C.17-4 Longitudinal Displacement of Expansion Joints	315
Figure D.2-1 Longitudinal Displacement of Expansion Joints	317
Figure D.3-1 Total Relative Displacement at Piers.....	318
Figure D.3-2 Transverse Displacement Envelope of Bridge Deck	319

Figure D.3-3 Plastic Rotations at the Top of the Columns.....	319
Figure D.3-4 Plastic Rotations at the Bottom of the Columns.....	320
Figure D.3-5 Damage at Top of Columns	320
Figure D.3-6 Damage at Bottom of Columns	321
Figure D.3-7 Hysteresis Plots for the Center Column of Pier 2.....	321
Figure D.3-8 Longitudinal Displacement of Expansion Joints	323
Figure D.4-1 Total Relative Displacement at Piers.....	324
Figure D.4-2 Transverse Displacement Envelope of Bridge Deck	325
Figure D.4-3 Plastic Rotations at Top of Columns	325
Figure D.4-4 Damage at Top of Columns	326
Figure D.4-5 Hysteresis Plots for the Center Column of Pier 2.....	326
Figure D.4-6 Longitudinal Displacement of Expansion Joints	328
Figure D.5-1 Total Relative Displacement at Piers.....	329
Figure D.5-2 Transverse Displacement Envelope of Bridge Deck	330
Figure D.5-3 Plastic Rotations at Top of Columns	330
Figure D.5-4 Plastic Rotations at Bottom of Column	331
Figure D.5-5 Damage at Top of Columns	331
Figure D.5-6 Damage at Bottom of Columns	332
Figure D.5-7 Hysteresis Plots for the Center Column of Pier 2.....	332
Figure D.5-8 Longitudinal Displacement of Expansion Joints	334
Figure D.6-1 Total Relative Displacement at Piers.....	335
Figure D.6-2 Plastic Rotations at the Top of the Columns.....	336
Figure D.6-3 Damage at Top of Columns	336

Figure D.6-4 Hysteresis Plots for the Center Column of Pier 2.....	337
Figure D.6-5 Longitudinal Displacement of Expansion Joints	339
Figure D.7-1 Total Relative Displacement at Piers.....	340
Figure D.7-2 Transverse Displacement Envelope of Bridge Deck	341
Figure D.7-3 Plastic Rotations at the Top of Columns	341
Figure D.7-4 Plastic Rotations at the Bottom of Columns	342
Figure D.7-5 Damage at Top of Columns	342
Figure D.7-6 Damage at Bottom of Columns	343
Figure D.7-7 Hysteresis Plots for the Center Column of Pier 2.....	343
Figure D.7-8 Longitudinal Displacement of Expansion Joints	345
Figure D.8-1 Total Relative Displacement at Piers.....	346
Figure D.8-2 Transverse Displacement Envelope of Bridge Deck	347
Figure D.8-3 Plastic Rotations at the Top of the Columns.....	347
Figure D.8-4 Plastic Rotations at the Bottom of the Columns.....	348
Figure D.8-5 Damage at the Top of Columns.....	348
Figure D.8-6 Damage at Bottom of Columns	349
Figure D.8-7 Hysteresis Plots of the Center Column at Pier 2	349
Figure D.8-8 Longitudinal Displacement of Expansion Joints	351
Figure D.9-1 Total Relative Displacement at Piers.....	352
Figure D.9-2 Transverse Displacement Envelope of Bridge Deck	353
Figure D.9-3 Plastic Rotations at the Top of the Columns.....	353
Figure D.9-4 Plastic Rotations at the Bottom of the Columns.....	354
Figure D.9-5 Damage at the Top of Columns.....	354

Figure D.9-6 Damage at the Bottom of Columns	355
Figure D.9-7 Hysteresis Plots for the Center Column of Pier 2.....	355
Figure D.10-1 Total Relative Displacement at Piers.....	357
Figure D.10-2 Transverse Displacement Envelope of Bridge Deck	358
Figure D.10-3 Plastic Rotations at the Top of the Columns.....	358
Figure D.10-4 Plastic Rotations at the Bottom of the Columns.....	359
Figure D.10-5 Damage at the Top of Columns.....	359
Figure D.10-6 Damage at the Bottom of Columns	360
Figure D.10-7 Hysteresis Plots for the Center Column of Pier 2.....	360
Figure D.11-1 Total Relative Displacement at Piers.....	362
Figure D.11-2 Transverse Displacement Envelope of Bridge Deck	363
Figure D.11-3 Plastic Rotations at the Top of the Columns.....	363
Figure D.11-4 Plastic Rotations at the Bottom of the Columns.....	364
Figure D.11-5 Damage at the Top of the Columns	364
Figure D.11-6 Damage at the Bottom of Columns	365
Figure D.11-7 Hysteresis Plots for the Center Column of Pier 2.....	365
Figure D.11-8 Longitudinal Displacement of Expansion Joints	367
Figure D.12-1 Total Relative Displacement at Piers.....	368
Figure D.12-2 Transverse Displacement Envelope of Bridge Deck	369
Figure D.12-3 Plastic Rotations at the Top of the Columns.....	369
Figure D.12-4 Plastic Rotations at the Bottom of the Columns.....	370
Figure D.12-5 Damage at the Top of the Columns	370
Figure D.12-6 Damage at the Bottom of Columns.....	371

Figure D.12-7 Hysteresis Plots for the Center Column of Pier 2..... 371

Figure D.12-8 Longitudinal Displacement of Expansion Joints 373

Figure D.13-1 Total Relative Displacement at Piers..... 374

Figure D.13-2 Transverse Displacement Envelope of Bridge Deck 375

Figure D.13-3 Plastic Rotations at the Top of the Columns..... 375

Figure D.13-4 Plastic Rotations at the Bottom of the Columns..... 376

Figure D.13-5 Damage at the Top of the Columns 376

Figure D.13-6 Damage at the Bottom of Columns 377

Figure D.13-7 Hysteresis Plots for the Center Column of Pier 2..... 377

Figure D.14-1 Total Relative Displacement at Piers..... 379

Figure D.14-2 Transverse Displacement Envelope of Bridge Deck 380

Figure D.14-3 Plastic Rotations at the Top of the Columns..... 380

Figure D.14-4 Plastic Rotations at the Bottom of the Columns..... 381

Figure D.14-5 Damage at the Top of the Columns 381

Figure D.14-6 Damage at the Bottom of Columns 382

Figure D.14-7 Hysteresis Plots for the Center Column of Pier 2..... 382

CHAPTER 1

Introduction

1.1 Pre-1970 Bridge Column Design

After the 1971 San Fernando earthquake, which caused substantial damage to highway bridges, bridge column design was changed to account for the evident lack of strength and ductility. It was found that the transverse steel specified for the plastic hinge region was not sufficient to supply the necessary confinement. Typically, the transverse reinforcement consisted of No. 3 or No. 4 reinforcing hoops, spaced every 12 inches. This resulted in transverse reinforcing ratios of 0.05% to 0.12%.

Researchers also identified problems with the lap splicing of the longitudinal reinforcement at the base of the column. Typically, the lap splices were placed at the base of the column, which is the location of the plastic hinge region. This, coupled with the fact that the lap splices were typically between 20 to 35 times the diameter of the reinforcing bar, led to many failures due to slipping of the splices.

At that time, designers changed their practices to account for these insufficiencies. It is now typical to provide spirals for the transverse reinforcement within the plastic hinge region, designed as a minimum of No. 3 bars with center-to-center spacing that cannot exceed 4 inches (AASHTO, 1998). It is also necessary to have the lap splice of the longitudinal reinforcing located within the middle half of the column, away from the plastic hinge regions. The lap splices must have a length of 60 times the diameter of the longitudinal bar, and be fully welded (AASHTO, 1998).

For reasons of economy, it was not possible to replace or retrofit all of the older bridges after these new developments. Thus, it is still necessary to understand the response that these older bridges will have to earthquake loading. There is very little information about how these lightly reinforced concrete bridges will respond to long-duration ground motions. With the possibility of a large-scale long-duration earthquake in Western Washington State, it is necessary to assess the response of these older bridges.

1.2 Research Objectives

The objectives of this research project were as follows:

- Analyze the response and damage in two bridges typical of construction in Washington State in short and long-duration earthquakes.
- Determine the response of these two bridge models with variations in the abutment and column spring stiffnesses.

These objectives were accomplished through the following tasks:

- Calibrate a theoretical damage model for poorly confined concrete columns.
- Implement the theoretical damage model into the computer program WSU-NEABS.
- Test and validate the changes implemented in the computer program.
- Model WSDOT Bridges 5/518 and 5/826.
- Analyze the two bridge models using long-duration time histories.
- Analyze the two bridge models using short-duration time histories and compare the results to those of the long-duration time histories.

- Investigate the sensitivity of the bridges to a variation of the abutment spring stiffness.
- Investigate the sensitivity of the bridges to a variation of the column soil spring stiffness.

1.3 Seismicity of Western Washington State

The Cascadia Subduction Zone (CSZ) is the boundary where the Juan de Fuca oceanic plate and the North American continental plate meet (see Figure 1.2-1 and Figure 1.2-2). The sliding or slip of the locked interface of the Juan de Fuca plate and North American plate can create mega-earthquakes, which have the potential of occurring approximately every 500 years (NRCan, 2004).

Two other modes of seismic activity are also possible. These two modes do not create earthquakes that are as large as those produced by the rupturing of the plate interface, however. The first of these modes is the cracking of the subducting plate due to tension stresses caused by the shrinking of the plate. These are deeper earthquakes that occur at depths between 18 miles and 44 miles, and reach magnitudes of up to 7+ (PNSN, 2004).

The final mode of seismic activity takes place in the shallower continental plate. These earthquakes occur up to a depth of 16 miles and also have magnitudes of up to 7+. These earthquakes occur due to fracturing in the plate as it adjusts to the stresses and movements caused by the subducting plate (PNSN, 2004)

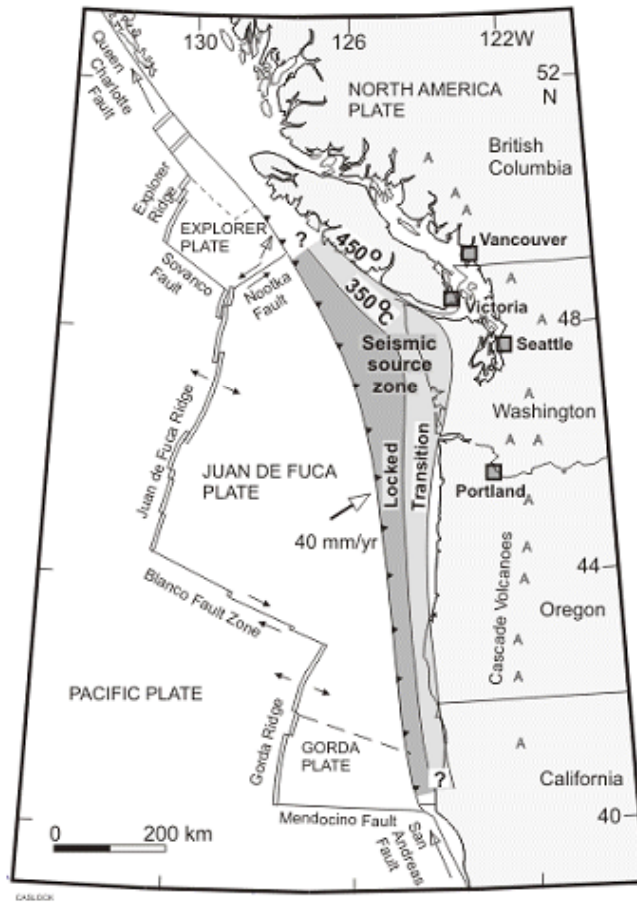


Figure 1.2-1 The Cascadia Subduction Zone Boundary (NRCan, 2004)

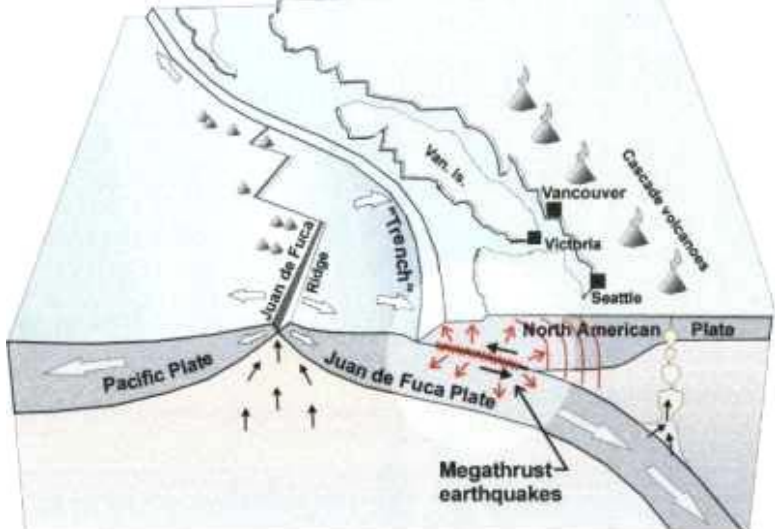


Figure 1.2-2 The Cascadia Subduction Zone (NRCan, 2004)

1.4 Program Modification

The program WSU-NEABS (WSU-Nonlinear Earthquake Analysis of Bridge Systems) was modified to add an additional damage model. This was done with the understanding that long-duration earthquakes cause bridge structures to undergo many more loading cycles than those of a short duration event. Kunnath et al (1997) proposed the damage model that was implemented in the program. The model, which is based on low-cycle fatigue, was calibrated from testing done by Stapleton (2004).

The program was also modified to account for the additional loss of stiffness due to damage, which is observed in lightly reinforced concrete members. This modification included an addition that allows for degradation of stiffness during the unloading phase. It also included an increase in the degradation of stiffness for the reloading branch of the hysteresis rule to mimic the pinching effect.

1.5 Bridge Modeling

Two pre-1971 Washington State Department of Transportation (WSDOT) bridges were modeled using WSU-NEABS. The two bridges, Bridges 5/518 and 5/826, are located in Western Washington State. They were chosen for this study because they represent typical 1950's and 1960's WSDOT Bridges, which do not provide the confinement needed in the plastic hinge region of the columns. They also have lap splices of the longitudinal steel in the plastic hinge region of only 35 times the diameter of the bars. The modeling of the bridges is discussed in more detail in Chapter 4.

1.6 Bridge Analysis

The two bridges were analyzed using a suite of ten different earthquakes. All of the earthquake time-history records were modified to fit a target acceleration spectrum for Western Washington State. Six of the records were from long-duration events and the last four were from short-duration events. The records were from earthquakes in Llolleo, Peru; Moquegua, Chile; Mexico City, Mexico; Kobe, Japan; and Olympia, Washington. The seismic excitation is discussed in more detail in Chapter 4.

The response of the bridges using the long-duration records was compared to that of the short-duration record response. Selected earthquakes were also used to determine the sensitivity of the bridges to a variation in the abutment and column soil spring stiffness.

Chapter Two

Literature Review

2.1 Introduction

Reinforced concrete bridge seismic design changed in 1971 with the recognition of inadequate design methods for confinement and lap splices. The change of seismic design criteria to account for the deficiency of strength and ductility found in the columns due to the lack of reinforcing was made at this time. Without adequate reinforcing, these columns cannot withstand major earthquakes.

There has been a large emphasis placed on research to understand how these lightly reinforced columns will respond to different levels and types of earthquake loading. Many methods of analysis have been tested to account for the non-linear behavior that is found in reinforced concrete members. One of the major areas of research has been to determine how to model the damage that accumulates in reinforced concrete.

2.2 Current Damage Analysis Methods

Current seismic analysis of reinforced concrete members under cyclic loading and random earthquake loading is accomplished using many differing techniques. There have been numerous proposed and tested models, none of which have completely solved the issue of modeling a material that behaves in a non-linear manner. One of the major difficulties is how to correctly model the accumulation of damage over time.

Damage in beam-column members is caused by many different mechanisms. The main cause of damage is concrete crushing and cracking. Under extreme loading,

damage can also involve buckling of the longitudinal steel, diagonal shear cracking, and deformations in the connection regions of the member usually caused by bond slip. These mechanisms cause a strength and stiffness degradation in the member.

A damage model is needed to accurately quantify the amount of damage that is sustained during this random loading. The effect of damage is included through the use of damage coefficients, which typically range from zero to one. If the damage coefficient is zero, there is no damage in the structural element and if the coefficient is one, the structural element is completely damaged. Values in between provide a measure of the amount of damage that the member has undergone.

There are five basic methods that have been used to model the damage: damage models that use strength and stiffness degradation as a basis; those that are based on displacement or deformation; models that are based on energy dissipation; hybrid damage models that combine aspects of the previous models; and damage models that are grounded in more complex theories of low-cycle fatigue (Kunnath et al. 1997). A review of these methods can be found in the literature (Williams and Sexsmith 1995).

2.2.1 Damage Models Based on Strength and Stiffness Degradation

Damage based on stiffness and strength deterioration is an issue that relates to deformation. The deformation demand is taken into account by evaluating physical properties such as maximum strains or curvatures. Under monotonic loading, peak values of displacement or rotation are important parameters.

Cumulative damage models based on strength and stiffness degradation are closely related to the hysteretic behavior of the concrete member. Structural damage is

generally understood to be a stiffness softening phenomenon caused by material deterioration. Such softening in nonlinear structural response is mirrored in the load-displacement diagram by a change in elastic slope (Kratzig et al. 2000).

This type of formulation is used in the program IDARC (Kunnath et al. 1992). The first edition of IDARC used a trilinear monotonic moment-curvature relationship. This was used along with a hysteresis law defined by three parameters. The three parameters are the stiffness degradation, the strength degradation, and pinching. The stiffness degradation is controlled by the parameter α , which defines the target unloading point in terms of the yield moment. See Figure 2.2-1(a).

The strength degradation is controlled by the equation:

$$M_m(i+1) = M_m(i) \left(1 - \beta_e \frac{\int dE}{M_y \phi_u} \beta_d \mu_\phi \right) \quad (2.1)$$

between cycles i and $(i+1)$, where the integral of dE is the accumulated hysteretic energy. See Figure 2.2-1(b). The pinching parameter is controlled by the parameter γ , which defines a reduced target point for the unloading path when the $M = 0$ axis is crossed. See Figure 2.2-1(c). One of the major disadvantages of this model is the fact that these parameters must be tuned to account for differing structural types and material properties.

Another method, much the same, was used in an analysis of older reinforced concrete columns (Pincheira et al 1999). The model presented is based on the theories of lumped plasticity and it accounts for shear and flexural strength and stiffness degradation.

It is able to account for the nonlinear response in both flexure and shear by the superposition of each separate hysteretic law.

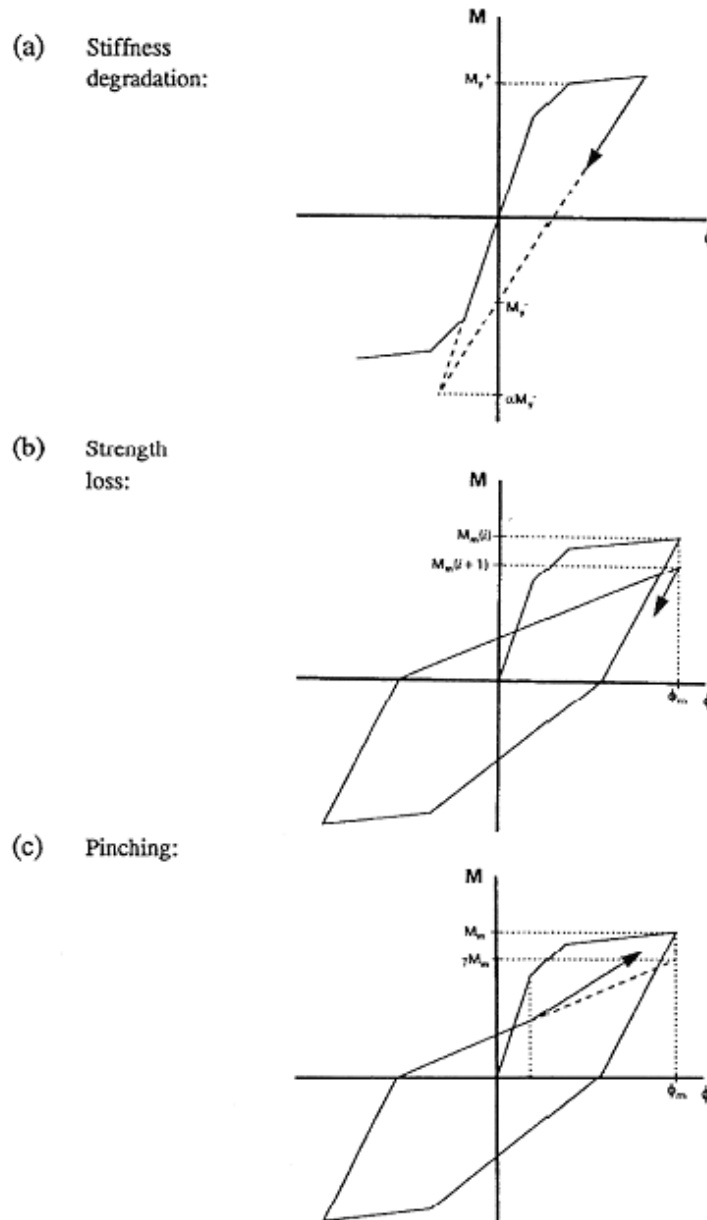
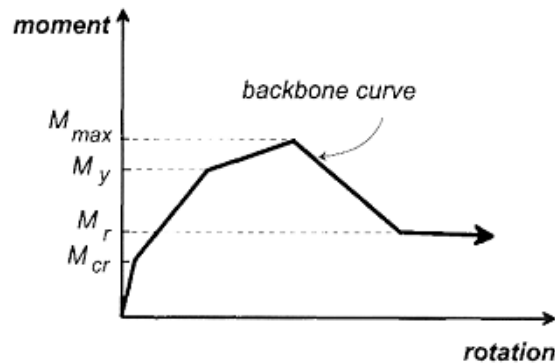
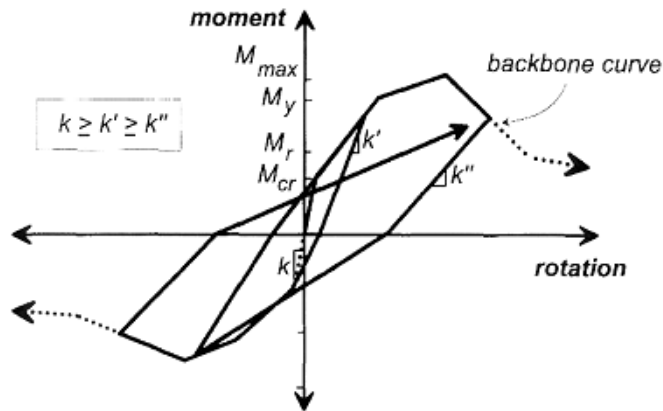


**Figure 2.2-1 Hysteresis Behavior of Concrete as Modeled in IDARC
(Williams and Sexsmith 1997)**

Flexural strength degradation was accounted for by adding a section of negative slope to the moment-rotation backbone curve as shown in Figure 2.2-2(a). This degradation continues until a residual moment is reached and, at this point, the backbone curve continues at a very slight negative slope. The stiffness degradation was accounted for by reducing the slope of the unloading stiffness as shown in Figure 2.2-2(b). Note that k' is larger than k'' .



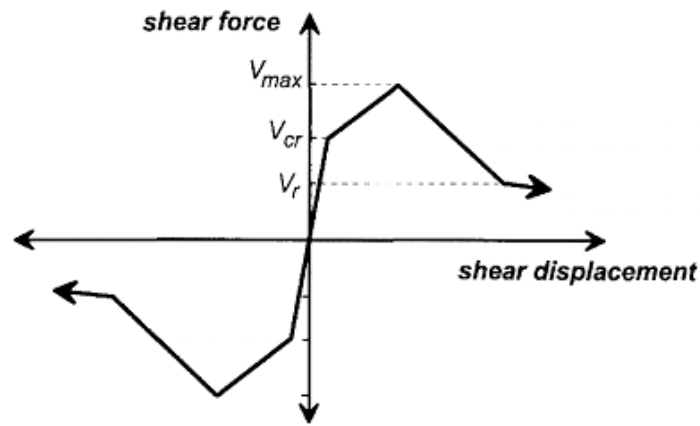
(a) Backbone curve



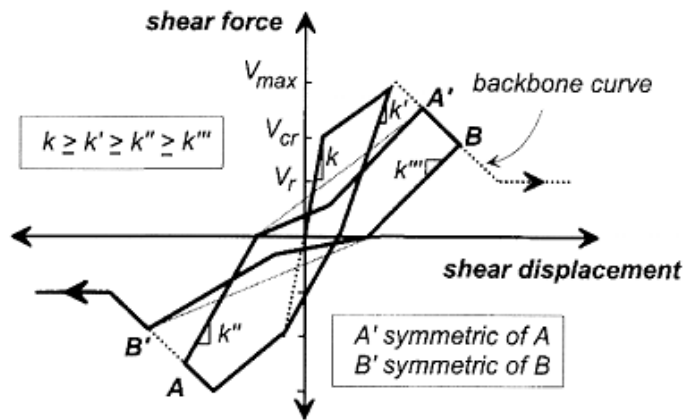
(b) Hysteretic laws

Figure 2.2-2. Moment and Rotation Relation: (a) Backbone Curve; (b) Hysteretic Laws (Pincheria et al 1999)

Much like the moment-rotation backbone curve, the shear force/deformation backbone curve shows the strength degradation as a section of negative slope. See Figure 2.2-3(a). It is also followed by a section of very small negative slope after a residual shear value has been reached. The shear stiffness component of the model was accounted for by a reduced unloading stiffness. For both flexure and shear, identical behavior is assumed for both directions of loading.



(a) Backbone curve



(b) Hysteretic laws

Figure 2.2-3. Shear Force and Displacement Relation: (a) Backbone Curve; (b) Hysteretic Laws (Pincheria et al 1999)

The definition of these backbone curves was based on existing material models and generally accepted theories of reinforced concrete. The response of the reinforced concrete column was based on flexural strength and deformation, anchorage slip, and shear strength and deformation. Moment-rotation backbone curves were found by using a plane section analysis with measured material properties of both the concrete and the steel.

Approximate procedures have been developed to account for anchorage slip. These procedures were used to calculate rigid-body rotations due to the bar slip. The backbone for the shear behavior was determined by using the Modified Compression Field Theory. With this theory, the shear force and deformation response of reinforced concrete members may be calculated.

Another damage model based on strength and stiffness degradation was proposed by Sivaselvan and Reinhorn (2000). They created a model that is defined by a smooth hysteretic function instead of a polygonal or piecewise hysteretic function. A polygonal hysteretic function is one that is broken into different pieces, which mirror actual behavioral stages of a member such as elastic, cracking, yielding, stiffness and strength degradation, and crack closure. The smooth hysteretic function differs in that it has a continual change in stiffness due to yielding, but sharp changes due to unloading and degrading behavior.

The model that Sivaselvan and Reinhorn (2000) propose is a variation of those created by Bouc (1967) and modified by Wen (1976), Baber and Noori (1985), Casciati (1989), and Reinhorn et al. (1995). It consists of two springs, which model the plain hysteretic behavior and the post-yield hardening of a member. One spring is linearly

elastic while the other changes stiffness after yielding occurs. This is modified to allow for stiffness degradation, strength degradation, pinching, and gap-closing behavior.

With increasing deformation, the elastic stiffness of a member degrades and this phenomenon has been accurately modeled using the pivot rule (Park et al. 1987). This rule states that the load-reversal branches target a pivot point that is located on the initial elastic branch at a distance of αM_y . See Figure 2.2-4(a). In this case, α is the stiffness degradation parameter, and the stiffness degradation factor K_{cur} , is given by the equation:

$$K_{cur} = R_k K_o = \frac{M_{cur} + \alpha M_y}{(K_o \phi_{cur} + \alpha M_y)} K_o \quad (2.2)$$

where M_{cur} = current moment; ϕ_{cur} = current curvature; K_o = initial elastic stiffness.

Stiffness degradation only occurs in the hysteretic spring, therefore only the hysteretic stiffness is modified and it is given by:

$$K_{hysteretic} = (R_k - a) \left[1 - \left(\frac{M^*}{M_y} \right)^N \left(\eta_1 \operatorname{sgn}(M^* \dot{\phi}) + \eta_2 \right) \right] \quad (2.3)$$

The strength degradation is modeled by reducing the capacity in the backbone curve. See Figure 2.2-4(b). “ The strength degradation rule can be formulated to include an envelope degradation, which occurs when the maximum deformation attained in the past is exceeded, and a continuous energy-based degradation. The strength degradation rule is given by the equation:

$$M_{y\ +/-} = M_{yo\ +/-} \left[1 - \left(\frac{\phi_{max\ +/-}}{\phi_u\ +/-} \right)^{\frac{1}{\beta_1}} \right] \left[1 - \frac{\beta_2}{(1 - \beta_2)} \frac{H}{H_{ult}} \right] \quad (2.4)$$

where M_y = yield moment; M_{yo} = initial yield moment; ϕ_{max} = maximum curvature; ϕ_u = ultimate curvature; H = hysteretic energy dissipated; H_{ult} = hysteretic energy dissipated when loaded monotonically to the ultimate curvature without degradation; β_1 = ductility-based strength degradation parameter; β_2 = energy-based strength degradation parameter” (Sivaselvan and Reinhorn 2000).

An additional spring is added to the system in series with the hysteretic spring to account for pinching. “The stiffness of the slip-lock spring can be written:

$$K_{slip-lock} = \left[\sqrt{\frac{2}{\pi}} \frac{s}{M_{\sigma}^*} \exp \left[\frac{1}{-2} \left(\frac{M^* - \overline{M}^*}{M_{\sigma}^*} \right)^2 \right] \right]^{-1} \quad (2.5)$$

where s = slip length = $R_s(\phi_{max}^+ - \phi_{max}^-)$; $M_{\sigma}^* = \sigma M_y^*$ = measure of the moment range over which slip occurs; $\overline{M}^* = \lambda M_y^*$ = mean moment level on either side about which slip occurs; R_s , σ , and λ = parameters of the model; and ϕ_{max}^+ and ϕ_{max}^- = maximum curvatures reached on the positive and negative sides, respectively, during the response” (Sivaselvan and Reinhorn 2000). There is also a gap-closing spring that can be added in parallel to model the stiffening effect when gaps close.

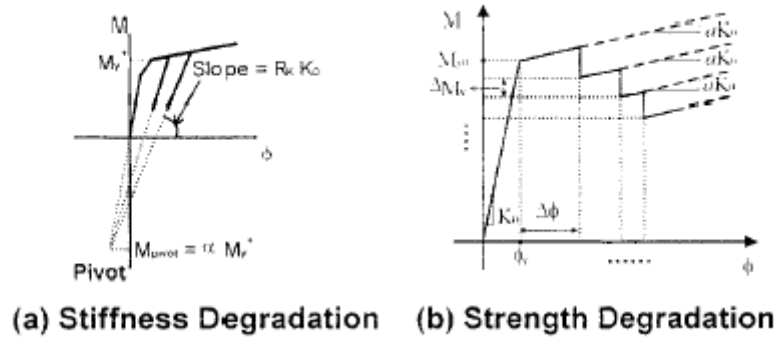


Figure 2.2-4. Stiffness and Strength Degradation (Sivaselvan et al 2000)

2.2.2 Damage Models Based on Measures of Deformation and/or Ductility

Williams and Sexsmith (1995) reviewed damage based on deformation. It is generally accepted that damage based on cycles of deformation is a low-cycle fatigue phenomenon. Degradation is assumed to evolve by the accumulation of plastic deformation. They refer to Stephens and Yao (1987), who proposed a damage model that was based entirely on displacement ductility. Figure 2.2-5 shows how positive and negative displacement increments are defined. “The damage index is:

$$D = \sum \left(\frac{\Delta\delta^+}{\Delta\delta_f} \right)^{1-br} \quad (2.6)$$

where $r = \Delta\delta^+/\Delta\delta^-$, $\Delta\delta_f$ is the value of $\Delta\delta^+$ in a single-cycle test to failure and b is a constant. Stephens and Yao recommend taking $\Delta\delta_f$ as 10% of the story height and b as 0.77” (Williams and Sexsmith 1995).

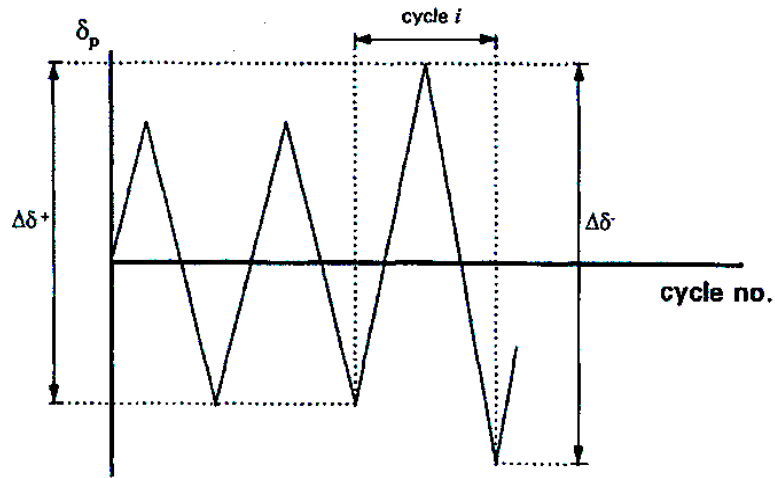


Figure 2.2-5 Plastic Displacement Increments (Stephens and Yao 1987)

Wang and Shah (1987) also developed a cumulative damage model based on deformation. Their model is based on the maximum deformation in a cycle and the accumulation of the damage is assumed to be proportional to the damage that has already occurred, “resulting in the following expression for the damage index:

$$D = \frac{\exp(sb) - 1}{\exp(s) - 1} \quad (2.7a)$$

$$b = c \sum_i \frac{\delta_{m,i}}{\delta_f} \quad (2.7b)$$

where s and c are user-defined constants and the parameter b is a scaled cumulative displacement ductility” (Williams and Sexsmith 1995). Wang and Shah tested two beam-column joints to calibrate their damage model and found that $c = 0.1$ and $\delta_f = 5\delta_y$. “The parameter s depends on the span-depth ratio and the level of shear reinforcement, with a value of 1.0 recommended for a heavily reinforced joint and -1.0 for a poorly reinforced

joint. The index is basically a measure of strength degradation, with the yield load in a deformation cycle given by the maximum load in the previous cycle multiplied by $(1-D)$ ” (Williams and Sexsmith 1995). See Figure 2.2-6.

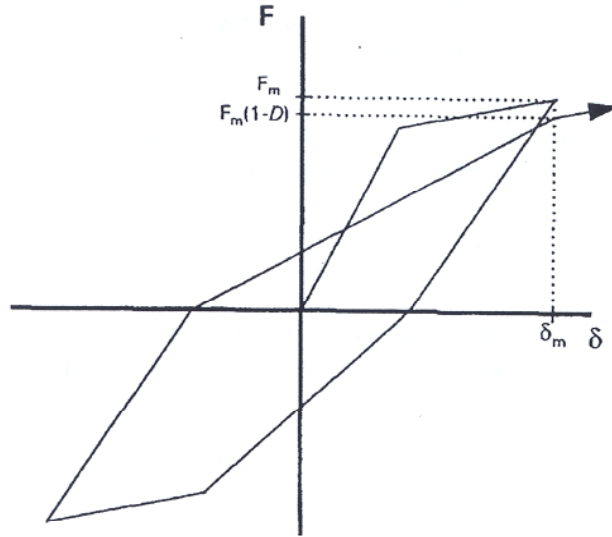


Figure 2.2-6. Physical Meaning of Wang and Shah (1987) Damage Index

Because damage based on deformation and ductility is a low-cycle fatigue phenomenon, the familiar Coffin-Manson law can be used. Jeong and Iwan (1988) calibrated the Coffin-Manson law to experimental data that was obtained from tests of reinforced concrete columns. They used the relationship:

$$n_f \mu^s = c \quad (2.8)$$

where the constants s and c were taken as 6 and 416, respectively, and the n_f factor is the number of cycles to failure at a specific level of deformation. The damage index was then found using Miner's rule, where:

$$D = \sum_i \frac{n_i}{n_{f,i}} = \frac{n_i \mu_i^s}{c} \quad (2.9)$$

Mander and Cheng (1995) derived a mechanics-based damage index that is related to the local section curvature at the plastic hinge in terms of the strain in the rebar (Kunnath et al. 1997). This is expressed as:

$$\phi_p D = \frac{0.113}{1 - \frac{2d}{D}} N_f^{-0.5} \quad (2.10)$$

“The above expression is derived from the plastic strain vs. fatigue life relationship obtained from actual testing of steel reinforcing bars (Mander et al., 1994) and the relationship between curvature and strain in a reinforced concrete circular cross-section assuming a linear strain profile.” (Kunnath et al. 1997) In the equation, ϕ_p is the plastic curvature, D is the column diameter, d is the cover depth, and N_f is the number of cycles to the appearance of the first fatigue crack in the steel.

Manfredi and Pecce (1996) introduced a damage model based on low-cycle fatigue in terms of ductility. The damage index has the expression:

$$D = A \sum_{i=1}^{N_i} \mu_i^b \quad (2.11)$$

where A and b are experimental parameters, N_i is the number of cycles, and $\mu_i = (\delta_i - \delta_y) / \delta_y$ is the ductility under the loading of the i th cycle. As is typical, failure is reached when $D = 1$. The value b is a measure of the sensitivity to damage. A low b value means the element is more sensitive to damage than for a higher b value.

2.2.3 Damage Models Based on Energy Dissipation

The earliest damage model based on energy absorption was introduced by Gosain et al (1977). The damage index is defined as:

$$D_e = \sum_i \frac{F_i \delta_i}{F_y \delta_y} \quad (2.12)$$

Gosain assumed that once the peak force has dropped below 75% of the yield value, the remaining capacity of the member is negligible. Therefore, only the hysteresis loops where $F_i / F_y \geq 0.75$ are included. (Williams and Sexsmith 1995)

A more familiar energy based damage model was developed by Kratzig et al (1989). The model is based on primary and follower half-cycles. See Figure 2.2-7. A primary half-cycle is the half-cycle in which the maximum deformation is contained.

Any subsequent half-cycle is a follower half-cycle, unless it exceeds the previous maximum deformation. Positive and negative half-cycles are calculated separately, where the accumulated damage for the positive half-cycle is:

$$D^+ = \frac{\sum E_{p,i}^+ + \sum E_i^+}{E_f^i + \sum E_i^+} \quad (2.13)$$

E_{pi} is the energy in a primary half-cycle, E_i is the energy in a follower half-cycle, and E_f is the energy dissipated in a monotonic pushover test to failure.

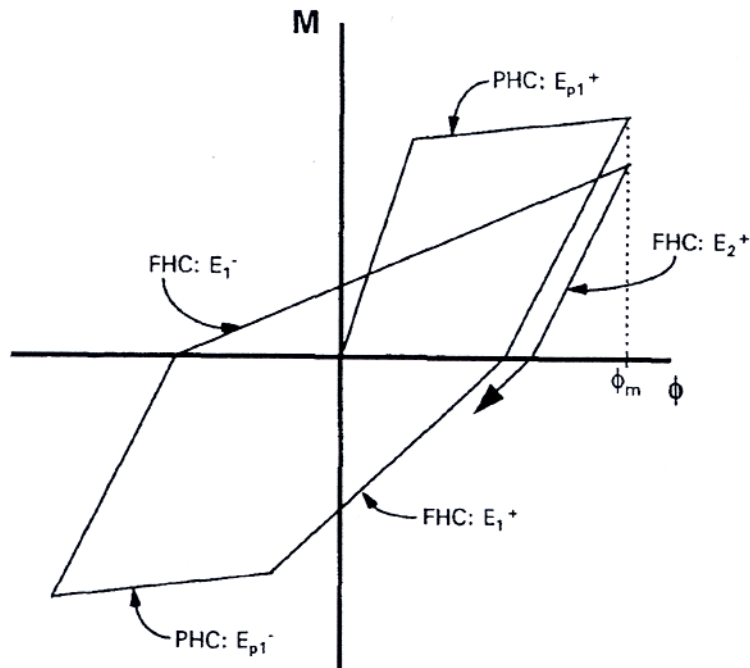


Figure 2.2-7 Primary (PHC) and Follower (FHC) Half-cycles (Kratzig et al 1989)

The same calculation is done for the negative cycles, and then the total damage index is found by:

$$D = D^+ + D^- - D^+ D^- \quad (2.14)$$

Noting that the follower cycles are included in the numerator and the denominator suggests that they contribute to the damage far less than the primary cycles do. This allows the model to account for both deformation and fatigue type damage. (Williams and Sexsmith 1995)

Other models based on energy dissipation are founded in fracture and continuum damage mechanics. One such model was proposed by Florez-Lopez et al (1998). This model was manipulated from that proposed by Marigo (1985), which was based on an extension of the Griffith criterion to include fatigue type damage. The model is given by:

$$d_i = \frac{G_i^\alpha}{R^\alpha \frac{\delta R}{\delta d_i}} \langle G_i \rangle \quad \text{if } G_i \geq G_{cr} \quad (2.15(a))$$

$$d_i = 0 \quad \text{otherwise} \quad (2.15(b))$$

where $R(d_i)$ is the crack resistance term, G_i is the energy release rate, and $G_{cr} = R(0)$.

During a monotonic test, this model will give the same damage evolution as the Griffith law, but when the loading becomes non-monotonic, they differ because of the accumulation due to fatigue.

2.2.4 Damage Models Based on Hybrid Formulations

The most common hybrid formulation is the Park-Ang Model (1985). Williams and Sexsmith (1995) reviewed this as well. The model uses a combination of deformation and energy dissipation. The damage coefficient is defined as:

$$D = \frac{\delta_m}{\delta_u} + \beta_e \frac{\int dE}{F_y \phi_u} \quad (2.16)$$

The first term is the one that takes the damage caused by deformation into account, while the cumulative damage is accounted for by the second term, which is the energy term.

The value β_e is a strength deterioration parameter. The authors suggested these guidelines for the damage index:

$D < 0.1$	No damage or localized minor cracking
$0.1 \leq D < 0.25$	Minor damage – light cracking throughout
$0.25 \leq D < 0.4$	Moderate damage – severe cracking, localized spalling
$0.4 \leq D < 1.0$	Severe damage – crushing of concrete, reinforcement exposed
$D \geq 1.0$	Collapsed

Ang revised this in 1993 so that $D = 0.8$ represents collapse.

The Park-Ang model was modified by Kunnath et al (1992) so that moment-curvature is used instead of force-displacement. The index is:

$$D = \frac{\phi_m - \phi_y}{\phi_u - \phi_y} + \beta_e \frac{\int dE}{M_y \phi_u} \quad (2.17)$$

These damage indices are used because they are easy to implement, but they are not without their problems. It is difficult to determine what the ultimate deformation and strength deterioration parameter should be. There have been many studies to determine what the deterioration parameter should be, with differing results, which makes it somewhat arbitrary (Williams and Sexsmith 1995).

A hybrid formulation was proposed by Bracci et al (1989), where a damage potential, D_P , was defined as the area enclosed by the monotonic force-displacement curve and the fatigue failure envelope. See Figure 2.2-8(a). The strength damage, D_S , is the area between the monotonic curve and the degraded force-displacement curve. This degradation causes permanent deformations, which induces deformation damage D_d .

For simplicity, Bracci et al used a simplified bilinear moment-curvature relationship, as is shown in Figure 2.2-8(b). Therefore, the proportionate strength loss and proportionate plastic deformation are:

$$D_M = \frac{\Delta M}{M_y} \quad (2.18a)$$

$$D_\phi = \frac{\phi_m - \phi_y}{\phi_f - \phi_y} \quad (2.18b)$$

The damage index can then be defined as:

$$D = \frac{D_s + D_d}{D_P} = \frac{\Delta M(\phi_f - \phi_y) + (M_y - \Delta M)(\phi_m - \phi_y)}{M_y(\phi_f - \phi_y)} = D_M + D_\phi - D_M D_\phi \quad (2.19)$$

“Bracci et al suggested a calculation method for D_ϕ in which the value of the yield curvature is modified after each cycle, taking account of both plastic deformations and the effect of stiffness degradation” (Williams and Sexsmith 1995). See Figure 2.2-8(c).

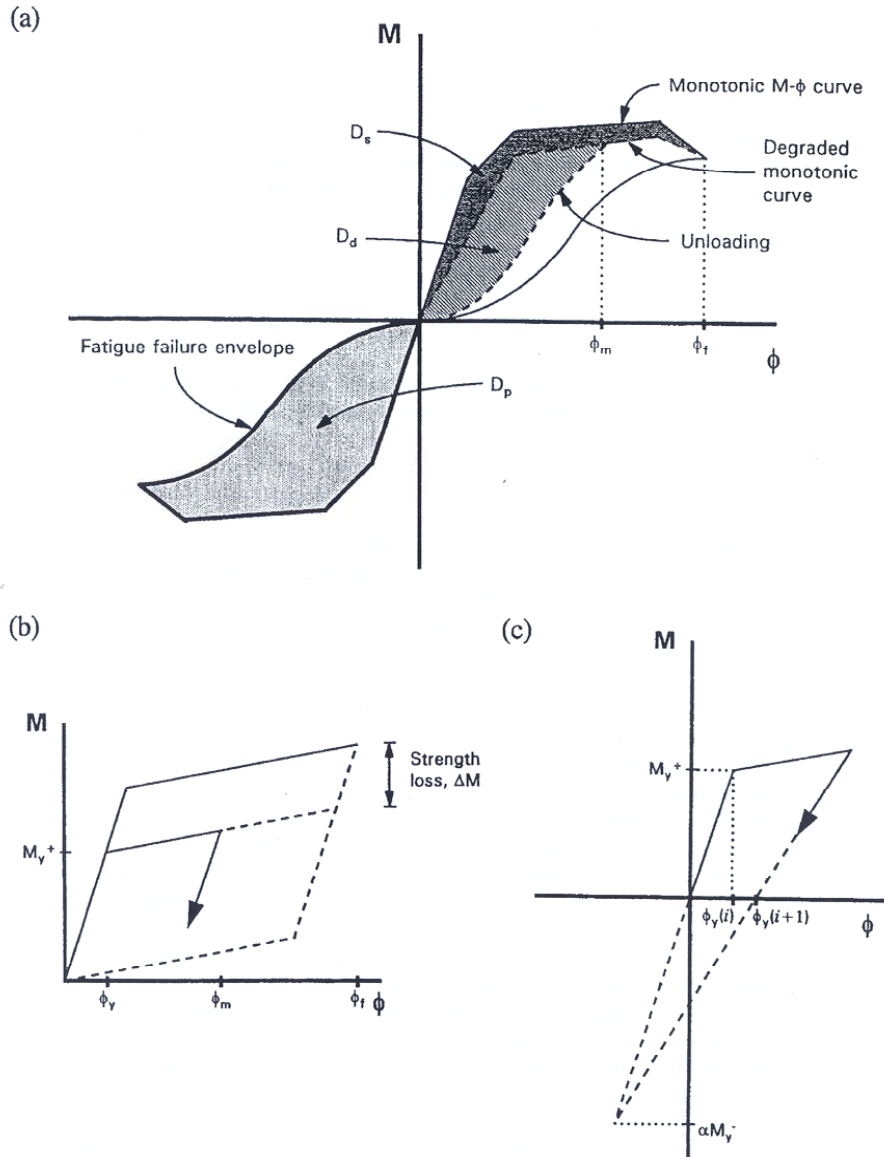


Figure 2.2-8. Moment – Curvature Characteristics for Damage Index (Bracci et al 1989)

The degradation of strength is defined as:

$$\Delta M = \frac{\int dE}{\phi_y} \quad (2.20)$$

where “the constant c is defined by a regression equation in terms of the axial load, the longitudinal and confinement steel ratios, and the material strengths” (Williams and Sexsmith 1995). Bracci et al suggested these guidelines for the damage index:

$D < 0.33$	Serviceable
$0.33 \leq D < 0.66$	Repairable
$0.66 \leq D < 1.0$	Irreparable
$D \geq 1.0$	Collapsed

2.2.5 Damage Models Based on More Complex Fatigue Models

Williams and Sexsmith (1995) considered a complex fatigue model proposed by Chung et al (1987, 1989a). “Given a monotonic moment-curvature curve with failure point (M_f, ϕ_f) , the moment reduction at failure ΔM_f is defined as shown” in Figure 2.2-9(a). (Williams and Sexsmith 1995) The loss of strength in a cycle is then:

$$\Delta M_i = \Delta M_f \left(\frac{\phi_i - \phi_y}{\phi_f - \phi_y} \right)^{1.5} \quad (2.21)$$

Because of the exponent of 1.5, the larger plastic deformations will cause much more damage than smaller ones. The moment-curvature failure envelope is shown in Figure 2.2-9(b) and is defined as:

$$M_{f,i} = M_f 2 \frac{\Phi_i}{\Phi_i + 1} \quad (2.22a)$$

$$\Phi_i = \frac{\phi_i}{\phi_f} \quad (2.22b)$$

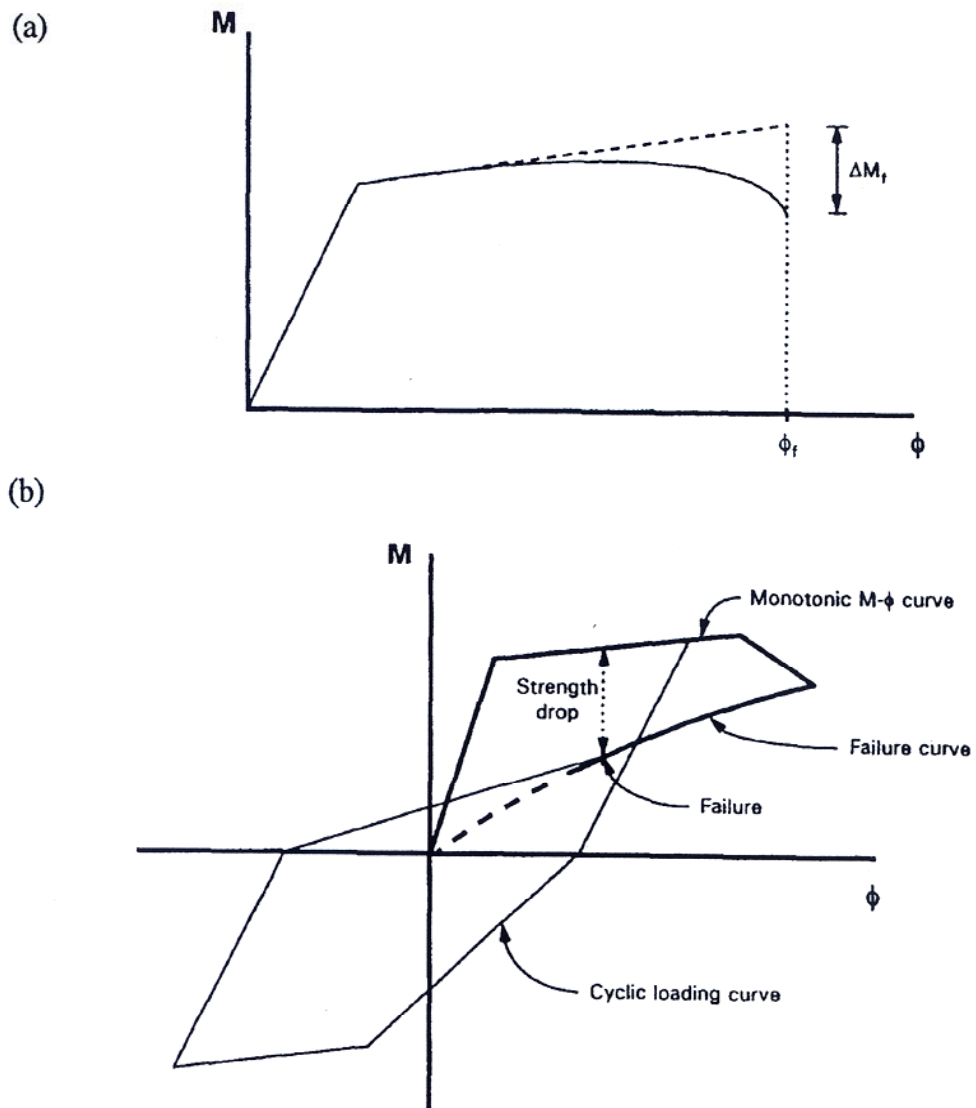


Figure 2.2-9 Definitions of Failure Under (a) Monotonic and (b) Cyclic Loading (Chung et al 1987)

The figure also shows that failure occurs when the moment-curvature curve intersects the failure envelope. The number of cycles to failure at a constant deformation level is defined by:

$$n_{f,i} = \frac{(M_i - M_{f,i})}{\Delta M_i} \quad (2.23)$$

In this formulation, positive and negative cycles are considered separately. The damage index is calculated using Miner's rule, with the addition of weighting:

$$D = \sum \left[\left(w_i^+ \right) \frac{n_i^+}{n_{f,i}^+} + w_i^- \frac{n_i^-}{n_{f,i}^-} \right] \quad (2.24)$$

The weights are:

$$w_i^+ = \left(\frac{\sum_{j=1}^{n_i^+} k_{ij}^+}{n_i^+ k_{i,ave}^+} \right) \frac{\phi_i^+ \phi_{i-1}^+}{2\phi_i^+} \quad (2.25)$$

“where $k_{i,ave}$ is the average stiffness for a specimen cycled to failure at amplitude i and the subscript j refers to the j th cycle at amplitude level i ” (Williams and Sexsmith 1995).

The weighting is exactly the same for the negative loading cycles. The first term

decreases the damaging effect of repeated cycles at a specific level and the second term takes into account the energy absorbed in a cycle.

Mander and Cheng (1995), developed a damage model based on longitudinal rebar fracture from low-cycle fatigue (Kunnath et al 1997). The Coffin-Manson law was implemented such that:

$$\varepsilon_p = \varepsilon_f' (2N_f)^c \quad (2.26)$$

where ε_p is the plastic strain amplitude, ε_f' and c are material constants to be determined from fatigue tests, and $2N_f$ is the number of cycles to failure. Experimentation was done and an experimental fit to the expression was found to be:

$$\varepsilon_p = 0.08(2N_f)^{-0.5} \quad (2.27)$$

The same expression was found using total strain:

$$\varepsilon_T = 0.08(2N_f)^{-0.33} \quad (2.28)$$

The damage index is then:

$$D = \sum \frac{1}{2N_f} \quad (2.29)$$

Kunnath et al (1997), modified the Coffin-Manson expression after doing fatigue tests of reinforced concrete columns. After experimental fitting, the expression was:

$$\varepsilon_p = 0.074(2N_f)^{-0.5} \quad (2.30)$$

The difference in the ε_f terms from Mander and Cheng is due to the loss of confinement and concrete fatigue.

2.3 Additional Topics

Some other topics that are important to this study are the importance of earthquake duration, soil-structure interaction, and methods of quantifying the damage in concrete columns. Two papers by Zhang et al (2004), discuss the importance of incorporating soil-structure interaction when modeling bridge structures. The conclusion was drawn that when soil-structure interaction is neglected, the response and forces in the bridge model were inaccurate.

Work was done by Williamson (2003), Bozorgnia et al (2003), and Lindt et al (2004) where the effect of long-duration earthquakes was considered. All three determined that it is important to provide a damage model that allows damage accumulation due to cyclic loading. The work by Bozorgnia et al (2003) also determined that the effects from aftershocks should be accounted for as well. It is also of interest to note that the study by Lindt et al (2004) was done using a Monte Carlo simulation in a suite of structurally different hypothetical structures.

The last paper, by Lehman et al (2004), was a study in performance-based seismic design. Research was performed to quantify the degree of damage in well-confined, circular cross-section, reinforced concrete bridge columns. The progression of damage in the columns is discussed and related to displacements and strain levels.

CHAPTER 3

WSU-NEABS Computer Program

3.1 The History of the Computer Program WSU-NEABS

The computer program WSU-NEABS (WSU-Nonlinear Earthquake Analysis of Bridge Systems) was selected for use in this project. Originally developed in 1973 with the name NEABS (Tseng and Penzien, 1973), it has been modified at Washington State University a number of times to enable it to more effectively model the actual nonlinear behavior of bridge systems (Cofer et al, 1994), (Zhang,1996).

Tseng and Penzien developed the original program, for which only an elasto-perfectly plastic beam-column and an expansion joint were available for nonlinear analysis. This program was developed to model three-dimensional, multi-span bridges, such as those that had been affected in the 1971 San Fernando earthquake. Kawashima and Penzien modified the program in 1976 and Imbsen, Nutt, and Penzien modified it again in 1978 (Zhang, 1996). NEABS was later enhanced in 1986 to allow kinematic hardening in the beam-column element and also changed to allow for a tie bar element in the nonlinear expansion joint.

Cofer et al (1994) modified the program once again to account for soil-structure interaction. They developed a nonlinear spring/damper/mass Discrete Foundation element. This element incorporates a spring and damper in all six local degrees-of-freedom. Mass and mass moments of inertia can be lumped to each node or separately to each degree-of freedom. The damper is a linear viscous dashpot and the spring has the ability to be nonlinear.

Zhang (1996) refined the nonlinear beam-column to include softening behavior and an improved hysteretic rule for cyclic loading. The softening behavior allows the bending moment to degrade as damage develops. The improved hysteretic rule includes the degradation of stiffness that is observed when beam-columns deteriorate.

WSU-NEABS also incorporates a linear elastic curved beam member and a linear elastic boundary spring. The linear elastic boundary spring allows spring stiffnesses in all six degrees-of-freedom. This can be used as a simplified soil-structure spring when all the soil properties are not sufficiently known to effectively use the Discrete Foundation element.

The program allows for many other options to accurately model and analyze discrete bridge systems. For example, WSU-NEABS can handle applied dynamic loading or prescribed loading at individual nodes. Multiple dynamic loadings can be applied at the same time in the x , y , and z directions.

Lumped or concentrated masses can be applied to nodes, or a mass density can be defined for the individual elements. If a mass density is defined, then the correct mass is calculated for the beam or column elements and applied to the two end nodes of the element. Applying a mass density is a convenient way of correctly modeling the mass of the system.

A direct step-by-step integration method is used in WSU-NEABS to solve the equation of motion. The program is capable of using either a constant acceleration method or a linear acceleration method. It is also capable of using a constant stiffness iteration method or a tangent stiffness iteration method.

3.2 Review of the Previous Beam-Column Element

To understand the modifications that were implemented in WSU-NEABS, it is necessary to understand the previous beam-column element. The previous beam-column element included softening hinges where the bending moment capacity degrades as damage develops. This can be seen in the Moment-Curvature ($M-\phi$) curve as shown in Figure 3.2-1 (Zhang, 1996).

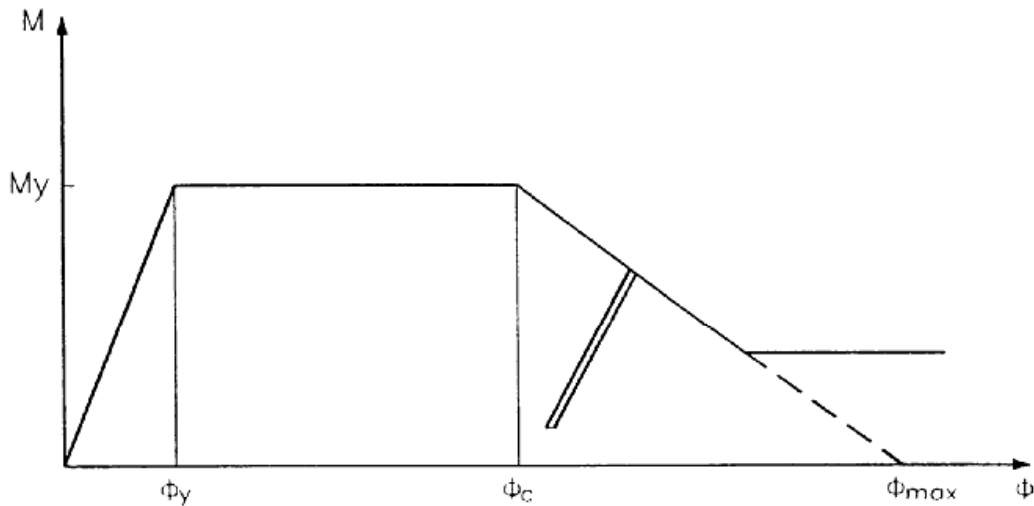


Figure 3.2-1 Moment vs. Curvature Relationship (Zhang 1996)

3.2.1 Previous Damage Coefficient

To derive the stiffness matrix for the softening branch of the $M-\phi$ curve, a damage coefficient is needed. This damage coefficient, D , as previously noted in Chapter 2, varies from zero to one. When D equals zero, there is no damage in the structural member and when D equals one, the structural element is totally damaged. In WSU-NEABS, the damage coefficient is limited to a value of D_{max} (Zhang, 1996). The damage coefficient is calculated as

$$D = \frac{\theta_p - \theta_{cp}}{\theta_{max} - \theta_{cp}}, \quad 0 \leq D \leq D_{max} \leq 1 \quad (3.1)$$

where θ_p is the total plastic rotation angle, θ_{cp} is the critical plastic rotation angle where softening begins, and θ_{max} is the maximum theoretical plastic rotation angle. The values for θ_{cp} and θ_{max} can be calculated by:

$$\theta_{cp} = l_p (\phi_c - \phi_y) \quad (3.2a)$$

$$\theta_{max} = l_p (\phi_{max} - \phi_y) \quad (3.2b)$$

where l_p is the theoretical plastic hinge length and ϕ_{max} is the curvature for which the maximum moment capacity is zero, theoretically. The maximum moment that can then be reached is:

$$M = (1 - D)M_y \quad (3.3)$$

where M_y is the yield moment.

3.2.2 Yield Function

The yield function in WSU-NEABS is based on the Bresler Equation (Bresler, 1960) for biaxial bending. The equation is:

$$\left(\frac{M_{yu}}{M_{yp}}\right)^2 + \left(\frac{M_{zu}}{M_{zp}}\right)^2 = 1 \quad (3.4)$$

where M_{yu} and M_{zu} are the ultimate moment values about the y-axis and the z-axis, respectively, for a fixed value of P_u . M_{yp} and M_{zp} are the ultimate moment values on the y-axis and z-axis for the same fixed value of P_u when they are each applied separately (Zhang, 1996).

By looking at interaction diagrams for reinforced concrete columns, it is understood that the level of axial load has a great impact on the moment capacity. Therefore, to consider this influence of axial load, P_u , M_{yp} and M_{zp} are calculated using the equations:

$$M_{zp} = M_{z0} \left(1 + a_1 \left(\frac{P_u}{P_0} \right) + a_2 \left(\frac{P_u}{P_0} \right)^2 + a_3 \left(\frac{P_u}{P_0} \right)^3 \right), \quad P_0 < P_u < P_t \quad (3.5a)$$

$$M_{yp} = M_{y0} \left(1 + b_1 \left(\frac{P_u}{P_0} \right) + b_2 \left(\frac{P_u}{P_0} \right)^2 + b_3 \left(\frac{P_u}{P_0} \right)^3 \right), \quad P_0 < P_u < P_t \quad (3.5b)$$

“where P_t is the ultimate axial tensile force, P_0 is the ultimate axial compressive force, M_{y0} and M_{z0} are yielding moments about the y and z axes, respectively, in pure bending, and $a_1, a_2, a_3, b_1, b_2,$ and b_3 are constants” (Zhang, 1996). The yield surface is shown in Figure 3.2-2.

To account for softening, Zhang (1996) modified the program such that the yield surface is no longer a stationary surface. As the plastic deformation increases, the yield stress level decreases. Thus, the radius of the yield surface contracts. This is shown in Figure 3.2-3 for a constant level of axial load. The equation of this yield function with softening included is:

$$\left(\frac{M_{yu}}{M_{yp}}\right)^2 + \left(\frac{M_{zu}}{M_{zp}}\right)^2 = (1 - D)^2 \quad (3.6)$$

where D is the previously defined damage coefficient (Zhang, 1996).

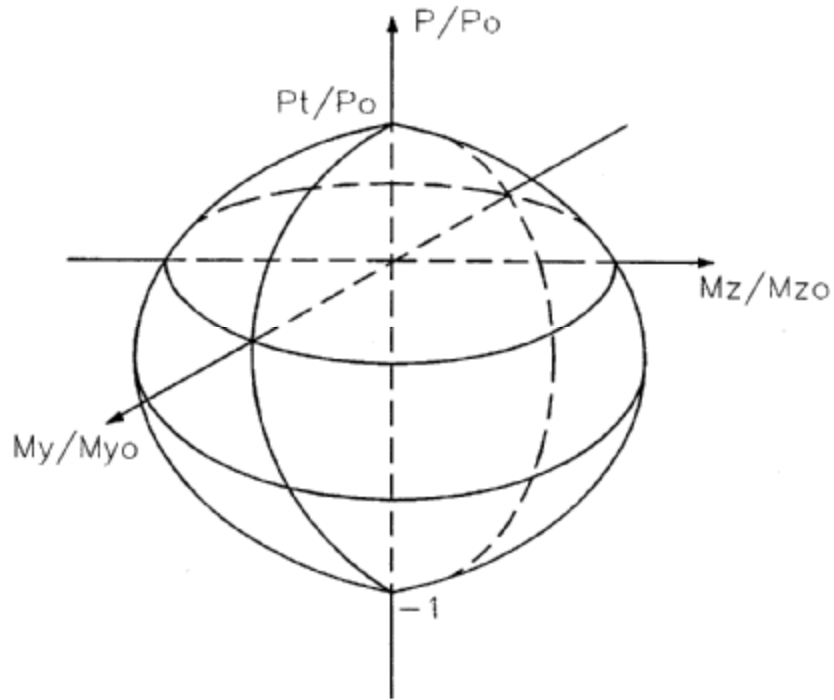


Figure 3.2-2 Generalized Yield Surface (Zhang 1996)

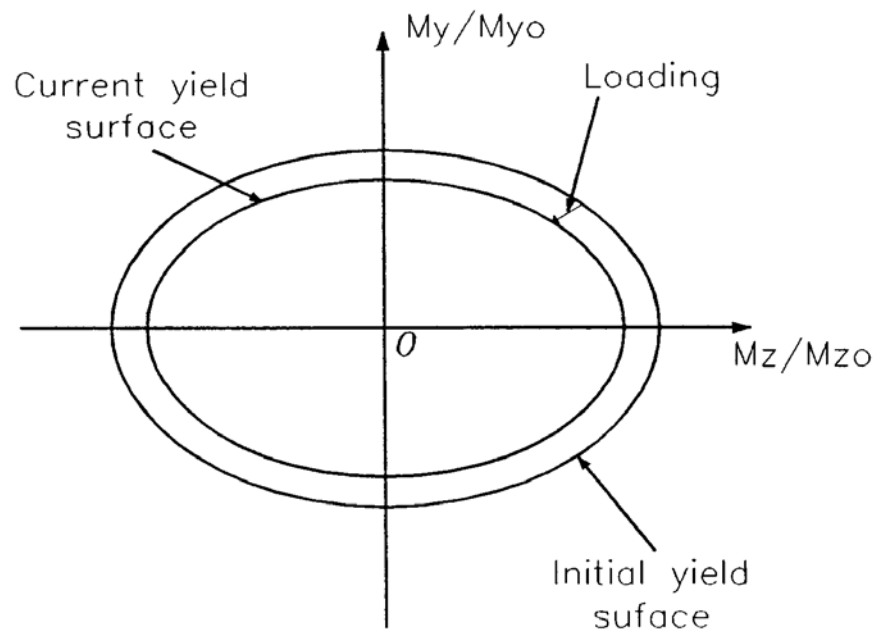


Figure 3.2-3 Yield Curve of Isotropic Strain Softening Material at a Constant Level of Axial Force(Zhang 1996)

The hysteresis model for the previous version of WSU-NEABS is shown in Figure 3.2-4. The model did not allow for a stiffness degradation of the unloading portion of the curve. That is, the stiffness during unloading was the same as the initial elastic stiffness. However, it is known that the unloading portion of the curve will decrease in stiffness with the increase in damage. Therefore, this has been corrected to allow for stiffness degradation. This addition to the program is discussed in the following section.

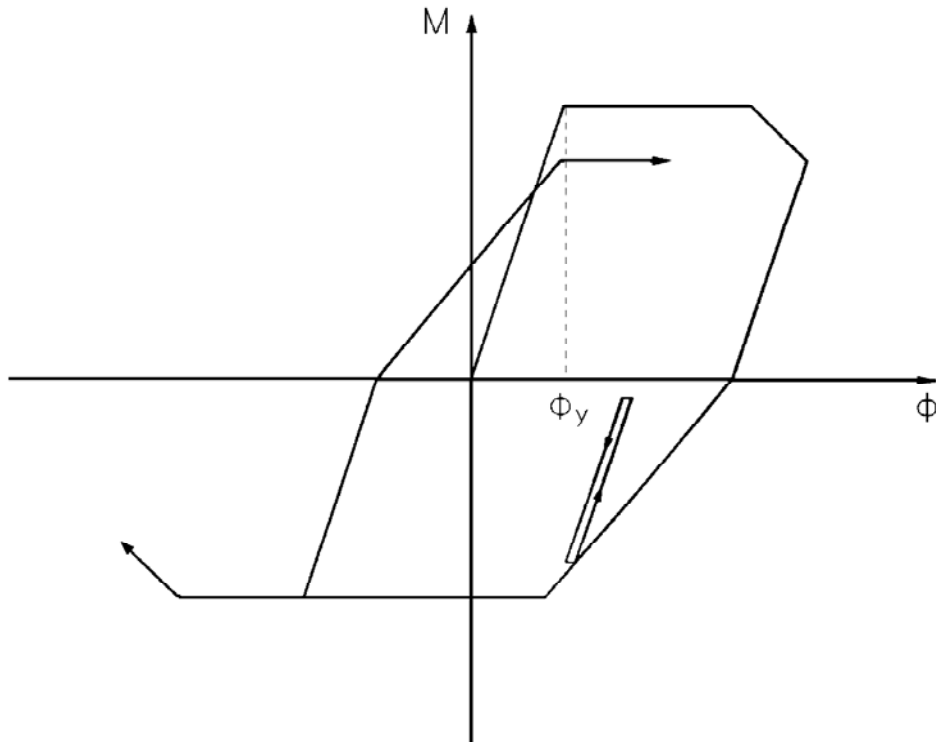


Figure 3.2-4 Hysteresis Model for the Previous Beam-Column Element (Zhang 1996)

3.3 Modification of WSU-NEABS

With the understanding that long duration earthquakes cause bridge structures to undergo many more loading cycles than for a short duration event, an additional source of damage within the model was necessary.

3.3.1 Modification of the Damage Model

The new damage accumulation index is based solely on cycles of the plastic rotation found in the plastic hinge region. The damage model proposed by Kunnath

(1997) was implemented into the NEABS program to account for this additional damage. See Chapter Two Section 2.2.5.

The basis of this damage model is the Coffin-Manson (Manson, 1953) equation:

$$\varepsilon_p = \varepsilon_f' (2N_f)^c \quad (3.7)$$

where ε_p is the plastic strain amplitude, $2N_f$ is the total number of cycles to failure, and ε_f' and c are material constants found from fatigue testing. If it is assumed that the rotation takes place about the center of the plastic hinge, the plastic strain amplitude can be found using the equation:

$$\varepsilon_p = \frac{\theta_p}{l_p} * \frac{D'}{2} \quad (3.8)$$

where θ_p is plastic rotation, l_p is the plastic hinge length, and D' is the distance between the extreme steel. By knowing the two material constants and solving for the plastic strain amplitude, the total number of cycles to failure can then be computed. Once this is known, Miner's Rule can be used to determine the damage coefficient D using the equation:

$$D = \sum \frac{1}{2N_f} \quad (3.9)$$

In the previous work done by Kunnath, the damage model was calibrated using well-confined concrete columns. Experimental results are also necessary to obtain damage data for the poorly confined columns considered here. Thus, poorly-confined specimens were tested by Stapleton (2004) to calibrate the model for this research. Four specimens were tested under constant amplitude displacements of 1.5, 2.5, 3.0, and 4.0 times the yield displacement. The new cumulative damage expression was derived based on experimental fitting of the Coffin-Manson fatigue expression using the results from the testing. See Figure3.3-1.

The calibrated equation was found to be:

$$\varepsilon_p = 0.0387(2N_f)^{-0.358} \quad (3.10)$$

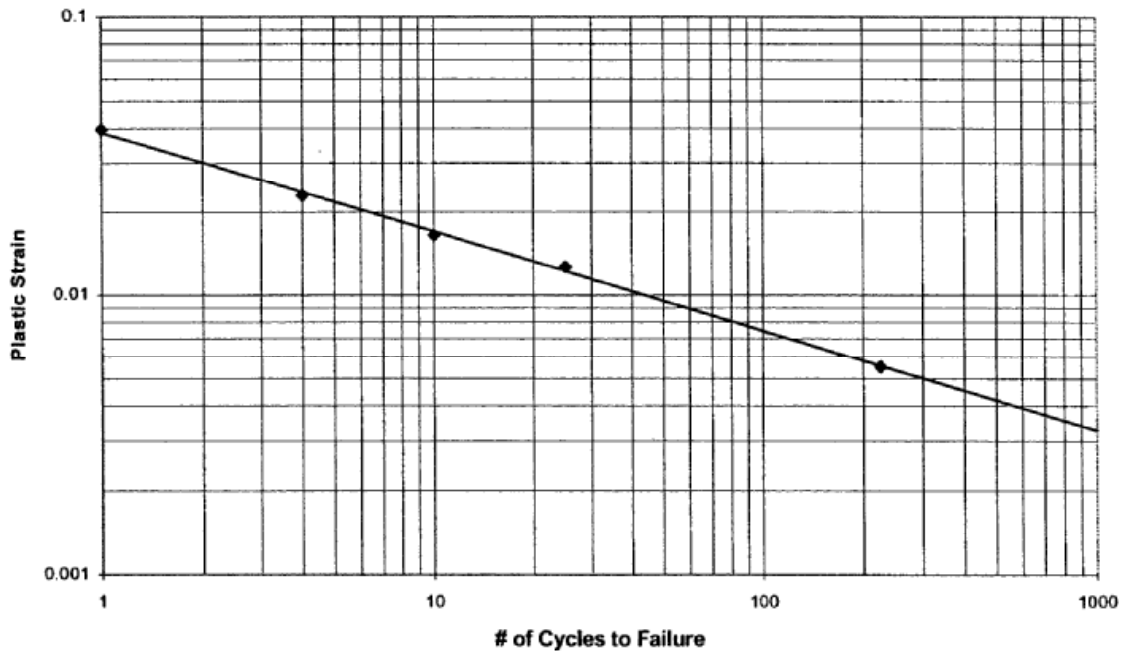


Figure 3.3-1 Results of Constant Amplitude Testing (Stapleton 2004)

This relationship was then implemented into WSU-NEABS. The program was given the capability to detect a peak in the plastic rotation, which would constitute a half-cycle. Once a half-cycle is detected, the above equation is used to determine the amount of damage that is incurred. This damage is then added to the total damage and is summed for each half-cycle for the duration of the seismic event.

It is important to understand that loading cycles that do not cause any plastic deformation will not cause any damage. This assumption was made because the tests by Stapleton at a constant amplitude of $1.5\Delta_y$ were shut off after 150 cycles because failure had not been reached. At 150 cycles, the test columns showed no meaningful signs of damage or deterioration. This was also found to be true by Kunnath (1997), where the test of the column at a constant displacement level of 2 times the yield displacement was shut down after 150 cycles. There were also no meaningful signs of damage or deterioration.

3.3.2 Modification of the Hysteresis Model for the Beam-Column Element

The previous version of the program allowed for a slight reloading stiffness degradation, but the testing results show that a greater reloading stiffness degradation is needed to properly model the pinching behavior that has been shown to occur in poorly confined concrete columns. The testing also shows that, as damage accumulates due to cyclic loading, the unloading stiffness will degrade. Because the previous version of the program did not allow for this degradation, an algorithm for it has been added to more accurately model the true behavior of these columns. The application of these changes is

illustrated by the moment vs. curvature curve shown in Figure 3.3-2. Note that the unloading stiffness, k'' , is less than the initial elastic stiffness k' .

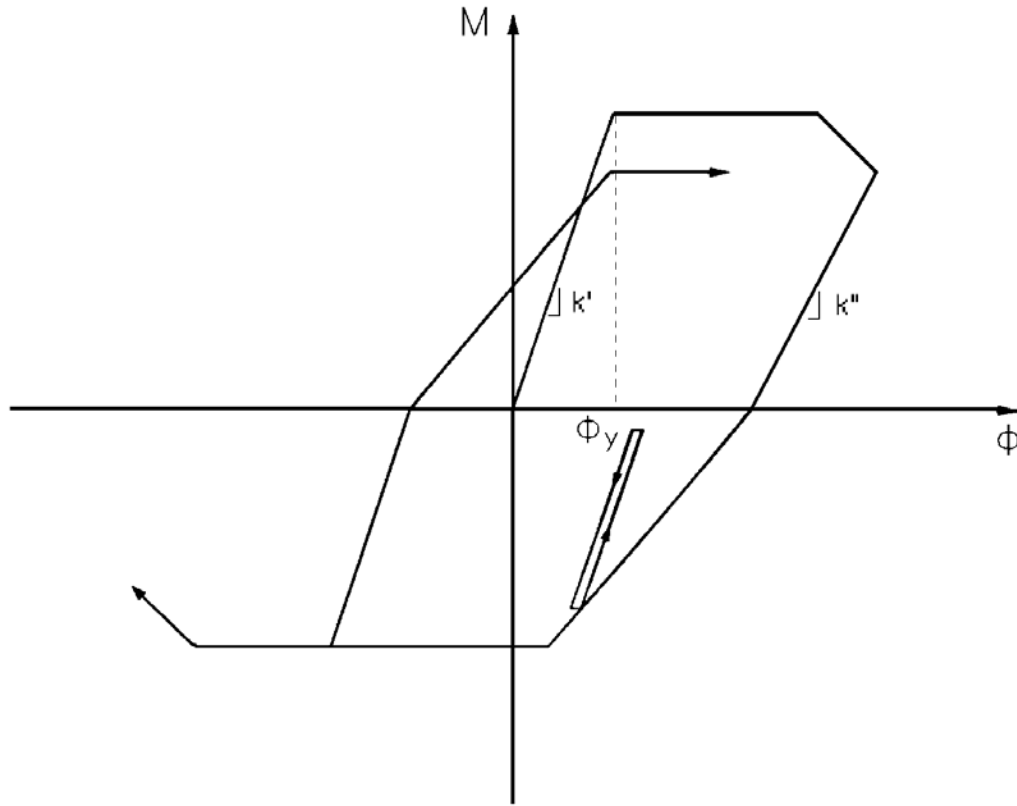


Figure 3.3-2 Hysteresis Model for the Beam-Column

During the elastic loading stage, there is no degradation due to damage. Therefore, the flexural capacities about the y and z -axes are those for a fully continuous member. As damage accumulates, the end conditions about the y and z -axes are considered to vary between fully continuous and fully hinged for the unloading and reloading stages (Zhang, 1996). A special damage coefficient, which was calibrated to tests, is used to define the loss of elastic stiffness of the member.

“Let $\underline{k}_{m iy}^e$, $\underline{k}_{m iz}^e$, $\underline{k}_{m jy}^e$, and $\underline{k}_{m jz}^e$ be the release matrices about the y and z -axes at the i and j ends, respectively. The difference between the elastic stiffness matrix and any one

of these release matrices equals the elastic matrix for pinned end conditions. For instance, the matrix $\underline{k}^e - \underline{k}_{miz}^e$ is the elastic matrix for which the rotational stiffness about the z -axis at the i -end is released” (Zhang, 1996). However, \underline{k}_{miy}^e , \underline{k}_{miz}^e , $\underline{k}_{m jy}^e$, and \underline{k}_{mjz}^e are coupled, therefore the matrix condensation method must be used to derive the stiffness degradation matrix.

This is the process in which the damage coefficient, D , is used. It should be noted that in this process, D is the actual damage found in the plastic hinge and D^* is just a coefficient used in this process. The beam-column element is divided into two sub-elements corresponding to ends i and j , where the degradation stiffness for each element is defined as:

$$\underline{k}_1^{ed} = \underline{k}_1^e - D^*_1 \underline{k}_{miy}^e - D^*_1 \underline{k}_{miz}^e \quad (3.11a)$$

$$\underline{k}_2^{ed} = \underline{k}_2^e - D^*_2 \underline{k}_{m jy}^e - D^*_2 \underline{k}_{mjz}^e \quad (3.11b)$$

In the previous version of the program, D^*_1 and D^*_2 were simply the damage coefficients for the two ends of the element. Here, D^*_1 and D^*_2 are now functions of the damage coefficients, which change, depending on the stage of the hysteresis. For the unloading stage of the hysteresis:

$$D_{ratio} = \frac{D_{1or2}}{D_{max}} \quad (3.12)$$

$$D_{1or2}^* = 0.15D_{ratio} + 0.7 \quad (3.13)$$

For the reloading stage of the hysteresis:

$$D_{1or2}^* = \left(-0.333(D_{ratio}^2)\right) + (0.4433D_{ratio}) + 0.85 \quad (3.14)$$

These functions allow for a decrease in stiffness only when damage has occurred. Tests show that once damage does occur, there is a slight change in the unloading stiffness but a more drastic change in the reloading stiffness of the member. These formulations mimic that type of behavior. For the unloading stage, D_1^* and D_2^* vary linearly from 0.7 to 0.85 and for the reloading stage they vary quadratically from 0.85 to 0.96. The effect of this variation on the reloading stiffness and the unloading stiffness of a column can be seen in Figure 3.3-3 and Figure 3.3-4. These figures show the change in stiffness due to the variation of D_1^* and D_2^* .

The value of D_1^* and D_2^* varies linearly at a much lower level during unloading, therefore the unloading stiffness will only change slightly. However, the reloading stiffness is designed to change quite quickly at first and then level off because it is modeled as a quadratic function. The tests by Stapleton (2004) were used to calibrate these functions.

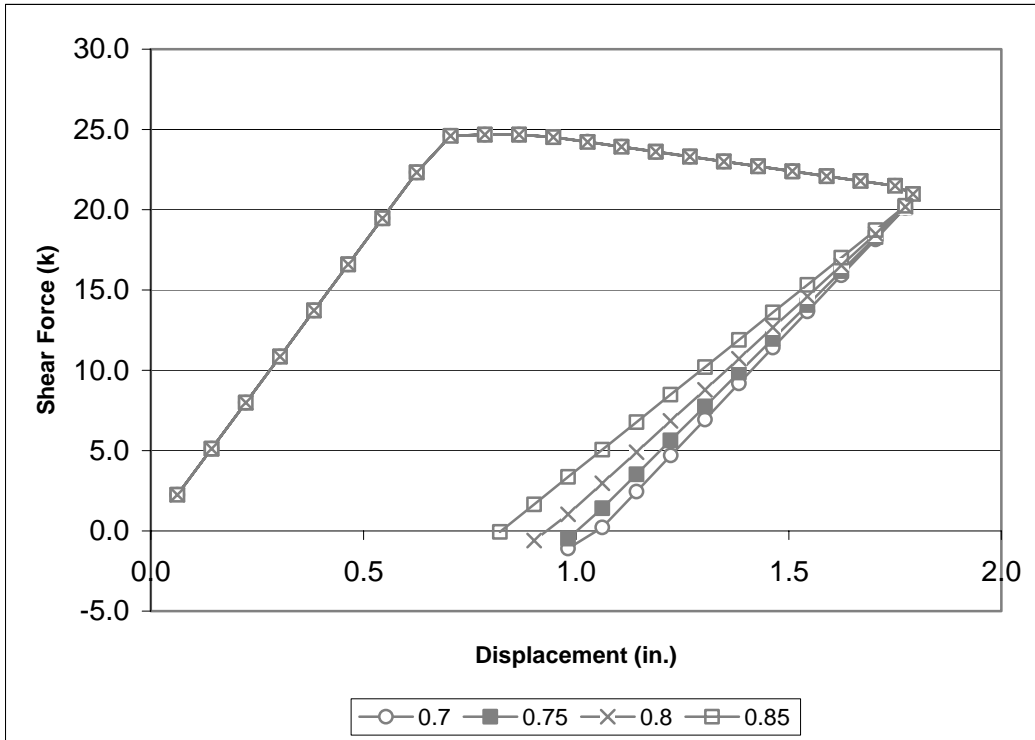


Figure 3.3-3 Effect on the Unloading Stiffness with the Variation of D_1^* and D_2^*

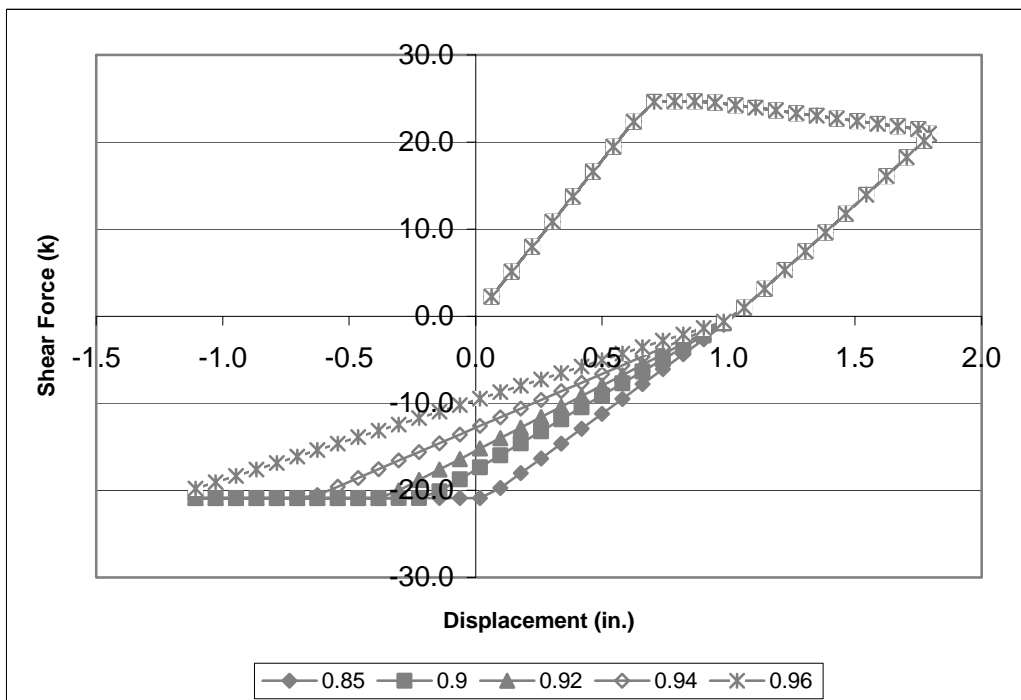


Figure 3.3-4 Effect on the Reloading Stiffness with the Variation of D_1^* and D_2^*

3.4 Examples

The modifications were implemented into the program and example studies were performed. The purpose of this testing was to insure that the changes made to the program had changed its performance in an acceptable manner. These analyses were conducted using models created to simulate actual testing specimens from the work of Stapleton (2004) and Kunnath (1997). Additional analyses were also conducted to determine how the damage coefficient compares to the level of physical damage. These were done using the same models and earthquake displacement records.

3.4.1 Example 1

In this example, a single column was modeled, as shown in Figure 3.4-1, to represent the actual test column used by Stapleton(2004). The column is fixed at the base and it is attached to an elastic boundary spring at the top to ensure that it remains stable during softening. The column model consists of three beam-column elements. The two at the bottom are nonlinear elements and the third element is a linear elastic element. The very bottom element is half the length of the plastic hinge, so the rotation takes place about the center of the plastic hinge. The nonlinear element above that is there to represent the splice region. The structural properties of the column are tabulated in Table 3.4-1.

The actual test by Stapleton (2004) was a displacement-controlled test. Thus, the lateral stiffness of the elastic boundary spring was set equal to 10,000 times that of the stiffness of the column. That is:

$$k_s = \frac{3EI}{l^3} * 10000$$

The force applied to the top of the column was calculated such that the desired displacement would be achieved. This method was used to insure that the correct displacement would be reached during each cycle.

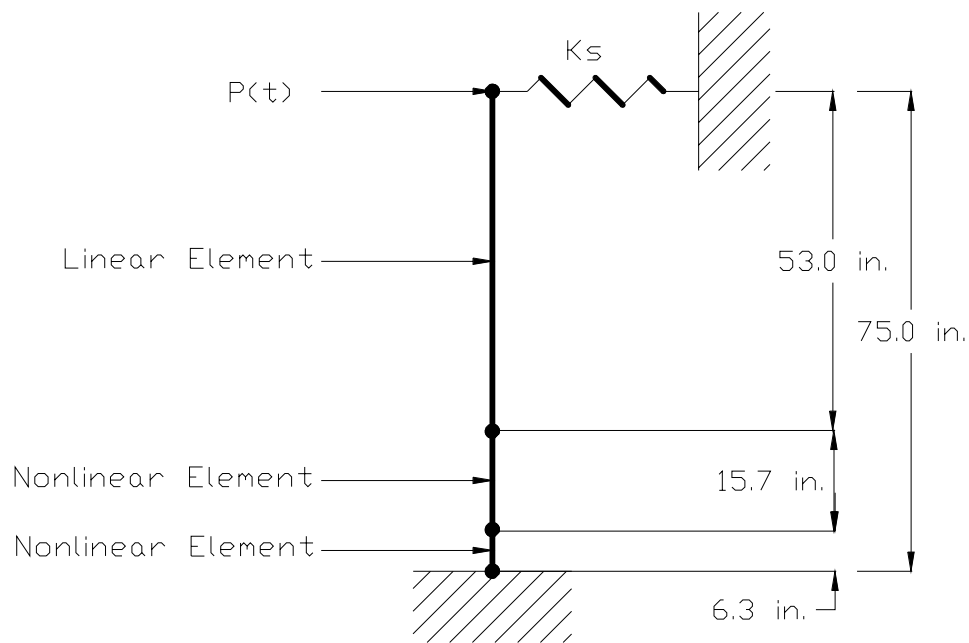


Figure 3.4-1 Structural Model of Single Column

Table 3.4-1 Structural Properties of Column

Young's Modulus (ksi)	Poisson Ratio	Unit Weight (lb/in ³)	M_{y0} (k-in)	P_0	P_t / P_0	a_1	a_2	a_3
4030	0.18	0.224E-06	1168	1476	0.1021	-9.576	-15.89	-5.340

Figure 3.4-2 shows the comparison of the actual test results to those computed by WSU-NEABS. With the accumulation of damage, a drop in strength after each cycle is observed. The initial stiffness is modeled very closely, but as the displacement increases, the two begin to diverge. The maximum shear forces that are reached by the two models are virtually the same, but the computer model shows strength degradation in the first cycle, which is due to softening behavior, whereas the experimental specimen does not. However, after the first cycle, the computer model only shows strength degradation due to the cyclic behavior and not softening. With this degradation in strength during the first cycle, the shear force differs by 11%. After this initial degradation, the shear forces in the computer model are quite similar to those obtained from the tests.

It is also worthwhile to note the stiffness degradation in the unloading and reloading stages. The initial reloading stiffness in the computer model is stiffer than the experiment, but it eventually closes in on the approximate stiffness after a few cycles. The stiffness degradation does not occur as quickly in the computer model because it is dependent on the level of damage, which takes a few cycles to accumulate. Therefore, the area enclosed in the hysteresis loops for this model is greater than the experiment, which suggests that the computer model dissipates more energy than the experiment.

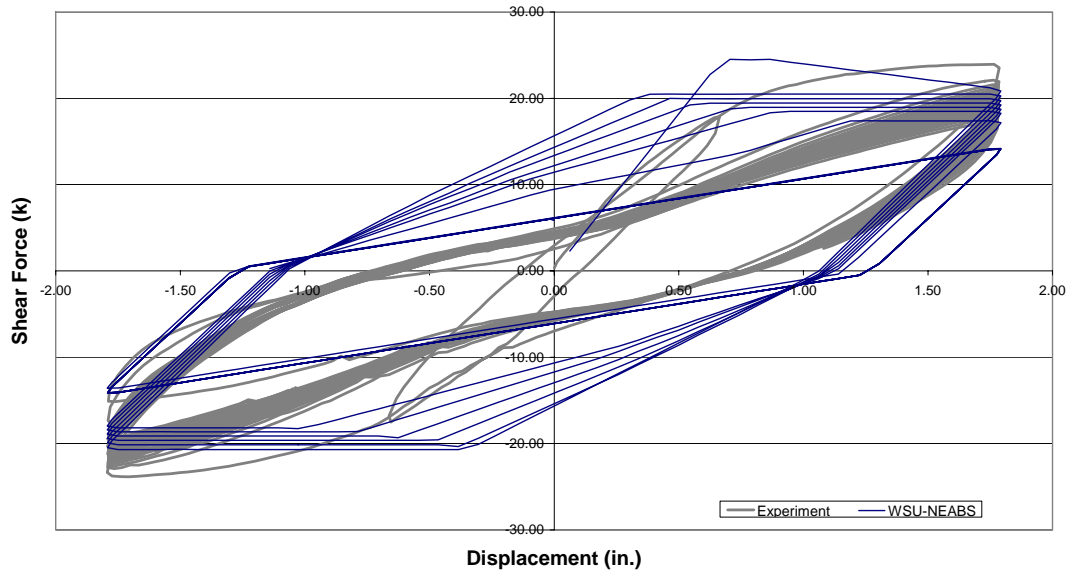


Figure 3.4-2 Constant Amplitude Comparison from Experiment (Stapleton, 2004) and WSU-NEABS

3.4.2 Example 2

In this example, the same column was modeled, as given in Figure 3.4-1. The material properties were kept the same and only the loading protocol was changed to simulate a standard cyclic test in which the amplitude increases throughout the test. Table 3.4-2 shows the actual displacements and the corresponding displacement ductility. Figure 3.4-2 shows the comparison of the actual test to that computed by WSU-NEABS.

Table 3.4-2 Summary of Standard Cyclic Protocol (Stapleton 2004)

Cycle Number	Displacement Level	Corresponding Ductility
1	0.171 in.	$0.25\Delta_y$
2 through 4	0.341 in.	$0.5\Delta_y$
5 through 7	0.512 in.	$0.75\Delta_y$
8 through 10	0.682 in.	$1.0\Delta_y$
11 through 13	1.57 in.	$2.3\Delta_y$
14 through 16	2.46 in.	$3.6\Delta_y$
17 through 19	3.41 in.	$5.0\Delta_y$

The initial stiffness is modeled very closely, and the maximum shear forces found in both models are virtually the same. The computer model shows a degradation of strength that is greater than the experiment shows. This degradation in strength causes a difference in shear force of up to 20%. The energy dissipated by the column is also overestimated because the stiffness of the computer model does not degrade as quickly as the experiment.

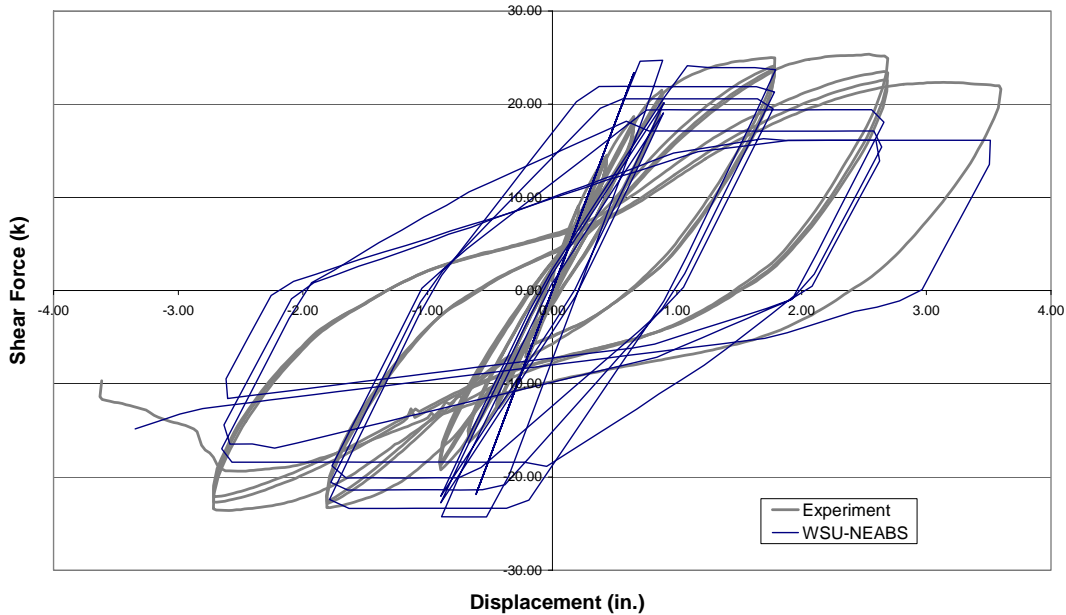


Figure 3.4-3 Changing Amplitude Comparison from experiment (Stapleton, 2004) and WSU-NEABS

3.4.3 Example 3

In this example, a single column was modeled, to represent the actual test column used by Kunnath (1997). The model was developed just like the model in Figure 3.4-1, except that the height of the column was 54 inches. The structural properties of the column are tabulated in Table 3.4-3. Figure 3.4-4 and Figure 3.4-5 shows the comparison of the actual test to that computed by WSU-NEABS.

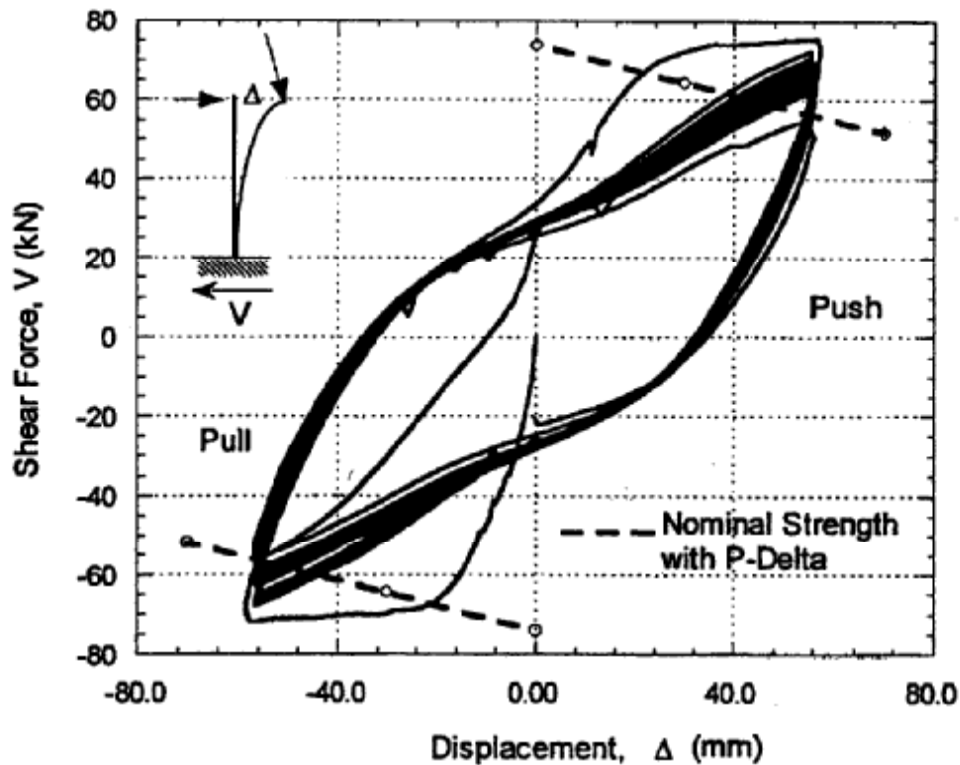


Figure 3.4-4 Kunnath's Test Results (Kunnath 1997)

Table 3.4-3 Structural Properties of Column

Young's Modulus (ksi)	Poisson Ratio	Unit Weight (lb/in ³)	M _{y0} (k-in)	P ₀	P _t / P ₀	a ₁	a ₂	a ₃
3604	0.18	0.224E-06	698	491	.3142	-2.216	-3.109	.3142

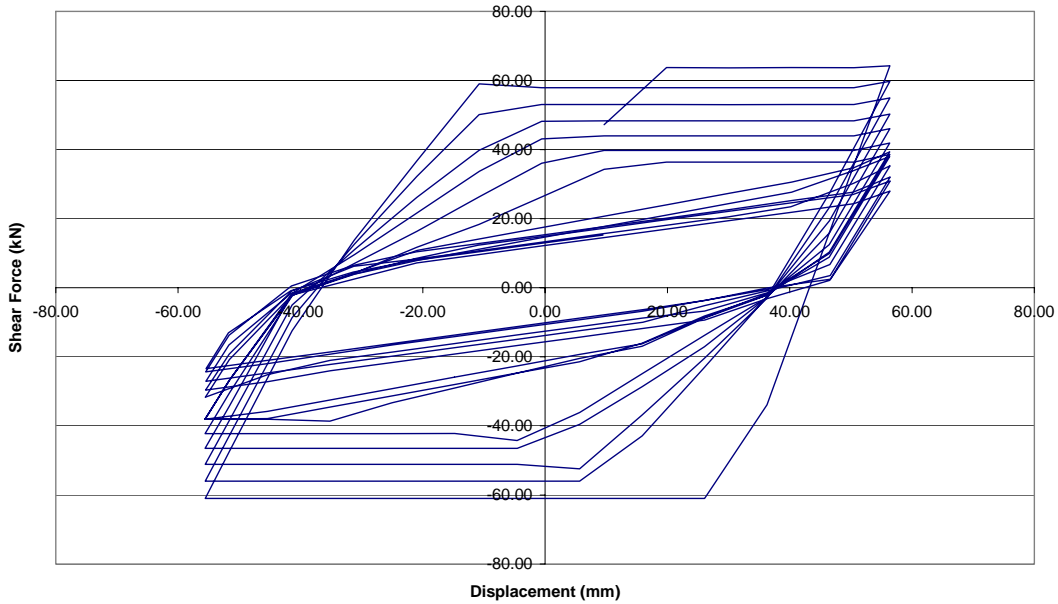


Figure 3.4-5 WSU-NEABS Simulation of Kunnath's Test

These results compare to those of this experiment much like they did for the previous tests in that the model reproduces the initial shear force very well and it also captures the stiffness degradation. It does not degrade in stiffness as quickly as the test specimen but part of this is due to the fact that this is a well-confined specimen, without damage in the first cycle. The greatest difference between the model and test results is the relatively large level of damage achieved in the model. Again this is due to the fact that damage coefficients for unconfined columns were used. Also, the computer model has a long yielding plateau at the maximum shear for during each cycle, whereas the experiment only shows the yield plateau during the first cycle.

With this difference and the fact that the stiffness of the computer model does not degrade as quickly, the computer model initially overestimates the amount of energy dissipated in the column. Even with the differences in all of these examples, the computer model does a reasonable job modeling the actual response of the experiments.

3.4.4 Damage Level Comparison

One of the specimens tested by Stapleton (2004) used a displacement record that was developed using an example earthquake. This same displacement record was used in the column model as shown in Figure 3.4-1. The computer model of the column had a damage coefficient of 0.34 after the analysis. According to the damage guidelines from Section 2.2.4, this would suggest that there would be minor to moderate damage, which would range from severe cracking to localized spalling. Figure 3.4-6 shows a picture of the test specimen after the test, where localized spalling is shown at the base of the column. This would indicate these damage guidelines can be used for the work in this study.



Figure 3.4-6 Final State of Damage for Column

Chapter 4

Seismic Analysis of Bridges Under Long-Duration Loading

4.1 WSDOT Bridge 5/518

To investigate the effects of long duration earthquakes on lightly reinforced concrete bridges, a three-dimensional model was analyzed using dynamic methods. The objective was to accurately model the bridge, as it is currently constructed, and then analyze the bridge model under seismic excitation.

4.1.1 Introduction

The bridge shown in Figure 4.1-1 is located at milepost 153.15 on 178th Street in King County of Washington State. It was constructed in 1964 to carry South 178th Street over Interstate 5. It was chosen for this study because it represents a typical highway over pass built before 1971, and thus is poorly detailed in the plastic hinge region with respect to the transverse reinforcement.

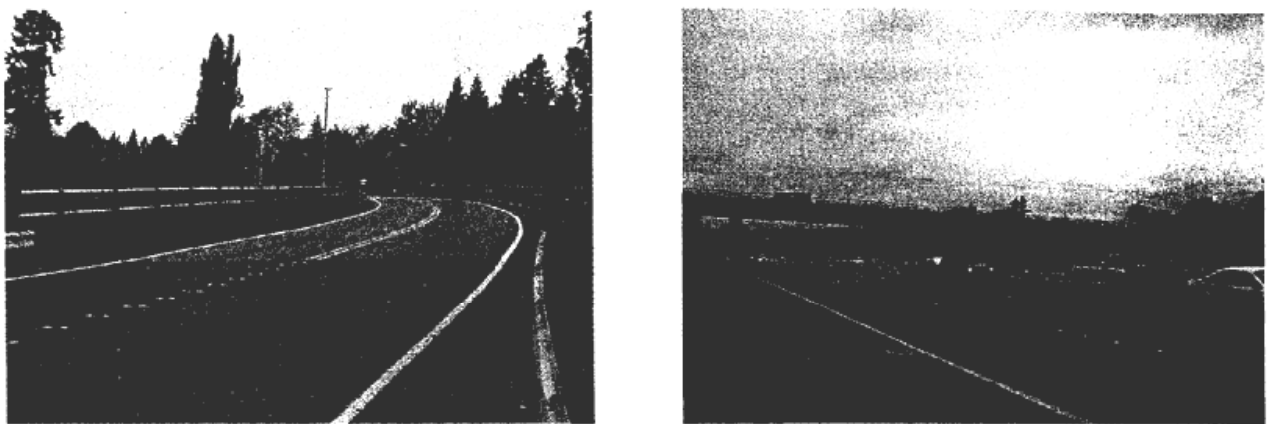


Figure 4.1-1 Bridge 5/518

4.1.2 Description of the Bridge

The plan and elevation of the bridge are shown in Figure 4.1-2. The bridge is 322 feet long and has four spans. The two middle spans are both 101.5 feet long, while the two end spans are 69 and 50 feet long, respectively. The reinforced concrete deck, which provides the main transverse stiffness of the superstructure, is discontinuous at all supports. It is 26 feet wide and has a thickness of 5.75 inches. The deck was supported by six prestressed concrete I-girders that are 4 feet 10 inches deep. These I-girders are spaced at 5 feet 5 inches on center.

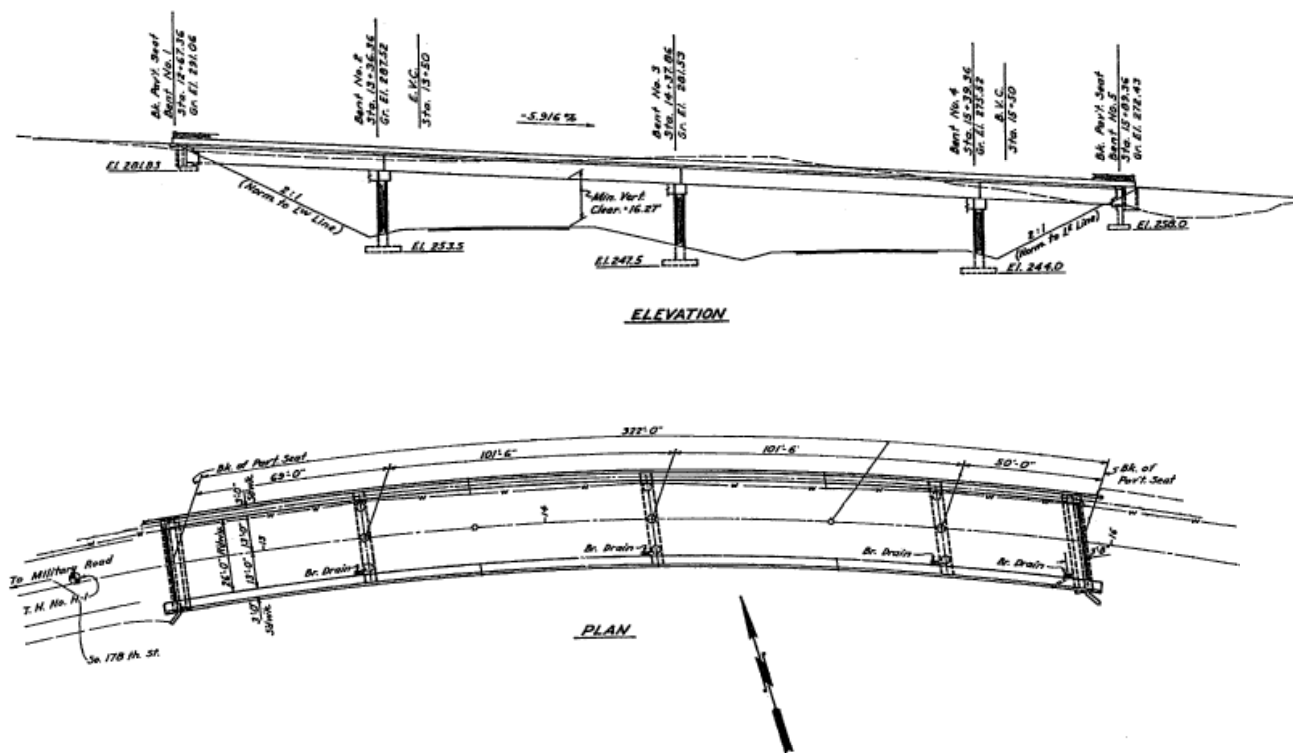


Figure 4.1-2 Plan and Profile Views of Bridge 5/518

The I-girders rest on the crossbeam and abutments with a grout pad topped with a rubber pad for the bearing. See Figure 4.1-3. Because the spans are discontinuous,

expansion joints of 1.5 inches were constructed between the spans. The expansion joints were filled with Gates Standard rubber joint filler.

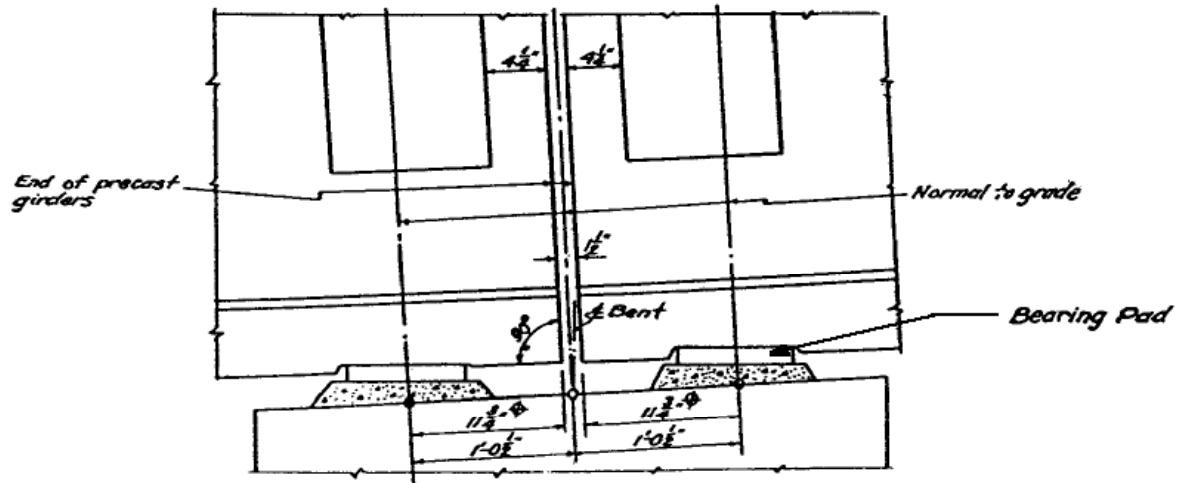


Figure 4.1-3 Bearing of I-Girders

The crossbeams were cast monolithically with the three columns at each bent as shown in Figure 4.1-4. Each crossbeam has a total length of 30 feet, a width of 48 inches, and a depth of 39 inches. There are six No. 10 and four No. 8 bars at the top and four No. 6 and four No. 7 bars at the bottom of each crossbeam. There are also four No. 5 bars along the sides. The confinement was provided by placing No. 5 stirrups at varying spacing to account for shear. See Figure 4.1-5.

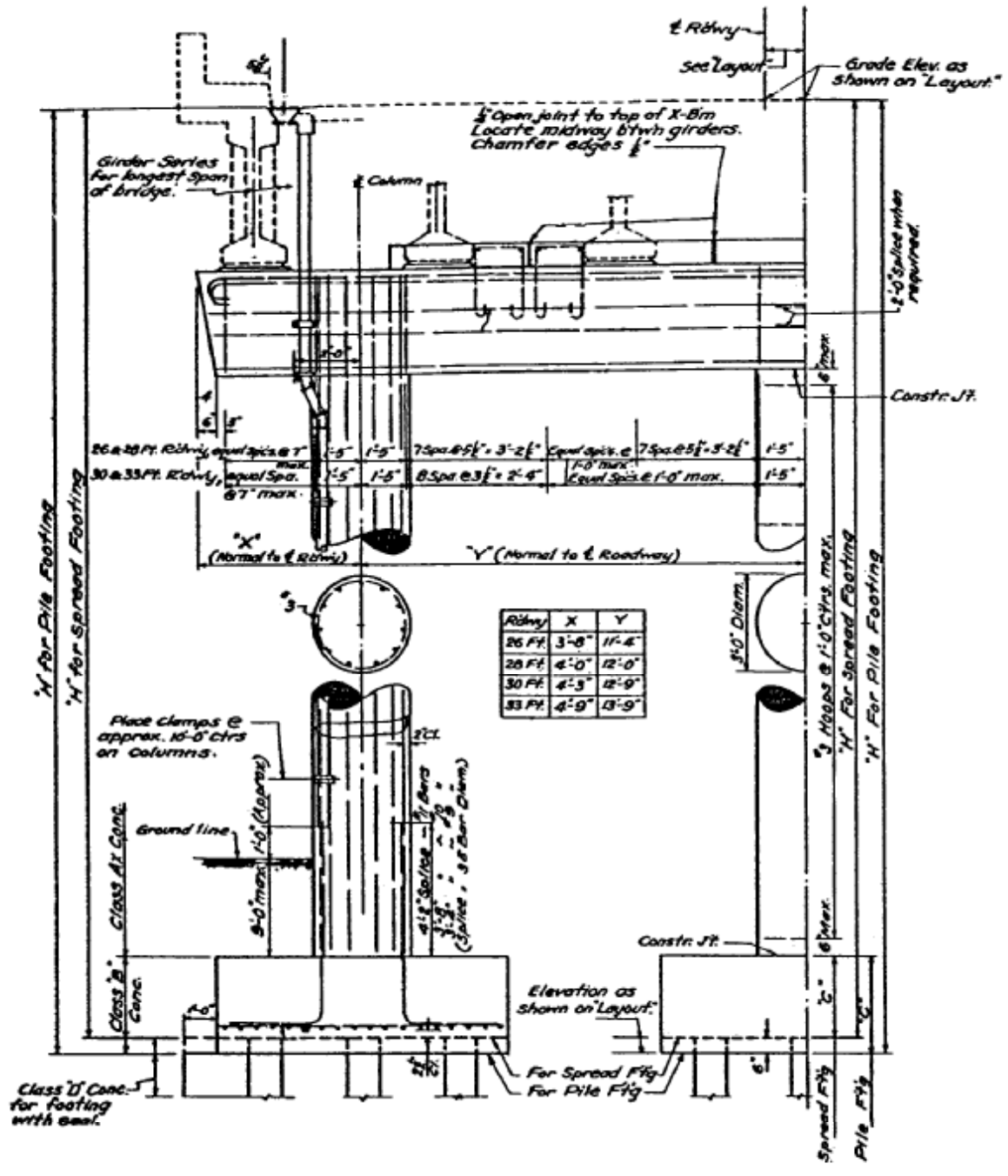


Figure 4.1-4 Intermediate Bent Cross Section

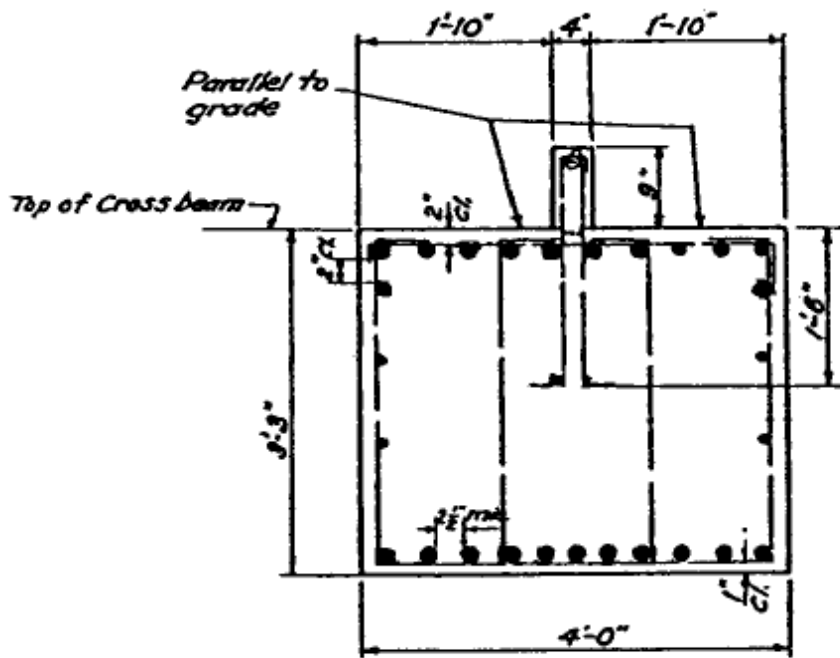
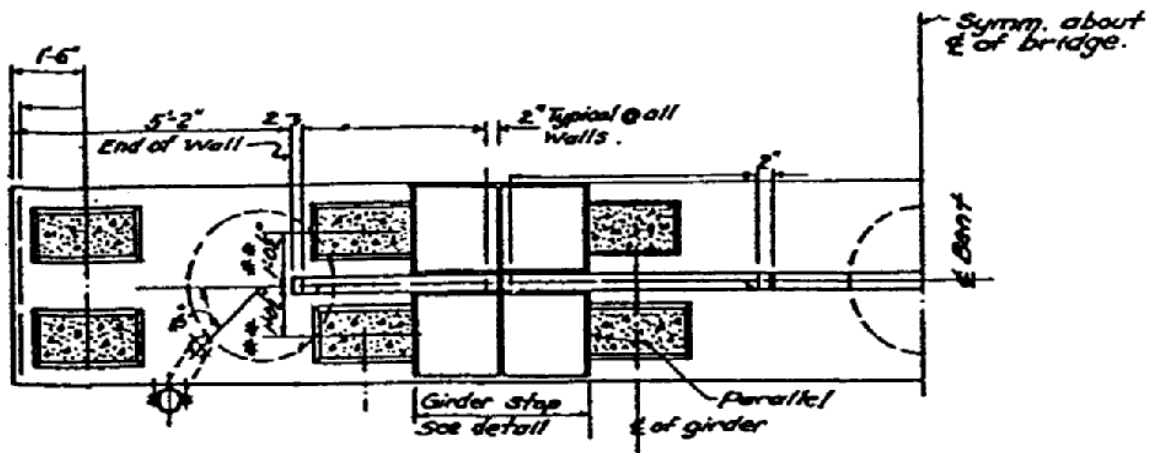


Figure 4.1-5 Cross Section of Cross Beam

Each crossbeam also has two end bent interior girder stops per bent and four intermediate bent girder stops per bent. The end bent interior girder stops are located at the inside face of the girders, while the intermediate bent girder stops are located between girders. See Figure 4.1-6. The deck and crossbeams provide a very stiff superstructure, much stiffer than the supporting columns.

The three interior bent columns are all supported on spread footings. These columns have clear heights of approximately 24 feet. They have a centerline spacing of 11.3 feet in the lateral direction. Compacted fill surrounds the columns at a height of

approximately 4 feet from the column base. All of the columns are circular with a diameter of 36 inches. They are reinforced longitudinally with eleven No. 11 reinforcing bars that are spaced evenly around the cross-section perimeter with a clear cover of two inches.



Fit flush with girder flange.

*$\frac{1}{2}$ " x 7" Asphaltic filler.
Fasten to concrete with
4d galv. nails @ 8" ctrs,
staggered. Min. edge dist. $1\frac{1}{2}$ "*

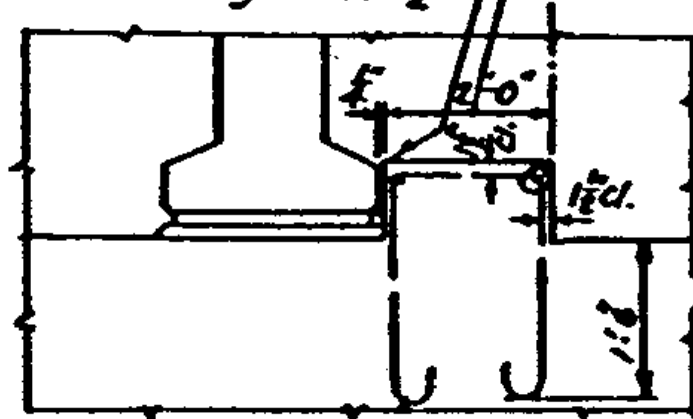


Figure 4.1-6 Girder Stop Details

The longitudinal bars extend into the crossbeam without a splice. This provides a longitudinal reinforcement ratio of 1.68%. Lap splices of 50 inches (35 longitudinal bar diameters) were used at the bases of the columns. The columns are reinforced in the transverse direction with No. 3 bars spaced every 12 inches. The hoops have an overlap of 21 inches and have no hooks. The transverse reinforcement ratio is 0.14%, which is very small compared to today's standards. This small transverse-reinforcing ratio, combined with a lap splice of this length, has been proven to be a problem in the past. A plastic hinge will form at the base of the column and the splice will breakdown during a major earthquake (Zhang, 1996).

The spread footings are 15 feet by 18 feet in the plan view and are 2 feet 3 inches thick. They are reinforced in the bottom layer with 25 No. 10 bars in the 15-foot dimension and 29 No. 9 bars in the 18-foot dimension. The columns are tied into the footing with 90° angles on the bottoms.

The concrete used in the footings and abutment walls is a WSDOT Class B mix with a compressive strength of $f'_c = 3000 \text{ psi}$. All other concrete used in the bridge, besides that used for the prestressed girders, is a WSDOT Class A mix with a compressive strength of $f'_c = 4000 \text{ psi}$. The steel used in this bridge is Grade 40 with a yield strength of $f_y = 40,000 \text{ psi}$.

4.1.3 Structural Model

A representation of the bridge model used in this study is shown in Figure 4.1-7 and Figure 4.1-8. The longitudinal beam and the crossbeams are modeled as very stiff beams. The longitudinal beam can be considered almost rigid because the deck and I-girders are composite, which creates a very stiff superstructure. The crossbeam is much stiffer than the columns so it can also be considered almost rigid. By having a very stiff crossbeam, the load from the longitudinal beam is evenly distributed between the columns, which helps to get the correct axial force in the columns. The columns are modeled with nonlinear beam-column elements. All members are given an appropriate cross-sectional area and mass density so as to model the mass and stiffness correctly.

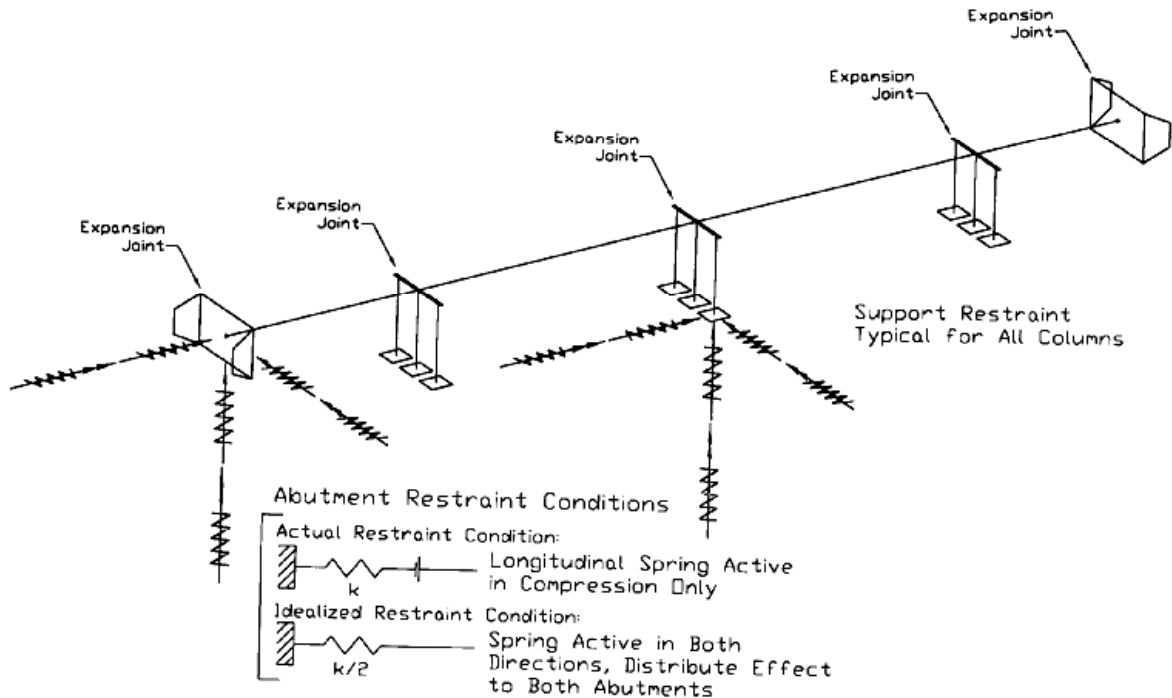


Figure 4.1-7 Structural Model of Bridge 5/518

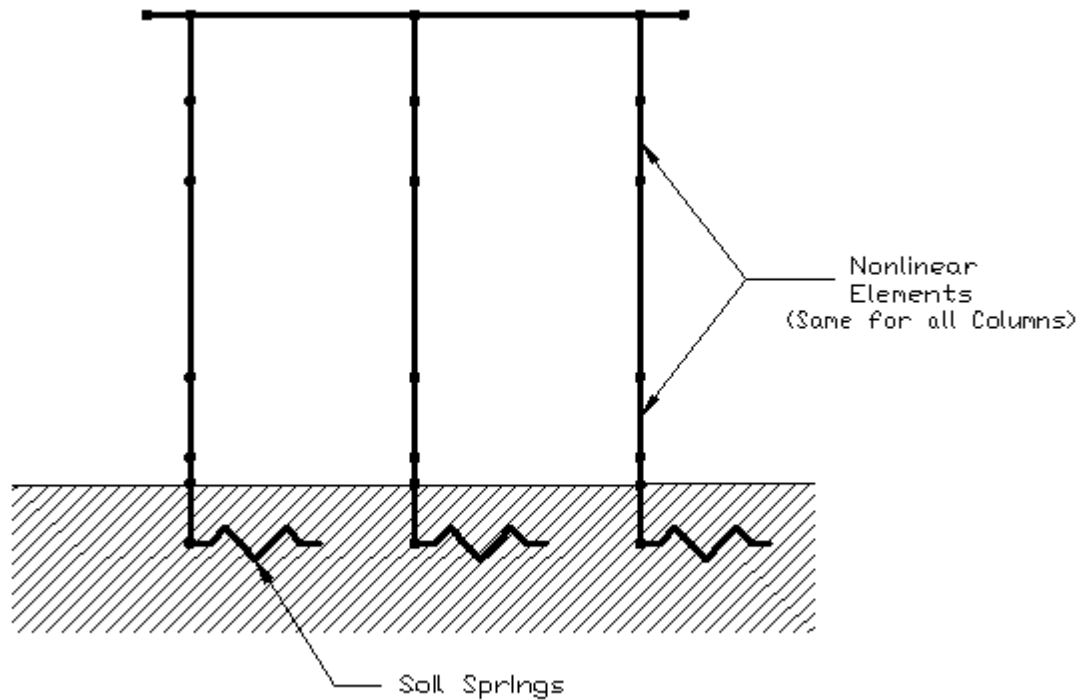


Figure 4.1-8 Bent from Structural Model

Because cracking will occur, the effective moment of inertia, I_{eff} , should be used. The effective moment of inertia was determined by using the cross sectional analysis program MPHI2C, developed by Marsh (1991). By plotting the moment versus curvature that is given from MPHI2C, the effective stiffness can be computed by taking a bilinear representation of the plot. (see Figure 4.1-9) The slope of the first line of the bilinear representation gives the effective EI value and by knowing E , the effective moment of inertia can be specified.

A preliminary value of I_{eff} , the traditional value of $\frac{1}{2} I_{gross}$, was used, but it was found to be too stiff compared to the actual tests by Stapleton (2004). Therefore the stiffness, EI , was matched to the actual test by Stapleton (2004), and I_{eff} was found to be approximately $\frac{1}{4} I_{gross}$. This value was used in all of the analyses. This is also

comparable to the I_{eff} values suggested in Figure 4.1-10 by Priestley (2003), when the axial load ratio is approximately 0.06 and ρ_l is approximately 0.01.

The parameters needed by WSU-NEABS to define the axial force-moment interaction curve were also found using MPHI2C. A summary of the structural properties of the longitudinal beam, crossbeam, and columns is shown in Table 4.1-1 and Table 4.1-2.

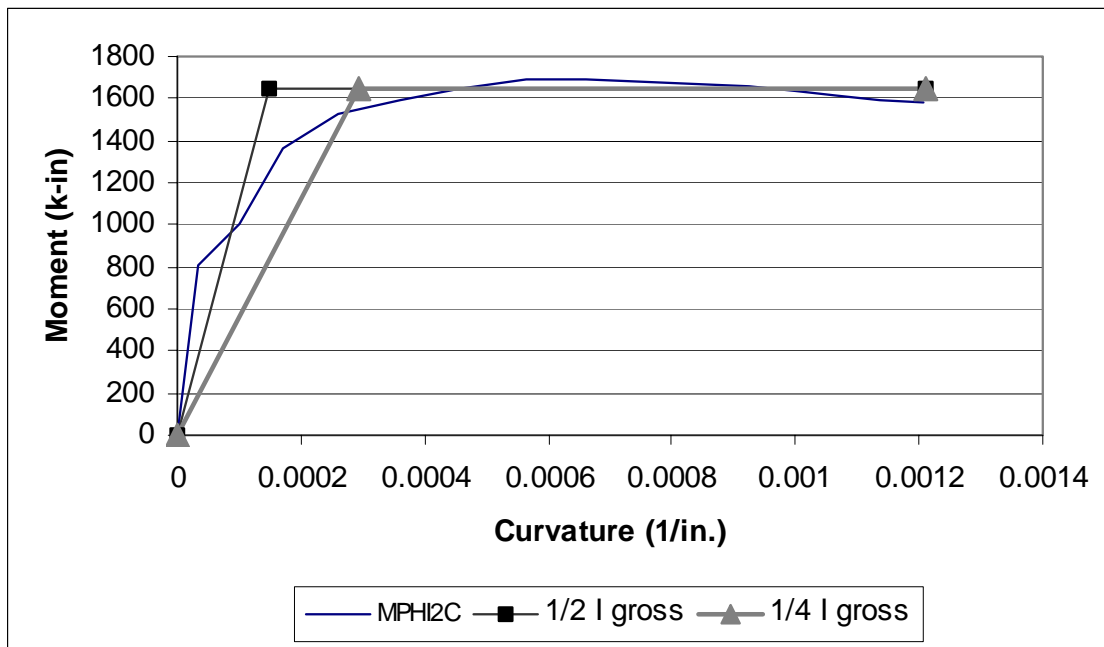


Figure 4.1-9 Bilinear Representation of Moment-Curvature

Table 4.1-1 Structural Properties for Columns, Crossbeams, and Deck Beams

	Young's Modulus (ksi)	Poisson Ratio	Unit Weight (kips / in ³)	Axial Area (in ²)	Shear Area (in ²)	Bending Inertia (in ⁴)	Torsional Inertia (in ⁴)
Columns	3604	0.18	2.224E-5	1018	1018	20000	164900
Crossbeam	360400	0.18	2.224E-5	1872	1872	6.187E+8	1.131E+7
Deck Beam	360400	0.18	2.224E-5	7134	7134	1.193E+8	1.207E+7

Table 4.1-2 Yield Function Constants for the Columns

M_{20} ($k-in$)	P_0 ($kips$)	P_t / P_0	a_0	a_1	a_2	a_3
9673	6107	.1609	1.0	-8.461	-13.35	-3.888

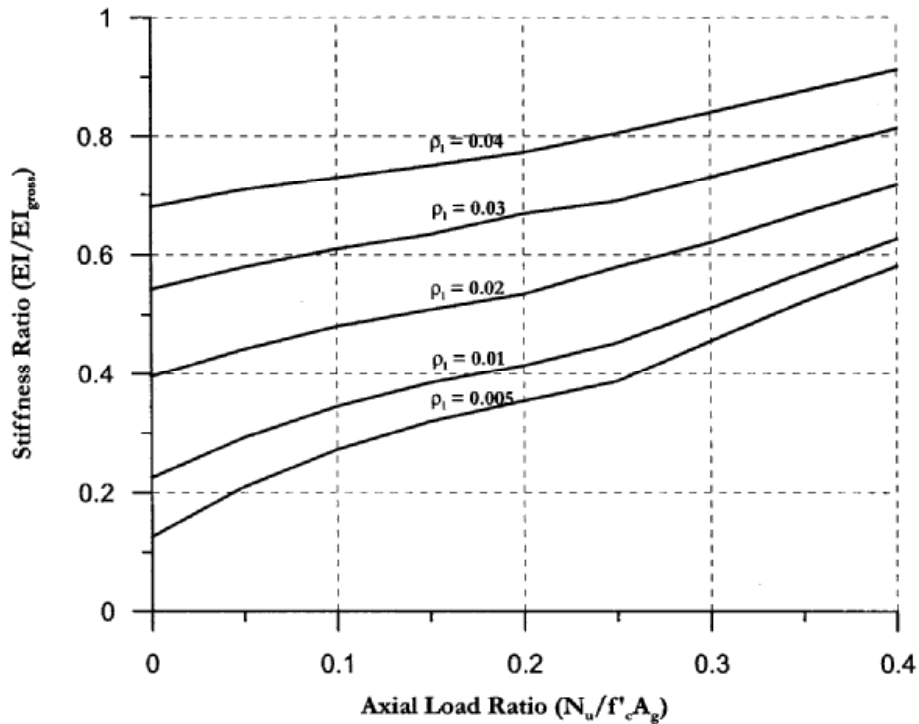


Figure 4.1-10 Effective Stiffness of Circular Bridge Columns (Priestley, 2003)

A boundary spring was used to consider the influence of soil-structure interaction. Table 4.1-3 gives the soil stiffness properties for the six degrees of freedom considered for the spring. Springs were attached to all columns and the two abutments. The soil stiffness properties for the abutment springs were computed using the Caltrans seismic design criteria (Caltrans, 2004). The soil stiffness properties for the column supports were computed using WSDOT Bridge Design Manual (WSDOT, 2002).

Table 4.1-3 Stiffness Properties for Soil Springs (k/in)

Location	Translation X	Translation Y	Translation Z	Rotation X	Rotation Y	Rotation Z
West Abutment	836.4	111.1	25320	1.0E+7	1.0E+7	1.748E+6
Pier 1	7120	7120	30470	574600	932000	128600
Pier 2	7474	7474	31840	727800	101500	140500
Pier 3	6736	6736	28960	440900	858800	117100
East Abutment	836.4	111.1	25320	1.0E+7	1.0E+7	1.748E+6

Rayleigh damping is used in NEABS, where $[C] = \alpha[M] + \beta[k]$. In this formulation, α and β are constants and this allows for a linear combination of the system mass matrix $[M]$ and the stiffness matrix $[k]$ to solve for the damping matrix $[C]$. The two damping factors, α and β , are found by:

$$\begin{Bmatrix} \alpha \\ \beta \end{Bmatrix} = \frac{2\xi}{\omega_i + \omega_j} \begin{Bmatrix} \omega_i \omega_j \\ 1 \end{Bmatrix} \quad (4.1)$$

where ω_i and ω_j are two control natural frequencies and ξ is the damping ratio. It must also be assumed that the two control frequencies have the same damping ratio for this formulation to work. Typically, ω_i is the fundamental natural frequency and ω_j is set to capture 90 –95% mass participation. For reasons of simplification, it is assumed that the fundamental natural frequency controls the dynamic response of the structure. Therefore $\omega_i = \omega_j = \omega$ and the above equation becomes:

$$\begin{Bmatrix} \alpha \\ \beta \end{Bmatrix} = \xi \begin{Bmatrix} \omega \\ 1 \\ \omega \end{Bmatrix} \quad (4.2)$$

The natural period was calculated assuming that the columns were fixed at their bases and that they remained elastic. The damping factors were found using this natural frequency and the assumption that the damping ratio was 5%.

Idealized expansion joint elements, as seen in Figure 4.1-11 and Figure 4.1-12, were used at each of the two abutments and at each pier. Each abutment expansion joint was idealized with one expansion joint element. The expansion joint element accounted for the stiffness in all six degrees of freedom. The expansion joints at the piers were idealized using three separate expansion joint elements. See Figure 4.1-13.

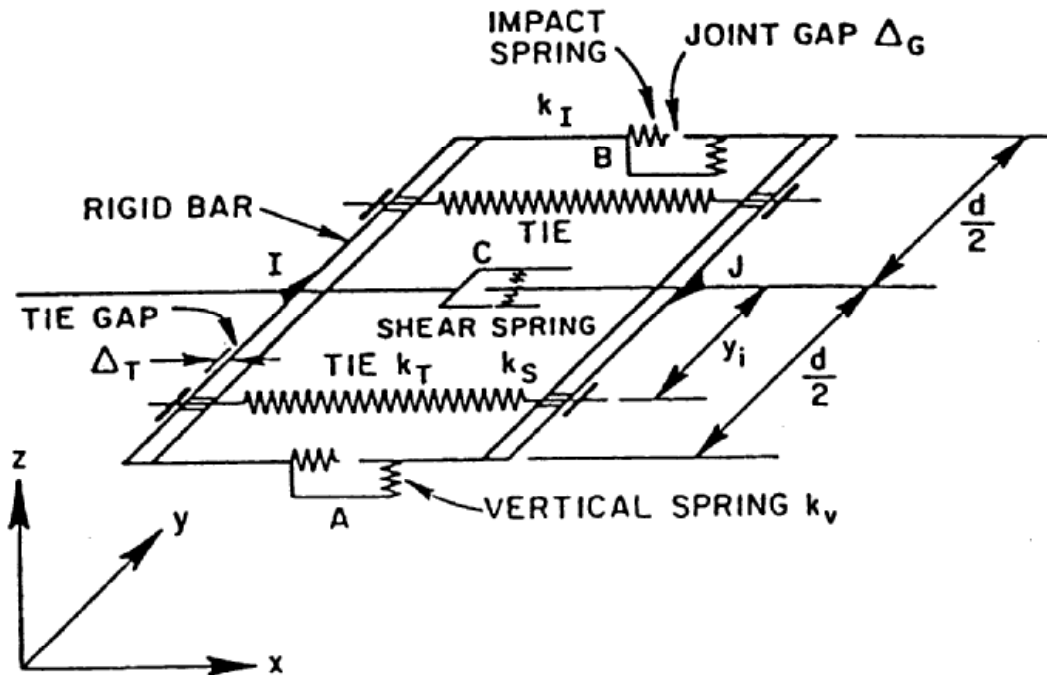


Figure 4.1-11 Idealized Expansion Joint

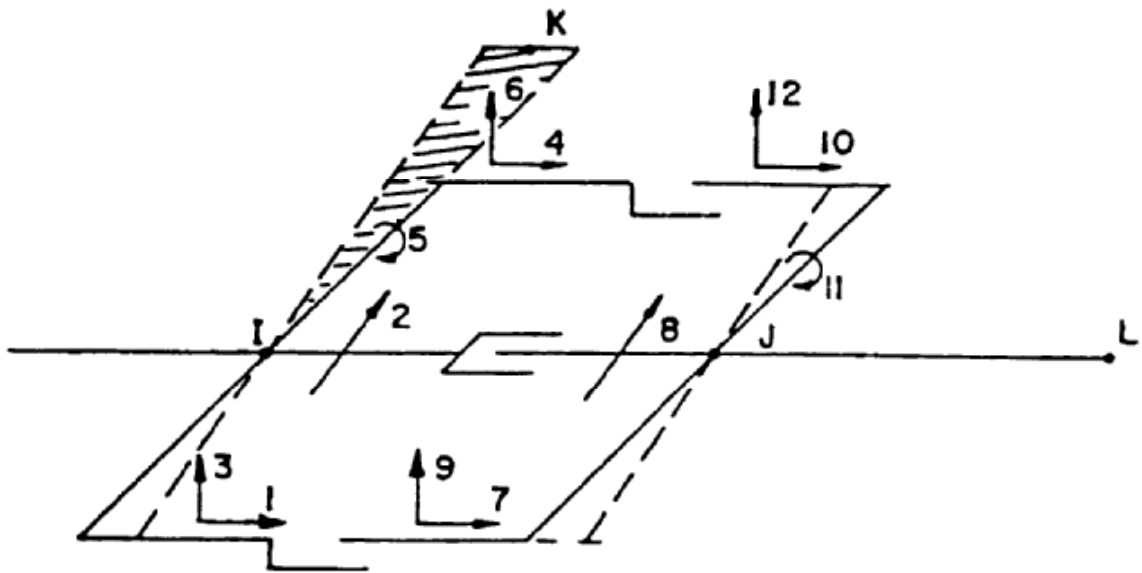


Figure 4.1-12 Expansion Joint Coordinate System

Element number one and number two provide the support between the longitudinal deck beam and the column crossbeam. These elements modeled the effects of the bearing pads and provided for vertical support and relative movements between the crossbeam and the deck beam. The third element in the figure spans between the two deck beams and accounts for the increased stiffness when the gap closes between the deck beams. The impact spring used in element three was assumed to have the axial stiffness of the superstructure. The nonlinear properties that were used for modeling the idealized expansion joint are tabulated in Table 4.1-4.

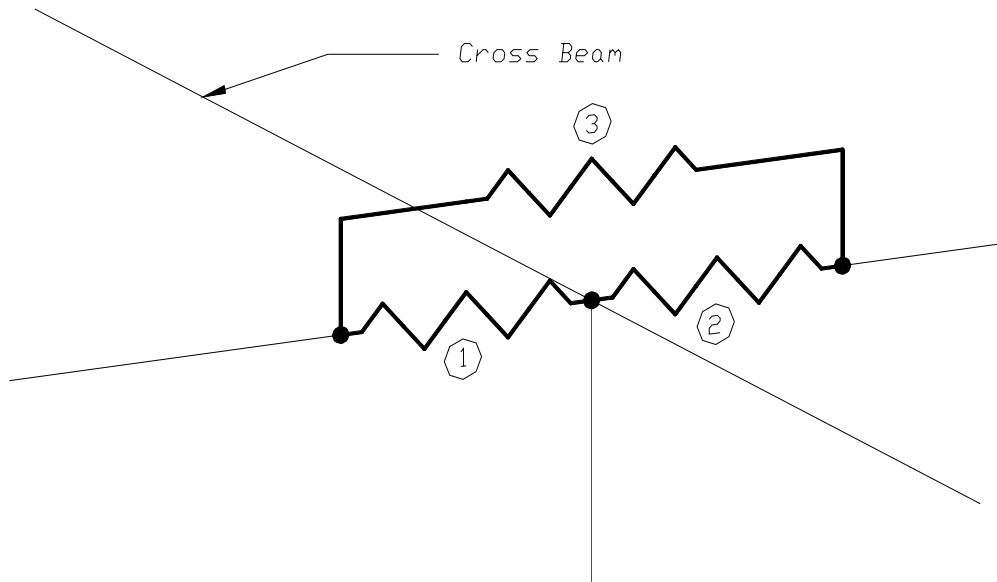


Figure 4.1-13 Idealized Expansion Joints at Intermediate Piers

Table 4.1-4 Input Parameters for Expansion Joints

	Support	Impacting Hinge
Bearing Type	Bearing Pad	NA
Element Width (in.), d	324.00	324.00
Skew (degrees)	0.00	0.00
Impacting Spring Stiffness (kips/in.), k_I	1.00	2.21×10^4
Bearing Friction Stiffness (kips/in.), k_F	1.00	1.00
Coefficient of Friction of Bearing, c_F	0.02	0.00
Stiffness of Tie Bar (kips/in.), k_T	NA	NA
Tie Bar Yield Force (kips), Y_T	NA	NA
Tie Bar Gap (in.), G_T	NA	NA
Seat Gap (in.), G_S	0.00	1.50
Number of Tie Bars	0	0
Vertical Stiffness (kips/in.), k_3, k_6	1.00×10^7	0.00
Longitudinal Stiffness (kips/in.), k_1, k_4	123.30	0.00
Transverse Stiffness (kips/in.), k_2	123.30	0.00
Rotational Stiffness (kips/in.), k_5	0.00	0.00

4.1.4 Seismic Excitation

A suite of ten earthquakes was used in the time-history analysis. Six of these earthquakes were long-duration events while the other four were short-duration events. Because there are no records of large inter-plate subduction zone earthquakes in Western Washington State, two earthquake records from South American inter-plate subduction zone earthquakes were used. The two earthquakes were the 1985 Llole, Chile earthquake record ($M = 7.9$) and the 2001 Moquegua, Peru earthquake record ($M = 8.4$).

These earthquake records were modified to fit a target acceleration spectrum for Western Washington State. Three attenuation relationships were reviewed by Stapleton (2004); Youngs et al (1997), Atkinson and Boore (2003), and Gregor et al (2002). Figure 4.1-14 shows the 5% damped acceleration spectrum for each of the three attenuation relationships. The spectra shown in this figure have been linearly scaled by a factor of two to develop a record that would emulate an extreme event and create damage in the bridge columns. Gregor et al (2002) predicts low spectral accelerations for periods from 0 to 1 seconds and high spectral accelerations beyond 1.5 seconds. Youngs et al (1997) may over estimate the peak spectral acceleration because it lacks a near-source saturation term (Stapleton, 2004). After reviewing the three different attenuation relationships, the Atkinson and Boore (2003) relationship was chosen for use as the target spectrum.

Figure 4.1-15 shows the target acceleration spectrum, the original acceleration spectrum of the East-West ground motions of the 2001 Peru Earthquake, and the modified spectrum of the Peru Earthquake. Figure 4.1-16 shows the entire modified time history of the E-W Peru Earthquake record. The earthquake record duration has been bracketed from the first cycle greater than 0.05g to the last cycle greater than 0.05g.

Figures 4.1-17 and Figure 4.1-18 show the North-South acceleration spectra and the modified and bracketed time history for the N-S 2001 Peru Earthquake.

The same was done for the 1985 Chile Earthquake. Figures 4.1-19 through 4.1-22 show the show the spectral acceleration and the modified and bracketed time histories for the Chile E-W and N-S records. These modified earthquakes account for two of the earthquakes in the suite of ten. The time histories from the unscaled acceleration spectra for both earthquakes were also used to account for two more of the earthquakes in the suite.

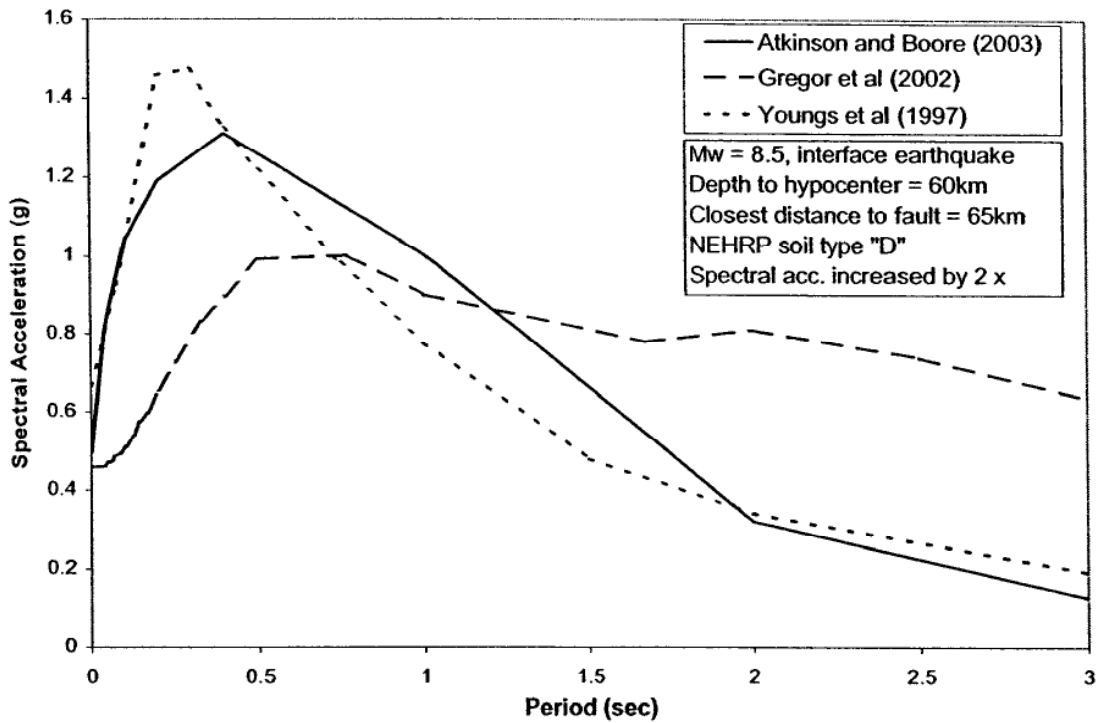


Figure 4.1-14 Acceleration Spectra Developed from Attenuation Relationships (Stapleton 2004)

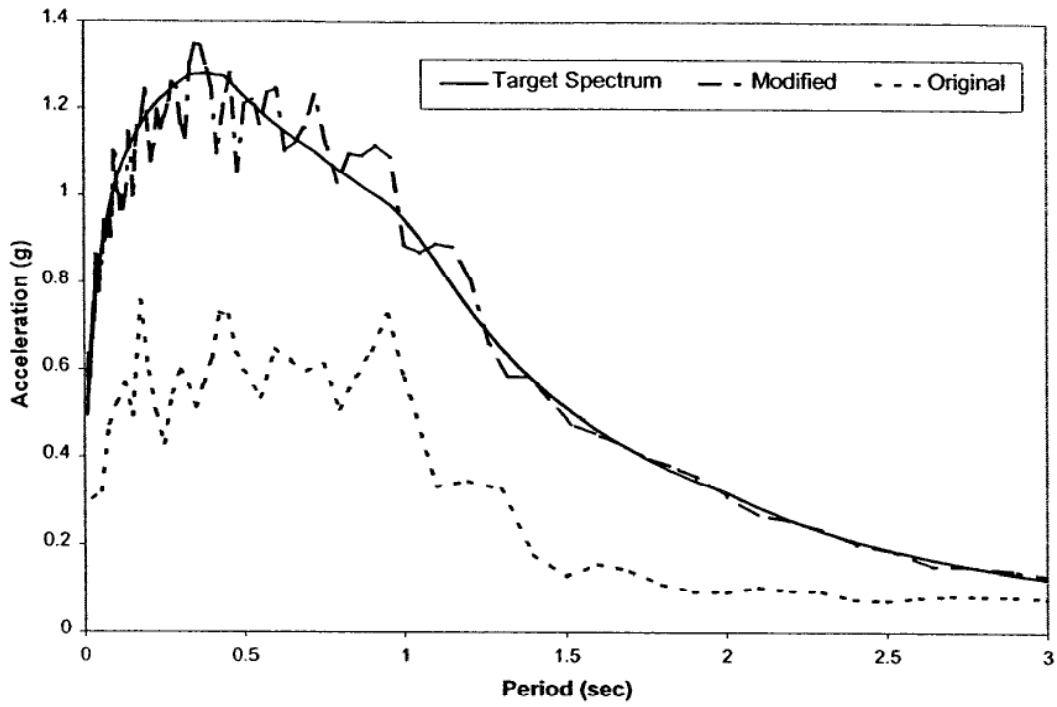


Figure 4.1-15 E-W Peru Spectral Acceleration (Stapleton 2004)

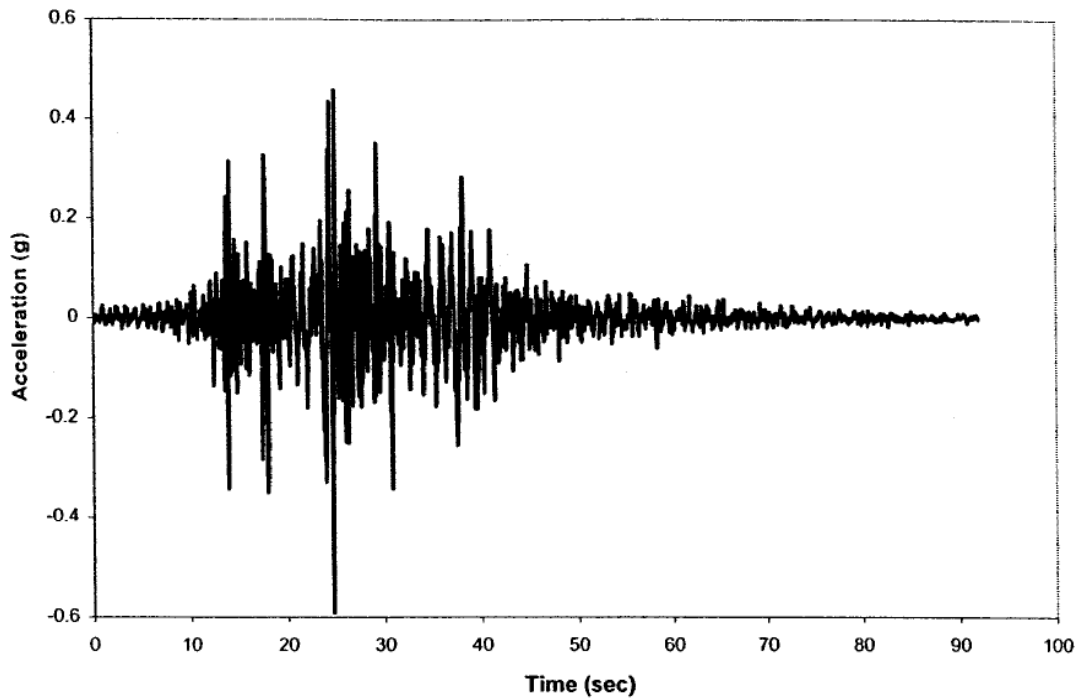


Figure 4.1-16 Modified Peru Earthquake, E-W Time History (Stapleton 2004)

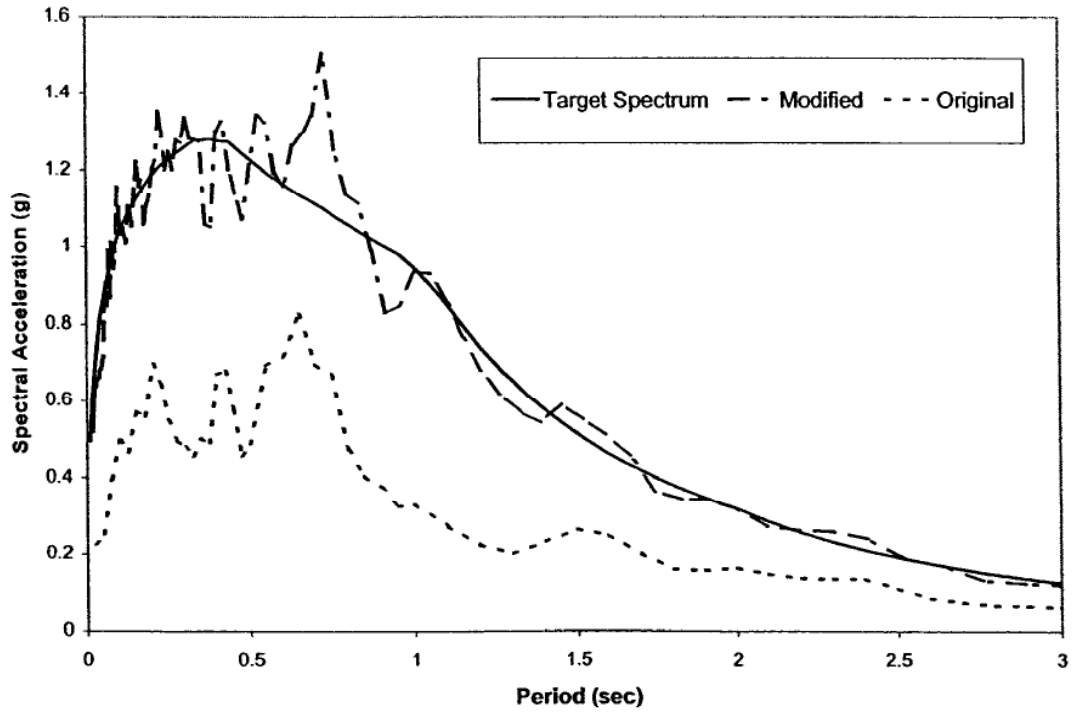


Figure 4.1-17 N-S Peru Spectral Acceleration (Stapleton 2004)

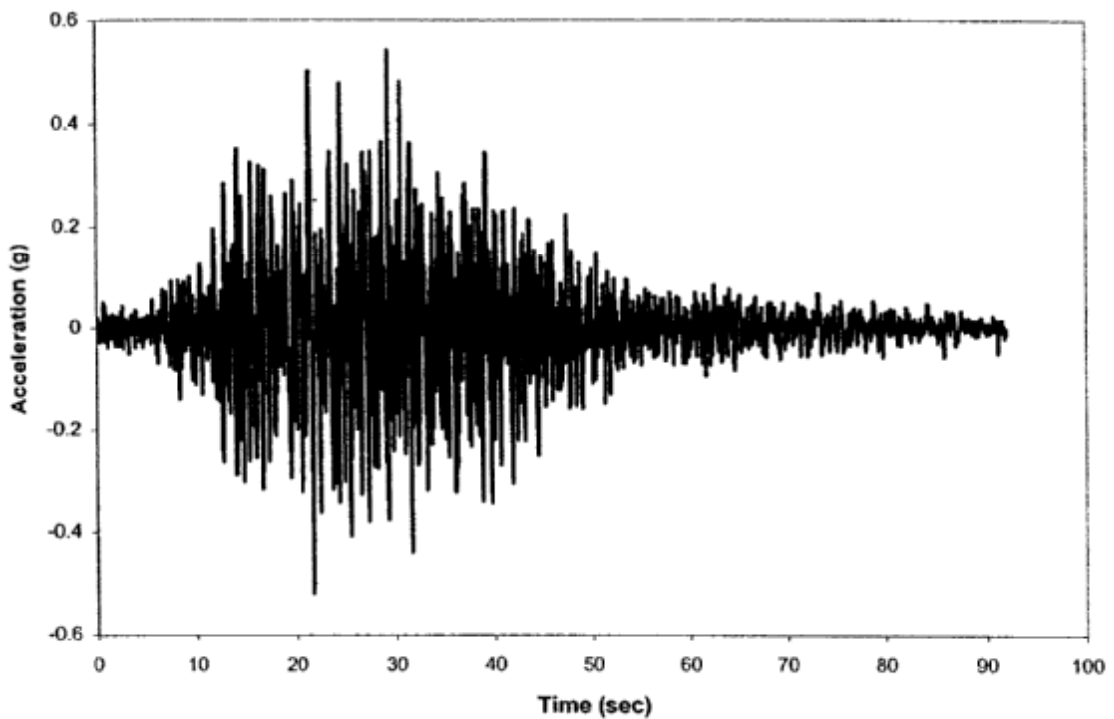


Figure 4.1-18 Modified Peru Earthquake, N-S Time History (Stapleton 2004)

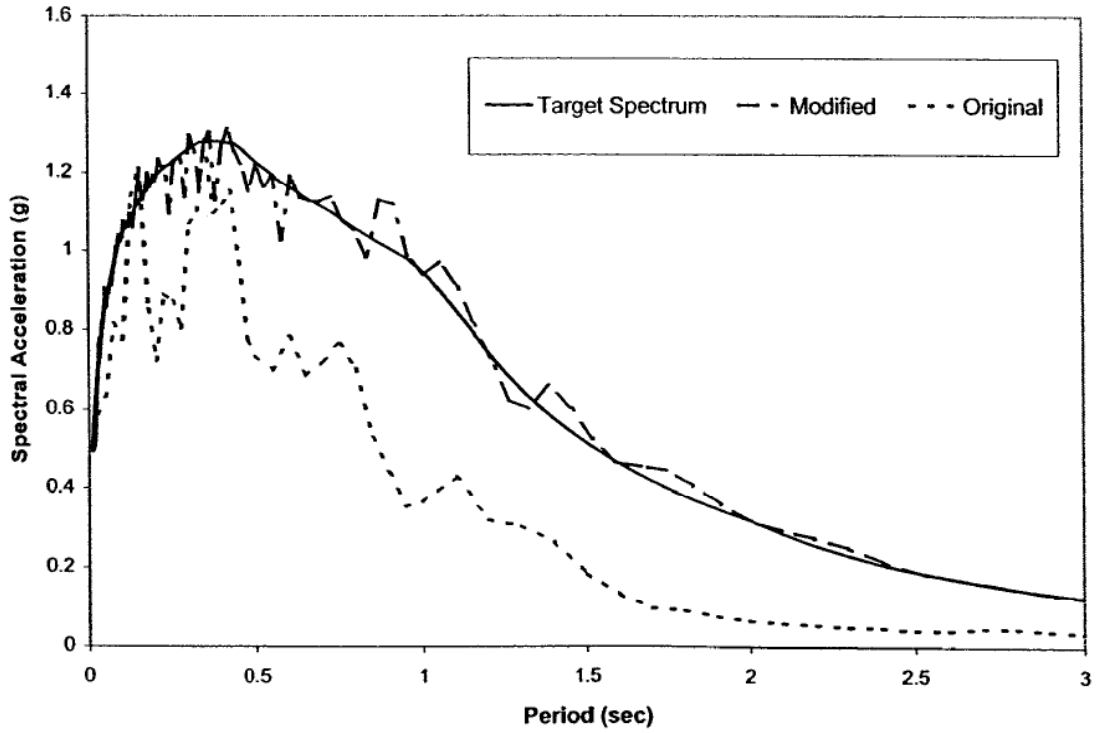


Figure 4.1-19 E-W Chile Spectral Acceleration adapted from Stapleton (2004)

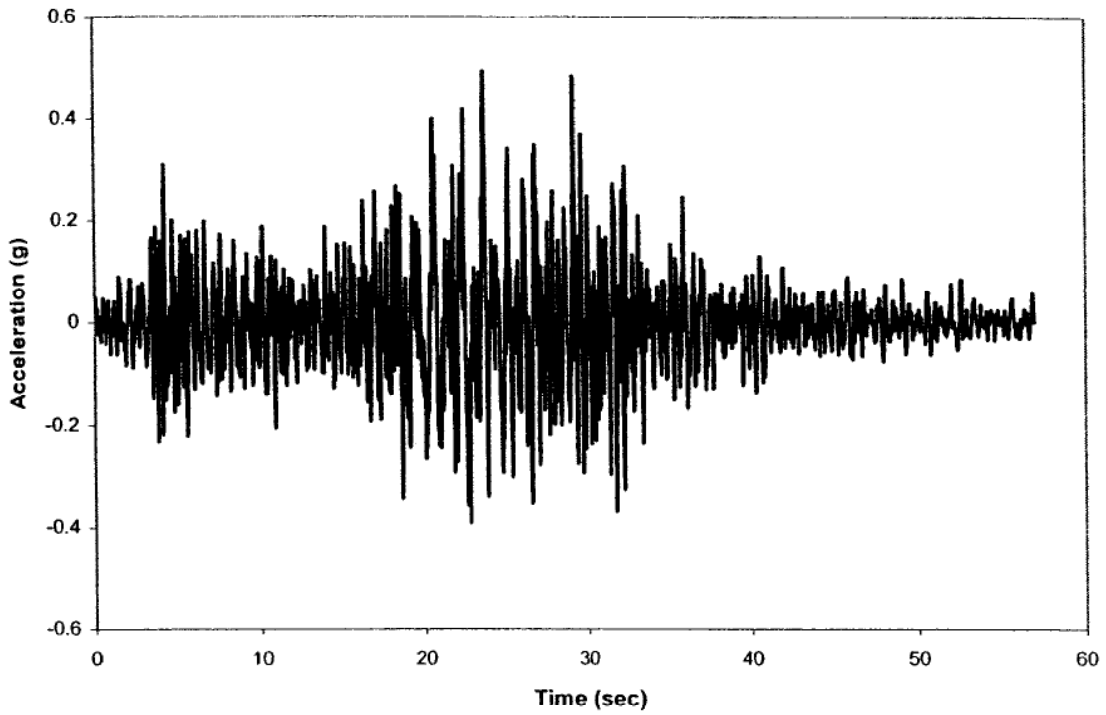


Figure 4.1-20 Modified Chile Earthquake, E-W Time History (Stapleton 2004)

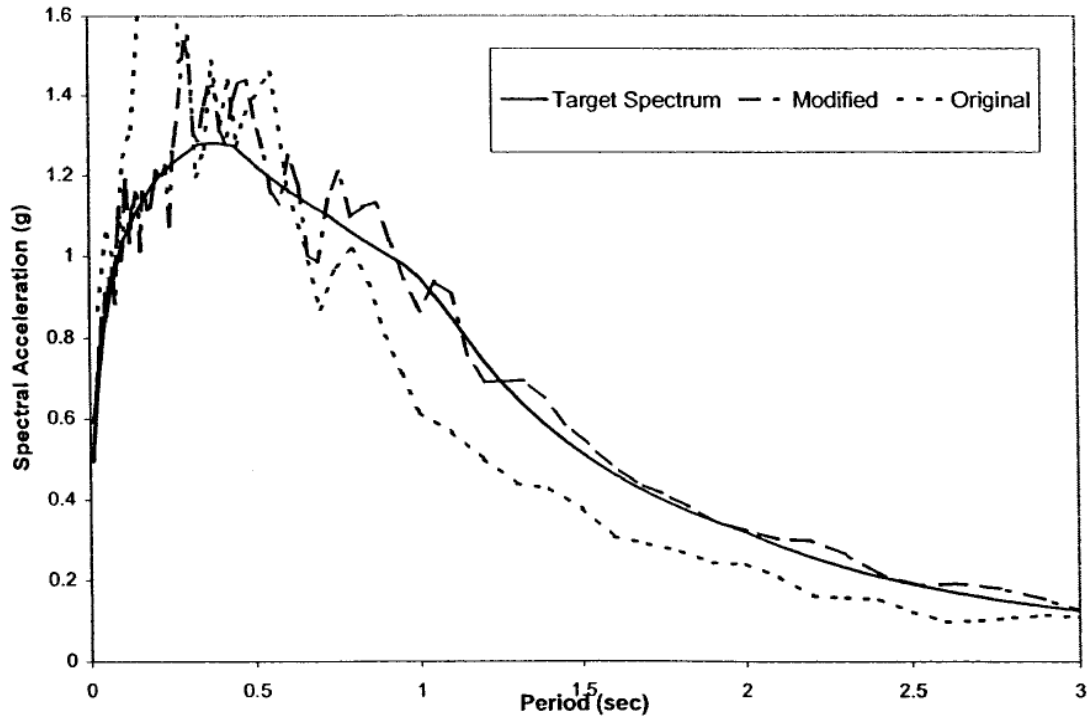


Figure 4.1-21 N-S Chile Spectral Acceleration (Stapleton 2004)

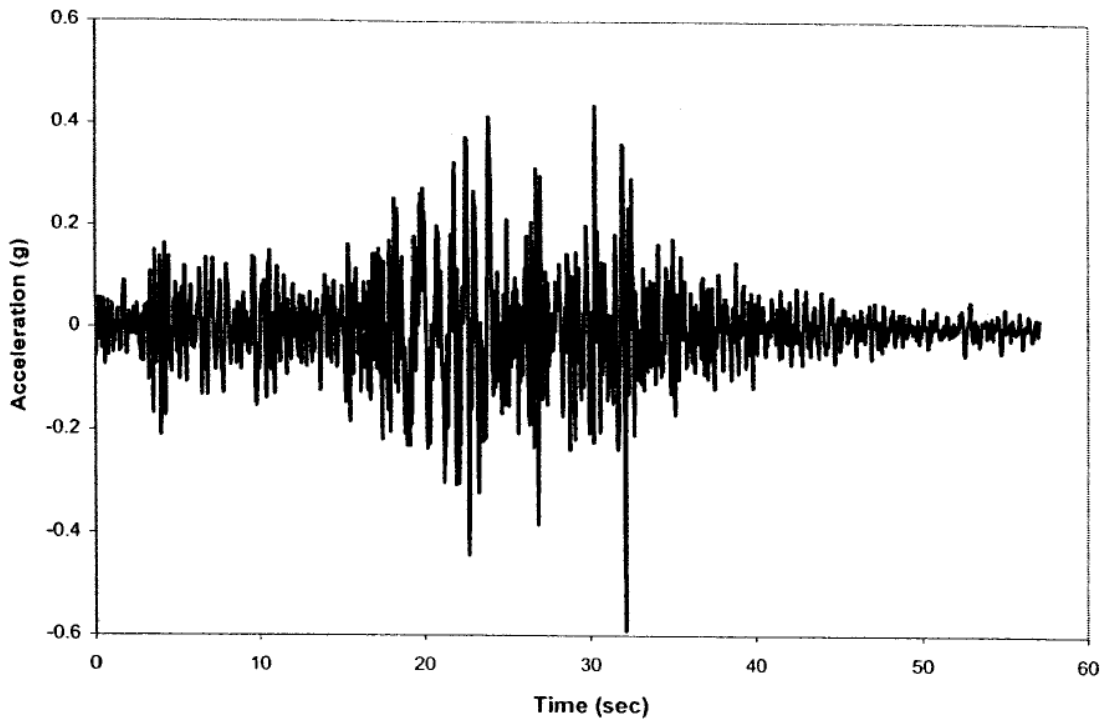


Figure 4.1-22 Modified Chile Earthquake, N-S Time History (Stapleton 2004)

Figures 4.1-23, 4.1-24, and 4.1-25 show the target acceleration spectrum used in this study compared with spectra from Frankel et al (1996) for Seattle, Olympia, and Grey's Harbor, WA. The target spectrum is compared with different return period ground motions. The fundamental period of the bridges used in this study are approximately one second.

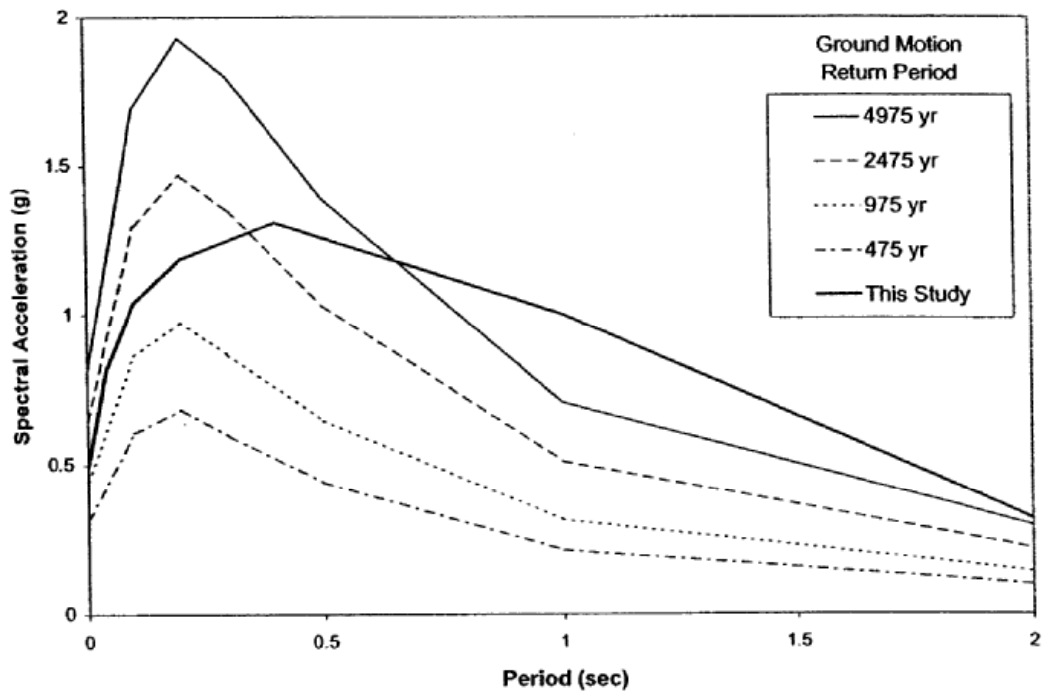


Figure 4.1-23 5% Damped Spectral Accelerations for Seattle, WA (Frankel, 1996)

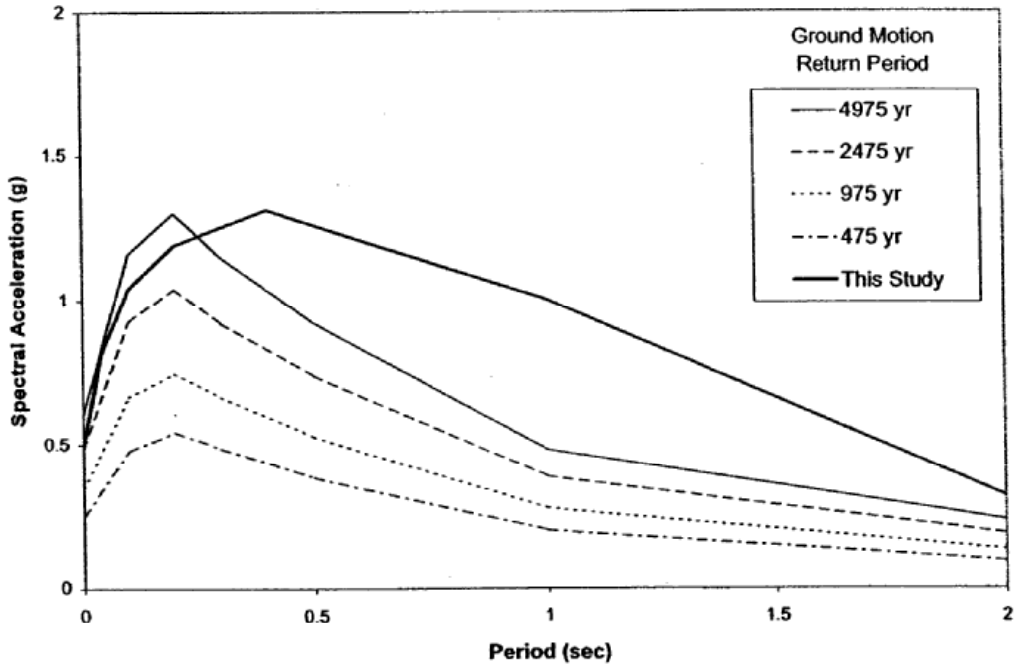


Figure 4.1-24 5% Damped Spectral Accelerations for Olympia, WA (Frankel, 1996)

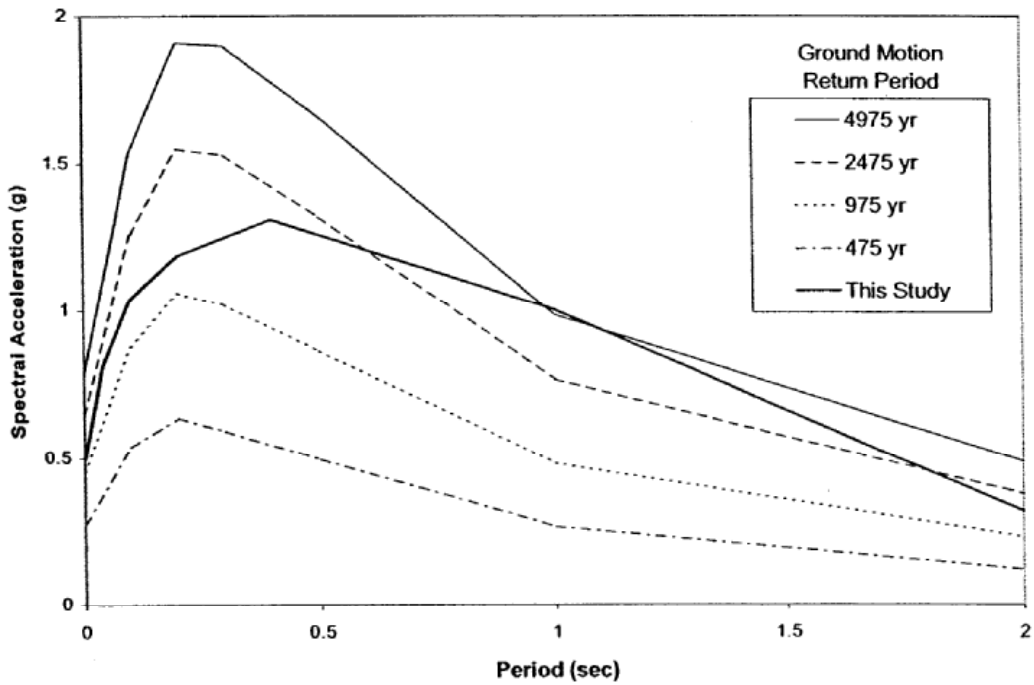


Figure 4.1-25 5% Damped Spectral Accelerations for Grey's Harbor, WA (Frankel, 1996)

The Washington State Department of Transportation (WSDOT) supplied the last six earthquake time histories. All six of these time histories were modified to fit an acceleration spectrum representative of the Seattle area. The six time histories come from three different earthquakes. Each earthquake has time histories that have been scaled for a 475 and a 950 year return period, respectively.

The first of these three earthquakes was a long-duration earthquake from the 1985 Mexico City Earthquake. The last two are short-duration earthquake from the 1995 Kobe Earthquake and the 1949 Olympia Earthquake. All of the time histories for these earthquakes can be found in Appendix A.

4.2 WSDOT Bridge 5/826

A second bridge was chosen for this study to help understand the effects of long duration earthquakes on lightly reinforced concrete bridges. The bridge is WSDOT Bridge 5/826 and it was modeled in much the same way as the previous bridge.

4.2.1 Introduction

The bridge shown in Figure 4.2-1 is located at milepost 261.51 on Smith Road in King County of Washington State. It was constructed in 1972 to carry Smith Road over Interstate 5. This bridge is also a lightly reinforced bridge as well as having splices in the plastic hinge region.



Figure 4.2-1 Bridge 5/826

4.2.2 Description of the Bridge

The plan and elevation of the bridge are shown in Figures 4.2-2 and 4.2-3. The bridge is 369 feet long and has four spans. The two middle spans are both 121 feet long, while the two end spans are 57 and 70 feet long, respectively. The reinforced concrete deck, which provides the main transverse stiffness of the super structure, is continuous at all interior supports. It is 40 feet wide and has a thickness of 7.0 inches. The deck is supported by six prestressed concrete I-girders that are 6 feet 1.5 inches deep. These I-girders are spaced at 7 feet 4 inches on center. The I-girders rest on the abutments on top of a grout pad topped with a 2.5 inch laminated elastomeric bearing pad. At the intermediate piers, the I-girders are cast into the crossbeam, which provides a very stiff superstructure. The provided superstructure is then much stiffer than the supporting columns.

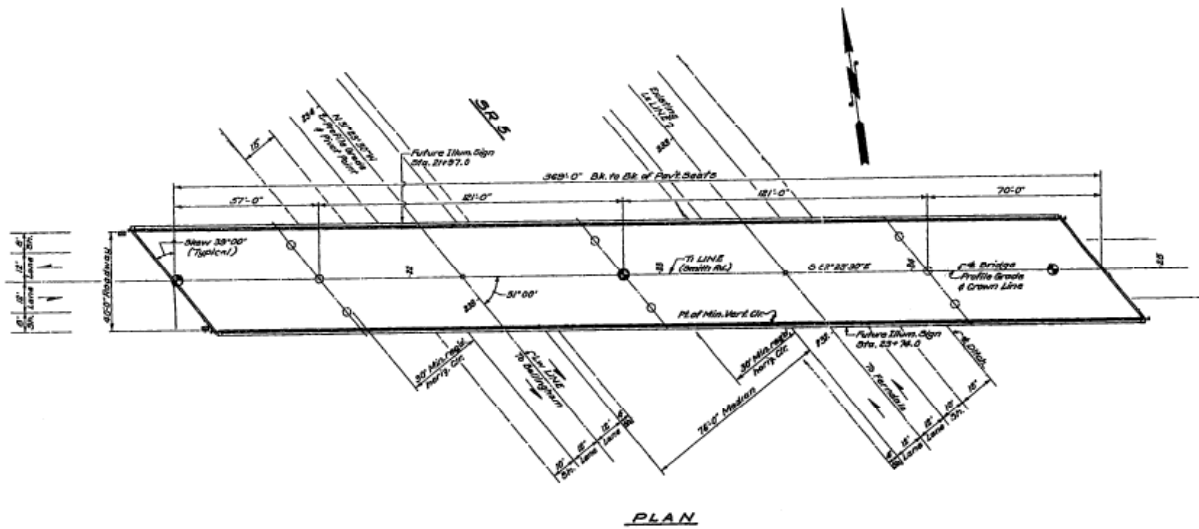


Figure 4.2-2 Plan View of Bridge 5/826

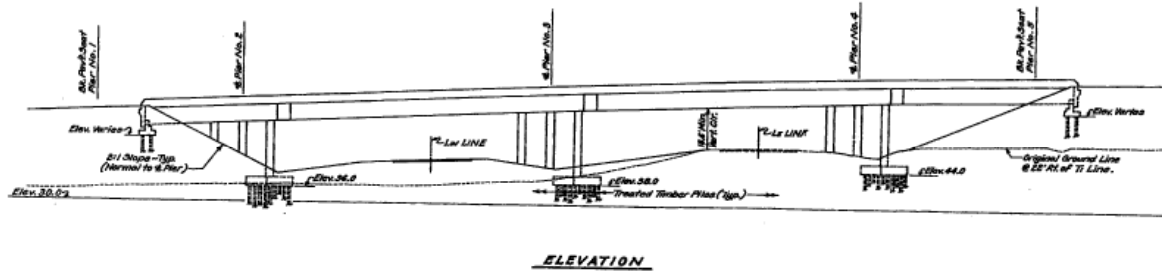


Figure 4.2-3 Elevation View of Bridge 5/826

The crossbeam was cast monolithically with the three columns at each bent. The crossbeam has a total length of 50 feet 2.25 inches, a width of 48 inches, and a depth of 6 feet 11 inches. See Figure 4.2-4. The crossbeams at piers No. two and four are reinforced with ten No. 10 bars at the top and eight No. 8 bars in the bottom. Pier No. 3 is reinforced with ten No. 10 bars in the top and eight No. 9 bars in the bottom. All piers also have eight No. 6 reinforcing bars along each side of the crossbeam. An inner and

outer reinforcing hoop provided confinement. The hoops are No. 5 reinforcing bars at varying spacing along the length of the crossbeam to account for shear.

All nine of the columns at the interior bents are supported on pile caps placed on top of driven piles. The columns have clear heights of 23.5 feet at pier No. 2, 22 feet at pier No. 3, and 24.5 feet at pier No. 4. They have a centerline spacing of 19.5 feet in the lateral direction. Compacted fill surrounds the columns to a height of approximately 4 feet. All of the columns are circular with diameters of 36 inches. They are reinforced longitudinally with seventeen No. 11 reinforcing bars that are evenly spaced around the cross-section perimeter with a clear cover of 1.5 inches. The longitudinal bars extend into the crossbeam without a splice.

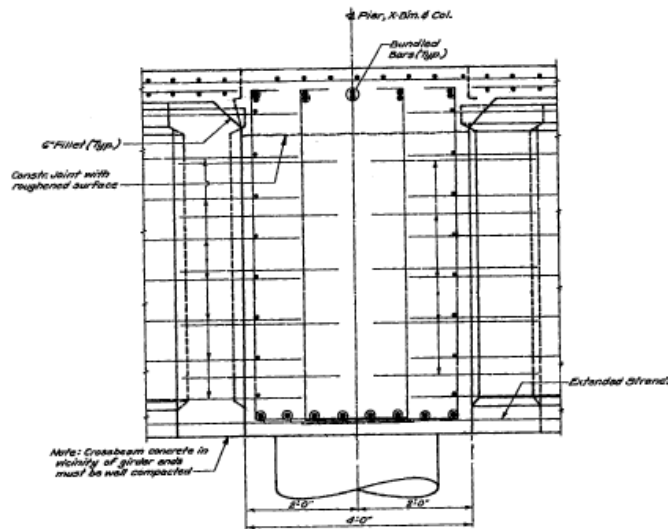


Figure 4.2-4 Cross Section of Cross Beam of Bridge 5/826

The columns have a longitudinal reinforcement of 2.6%. Lap splices of 63 inches were used at the base of the columns. The columns are reinforced in the transverse direction with No. 4 bars spaced every 6 inches. The hoops have an overlap of 24 inches

and have no hooks. The transverse reinforcement ratio is 0.4%. All column details are shown in Figure 4.2-5.

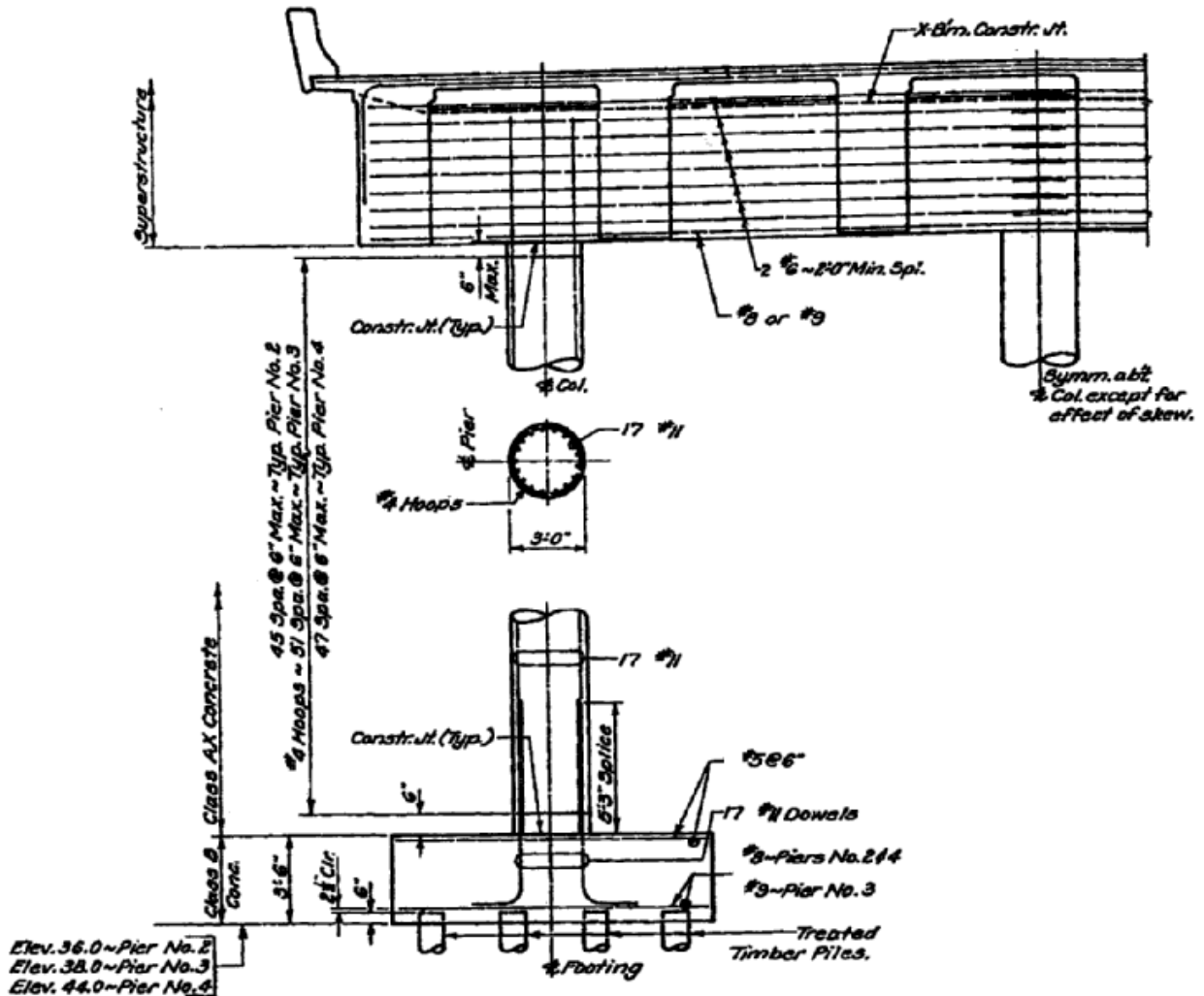


Figure 4.2-5 Column Cross Section of Bridge 5/826

Each column is on a separate foundation consisting of a pile cap that is cast monolithically with the column. The pile caps are all 12 feet 9 inches square in the plan view and 3 feet 6 inches thick. The pile caps at Pier No. 3 are supported on 16 treated

timber piles. There are four rows of four piles with centerline spacings of 3 feet 3 inches. The pile caps at piers 2 and 4 are supported on 14 driven piles. There are four rows with three piles in the first and fourth rows and four piles in the middle two rows. See Figure 4.2-6.

The pile caps contain two mats of steel placed in the top and bottom of the elevation. The mat at the top consists of No. 5 bars running in both directions, spaced every 6 inches for the pile caps at all piers. The mat in the bottom of the pile caps at piers 2 and 4 consists of No. 8 bars running in both directions, spaced every 6 inches. The mat in the bottom of the pile caps at pier No. 3 consists of No. 9 bars running in both directions, spaced every 6 inches.

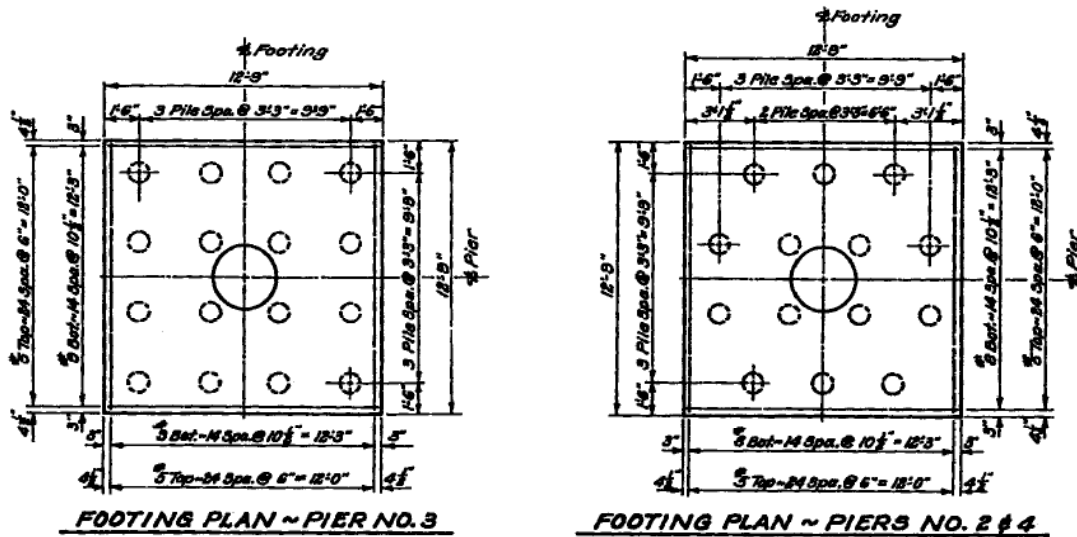


Figure 4.2-6 Column Footing Plans for Bridge 5/826

The abutments are set on driven piles. The pile caps at the abutments are 6 feet 3 inches by 56 feet 6.5 inches in the plan view, and they are 2 feet thick. The pile caps are

supported on 20 treated timber driven piles. There are 10 rows of two piles each, along the length of the abutment. See Figure 4.2-7 for the abutment details.

The pile cap has two mats of steel located at the top and bottom with clear covers of 2 inches at the top and 2.5 inches at the bottom. The steel mats consist of No. 6 bars running in both directions, spaced at 12 inches. The abutment pile caps are cast monolithically with the abutment walls and have two No. 5 bars spaced every foot, running up into the wall.

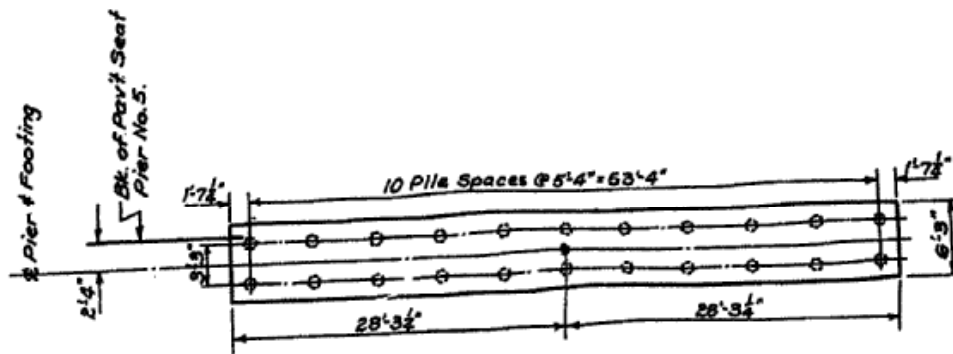


Figure 4.2-7 Abutment Footing Plan for Bridge 5/826

The concrete used in the pile caps and abutment walls is a WSDOT Class B mix with a compressive strength of $f'_c = 3000 \text{ psi}$. All other concrete used in the bridge, besides that used for the prestressed girders, is a WSDOT Class AX mix with a compressive strength of $f'_c = 4000 \text{ psi}$. The reinforcing steel used in this bridge is Grade 40 with a yield strength of $f_y = 40,000 \text{ psi}$.

4.2.3 Structural Model

A drawing of the bridge model used in this study is shown in Figure 4.2-8. The longitudinal deck beams and the crossbeams are modeled as very stiff beams. Like Bridge 5/518, the longitudinal beam can be considered almost rigid because of the composite action of the deck and I-girders. Because the crossbeam is much stiffer than the columns, it can be considered almost rigid as well. The columns are modeled with nonlinear beam-column elements and are given an appropriate cross sectional area and mass density. A summary of the structural properties of the longitudinal deck beam, crossbeams, and columns is shown in Table 4.2-1 and Table 4.2-2.

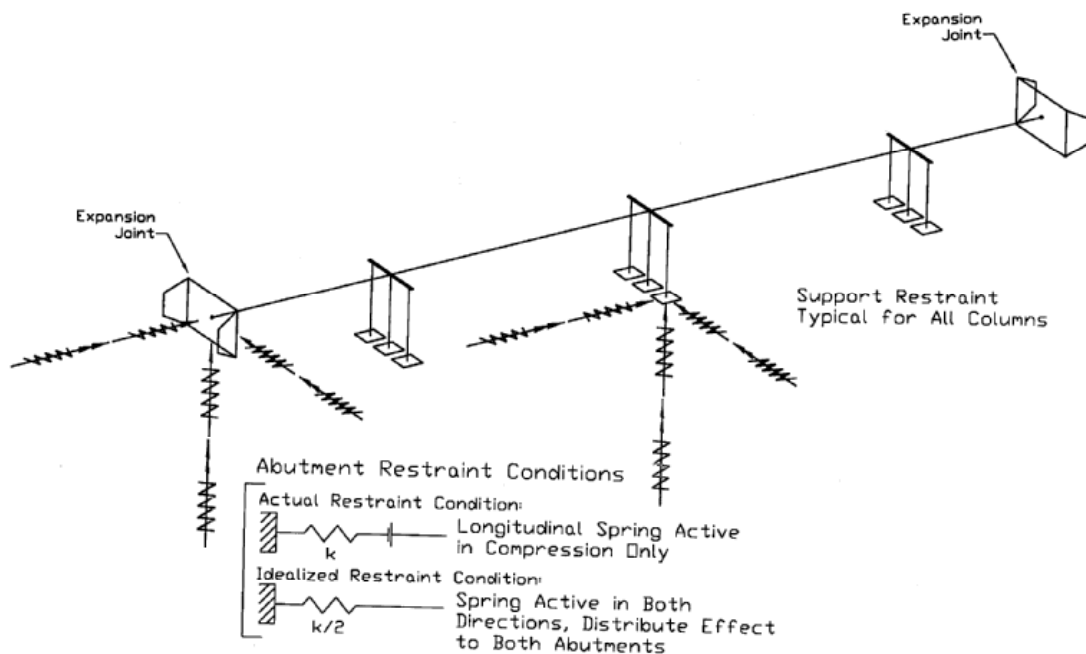


Figure 4.2-8 Structural Model of Bridge 5/826

Table 4.2-1 Structural Properties for Columns and Crossbeams

	Young's Modulus (ksi)	Poisson Ratio	Unit Weight (kips / in ³)	Axial Area (in ²)	Shear Area (in ²)	Bending Inertia (in ⁴)	Torsional Inertia (in ⁴)
Columns	3604	0.18	2.224E-5	1018	1018	20000	164900
Crossbeam	360400	0.18	2.224E-5	3984	3984	412200	1.537E+6
Deck Beam	360400	0.18	2.224E-5	8423	8423	1.000E+8	1.000E+8

Table 4.2-2 Yield Function Constants for the Columns

M_{20} (k - in)	P_0 (kips)	P_t / P_0	a_0	a_1	a_2	a_3
14110	6107	0.1895	1.0	-4.248	-5.404	-.1561

Boundary springs are used to consider the influence of soil-structure interaction. The soil stiffness properties for the six degrees of freedom are listed in Table 4.2-3. Springs were attached at all columns and the two abutments. The soil stiffness properties were obtained using the WSDOT Bridge Design Manual (WSDOT, 2002).

Table 4.2-3 Stiffness Properties for Soil Springs (k/in)

Location	Translation X	Translation Y	Translation Z	Rotation X	Rotation Y	Rotation Z
West Abutment	1049	1049	5280	1.00E+7	1.00E+7	1.00E+8
Pier 1	1442	1442	2639	3440000	4444000	1.00E+8
Pier 2	1690	1690	3016	5734000	5734000	1.00E+8
Pier 3	1129	1129	2639	3440000	4444000	1.00E+8
East Abutment	1172	1172	5808	1.00E+7	1.00E+7	1.00E+8

Rayleigh damping was used for this bridge model and coefficient values were assigned as was previously explained in section 4.1.3. Because the deck of this bridge is continuous, expansion joints were only needed at the two abutments. Each abutment expansion joint was idealized with one expansion joint element. The expansion joint element accounted for the stiffness in all six degrees of freedom. The expansion joint element allows for a 1.5 inch seat gap and has an impact spring that accounts for the increased stiffness when the gap closes. This impact spring was assumed to have the same axial stiffness as the longitudinal deck beam. The nonlinear properties of the expansion joints are tabulated in Table 4.2-4.

Table 4.2-4 Input Parameters for Expansion Joints

	Support	Impacting Hinge
Bearing Type	Bearing Pad	NA
Element Width (<i>in.</i>), d	440.20	440.20
Skew (<i>degrees</i>)	0.00	0.00
Impacting Spring Stiffness (<i>kips/in.</i>), k_I	1.00	2.21×10^4
Bearing Friction Stiffness (<i>kips/in.</i>), k_F	1.00	1.00
Coefficient of Friction of Bearing, c_F	0.02	0.00
Stiffness of Tie Bar (<i>kips/in.</i>), k_T	NA	NA
Tie Bar Yield Force (<i>kips</i>), Y_T	NA	NA
Tie Bar Gap (<i>in.</i>), G_T	NA	NA
Seat Gap (<i>in.</i>), G_S	0.00	1.50
Number of Tie Bars	0	0
Vertical Stiffness (<i>kips/in.</i>), k_3, k_6	1.00×10^7	0.00
Longitudinal Stiffness (<i>kips/in.</i>), k_1, k_4	123.30	0.00
Transverse Stiffness (<i>kips/in.</i>), k_2	123.30	0.00
Rotational Stiffness (<i>kips/in.</i>), k_5	0.00	0.00

4.2.4 Seismic Excitation

The same seismic excitation was used for this bridge as was used on Bridge 5/518.

Chapter 5

Analytical Results and Interpretation

5.1 Introduction

Presented in this chapter are selected time history analysis results from the nonlinear finite element analysis of WSDOT Bridges 5/518 and 5/826. The results include the displacement at the top of the piers, the plastic rotation of the plastic hinges at the top of the columns, the damage corresponding to the plastic rotation found in the plastic hinges, column moment, column shear, and displacement of the expansion joints.

5.2 Bridge 5/518

The results from analyses using the modified Peru and modified Chile earthquakes and the model of Bridge 5/518 are presented here. These two cases were chosen because they are the two extreme cases, and they show the most information about the response of the bridge with respect to the new damage model.

5.2.1 Modified Peru Earthquake

Figures 5.2-1 through 5.2-3 show the total displacement time histories at the top of the intermediate piers, where relative displacement is the difference between displacement at the top versus that at the column base. The total relative displacement was found by taking the square root of the sum of the squares of the longitudinal and transverse displacements. The figures show that the total relative displacements at the center pier are much larger than those of the outer piers. This can be seen by looking at the displacement envelope shown in Figure 5.2-4, where the maximum relative transverse

displacements at each pier are plotted. The greater displacement at the center pier is not surprising since the abutments provide some restraint in the transverse direction. The figure also shows that most of the displacement is in the transverse direction. This is because the period of the bridge in the transverse direction is much greater than it is in the longitudinal direction. The longitudinal displacements are similar for all three piers because the deck is virtually rigid compared to the columns.

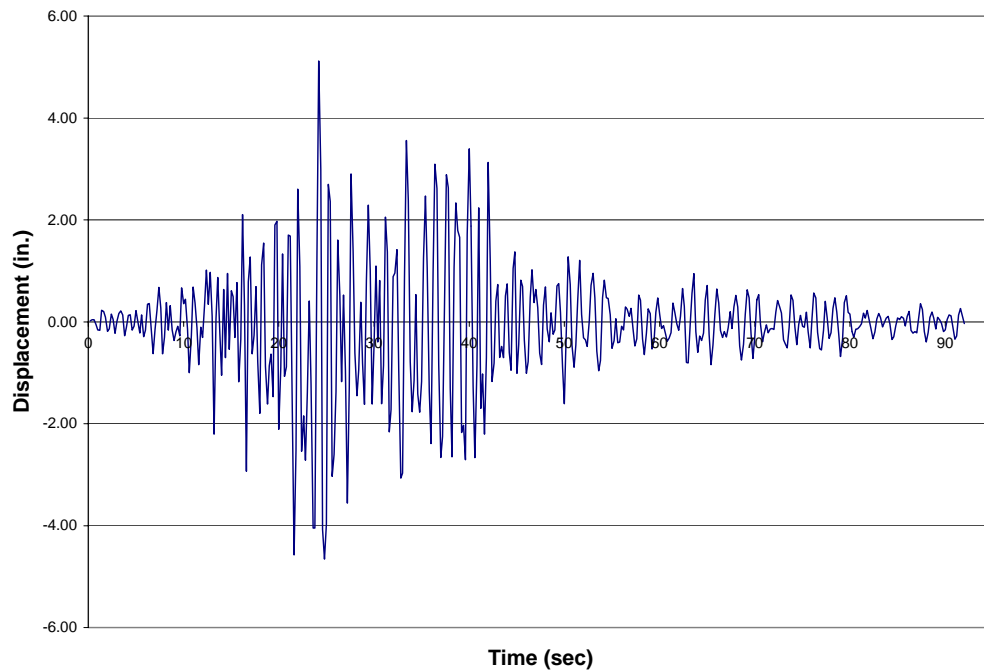


Figure 5.2-1 Total Relative Displacement at Pier 1, Modified Peru Earthquake

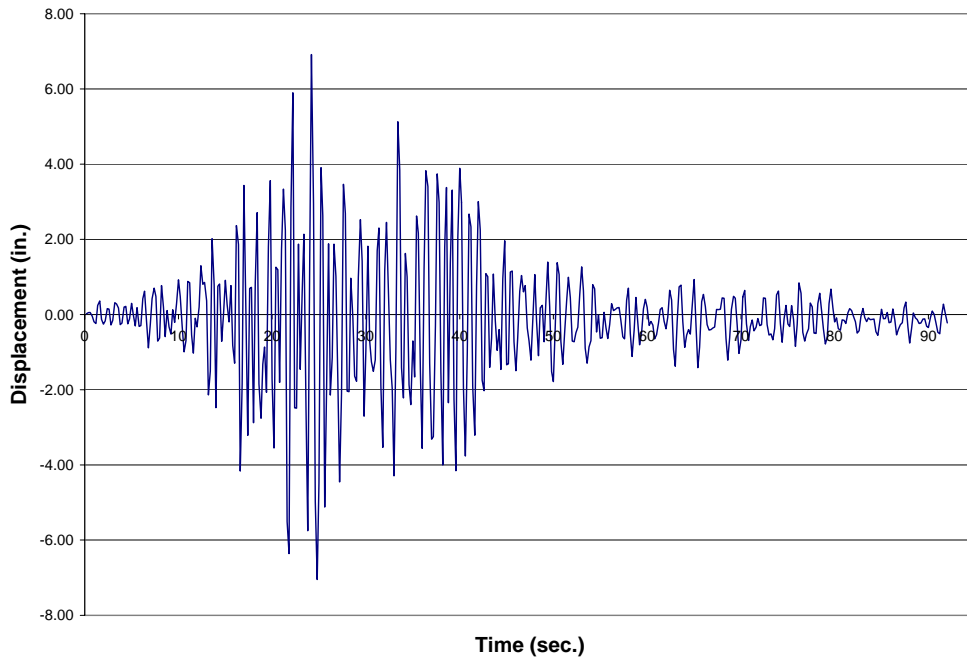


Figure 5.2-2 Total Relative Displacement at Pier 2, Modified Peru Earthquake

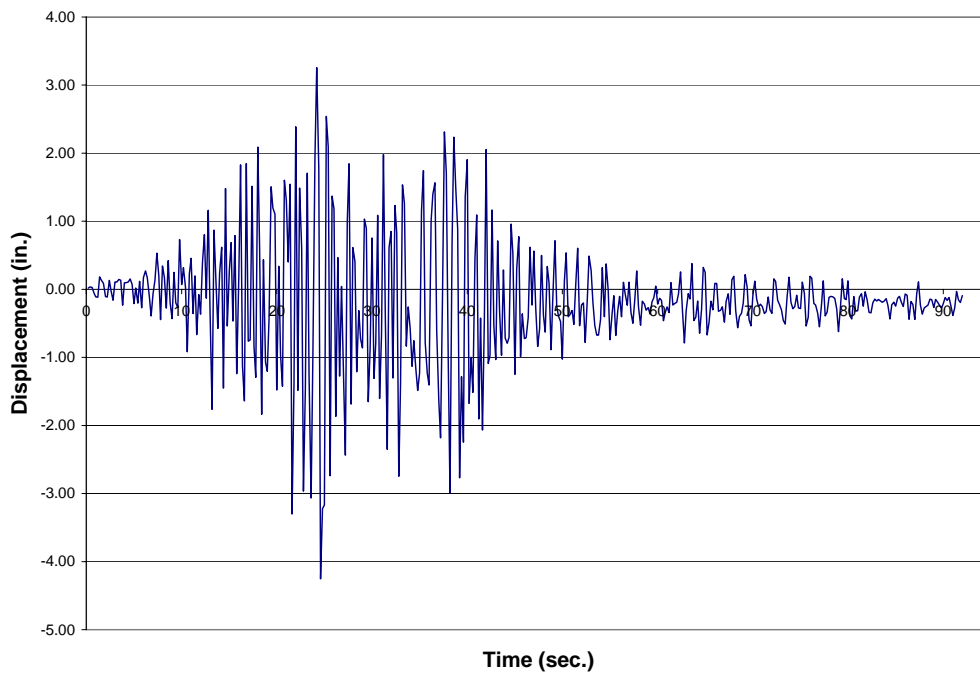


Figure 5.2-3 Total Relative Displacement at Intermediate Pier 3, Modified Peru Earthquake

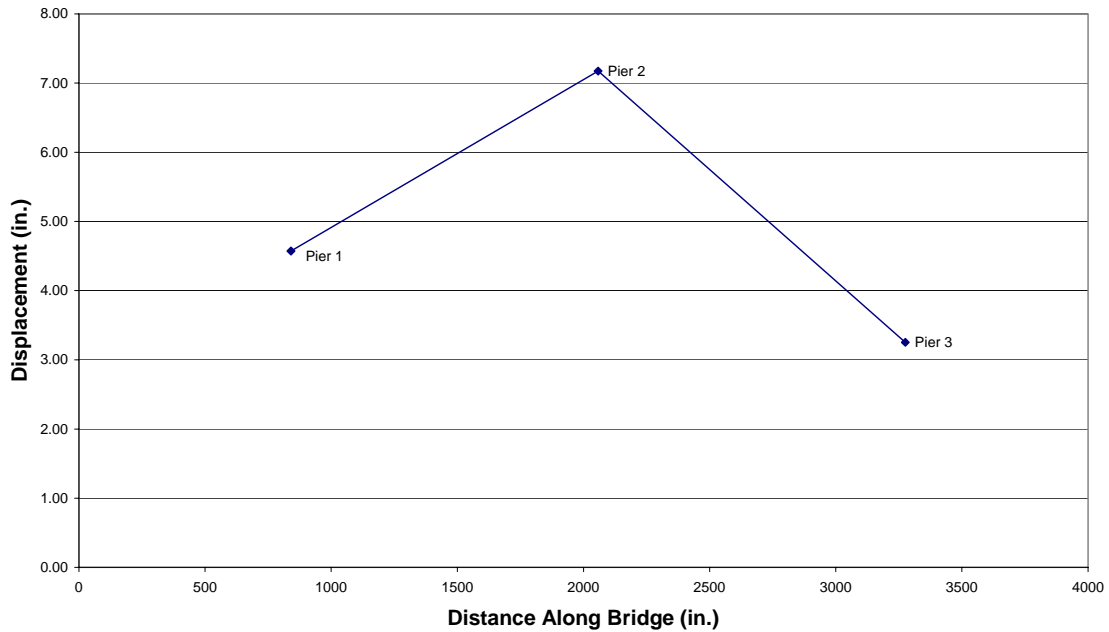


Figure 5.2-4 Transverse Displacement Envelope of Bridge Deck, Modified Peru Earthquake

Because the foundation springs at the bottom of every column allowed for slight rotations, the plastic rotation was confined to plastic hinges at the top of the columns. Table 5.2-1 shows the maximum moments at the top and bottom of all of the columns. It should be noted that yielding limits the amount of moment that can be developed in the columns, and the yield level depends on the level of axial force.

Table 5.2-1 Maximum Moment (kip-in) at the Top and Bottoms of Columns, Modified Peru Earthquake

Pier No.	Column	Moment	
		Top	Bottom
1	1	16505.3	6238.4
	2	15250.7	6614.5
	3	17633.1	6953.7
2	1	16851.3	10623.2
	2	16070.4	10370.0
	3	18220.6	10447.8
3	1	15732.8	6942.7
	2	14892.5	6761.1
	3	15811.3	6671.8

Because the displacements at the center pier were larger than those at the outer piers, the plastic rotations in the plastic hinges found in that pier were larger, as shown in Figure 5.2-5. Pier 1 and Pier 3 are the outer piers, and the center pier is Pier 2. It should also be noted that the columns in the center pier have many more plastic rotation cycles than the columns of the other piers.

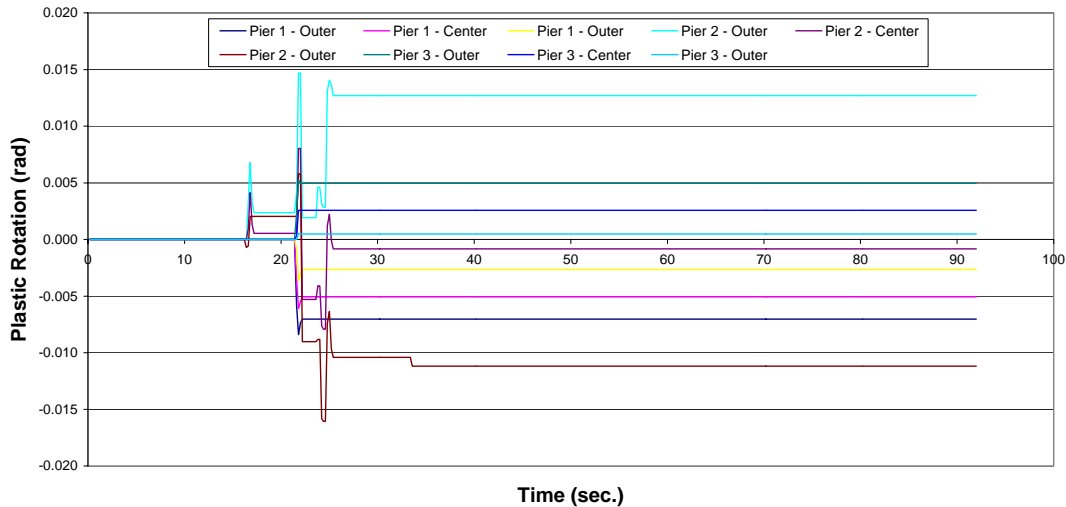


Figure 5.2-5 Plastic Rotations at the Top of the Columns, Modified Peru Earthquake

Due to the fact that the columns in the center pier experienced larger plastic rotations and more plastic rotation cycles than those of the outer piers, the columns in the center pier also accumulated more damage, as shown in Figure 5.2-6. The levels of damage in the columns at Pier 1 are less than those of the columns at Pier 3. This is due to the fact that the span that connects to Pier 1 is the shorter of the two end spans, and therefore allows for less displacement.

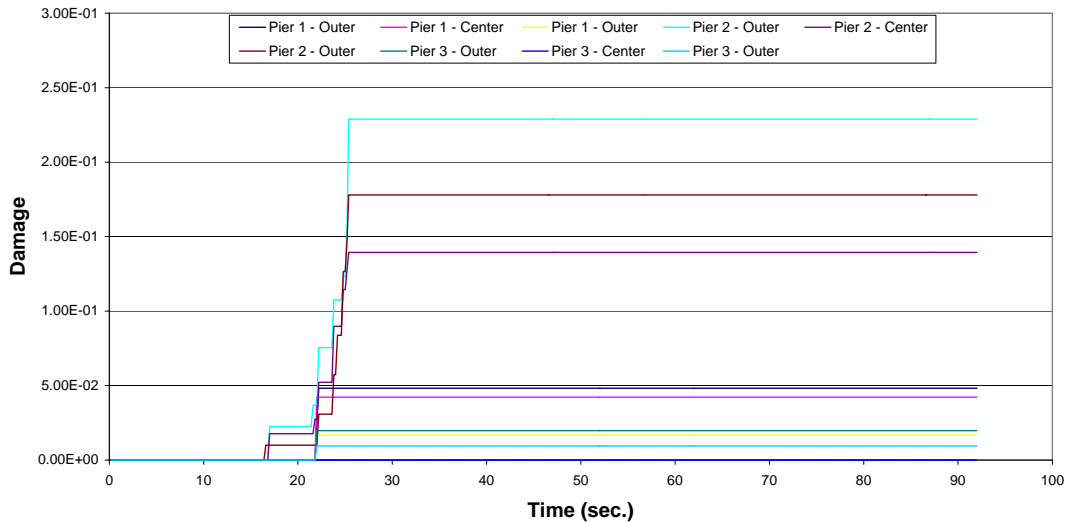


Figure 5.2-6 Damage at the Top of the Columns, Modified Peru Earthquake

The damage coefficients for the columns at the center pier ranged in value between 0.14 and 0.23, which would indicate that there is light cracking throughout the column section. The damage coefficients in the columns at the other piers are at or below 0.05, which would suggest only minor cracking. The indicated damage is small enough that localized spalling would not occur. By looking at the shear versus displacement hysteresis plots, as shown in Figures 5.2-7 and 5.2-8, it can also be seen that the demand

on the columns is not very large. In the longitudinal direction, the hysteresis loops only open slightly, which would suggest that there was only minor yielding. The hysteresis loops for the transverse direction open more, but they also show little significant yielding, which is consistent with the accumulated damage. Figure 5.2-8 also shows that, as the damage accumulated and the hysteresis loops opened, the stiffness was reduced.

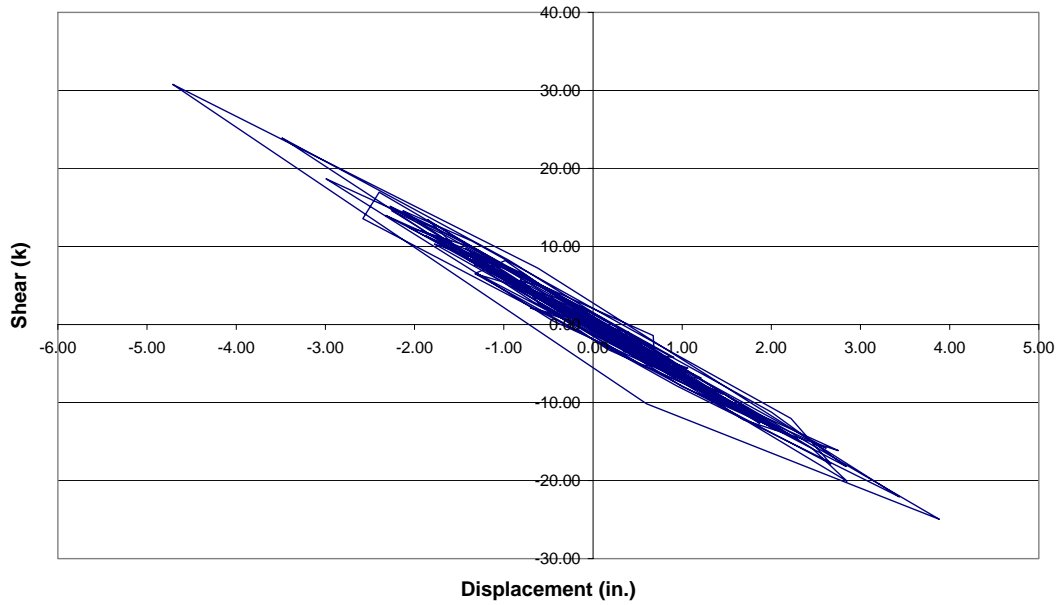


Figure 5.2-7 Longitudinal Hysteresis Plot for the Center Column of Pier 2, Modified Peru Earthquake

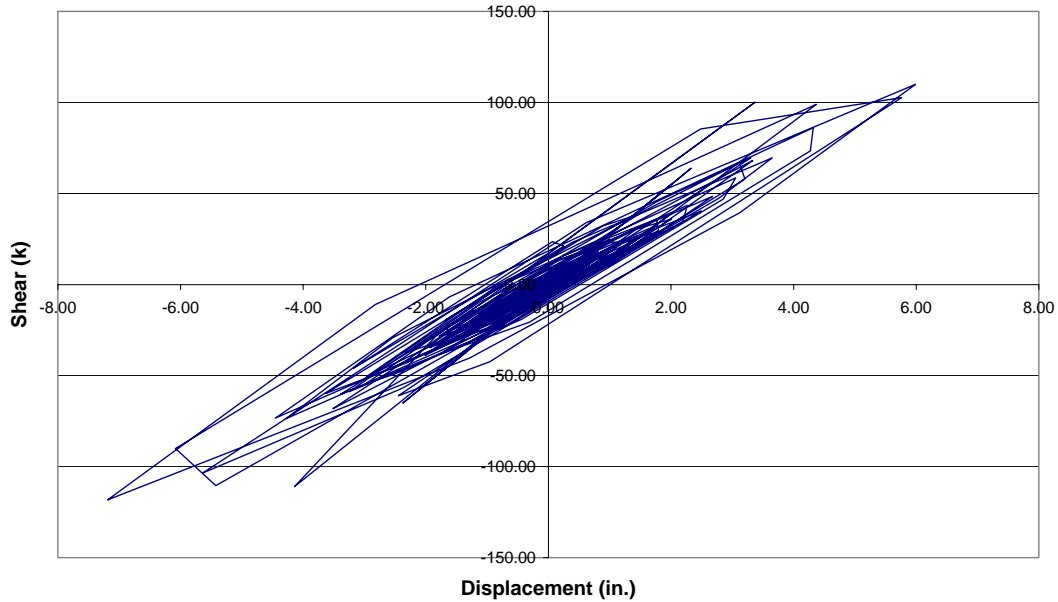


Figure 5.2-8 Transverse Hysteresis Plot for the Center Column of Pier 2, Modified Peru Earthquake

The maximum shear values at the top and bottom of the columns are shown in Table 5.2-2. The shear values are different at the top and bottom because the soil spring at the base of the column allows for some column rotation, which causes a variation in local force components. The shear capacity of the columns was based solely on the concrete for simplicity and was determined according to Kowalsky and Priestley (2000):

$$V_c = 2.8\sqrt{f'_c} * A_e$$

where A_e is taken as 80% of the gross area of the column and f'_c was taken as 6000 *psi*. The specification for the bridge requires $f'_c = 4000$ *psi*, but Priestley (1996) recommends using $1.5 * f'_c$ as being more representative of the actual concrete strength in older bridges. This gives a final shear capacity of 171.6 kips for the columns. Since the maximum shear in the columns was 128 kips, the shear capacity was not exceeded.

Columns with smaller aspect ratios than those that are found in this bridge should be investigated further.

Table 5.2-2 Maximum Shear (kips) in the Columns, Modified Peru Earthquake

Pier No.	Column	Shear			
		Top	Demand/ Capacity	Bottom	Demand/ Capacity
1	1	87.27	0.51	93.90	0.55
	2	92.49	0.54	98.36	0.57
	3	102.04	0.59	112.25	0.65
2	1	114.79	0.67	123.03	0.72
	2	104.13	0.61	118.73	0.69
	3	116.11	0.68	127.76	0.75
3	1	92.52	0.54	91.52	0.53
	2	76.07	0.46	99.86	0.58
	3	95.75	0.56	101.32	0.59

The maximum abutment forces in the transverse and longitudinal directions are found in Table 5.2-3. The shear capacity of the abutments was determined according to the AASHTO Bridge Design Specifications (AASHTO, 1998), where the nominal shear strength is calculated by:

$$V_n \leq 0.2f'_c A_{cv}$$

where A_{cv} is the area of the concrete engaged in shear transfer. The value of A_{cv} in the longitudinal direction for this bridge is 3744 in², which incorporates the cross section of the thinnest portion of the abutment wall. This gives a nominal shear capacity of 3370 kips. The shear forces in the abutments in the longitudinal direction were not near the

capacity limit, therefore the abutment is considered capable of resisting the seismic demands.

The value of A_{cv} in the transverse direction for this bridge is 1620 in², which incorporates the cross section of the girder stops along the crossbeam. This gives a nominal shear capacity of 1458 kips. This is also much greater than the actual force seen by the abutment in the analysis.

Table 5.2-3 Maximum Shear (kips) at the Abutments, Modified Peru Earthquake

Abutment	Shear			
	Longitudinal	Demand/ Capacity	Transverse	Demand/ Capacity
West	1840	0.55	245	0.17
East	1470	0.44	196	0.13

By looking at the relative longitudinal displacement of the expansion joints, it can be determined if there will be pounding at the abutments and piers. Figure 5.2-9 shows the relative longitudinal displacement at the West abutment. It should be noted that when the relative displacement is negative, the expansion joint is closing. The expansion joint has a gap of 1.5 inches, so it can be seen that pounding occurs at the West abutment. Pounding occurs at all of the piers and at the other abutment, as well. The plots for the other abutment and piers can be found in Appendix C. It was within the scope of this project to determine if pounding occurs but not to quantify the damage due to pounding. Further research should be done to determine those effects.

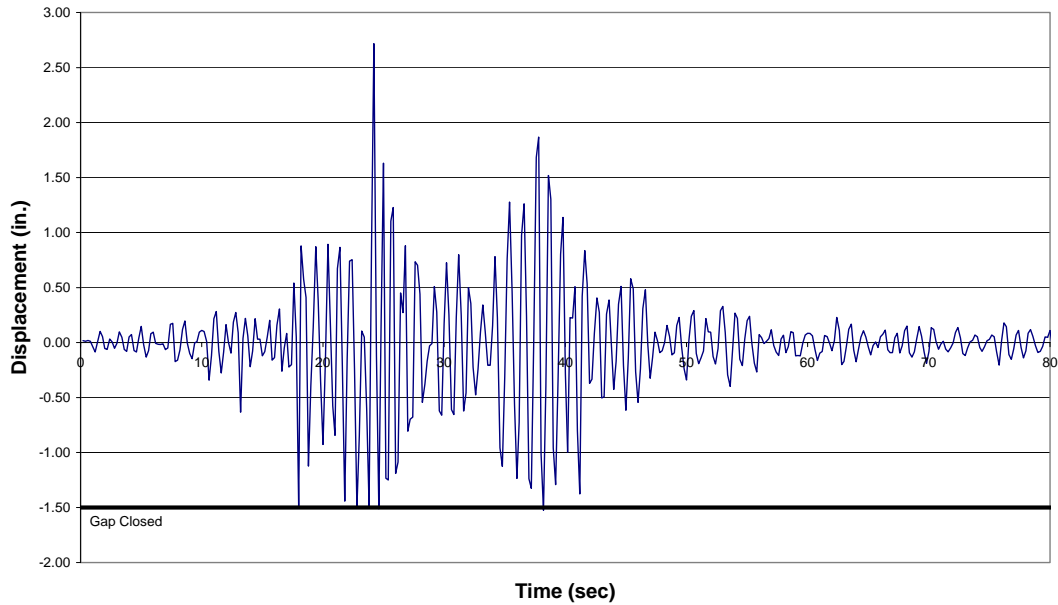


Figure 5.2-9 Relative Longitudinal Displacement at the West Abutment, Modified Peru Earthquake

The maximum displacement that the bearing pads can withstand was determined by the equation (Priestley, 1996):

$$x_b = h\gamma_s$$

where h is the thickness of the bearing pad and γ_s is the allowable shear strain. The maximum shear strain, γ_s , is taken conservatively as:

$$\gamma_s = 0.2\varepsilon_{tu}$$

where ε_{tu} is the failure tensile strain. An average ε_{tu} value of 5.75 was assumed (Priestley, 1996), and the thickness of the bearing pad is 1.25 inches. This gives an

allowable displacement of 1.44 inches while the actual displacement is predicted to be 2.72 inches. It should be noted that conservative values have been used, but they imply that a failure of the bearing pad could occur.

After such a large earthquake, the bridge appears to be in good condition. The columns do not accumulate excessive damage and they are capable of resisting the shear demands. The abutments are also able to resist the shear demands in both the longitudinal and transverse directions. The two main concerns would be the pounding of the expansion joints that occurs at the abutments and piers and a possible failure of the bearing pads.

5.2.2 Modified Chile Earthquake

Figures 5.2-10 through 5.2-12 show the relative displacement time histories at the top of the intermediate piers. The figures show that the total relative displacements at the center pier are much larger than those of the outer piers. This can be seen by looking at the transverse displacement envelope shown in Figure 5.2-13. The figure also shows that most of the displacement is in the transverse direction. This is because the period of the bridge in the transverse direction is much greater than it is in the longitudinal direction.

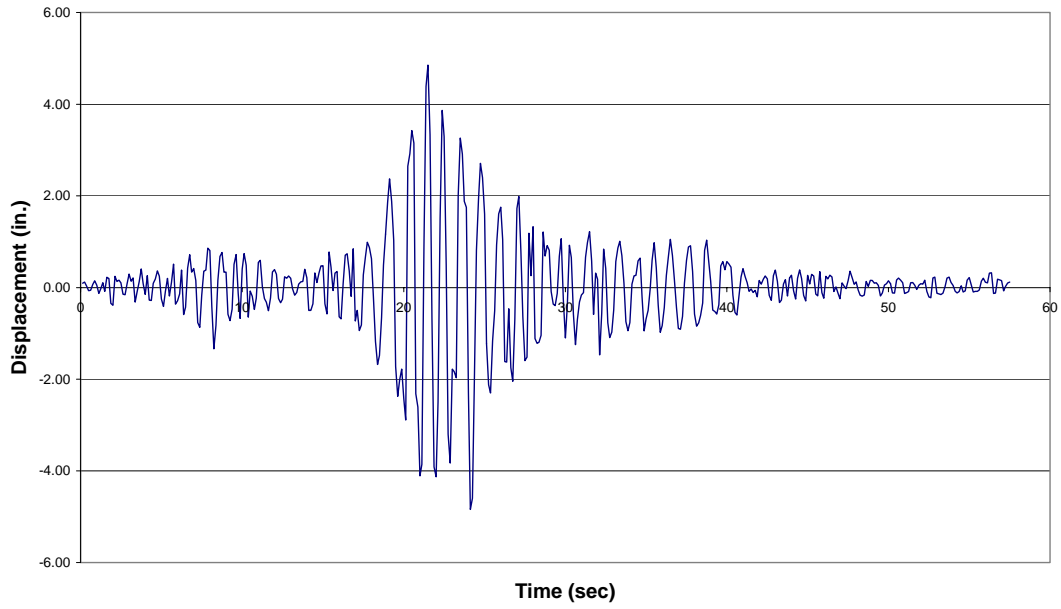


Figure 5.2-10 Total Relative Displacement at Pier 1, Modified Chile Earthquake

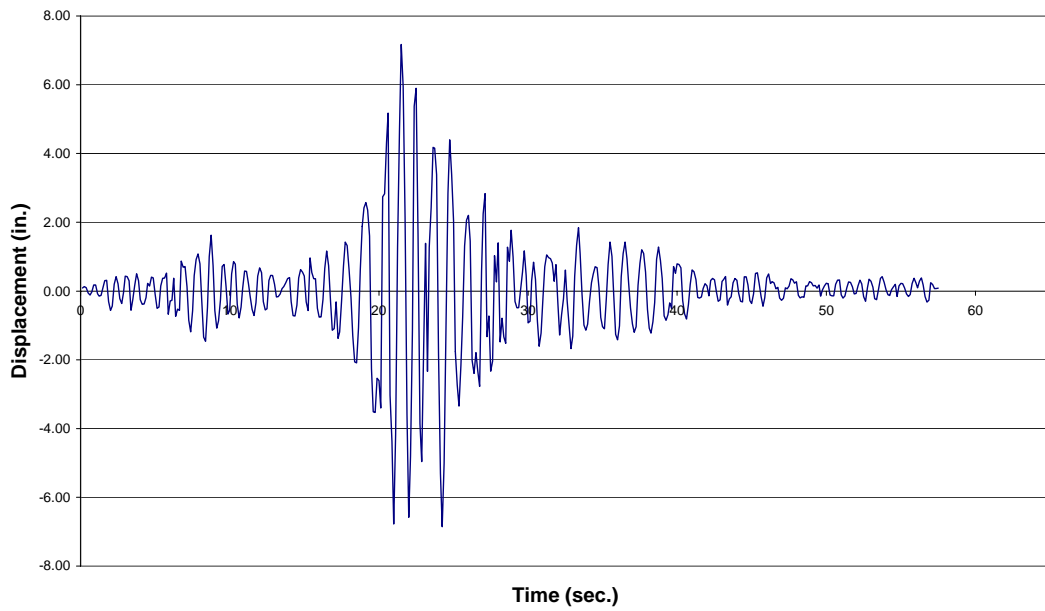


Figure 5.2-11 Total Relative Displacement at Pier 2, Modified Chile Earthquake

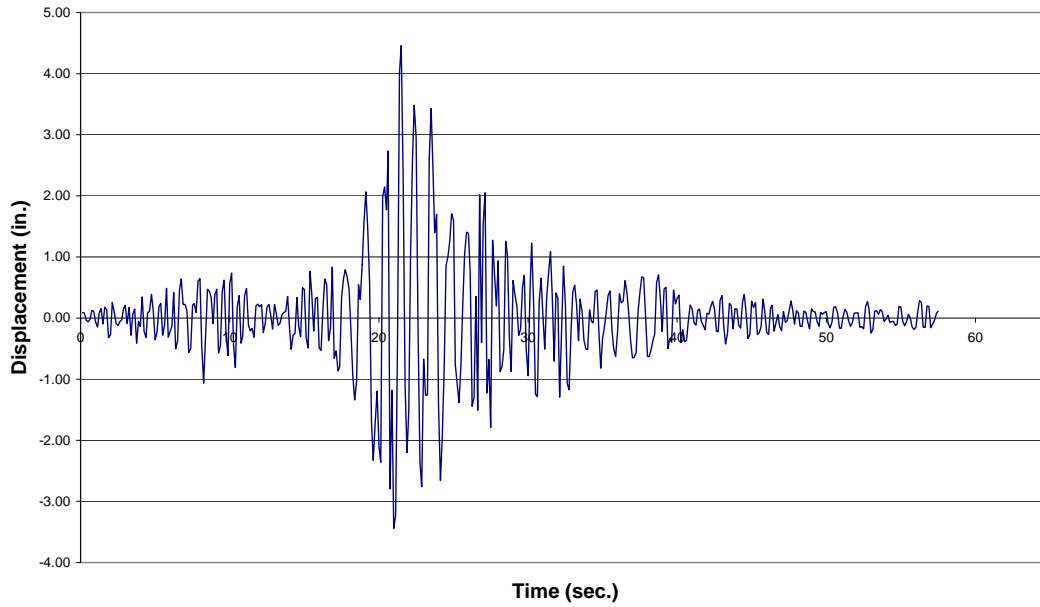


Figure 5.2-12 Total Relative Displacement at Pier 3, Modified Chile Earthquake

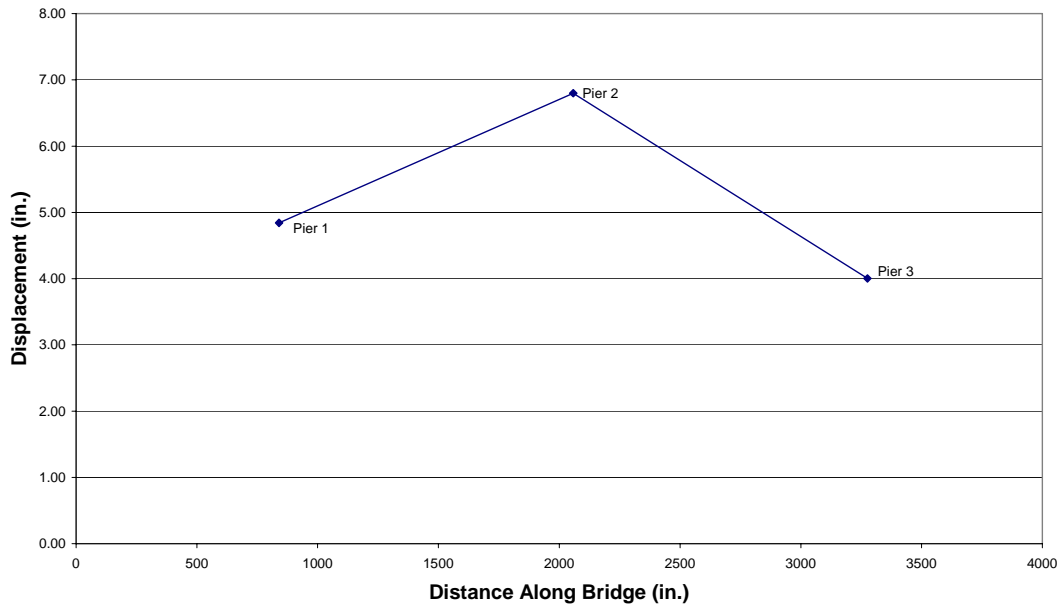


Figure 5.2-13 Transverse Relative Displacement Envelope of Bridge Deck, Modified Chile Earthquake

Because the foundation springs at the base of every column allow for slight rotations, the plastic rotation was confined to the plastic hinges at the top of the columns.

Table 5.2-4 shows the maximum moments at the top and bottom of all the columns.

Table 5.2-4 Maximum Moment (kip-in) at the Top and Bottoms of Columns, Modified Chile Earthquake

Pier No.	Column	Moment	
		Top	Bottom
1	1	12985.0	6265.1
	2	15277.5	6150.9
	3	11544.9	6118.8
2	1	17242.5	10705.8
	2	15090.2	10699.9
	3	16654.8	10303.6
3	1	17404.0	4970.1
	2	14914.9	5524.5
	3	15949.7	6113.1

Because the displacements at the center pier were larger than those at the outer piers, the plastic rotations in the plastic hinges found in that pier were larger, as shown in Figure 5.2-14. The columns in the center pier also have more plastic rotation cycles than do the other piers, which causes more damage.

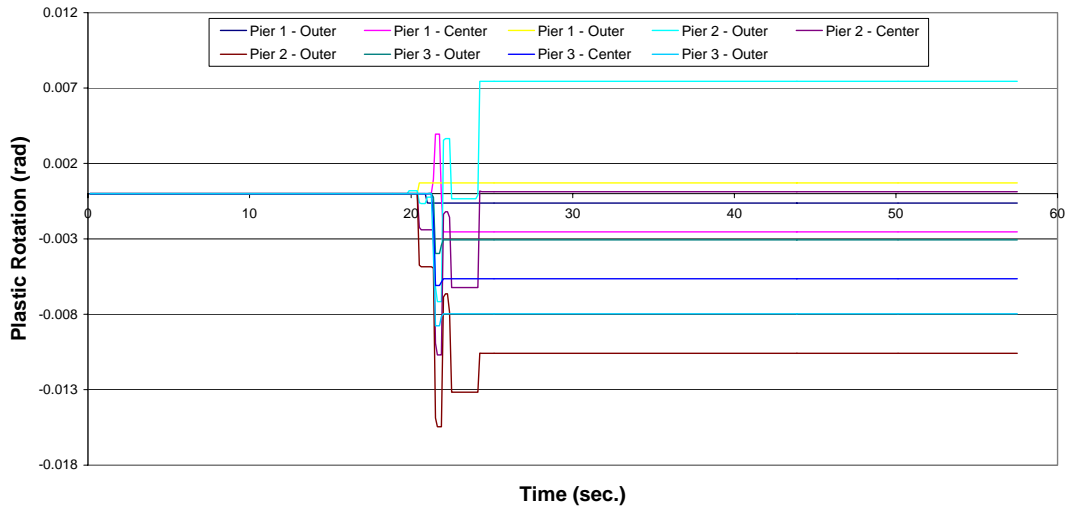


Figure 5.2-14 Plastic Rotations at the Top of the Columns, Modified Chile Earthquake

Due to the fact that the columns in the center pier experienced larger plastic rotations and more plastic rotation cycles, the columns in the center pier accumulated the most damage as shown in Figure 5.2-15.

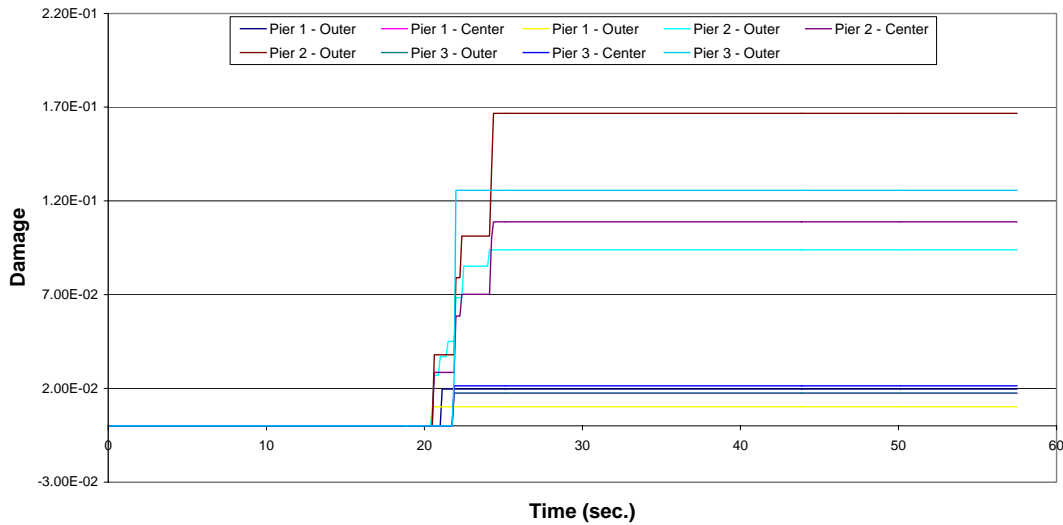


Figure 5.2-15 Damage at the Top of the Columns, Modified Chile Earthquake

The damage coefficients for the columns at the center pier and an outer column at Pier 3 ranged in value between 0.167 and 0.094, which indicates that there is anywhere from localized minor cracking to light cracking throughout the column section. The damage coefficients in all of the other columns are at or below 0.03, which would suggest negligible cracking. It should be noted that all columns had damage, although the figure only shows traces for eight of the nine columns. The center column of Pier 1 plots underneath other columns, with damage levels of about 0.02. All indicated damage levels are small enough that localized spalling would not occur. Figure 5.2-16 shows the estimated damage that would be seen in the columns. This picture was taken after the modified Chile displacement record was applied to the test specimen from the testing done by Stapleton (2004). It shows very little damage.



Figure 5.2-16 Final State of Damage in Column

By looking at the shear versus displacement hysteresis plots, as shown in Figure 5.2-17 and 5.2-18, it can also be seen that the demand on the columns is not very large. In the longitudinal direction, the hysteresis loops only open slightly, which would suggest that there was only minor yielding. The hysteresis loops for the transverse direction open more, but they also show little significant yielding, which is consistent with the accumulated damage.

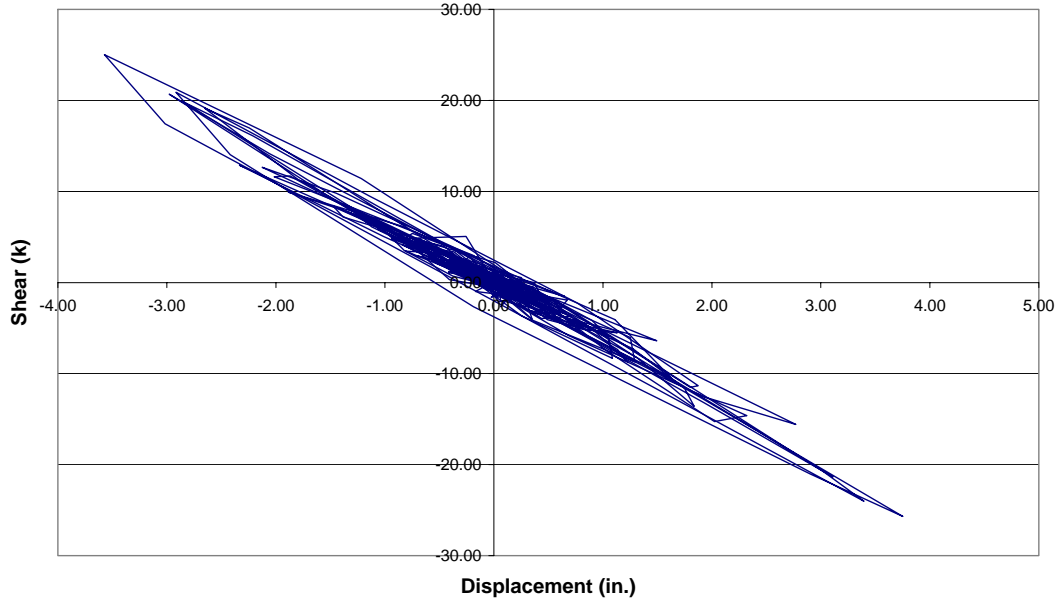


Figure 5.2-17 Longitudinal Hysteresis Plot for the Center Column of Pier 2, Modified Chile Earthquake

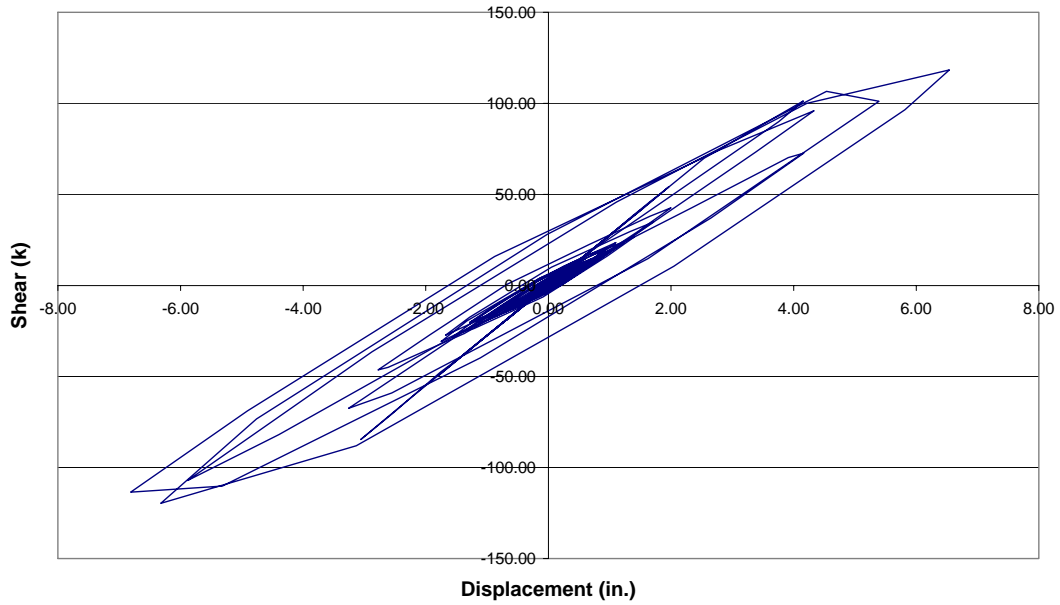


Figure 5.2-18 Transverse Hysteresis Plot for the Center Column of Pier 2, Modified Chile Earthquake

The maximum shear values at the top and bottom of the columns are shown in Table 5.2-5. The shear capacity of the column due only to the concrete is 171.6 kips. Since the maximum shear in the columns was 131 kips, the shear capacity was not exceeded. Columns with smaller aspect ratios than those that are found in this bridge should be investigated further.

Table 5.2-5 Maximum Shear (kips) in the Columns, Modified Chile Earthquake

Pier No.	Column	Shear			
		Top	Demand/ Capacity	Bottom	Demand/ Capacity
1	1	80.42	0.47	81.47	0.48
	2	87.33	0.51	101.56	0.59
	3	73.36	0.43	73.80	0.43
2	1	115.73	0.67	130.14	0.76
	2	109.33	0.64	120.23	0.70
	3	117.29	0.68	131.19	0.77
3	1	94.03	0.55	115.90	0.68
	2	84.82	0.49	110.36	0.64
	3	82.09	0.48	100.95	0.59

The maximum abutment forces in the transverse and longitudinal directions are found in Table 5.2-6. The shear capacity of the abutments in the transverse and longitudinal directions is 3370 kips and 1458 kips, respectively. With a maximum demand of only 1440 kips and 414 kips, respectively, the abutments are considered capable of resisting the seismic demands.

Table 5.2-6 Maximum Shear (kips) at the Abutments, Modified Chile Earthquake

Abutment	Shear			
	Longitudinal	Demand/ Capacity	Transverse	Demand/ Capacity
West	1360	0.41	414	0.28
East	1440	0.43	248	0.17

By looking at the relative longitudinal displacement of the expansion joints, it can be determined if there will be pounding at the abutments and piers. Figure 5.2-19 shows the relative longitudinal displacement at the West abutment. It can be seen in this plot that pounding does occur at the West abutment. Pounding occurs at all of the piers and both abutments. The plots for the abutments and other piers can be found in Appendix C.

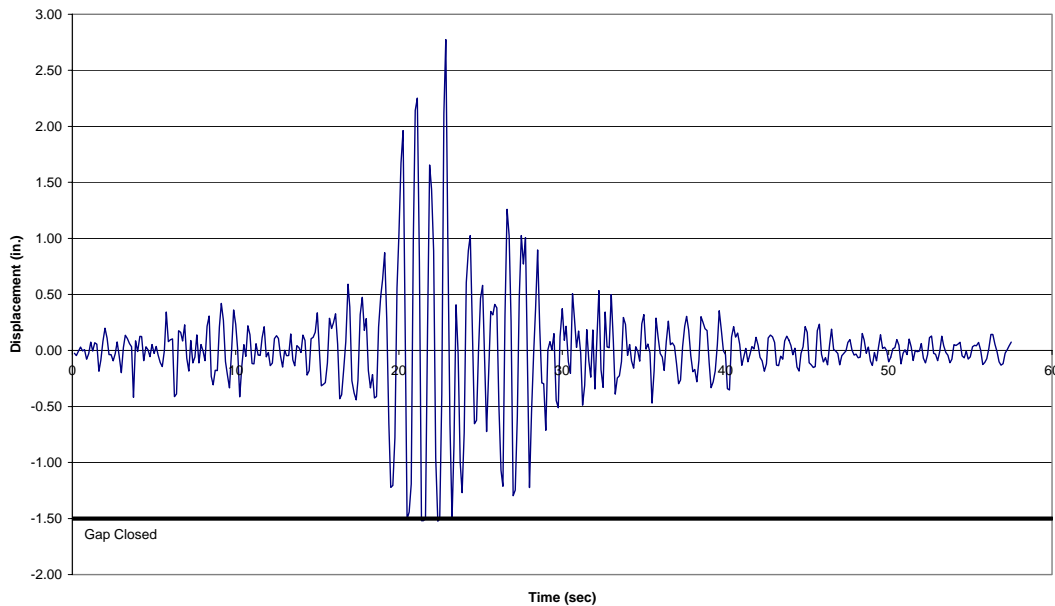


Figure 5.2-19 Relative Longitudinal Displacement at the West Abutment, Modified Chile Earthquake

The allowable displacement of the bearing pads is conservatively 1.44 inches, while the actual maximum displacement is predicted to be 2.78 inches. This implies that a bearing pad failure could occur.

After this earthquake, the bridge remains in good condition. The columns do not accumulate excessive damage and they are capable of resisting the shear demands. The abutments are also able to resist the shear demands in both the longitudinal and transverse directions. Again, the two main concerns would be the pounding of the expansion joints that occurs at the abutments and piers, and failure of the bearing pads.

5.3 Bridge 5/826

The results from analyses using the modified Peru and modified Chile earthquakes and the model of Bridge 5/826 are presented here. These two cases were chosen because they are the two extreme cases, and they show the most information about the response of the bridge with respect to the new damage model.

5.3.1 Modified Peru Earthquake

Figures 5.3-1 through 5.3-3 show the total displacement time histories at the top of the intermediate piers. The figures show that the total displacement at all of the piers is virtually the same. This is due to the fact that the bridge deck is continuous, thereby acting as a very stiff, nearly rigid beam. This can be seen by looking at the transverse displacement envelope shown in Figure 5.3-4.

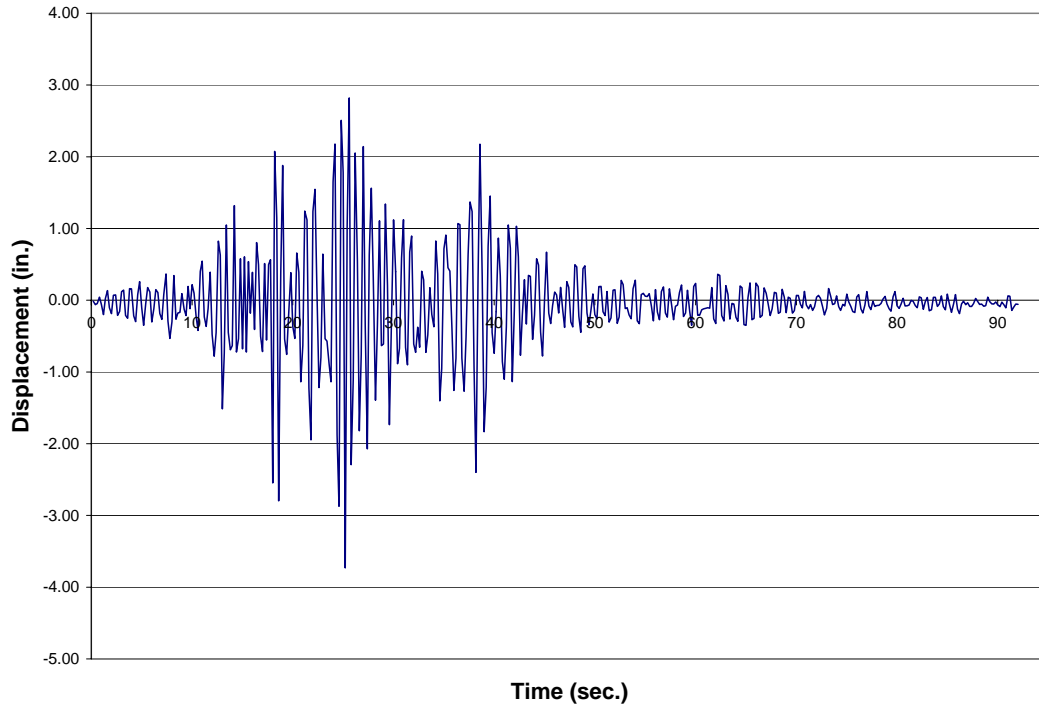


Figure 5.3-1 Total Relative Displacement at Pier 1, Modified Peru Earthquake

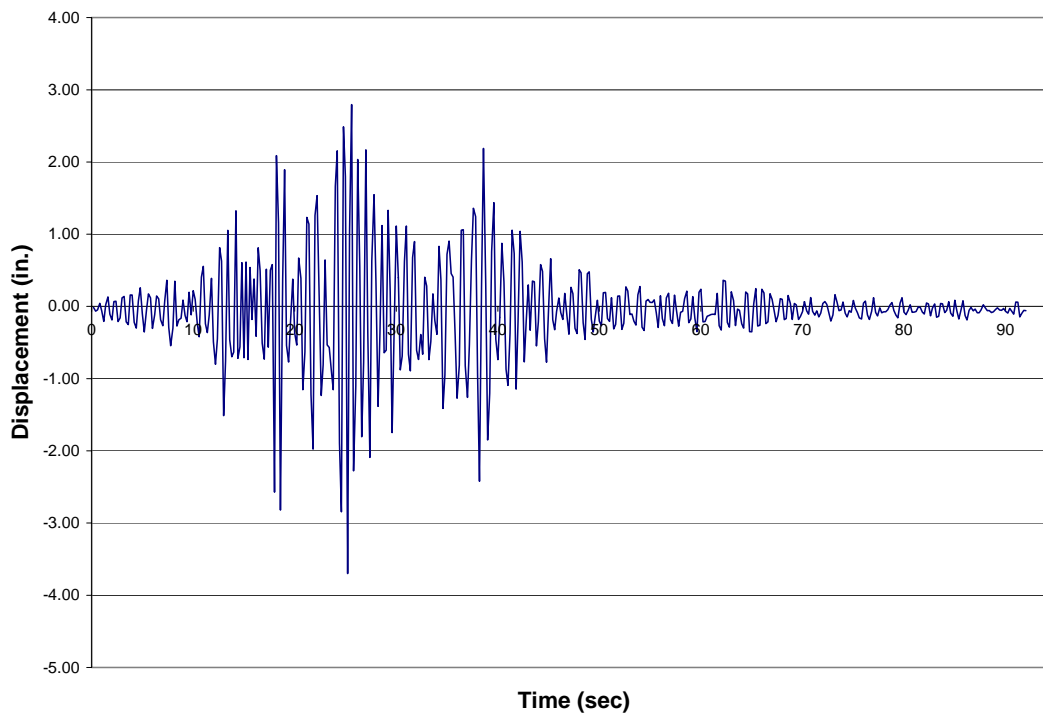


Figure 5.3-2 Total Relative Displacement at Pier 2, Modified Peru Earthquake

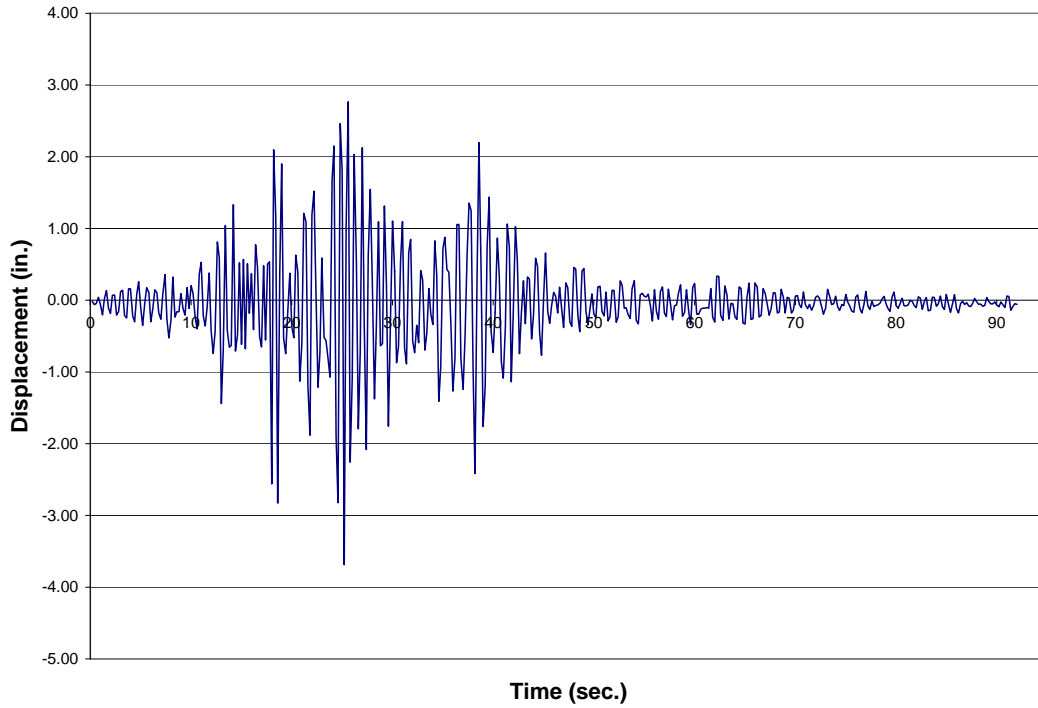


Figure 5.3-3 Total Relative Displacement at Pier 3, Modified Peru Earthquake

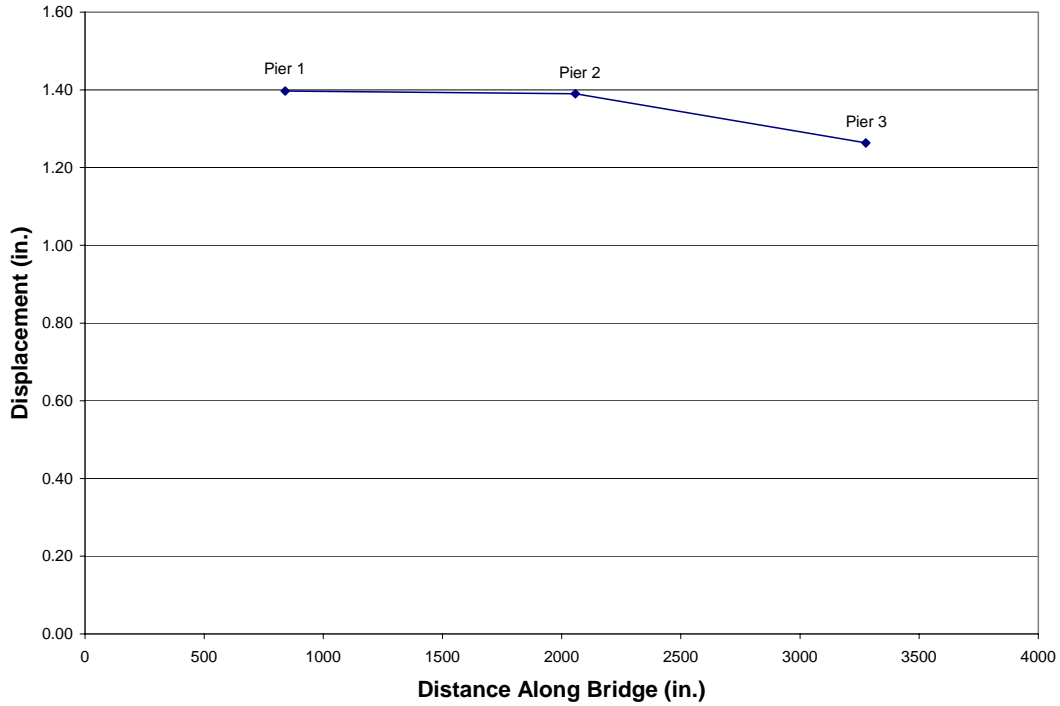


Figure 5.3-4 Transverse Relative Displacement Envelope of Bridge Deck, Modified Peru Earthquake

Table 5.3-1 shows the maximum moments at the top and bottom of all the columns. Because of the relatively high transverse reinforcement ratio found in this bridge, the yield moment is also relatively high and, therefore, only slight yielding occurred in the columns. There was no accumulated damage because there was not a reversal of the plastic rotation which would denote a cycle. By looking at the shear versus displacement hysteresis plots as shown in Figure 5.3-5 and 5.3-6, it can be seen that only slight yielding occurred.

Table 5.3-1 Maximum Moment (kip-in) at the Top and Bottoms of Columns, Modified Peru Earthquake

Pier No.	Column	Moment	
		Top	Bottom
1	1	17970.8	15310.8
	2	17951.5	15311.2
	3	17892.8	15281.7
2	1	14510.6	13070.8
	2	14471.5	13051.25
	3	14383.2	13002.0
3	1	16421.1	14171.06
	2	16401.7	14171.38
	3	16322.6	14131.7

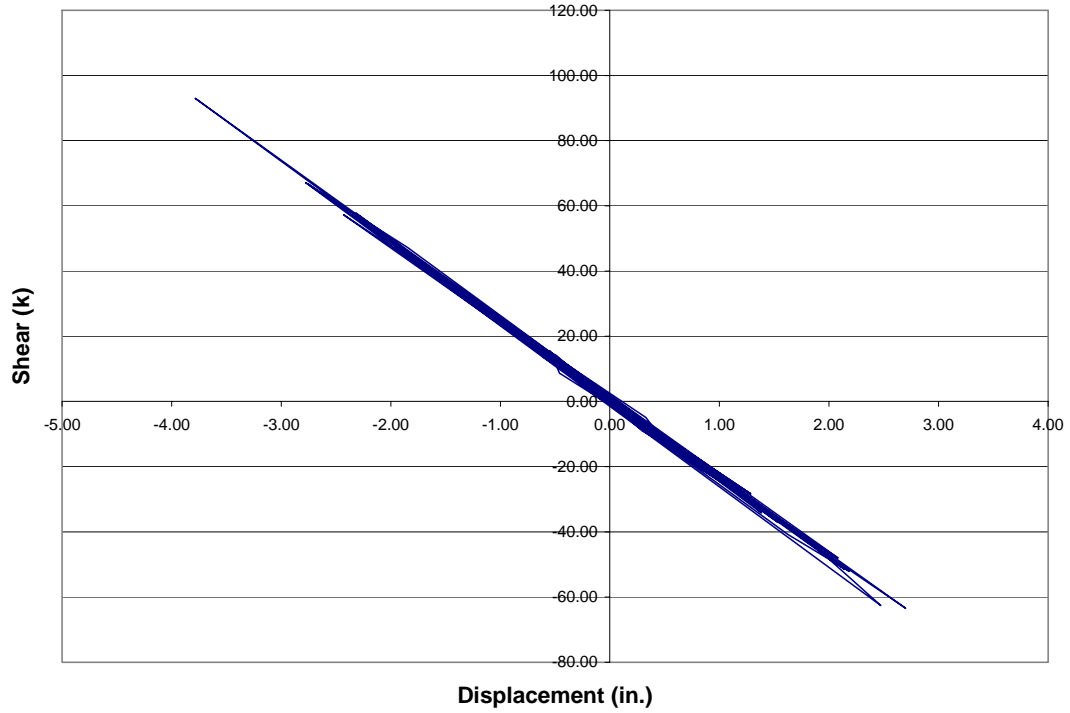


Figure 5.3-5 Longitudinal Hysteresis Plot for the Center Column of Pier 2, Modified Peru Earthquake

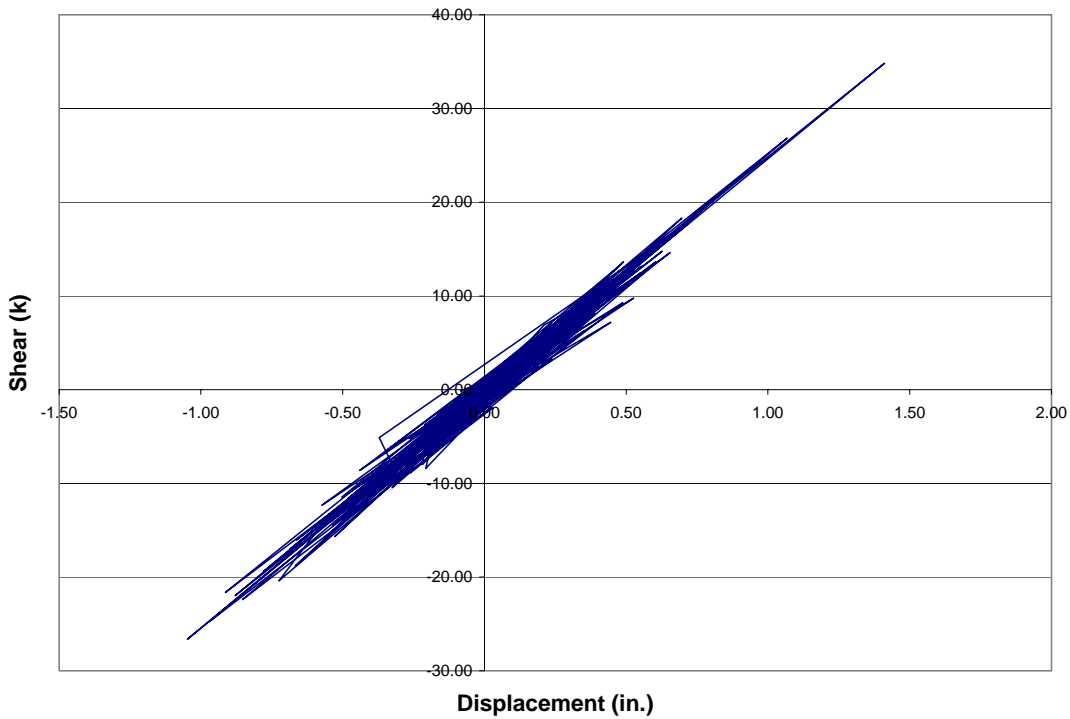


Figure 5.3-6 Transverse Hysteresis plot for the Center Column of Pier 2, Modified Peru Earthquake

The maximum shear values at the top and bottom of the columns are shown in Table 5.3-2. The shear capacity of the columns based solely on the concrete was determined according to Kowalsky and Priestley (2000):

$$V_c = 3.4\sqrt{f'_c} * A_e$$

where f'_c was taken as 6000 *psi*. The value of 3.4 has changed from the previous bridge, where it was 2.8, because this value is dependent on the ductility demand of the column. This gives a final shear capacity of 214.5 kips. Since the maximum shear in the columns was only 127 kips, the shear capacity was not exceeded.

Table 5.3-2 Maximum Shear (kips) in the Columns, Modified Peru Earthquake

Pier No.	Column	Shear			
		Top	Demand/ Capacity	Bottom	Demand/ Capacity
1	1	113.91	0.53	126.50	0.59
	2	113.81	0.53	126.40	0.59
	3	113.32	0.53	126.01	0.59
2	1	79.40	0.37	93.73	0.44
	2	79.22	0.37	93.52	0.44
	3	78.73	0.37	93.04	0.44
3	1	98.68	0.46	111.90	0.52
	2	98.58	0.46	111.81	0.52
	3	98.07	0.46	111.31	0.52

The maximum abutment forces in the transverse and longitudinal directions are found in Table 5.3-3. The value of A_{cv} in the longitudinal direction for this bridge is 5760 in², which incorporates the cross section of the thinnest portion of the abutment wall. This gives a nominal shear capacity of 5184 kips. None of the shear forces in the longitudinal direction were near this value, therefore the abutment is considered capable of resisting the seismic demands. The value of A_{cv} in the transverse direction for this bridge is 6047 in², which gives a nominal shear capacity of 5443 kips.

Table 5.3-3 Maximum Shear (kips) at the Abutments, Modified Peru Earthquake

Abutment	Shear			
	Longitudinal	Demand/ Capacity	Transverse	Demand/ Capacity
West	1230	0.21	1490	0.27
East	2580	0.45	1410	0.26

By looking at the relative longitudinal displacement of the expansion joints, it can be determined if there will be pounding at the abutments. Figure 5.3-7 shows the relative longitudinal displacement at the West abutment. The expansion joint has a gap of 1.5 inches, so it can be seen that there is pounding at the West abutment. Pounding also occurs at the East abutment, as can be seen in Figure 5.3-8.

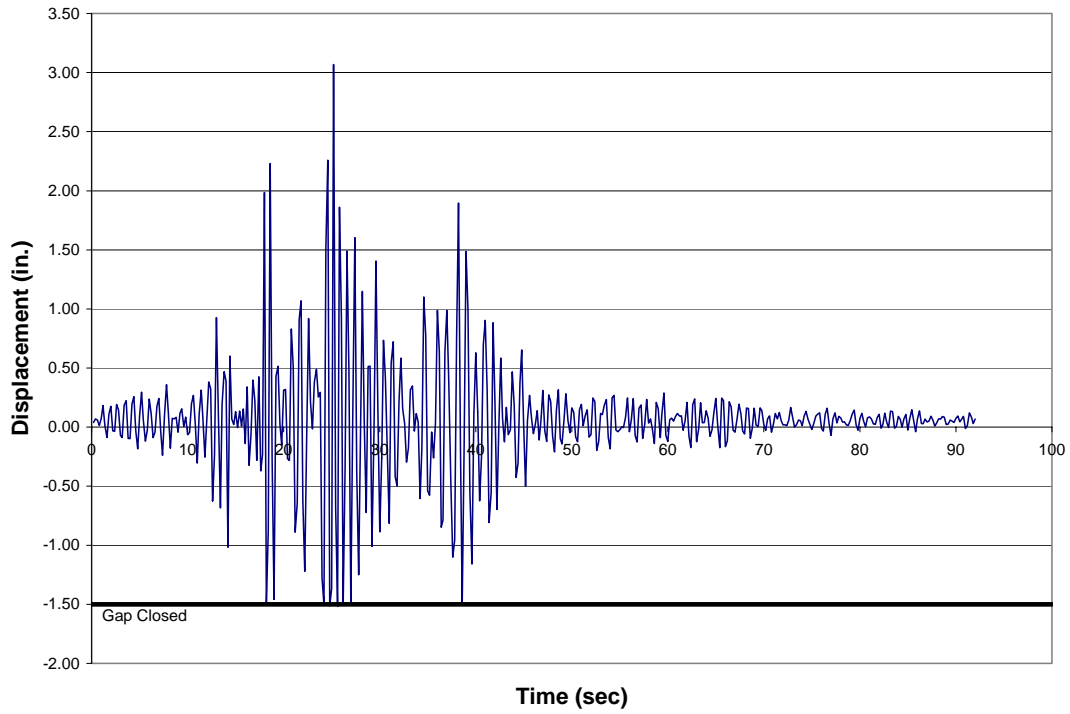


Figure 5.3-7 Relative Longitudinal Displacement at the West Abutment, Modified Peru Earthquake

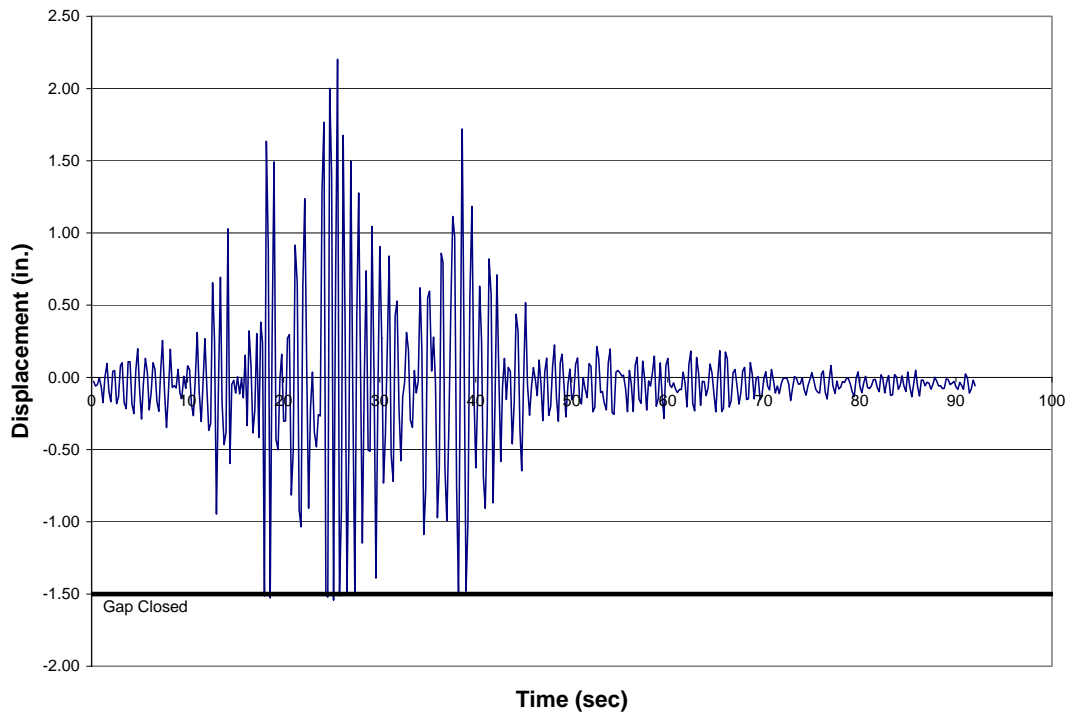


Figure 5.3-8 Relative Longitudinal Displacement at the East Abutment, Modified Peru Earthquake

For the bearing pads, an average ε_{tu} value of 5.75 was assumed, and the thickness of the bearing pad is 2.5 inches. This gives an allowable displacement of 2.88 inches, while the maximum displacement is predicted to be 3.1 inches. It should be noted that conservative values have been used, but this would imply that a possible failure of the bearing pad could occur.

The bridge appears to be in good condition after such a large event. The columns did not accumulate any damage and they are capable of resisting the shear demands. The abutments were also able to resist the shear demands in the longitudinal and transverse directions. Again, the two main concerns would be the pounding at the abutments and the possible failure of the bearing pads.

5.3.2 Modified Chile Earthquake

Figures 5.3-9 through 5.3-11 show the total displacement time histories at the top of the intermediate piers. The figures show that the total displacement at all of the piers is virtually the same. This can also be seen by looking at the transverse displacement envelope shown in Figure 5.3-12.

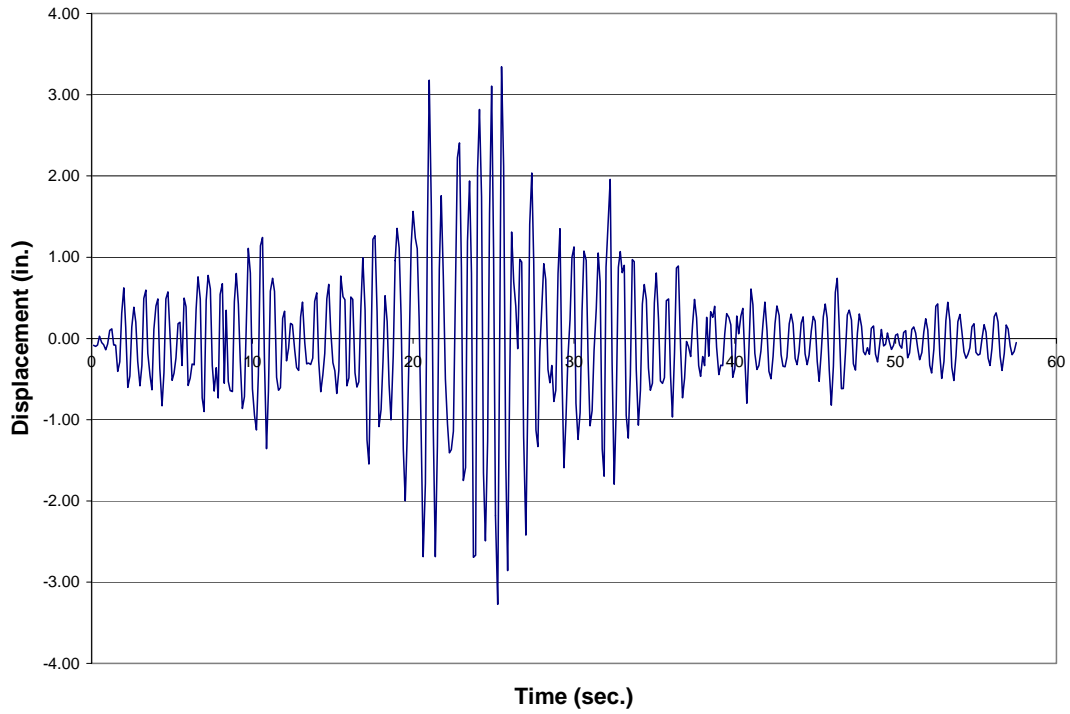


Figure 5.3-9 Total Relative Displacement at Pier 1, Modified Chile Earthquake

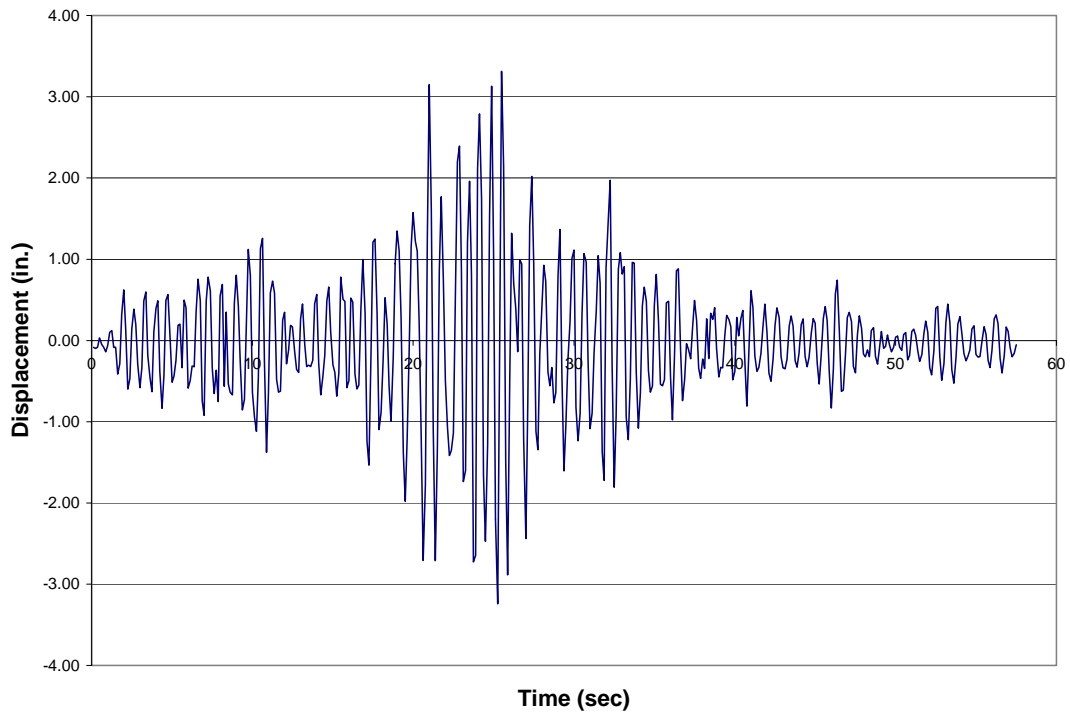


Figure 5.3-10 Total Relative Displacement at Pier 2, Modified Chile Earthquake

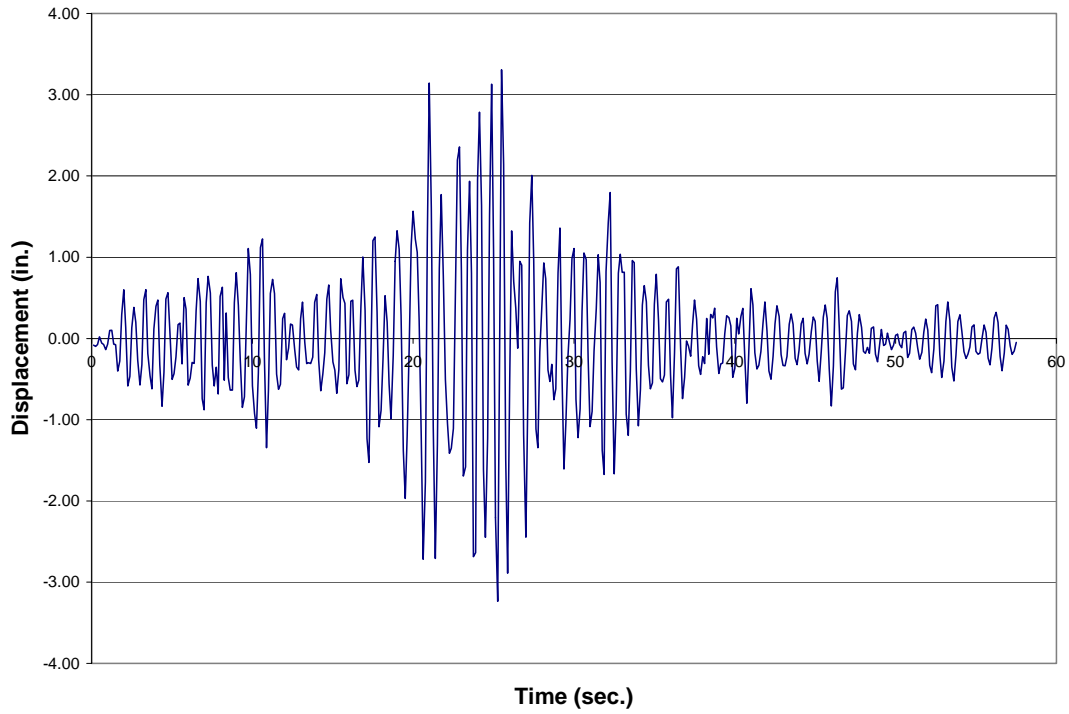


Figure 5.3-11 Total Relative Displacement at Pier 3, Modified Chile Earthquake

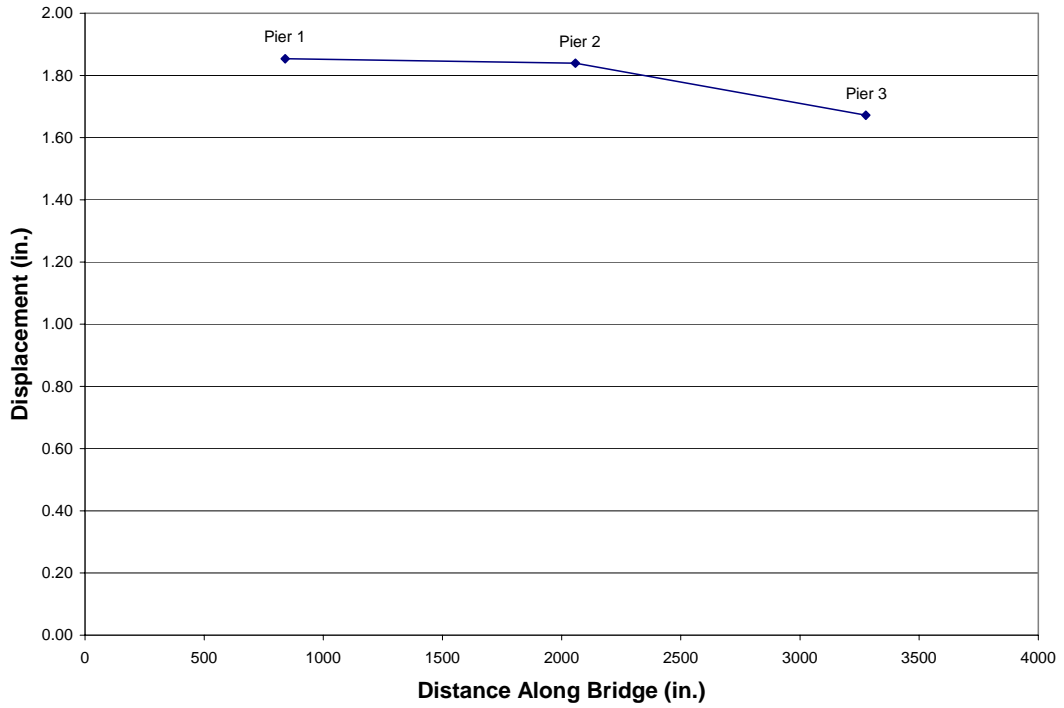


Figure 5.3-12 Transverse Displacement Envelope of Bridge Deck, Modified Chile Earthquake

Table 5.3-4 Maximum Moment (kip-in) at the Top and Bottoms of Columns, Modified Chile Earthquake

Pier No.	Column	Moment	
		Top	Bottom
1	1	15810.6	13441.0
	2	15791.2	13431.4
	3	15702.3	13391.83
2	1	12780.3	11470.9
	2	12741.1	11451.4
	3	12780.0	11470.0
3	1	14440.6	12441.0
	2	14510.1	12470.1
	3	14520.0	12480.0

Table 5.3-4 shows the maximum moment at the top and bottom of all columns. Again, there was only slight yielding in the columns. By looking at the shear force versus displacement hysteresis plots as shown in Figure 5.3-13 and 5.3-14, it can be seen that slight yielding occurred.

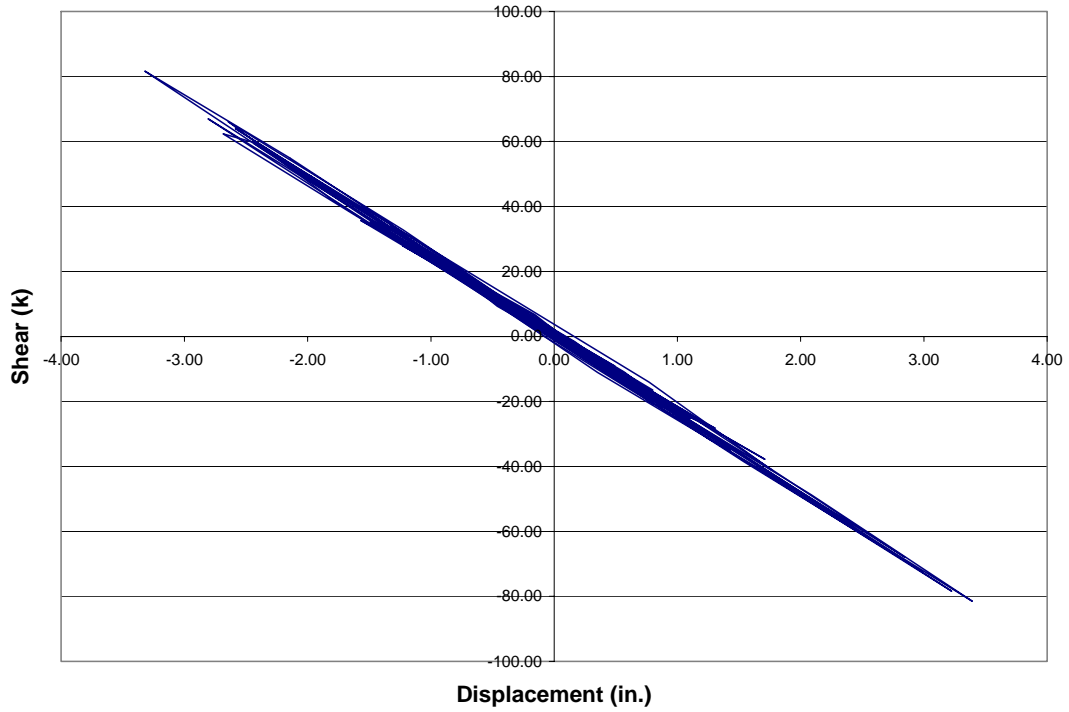


Figure 5.3-13 Longitudinal Hysteresis Plot for the Center Column of Pier 2, Modified Chile Earthquake

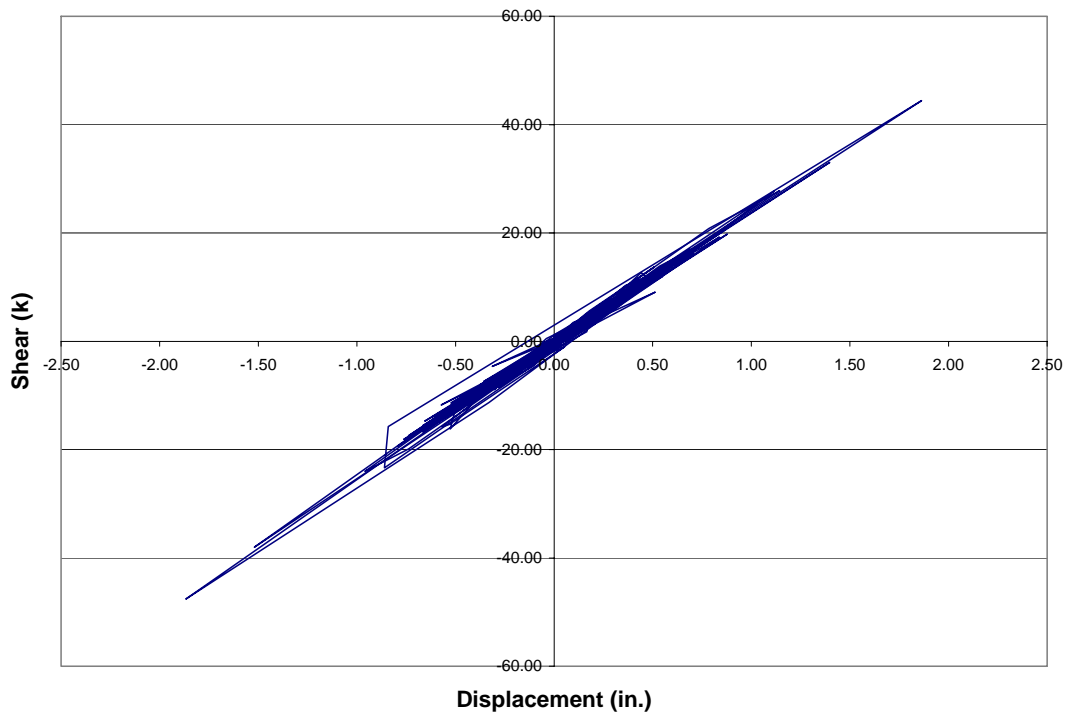


Figure 5.3-14 Transverse Hysteresis Plot for the Center Column of Pier 2, Modified Chile Earthquake

The maximum shear values at the top and bottom of the columns are shown in Table 5.3-5. The shear capacity of the column due only to the concrete is 214.5 kips. Since the maximum shear in the columns was 111 kips, the shear capacity was not exceeded. Columns with smaller aspect ratios than those that are found in this bridge should be investigated further.

Table 5.3-5 Maximum Shear (kips) in the Columns, Modified Chile Earthquake

Pier No.	Column	Shear			
		Top	Demand/ Capacity	Bottom	Demand/ Capacity
1	1	100.70	0.47	110.91	0.52
	2	100.61	0.47	110.81	0.52
	3	100.21	0.47	110.42	0.52
2	1	70.59	0.33	82.27	0.38
	2	70.34	0.33	82.07	0.38
	3	70.14	0.33	81.66	0.38
3	1	87.34	0.41	98.16	0.46
	2	87.38	0.41	98.07	0.46
	3	87.49	0.41	97.87	0.46

The maximum abutment forces in the transverse and longitudinal directions are found in Table 5.3-6. The shear capacity of the abutment in the longitudinal direction is 5184 kips. The capacity in the transverse direction is so large that it will not be a factor. With a maximum shear demand of only 2060 *kips*, the abutments are considered capable of resisting the seismic demands.

Table 5.3-6 Maximum Shear (kips) at the Abutments, Modified Chile Earthquake

Abutment	Shear			
	Longitudinal	Demand/ Capacity	Transverse	Demand/ Capacity
West	1930	0.37	1980	0.36
East	2060	0.40	1870	0.34

By looking at the relative longitudinal displacement of the expansion joints, it can be determined if there will be pounding at the abutments. Figures 5.3-15 and 5.3-16 show the relative longitudinal displacement at the West and East abutments, respectively. It can be seen in this plot that pounding is likely to occur at both abutments.

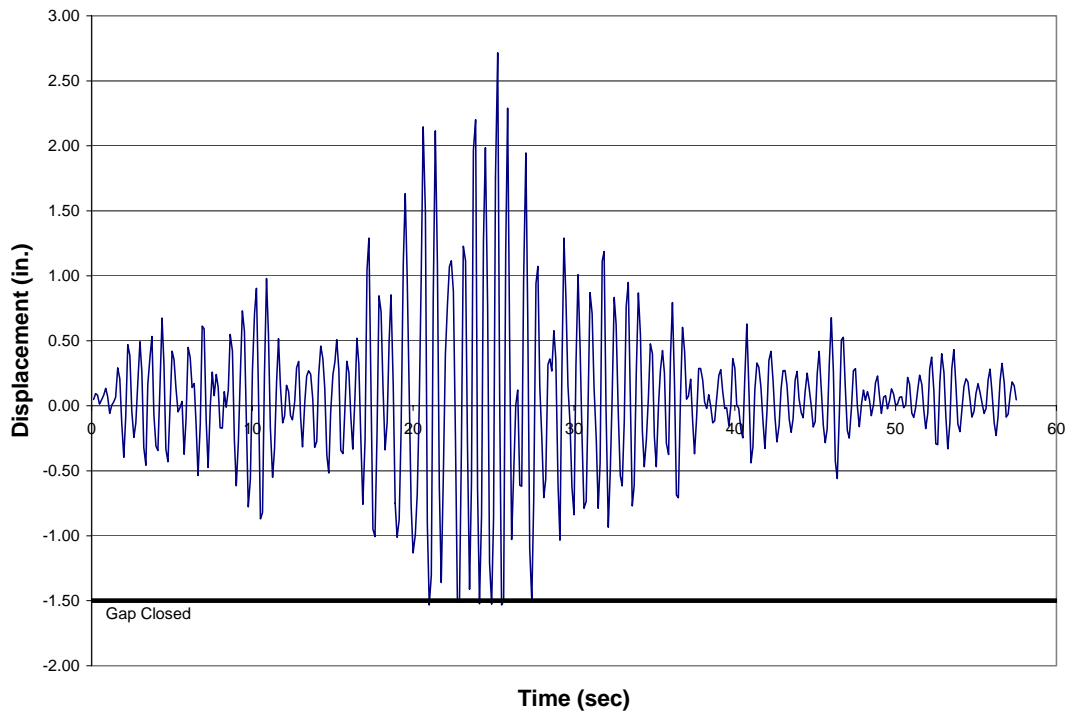


Figure 5.3-15 Relative Longitudinal Displacement at the West Abutment, Modified Chile Earthquake

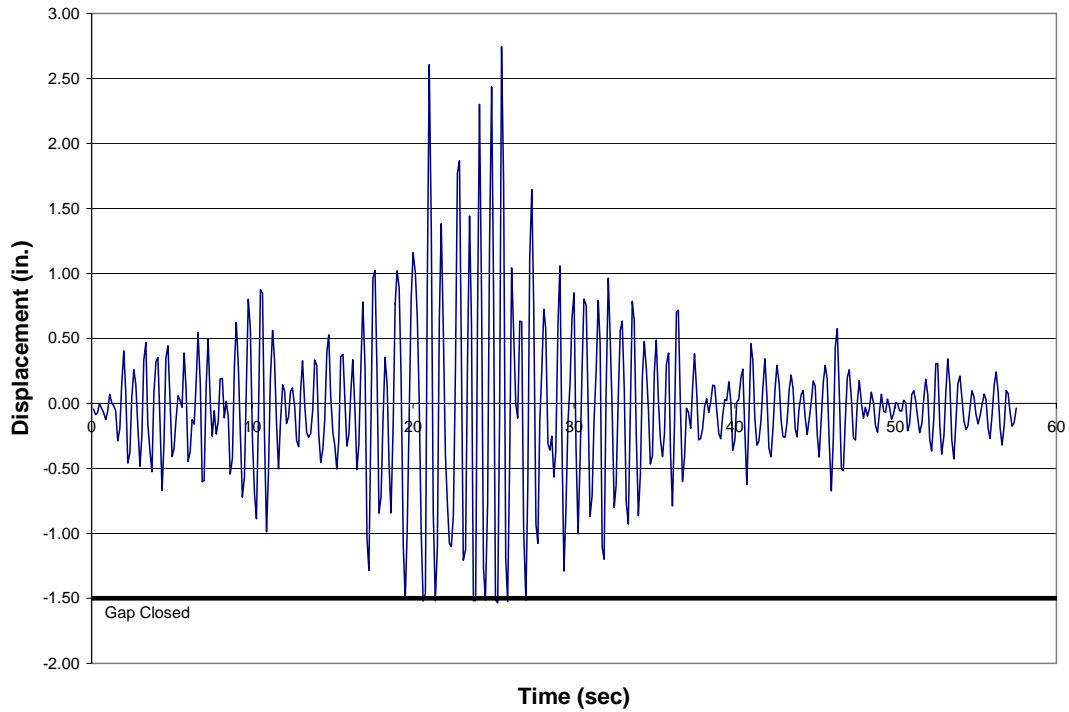


Figure 5.3-16 Relative Longitudinal Displacement at the East Abutment, Modified Chile Earthquake

The allowable displacement of the bearing pads is conservatively 2.88 inches, while the actual maximum displacement is predicted to be 2.75 inches. This is very close to the failure threshold and implies that a possible failure of the bearing pad could occur.

The bridge seems to be in good condition after such a large event. The columns did not accumulate any damage and they are capable of resisting the shear demands. The abutments were also able to resist the shear demands in the longitudinal and transverse directions. Again, the two main concerns would be the pounding at the abutments and the possible failure of the bearing pads.

5.4 Summary of all other Earthquakes

Presented in this section are the summaries of the time history analysis results from the nonlinear finite element spine models of WSDOT Bridges 5/518 and 5/826. All of the time history plots and tables for these analyses can be found in Appendix C.

5.4.1 Bridge 5/518

The summaries of the results using the unmodified Peru, unmodified Chile, Mexico City 475 and 950, Olympia 475 and 950, and the Kobe 475 and 950 earthquakes applied to the model of Bridge 5/518 are presented here. The summaries of the results can be found in Tables 5.4-1 through 5.4-8.

Table 5.4-1 Results from the Unmodified Peru Earthquake

Displacements					
Pier	Max. Transverse Displacement (<i>in.</i>)		Comments:		
Pier 1	2.63				
Pier 2	4.77				
Pier 3	2.12				
Maximum Damage					
Column	Damage Level		Comments:		
Pier 2 – Center Column	0.019		Light Cracking		
Maximum Column Shear					
Column	Shear (<i>kips</i>)	Capacity (<i>kips</i>):	Demand/ Capacity		
Pier 2 – Center Column	100.8	214.5	0.47		
Maximum Abutment Shear					
Abutment	Longitudinal Shear (<i>kips</i>)	Transverse Shear (<i>kips</i>)	Long. Capacity (<i>kips</i>)	Trans. Capacity (<i>kips</i>)	Failure (Y/N)
West	294	103	3370	1458	N
East	299	75	3370	1458	N
Expansion Joints					
Expansion Joint	Pounding (Y/N)		Comments:		
West Abutment	N				
East Abutment	N				
Pier 1	Y		Only at one edge		
Pier 2	N				
Pier 3	N				
Bearing Pads					
Pier	Max. Displacement (<i>in.</i>)	Allowable Displacement (<i>in.</i>)	Failure (Y/N)		
West Abutment	1.31	1.44	N		

Table 5.4-2 Results from the Unmodified Chile Earthquake

Displacements					
Pier	Max. Transverse Displacement (<i>in.</i>)		Comments:		
Pier 1	2.59				
Pier 2	4.38				
Pier 3	2.10				
Maximum Damage					
Column	Damage Level		Comments:		
Pier 2 – Center Column	0.031		Light Cracking		
Maximum Column Shear					
Column	Shear (<i>kips</i>)	Capacity (<i>kips</i>):	Demand/ Capacity		
Pier 2 – Center Column	113.0	214.5	0.53		
Maximum Abutment Shear					
Abutment	Longitudinal Shear (<i>kips</i>)	Transverse Shear (<i>kips</i>)	Long. Capacity (<i>kips</i>)	Trans. Capacity (<i>kips</i>)	Failure (Y/N)
West	433	114	3370	1458	N
East	489	133	3370	1458	N
Expansion Joints					
Expansion Joint	Pounding (Y/N)		Comments:		
West Abutment	Y		One edge only		
East Abutment	Y		One edge only		
Pier 1	Y		One edge only		
Pier 2	N				
Pier 3	Y		One edge only		
Bearing Pads					
Pier	Max. Displacement (<i>in.</i>)	Allowable Displacement (<i>in.</i>)	Failure (Y/N)		
West Abutment	1.51	1.44	Y		

Table 5.4-3 Results from the Mexico City 475-Year Earthquake

Displacements					
Pier	Max. Transverse Displacement (<i>in.</i>)		Comments:		
Pier 1	2.08				
Pier 2	2.57				
Pier 3	1.78				
Maximum Damage					
Column	Damage Level		Comments:		
N/A	N/A		No damage in columns		
Maximum Column Shear					
Column	Shear (<i>kips</i>)	Capacity (<i>kips</i>):	Demand/ Capacity		
Pier 2 – Center Column	69.6	214.5	0.32		
Maximum Abutment Shear					
Abutment	Longitudinal Shear (<i>kips</i>)	Transverse Shear (<i>kips</i>)	Long. Capacity (<i>kips</i>)	Trans. Capacity (<i>kips</i>)	Failure (Y/N)
West	219	51	3370	1458	N
East	171	66	3370	1458	N
Expansion Joints					
Expansion Joint	Pounding (Y/N)		Comments:		
West Abutment	N				
East Abutment	N				
Pier 1	N				
Pier 2	N				
Pier 3	N				
Bearing Pads					
Pier	Max. Displacement (<i>in.</i>)	Allowable Displacement (<i>in.</i>)	Failure (Y/N)		
Pier 3	0.88	1.44	N		

Table 5.4-4 Results from the Mexico City 950-Year Earthquake

Displacements					
Pier	Max. Transverse Displacement (<i>in.</i>)		Comments:		
Pier 1	2.72				
Pier 2	3.52				
Pier 3	2.33				
Maximum Damage					
Column	Damage Level		Comments:		
Pier 2 – Outer Column	0.019		Light Cracking		
Maximum Column Shear					
Column	Shear (<i>kips</i>)	Capacity (<i>kips</i>):	Demand/ Capacity		
Pier 2 – outer Column	110.26	214.5	0.52		
Maximum Abutment Shear					
Abutment	Longitudinal Shear (<i>kips</i>)	Transverse Shear (<i>kips</i>)	Long. Capacity (<i>kips</i>)	Trans. Capacity (<i>kips</i>)	Failure (Y/N)
West	344	98.3	3370	1458	N
East	289	124	3370	1458	N
Expansion Joints					
Expansion Joint	Pounding (Y/N)		Comments:		
West Abutment	Y		One edge only		
East Abutment	N				
Pier 1	N				
Pier 2	N				
Pier 3	N				
Bearing Pads					
Pier	Max. Displacement (<i>in.</i>)	Allowable Displacement (<i>in.</i>)	Failure (Y/N)		
Pier 3	1.50	1.44	Y		

Table 5.4-5 Results from the Olympia 475-Year Earthquake

Displacements					
Pier	Max. Transverse Displacement (<i>in.</i>)		Comments:		
Pier 1	2.08				
Pier 2	2.85				
Pier 3	1.72				
Maximum Damage					
Column	Damage Level		Comments:		
N/A	N/A		No damage in columns		
Maximum Column Shear					
Column	Shear (<i>kips</i>)	Capacity (<i>kips</i>):	Demand/ Capacity		
Pier 2 - Outer	73.3	214.5	0.34		
Maximum Abutment Shear					
Abutment	Longitudinal Shear (<i>kips</i>)	Transverse Shear (<i>kips</i>)	Long. Capacity (<i>kips</i>)	Trans. Capacity (<i>kips</i>)	Failure (Y/N)
West	231	80	3370	1458	N
East	188	90	3370	1458	N
Expansion Joints					
Expansion Joint	Pounding (Y/N)		Comments:		
West Abutment	N				
East Abutment	N				
Pier 1	N				
Pier 2	N				
Pier 3	N				
Bearing Pads					
Pier	Max. Displacement (<i>in.</i>)	Allowable Displacement (<i>in.</i>)	Failure (Y/N)		
West Abutment	1.02	1.44	N		

Table 5.4-6 Results from the Olympia 950-Year Earthquake

Displacements					
Pier	Max. Transverse Displacement (<i>in.</i>)		Comments:		
Pier 1	2.96				
Pier 2	4.20				
Pier 3	2.53				
Maximum Damage					
Column	Damage Level		Comments:		
Pier 2 – Outer Column	0.017		Light Cracking		
Maximum Column Shear					
Column	Shear (<i>kips</i>)	Capacity (<i>kips</i>):	Demand/ Capacity		
Pier 2 – Outer Column	108.8	214.5	0.51		
Maximum Abutment Shear					
Abutment	Longitudinal Shear (<i>kips</i>)	Transverse Shear (<i>kips</i>)	Long. Capacity (<i>kips</i>)	Trans. Capacity (<i>kips</i>)	Failure (Y/N)
West	449	148	3370	1458	N
East	336	196	3370	1458	N
Expansion Joints					
Expansion Joint	Pounding (Y/N)		Comments:		
West Abutment	Y		One edge only		
East Abutment	N				
Pier 1	Y				
Pier 2	N				
Pier 3	Y				
Bearing Pads					
Pier	Max. Displacement (<i>in.</i>)	Allowable Displacement (<i>in.</i>)	Failure (Y/N)		
Pier 3	1.57	1.44	Y		

Table 5.4-7 Results from the Kobe 475-Year Earthquake

Displacements					
Pier	Max. Transverse Displacement (<i>in.</i>)		Comments:		
Pier 1	2.24				
Pier 2	3.51				
Pier 3	1.94				
Maximum Damage					
Column	Damage Level		Comments:		
N/A	N/A		No damage in columns		
Maximum Column Shear					
Column	Shear (<i>kips</i>)	Capacity (<i>kips</i>):	Demand/ Capacity		
Pier 2 – Outer Column	83.4	214.5	0.39		
Maximum Abutment Shear					
Abutment	Longitudinal Shear (<i>kips</i>)	Transverse Shear (<i>kips</i>)	Long. Capacity (<i>kips</i>)	Trans. Capacity (<i>kips</i>)	Failure (Y/N)
West	326	74	3370	1458	N
East	240	78	3370	1458	N
Expansion Joints					
Expansion Joint	Pounding (Y/N)		Comments:		
West Abutment	Y		One edge only		
East Abutment	N				
Pier 1	Y		One edge only		
Pier 2	N				
Pier 3	Y		One edge only		
Bearing Pads					
Pier	Max. Displacement (<i>in.</i>)	Allowable Displacement (<i>in.</i>)	Failure (Y/N)		
West Abutment	1.51	1.44	Y		

Table 5.4-8 Results from the Kobe 950-Year Earthquake

Displacements					
Pier	Max. Transverse Displacement (<i>in.</i>)		Comments:		
Pier 1	2.88				
Pier 2	4.91				
Pier 3	2.52				
Maximum Damage					
Column	Damage Level		Comments:		
Pier 2 – Outer Column	0.020		Light Cracking		
Maximum Column Shear					
Column	Shear (<i>kips</i>)	Capacity (<i>kips</i>):	Demand/ Capacity		
Pier 2 – Outer Column	118	214.5	0.55		
Maximum Abutment Shear					
Abutment	Longitudinal Shear (<i>kips</i>)	Transverse Shear (<i>kips</i>)	Long. Capacity (<i>kips</i>)	Trans. Capacity (<i>kips</i>)	Failure (Y/N)
West	563	156	3370	1458	N
East	673	121	3370	1458	N
Expansion Joints					
Expansion Joint	Pounding (Y/N)		Comments:		
West Abutment	Y		One edge only		
East Abutment	Y		One edge only		
Pier 1	Y		One edge only		
Pier 2	N				
Pier 3	Y		One edge only		
Bearing Pads					
Pier	Max. Displacement (<i>in.</i>)	Allowable Displacement (<i>in.</i>)	Failure (Y/N)		
Pier 3	1.65	1.44	Y		

5.4.2 Bridge 5/826

The summaries of the results using the unmodified Peru, unmodified Chile, Mexico City 475 and 950, Olympia 475 and 950, and the Kobe 475 and 950 earthquakes applied to the model of Bridge 5/826 are presented here. The summaries of the results can be found in Tables 5.4-9 through 5.4-16.

Table 5.4-9 Results from the Unmodified Peru Earthquake

Displacements					
Pier	Max. Transverse Displacement (<i>in.</i>)		Comments:		
Pier 1	0.70				
Pier 2	0.70				
Pier 3	0.64				
Maximum Damage					
Column	Damage Level		Comments:		
N/A	N/A		No damage in columns		
Maximum Column Shear					
Column	Shear (<i>kips</i>)		Capacity (<i>kips</i>):	Demand/ Capacity	
Pier 1 – Outer Column	74.8		214.5	0.35	
Maximum Abutment Shear					
Abutment	Longitudinal Shear (<i>kips</i>)	Transverse Shear (<i>kips</i>)	Long. Capacity (<i>kips</i>)	Trans. Capacity (<i>kips</i>)	Failure (Y/N)
West	68.6	74.8	5184	5443	N
East	80.6	71.3	5184	5443	N
Expansion Joints					
Expansion Joint	Pounding (Y/N)		Comments:		
West Abutment	Y				
East Abutment	Y				
Bearing Pads					
Abutment	Max. Displacement (<i>in.</i>)		Allowable Displacement (<i>in.</i>)	Failure (Y/N)	
East	1.81		2.88	N	

Table 5.4-10 Results from the Unmodified Chile Earthquake

Displacements					
Pier	Max. Transverse Displacement (<i>in.</i>)		Comments:		
Pier 1	0.93				
Pier 2	0.92				
Pier 3	0.84				
Maximum Damage					
Column	Damage Level		Comments:		
N/A	N/A		No damage in columns		
Maximum Column Shear					
Column	Shear (<i>kips</i>)	Capacity (<i>kips</i>):	Demand/ Capacity		
Pier 3 – Center Column	64.5	214.5	0.30		
Maximum Abutment Shear					
Abutment	Longitudinal Shear (<i>kips</i>)	Transverse Shear (<i>kips</i>)	Long. Capacity (<i>kips</i>)	Trans. Capacity (<i>kips</i>)	Failure (Y/N)
West	373	998	5184	5443	N
East	484	939	5184	5443	N
Expansion Joints					
Expansion Joint	Pounding (Y/N)		Comments:		
West Abutment	N				
East Abutment	Y				
Bearing Pads					
Abutment	Max. Displacement (<i>in.</i>)	Allowable Displacement (<i>in.</i>)	Failure (Y/N)		
West	1.58	2.88	N		

Table 5.4-11 Results from the Mexico City 475-Year Earthquake

Displacements					
Pier	Max. Transverse Displacement (<i>in.</i>)		Comments:		
Pier 1	1.80				
Pier 2	1.81				
Pier 3	1.78				
Maximum Damage					
Column	Damage Level		Comments:		
N/A	N/A		No damage in columns		
Maximum Column Shear					
Column	Shear (<i>kips</i>)	Capacity (<i>kips</i>):	Demand/ Capacity		
Pier 1 – Outer Column	60.8	214.5	0.28		
Maximum Abutment Shear					
Abutment	Longitudinal Shear (<i>kips</i>)	Transverse Shear (<i>kips</i>)	Long. Capacity (<i>kips</i>)	Trans. Capacity (<i>kips</i>)	Failure (Y/N)
West	367	688	5184	5443	N
East	377	656	5184	5443	N
Expansion Joints					
Expansion Joint	Pounding (Y/N)		Comments:		
West Abutment	Y				
East Abutment	N				
Bearing Pads					
Abutment	Max. Displacement (<i>in.</i>)	Allowable Displacement (<i>in.</i>)	Failure (Y/N)		
West	3.07	2.88	Y		

Table 5.4-12 Results from the Mexico City 950-Year Earthquake

Displacements					
Pier	Max. Transverse Displacement (<i>in.</i>)		Comments:		
Pier 1	2.36				
Pier 2	2.38				
Pier 3	2.34				
Maximum Damage					
Column	Damage Level		Comments:		
N/A	N/A		No damage in columns		
Maximum Column Shear					
Column	Shear (<i>kips</i>)	Capacity (<i>kips</i>):	Demand/ Capacity		
Pier 1 – Outer Column	80.6	214.5	0.38		
Maximum Abutment Shear					
Abutment	Longitudinal Shear (<i>kips</i>)	Transverse Shear (<i>kips</i>)	Long. Capacity (<i>kips</i>)	Trans. Capacity (<i>kips</i>)	Failure (Y/N)
West	748	1400	5184	5443	N
East	952	1290	5184	5443	N
Expansion Joints					
Expansion Joint	Pounding (Y/N)		Comments:		
West Abutment	Y				
East Abutment	Y				
Bearing Pads					
Abutment	Max. Displacement (<i>in.</i>)	Allowable Displacement (<i>in.</i>)	Failure (Y/N)		
West	1.91	2.88	N		

Table 5.4-13 Results from the Olympia 475-Year Earthquake

Displacements					
Pier	Max. Transverse Displacement (<i>in.</i>)		Comments:		
Pier 1	1.93				
Pier 2	1.95				
Pier 3	1.93				
Maximum Damage					
Column	Damage Level		Comments:		
N/A	N/A		No damage in columns		
Maximum Column Shear					
Column	Shear (<i>kips</i>)	Capacity (<i>kips</i>):	Demand/ Capacity		
Pier 1 – Outer Column	64.9	214.5	0.30		
Maximum Abutment Shear					
Abutment	Longitudinal Shear (<i>kips</i>)	Transverse Shear (<i>kips</i>)	Long. Capacity (<i>kips</i>)	Trans. Capacity (<i>kips</i>)	Failure (Y/N)
West	365	1030	5184	5443	N
East	542	974	5184	5443	N
Expansion Joints					
Expansion Joint	Pounding (Y/N)		Comments:		
West Abutment	Y				
East Abutment	N				
Bearing Pads					
Abutment	Max. Displacement (<i>in.</i>)	Allowable Displacement (<i>in.</i>)	Failure (Y/N)		
West	2.71	2.88	N		

Table 5.4-14 Results from the Olympia 950-Year Earthquake

Displacements					
Pier	Max. Transverse Displacement (<i>in.</i>)		Comments:		
Pier 1	2.26				
Pier 2	2.28				
Pier 3	2.25				
Maximum Damage					
Column	Damage Level		Comments:		
N/A	N/A		No damage in columns		
Maximum Column Shear					
Column	Shear (<i>kips</i>)	Capacity (<i>kips</i>):	Demand/ Capacity		
Pier 1 – Outer Column	77.0	214.5	0.36		
Maximum Abutment Shear					
Abutment	Longitudinal Shear (<i>kips</i>)	Transverse Shear (<i>kips</i>)	Long. Capacity (<i>kips</i>)	Trans. Capacity (<i>kips</i>)	Failure (Y/N)
West	701	1450	5184	5443	N
East	871	1340	5184	5443	N
Expansion Joints					
Expansion Joint	Pounding (Y/N)		Comments:		
West Abutment	Y				
East Abutment	N				
Bearing Pads					
Abutment	Max. Displacement (<i>in.</i>)	Allowable Displacement (<i>in.</i>)	Failure (Y/N)		
West	3.08	2.88	Y		

Table 5.4-15 Results from the Kobe 475-Year Earthquake

Displacements					
Pier	Max. Transverse Displacement (<i>in.</i>)		Comments:		
Pier 1	2.21				
Pier 2	2.23				
Pier 3	2.18				
Maximum Damage					
Column	Damage Level		Comments:		
N/A	N/A		No damage in columns		
Maximum Column Shear					
Column	Shear (<i>kips</i>)	Capacity (<i>kips</i>):	Demand/ Capacity		
Pier 1 – Outer Column	71.69	214.5	0.33		
Maximum Abutment Shear					
Abutment	Longitudinal Shear (<i>kips</i>)	Transverse Shear (<i>kips</i>)	Long. Capacity (<i>kips</i>)	Trans. Capacity (<i>kips</i>)	Failure (Y/N)
West	648	1060	5184	5443	N
East	566	1010	5184	5443	N
Expansion Joints					
Expansion Joint	Pounding (Y/N)		Comments:		
West Abutment	Y				
East Abutment	Y				
Bearing Pads					
Abutment	Max. Displacement (<i>in.</i>)	Allowable Displacement (<i>in.</i>)	Failure (Y/N)		
West	3.07	2.88	Y		

Table 5.4-16 Results from the Kobe 950-Year Earthquake

Displacements					
Pier	Max. Transverse Displacement (<i>in.</i>)		Comments:		
Pier 1	3.00				
Pier 2	3.02				
Pier 3	2.96				
Maximum Damage					
Column	Damage Level		Comments:		
N/A	N/A		No damage in columns		
Maximum Column Shear					
Column	Shear (<i>kips</i>)	Capacity (<i>kips</i>):	Demand/ Capacity		
Pier 1 – Center Column	97.8	214.5	0.46		
Maximum Abutment Shear					
Abutment	Longitudinal Shear (<i>kips</i>)	Transverse Shear (<i>kips</i>)	Long. Capacity (<i>kips</i>)	Trans. Capacity (<i>kips</i>)	Failure (Y/N)
West	1440	1420	5184	5443	N
East	1140	1260	5184	5443	N
Expansion Joints					
Expansion Joint	Pounding (Y/N)		Comments:		
West Abutment	Y				
East Abutment	Y				
Bearing Pads					
Abutment	Max. Displacement (<i>in.</i>)	Allowable Displacement (<i>in.</i>)	Failure (Y/N)		
West	3.07	2.88	Y		

These summaries show that the bridges are in good condition. The columns accumulated very little damage and were capable of resisting the shear demands. The abutments were also capable of resisting the shear demand in the longitudinal and transverse directions. The two main concerns for all of the bridges were pounding and possible failures of the bearing pads.

Chapter 6

Soil-Structure Parametric Study and Bent Model Comparison

6.1 Introduction

The purpose of this study was to determine the effects that the stiffness of the column footing soil springs and the abutment soil springs have on the response of the bridge model. Many times, nonlinear time history analyses are performed on simplified models with fixed column bases and rollers at the abutments. Therefore, analyses were performed to determine how boundary conditions affect the response of the bridge. A bent model was also constructed to see if it could effectively model one of the bridge piers.

Presented in this chapter are selected time history analysis results from the nonlinear finite element spine model of WSDOT 5/518 and 5/826, and the bent model. The main portion of the study was performed using Bridge 5/518 and the modified Peru earthquake. The results include the displacement at the top of the piers, the plastic rotation of the plastic hinges at the top and bottom of the columns, the damage corresponding to the plastic rotation found in the plastic hinges, column moment, column shear, and behavior of the expansion joints.

6.2 Soil-Structure Parametric Study Protocol

The analysis protocol for this study was centered on the response of Bridge 5/518 to the modified Peru earthquake. Six different analyses were performed using this bridge, for which the stiffness of the column soil spring, the abutment soil spring, or both were varied. The entire analysis protocol is listed in Table 6.2-1, where the initial

stiffness values of the column base and abutment soil springs were taken from the bridge model used in Chapter 5. To evaluate the effect of a different earthquake, the combination of foundation spring stiffness values that resulted in the highest level of column damage was determined from the previous six cases. These were applied to Bridge 5/518, and it was re-analyzed with the modified Chile earthquake.

Table 6.2-1 Analysis Protocol

Run No.	Bridge	Earthquake	Column Base Soil Spring Stiffness	Abutment Soil Spring Stiffness
1	5/518	Modified Peru	Fixed	Roller – Both Directions
2	5/518	Modified Peru	Fixed	Roller – Longitudinal Only
3	5/518	Modified Peru	Unchanged	Increase by a factor of 10
4	5/518	Modified Peru	Unchanged	Roller – Longitudinal Only
5	5/518	Modified Peru	Decrease by a factor of 10	Unchanged
6	5/518	Modified Peru	Fixed	Unchanged
7	5/518	Modified Chile	Fixed	Roller – Both Directions
8	5/826	Modified Peru	Fixed	Roller – Longitudinal Only
9	5/826	Modified Peru	Fixed	Roller – Both Directions
10	5/518	Olympia 950-Year	Fixed	Roller – Both Directions
11	5/518	Kobe 950-Year	Fixed	Roller – Both Directions
12	5/826	Olympia 950-Year	Fixed	Roller – Both Directions
13	5/826	Kobe 950-Year	Fixed	Roller – Both Directions

The response of Bridge 5/826 to the modified Peru earthquake was also analyzed for the case in which the column bases were fixed and rollers were used at the abutments. Two cases were investigated; the first of which only allowed for rollers in the longitudinal direction. The other case allowed for rollers in both directions. The last four analyses used both bridge models where the Olympia 950-year and Kobe 950-year earthquakes were applied. In all four of these cases, the columns were fixed at their bases and the abutments had rollers in both directions.

6.3 Results and Interpretation

The results from the analyses using the modified Peru and modified Chile earthquakes and the models of Bridges 5/518 and 5/826 are presented here. These results are compared to the results from their respective base cases found in Chapter 5.

6.3.1 Run No. 1

The results from the response of Bridge 5/518, with fixed columns and rollers at the abutments in both directions, to the modified Peru earthquake are presented here. Figures 6.3-1 through 6.3-3 show the total relative displacement time histories at the top of the intermediate piers. The total relative displacement levels did not change significantly. The displacements in the positive direction are slightly larger and the displacements in the negative direction are slightly less than those found in the base case. The greatest difference is the residual displacement of three inches that was not there in the base case. The bridge deck displacement envelope shows that the transverse displacement at the piers is actually 2 to 3 inches less. Because the total displacement did

not change substantially, but the transverse displacements decreased by 2-3 inches, there was a significant increase in the longitudinal displacement.

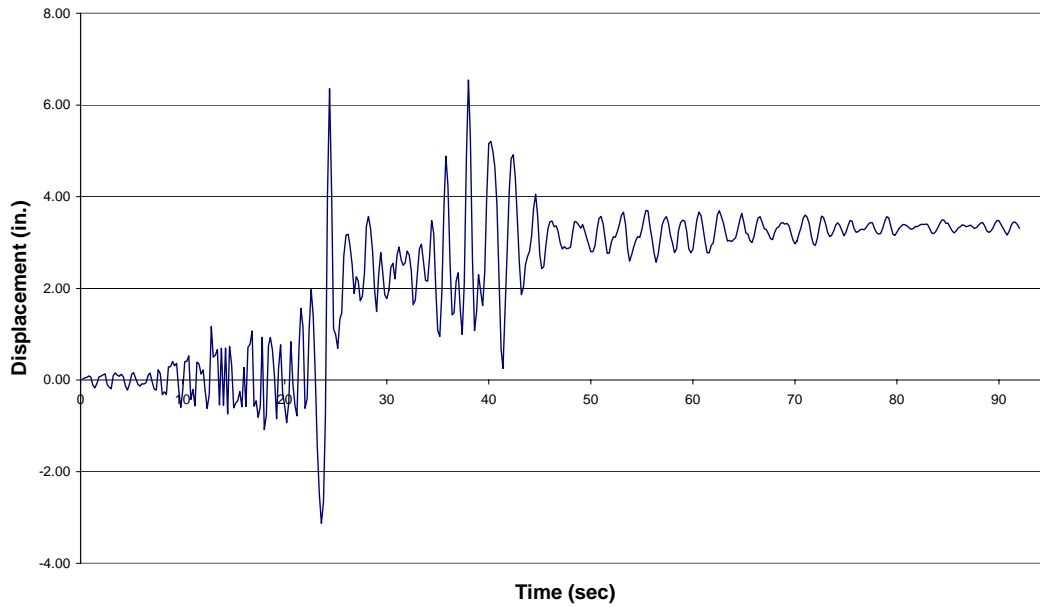


Figure 6.3-1 Total Displacement at Pier 1, Modified Peru Earthquake, Bridge 5/518

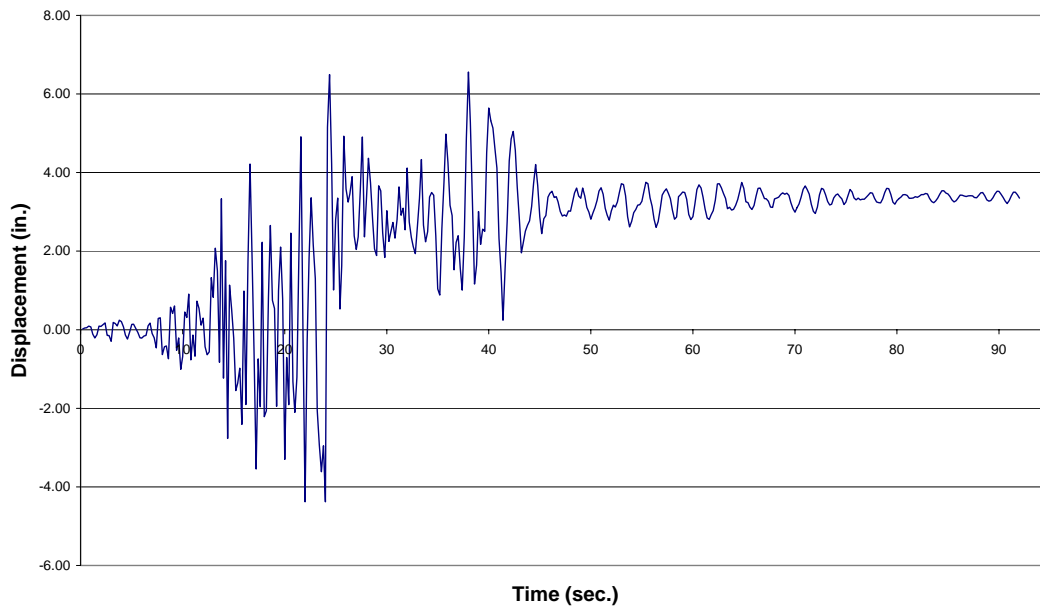


Figure 6.3-2 Total Displacement at Pier 2, Modified Peru Earthquake, Bridge 5/518

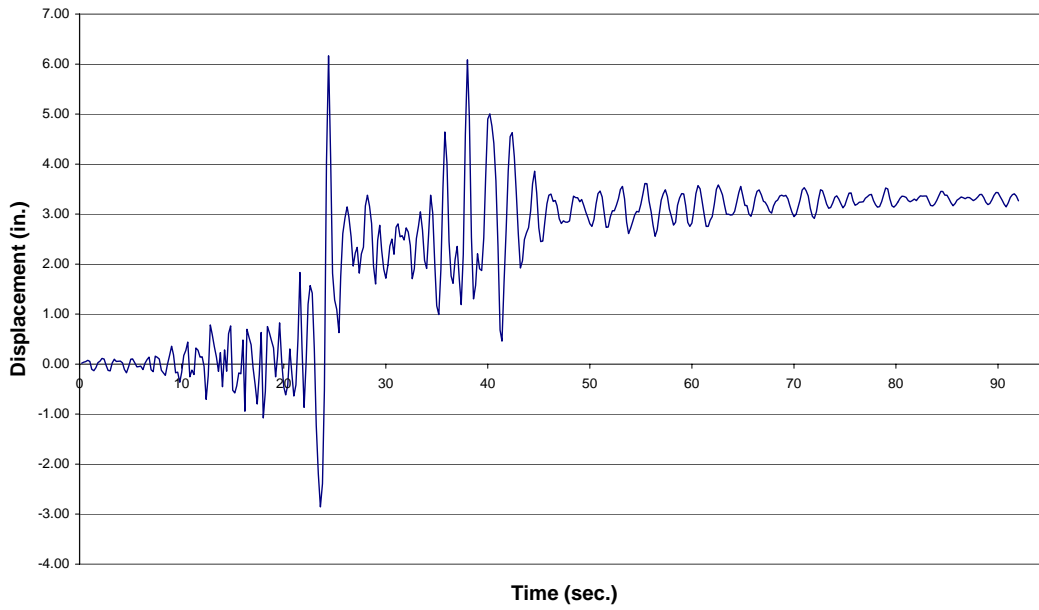


Figure 6.3-3 Total Displacement at Pier 3, Modified Peru Earthquake, Bridge 5/518

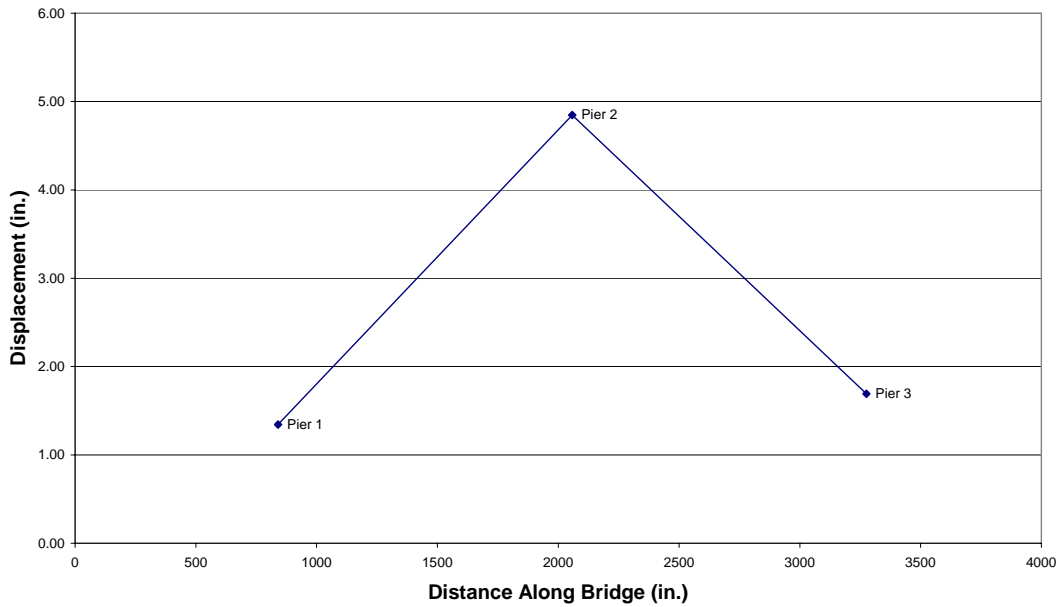


Figure 6.3-4 Transverse Displacement Envelope of Bridge Deck, Modified Peru Earthquake, Bridge 5/518

Table 6.3-1 shows the maximum moments at the top and bottom of all the columns. It should be noted that yielding limits the amount of moment that can be developed in the columns, and the yield level depends on the level of axial load.

Table 6.3-1 Maximum Moment (kip-in) at the Top and Bottoms of Columns, Modified Peru Earthquake, Bridge 5/518

Pier No.	Column	Moment	
		Top	Bottom
1	1	10434.6	13706.6
	2	10684.1	12864.4
	3	11957.7	13316.3
2	1	17360.1	15453.7
	2	15560.9	13611.4
	3	16275.5	14950.9
3	1	16016.7	13753.0
	2	14864.0	12805.8
	3	17355.7	15236.7

Because the columns have been fixed at their base, yielding occurs there first as shown by the plastic rotation plot in Figure 6.3-5. Yielding also occurs at the top of the columns at Pier 2 as shown in Figure 6.3-6. This is much different than the results of the base case, in which yielding only occurred at the top of the column.

There is more accumulated damage in the columns than there was for the base case, as shown in Figures 6.3-7 and 6.3-8. The damage coefficients for the bottom of the columns at the center pier ranged in value between 0.188 and 0.146, which insinuates minor cracking to light cracking throughout the column section. The damage coefficients for the top of the center columns ranged in value between 0.073 and 0.022, which suggests minor cracking.

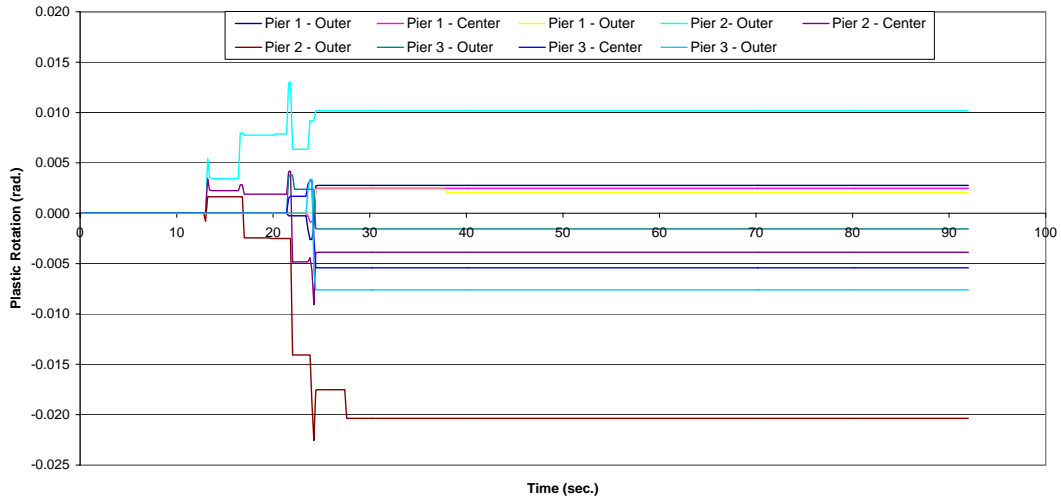


Figure 6.3-5 Plastic Rotations at the Bottom of the Columns, Modified Peru Earthquake, Bridge 5/518

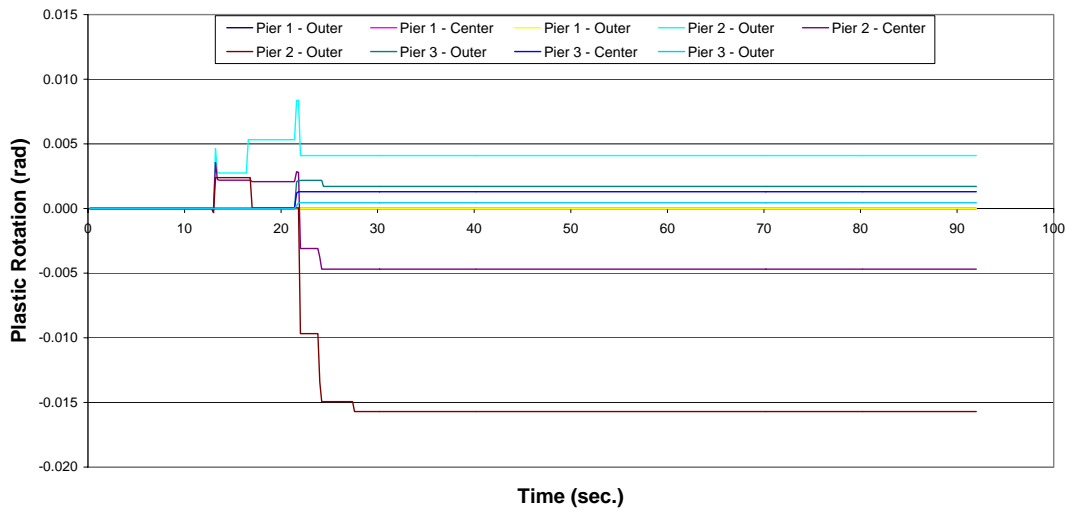


Figure 6.3-6 Plastic Rotations at the Top of the Columns, Modified Peru Earthquake, Bridge 5/518

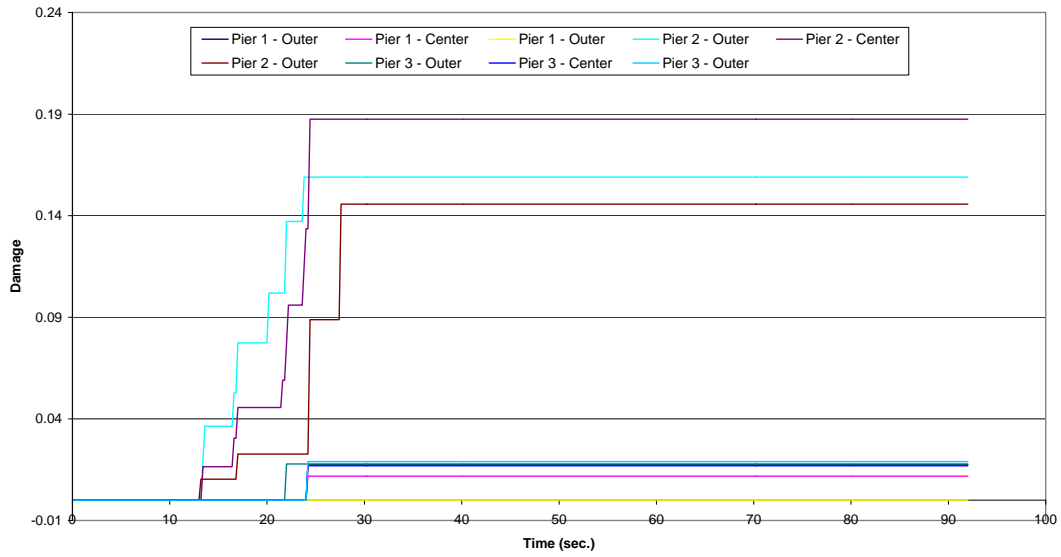


Figure 6.3-7 Damage at the Bottom of the Columns, Modified Peru Earthquake, Bridge 5/518

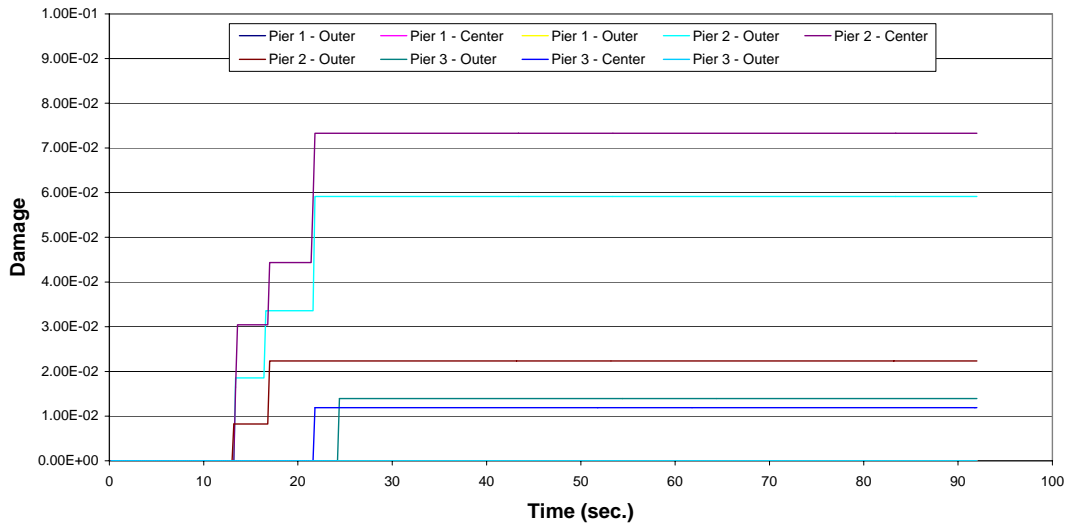


Figure 6.3-8 Damage at the Top of the Columns, Modified Peru Earthquake, Bridge 5/518

By looking at the shear versus displacement hysteresis plots, as shown in Figures 6.3-9 and 6.3-10, much more plasticity is shown occurring at the plastic hinges than for the base case. This can be seen in the opening of the hysteresis loops. It is also interesting to note the residual displacement found in the longitudinal hysteresis loops.

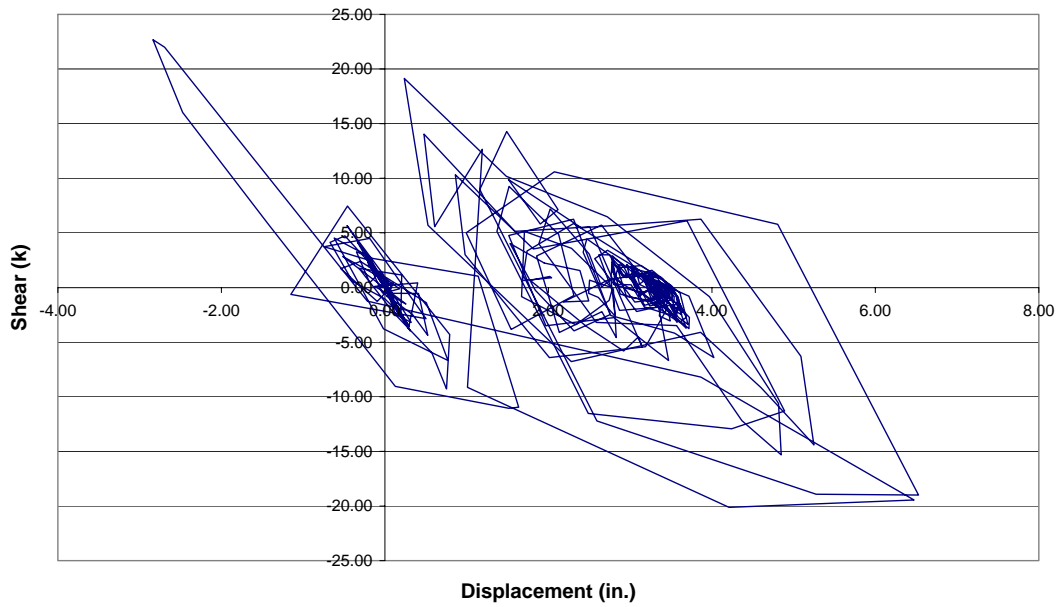


Figure 6.3-9 Longitudinal Hysteresis Plot for the Center Column of Pier 2, Modified Peru Earthquake, Bridge 5/518

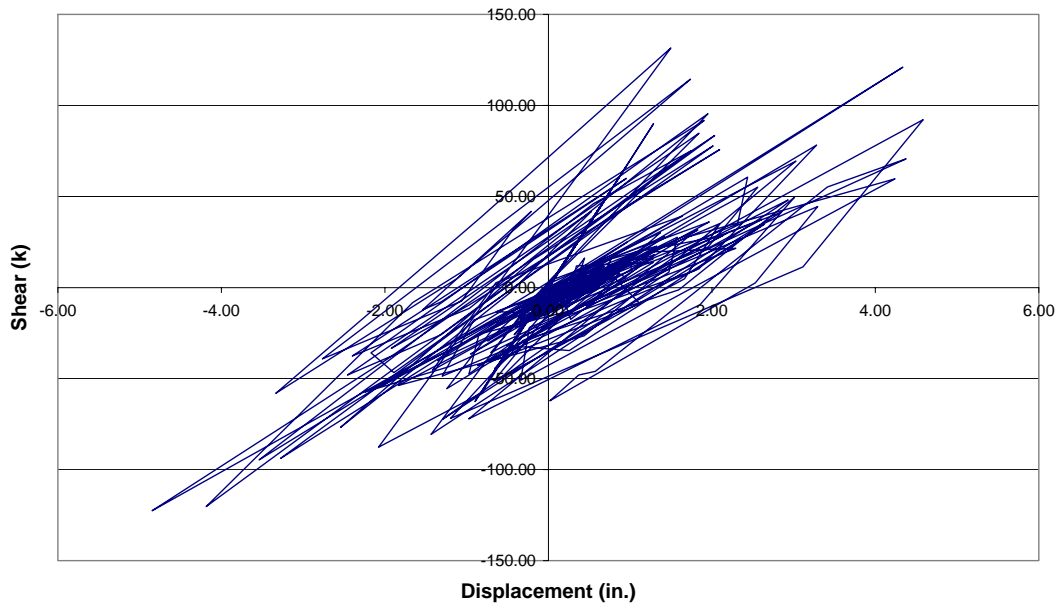


Figure 6.3-10 Transverse Hysteresis plot for the Center Column of Pier 2, Modified Peru Earthquake, Bridge 5/518

The maximum shear values at the top and bottom of the columns are shown in Table 6.3-2. The shear capacity of the columns is 171.6 kips, and the maximum actual shear found in the columns was 178 kips. This would suggest that there could be a possible shear failure in at least one of the columns. The shear values in the columns increased from those found in the base case.

Table 6.3-2 Maximum Shear (kips) in the Columns, Modified Peru Earthquake, Bridge 5/518

Pier No.	Column	Shear			
		Top	Demand/ Capacity	Bottom	Demand/ Capacity
1	1	93.39	0.54	94.72	0.55
	2	98.91	0.58	92.87	0.54
	3	107.23	0.63	109.61	0.64
2	1	145.31	0.85	147.51	0.86
	2	127.60	0.74	131.60	0.77
	3	138.07	0.80	143.49	0.84
3	1	156.04	0.91	143.43	0.84
	2	139.71	0.81	142.01	0.83
	3	164.10	0.96	177.74	1.04

By looking at the relative longitudinal displacement of the expansion joints, it can be determined if there will be pounding at the piers. Figure 6.3-11 shows the relative longitudinal displacement at Pier 1. It was found that pounding occurs at all three piers. However, with the increased displacement at the abutments, the pounding at the piers has been reduced.

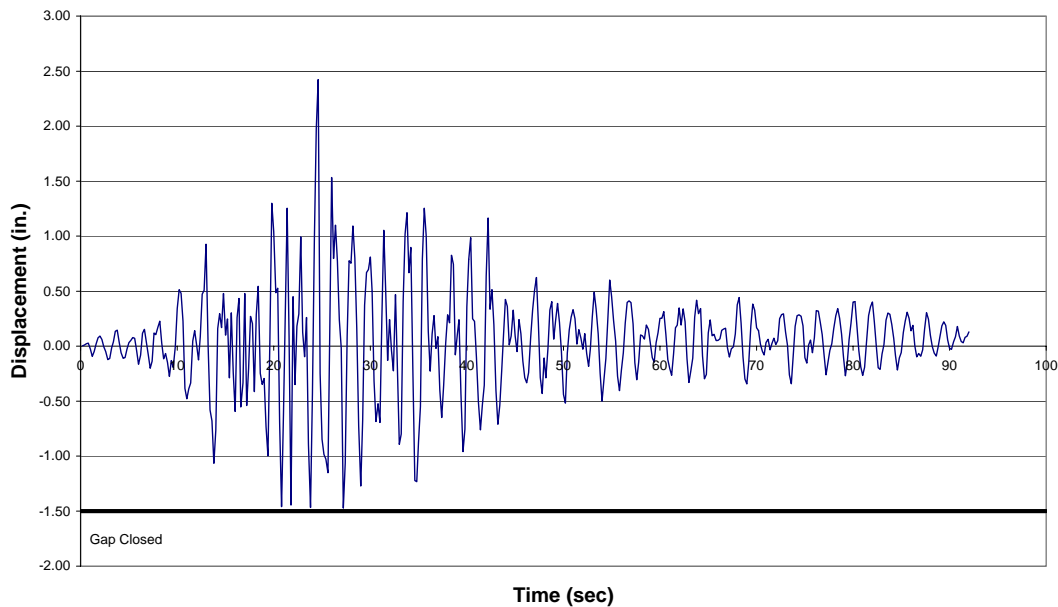


Figure 6.3-11 Relative Longitudinal Displacement at Pier 1, Modified Peru Earthquake, Bridge 5/518

The maximum displacement that the bearing pads can withstand is 1.44 inches. The actual maximum displacement is predicted to be 1.89 inches, which would suggest a possible bearing pad failure. The maximum displacements of the expansion joints are less than those of the base case, which would suggest that there would be fewer bearing pad failures.

6.2.2 Run No. 2

The results from the response of Bridge 5/518, with fixed columns and rollers in the longitudinal direction only, to the modified Peru earthquake are presented here. Table 6.3-3 summarizes the results from this time history analysis. All of the time history plots and tables for this analysis can be found in Appendix D.

Table 6.3-3 Results from the Modified Peru Earthquake, Bridge 5/518, Run No. 2

Max. Displacement					
Pier	Total Displacement (<i>in.</i>)			Comments:	
Pier 1	7.04				
Pier 2	6.99				
Pier 3	6.55				
Damage Levels					
Column	Max at Top	Comments:	Max at Bottom	Comments:	
1	0.014	Minor Cracking	.034	Minor Cracking	
2	0.011	Minor Cracking	.012	Minor Cracking	
3	0.007	Minor Cracking	.063	Minor Cracking	
4	0.085	Minor Cracking	.212	Medium Cracking	
5	0.116	Medium Cracking	.124	Medium Cracking	
6	0.070	Minor Cracking	.182	Medium Cracking	
7	N/A	No Damage	.013	Minor Cracking	
8	N/A	No Damage	.007	Minor Cracking	
9	N/A	No Damage	.036	Minor Cracking	
Maximum Column Shear					
Column	Shear (<i>kips</i>)	Capacity (<i>kips</i>)	Demand/Capacity		
Pier 2 – Outer Column	150.1	171.6	0.87		
Maximum Abutment Shear					
Abutment	Longitudinal Shear (<i>kips</i>)	Transverse Shear (<i>kips</i>)	Long. Capacity (<i>kips</i>)	Trans. Capacity (<i>kips</i>)	Failure (Y/N)
West	N/A	N/A	3370	1458	N/A
East	N/A	N/A	3370	1458	N/A
Expansion Joints					
Expansion Joint	Pounding (Y/N)		Comments:		
West Abutment	N/A				
East Abutment	N/A				
Pier 1	N				
Pier 2	N				
Pier 3	N				
Bearing Pads					
Pier	Max. Displacement (<i>in.</i>)		Allowable Displacement (<i>in.</i>)	Failure (Y/N)	
Pier 2	0.88		1.44	N	

The total relative displacements are larger than those of the base case because the roller allows for much more displacement in the longitudinal direction. However, the displacements in the transverse direction actually decrease by over two inches. This is the reason why the total relative displacements at the piers are virtually the same value.

It is interesting to note that, unlike the base case, for which damage only occurred at the top of the columns, damage occurred at the bottom of the columns and also at the top of the columns. The total accumulated damage in the columns increased from those seen in the base case. The shear in the columns also increased by up to 30% compared to those of the base case.

By allowing more displacement in the abutments, the pounding at the piers was eliminated. With the corresponding decrease in the relative displacement at the expansion joints, the analysis indicates that the bearing pads will be able to withstand the displacements.

6.3.3 Run No. 3

The results from the response of Bridge 5/518, where the column base soil stiffness was left unchanged from the base case and the abutment soil spring stiffness was increased by a factor of ten, to the modified Peru earthquake are presented here. Table 6.3-4 summarizes the results from this time history analysis. All of the time history plots and tables for this analysis can be found in Appendix D.

Table 6.3-4 Results from the Modified Peru Earthquake, Bridge 5/518, Run No. 3

Max. Displacement					
Pier	Total Displacement (<i>in.</i>)			Comments:	
Pier 1	4.63				
Pier 2	7.02				
Pier 3	3.53				
Damage Levels					
Column	Max at Top	Comments:	Max at Bottom	Comments:	
1	0.019	Minor cracking	N/A	No damage	
2	0.015	Minor cracking	N/A	No damage	
3	0.008	Minor cracking	N/A	No damage	
4	0.118	Medium cracking	N/A	No damage	
5	0.095	Minor cracking	N/A	No damage	
6	0.193	Medium cracking	N/A	No damage	
7	N/A	No damage	N/A	No damage	
8	N/A	No damage	N/A	No damage	
9	N/A	No damage	N/A	No damage	
Maximum Column Shear					
Column	Shear (<i>kips</i>)	Capacity (<i>kips</i>)	Demand/Capacity		
Pier 2 – Outer Column	124.30	171.6	0.72		
Maximum Abutment Shear					
Abutment	Longitudinal Shear (<i>kips</i>)	Transverse Shear (<i>kips</i>)	Long. Capacity (<i>kips</i>)	Trans. Capacity (<i>kips</i>)	Failure (Y/N)
West	1230	205	3370	1458	N
East	1280	318	3370	1458	N
Expansion Joints					
Expansion Joint	Pounding (Y/N)			Comments:	
West Abutment	Y				
East Abutment	Y				
Pier 1	Y				
Pier 2	Y				
Pier 3	Y				
Bearing Pads					
Pier	Max. Displacement (<i>in.</i>)		Allowable Displacement (<i>in.</i>)	Failure (Y/N)	
West Abutment	2.37		1.44	Y	

By increasing the soil stiffness at the abutments, the total relative displacements at the piers decreased by half an inch. This is expected because the stiffer soil spring at the abutments provides more restraint in the longitudinal and transverse directions. With the reduction of displacement, the damage that occurs in the columns is decreased slightly. The columns in Pier 3 accumulate no damage and the columns at Pier 2 have damage coefficients at or below 0.193. It is also necessary to note that the columns that do have damage only have damage at the top.

The shear in the columns was slightly reduced by making these changes, as well. The shear in the abutments shows that overall, the shear decreases. But this is caused by the fact that these maximum values are due to spikes in force created from pounding at the expansion joints. With the increased stiffness of the abutments, the pounding there decreased. Therefore, the shear-force maximum values decreased, overall.

6.3.4 Run No. 4

The results from the response of Bridge 5/518, for which the column base soil stiffness was left unchanged from the base case and the abutments were changed to rollers in the longitudinal direction only, to the modified Peru earthquake are presented here. Table 6.3-5 summarizes the results from this time history analysis. All of the time history plots and tables for this analysis can be found in Appendix D.

Table 6.3-5 Results from the Modified Peru Earthquake, Bridge 5/518, Run No. 4

Max. Displacement					
Pier	Total Displacement (<i>in.</i>)			Comments:	
Pier 1	5.48				
Pier 2	7.47				
Pier 3	5.17				
Damage Levels					
Column	Max at Top	Comments:	Max at Bottom	Comments:	
1	0.037	Minor cracking	N/A	No damage	
2	0.029	Minor cracking	N/A	No damage	
3	0.015	Minor cracking	N/A	No damage	
4	0.123	Minor cracking	N/A	No damage	
5	0.154	Minor cracking	N/A	No damage	
6	0.154	Minor cracking	N/A	No damage	
7	N/A	No damage	N/A	No damage	
8	N/A	No damage	N/A	No damage	
9	0.009	Minor cracking	N/A	No damage	
Maximum Column Shear					
Column	Shear (<i>kips</i>)	Capacity (<i>kips</i>)	Demand/Capacity		
Pier 2 – Outer Column	133.94	171.6	0.78		
Maximum Abutment Shear					
Abutment	Longitudinal Shear (<i>kips</i>)	Transverse Shear (<i>kips</i>)	Long. Capacity (<i>kips</i>)	Trans. Capacity (<i>kips</i>)	Failure (Y/N)
West	N/A	N/A	3370	1458	N
East	N/A	N/A	3370	1458	N
Expansion Joints					
Expansion Joint	Pounding (Y/N)		Comments:		
West Abutment	N/A				
East Abutment	N/A				
Pier 1	N				
Pier 2	N				
Pier 3	Y		One edge only		
Bearing Pads					
Pier	Max. Displacement (<i>in.</i>)		Allowable Displacement (<i>in.</i>)	Failure (Y/N)	
Pier 2	1.41		1.44	N	

By allowing a roller at the abutments, the total relative displacements at the piers increased slightly. This is expected because the rollers at the abutments do not restrain the bridge in the longitudinal direction. The columns in Pier 2 have the most damage and the damage coefficients range between 0.154 and 0.123. It is necessary to note that the columns only have damage at their tops. The shear in the columns stayed virtually the same as the base case. With the rollers at the abutments, the longitudinal displacement at the expansion joints decreased greatly. The model shows only one occurrence of an expansion joint closing.

6.3.5 Run No. 5

The results from the response of Bridge 5/518, for which the column base soil stiffness was decreased by a factor of ten from the base case and the abutment soil spring stiffness was unchanged, to the modified Peru earthquake are presented here. Table 6.3-6 summarizes the results from this time history analysis. All of the time history plots and tables for this analysis can be found in Appendix D.

Table 6.3-6 Results from the Modified Peru Earthquake, Bridge 5/518, Run No. 5

Max. Displacement					
Pier	Total Displacement (<i>in.</i>)			Comments:	
Pier 1	6.86				
Pier 2	9.24				
Pier 3	4.54				
Damage Levels					
Column	Max at Top	Comments:	Max at Bottom	Comments:	
1	0.021	Minor cracking	N/A	No damage	
2	0.033	Minor cracking	N/A	No damage	
3	0.024	Minor cracking	N/A	No damage	
4	0.062	Minor cracking	N/A	No damage	
5	0.072	Minor cracking	N/A	No damage	
6	0.070	Minor cracking	N/A	No damage	
7	N/A	No damage	N/A	No damage	
8	N/A	No damage	N/A	No damage	
9	N/A	No damage	N/A	No damage	
Maximum Column Shear					
Column	Shear (<i>kips</i>)	Capacity (<i>kips</i>)	Demand/Capacity		
Pier 2 – Outer Column	104.23	171.6	0.61		
Maximum Abutment Shear					
Abutment	Longitudinal Shear (<i>kips</i>)	Transverse Shear (<i>kips</i>)	Long. Capacity (<i>kips</i>)	Trans. Capacity (<i>kips</i>)	Failure (Y/N)
West	1950	309	3370	1458	N
East	1730	188	3370	1458	N
Expansion Joints					
Expansion Joint	Pounding (Y/N)		Comments:		
West Abutment	Y				
East Abutment	Y				
Pier 1	Y				
Pier 2	Y				
Pier 3	Y				
Bearing Pads					
Pier	Max. Displacement (<i>in.</i>)		Allowable Displacement (<i>in.</i>)	Failure (Y/N)	
West Abutment	2.55		1.44	Y	

By decreasing the soil stiffness at the columns, the total relative displacements at the piers increased by up to two inches. There is also considerable residual displacement, which did not appear in the base case. This is expected because the decreased stiffness does not provide as much restraint. Therefore, the rotations at the column bases are increased. By allowing increased displacement in the structure, the damage in the columns decreased. The damage coefficients at Pier 2 for the base case ranged from 0.223 and 0.139, while, for this case they ranged from 0.072 and 0.062. The damage in the columns was confined to the top.

The shear in the columns was reduced considerably, and in some columns it was reduced by up to 50%. The shear in the abutments increased by up to 30% with this change. Pounding occurs at the all of the abutments and piers, which is the same as the base case.

6.3.6 Run No. 6

The results from the response of Bridge 5/518, where the column bases were fixed and the abutment soil spring stiffness was unchanged, to the modified Peru earthquake are presented here. Table 6.3-7 summarizes the results from this time history analysis. All of the time history plots and tables for this analysis can be found in Appendix D.

Table 6.3-7 Results from the Modified Peru Earthquake, Bridge 5/518, Run No. 6

Max. Displacement					
Pier	Total Displacement (<i>in.</i>)			Comments:	
Pier 1	3.62				
Pier 2	4.97				
Pier 3	3.27				
Damage Levels					
Column	Max at Top	Comments:	Max at Bottom	Comments:	
1	0.037	Minor cracking	0.020	Minor cracking	
2	0.024	Minor cracking	0.038	Minor cracking	
3	0.026	Minor cracking	0.030	Minor cracking	
4	0.097	Minor cracking	0.214	Medium cracking	
5	0.071	Minor cracking	0.175	Medium cracking	
6	0.013	Minor cracking	0.156	Medium cracking	
7	N/A	No damage	0.018	Minor cracking	
8	N/A	No damage	0.030	Minor cracking	
9	N/A	No damage	0.030	Minor cracking	
Maximum Column Shear					
Column	Shear (<i>kips</i>)	Capacity (<i>kips</i>)	Demand/Capacity		
Pier 1 – Outer Column	152.5	171.6	0.90		
Maximum Abutment Shear					
Abutment	Longitudinal Shear (<i>kips</i>)	Transverse Shear (<i>kips</i>)	Long. Capacity (<i>kips</i>)	Trans. Capacity (<i>kips</i>)	Failure (Y/N)
West	1800	202	3370	1458	N
East	1740	147	3370	1458	N
Expansion Joints					
Expansion Joint	Pounding (Y/N)			Comments:	
West Abutment	Y				
East Abutment	Y				
Pier 1	Y			One edge only	
Pier 2	Y			One edge only	
Pier 3	Y			One edge only	
Bearing Pads					
Pier	Max. Displacement (<i>in.</i>)		Allowable Displacement (<i>in.</i>)	Failure (Y/N)	
Pier 3	2.68		1.44	Y	

By fixing the columns at their bases, the total relative displacements at the piers decreased by almost two inches. This is expected because the fixed foundations provide increased restraint in the transverse and longitudinal directions. Although this effect decreases displacements, it increases the forces in the columns and therefore the total accumulated damage in the columns increases. It should be noted that it also causes damage to occur at both the top and the bottom of the columns. So, overall, the columns are damaged much more than in the base case.

The shear in the columns was increased by up to 35%, while the shear in the abutments was decreased slightly by this change. The frequency of pounding at the abutments and piers decreased with this change, but it still occurs.

6.3.7 Run No. 7

The results from the response of Bridge 5/518, where the “worst case” combination of support properties was used, to the modified Chile earthquake are presented here. The “worst case” combination was found to be fixed column bases and rollers in both directions at the abutments. Table 6.3-8 summarizes the results from this time history analysis. All of the time history plots and tables for this analysis can be found in Appendix D.

Table 6.3-8 Results from the Modified Chile Earthquake, Bridge 5/518, Run No. 7

Max. Displacement					
Pier	Total Displacement (<i>in.</i>)			Comments:	
Pier 1	4.72				
Pier 2	5.39				
Pier 3	4.70				
Damage Levels					
Column	Max at Top	Comments:	Max at Bottom	Comments:	
1	N/A	No damage	0.082	Minor cracking	
2	N/A	No damage	0.045	Minor cracking	
3	N/A	No damage	0.045	Minor cracking	
4	0.013	Minor cracking	0.185	Medium cracking	
5	0.017	Minor cracking	0.133	Medium cracking	
6	0.032	Minor cracking	0.133	Medium cracking	
7	N/A	No damage	0.069	Minor Cracking	
8	N/A	No damage	0.069	Minor cracking	
9	N/A	No damage	0.074	Minor cracking	
Maximum Column Shear					
Column	Shear (<i>kips</i>)	Capacity (<i>kips</i>)	Demand/Capacity		
Pier 2 – Outer Column	148.06	171.6	0.86		
Maximum Abutment Shear					
Abutment	Longitudinal Shear (<i>kips</i>)	Transverse Shear (<i>kips</i>)	Long. Capacity (<i>kips</i>)	Trans. Capacity (<i>kips</i>)	Failure (Y/N)
West	N/A	N/A	3370	1458	N
East	N/A	N/A	3370	1458	N
Expansion Joints					
Expansion Joint	Pounding (Y/N)		Comments:		
West Abutment	N/A				
East Abutment	N/A				
Pier 1	N				
Pier 2	N				
Pier 3	N				
Bearing Pads					
Pier	Max. Displacement (<i>in.</i>)		Allowable Displacement (<i>in.</i>)	Failure (Y/N)	
Pier 3	2.43		1.44	Y	

By fixing the column bases, the total relative displacements at the piers are decreased from those of the base case. The total displacements are decreased the most at Pier 2, but only slightly at the other piers. The transverse displacements are decreased by up to three inches. This happens because there is more displacement in the longitudinal direction because of the rollers at the abutments.

It is interesting to note that unlike the base case, for which damage only occurred at the top of the columns, damage occurred at both the bottom of the columns and the top of the columns. The damage levels at the ends of the columns also increased from those in the base case. The shear in the columns also increased by up to 30%.

By allowing more displacement in the abutments, the pounding at the piers was reduced. Pounding occurs at only one of the three piers, but it has been reduced considerably. The analysis indicated that there would still be a possible failure of the bearing pads, however.

6.3.8 Run No. 8

The results from the response of Bridge 5/826, for which the column bases were fixed and the abutments were changed to rollers in the longitudinal direction only, to the modified Peru earthquake are presented here. Table 6.3-9 summarizes the results from this time history analysis. All of the time history plots and tables for this analysis can be found in Appendix D.

Table 6.3-9 Results from the Modified Peru Earthquake, Bridge 5/826, Run No. 8

Max. Displacement					
Pier	Total Displacement (<i>in.</i>)			Comments:	
Pier 1	4.49				
Pier 2	4.50				
Pier 3	4.50				
Damage Levels					
Column	Max at Top	Comments:	Max at Bottom	Comments:	
1	N/A	No damage	0.047	Minor cracking	
2	0.048	Minor cracking	0.058	Minor cracking	
3	0.032	Minor cracking	0.056	Minor cracking	
4	0.010	Minor cracking	0.012	Minor cracking	
5	0.008	Minor cracking	N/A	No damage	
6	0.008	Minor cracking	0.011	Minor cracking	
7	0.026	Minor cracking	0.018	Minor cracking	
8	0.042	Minor cracking	0.042	Minor cracking	
9	0.018	Minor cracking	0.040	Minor cracking	
Maximum Column Shear					
Column	Shear (<i>kips</i>)	Capacity (<i>kips</i>)	Demand/Capacity		
Pier 1 – Center Column	184.70	171.6	1.07		
Maximum Abutment Shear					
Abutment	Longitudinal Shear (<i>kips</i>)	Transverse Shear (<i>kips</i>)	Long. Capacity (<i>kips</i>)	Trans. Capacity (<i>kips</i>)	Failure (Y/N)
West	N/A	N/A	5184	5443	N
East	N/A	N/A	5184	5443	N
Expansion Joints					
Expansion Joint	Pounding (Y/N)		Comments:		
West Abutment	N/A				
East Abutment	N/A				
Pier 1	N/A				
Pier 2	N/A				
Pier 3	N/A				
Bearing Pads					
Pier	Max. Displacement (<i>in.</i>)		Allowable Displacement (<i>in.</i>)	Failure (Y/N)	
N/A	N/A		2.88	N	

By fixing the columns at their bases and allowing a roller at the abutments, the total relative displacement increased by around an inch. This is expected because the abutment is not there to provide restraint. Because of this increased displacement and the fact that the columns were fixed at their bases, damage occurred at the top and bottom of certain columns. The base case did not have any damage in any of the columns. Also, with this change, the shear in the columns increased drastically, and at least two of the columns would possibly fail in shear.

6.3.9 Run No. 9

The results from the response of Bridge 5/826, for which the column bases were fixed and the abutments were changed to rollers in both directions, to the modified Peru earthquake are presented here. Table 6.3-10 summarizes the results from this time history analysis. All of the time history plots and tables for this analysis can be found in Appendix D.

Table 6.3-10 Results from the Modified Peru Earthquake, Bridge 5/826, Run No. 9

Max. Displacement					
Pier	Total Displacement (<i>in.</i>)			Comments:	
Pier 1	7.21				
Pier 2	7.25				
Pier 3	7.80				
Damage Levels					
Column	Max at Top	Comments:	Max at Bottom	Comments:	
1	N/A	No damage	N/A	Minor cracking	
2	0.030	Minor cracking	0.063	Minor cracking	
3	0.029	Minor cracking	0.034	Minor cracking	
4	0.077	Minor cracking	0.039	Minor cracking	
5	0.017	Minor cracking	0.016	Minor cracking	
6	0.057	Minor cracking	0.045	Minor cracking	
7	0.071	Minor cracking	0.057	Minor cracking	
8	0.070	Minor cracking	0.086	Minor cracking	
9	0.073	Minor cracking	0.079	Minor cracking	
Maximum Column Shear					
Column	Shear (<i>kips</i>)	Capacity (<i>kips</i>)	Demand/Capacity		
Pier 1 – Outer Column	161.43	171.6	0.94		
Maximum Abutment Shear					
Abutment	Longitudinal Shear (<i>kips</i>)	Transverse Shear (<i>kips</i>)	Long. Capacity (<i>kips</i>)	Trans. Capacity (<i>kips</i>)	Failure (Y/N)
West	N/A	N/A	5184	5443	N
East	N/A	N/A	5184	5443	N
Expansion Joints					
Expansion Joint	Pounding (Y/N)		Comments:		
West Abutment	N/A				
East Abutment	N/A				
Pier 1	N/A				
Pier 2	N/A				
Pier 3	N/A				
Bearing Pads					
Pier	Max. Displacement (<i>in.</i>)		Allowable Displacement (<i>in.</i>)	Failure (Y/N)	
N/A	N/A		2.88	N	

By allowing rollers in both directions at the abutments, the total relative displacements increased considerably over those in the base case. There were also residual displacements of up to four inches at Pier 1 and two inches at Pier 2. With this increase in displacement, there is now damage at both ends of the columns, where there was no damage in any of the columns in the base case. The shear in the columns increased by up to 30%, but not to a level of failure.

6.3.10 Run No. 10

The results from the response of Bridge 5/518, for which the column bases were fixed and the abutment were changed to rollers in both directions, to the Olympia 950-year earthquake are presented here. Table 6.3-11 summarizes the results from this time history analysis. All of the time history plots and tables for this analysis can be found in Appendix D.

Table 6.3-11 Results from the Olympia 950-Year EQ, Bridge 5/518, Run No. 10

Max. Displacement					
Pier	Total Displacement (<i>in.</i>)			Comments:	
Pier 1	2.61				
Pier 2	4.10				
Pier 3	2.20				
Damage Levels					
Column	Max at Top	Comments:	Max at Bottom	Comments:	
1	N/A	No damage	N/A	No damage	
2	N/A	No damage	N/A	No damage	
3	N/A	No damage	N/A	No damage	
4	0.013	Minor cracking	0.042	Minor cracking	
5	0.008	Minor cracking	0.013	Minor cracking	
6	0.016	Minor cracking	0.071	Minor cracking	
7	N/A	No damage	N/A	No damage	
8	N/A	No damage	N/A	No damage	
9	N/A	No damage	N/A	No damage	
Maximum Column Shear					
Column	Shear (<i>kips</i>)	Capacity (<i>kips</i>)	Demand/Capacity		
Pier 2 – Outer Column	147.8	171.6	0.86		
Maximum Abutment Shear					
Abutment	Longitudinal Shear (<i>kips</i>)	Transverse Shear (<i>kips</i>)	Long. Capacity (<i>kips</i>)	Trans. Capacity (<i>kips</i>)	Failure (Y/N)
West	N/A	N/A	3370	1458	N
East	N/A	N/A	3370	1458	N
Expansion Joints					
Expansion Joint	Pounding (Y/N)		Comments:		
West Abutment	N/A				
East Abutment	N/A				
Pier 1	N				
Pier 2	N				
Pier 3	N				
Bearing Pads					
Pier	Max. Displacement (<i>in.</i>)		Allowable Displacement (<i>in.</i>)	Failure (Y/N)	
Pier 3	0.83		1.44	N	

By allowing rollers at the abutments the total relative displacement did not change significantly, but the shear in the columns increased by up to 37%. By allowing more displacement at the abutments, the pounding at the piers was eliminated. The displacement at the piers was reduced enough that the bearing pads are predicted to be able to withstand the demand.

6.3.11 Run No. 11

The results from the response of Bridge 5/518, for which the column bases were fixed and the abutments were changed to rollers in both directions, to the Kobe 950-year earthquake are presented here. Table 6.3-12 summarizes the results from this time history analysis. All of the time history plots and tables for this analysis can be found in Appendix D.

Table 6.3-12 Results from the Kobe 950-Year EQ, Bridge 5/518, Run No. 11

Max. Displacement					
Pier	Total Displacement (<i>in.</i>)			Comments:	
Pier 1	2.59				
Pier 2	3.73				
Pier 3	2.21				
Damage Levels					
Column	Max at Top	Comments:	Max at Bottom	Comments:	
1	N/A	No damage	N/A	No damage	
2	N/A	No damage	N/A	No damage	
3	N/A	No damage	N/A	No damage	
4	0.020	Minor cracking	0.019	Minor cracking	
5	0.036	Minor cracking	0.035	Minor cracking	
6	0.040	Minor cracking	0.027	Minor cracking	
7	N/A	No damage	N/A	No damage	
8	N/A	No damage	N/A	No damage	
9	N/A	No damage	N/A	No damage	
Maximum Column Shear					
Column	Shear (<i>kips</i>)	Capacity (<i>kips</i>)	Demand/Capacity		
Pier 2 – Outer Column	143.0	171.6	0.83		
Maximum Abutment Shear					
Abutment	Longitudinal Shear (<i>kips</i>)	Transverse Shear (<i>kips</i>)	Long. Capacity (<i>kips</i>)	Trans. Capacity (<i>kips</i>)	Failure (Y/N)
West	N/A	N/A	3370	1458	N
East	N/A	N/A	3370	1458	N
Expansion Joints					
Expansion Joint	Pounding (Y/N)		Comments:		
West Abutment	N/A				
East Abutment	N/A				
Pier 1	N				
Pier 2	N				
Pier 3	N				
Bearing Pads					
Pier	Max. Displacement (<i>in.</i>)		Allowable Displacement (<i>in.</i>)	Failure (Y/N)	
Pier 3	0.98		1.44	N	

By allowing rollers at the abutments, the total relative displacement did not change significantly, but the shear in the columns increased by up to 99% at Pier 1. The shear force in the columns at Pier 2 and 3 increased by only 20%. The damage now occurs at the top and bottom of the columns and the accumulated damage increased from the base case. Even with the great increase in shear force in the column of Pier 1, none of the columns are predicted to fail in shear. Because the rollers at the abutments allow for more displacement, the pounding at the piers was eliminated. The bearing pads at the piers are predicted to be able to withstand the seismic demands.

6.3.12 Run No. 12

The results from the response of Bridge 5/826, for which the column bases were fixed and the abutment were changed to rollers in both directions, to the Olympia 950-year earthquake are presented here. Table 6.3-13 summarizes the results from this time history analysis. All of the time history plots and tables for this analysis can be found in Appendix D.

Table 6.3-13 Results from the Olympia 950-Year EQ, Bridge 5/826, Run No. 12

Max. Displacement					
Pier	Total Displacement (<i>in.</i>)			Comments:	
Pier 1	3.36				
Pier 2	3.44				
Pier 3	3.56				
Damage Levels					
Column	Max at Top	Comments:	Max at Bottom	Comments:	
1	0.017	Minor cracking	N/A	No damage	
2	0.016	Minor cracking	N/A	No damage	
3	0.017	Minor cracking	0.057	Minor cracking	
4	N/A	No damage	N/A	No damage	
5	N/A	No damage	N/A	No damage	
6	N/A	No damage	N/A	No damage	
7	N/A	No damage	N/A	No damage	
8	N/A	No damage	N/A	No damage	
9	N/A	No damage	N/A	No damage	
Maximum Column Shear					
Column	Shear (<i>kips</i>)	Capacity (<i>kips</i>)	Demand/Capacity		
Pier 1 – Outer Column	143.3	171.6	0.84		
Maximum Abutment Shear					
Abutment	Longitudinal Shear (<i>kips</i>)	Transverse Shear (<i>kips</i>)	Long. Capacity (<i>kips</i>)	Trans. Capacity (<i>kips</i>)	Failure (Y/N)
West	N/A	N/A	5184	5443	N
East	N/A	N/A	5184	5443	N
Expansion Joints					
Expansion Joint	Pounding (Y/N)		Comments:		
West Abutment	N/A				
East Abutment	N/A				
Pier 1	N/A				
Pier 2	N/A				
Pier 3	N/A				
Bearing Pads					
Pier	Max. Displacement (<i>in.</i>)		Allowable Displacement (<i>in.</i>)	Failure (Y/N)	
N/A	N/A		2.88	N/A	

With rollers at the abutments, the total relative displacement increased by up to one inch. The shear force in the columns was increased by up to 86%, but not to a level that would cause failure. The damage in the columns is at levels that cause only minor damage, whereas the base case did not have any damage at all.

6.3.13 Run No. 13

The results from the response of Bridge 5/826, for which the column bases were fixed and the abutment were changed to rollers in both directions, to the Kobe 950-year earthquake are presented here. Table 6.3-14 summarizes the results from this time history analysis. All of the time history plots and tables for this analysis can be found in Appendix D.

Table 6.3-14 Results from the Kobe 950-Year EQ, Bridge 5/826, Run No. 13

Max. Displacement					
Pier	Total Displacement (<i>in.</i>)			Comments:	
Pier 1	4.10				
Pier 2	4.04				
Pier 3	3.98				
Damage Levels					
Column	Max at Top	Comments:	Max at Bottom	Comments:	
1	0.014	Minor cracking	0.015	Minor cracking	
2	N/A	No damage	0.027	Minor cracking	
3	N/A	No damage	0.013	Minor cracking	
4	N/A	No damage	N/A	No damage	
5	N/A	No damage	N/A	No damage	
6	N/A	No damage	N/A	No damage	
7	N/A	No damage	0.009	Minor cracking	
8	N/A	No damage	0.007	Minor cracking	
9	0.015	Minor cracking	0.017	Minor cracking	
Maximum Column Shear					
Column	Shear (<i>kips</i>)	Capacity (<i>kips</i>)	Demand/Capacity		
Pier 1 – Outer Column	144.7	171.6	0.84		
Maximum Abutment Shear					
Abutment	Longitudinal Shear (<i>kips</i>)	Transverse Shear (<i>kips</i>)	Long. Capacity (<i>kips</i>)	Trans. Capacity (<i>kips</i>)	Failure (Y/N)
West	N/A	N/A	5184	5443	N
East	N/A	N/A	5184	5443	N
Expansion Joints					
Expansion Joint	Pounding (Y/N)		Comments:		
West Abutment	N/A				
East Abutment	N/A				
Pier 1	N/A				
Pier 2	N/A				
Pier 3	N/A				
Bearing Pads					
Pier	Max. Displacement (<i>in.</i>)		Allowable Displacement (<i>in.</i>)	Failure (Y/N)	
N/A	N/A		2.88	N/A	

The total relative displacement was increased by up to one inch. The shear force in the columns is increased by up to 48%. This does not increase it to a level that would cause a shear failure in the columns, however. The damage in the columns is at levels that cause only minor damage, whereas the base case did not have any damage at all.

In this study it is seen that besides increasing the damage, fixing the column bases caused the damage to occur at the top and bottom of the columns, whereas the damage occurred at the top of the columns when soil springs were used. The fixed-roller cases also increased the level of shear in the columns to a point at which some of them could possibly fail. It is also predicted that pounding will occur and that there could be bearing pad failures.

This study also showed that a variation in the abutment stiffness, while the column base stiffnesses were left unchanged, affected the pounding and bearing pad behavior. By allowing a roller at the abutment, the pounding and occurrences of bearing pad failures decreased. When the abutment stiffness is left unchanged and the column base stiffnesses were varied, there was a greater variation in the column damage and shear force in the columns.

6.4 Bent Model Comparison

A bent model was constructed to model the center pier of Bridge 5/518. This model was then analyzed to determine if a bent model can accurately model the response of the bridge, or if the entire bridge model is necessary. If a bent model could be used, it would drastically cut down the time it takes to construct and execute the model. This

would allow for the use of probabilistic studies to be conducted to determine if long-duration earthquakes are truly more damaging.

Two models were used for this study, the first was fixed at the base of the columns and the second had soil springs at the base of the columns. The modified Peru earthquake was used in this study, with accelerations in the transverse and vertical directions only.

Figure 6.4-1 shows the relative transverse displacement at the top of the center pier of the bridge model. Figure 6.4-2 shows the relative transverse displacement of the bent model. The comparison of the two figures shows that the relative peak displacements of the bent model are less than those of the bridge pier.

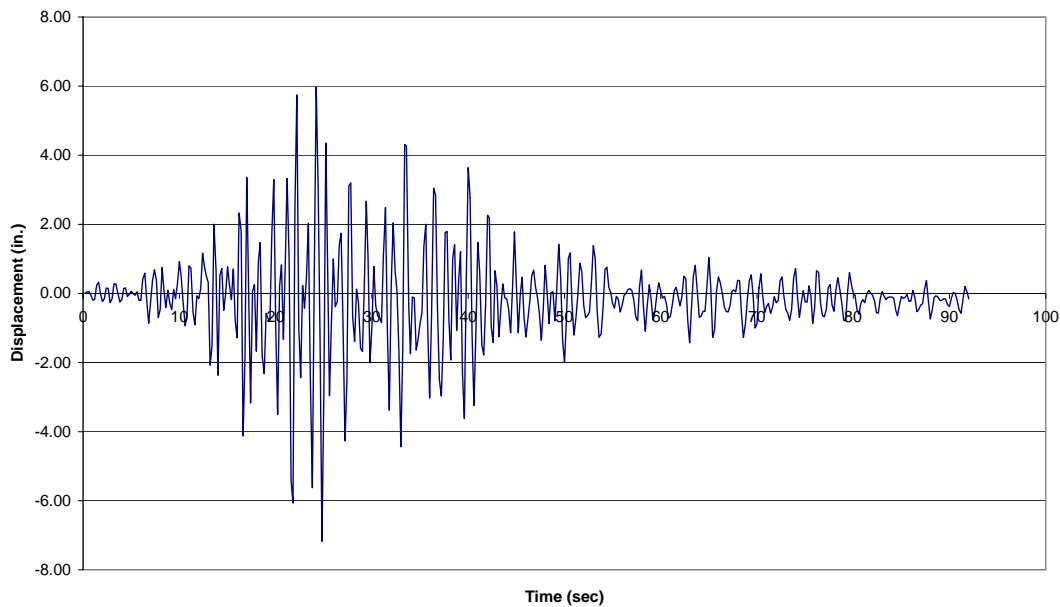


Figure 6.4-1 Relative Transverse Displacement of Bridge Pier

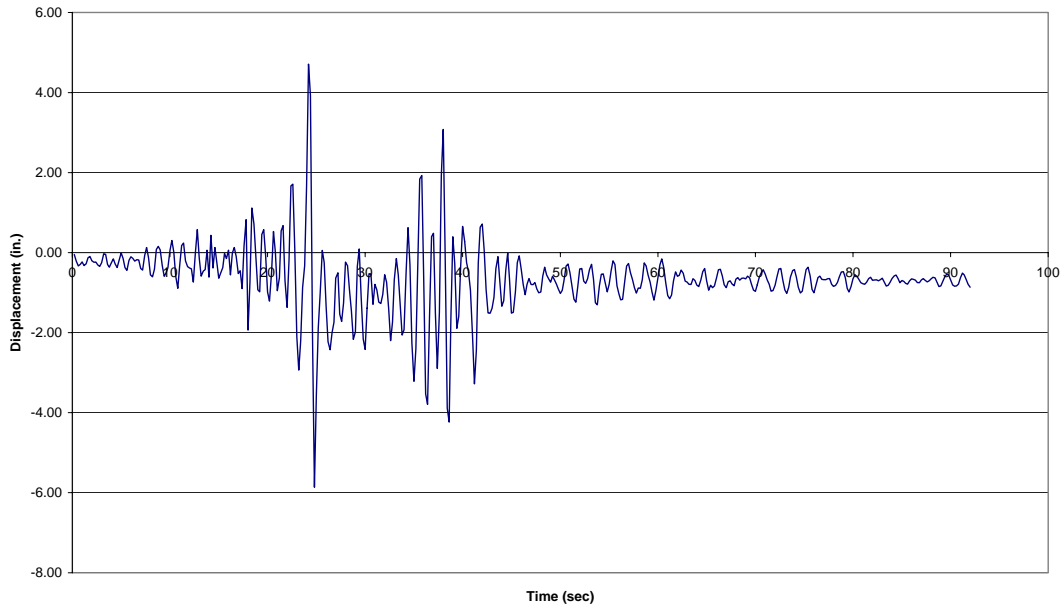


Figure 6.4-2 Relative Transverse Displacement of Bent Model

The most noticeable difference in the displacement time histories is the fact that the bent model has a residual displacement of around one-inch. The displacement time-history of the bridge pier shows a residual displacement that is so small it is negligible. The maximum moment at the top and bottom of the columns is shown in Table 6.4-1. It can be seen that the moment levels in the pier of the bridge model are greater than those of the bent model in every case. It should be noted that yielding limits the level of moment that can be developed in the columns, and the yield level depends on the level of axial force.

Table 6.4-1 Maximum Moment (kip-in) at the Top and Bottoms of Columns

Model	Column	Moment	
		Top	Bottom
Bridge Pier	1	16851	10623
	2	16070	10370
	3	18220	10447
Bent Model	1	12170	8877
	2	14600	11040
	3	13610	11280

Figures 6.4-3 and 6.4-4 show the plastic rotation that occurred in the columns of the center pier of the bridge model. Figures 6.4-5 and 6.4-6 show the plastic rotation that occurred in the columns of the bent model. The plots show significant differences in the plastic behavior of the two models. This is also reflected in the plots of the damage as shown in Figures 6.4-7 through 6.4-9. There was no calculated damage at the bottom of the columns of the pier from the bridge model because there was not a reversal in the plastic rotation, which would denote a cycle.

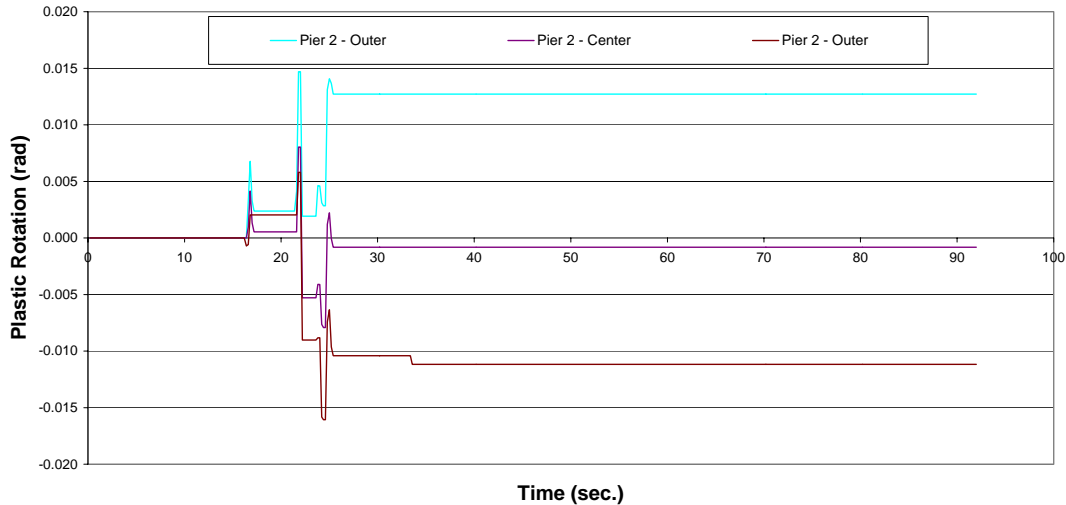


Figure 6.4-3 Plastic Rotations at the Top of the Columns for the Bridge Pier

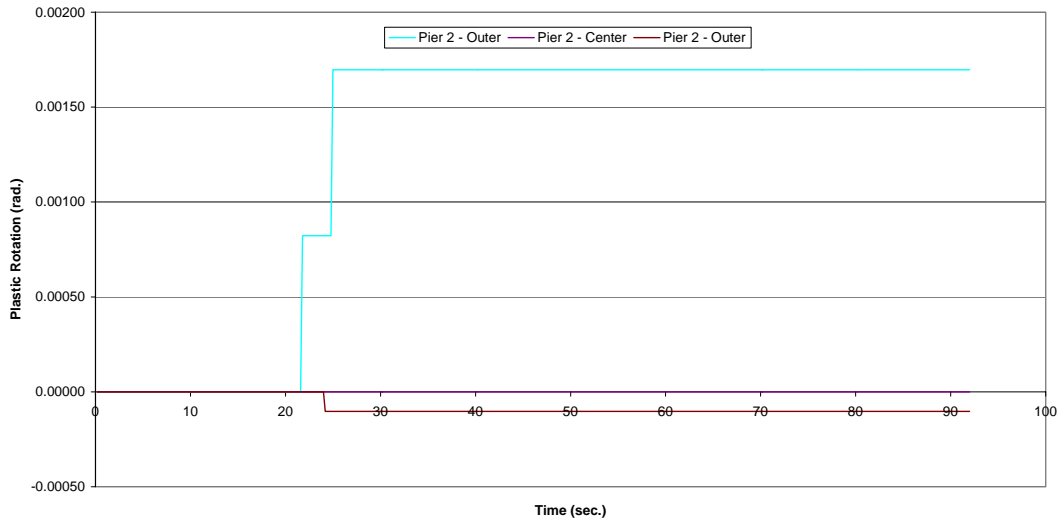


Figure 6.4-4 Plastic Rotations at the Bottom of the Columns for the Bridge Pier

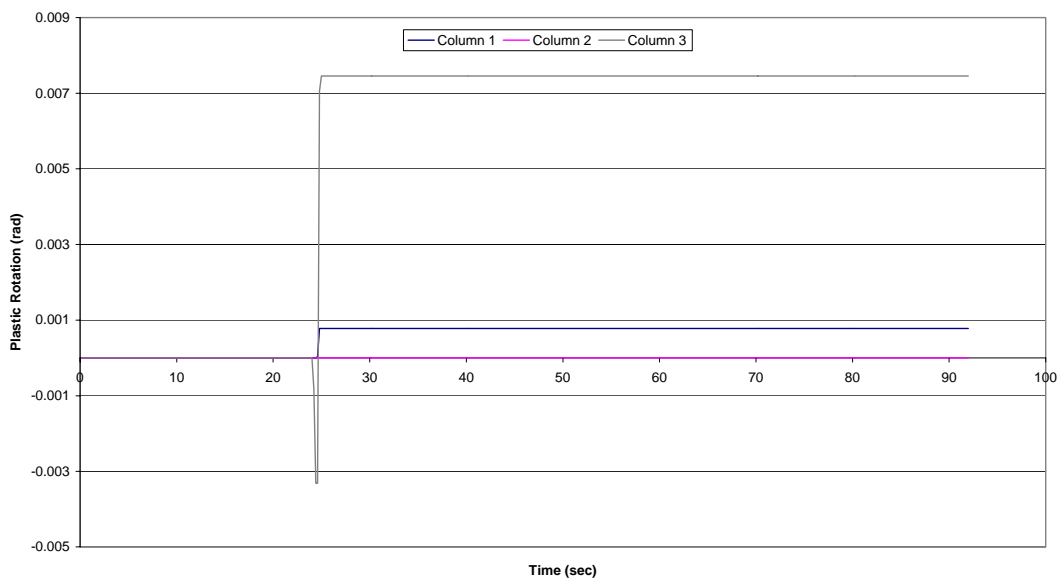


Figure 6.4-5 Plastic Rotations at the Top of the Columns for the Bent Model

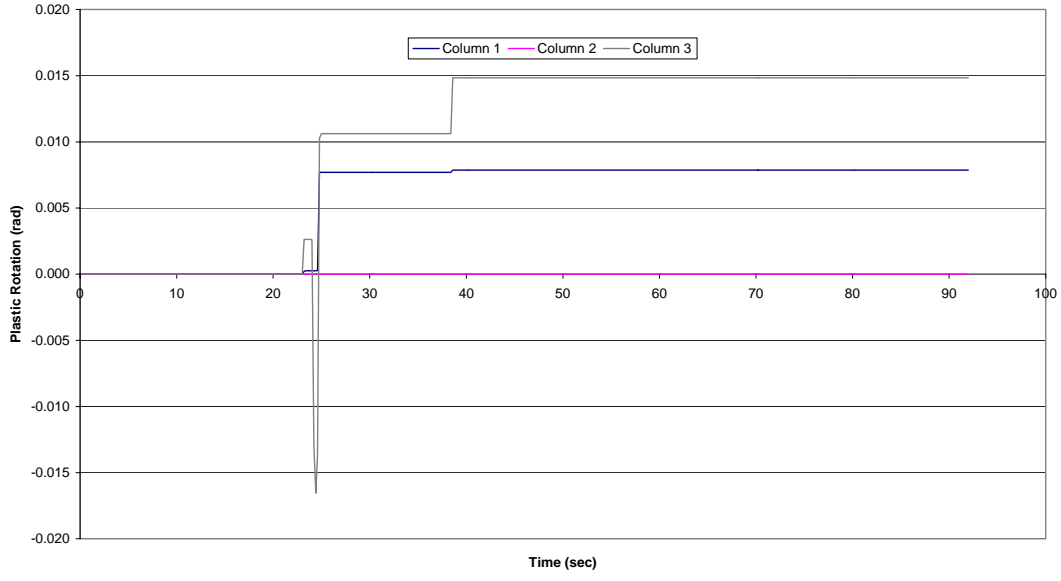


Figure 6.4-6 Plastic Rotations at the Bottom of the Columns for the Bent Model

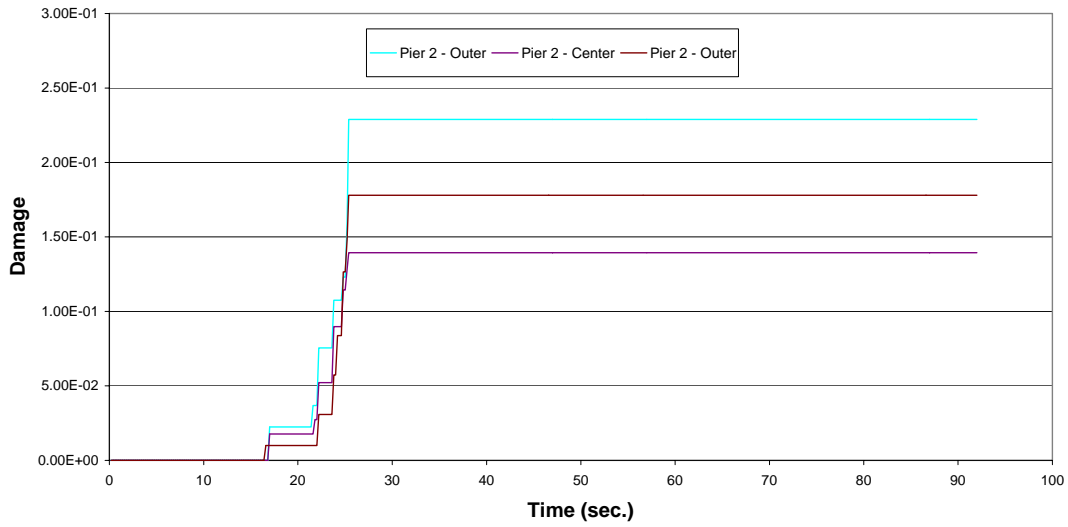


Figure 6.4-7 Damage at the Top of the Columns for the Bridge Pier

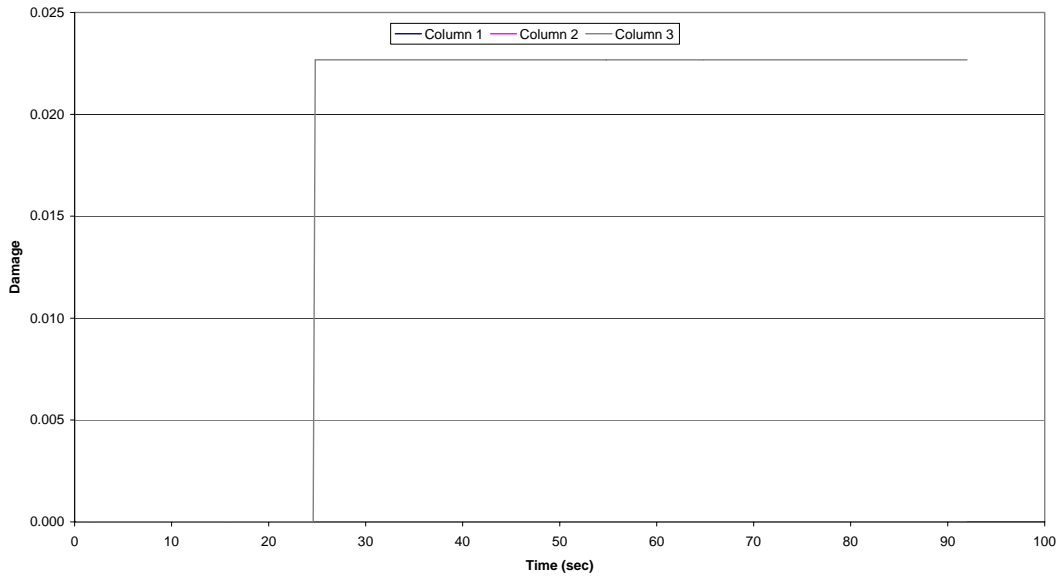


Figure 6.4-8 Damage at the Top of the Columns for the Bent Model

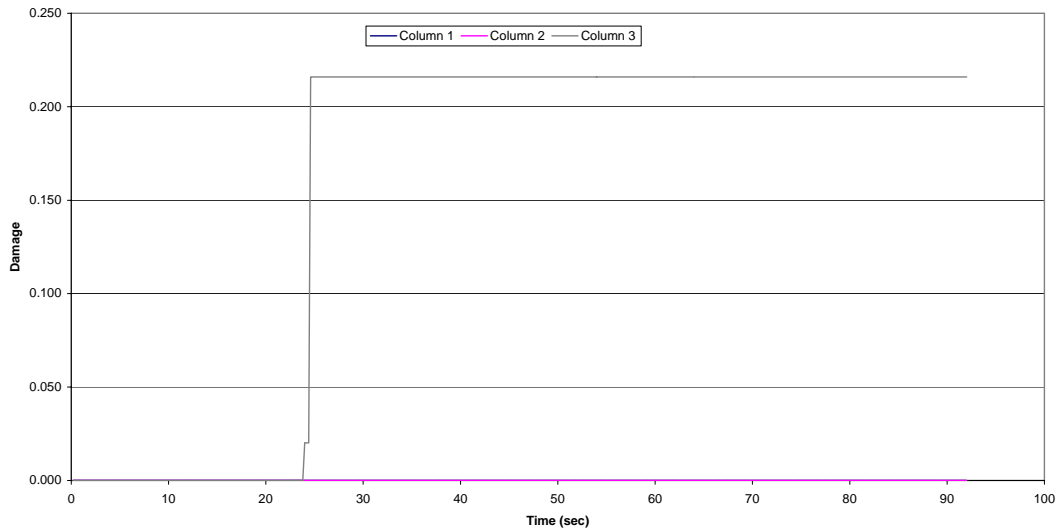


Figure 6.4-9 Damage at the Bottom of the Columns for the Bent Model

The damage in the bent model is at nearly the same level as the bridge pier, but the biggest difference is that the bent model only shows damage in one of the outer columns. The major portion of the damage in the bent model was at the bottom of the

column, but it was at the top of the column in the bridge pier. The differences in damage and the fact that the other columns of the bent model do not accumulate damage, is most likely attributed to the fact that the bent model does not incorporate ground accelerations in the longitudinal direction.

The maximum shear values at the top and bottom of the columns are shown in Table 6.4-2. The shear values compare fairly closely for the two different cases. The shear in the columns of the pier from the bridge model are slightly higher than those of the bent model, but none of them are at the level of failure.

Table 6.4-2 Maximum Shear (kips) at the Top and Bottoms of Columns

Model	Column	Shear			
		Top	Demand/ Capacity	Bottom	Demand/ Capacity
Bridge Pier	1	114.79	0.67	123.03	0.72
	2	104.14	0.61	118.73	0.69
	3	116.11	0.68	127.76	0.74
Bent Model	1	96.69	0.56	99.67	0.58
	2	118.80	0.69	118.7	0.69
	3	105.7	0.62	90.96	0.53

Chapter 7

Summary and Conclusions

7.1 Summary

The computer program WSU–NEABS (WSU-Nonlinear Earthquake Analysis of Bridge Systems) was modified to allow for damage accumulation in the columns based solely on cycles of plastic rotation. The new damage model was calibrated from testing done by Stapleton (2004) and then implemented into the program. The modified program with the new damage model was then tested using models created to simulate actual test specimens from the work of Stapleton (2004) and Kunnath (1997).

Two existing highway bridges were modeled using finite element spine models and then analyzed with the modified version of the nonlinear analysis program. The analyses were done in two stages, the first of which included a suite of ten earthquakes. The ten earthquakes were applied to the two bridge models, while the soil stiffness at the column bases and the abutments, based on existing soil conditions, were held constant. The second stage of the analyses involved a parametric study, in which the soil properties at the column bases and abutments were varied. In each case, the response of the bridge was then compared to that of the base case in the first stage.

A single bent model was also constructed to model the center pier of Bridge 5/518. This model was then analyzed to determine if a bent model can be used to approximate the response of the bridge or if the entire bridge model is necessary.

7.2 Analyses with Constant Soil Stiffness

Table 7.2-1 shows a summary of the response of Bridge 5/518 to all ten earthquakes. The modified Peru earthquake caused the most damage, but it is only at a level that would cause light cracking throughout the column section. It is interesting to note that, besides the two modified earthquakes, which are extreme cases, damage only occurs in the center pier or does not occur at all. This would suggest that the center pier would be the most important pier to retrofit.

Table 7.2-1 Summary of Results for Bridge 5/518

Earthquake	Max. Damage Level	Piers Damaged	Max. Column Shear Demand/ Capacity	Max. Abutment Demand/ Capacity	Pounding (Y/N)	Bearing Pad Failure (Y/N)
Modified Peru	0.229	1,2,3	0.75	0.55	Y	Y
Unmodified Peru	0.019	2	0.47	0.09	Y	N
Modified Chile	0.167	1,2,3	0.77	0.43	Y	Y
Unmodified Chile	0.031	2	0.53	0.15	Y	Y
Mexico City - 475	0.000	N/A	0.32	0.06	N	N
Mexico City- 950	0.019	2	0.52	0.10	Y	Y
Olympia - 475	0.000	N/A	0.34	0.07	N	N
Olympia - 950	0.017	2	0.51	0.13	Y	Y
Kobe – 475	0.000	N/A	0.39	0.10	Y	Y
Kobe – 950	0.020	2	0.55	0.20	Y	Y

Although the damage in the columns is at a level that would only cause minor damage, there are two other issues that are of concern. Pounding occurs in almost every

case and possible bearing pad failures could occur during the majority of the earthquakes. This suggests that retrofitting of the expansion joints is needed.

The shear levels in the columns and the abutments are all below their capacities. Under the loading of the more extreme modified earthquakes, the shear in the columns reaches a level that would cause problems for those that have smaller aspect ratios. The levels of shear in the abutments are all well below their capacity, and this type of failure does not seem to be of much concern.

With one of the major issues of this research being long-duration earthquakes, it should be noted that for the cases for which long-duration events were applied, there was more accumulated damage than for those in which a short-duration event was applied. However, this is not all due to the fact that it is a long-duration event. It seems that the more important issue is the amplitude of the ground motion and the duration of strong motion that actually causes yielding.

Long-duration events in the Puget Sound region of Washington State have many more loading cycles, but most of those cycles are not at levels that cause yielding and, hence, do not affect damage. Therefore, it is necessary to do a more in-depth study of the general behavior of long and short-duration earthquakes. This should be done to determine if it is a general trend for long-duration events to have greater amplitudes and longer strong motion durations that cause yielding. If this is true, then it can be stated that long-duration earthquakes are truly more damaging than short-duration earthquakes. It should also be noted that typically, as the magnitude of the earthquake increases, the duration of the event increases as well.

Better understanding of damaged columns under elastic loading is also necessary to determine if long-duration events are more damaging. Research should be performed to determine if there is any hysteretic action that occurs when the damaged columns are acting elastically. If there is hysteretic action in this situation, then long-duration events would have more damage than short-duration earthquakes, and this would need to be included in the damage model.

Table 7.2-2 shows a summary of the response of Bridge 5/826 to all ten earthquakes. It is seen that none of the earthquakes cause damage in the columns, and only in the cases of the modified earthquakes was there slight yielding. This is due to the fact that this bridge has a higher transverse reinforcement ratio in the plastic hinge region of the columns. The bridge also has a continuous deck, which provides much more restraint in the transverse direction. Coupled with the fact that there are not any expansion joints at the intermediate piers to allow more longitudinal displacement, the total relative displacements of the columns decreased considerably from those of Bridge 5/518.

With this reduction in displacement, it can be seen that the shear demand at the abutments is increased in all cases, compared to that of Bridge 5/518, except those of the modified earthquakes. Although the shear demands in the abutments are increased, they are still well below their capacity. Conversely, the decrease in displacement reduced the shear level in the columns. This is dependent on the stiffness of the abutment because, as the stiffness increases, the abutment provides more restraint and the displacements decrease. It should be noted that there is pounding at the abutments in every case, and most of them could have bearing pad failures.

Table 7.2-2 Summary of Results for Bridge 5/826

Earthquake	Max. Damage Level	Piers Damaged	Max. Column Shear Demand/ Capacity	Max. Abutment Demand/ Capacity	Pounding (Y/N)	Bearing Pad Failure (Y/N)
Modified Peru	0.000	N/A	0.59	0.45	Y	Y
Unmodified Peru	0.000	N/A	0.35	0.16	Y	N
Modified Chile	0.000	N/A	0.52	0.40	Y	Y
Unmodified Chile	0.000	N/A	0.30	0.18	Y	N
Mexico City - 475	0.000	N/A	0.28	0.13	Y	Y
Mexico City- 950	0.000	N/A	0.38	0.26	Y	N
Olympia - 475	0.000	N/A	0.30	0.19	Y	N
Olympia - 950	0.000	N/A	0.36	0.27	Y	Y
Kobe – 475	0.000	N/A	0.33	0.19	Y	Y
Kobe – 950	0.000	N/A	0.46	0.28	Y	Y

7.3 Analyses with Varying Soil Stiffness

Table 7.3-1 shows the analysis protocol for this stage of the study. Tables 7.3-2 and 7.3-3 show summaries of the responses of the two bridges to the variation in support properties. It can be seen that, for these bridges, the cases with the most damage are those for which the columns were fixed and rollers were applied to the abutments. Even with this change, however, the damage is only at a level that would result in light to medium damage, but shear failures would occur.

Table 7.3-1 Analysis Protocol

Run No.	Bridge	Earthquake	Column Base Soil Spring Stiffness	Abutment Soil Spring Stiffness
1	5/518	Modified Peru	Fixed	Roller – Both Directions
2	5/518	Modified Peru	Fixed	Roller – Longitudinal Only
3	5/518	Modified Peru	Unchanged	Increase by a factor of 10
4	5/518	Modified Peru	Unchanged	Roller – Longitudinal Only
5	5/518	Modified Peru	Decrease by a factor of 10	Unchanged
6	5/518	Modified Peru	Fixed	Unchanged
7	5/518	Modified Chile	Fixed	Roller – Both Directions
8	5/826	Modified Peru	Fixed	Roller – Longitudinal Only
9	5/826	Modified Peru	Fixed	Roller – Both Directions
10	5/518	Olympia 950-Year	Fixed	Roller – Both Directions
11	5/518	Kobe 950-Year	Fixed	Roller – Both Directions
12	5/826	Olympia 950-Year	Fixed	Roller – Both Directions
13	5/826	Kobe 950-Year	Fixed	Roller – Both Directions

Table 7.3-2 Summary of Results for Bridge 5/518

Run No.	Max. Damage Level	Damage at Top or Bottom	Piers Damaged	Max. Column Shear Demand/ Capacity	Pounding (Y/N)	Bearing Pad Failure (Y/N)
1	0.188	Both	1,2,3	1.04	Y	Y
2	0.212	Both	1,2,3	0.87	N	N
3	0.193	Top	1,2	0.72	Y	N
4	0.154	Top	1,2,3	0.78	Y	N
5	0.072	Top	1,2	0.61	Y	Y
6	0.214	Both	1,2,3	0.90	Y	Y
7	0.185	Both	1,2,3	0.86	N	Y
10	0.071	Both	2	0.86	N	N
11	0.040	Both	2	0.83	N	N

Table 7.3-3 Summary of Results for Bridge 5/826

Run No.	Max. Damage Level	Damage at Top or Bottom	Piers Damaged	Max. Column Shear Demand/ Capacity	Pounding (Y/N)	Bearing Pad Failure (Y/N)
8	0.058	Both	1,2,3	1.07	N/A	N/A
9	0.086	Both	1,2,3	0.94	N/A	N/A
12	0.057	Both	1	0.84	N/A	N/A
13	0.027	Both	1,3	0.84	N/A	N/A

Besides increasing the damage, fixing the column bases caused the damage to occur at both the top and bottom of the columns, whereas the damage occurred only at the top of the columns when soil springs were used. The fixed-roller cases also increased the level of shear in the columns to a point at which some of them would likely fail. Predictions also show that pounding will occur and that there could be bearing pad failures.

This study also showed that a variation in the abutment stiffness, while the column base stiffnesses were left unchanged, affected the pounding and bearing pad behavior. By allowing a roller at the abutment, the pounding and occurrences of bearing pad failures decreased. When the abutment stiffness is left unchanged and the column base stiffnesses were varied, there was a greater variation in the column damage and shear force in the columns.

Using soil springs when modeling is more realistic than using fixed bases, although these results show that using fixed conditions at columns with roller conditions at abutments is a conservative estimate as far as the damage and shear in the columns is concerned. However, the model with soil springs applied at the columns and abutments better predicts pounding and possible bearing pad failure. Therefore, this should be investigated further to determine if retrofitting is necessary. In general, the use of spring supports to simulate soil conditions involves little extra effort, yet leads to increased accuracy in the results. Therefore, the use of springs to represent the supporting soil is recommended.

7.4 Bent Model Comparison

The bent model showed smaller relative transverse displacements than those from the center pier of the full bridge model. It also had residual displacement, while the residual displacement in the pier of the bridge model was negligible. This is due to the fact that the bent model does not have any restraint from abutments like the bridge model does. The damage found in the bent model was comparable to the bridge pier but it occurred at the bottom of the column rather than the top. The damage occurred in one of

the outer columns of the bent model, but in the full bridge model, there was considerable damage in all of the columns.

Most of these differences are likely due to the fact that the bent model only has ground accelerations in the transverse and vertical directions. The effects from the longitudinal response are totally ignored. Taking all of these differences into account, the bent model does a somewhat unsatisfactory job of capturing the response of the bridge pier.

7.5 Recommendations for Future Work

Further investigation into the bent model should be done. If the results are found to be satisfactory, then it could be utilized in a probabilistic study. A formulation with a variation of short and long-duration earthquakes could be applied to the bent model to help determine if long duration earthquakes are more damaging.

Work should also be done to determine what the effects of aftershocks would be to the model. It would be helpful to understand what the response of the model would be if an aftershock event followed a large damaging event. Further study would have to be done to develop an accurate aftershock record.

More research needs to be done to determine the effects that elastic loading cycles have after large damaging cycles have already occurred. The damage model that has been added to this program does not take this into account due to the fact that damage is only accumulated if inelastic behavior occurs. If it is found that elastic cycles cause damage after large inelastic cycles have occurred, this would need to be added to the current damage model. This issue has been brought up by other researchers, but the

study by Stapleton (2004) does not show that this is a major issue, although further research should be done to verify this.

This study also shows that soil-structure interaction has a large effect on the overall response of the bridge models. This should also be researched further with a more in-depth study. This study would be important because soil-structure interaction is one of the more random aspects of bridge modeling.

References

- American Association of State Highway and Transportation Officials (1998). *LRFD Bridge Design Specifications, 2nd Edition*. AASHTO.
- Atkinson, G.M. and Boore, D.M. (2003). “Empirical Ground-Motion Relations for Subduction Zone Earthquakes and Their Application to Cascadia and Other Regions.” *Bulletin of the Seismological Society of America*, 93(4), 1703-1729.
- Baber, T.T., and Noori, M.N. (1985). “Random Vibration of Degrading, Pinching Systems.” *Journal of Engineering Mechanics*, 111(8), 1010-1026.
- Bouc, R. (1967). “Forced Vibration of Mechanical Systems with Hysteresis.” *Proceedings of the 4th Conference on Non-Linear Oscillations*.
- Bozorgnia, Y., Bertero, V. (2003). “Damage Spectra: Characteristics and Applications to Seismic Risk Reduction.” *Journal of Structural Engineering, ASCE*, Vol. 129, No. 10, 1330-1340.
- Bracci, J.M., Reinhorn, A.M., Mander, J.B., and Kunnath, S.K. (1989). “Deterministic Model for Seismic Damage Evaluation of RC Structures.” *Technical Report NCEER-89-0033*, National Center for Earthquake Engineering Research, State University of New York, Buffalo NY.
- Bresler, B., “Design Criteria for Reinforced Columns under Axial Load and Biaxial Bending.” *American Concrete Institute*, Vol. 32, No. 5, November 1960.
- California Department of Transportation. *Seismic Design Criteria*. Sacramento, CA, Government Printing Office, 2004.

- Casciati, F. (1989). "Stochastic Dynamics of Hysteretic Media." *Structural Safety*, Amsterdam, 6, 259-269.
- Chung, Y.S., Meyer, C., and Shinozuka, M. (1987). "Seismic Damage Assessment of RC Members." *Technical Report NCEER-87-0022*, National Center for Earthquake Engineering Research, State University of New York, Buffalo NY.
- Chung, Y.S., Meyer, C., and Shinozuka, M. (1989a). "Modeling of Concrete Damage." *Structural Journal, American Concrete Institute*, Vol. 86, No. 3, 259-271.
- Cofer, W.F., McLean, D.I., and McGuire, J.W. (1994). "Analytical Modeling of Foundation for Seismic Analysis of Bridges." *Research Report T9234-02*, Washington State Department of Transportation, February 1994.
- Frankel, A., Mueller, C., Barnhard, T., Perkins, D., Leyendecker, E. V., Dickman, N., Hanson, S., and Hopper, M. (1996). National Seismic-Hazard Maps: Documentation, U.S. Geological Survey, U.S. Department of the Interior.
- Gosain, N.K., Brown, R.H., and Jirsa, J.O. (1977). "Shear Requirements for Load Reversals on RC Members." *Journal of Structural Engineering, ASCE*, Vol. 103, No. 7, 1461-1476.
- Gregor, N.J., Silva, W.J., Wong, I.G., and Youngs, R.R. (2002). "Ground-Motion Attenuation Relationships for Cascadia Subduction Zone Megathrust Earthquakes Based on a Stochastic Finite-Fault Model." *Bulletin of the Seismological Society of America*, 92(5), 1923-1932.

- Jeong, G.D., and Iwan, W.D. (1988). "Effect of Earthquake Duration on the Damage of Structures." *Earthquake Engineering and Structural Dynamics*, Vol. 16, No. 8, 1201-1211.
- Kowalsky, M.J., Priestley, M.J.N. (2000). "Improved Analytical Model for Shear Strength of Circular Reinforced Concrete Columns in Seismic Regions." *ACI Structural Journal*, 97(3), 388-397.
- Kratzig, W.B., Meyer, I.F., and Meskouris, K. (1989). "Damage Evolution in Reinforced Concrete Members Under Cyclic Loading." *Proc. 5th Int. Conf. on Structural Safety and Reliability (ICOSSAR 89)*, San Francisco CA, Vol. II, 795-802.
- Kratzig, W.B., Petryna, Y.S., and Stangenberg, F. (2000). "Measures of Structural Damage for Global Failure Analysis." *Int. Journal of Solids and Structures*, Vol. 37, 7393-7407.
- Kunnath, S.K., El-Bahy, A., Taylor, A.W., and Stone W.C. (1997). "Cumulative Seismic Damage of Reinforced Concrete Bridge Piers." *Technical Report NISTIR 6075*. Gaithersberg, MD: Building and Fire Research Laboratory, National Institute of Standards and Technology.
- Kunnath, S.K., Reinhorn, A.M., Lobo, R.F. (1992). "IDARC Version 3.0: A Program for the Inelastic Damage Analysis of RC Structures." *Technical Report NCEER-92-0022*, National Center for Earthquake Engineering Research, State University of New York, Buffalo NY.
- Lehman, D., Moehle, M., Mahin, S., Calderone, A., Henry, L. (2004). "Experimental Evaluation of the Seismic Performance of Reinforced Concrete Bridge Columns." *Journal of Structural Engineering, ASCE*, Vol. 130, No. 6, 869-879

- Lindt, J.W., Goh, G. (2004). "Earthquake Duration Effect on Structural Reliability." *Journal of Structural Engineering, ASCE*, Vol. 130, No. 5, 821-826
- Makris, N., Zhang, J. (2004). "Seismic Response Analysis of a Highway Overcrossing Equipped with Elastomeric Bearings and Fluid Dampers." *Journal of Structural Engineering, ASCE*, Vol. 130, No. 6, 830-845
- Mander, J.B., and Cheng, C.T. (1995). "Replaceable Hinge Detailing for Bridge Columns." *National Seismic Conference on Bridges and Highways*, San Diego, CA, December 10-13.
- Mander, J.B., Panthaki, A.M., and Kasalanati, A. (1994). "Low Cycle Fatigue Behavior of Reinforcing Steel." *Journal of Materials in Civil Engineering, ASCE*, 6(4),453-468
- Manfredi, G. and Pecce, M (1997). "Low Cycle Fatigue of RC Beams in NSC and HSC." *Engineering Structures*, Vol. 19, No. 3, 217-223.
- Manson, S. S., (1953). "Behavior of Materials under Conditions of Thermal Stress." *Heat Transfer Symposium*, University of Michigan Engineering Research Institute, Ann Arbor, Michigan, pp. 9-75
- Marigo, J.J. (1985). "Modeling of Brittle and Fatigue Damage for Elastic Materials by Growth of Microvoids." *Engineering Fracture Mechanics*, 21(4), 861-874.
- Marsh, M.L. (1991). "Effects of Flexural Strength Variations on the Seismic Performance of Reinforced Concrete Multiple Column Bridge Bents, *Doctoral Thesis*, University of Washington.
- NRCan (2004). "Earthquake Processes: Cascadia Subduction Zone." Natural Resources Canada. Accessed online at: <http://www.nrcan.gc.ca/geodyn/cascadia.htm>

- Park, Y.J., Reinhorn, A.M., and Kunnath, S.K. (1987). "IDARC: Inelastic Damage Analysis of Reinforced Concrete Frame-Shear Wall Structures." *Technical Report NCEER-87-0008*, State University of New York, Buffalo NY.
- Pincheria, J.A., Dotiwala, F.S., and D'Souza, J.T. (1999). "Seismic Analysis of Older Reinforced Concrete Columns." *Earthquake Spectra, EERI*, Vol. 15, No. 2, 245-272.
- PNSN (2004). "Deep Quakes in Washington and Oregon." Pacific Northwest Seismograph Network, University of Washington. Accessed online at:
http://www.pnsn.org/INFO_GENERAL/platecontours.html
- Priestley, M.J.N., Seible, F., Calvi, G.M. (1996). *Seismic Design and Retrofit of Bridges*. New York. John Wiley & Sons.
- Priestley, M.J.N. (2003). "Myths and Fallacies in Earthquake Engineering, Revisited." *The Mallet Milne Lecture*. Rose School, Pavia, Italy.
- Sivaselvan, M.V., and Reinhorn, A.M. (2000). "Hysteretic Models for Deteriorating Inelastic Structures." *Journal of Engineering Mechanics*, Vol. 126, No. 6, 633-640.
- Stapleton, S.E. (2004). "Performance of Poorly Confined Reinforced Concrete Columns in Long-Duration Earthquakes." *Masters Thesis*, Washington State University.
- Stephens, J.E., and Yao, J.T.P. (1987). "Damage Assessment Using Response Measurement." *Journal of Structural Engineering, ASCE*, Vol. 113, No. 4, 787-801.
- Thomson, E., Bendito, A., and Florez-Lopez, J. (1998). "Simplified Model of Low Cycle Fatigue for RC Frames." *Journal of Structural Engineering*, Vol. 124, No. 9, 1082-1085.

- Tseng, W., Penzien, J. (1973). "Analytical Investigations of the Seismic Response of Long Multi-Span Highway Bridges." *Earthquake Engineering Research Center*, University of California, Berkeley, California.
- Wang, M.L., and Shah, S.P. (1987). "Reinforced Concrete Hysteresis Model Based in the Damage Concept." *Earthquake Engineering and Structural Dynamics*, Vol. 15, No. 5, 255-268.
- Washington State Department of Transportation. *Bridge Design Manual*. Olympia, WA, Government Printing Office, 2002.
- Wen, Y.K. (1976). "Method for Random Vibration of Hysteretic Characteristics of Structures." *Journal of Engineering Mechanics, ASCE*, 116(8), 1798-1811.
- Williams, M.S., and Sexsmith, R.G. (1995). "Seismic Damage Indices for Concrete Structures: A State-of-the-Art Review." *Earthquake Spectra, EERI*, Vol. 11, No. 2, 319-349.
- Williamson, E.B. (2003). "Evaluation of Damage and P-Delta Effects for Systems Under Earthquake Excitation." *Journal of Structural Engineering, ASCE*, Vol. 129, No. 8, 1036-1046
- Youngs, R.R., Chiou, S.J., Silva, W.J., and Humphrey, J.R. (1997). "Strong Ground Motion Attenuation Relationships for Subduction Zone Earthquakes." *Seismological Research Letter*, 68(1), 58-73.
- Zhang, J., Makris, N., Delis, T. (2004). "Structural Characterization of Modern Highway Overcrossings – Case Study." *Journal of Structural Engineering, ASCE*, Vol. 130, No.6, 846-860

Zhang, Y. (1996). "Analytical Evaluation of Retrofit Strategies for Multi-Column Bridges." *Doctoral Thesis*, Washington State University.

Appendix A

Additional Time Histories Used in Study

Original Peru Earthquake

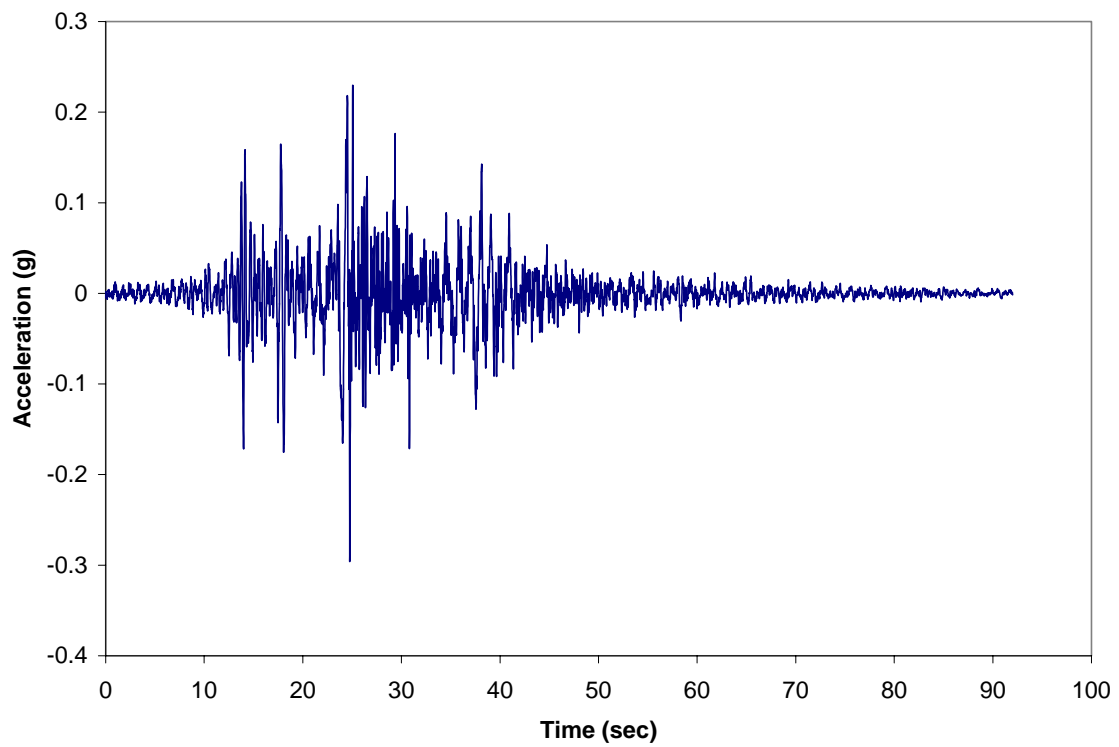


Figure A-1: Original Peru Earthquake, E-W Time History

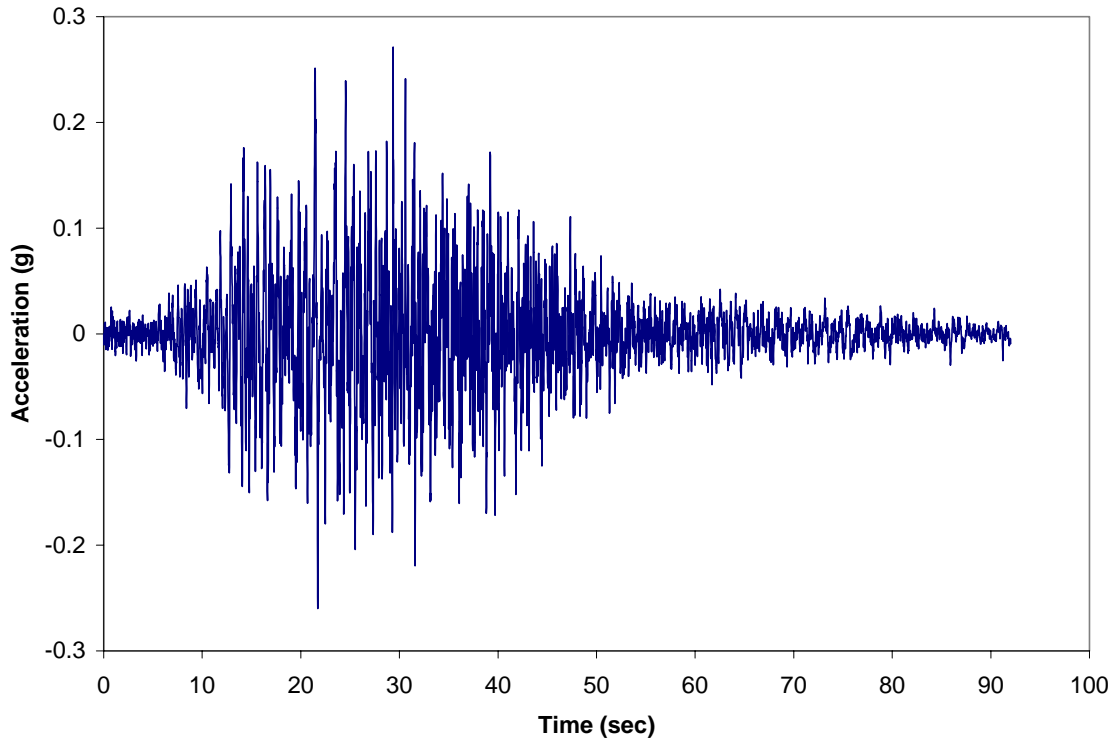


Figure A-2: Original Peru Earthquake, N-S Time History

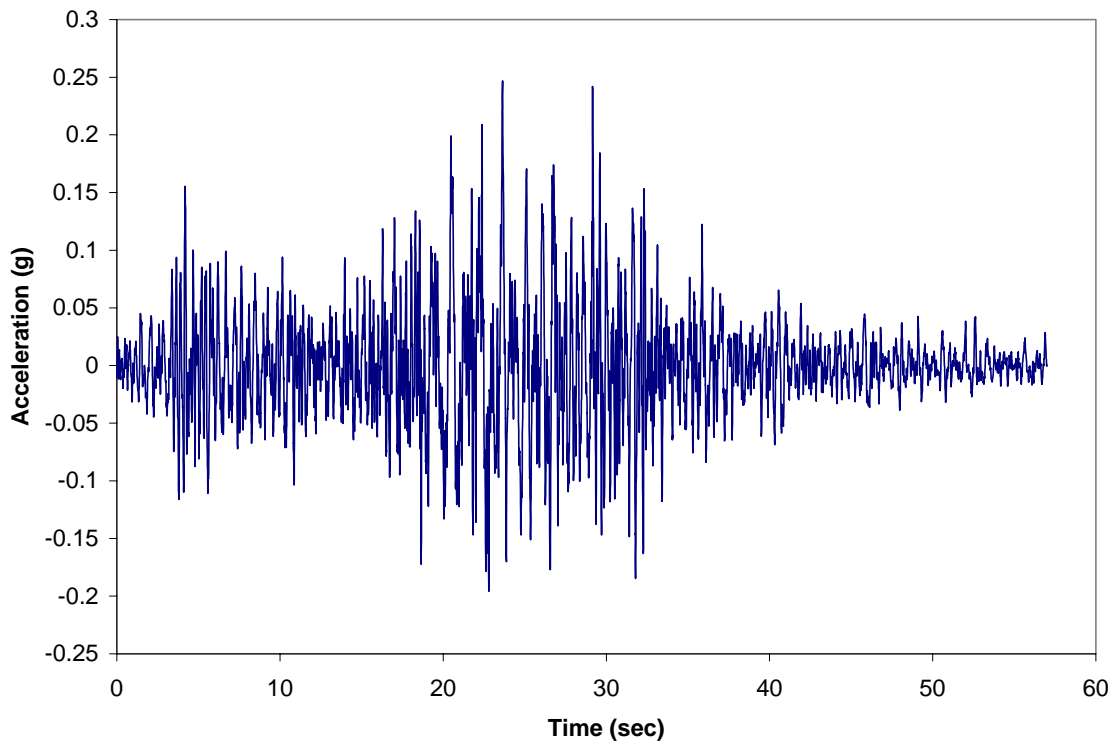


Figure A-3: Original Chile Earthquake, E-W Time History

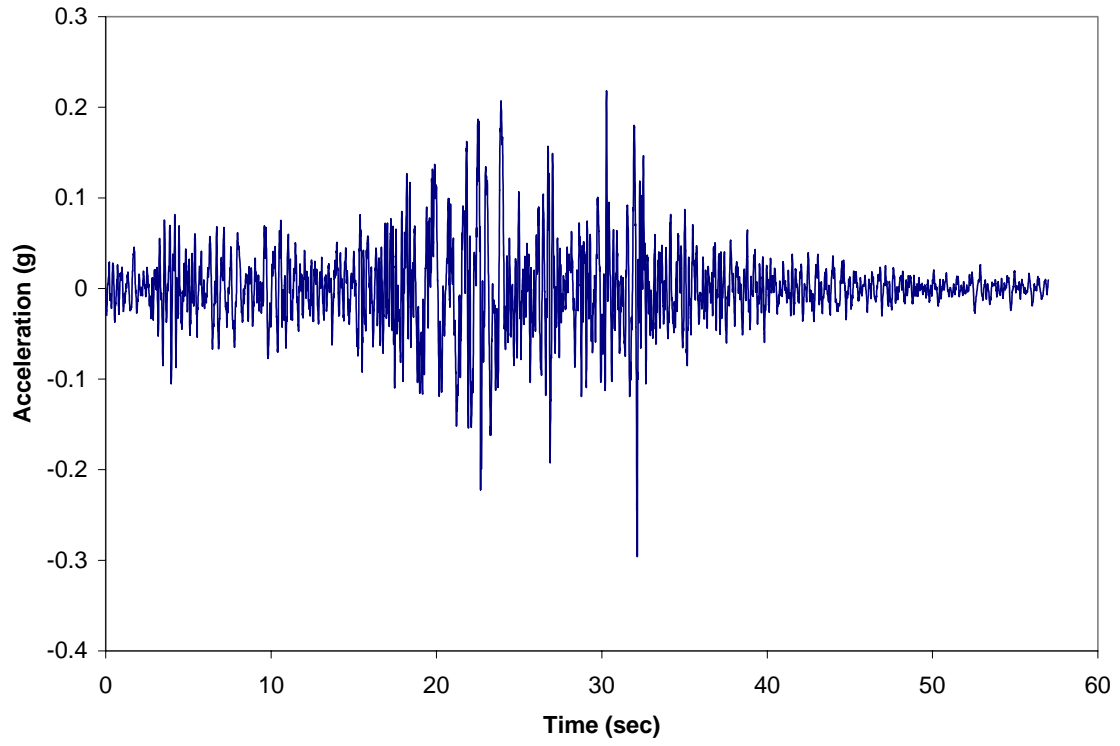


Figure A-4: Original Chile Earthquake, N-S Time History

1985 Mexico City Earthquake

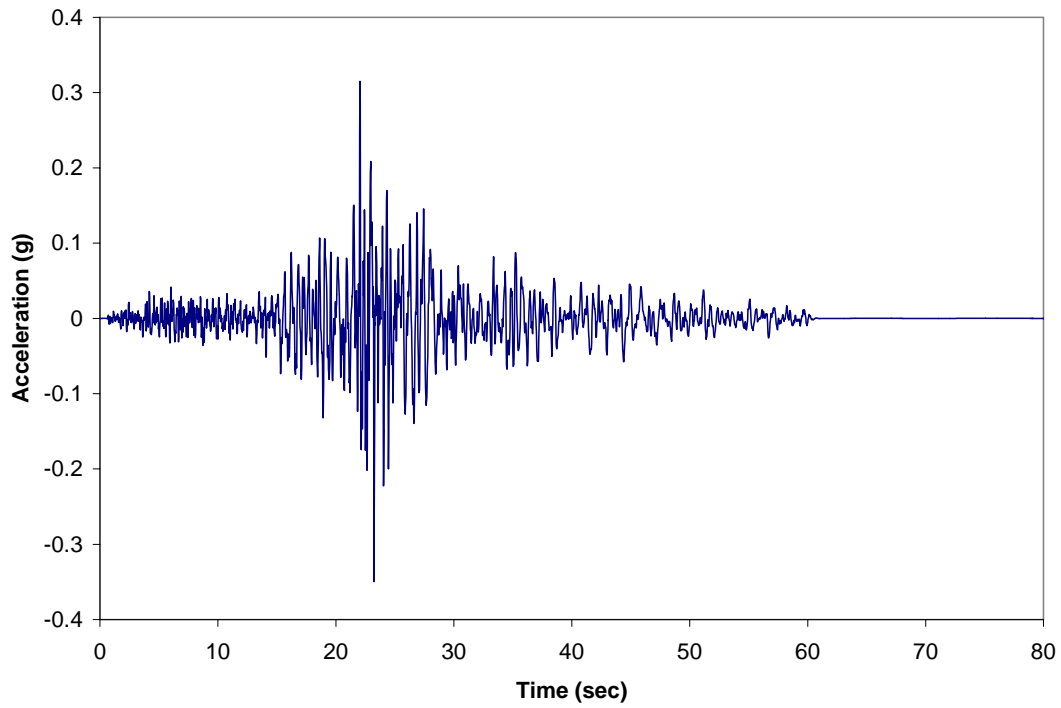


Figure A-5: 475 Year Mexico City Earthquake, E-W Time History

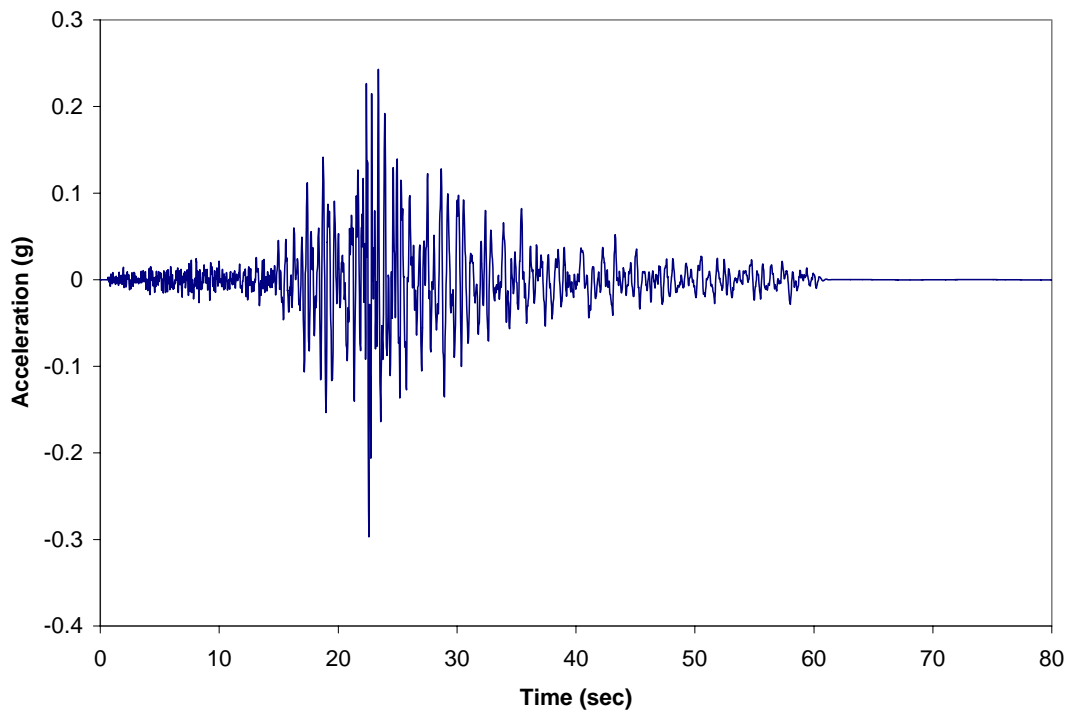


Figure A-6: 475 Year Mexico City Earthquake, N-S Time History

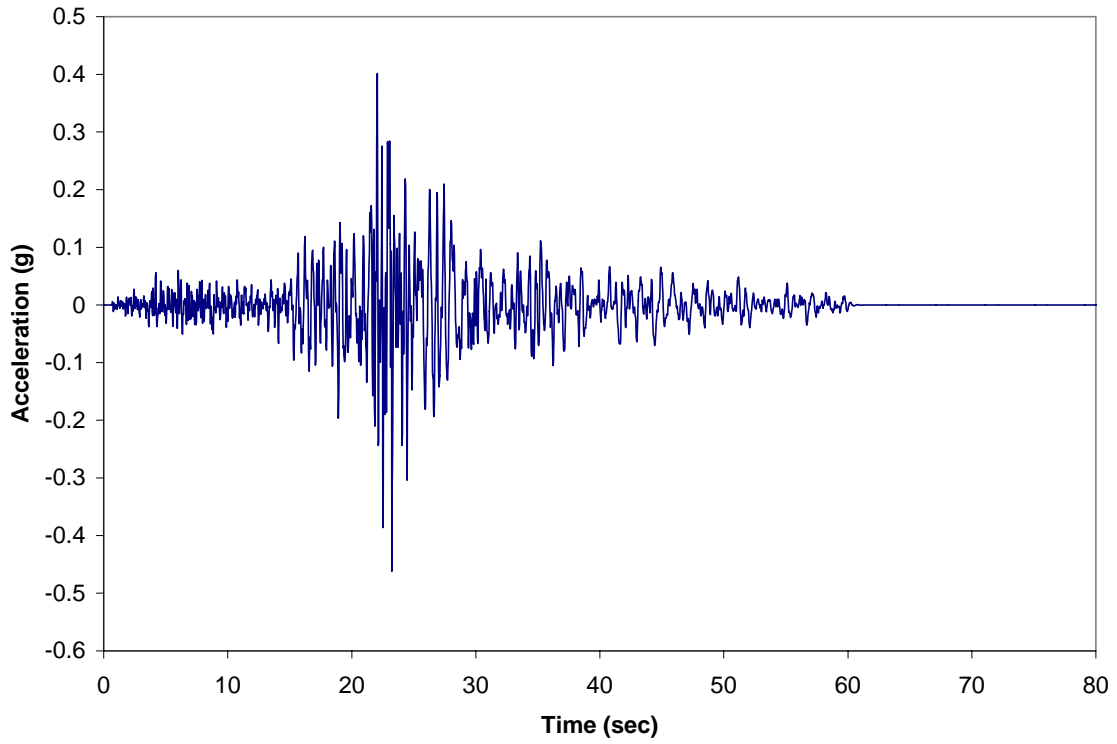


Figure A-7: 950 Year Mexico City Earthquake, E-W Time History

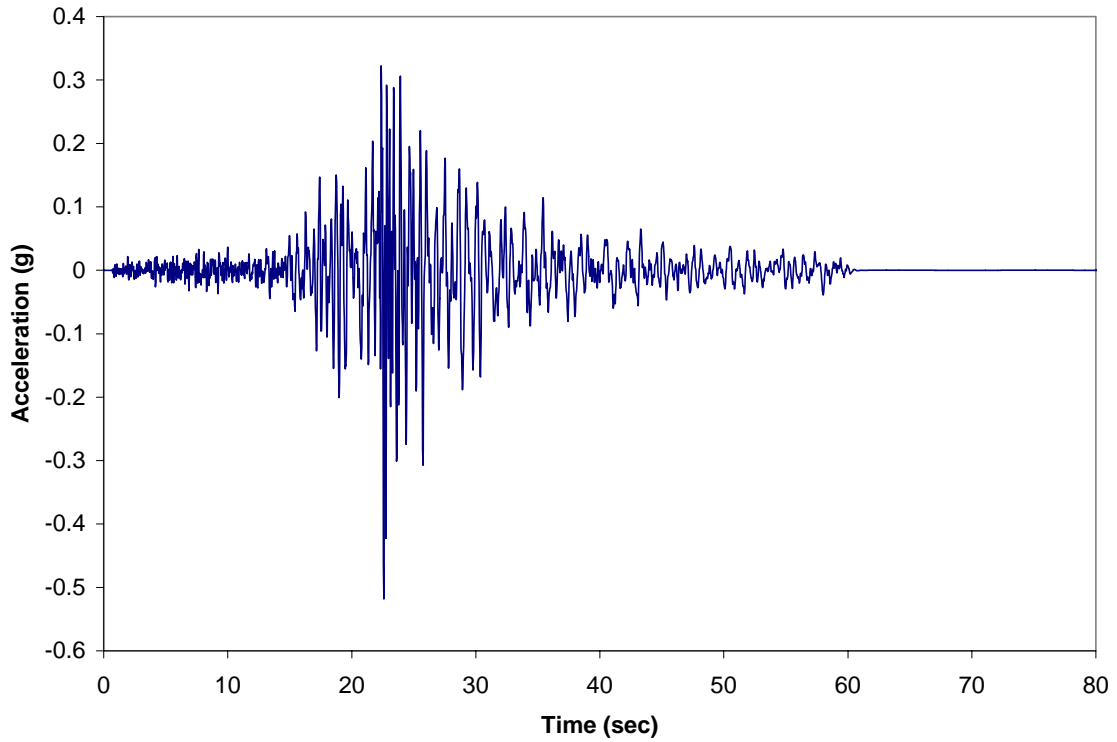


Figure A-8: 950 Year Mexico City Earthquake, N-S Time History

1996 Kobe Earthquake

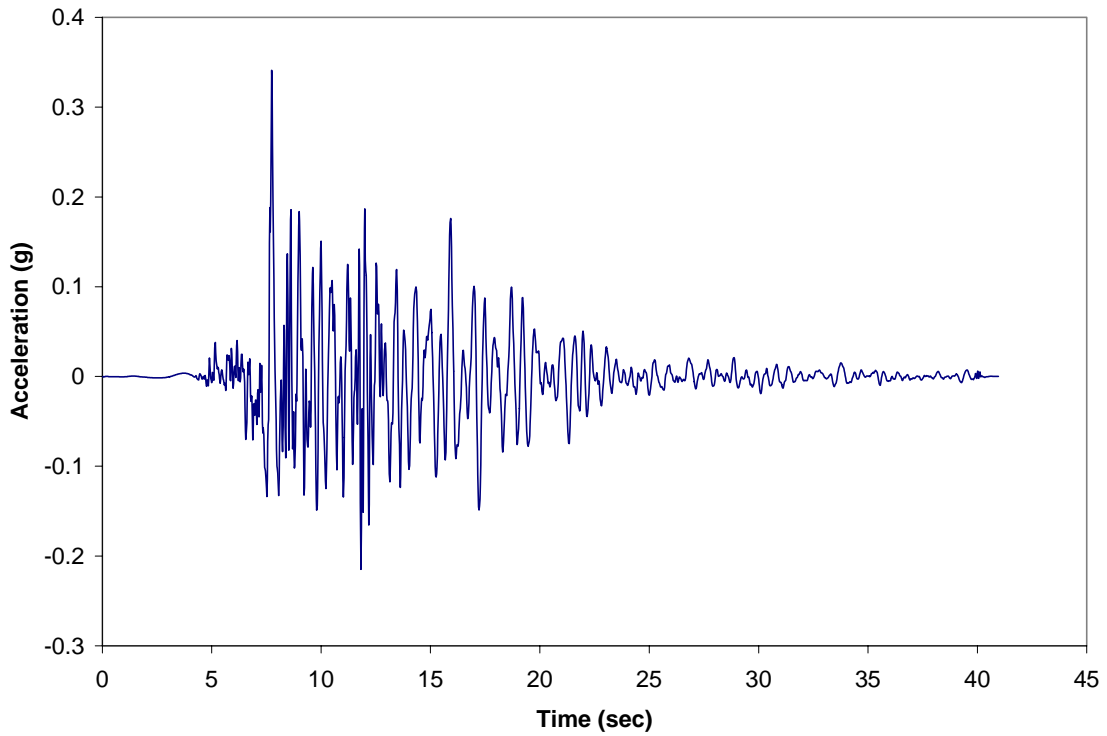


Figure A-9: 475 Year Kobe Earthquake, E-W Time History

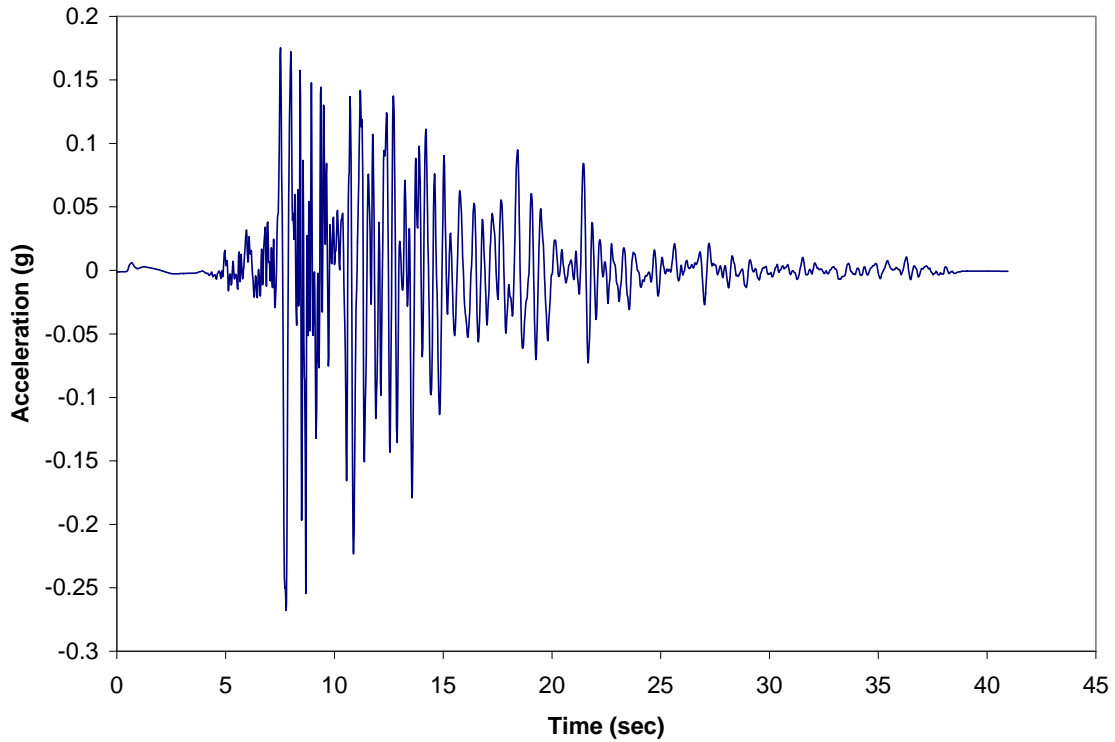


Figure A-10: 475 Year Kobe Earthquake, N-S Time History

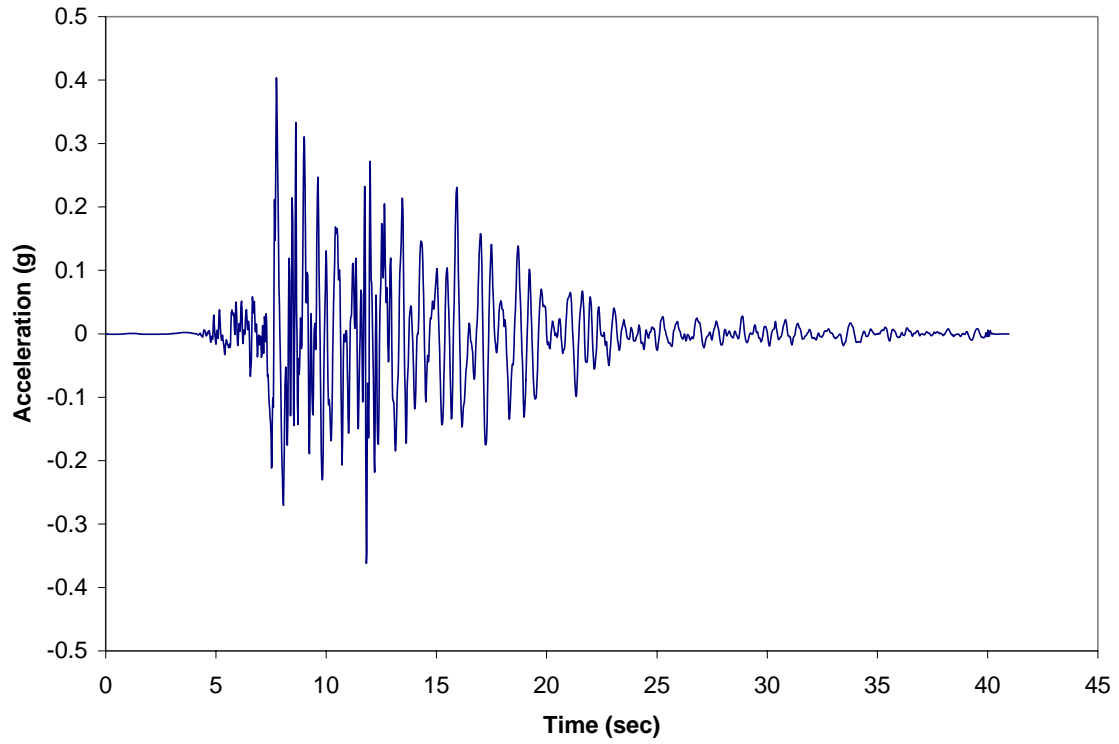


Figure A-11: 950 Year Kobe Earthquake, E-W Time History

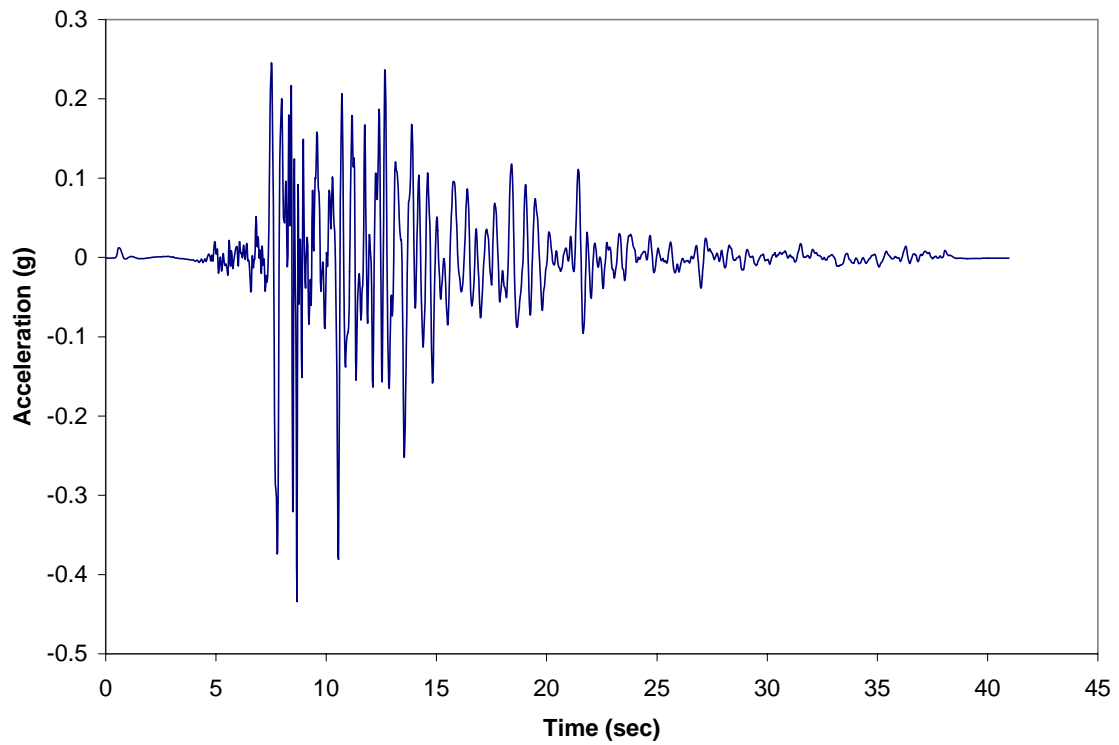


Figure A-12: 950 Year Kobe Earthquake, N-S Time History

1949 Olympia Earthquake

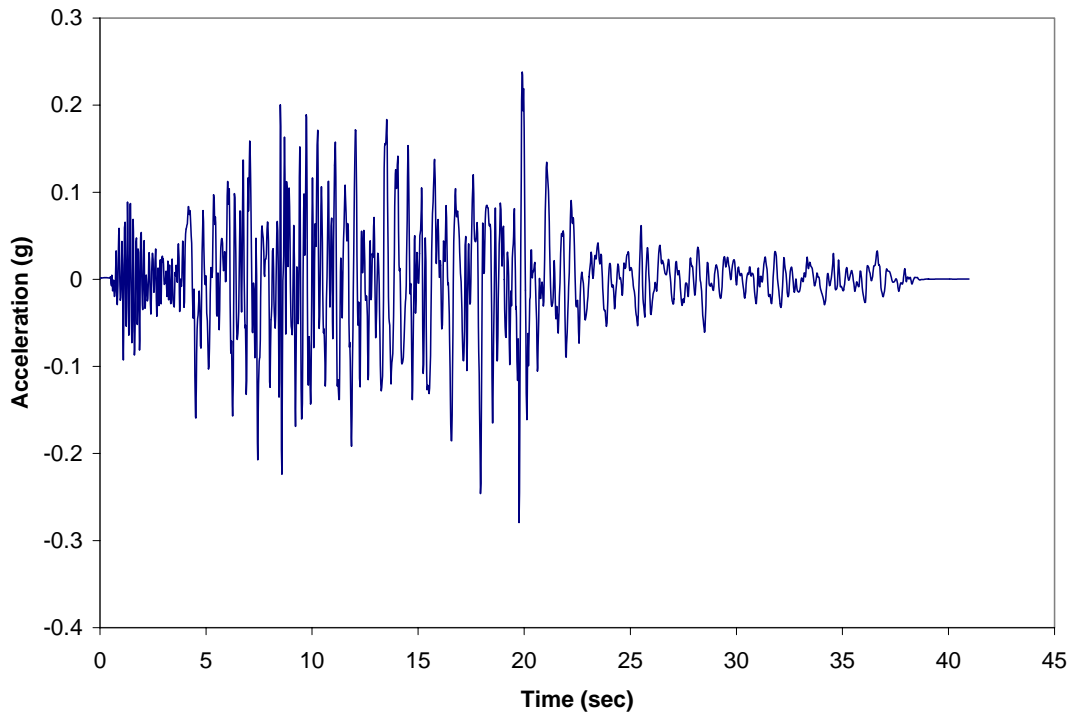


Figure A-13: 475 Year Olympia Earthquake. E-W Time History

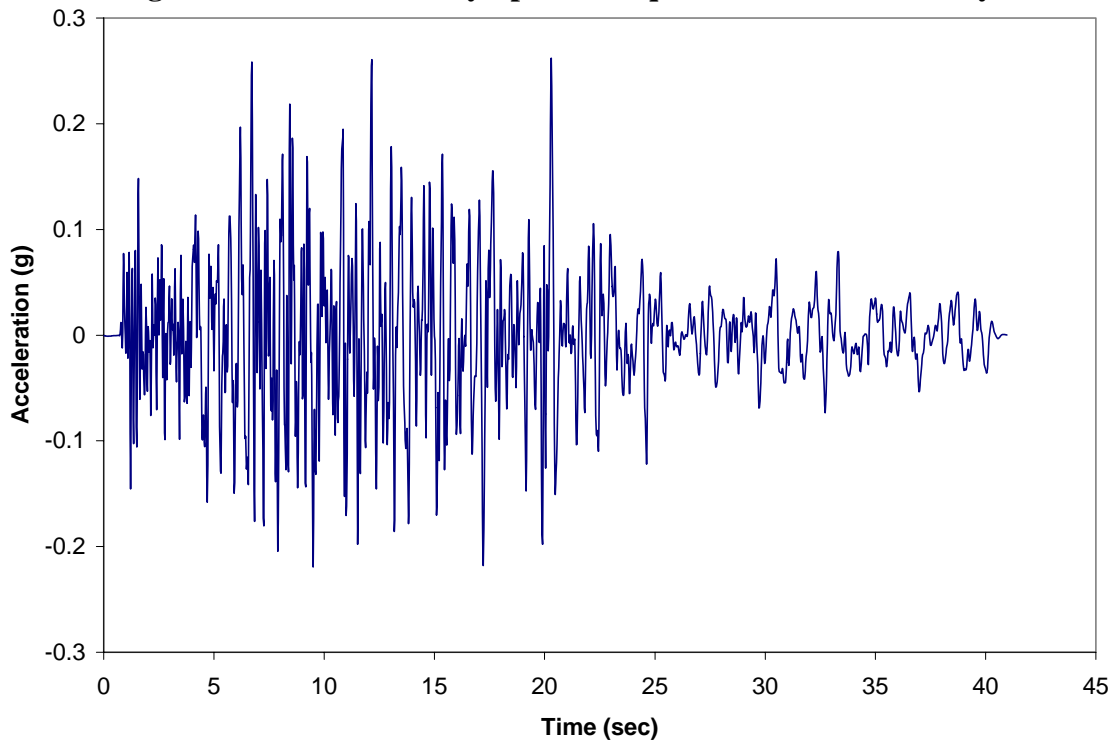


Figure A-14: 475 Year Olympia Earthquake, N-S Time History

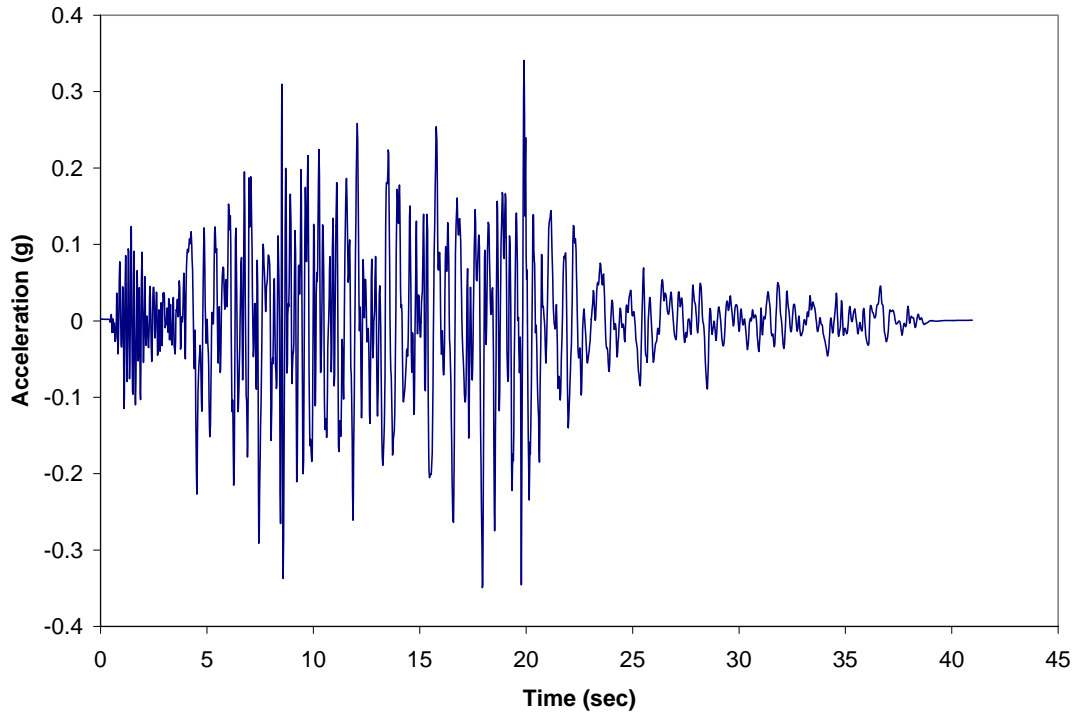


Figure A-15: 950 Year Olympia Earthquake, E-W Time History

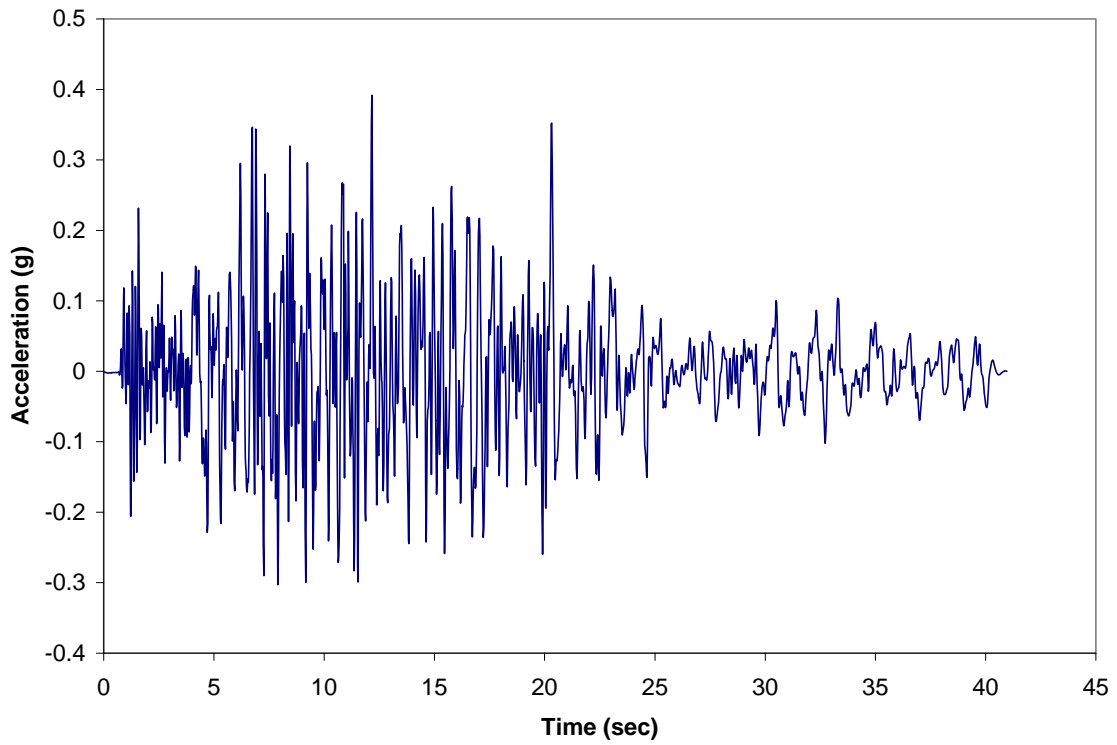


Figure A-16: 950 Year Olympia Earthquake, N-S Time History

Appendix B

Example WSU-NEABS Analysis

Bridge 5/518 Structural Model and Analysis Control Input File, "INPUT"

```
SpineBridgel
118 3 106 3 2 9205 20 .5692E+00 .4392E-02
1 0 0 0 0 0 0- .2058E+04 .0000E+00 .0000E+00
2 0 0 0 0 0 0- .2046E+04 .0000E+00 .0000E+00
3 0 0 0 0 0 0- .1839E+04 .0000E+00 .0000E+00
4 0 0 0 0 0 0- .1632E+04 .0000E+00 .0000E+00
5 0 0 0 0 0 0- .1425E+04 .0000E+00 .0000E+00
6 0 0 0 0 0 0- .1219E+04 .0000E+00 .0000E+00
7 0 0 0 0 0 0- .1217E+04 .0000E+00 .0000E+00
8 0 0 0 0 0 0- .9015E+03 .0000E+00 .0000E+00
9 0 0 0 0 0 0- .6090E+03 .0000E+00 .0000E+00
10 0 0 0 0 0 0- .3045E+03 .0000E+00 .0000E+00
11 0 0 0 0 0 0- .7500E+00 .0000E+00 .0000E+00
12 0 0 0 0 0 0 .7500E+00 .0000E+00 .0000E+00
13 0 0 0 0 0 0 .3045E+03 .0000E+00 .0000E+00
14 0 0 0 0 0 0 .6090E+03 .0000E+00 .0000E+00
15 0 0 0 0 0 0 .9015E+03 .0000E+00 .0000E+00
16 0 0 0 0 0 0 .1217E+04 .0000E+00 .0000E+00
17 0 0 0 0 0 0 .1219E+04 .0000E+00 .0000E+00
18 0 0 0 0 0 0 .1368E+04 .0000E+00 .0000E+00
19 0 0 0 0 0 0 .1518E+04 .0000E+00 .0000E+00
20 0 0 0 0 0 0 .1668E+04 .0000E+00 .0000E+00
21 0 0 0 0 0 0 .1818E+04 .0000E+00 .0000E+00
22 0 0 0 0 0 0 .1830E+04 .0000E+00 .0000E+00
23 0 0 0 0 0 0 0- .1218E+04 .1620E+03 .0000E+00
24 0 0 0 0 0 0 0- .1218E+04 .1357E+03 .0000E+00
25 0 0 0 0 0 0 0- .1218E+04 .0000E+00 .0000E+00
26 0 0 0 0 0 0 0- .1218E+04- .1357E+03 .0000E+00
27 0 0 0 0 0 0 0- .1218E+04- .1620E+03 .0000E+00
28 0 0 0 0 0 0 0 .0000E+00 .1620E+03 .0000E+00
29 0 0 0 0 0 0 0 .0000E+00 .1357E+03 .0000E+00
30 0 0 0 0 0 0 0 .0000E+00 .0000E+00 .0000E+00
31 0 0 0 0 0 0 0 .0000E+00- .1357E+03 .0000E+00
32 0 0 0 0 0 0 0 .0000E+00- .1620E+03 .0000E+00
33 0 0 0 0 0 0 0 .1218E+04 .1620E+03 .0000E+00
34 0 0 0 0 0 0 0 .1218E+04 .1357E+03 .0000E+00
35 0 0 0 0 0 0 0 .1218E+04 .0000E+00 .0000E+00
36 0 0 0 0 0 0 0 .1218E+04- .1357E+03 .0000E+00
37 0 0 0 0 0 0 0 .1218E+04- .1620E+03 .0000E+00
38 0 0 0 0 0 0 1- .2058E+04 .0000E+00- .2340E+02
39 0 0 0 0 0 0 1 .1830E+04 .0000E+00- .2340E+02
40 0 0 0 0 0 0 0- .1218E+04 .1357E+03- .2000E+03
41 0 0 0 0 0 0 0- .1218E+04 .0000E+00- .2000E+03
42 0 0 0 0 0 0 0- .1218E+04- .1357E+03- .2000E+03
43 0 0 0 0 0 0 0- .1218E+04 .1357E+03- .2184E+03
44 0 0 0 0 0 0 0- .1218E+04 .0000E+00- .2184E+03
45 0 0 0 0 0 0 0- .1218E+04- .1357E+03- .2184E+03
46 0 0 0 0 0 0 0- .1218E+04 .1357E+03- .2665E+03
47 0 0 0 0 0 0 0- .1218E+04 .0000E+00- .2665E+03
48 0 0 0 0 0 0 0- .1218E+04- .1357E+03- .2665E+03
49 0 0 0 0 0 0 0- .1218E+04 .1357E+03- .2825E+03
50 0 0 0 0 0 0 0- .1218E+04 .0000E+00- .2825E+03
51 0 0 0 0 0 0 0- .1218E+04- .1357E+03- .2825E+03
52 0 0 0 0 0 0 1- .1218E+04 .1357E+03- .3185E+03
```

53	0	0	0	0	0	1-	.1218E+04	.0000E+00-	.3185E+03
54	0	0	0	0	0	1-	.1218E+04-	.1357E+03-	.3185E+03
55	0	0	0	0	0	0	.0000E+00	.1357E+03-	.1000E+03
56	0	0	0	0	0	0	.0000E+00	.0000E+00-	.1000E+03
57	0	0	0	0	0	0	.0000E+00-	.1357E+03-	.1000E+03
58	0	0	0	0	0	0	.0000E+00	.1357E+03-	.2184E+03
59	0	0	0	0	0	0	.0000E+00	.0000E+00-	.2184E+03
60	0	0	0	0	0	0	.0000E+00-	.1357E+03-	.2184E+03
61	0	0	0	0	0	0	.0000E+00	.1357E+03-	.2666E+03
62	0	0	0	0	0	0	.0000E+00	.0000E+00-	.2666E+03
63	0	0	0	0	0	0	.0000E+00-	.1357E+03-	.2666E+03
64	0	0	0	0	0	0	.0000E+00	.1357E+03-	.2826E+03
65	0	0	0	0	0	0	.0000E+00	.0000E+00-	.2826E+03
66	0	0	0	0	0	0	.0000E+00-	.1357E+03-	.2826E+03
67	0	0	0	0	0	0	.0000E+00	.1357E+03-	.3186E+03
68	0	0	0	0	0	0	.0000E+00	.0000E+00-	.3186E+03
69	0	0	0	0	0	0	.0000E+00-	.1357E+03-	.3186E+03
70	0	0	0	0	0	0	.1218E+04	.1357E+03-	.1000E+03
71	0	0	0	0	0	0	.1218E+04	.0000E+00-	.1000E+03
72	0	0	0	0	0	0	.1218E+04-	.1357E+03-	.1000E+03
73	0	0	0	0	0	0	.1218E+04	.1357E+03-	.1900E+03
74	0	0	0	0	0	0	.1218E+04	.0000E+00-	.1900E+03
75	0	0	0	0	0	0	.1218E+04-	.1357E+03-	.1900E+03
76	0	0	0	0	0	0	.1218E+04	.1357E+03-	.2377E+03
77	0	0	0	0	0	0	.1218E+04	.0000E+00-	.2377E+03
78	0	0	0	0	0	0	.1218E+04-	.1357E+03-	.2377E+03
79	0	0	0	0	0	0	.1218E+04	.1357E+03-	.2525E+03
80	0	0	0	0	0	0	.1218E+04	.0000E+00-	.2525E+03
81	0	0	0	0	0	0	.1218E+04-	.1357E+03-	.2525E+03
82	0	0	0	0	0	0	.1218E+04	.1357E+03-	.2885E+03
83	0	0	0	0	0	0	.1218E+04	.0000E+00-	.2885E+03
84	0	0	0	0	0	0	.1218E+04-	.1357E+03-	.2885E+03
85	1	1	1	1	1	1-	.2058E+04	.2000E+03	.0000E+00
86	1	1	1	1	1	1-	.1219E+04	.2000E+03	.0000E+00
87	1	1	1	1	1	1-	.7500E+00	.2000E+03	.0000E+00
88	1	1	1	1	1	1	.1217E+04	.2000E+03	.0000E+00
89	1	1	1	1	1	1	.1830E+04	.2000E+03	.0000E+00
90	1	1	1	1	1	1	.1830E+04-	.2000E+03	.0000E+00
91	1	1	1	1	1	1-	.1218E+04	.2000E+03	.0000E+00
92	1	1	1	1	1	1	.0000E+00	.2000E+03	.0000E+00
93	1	1	1	1	1	1	.1218E+04	.2000E+03	.0000E+00
94	1	1	1	1	1	1-	.1218E+04	.1800E+03-	.3185E+03
95	1	1	1	1	1	1-	.1210E+04	.1357E+03-	.3185E+03
96	1	1	1	1	1	1-	.1210E+04	.0000E+00-	.3185E+03
97	1	1	1	1	1	1-	.1210E+04-	.1357E+03-	.3185E+03
98	1	1	1	1	1	1	.0000E+00	.1800E+03-	.3185E+03
99	1	1	1	1	1	1	.8000E+01	.1357E+03-	.3185E+03
100	1	1	1	1	1	1	.8000E+01	.0000E+00-	.3185E+03
101	1	1	1	1	1	1	.8000E+01-	.1357E+03-	.3185E+03
102	1	1	1	1	1	1	.1218E+04	.1800E+03-	.2885E+03
103	1	1	1	1	1	1	.1224E+04	.1357E+03-	.2885E+03
104	1	1	1	1	1	1	.1224E+04	.0000E+00-	.2885E+03
105	1	1	1	1	1	1	.1224E+04-	.1357E+03-	.2885E+03
106	1	1	1	1	1	1-	.2058E+04	.1000E+02-	.2340E+02
107	1	1	1	1	1	1-	.2050E+04	.0000E+00-	.2340E+02
108	1	1	1	1	1	1	.1830E+04	.1000E+02-	.2340E+02
109	1	1	1	1	1	1	.1838E+04	.0000E+00-	.2340E+02
110	0	0	0	0	0	0-	.1218E+04	.1357E+03-	.5200E+02
111	0	0	0	0	0	0-	.1218E+04	.0000E+00-	.5200E+02
112	0	0	0	0	0	0-	.1218E+04-	.1357E+03-	.5200E+02
113	0	0	0	0	0	0	.0000E+00	.1357E+03-	.5200E+02
114	0	0	0	0	0	0	.0000E+00	.0000E+00-	.5200E+02
115	0	0	0	0	0	0	.0000E+00-	.1357E+03-	.5200E+02
116	0	0	0	0	0	0	.1218E+04	.1357E+03-	.5200E+02
117	0	0	0	0	0	0	.1218E+04	.0000E+00-	.5200E+02
118	0	0	0	0	0	0	.1218E+04-	.1357E+03-	.5200E+02
2	84	6	0	3	15				
1		.1000E+07	.1800E+00	.0000E+00					
2		.3604E+04	.1800E+00	.2240E-06					
3		.3604E+06	.1800E+00	.2240E-06					
1		.1018E+04	.8553E+03	.8553E+03		.1649E+06	.8245E+05	.8245E+05	


```

2 .7134E+04 .7134E+04 .7134E+04 .1101E+06 .4257E+07 .1193E+09
3 .1872E+04 .1872E+04 .1872E+04 .1114E+08 .6161E+09 .4977E+09
4 .1872E+04 .1872E+04 .1872E+04 .1207E+08 .6532E+09 .5537E+09
5 .1872E+04 .1872E+04 .1872E+04 .1072E+08 .5868E+09 .4852E+09
6 .1018E+04 .1018E+04 .1018E+04 .1649E+06 .2000E+05 .2000E+05
.0000E+00 .0000E+00 .0000E+00 .0000E+00
.0000E+00 .0000E+00 .0000E+00 .0000E+00
-.3864E+03 .0000E+00 .0000E+00 .0000E+00
1 .1111E+04 .1580E+05 .1327E+05 .1014E+00
.1000E+01-.7881E+01-.1024E+02-.1356E+01 .1000E+01-.7881E+01-.1024E+02-.1356E+01
.5000E+02 .9000E+02 .8000E+00 .5000E+02 .9000E+02 .6000E+00 .1796E+02 .3870E-01
2 .1111E+04 .1687E+05 .1426E+05 .1014E+00
.1000E+01-.7880E+01-.1024E+02-.1360E+01 .1000E+01-.7880E+01-.1024E+02-.1360E+01
.5000E+02 .9000E+02 .8000E+00 .5000E+02 .9000E+02 .8000E+00 .1796E+02 .3870E-01
3 .1111E+04 .1493E+05 .1258E+05 .1014E+00
.1000E+01-.7880E+01-.1024E+02-.1360E+01 .1000E+01-.7880E+01-.1024E+02-.1360E+01
.5000E+02 .9000E+02 .8000E+00 .5000E+02 .9000E+02 .8000E+00 .1796E+02 .3870E-01
4 .6107E+04 .9673E+04 .9673E+04 .1600E+00
.1000E+01-.8461E+01-.1335E+02-.3888E+01 .1000E+01-.8461E+01-.1335E+02-.3888E+01
.3626E-01 .2614E+00 .8200E+00 .3626E-01 .2614E+00 .8200E+00 .1796E+02 .3870E-01
5 .6107E+04 .9673E+04 .9673E+04 .1600E+00
.1000E+01-.8461E+01-.1335E+02-.3888E+01 .1000E+01-.8461E+01-.1335E+02-.3888E+01
.3626E-01 .2614E+00 .7700E+00 .3626E-01 .2614E+00 .7700E+00 .1796E+02 .3870E-01
6 .6107E+04 .9673E+04 .9673E+04 .1600E+00
.1000E+01-.8461E+01-.1335E+02-.3888E+01 .1000E+01-.8461E+01-.1335E+02-.3888E+01
.3626E-01 .2614E+00 .7700E+00 .3626E-01 .2614E+00 .7700E+00 .1796E+02 .3870E-01
7 .6107E+04 .9673E+04 .9673E+04 .1600E+00
.1000E+01-.8461E+01-.1335E+02-.3888E+01 .1000E+01-.8461E+01-.1335E+02-.3888E+01
.3626E-01 .2614E+00 .7300E+00 .3626E-01 .2614E+00 .7300E+00 .1796E+02 .3870E-01
8 .6107E+04 .9673E+04 .9673E+04 .1600E+00
.1000E+01-.8461E+01-.1335E+02-.3888E+01 .1000E+01-.8461E+01-.1335E+02-.3888E+01
.3626E-01 .2614E+00 .8300E+00 .3626E-01 .2614E+00 .8300E+00 .1796E+02 .3870E-01
9 .6107E+04 .9673E+04 .9673E+04 .1600E+00
.1000E+01-.8461E+01-.1335E+02-.3888E+01 .1000E+01-.8461E+01-.1335E+02-.3888E+01
.3626E-01 .2614E+00 .7900E+00 .3626E-01 .2614E+00 .7900E+00 .1796E+02 .3870E-01
10 .6107E+04 .1215E+05 .1215E+05 .1609E+00
.1000E+01-.6336E+01-.9664E+01-.2328E+01 .1000E+01-.6336E+01-.9664E+01-.2328E+01
.3626E-01 .2614E+00 .8200E+00 .3626E-01 .2614E+00 .8200E+00 .1796E+02 .3870E-01
11 .6107E+04 .1215E+05 .1215E+05 .1609E+00
.1000E+01-.6336E+01-.9664E+01-.2328E+01 .1000E+01-.6336E+01-.9664E+01-.2328E+01
.3626E-01 .2614E+00 .7700E+00 .3626E-01 .2614E+00 .7700E+00 .1796E+02 .3870E-01
12 .6107E+04 .1215E+05 .1215E+05 .1609E+00
.1000E+01-.6336E+01-.9664E+01-.2328E+01 .1000E+01-.6336E+01-.9664E+01-.2328E+01
.3626E-01 .2614E+00 .8300E+00 .3626E-01 .2614E+00 .8300E+00 .1796E+02 .3870E-01
13 .6107E+04 .1215E+05 .1215E+05 .1609E+00
.1000E+01-.6336E+01-.9664E+01-.2328E+01 .1000E+01-.6336E+01-.9664E+01-.2328E+01
.3626E-01 .2614E+00 .7700E+00 .3626E-01 .2614E+00 .7700E+00 .1796E+02 .3870E-01
14 .6107E+04 .1215E+05 .1215E+05 .1609E+00
.1000E+01-.6336E+01-.9664E+01-.2328E+01 .1000E+01-.6336E+01-.9664E+01-.2328E+01
.3626E-01 .2614E+00 .8300E+00 .3626E-01 .2614E+00 .8300E+00 .1796E+02 .3870E-01
15 .6107E+04 .1215E+05 .1215E+05 .1609E+00
.1000E+01-.6336E+01-.9664E+01-.2328E+01 .1000E+01-.6336E+01-.9664E+01-.2328E+01
.3626E-01 .2614E+00 .7900E+00 .3626E-01 .2614E+00 .7900E+00 .1796E+02 .3870E-01
1 2 3 85 3 2 0 0 0 000000000000 0
2 3 4 85 3 2 0 0 0 000000000000 0
3 4 5 85 3 2 0 0 0 000000000000 0
4 5 6 85 3 2 0 0 0 000000000000 0
5 7 8 85 3 2 0 0 0 000000000000 0
6 8 9 85 3 2 0 0 0 000000000000 0
7 9 10 85 3 2 0 0 0 000000000000 0
8 10 11 85 3 2 0 0 0 000000000000 0
9 12 13 85 3 2 0 0 0 000000000000 0
10 13 14 85 3 2 0 0 0 000000000000 0
11 14 15 85 3 2 0 0 0 000000000000 0
12 15 16 85 3 2 0 0 0 000000000000 0
13 17 18 85 3 2 0 0 0 000000000000 0
14 18 19 85 3 2 0 0 0 000000000000 0
15 19 20 85 3 2 0 0 0 000000000000 0
16 20 21 85 3 2 0 0 0 000000000000 0
17 23 24 2 3 3 0 0 0 000000000000 0
18 24 25 2 3 3 0 0 0 000000000000 0

```

19	25	26	2	3	3	0	0	0	0000000000000	0
20	26	27	2	3	3	0	0	0	0000000000000	0
21	28	29	2	3	4	0	0	0	0000000000000	0
22	29	30	2	3	4	0	0	0	0000000000000	0
23	30	31	2	3	4	0	0	0	0000000000000	0
24	31	32	2	3	4	0	0	0	0000000000000	0
25	33	34	2	3	5	0	0	0	0000000000000	0
26	34	35	2	3	5	0	0	0	0000000000000	0
27	35	36	2	3	5	0	0	0	0000000000000	0
28	36	37	2	3	5	0	0	0	0000000000000	0
29	1	38	3	1	1	0	0	0	0000000000000	0
30	49	52	55	1	1	0	0	0	0000000000000	0
31	50	53	56	1	1	0	0	0	0000000000000	0
32	51	54	57	1	1	0	0	0	0000000000000	0
33	64	67	69	1	1	0	0	0	0000000000000	0
34	65	68	71	1	1	0	0	0	0000000000000	0
35	66	69	72	1	1	0	0	0	0000000000000	0
36	79	82	67	1	1	0	0	0	0000000000000	0
37	80	83	65	1	1	0	0	0	0000000000000	0
38	81	84	66	1	1	0	0	0	0000000000000	0
39	22	39	35	1	1	0	0	0	0000000000000	0
40	24	110	55	1	1	0	0	0	0000000000000	0
41	25	111	30	1	1	0	0	0	0000000000000	0
42	26	112	31	1	1	0	0	0	0000000000000	0
43	40	43	29	2	6	0	0	0	0000000000000	0
44	41	44	30	2	6	0	0	0	0000000000000	0
45	42	45	31	2	6	0	0	0	0000000000000	0
46	43	46	29	2	6	0	0	0	0000000000000	5
47	44	47	30	2	6	0	0	0	0000000000000	4
48	45	48	31	2	6	0	0	0	0000000000000	5
49	46	49	29	2	6	0	0	0	0000000000000	0
50	47	50	30	2	6	0	0	0	0000000000000	0
51	48	51	31	2	6	0	0	0	0000000000000	0
52	29	113	24	1	1	0	0	0	0000000000000	0
53	30	114	25	1	1	0	0	0	0000000000000	0
54	31	115	26	1	1	0	0	0	0000000000000	0
55	55	58	40	2	6	0	0	0	0000000000000	0
56	56	59	41	2	6	0	0	0	0000000000000	0
57	57	60	42	2	6	0	0	0	0000000000000	0
58	58	61	40	2	6	0	0	0	0000000000000	7
59	59	62	25	2	6	0	0	0	0000000000000	6
60	60	63	26	2	6	0	0	0	0000000000000	7
61	61	64	24	2	6	0	0	0	0000000000000	0
62	62	65	25	2	6	0	0	0	0000000000000	0
63	63	66	26	2	6	0	0	0	0000000000000	0
64	34	116	29	1	1	0	0	0	0000000000000	0
65	35	117	30	1	1	0	0	0	0000000000000	0
66	36	118	31	1	1	0	0	0	0000000000000	0
67	70	73	29	2	6	0	0	0	0000000000000	0
68	71	74	30	2	6	0	0	0	0000000000000	0
69	72	75	31	2	6	0	0	0	0000000000000	0
70	73	76	29	2	6	0	0	0	0000000000000	9
71	74	77	30	2	6	0	0	0	0000000000000	8
72	75	78	31	2	6	0	0	0	0000000000000	9
73	76	79	29	2	6	0	0	0	0000000000000	0
74	77	80	30	2	6	0	0	0	0000000000000	0
75	78	81	31	2	6	0	0	0	0000000000000	0
76	110	40	55	2	6	0	0	0	0000000000000	11
77	111	41	30	2	6	0	0	0	0000000000000	10
78	112	42	31	2	6	0	0	0	0000000000000	11
79	113	55	24	2	6	0	0	0	0000000000000	13
80	114	56	25	2	6	0	0	0	0000000000000	12
81	115	57	26	2	6	0	0	0	0000000000000	13
82	116	70	29	2	6	0	0	0	0000000000000	15
83	117	71	30	2	6	0	0	0	0000000000000	14
84	118	72	31	2	6	0	0	0	0000000000000	15
4	11	5	0							
1	.8364E+03	.1111E+03	.2532E+05	.1000E+08	.1000E+08	.1748E+07				
2	.7120E+04	.7120E+04	.3047E+05	.5746E+06	.9320E+06	.1286E+06				
3	.7474E+04	.7474E+04	.3184E+05	.7278E+06	.1015E+07	.1405E+06				
4	.6736E+04	.6736E+04	.2896E+05	.4409E+06	.8588E+06	.1171E+06				

```

5 .8364E+03 .1111E+03 .2532E+05 .1000E+08 .1000E+08 .1748E+07
1 38 107 106 1 0
2 52 95 94 2 0
3 53 96 94 2 0
4 54 97 94 2 0
5 67 99 98 3 0
6 68 100 98 3 0
7 69 101 98 3 0
8 82 103 102 4 0
9 83 104 102 4 0
10 84 105 102 4 0
11 39 109 108 5 0
5 11 2 3
1 .1000E+01 .1000E+01 .1000E+01 .1000E+01 .1000E+01 .1000E+01
2 .1236E+03 .1236E+03 .1000E+08 .1236E+03 .1000E+08 .1000E+08
1 .2000E-01 .1000E+01 .0000E+00 .0000E+00 .0000E+00 .0000E+00 .1000E+01 0
.0000E+00 .0000E+00 .0000E+00 .0000E+00 .0000E+00 .0000E+00
2 .0000E+00 .1000E+01 .1500E+01 .0000E+00 .0000E+00 .0000E+00 .2210E+05 0
.0000E+00 .0000E+00 .0000E+00 .0000E+00 .0000E+00 .0000E+00
3 .2000E-01 .1000E+01 .1500E+01 .0000E+00 .0000E+00 .0000E+00 .2210E+05 0
.0000E+00 .0000E+00 .0000E+00 .0000E+00 .0000E+00 .0000E+00
1 1 2 85 25 545535 1 2 3 .3240E+03 .0000E+00 .2000E+08
2 6 25 86 30 545535 -1 2 1 .3240E+03 .0000E+00 .2000E+08
3 25 7 91 30 545535 1 2 1 .3240E+03 .0000E+00 .2000E+08
4 11 30 87 35 545535 -1 2 1 .3240E+03 .0000E+00 .2000E+08
5 30 12 92 35 545535 1 2 1 .3240E+03 .0000E+00 .2000E+08
6 16 35 88 22 545535 -1 2 1 .3240E+03 .0000E+00 .2000E+08
7 35 17 93 22 545535 1 2 1 .3240E+03 .0000E+00 .2000E+08
8 22 21 90 35 545535 1 2 3 .3240E+03 .0000E+00 .2000E+08
9 6 7 86 30 545535 1 1 2 .3240E+03 .0000E+00 .1000E+01
10 11 12 87 35 545535 1 1 2 .3240E+03 .0000E+00 .1000E+01
11 16 17 88 22 545535 1 1 2 .3240E+03 .0000E+00 .1000E+01

.1000E+01 .0000E+00 .0000E+00 .0000E+00
.1000E-01 0
20 .5000E-01
200 1 .1000E-01 .5000E-02
1 2 3 .5000E+00 .5000E+00 .5000E+00

4
1 1 2 3 4 5 6
2 1 2 3 4 5 6
21 1 2 3 4 5 6
22 1 2 3 4 5 6
28 1 2 3 4 5 6
29 1 2 3 4 5 6
30 1 2 3 4 5 6
31 1 2 3 4 5 6
32 1 2 3 4 5 6
52 1 2 3 4 5 6
53 1 2 3 4 5 6
54 1 2 3 4 5 6
56 1 2 3 4 5 6
59 1 2 3 4 5 6
62 1 2 3 4 5 6
65 1 2 3 4 5 6
67 1 2 3 4 5 6
68 1 2 3 4 5 6
69 1 2 3 4 5 6
82 1 2 3 4 5 6
83 1 2 3 4 5 6
84 1 2 3 4 5 6
110 1 2 3 4 5 6
111 1 2 3 4 5 6
112 1 2 3 4 5 6
113 1 2 3 4 5 6
114 1 2 3 4 5 6
115 1 2 3 4 5 6
116 1 2 3 4 5 6
117 1 2 3 4 5 6

```

118	1	2	3	4	5	6							
4													
2	46	1	2	3	4	5	6	7	8	9	10	11	12
2	47	1	2	3	4	5	6	7	8	9	10	11	12
2	48	1	2	3	4	5	6	7	8	9	10	11	12
2	58	1	2	3	4	5	6	7	8	9	10	11	12
2	59	1	2	3	4	5	6	7	8	9	10	11	12
2	60	1	2	3	4	5	6	7	8	9	10	11	12
2	70	1	2	3	4	5	6	7	8	9	10	11	12
2	71	1	2	3	4	5	6	7	8	9	10	11	12
2	72	1	2	3	4	5	6	7	8	9	10	11	12
2	76	1	2	3	4	5	6	7	8	9	10	11	12
2	77	1	2	3	4	5	6	7	8	9	10	11	12
2	78	1	2	3	4	5	6	7	8	9	10	11	12
2	79	1	2	3	4	5	6	7	8	9	10	11	12
2	80	1	2	3	4	5	6	7	8	9	10	11	12
2	81	1	2	3	4	5	6	7	8	9	10	11	12
2	82	1	2	3	4	5	6	7	8	9	10	11	12
2	83	1	2	3	4	5	6	7	8	9	10	11	12
2	84	1	2	3	4	5	6	7	8	9	10	11	12
4	1	1	2	3	4	5	6	7	8	9	10	11	12
4	11	1	2	3	4	5	6	7	8	9	10	11	12
5	1	1	2	3	4	5	6	7	8	9	10	11	12
5	2	1	2	3	4	5	6	7	8	9	10	11	12
5	3	1	2	3	4	5	6	7	8	9	10	11	12
5	4	1	2	3	4	5	6	7	8	9	10	11	12
5	5	1	2	3	4	5	6	7	8	9	10	11	12
5	6	1	2	3	4	5	6	7	8	9	10	11	12
5	7	1	2	3	4	5	6	7	8	9	10	11	12
5	8	1	2	3	4	5	6	7	8	9	10	11	12
5	9	1	2	3	4	5	6	7	8	9	10	11	12
5	10	1	2	3	4	5	6	7	8	9	10	11	12
5	11	1	2	3	4	5	6	7	8	9	10	11	12

Bridge 5/826 Structural Model and Analysis Control Input File, "INPUT"

```

SpineBridge2
92 3 82 3 2 9205 20 .5692E+00 .4392E-02
1 0 0 0 0 0 0 .0000E+00 .0000E+00 .0000E+00
2 0 0 0 0 0 0 .3420E+03 .0000E+00 .1638E+02
3 0 0 0 0 0 0 .6840E+03 .0000E+00 .3276E+02
4 0 0 0 0 0 0 .1168E+04 .0000E+00 .5464E+02
5 0 0 0 0 0 0 .1652E+04 .0000E+00 .7652E+02
6 0 0 0 0 0 0 .2136E+04 .0000E+00 .9840E+02
7 0 0 0 0 0 0 .2620E+04 .0000E+00 .1150E+03
8 0 0 0 0 0 0 .3104E+04 .0000E+00 .1316E+03
9 0 0 0 0 0 0 .3588E+04 .0000E+00 .1482E+03
10 0 0 0 0 0 0 .4008E+04 .0000E+00 .1588E+03
11 0 0 0 0 0 0 .4428E+04 .0000E+00 .1694E+03

```

12	0	0	0	0	0	0	.5058E+03	.2201E+03	.3276E+02
13	0	0	0	0	0	0	.5368E+03	.1818E+03	.3276E+02
14	1	1	1	1	1	1	.6840E+03	.0000E+00	.3276E+02
15	0	0	0	0	0	0	.8312E+03-	.1818E+03	.3276E+02
16	0	0	0	0	0	0	.8622E+03-	.2201E+03	.3276E+02
17	0	0	0	0	0	0	.1958E+04	.2201E+03	.9840E+02
18	0	0	0	0	0	0	.1989E+04	.1818E+03	.9840E+02
19	1	1	1	1	1	1	.2136E+04	.0000E+00	.9840E+02
20	0	0	0	0	0	0	.2283E+04-	.1818E+03	.9840E+02
21	0	0	0	0	0	0	.2314E+04-	.2201E+03	.9840E+02
22	0	0	0	0	0	0	.3410E+04	.2201E+03	.1482E+03
23	0	0	0	0	0	0	.3441E+04	.1818E+03	.1482E+03
24	1	1	1	1	1	1	.3588E+04	.0000E+00	.1482E+03
25	0	0	0	0	0	0	.3735E+04-	.1818E+03	.1482E+03
26	0	0	0	0	0	0	.3766E+04-	.2201E+03	.1482E+03
27	0	0	0	0	0	0	.5368E+03	.1818E+03-	.7990E+01
28	0	0	0	0	0	0	.5368E+03	.1818E+03-	.5809E+02
29	0	0	0	0	0	0	.5368E+03	.1818E+03-	.2270E+03
30	0	0	0	0	0	0	.5368E+03	.1818E+03-	.2799E+03
31	0	0	0	0	0	0	.5368E+03	.1818E+03-	.2899E+03
32	0	0	0	0	0	0	.6840E+03	.0000E+00-	.7990E+01
33	0	0	0	0	0	0	.6840E+03	.0000E+00-	.5809E+02
34	0	0	0	0	0	0	.6840E+03	.0000E+00-	.2270E+03
35	0	0	0	0	0	0	.6840E+03	.0000E+00-	.2799E+03
36	0	0	0	0	0	0	.6840E+03	.0000E+00-	.2899E+03
37	0	0	0	0	0	0	.8312E+03-	.1818E+03-	.7990E+01
38	0	0	0	0	0	0	.8312E+03-	.1818E+03-	.5809E+02
39	0	0	0	0	0	0	.8312E+03-	.1818E+03-	.2270E+03
40	0	0	0	0	0	0	.8312E+03-	.1818E+03-	.2799E+03
41	0	0	0	0	0	0	.8312E+03-	.1818E+03-	.2899E+03
42	0	0	0	0	0	0	.1989E+04	.1818E+03	.5765E+02
43	0	0	0	0	0	0	.1989E+04	.1818E+03	.7550E+01
44	0	0	0	0	0	0	.1989E+04	.1818E+03-	.1974E+03
45	0	0	0	0	0	0	.1989E+04	.1818E+03-	.2503E+03
46	0	0	0	0	0	0	.1989E+04	.1818E+03-	.2604E+03
47	0	0	0	0	0	0	.2136E+04	.0000E+00	.5765E+02
48	0	0	0	0	0	0	.2136E+04	.0000E+00	.7550E+01
49	0	0	0	0	0	0	.2136E+04	.0000E+00-	.1974E+03
50	0	0	0	0	0	0	.2136E+04	.0000E+00-	.2503E+03
51	0	0	0	0	0	0	.2136E+04	.0000E+00-	.2604E+03
52	0	0	0	0	0	0	.2283E+04-	.1818E+03	.5765E+02
53	0	0	0	0	0	0	.2283E+04-	.1818E+03	.7550E+01
54	0	0	0	0	0	0	.2283E+04-	.1818E+03-	.1974E+03
55	0	0	0	0	0	0	.2283E+04-	.1818E+03-	.2503E+03
56	0	0	0	0	0	0	.2283E+04-	.1818E+03-	.2604E+03
57	0	0	0	0	0	0	.3441E+04	.1818E+03	.1075E+03
58	0	0	0	0	0	0	.3441E+04	.1818E+03	.5735E+02
59	0	0	0	0	0	0	.3441E+04	.1818E+03-	.1236E+03
60	0	0	0	0	0	0	.3441E+04	.1818E+03-	.1765E+03
61	0	0	0	0	0	0	.3441E+04	.1818E+03-	.1866E+03
62	0	0	0	0	0	0	.3588E+04	.0000E+00	.1075E+03
63	0	0	0	0	0	0	.3588E+04	.0000E+00	.5735E+02
64	0	0	0	0	0	0	.3588E+04	.0000E+00-	.1236E+03
65	0	0	0	0	0	0	.3588E+04	.0000E+00-	.1765E+03
66	0	0	0	0	0	0	.3588E+04	.0000E+00-	.1866E+03
67	0	0	0	0	0	0	.3735E+04-	.1818E+03	.1075E+03
68	0	0	0	0	0	0	.3735E+04-	.1818E+03	.5735E+02
69	0	0	0	0	0	0	.3735E+04-	.1818E+03-	.1236E+03
70	0	0	0	0	0	0	.3735E+04-	.1818E+03-	.1765E+03
71	0	0	0	0	0	0	.3735E+04-	.1818E+03-	.1866E+03
72	1	1	1	1	1	1	-.1944E+03	.2401E+03	.0000E+00
73	1	1	1	1	1	1	.3635E+04	.2401E+03	.1588E+03
74	0	0	0	0	0	0	-.5000E+01	.0000E+00	.0000E+00
75	0	0	0	0	0	0	-.5000E+01	.0000E+00-	.2000E+02
76	0	0	0	0	0	0	.4433E+04	.0000E+00	.1694E+03
77	0	0	0	0	0	0	.4433E+04	.0000E+00	.1494E+03
78	1	1	1	1	1	1	.5318E+03	.1818E+03-	.2899E+03
79	1	1	1	1	1	1	.6790E+03	.0000E+00-	.2899E+03
80	1	1	1	1	1	1	.8262E+03-	.1818E+03-	.2899E+03
81	1	1	1	1	1	1	-.1472E+03	.1818E+03	.0000E+00
82	1	1	1	1	1	1	.2131E+04	.0000E+00-	.2604E+03

83	1	1	1	1	1	1	.2278E+04-	.1818E+03-	.2604E+03					
84	1	1	1	1	1	1	.3436E+04	.1818E+03-	.1866E+03					
85	1	1	1	1	1	1	.3583E+04	.0000E+00-	.1866E+03					
86	1	1	1	1	1	1	.3730E+04-	.1818E+03-	.1866E+03					
87	1	1	1	1	1	1-	.1000E+02	.0000E+04-	.2000E+02					
88	1	1	1	1	1	1	.4438E+04	.0000E+00	.1494E+03					
89	1	1	1	1	1	1-	.5000E+01-	.5000E+01-	.2000E+02					
90	1	1	1	1	1	1	.4433E+04-	.5000E+01	.1494E+03					
91	1	1	1	1	1	1	.1984E+04	.1818E+03-	.2604E+03					
92	1	1	1	1	1	1	.4281E+04	.1818E+03	.1694E+03					
2	69	4	0	3	12									
1							.1000E+08	.1800E+00	.0000E+00					
2							.3604E+06	.1800E+00	.2240E-06					
3							.3604E+04	.1800E+00	.2240E-06					
1							.1440E+05	.1440E+05	.1440E+05	.1000E+09	.1000E+09	.1000E+09		
2							.8423E+04	.8423E+04	.8423E+04	.1000E+09	.1000E+09	.1000E+09		
3							.3984E+04	.3984E+04	.3984E+04	.1530E+07	.4122E+06	.3334E+06		
4							.1018E+04	.1018E+04	.1018E+04	.1649E+06	.2000E+05	.2000E+05		
							.0000E+00	.0000E+00	.0000E+00					
							.0000E+00	.0000E+00	.0000E+00					
							-.3864E+03	.0000E+00	.0000E+00					
1							.6107E+04	.1590E+05	.1590E+05	.2218E+00				
							.1000E+01-	.3568E+01-	.4298E+01	.2693E+00	.1000E+01-	.3568E+01-	.4298E+01	.2693E+00
							.3626E-01	.2614E+00	.7600E+00	.3626E-01	.2614E+00	.7600E+00	.2044E+02	.3870E-01
2							.6107E+04	.1590E+05	.1590E+05	.2218E+00				
							.1000E+01-	.3568E+01-	.4298E+01	.2693E+00	.1000E+01-	.3568E+01-	.4298E+01	.2693E+00
							.3626E-01	.2614E+00	.7900E+00	.3626E-01	.2614E+00	.7900E+00	.2044E+02	.3870E-01
3							.6107E+04	.1590E+05	.1590E+05	.2218E+00				
							.1000E+01-	.3568E+01-	.4298E+01	.2693E+00	.1000E+01-	.3568E+01-	.4298E+01	.2693E+00
							.3626E-01	.2614E+00	.7100E+00	.3626E-01	.2614E+00	.7100E+00	.2044E+02	.3870E-01
4							.6107E+04	.1590E+05	.1590E+05	.2218E+00				
							.1000E+01-	.3568E+01-	.4298E+01	.2693E+00	.1000E+01-	.3568E+01-	.4298E+01	.2693E+00
							.3626E-01	.2614E+00	.7400E+00	.3626E-01	.2614E+00	.7400E+00	.2044E+02	.3870E-01
5							.6107E+04	.1590E+05	.1590E+05	.2218E+00				
							.1000E+01-	.3568E+01-	.4298E+01	.2693E+00	.1000E+01-	.3568E+01-	.4298E+01	.2693E+00
							.3626E-01	.2614E+00	.7500E+00	.3626E-01	.2614E+00	.7500E+00	.2044E+02	.3870E-01
6							.6107E+04	.1590E+05	.1590E+05	.2218E+00				
							.1000E+01-	.3568E+01-	.4298E+01	.2693E+00	.1000E+01-	.3568E+01-	.4298E+01	.2693E+00
							.3626E-01	.2614E+00	.7800E+00	.3626E-01	.2614E+00	.7800E+00	.2044E+02	.3870E-01
7							.6107E+04	.1411E+05	.1411E+05	.1895E+00				
							.1000E+01-	.4248E+01-	.5404E+01-	.1561E+00	.1000E+01-	.4248E+01-	.5404E+01-	.1561E+00
							.3626E-01	.2614E+00	.7600E+00	.3626E-01	.2614E+00	.7600E+00	.2044E+02	.3870E-01
8							.6107E+04	.1411E+05	.1411E+05	.1895E+00				
							.1000E+01-	.4248E+01-	.5404E+01-	.1561E+00	.1000E+01-	.4248E+01-	.5404E+01-	.1561E+00
							.3626E-01	.2614E+00	.7900E+00	.3626E-01	.2614E+00	.7900E+00	.2044E+02	.3870E-01
9							.6107E+04	.1411E+05	.1411E+05	.1895E+00				
							.1000E+01-	.4248E+01-	.5404E+01-	.1561E+00	.1000E+01-	.4248E+01-	.5404E+01-	.1561E+00
							.3626E-01	.2614E+00	.7100E+00	.3626E-01	.2614E+00	.7100E+00	.2044E+02	.3870E-01
10							.6107E+04	.1411E+05	.1411E+05	.1895E+00				
							.1000E+01-	.4248E+01-	.5404E+01-	.1561E+00	.1000E+01-	.4248E+01-	.5404E+01-	.1561E+00
							.3626E-01	.2614E+00	.7400E+00	.3626E-01	.2614E+00	.7400E+00	.2044E+02	.3870E-01
11							.6107E+04	.1411E+05	.1411E+05	.1895E+00				
							.1000E+01-	.4248E+01-	.5404E+01-	.1561E+00	.1000E+01-	.4248E+01-	.5404E+01-	.1561E+00
							.3626E-01	.2614E+00	.7400E+00	.3626E-01	.2614E+00	.7400E+00	.2044E+02	.3870E-01
12							.6107E+04	.1411E+05	.1411E+05	.1895E+00				
							.1000E+01-	.4248E+01-	.5404E+01-	.1561E+00	.1000E+01-	.4248E+01-	.5404E+01-	.1561E+00
							.3626E-01	.2614E+00	.7800E+00	.3626E-01	.2614E+00	.7800E+00	.2044E+02	.3870E-01
1	1	2	72	2	2	0	0	0	0	0000000000000	0			
2	2	3	72	2	2	0	0	0	0	0000000000000	0			
3	3	4	12	2	2	0	0	0	0	0000000000000	0			
4	4	5	12	2	2	0	0	0	0	0000000000000	0			
5	5	6	17	2	2	0	0	0	0	0000000000000	0			
6	6	7	17	2	2	0	0	0	0	0000000000000	0			
7	7	8	17	2	2	0	0	0	0	0000000000000	0			
8	8	9	22	2	2	0	0	0	0	0000000000000	0			
9	9	10	22	2	2	0	0	0	0	0000000000000	0			
10	10	11	22	2	2	0	0	0	0	0000000000000	0			
11	12	13	1	2	3	0	0	0	0	0000000000000	0			
12	13	3	1	2	3	0	0	0	0	0000000000000	0			
13	3	15	1	2	3	0	0	0	0	0000000000000	0			
14	15	16	1	2	3	0	0	0	0	0000000000000	0			

15	17	18	42	2	3	0	0	0	0000000000000	0
16	18	6	42	2	3	0	0	0	0000000000000	0
17	6	20	42	2	3	0	0	0	0000000000000	0
18	20	21	42	2	3	0	0	0	0000000000000	0
19	22	23	8	2	3	0	0	0	0000000000000	0
20	23	9	8	2	3	0	0	0	0000000000000	0
21	9	25	8	2	3	0	0	0	0000000000000	0
22	25	26	8	2	3	0	0	0	0000000000000	0
23	13	27	42	1	4	0	0	0	0000000000000	0
24	27	28	42	3	4	0	0	0	0000000000000	2
25	28	29	42	3	4	0	0	0	0000000000000	0
26	29	30	42	3	4	0	0	0	0000000000000	8
27	30	31	42	3	4	0	0	0	0000000000000	0
28	3	32	50	1	4	0	0	0	0000000000000	0
29	32	33	50	3	4	0	0	0	0000000000000	1
30	33	34	50	3	4	0	0	0	0000000000000	0
31	34	35	50	3	4	0	0	0	0000000000000	7
32	35	36	50	3	4	0	0	0	0000000000000	0
33	15	37	55	1	4	0	0	0	0000000000000	0
34	37	38	55	3	4	0	0	0	0000000000000	2
35	38	39	55	3	4	0	0	0	0000000000000	0
36	39	40	55	3	4	0	0	0	0000000000000	8
37	40	41	55	3	4	0	0	0	0000000000000	0
38	18	42	30	1	4	0	0	0	0000000000000	0
39	42	43	30	3	4	0	0	0	0000000000000	4
40	43	44	30	3	4	0	0	0	0000000000000	0
41	44	45	30	3	4	0	0	0	0000000000000	10
42	45	46	30	3	4	0	0	0	0000000000000	0
43	6	47	35	1	4	0	0	0	0000000000000	0
44	47	48	35	3	4	0	0	0	0000000000000	3
45	48	49	35	3	4	0	0	0	0000000000000	0
46	49	50	35	3	4	0	0	0	0000000000000	9
47	50	51	35	3	4	0	0	0	0000000000000	0
48	20	52	40	1	4	0	0	0	0000000000000	0
49	52	53	40	3	4	0	0	0	0000000000000	4
50	53	54	40	3	4	0	0	0	0000000000000	0
51	54	55	40	3	4	0	0	0	0000000000000	10
52	55	56	40	3	4	0	0	0	0000000000000	0
53	23	57	45	1	4	0	0	0	0000000000000	0
54	57	58	45	3	4	0	0	0	0000000000000	6
55	58	59	45	3	4	0	0	0	0000000000000	0
56	59	60	45	3	4	0	0	0	0000000000000	12
57	60	61	45	3	4	0	0	0	0000000000000	0
58	9	62	50	1	4	0	0	0	0000000000000	0
59	62	63	50	3	4	0	0	0	0000000000000	4
60	63	64	50	3	4	0	0	0	0000000000000	0
61	64	65	50	3	4	0	0	0	0000000000000	11
62	65	66	50	3	4	0	0	0	0000000000000	0
63	25	67	55	1	4	0	0	0	0000000000000	0
64	67	68	55	3	4	0	0	0	0000000000000	6
65	68	69	55	3	4	0	0	0	0000000000000	0
66	69	70	55	3	4	0	0	0	0000000000000	12
67	70	71	55	3	4	0	0	0	0000000000000	0
68	76	77	10	1	2	0	0	0	0000000000000	0
69	74	75	14	1	2	0	0	0	0000000000000	0
4	11	5	0							
1	.1049E+04	.1049E+04	.5280E+04	.1000E+08	.1000E+08	.1000E+08	.1000E+09			
2	.1442E+04	.1442E+04	.2639E+04	.3440E+07	.4444E+07	.1000E+09				
3	.1690E+04	.1690E+04	.3016E+04	.5734E+07	.5734E+07	.1000E+09				
4	.1129E+04	.1129E+04	.2639E+04	.3440E+07	.4444E+07	.1000E+09				
5	.1172E+04	.1172E+04	.5808E+04	.1000E+08	.1000E+08	.1000E+09				
1	75	87	89	1	0					
2	77	88	90	5	0					
3	31	78	36	2	0					
4	36	79	41	2	0					
5	41	80	36	2	0					
6	46	91	51	3	0					
7	51	82	56	3	0					
8	56	83	51	3	0					
9	61	84	66	4	0					
10	66	85	71	4	0					

```

11 71 86 66 4 0
5 2 1 1
1 .1236E+03 .1236E+03 .1000E+08 .1236E+03 .1000E+08 .1000E+08
1 .2000E-01 .1000E+01 .1500E+01 .0000E+00 .0000E+00 .0000E+00 .2210E+05 0
.0000E+00 .0000E+00 .0000E+00 .0000E+00 .0000E+00 .0000E+00
1 1 74 81 3 545545 -1 1 1 .4402E+03 .0000E+00 .2000E+08
2 11 76 92 10 545545 -1 1 1 .4402E+03 .0000E+00 .2000E+08

```

```

.1000E+01 .0000E+00 .0000E+00 .0000E+00
.1000E-01 0
20 .7000E-01
200 1 .5000E-01 .2500E-01
1 2 3 .1000E+01 .1000E+01 .1000E+01

```

```

4
1 1 2 3 4 5 6
11 1 2 3 4 5 6
27 1 2 3 4 5 6
31 1 2 3 4 5 6
32 1 2 3 4 5 6
36 1 2 3 4 5 6
37 1 2 3 4 5 6
41 1 2 3 4 5 6
42 1 2 3 4 5 6
46 1 2 3 4 5 6
47 1 2 3 4 5 6
51 1 2 3 4 5 6
52 1 2 3 4 5 6
56 1 2 3 4 5 6
57 1 2 3 4 5 6
61 1 2 3 4 5 6
62 1 2 3 4 5 6
66 1 2 3 4 5 6
67 1 2 3 4 5 6
71 1 2 3 4 5 6
74 1 2 3 4 5 6
76 1 2 3 4 5 6

```

```

4
2 24 1 2 3 4 5 6 7 8 9 10 11 12
2 26 1 2 3 4 5 6 7 8 9 10 11 12
2 29 1 2 3 4 5 6 7 8 9 10 11 12
2 31 1 2 3 4 5 6 7 8 9 10 11 12
2 34 1 2 3 4 5 6 7 8 9 10 11 12
2 36 1 2 3 4 5 6 7 8 9 10 11 12
2 39 1 2 3 4 5 6 7 8 9 10 11 12
2 41 1 2 3 4 5 6 7 8 9 10 11 12
2 44 1 2 3 4 5 6 7 8 9 10 11 12
2 46 1 2 3 4 5 6 7 8 9 10 11 12
2 49 1 2 3 4 5 6 7 8 9 10 11 12
2 51 1 2 3 4 5 6 7 8 9 10 11 12
2 54 1 2 3 4 5 6 7 8 9 10 11 12
2 56 1 2 3 4 5 6 7 8 9 10 11 12
2 59 1 2 3 4 5 6 7 8 9 10 11 12
2 61 1 2 3 4 5 6 7 8 9 10 11 12
2 64 1 2 3 4 5 6 7 8 9 10 11 12
2 66 1 2 3 4 5 6 7 8 9 10 11 12
4 1 1 2 3 4 5 6 7 8 9 10 11 12
4 2 1 2 3 4 5 6 7 8 9 10 11 12
5 1 1 2 3 4 5 6 7 8 9 10 11 12
5 2 1 2 3 4 5 6 7 8 9 10 11 12

```


Applied Seismic Excitation File, "RECORD"

* This is only the first 20 Seconds of the E-W Time History

Peru EW
9200 386.4000 .0100 .0000
-.010120 -.005035 .000818 .003828 .002401 -.001776 -.005401 -.006466
-.005354 -.003804 -.003465 -.005294 -.008987 -.012532 -.013099 -.009684
-.004743 -.002261 -.003630 -.006124 -.005837 -.001819 .003384 .006731
.007421 .006536 .005276 .004274 .004188 .005538 .007639 .008326
.005725 .000309 -.005087 -.007682 -.007088 -.005406 -.004966 -.006097
-.006959 -.005674 -.002422 .000601 .001406 .000066 -.001667 -.002383
-.002173 -.002040 -.002610 -.003733 -.004770 -.004991 -.003951 -.002197
-.001380 -.002994 -.006514 -.009411 -.009443 -.006851 -.003696 -.001347
.000699 .003178 .005132 .004375 .000030 -.006118 -.010971 -.012778
-.012196 -.011090 -.010447 -.009658 -.007611 -.004496 -.002100 -.001970
-.003012 -.001714 .004399 .013267 .019246 .018331 .012367 .007140
.006255 .007690 .007136 .003894 .002171 .006083 .014614 .022454
.025530 .024426 .022312 .020741 .018844 .016041 .013909 .014316
.016593 .017764 .015826 .011773 .008004 .005345 .002653 -.000958
-.004465 -.006145 -.005749 -.004873 -.005195 -.007111 -.010029 -.013310
-.016093 -.016735 -.013491 -.006570 .000941 .004994 .004063 .000451
-.002040 -.001844 -.000778 -.001651 -.004958 -.008329 -.009091 -.007219
-.005455 -.006604 -.010654 -.014738 -.015765 -.013090 -.008573 -.004548
-.002104 -.001334 -.002254 -.004748 -.007668 -.009120 -.008232 -.006433
-.006114 -.007937 -.009782 -.008806 -.004319 .001405 .005149 .005297
.002802 .000106 -.000606 .001284 .004644 .007409 .008170 .007410
.007274 .009457 .013024 .014478 .010869 .003219 -.003281 -.003339
.003756 .013254 .018927 .017926 .012138 .005327 -.000241 -.004477
-.007715 -.009603 -.009828 -.009123 -.008446 -.007422 -.004468 .000858
.006234 .007965 .004304 -.002892 -.009592 -.012510 -.010927 -.006835
-.003739 -.004579 -.009345 -.014484 -.015470 -.010998 -.004413 -.000537
-.000904 -.002776 -.002782 -.000868 .000146 -.001595 -.004557 -.005768
-.004377 -.002483 -.002387 -.004058 -.005682 -.006196 -.006172 -.006287
-.005886 -.004045 -.001470 -.000158 -.000496 .000276 .005520 .014733
.022600 .023299 .015946 .005446 -.001806 -.002835 .000895 .005922
.009459 .010216 .008318 .005235 .003305 .004127 .007201 .010516
.012819 .014779 .017588 .020565 .021025 .016825 .009012 .001521
-.001800 -.000152 .003900 .006591 .005737 .001936 -.002315 -.004799
-.005180 -.004872 -.005289 -.006336 -.006494 -.004384 -.000014 .005152
.008973 .009344 .005212 -.002142 -.008688 -.009978 -.005058 .001878
.004905 .001958 -.003166 -.004877 -.001443 .003726 .006154 .004589
.001145 -.002017 -.004952 -.009037 -.014591 -.020062 -.023309 -.023408
-.021179 -.018415 -.016557 -.015937 -.015794 -.015013 -.012950 -.010054
-.007797 -.007832 -.010475 -.013903 -.015235 -.013249 -.009914 -.008595
-.010237 -.011927 -.009773 -.003269 .003886 .007252 .005636 .001572
-.001181 -.000137 .005187 .013296 .020935 .024250 .021455 .014772
.009168 .008250 .011301 .014358 .014178 .010903 .007308 .005982
.007460 .010319 .012470 .012449 .010458 .008537 .009294 .013424
.018298 .019499 .014699 .006213 -.000609 -.002218 -.000272 -.000069
-.005128 -.013355 -.018672 -.016603 -.008143 .001394 .006708 .005541
-.001061 -.009828 -.016356 -.017145 -.012356 -.006574 -.005147 -.009032
-.013778 -.014400 -.010612 -.006531 -.005573 -.007139 -.008526 -.008764
-.009110 -.010402 -.011538 -.011208 -.009764 -.008269 -.006257 -.002250
.003116 .005903 .002617 -.004958 -.010065 -.007371 .001323 .008557
.008686 .003200 -.001535 -.001259 .002382 .004584 .002872 -.001028
-.003973 -.004793 -.004373 -.003482 -.001708 .001168 .003897 .004706
.003565 .002595 .003904 .007234 .010394 .011861 .012452 .013911
.016289 .017356 .015055 .010124 .005943 .005595 .009295 .014473
.018124 .018908 .017638 .016193 .016051 .017314 .018931 .019784
.019666 .018979 .017796 .015654 .012565 .009475 .007164 .004938
.001573 -.002384 -.004347 -.002905 -.000492 -.001397 -.006681 -.012642
-.015196 -.014855 -.015538 -.018808 -.021332 -.019367 -.014182 -.010975
-.012400 -.015383 -.015364 -.012349 -.010677 -.013171 -.017459 -.019134
-.017035 -.013866 -.011942 -.010477 -.007734 -.004477 -.003330 -.004998

-.006745	-.005757	-.002955	-.002191	-.005467	-.010244	-.012126	-.009745
-.005975	-.004462	-.005760	-.007461	-.007316	-.005355	-.002829	-.000299
.002437	.004781	.005009	.002061	-.002581	-.005569	-.004337	.000872
.007456	.012366	.013811	.011840	.008191	.005362	.005171	.007526
.010797	.013542	.015894	.018908	.022773	.026013	.026798	.024625
.020496	.015588	.010511	.005879	.002881	.002271	.002983	.002573
-.000244	-.004067	-.006329	-.006229	-.005180	-.004358	-.002828	.000776
.005323	.007354	.005032	.000935	-.000132	.003792	.009922	.014023
.014878	.014732	.015932	.018019	.018348	.014635	.006698	-.003576
-.012920	-.017854	-.016572	-.010844	-.005507	-.004985	-.009567	-.015407
-.018374	-.017844	-.016442	-.016646	-.018312	-.019785	-.020400	-.021028
-.022133	-.022481	-.020404	-.016034	-.011336	-.007958	-.005646	-.003296
-.000850	.000521	.000139	-.001140	-.001737	-.000745	.001979	.006309
.011566	.015821	.016926	.015013	.013345	.015184	.019740	.022274
.019208	.012409	.007384	.007138	.009060	.008248	.003051	-.003850
-.009122	-.011912	-.012712	-.010982	-.005771	.001284	.005769	.004593
-.000210	-.003224	-.001237	.003654	.006809	.005918	.002668	.000220
.000276	.002321	.004651	.005428	.003713	.000549	-.001048	.001398
.006589	.009259	.004633	-.006518	-.017654	-.022007	-.018284	-.010974
-.005420	-.003356	-.002852	-.001456	.001631	.005705	.009457	.011067
.008526	.001203	-.008380	-.015241	-.015412	-.009573	-.003197	-.002591
-.009660	-.019876	-.025513	-.021988	-.011858	-.002770	-.000935	-.006322
-.013896	-.019035	-.020877	-.020707	-.018622	-.013651	-.006805	-.001975
-.001986	-.004612	-.004480	.000307	.005157	.004000	-.003110	-.009162
-.007168	.003108	.015903	.025342	.029322	.028490	.024132	.018016
.012744	.010099	.009237	.007932	.006093	.006504	.011112	.017438
.020608	.019146	.017286	.020048	.026678	.030499	.026072	.015492
.006552	.004725	.008139	.010735	.009495	.007120	.007762	.011452
.014161	.012959	.009744	.008775	.011159	.013062	.009983	.001846
-.007071	-.013144	-.016914	-.021098	-.026006	-.028677	-.026768	-.022152
-.019203	-.019939	-.022092	-.022631	-.021891	-.022854	-.026423	-.029317
-.027840	-.023017	-.020026	-.022070	-.026120	-.026338	-.021091	-.014907
-.012786	-.014269	-.014677	-.011695	-.008373	-.008803	-.012395	-.014511
-.012247	-.007528	-.003570	-.000306	.004707	.011290	.015173	.012558
.004919	-.002311	-.005058	-.003278	.001156	.006594	.010748	.009940
.002421	-.007652	-.012254	-.007484	.001764	.006928	.005218	.001915
.003216	.009074	.014808	.017945	.020570	.024658	.028203	.028036
.025162	.024289	.027707	.031723	.030916	.024743	.018163	.015695
.016807	.017831	.017053	.016086	.016737	.018409	.019528	.020048
.020953	.021473	.018765	.011246	.001406	-.006181	-.009461	-.010475
-.011978	-.013939	-.014486	-.013713	-.014376	-.018045	-.021820	-.020861
-.014151	-.006258	-.002347	-.002518	-.002347	.001141	.005890	.007888
.006691	.006073	.009322	.015329	.020327	.022375	.022751	.022944
.022116	.018590	.013120	.008841	.007648	.007763	.006254	.003390
.002986	.007433	.013365	.013742	.004918	-.009247	-.020942	-.025902
-.026536	-.027893	-.031518	-.034174	-.031968	-.024735	-.016104	-.010326
-.009571	-.013680	-.020957	-.028763	-.034106	-.035068	-.032050	-.027476
-.023777	-.021582	-.019546	-.015880	-.009997	-.003155	.002394	.004989
.004825	.003807	.004367	.008168	.015522	.025048	.033538	.036840
.032662	.023363	.015427	.014425	.019648	.023982	.020259	.008288
-.004378	-.009299	-.005218	.000446	-.001462	-.013113	-.027680	-.036206
-.036211	-.033298	-.034386	-.040443	-.046294	-.046764	-.041284	-.032473
-.022004	-.009889	.002694	.012034	.014951	.012503	.009354	.009096
.011180	.012777	.013011	.014117	.018455	.025077	.030116	.030406
.026432	.021412	.017889	.015513	.012373	.007928	.004133	.003369
.005889	.009706	.012922	.015204	.016702	.016181	.011746	.003885
-.003029	-.003940	.001519	.007395	.006544	-.002165	-.012181	-.015605
-.010958	-.004187	-.001867	-.004624	-.007909	-.008480	-.008047	-.009832
-.012944	-.012493	-.005597	.004241	.010257	.009304	.004430	.000627
-.000178	.000868	.003102	.007370	.013222	.017035	.015055	.007983
.001114	-.000649	.003078	.009139	.014616	.018279	.019407	.017481
.013992	.012727	.016453	.023368	.028368	.028017	.023354	.017484
.012051	.007207	.004002	.004206	.007095	.008085	.002779	-.007670
-.016584	-.018267	-.014062	-.011216	-.015435	-.025169	-.033622	-.036351
-.035900	-.038345	-.045542	-.052401	-.052704	-.046838	-.041653	-.042188
-.045275	-.043471	-.034653	-.025192	-.022305	-.025386	-.027368	-.024268
-.020020	-.020295	-.023669	-.022367	-.011634	.004626	.019261	.030237
.040444	.049931	.053049	.045918	.034271	.029191	.034323	.040648
.036823	.023106	.011693	.012479	.021283	.024258	.013012	-.007148
-.023956	-.030785	-.030806	-.030338	-.031154	-.030808	-.028584	-.028114
-.032607	-.038886	-.038455	-.025902	-.005436	.012376	.021131	.024880

.032849	.047992	.062519	.065860	.056508	.044195	.040020	.045621
.053317	.055792	.053528	.051908	.053147	.053422	.048245	.038474
.029519	.024994	.022828	.018003	.008404	-.003023	-.011578	-.015679
-.017969	-.021884	-.027424	-.030916	-.029213	-.024035	-.021172	-.024730
-.032302	-.036937	-.034371	-.027911	-.025218	-.030341	-.039513	-.045200
-.043574	-.037416	-.031950	-.029184	-.026903	-.022632	-.017083	-.013210
-.012383	-.012574	-.010564	-.005721	-.001005	-.000154	-.003743	-.008290
-.009324	-.005594	.000028	.003838	.005289	.006987	.010790	.014798
.015351	.011671	.007272	.005926	.007298	.007749	.005349	.002423
.002587	.006363	.011147	.014771	.017377	.019204	.018309	.012060
.000771	-.011637	-.020907	-.025742	-.027418	-.027258	-.025421	-.021899
-.017238	-.011793	-.004973	.003660	.012794	.019657	.022514	.022447
.022320	.023978	.026982	.029994	.032895	.036778	.041830	.045638
.044371	.035996	.022530	.008844	-.000964	-.006521	-.010819	-.017189
-.026196	-.035146	-.040377	-.040597	-.038323	-.037909	-.041239	-.045172
-.043923	-.035110	-.023199	-.015899	-.016295	-.019362	-.017165	-.007483
.003962	.009948	.009278	.006750	.006576	.007713	.006446	.001876
-.002801	-.004309	-.002620	.000364	.004222	.010276	.018622	.026260
.029267	.026322	.019515	.011709	.003810	-.005279	-.016247	-.027410
-.035330	-.037834	-.036328	-.034633	-.034735	-.034139	-.028428	-.016936
-.004589	.003159	.007087	.014122	.029556	.050039	.065854	.070195
.065301	.058961	.056312	.056276	.055623	.054346	.055750	.061788
.069989	.075369	.074737	.068385	.058333	.046126	.033001	.021211
.013873	.012603	.015635	.018695	.018117	.013091	.005273	-.003410
-.012217	-.021277	-.030247	-.037758	-.042148	-.042905	-.041370	-.040052
-.040978	-.044660	-.050598	-.058783	-.070146	-.085248	-.102507	-.118464
-.130040	-.136366	-.137806	-.133617	-.121542	-.100659	-.074078	-.047737
-.025731	-.007391	.010348	.027616	.039729	.041361	.032629	.020224
.012166	.011490	.015230	.018827	.020758	.022827	.027294	.034578
.043527	.052673	.061025	.068321	.075179	.082263	.088593	.091004
.086840	.077630	.069012	.065384	.064827	.060633	.048781	.032922
.020767	.015412	.011590	.001200	-.017827	-.039112	-.053981	-.059314
-.059034	-.058967	-.061179	-.063186	-.061211	-.053412	-.040386	-.024002
-.006310	.010658	.024864	.034355	.037914	.036033	.031429	.027509
.025262	.021584	.012083	-.003766	-.020952	-.033706	-.041477	-.048556
-.057094	-.062603	-.058786	-.046959	-.037779	-.041234	-.054998	-.064849
-.057594	-.033077	-.002914	.021201	.036472	.047115	.056879	.065594
.071863	.075681	.077170	.074830	.067850	.059606	.056003	.058693
.061835	.057752	.045284	.029862	.014928	-.003843	-.032896	-.070491
-.105343	-.127021	-.135631	-.139443	-.144250	-.148175	-.147024	-.141357
-.135007	-.127740	-.112993	-.084951	-.046092	-.005410	.030909	.064828
.101683	.141465	.176969	.200643	.212143	.218270	.226187	.237090
.245929	.245914	.233257	.208897	.177620	.145788	.118407	.095753
.071881	.037716	-.011600	-.071154	-.128572	-.173320	-.203906	-.226134
-.245467	-.263243	-.279830	-.297991	-.319378	-.338423	-.343354	-.326135
-.290175	-.246516	-.202588	-.157062	-.105205	-.046499	.015768	.079753
.146503	.213640	.271117	.307312	.316847	.305580	.281794	.255786
.233524	.221094	.218273	.214981	.195949	.152489	.092165	.033189
-.010864	-.040776	-.065748	-.090511	-.110229	-.118022	-.114296	-.106718
-.101369	-.096579	-.086804	-.071711	-.060441	-.063173	-.078592	-.094560
-.100980	-.096372	-.089345	-.089446	-.097589	-.106806	-.110086	-.106849
-.102354	-.099516	-.096879	-.092740	-.088029	-.084015	-.077298	-.060464
-.029101	.012054	.051745	.081075	.099825	.113841	.126933	.136723
.139845	.137256	.134624	.139499	.149849	.157484	.155714	.145787
.137313	.136668	.137440	.124761	.090988	.045798	.008919	-.007671
-.009210	-.010730	-.022518	-.044144	-.069665	-.094199	-.114253	-.126062
-.128338	-.126701	-.130616	-.142631	-.151980	-.143012	-.111391	-.070192
-.037920	-.021397	-.012135	.000934	.018329	.031139	.033555	.031078
.035636	.054045	.082374	.110039	.127463	.130103	.118289	.095877
.069167	.044631	.025751	.011673	-.000187	-.010247	-.015944	-.015068
-.008712	.000086	.010202	.022695	.035999	.042238	.031929	.004371
-.027772	-.047571	-.049245	-.043822	-.047713	-.065690	-.086296	-.094513
-.087023	-.073237	-.062183	-.052074	-.035069	-.010497	.011293	.020302
.019824	.023971	.041464	.064352	.075315	.065290	.041932	.020840
.011429	.012713	.020158	.032002	.047806	.064071	.075019	.077482
.072615	.062012	.044708	.020031	-.007553	-.029386	-.039285	-.038189
-.031689	-.024844	-.020670	-.021847	-.029981	-.042146	-.050887	-.051006
-.046114	-.046163	-.057369	-.075979	-.092686	-.101728	-.103695	-.100516
-.090864	-.072474	-.047332	-.021804	-.000491	.018778	.042615	.074501
.109903	.138665	.152174	.148727	.133312	.113144	.093714	.078241
.069480	.069912	.078894	.089825	.092304	.079410	.053892	.026151

```

.004826 -.011066 -.029870 -.057044 -.087676 -.110108 -.116797 -.111198
-.103914 -.102853 -.107181 -.110102 -.106579 -.098651 -.093661 -.097078
-.105996 -.109867 -.099135 -.074695 -.048301 -.032175 -.027518 -.024258
-.012419 .007479 .026702 .039556 .049238 .060873 .071436 .070639
.053222 .027423 .008271 .002498 .002754 -.002406 -.014515 -.023076
-.016592 .005859 .033714 .053213 .056255 .043921 .024829 .009733
.004397 .004946 .001094 -.013786 -.034940 -.049702 -.049122 -.035677
-.019240 -.007095 .000821 .007953 .015677 .023086 .030328 .039123
.049454 .057456 .058287 .050726 .038343 .026499 .019327 .018878
.024754 .032598 .034402 .023712 .002708 -.017260 -.024724 -.018770
-.009447 -.006874 -.010987 -.013690 -.010318 -.006353 -.011167 -.026688
-.044545 -.054697 -.054816 -.050270 -.046350 -.042832 -.036000 -.024100
-.009498 .003398 .011029 .011822 .006535 -.001329 -.005836 -.000972
.016068 .042685 .071243 .091930 .097729 .089377 .076254 .070012
.074588 .082053 .080543 .067684 .055196 .057995 .078510 .103117
.114914 .108608 .091912 .073973 .055961 .033854 .007318 -.018180
-.037892 -.052763 -.065371 -.073439 -.072266 -.065555 -.069979 -.103254
-.165052 -.232126 -.275747 -.285197 -.272967 -.257155 -.241497 -.215415
-.172412 -.124053 -.092147 -.087572 -.099273 -.105397 -.093703 -.069614
-.045156 -.023422 .003786 .043522 .089890 .126722 .142325 .140903
.139380 .153686 .188165 .234396 .279037 .312039 .328699 .329290
.318675 .304630 .294036 .288929 .286523 .283156 .277741 .270934
.262185 .249154 .230249 .205792 .175475 .135870 .083524 .021716
-.037560 -.081461 -.107243 -.124739 -.146866 -.177691 -.211732 -.242501
-.269178 -.295762 -.321550 -.341580 -.350767 -.348232 -.341038 -.335326
-.330634 -.323101 -.309763 -.291543 -.266896 -.231458 -.181678 -.120651
-.059244 -.009980 .020656 .034833 .039705 .041973 .045210 .050560
.058323 .068509 .080335 .092405 .104189 .114455 .123437 .128873
.126339 .113948 .095412 .079758 .073929 .075272 .072822 .057948
.033500 .012175 .006209 .016969 .037638 .061784 .086275 .107063
.117876 .112199 .087823 .049079 .004833 -.034724 -.061080 -.070523
-.066209 -.056198 -.047335 -.040496 -.032454 -.022428 -.015251 -.016948
-.027595 -.040170 -.047030 -.047043 -.045526 -.047467 -.051303 -.049567
-.035310 -.008523 .022582 .045800 .051805 .039389 .016074 -.006480
-.019096 -.019277 -.010282 .003064 .017986 .034033 .050700 .064825
.070633 .063416 .044965 .025430 .017667 .026704 .044124 .054407
.048791 .032843 .019742 .016383 .017589 .013888 .002673 -.010799
-.022297 -.034613 -.052082 -.071335 -.081965 -.078327 -.067840 -.064217
-.072487 -.084017 -.087742 -.084046 -.084276 -.096957 -.117597 -.134020
-.139773 -.139460 -.140589 -.142954 -.138090 -.118625 -.086127 -.049482
-.017162 .007293 .023257 .029495 .025303 .014856 .007867 .012992
.029903 .049075 .060944 .065049 .069292 .080078 .094659 .103986
.102207 .091583 .078348 .065978 .054403 .044317 .038878 .039151
.039628 .031419 .011566 -.011858 -.025375 -.021566 -.005129 .011371
.016962 .008414 -.009883 -.029722 -.042934 -.044354 -.033609 -.015023
.004996 .021413 .032461 .038805 .041502 .040796 .036752 .030527
.024546 .020651 .018034 .013810 .007068 .002223 .006611 .022754
.043487 .056971 .058241 .054642 .057863 .070130 .080127 .073844
.048847 .016338 -.010242 -.026503 -.036237 -.042160 -.041255 -.030536

```

Analysis Results File, "OUTPUT"

** This is only Selected Portions of the OUTPUT*

SpineBridgel

```

number of nodal points      = 118
number of element types     = 3
number of total elements    = 106
number of time functions    = 3

```

```

ground motion input code = 2
number of time steps (dt) = 9205
dt multiplier for output = 20
damping factor alpha = 5.692E-01
damping factor beta = 4.392E-03

```

lnodal point data as input.....

Nodal number	boundary condition codes						nodal point coordinates			
	x	y	z	xx	yy	zz	x	y	z	
1	0	0	0	0	0	0	-2058.000	0.000	0.000	0
2	0	0	0	0	0	0	-2046.000	0.000	0.000	0
3	0	0	0	0	0	0	-1839.000	0.000	0.000	0
4	0	0	0	0	0	0	-1632.000	0.000	0.000	0
5	0	0	0	0	0	0	-1425.000	0.000	0.000	0
6	0	0	0	0	0	0	-1219.000	0.000	0.000	0
7	0	0	0	0	0	0	-1217.000	0.000	0.000	0
8	0	0	0	0	0	0	-901.500	0.000	0.000	0
9	0	0	0	0	0	0	-609.000	0.000	0.000	0
10	0	0	0	0	0	0	-304.500	0.000	0.000	0
11	0	0	0	0	0	0	-0.750	0.000	0.000	0
12	0	0	0	0	0	0	0.750	0.000	0.000	0
13	0	0	0	0	0	0	304.500	0.000	0.000	0
14	0	0	0	0	0	0	609.000	0.000	0.000	0
15	0	0	0	0	0	0	901.500	0.000	0.000	0
16	0	0	0	0	0	0	1217.000	0.000	0.000	0
17	0	0	0	0	0	0	1219.000	0.000	0.000	0
18	0	0	0	0	0	0	1368.000	0.000	0.000	0
19	0	0	0	0	0	0	1518.000	0.000	0.000	0
20	0	0	0	0	0	0	1668.000	0.000	0.000	0
21	0	0	0	0	0	0	1818.000	0.000	0.000	0
22	0	0	0	0	0	0	1830.000	0.000	0.000	0
23	0	0	0	0	0	0	-1218.000	162.000	0.000	0
24	0	0	0	0	0	0	-1218.000	135.700	0.000	0
25	0	0	0	0	0	0	-1218.000	0.000	0.000	0
26	0	0	0	0	0	0	-1218.000	-135.700	0.000	0
27	0	0	0	0	0	0	-1218.000	-162.000	0.000	0
28	0	0	0	0	0	0	0.000	162.000	0.000	0
29	0	0	0	0	0	0	0.000	135.700	0.000	0
30	0	0	0	0	0	0	0.000	0.000	0.000	0
31	0	0	0	0	0	0	0.000	-135.700	0.000	0
32	0	0	0	0	0	0	0.000	-162.000	0.000	0
33	0	0	0	0	0	0	1218.000	162.000	0.000	0
34	0	0	0	0	0	0	1218.000	135.700	0.000	0
35	0	0	0	0	0	0	1218.000	0.000	0.000	0
36	0	0	0	0	0	0	1218.000	-135.700	0.000	0
37	0	0	0	0	0	0	1218.000	-162.000	0.000	0
38	0	0	0	0	0	1	-2058.000	0.000	-23.400	0
39	0	0	0	0	0	1	1830.000	0.000	-23.400	0
40	0	0	0	0	0	0	-1218.000	135.700	-200.000	0
41	0	0	0	0	0	0	-1218.000	0.000	-200.000	0
42	0	0	0	0	0	0	-1218.000	-135.700	-200.000	0
43	0	0	0	0	0	0	-1218.000	135.700	-218.400	0
44	0	0	0	0	0	0	-1218.000	0.000	-218.400	0
45	0	0	0	0	0	0	-1218.000	-135.700	-218.400	0
46	0	0	0	0	0	0	-1218.000	135.700	-266.500	0
47	0	0	0	0	0	0	-1218.000	0.000	-266.500	0
48	0	0	0	0	0	0	-1218.000	-135.700	-266.500	0
49	0	0	0	0	0	0	-1218.000	135.700	-282.500	0
50	0	0	0	0	0	0	-1218.000	0.000	-282.500	0
51	0	0	0	0	0	0	-1218.000	-135.700	-282.500	0
52	0	0	0	0	0	1	-1218.000	135.700	-318.500	0
53	0	0	0	0	0	1	-1218.000	0.000	-318.500	0
54	0	0	0	0	0	1	-1218.000	-135.700	-318.500	0

55	0	0	0	0	0	0	0.000	135.700	-100.000	0
56	0	0	0	0	0	0	0.000	0.000	-100.000	0
57	0	0	0	0	0	0	0.000	-135.700	-100.000	0
58	0	0	0	0	0	0	0.000	135.700	-218.400	0
59	0	0	0	0	0	0	0.000	0.000	-218.400	0
60	0	0	0	0	0	0	0.000	-135.700	-218.400	0
61	0	0	0	0	0	0	0.000	135.700	-266.600	0
62	0	0	0	0	0	0	0.000	0.000	-266.600	0
63	0	0	0	0	0	0	0.000	-135.700	-266.600	0
64	0	0	0	0	0	0	0.000	135.700	-282.600	0
65	0	0	0	0	0	0	0.000	0.000	-282.600	0
66	0	0	0	0	0	0	0.000	-135.700	-282.600	0
67	0	0	0	0	0	0	0.000	135.700	-318.600	0
68	0	0	0	0	0	0	0.000	0.000	-318.600	0
69	0	0	0	0	0	0	0.000	-135.700	-318.600	0
70	0	0	0	0	0	0	1218.000	135.700	-100.000	0
71	0	0	0	0	0	0	1218.000	0.000	-100.000	0
72	0	0	0	0	0	0	1218.000	-135.700	-100.000	0
73	0	0	0	0	0	0	1218.000	135.700	-190.000	0
74	0	0	0	0	0	0	1218.000	0.000	-190.000	0
75	0	0	0	0	0	0	1218.000	-135.700	-190.000	0
76	0	0	0	0	0	0	1218.000	135.700	-237.700	0
77	0	0	0	0	0	0	1218.000	0.000	-237.700	0
78	0	0	0	0	0	0	1218.000	-135.700	-237.700	0
79	0	0	0	0	0	0	1218.000	135.700	-252.500	0
80	0	0	0	0	0	0	1218.000	0.000	-252.500	0
81	0	0	0	0	0	0	1218.000	-135.700	-252.500	0
82	0	0	0	0	0	0	1218.000	135.700	-288.500	0
83	0	0	0	0	0	0	1218.000	0.000	-288.500	0
84	0	0	0	0	0	0	1218.000	-135.700	-288.500	0
85	1	1	1	1	1	1	-2058.000	200.000	0.000	0
86	1	1	1	1	1	1	-1219.000	200.000	0.000	0
87	1	1	1	1	1	1	-0.750	200.000	0.000	0
88	1	1	1	1	1	1	1217.000	200.000	0.000	0
89	1	1	1	1	1	1	1830.000	200.000	0.000	0
90	1	1	1	1	1	1	1830.000	-200.000	0.000	0
91	1	1	1	1	1	1	-1218.000	200.000	0.000	0
92	1	1	1	1	1	1	0.000	200.000	0.000	0
93	1	1	1	1	1	1	1218.000	200.000	0.000	0
94	1	1	1	1	1	1	-1218.000	180.000	-318.500	0
95	1	1	1	1	1	1	-1210.000	135.700	-318.500	0
96	1	1	1	1	1	1	-1210.000	0.000	-318.500	0
97	1	1	1	1	1	1	-1210.000	-135.700	-318.500	0
98	1	1	1	1	1	1	0.000	180.000	-318.500	0
99	1	1	1	1	1	1	8.000	135.700	-318.500	0
100	1	1	1	1	1	1	8.000	0.000	-318.500	0
101	1	1	1	1	1	1	8.000	-135.700	-318.500	0
102	1	1	1	1	1	1	1218.000	180.000	-288.500	0
103	1	1	1	1	1	1	1224.000	135.700	-288.500	0
104	1	1	1	1	1	1	1224.000	0.000	-288.500	0
105	1	1	1	1	1	1	1224.000	-135.700	-288.500	0
106	1	1	1	1	1	1	-2058.000	10.000	-23.400	0
107	1	1	1	1	1	1	-2050.000	0.000	-23.400	0
108	1	1	1	1	1	1	1830.000	10.000	-23.400	0
109	1	1	1	1	1	1	1838.000	0.000	-23.400	0
110	0	0	0	0	0	0	-1218.000	135.700	-52.000	0
111	0	0	0	0	0	0	-1218.000	0.000	-52.000	0
112	0	0	0	0	0	0	-1218.000	-135.700	-52.000	0
113	0	0	0	0	0	0	0.000	135.700	-52.000	0
114	0	0	0	0	0	0	0.000	0.000	-52.000	0
115	0	0	0	0	0	0	0.000	-135.700	-52.000	0
116	0	0	0	0	0	0	1218.000	135.700	-52.000	0
117	0	0	0	0	0	0	1218.000	0.000	-52.000	0
118	0	0	0	0	0	0	1218.000	-135.700	-52.000	0

lcomplete nodal point data.....

Node number	boundary condition codes						nodal point coordinates		
	x	y	z	xx	yy	zz	x	y	z
1	0	0	0	0	0	0	-2058.000	0.000	0.000

2	0	0	0	0	0	0	-2046.000	0.000	0.000
3	0	0	0	0	0	0	-1839.000	0.000	0.000
4	0	0	0	0	0	0	-1632.000	0.000	0.000
5	0	0	0	0	0	0	-1425.000	0.000	0.000
6	0	0	0	0	0	0	-1219.000	0.000	0.000
7	0	0	0	0	0	0	-1217.000	0.000	0.000
8	0	0	0	0	0	0	-901.500	0.000	0.000
9	0	0	0	0	0	0	-609.000	0.000	0.000
10	0	0	0	0	0	0	-304.500	0.000	0.000
11	0	0	0	0	0	0	-0.750	0.000	0.000
12	0	0	0	0	0	0	0.750	0.000	0.000
13	0	0	0	0	0	0	304.500	0.000	0.000
14	0	0	0	0	0	0	609.000	0.000	0.000
15	0	0	0	0	0	0	901.500	0.000	0.000
16	0	0	0	0	0	0	1217.000	0.000	0.000
17	0	0	0	0	0	0	1219.000	0.000	0.000
18	0	0	0	0	0	0	1368.000	0.000	0.000
19	0	0	0	0	0	0	1518.000	0.000	0.000
20	0	0	0	0	0	0	1668.000	0.000	0.000
21	0	0	0	0	0	0	1818.000	0.000	0.000
22	0	0	0	0	0	0	1830.000	0.000	0.000
23	0	0	0	0	0	0	-1218.000	162.000	0.000
24	0	0	0	0	0	0	-1218.000	135.700	0.000
25	0	0	0	0	0	0	-1218.000	0.000	0.000
26	0	0	0	0	0	0	-1218.000	-135.700	0.000
27	0	0	0	0	0	0	-1218.000	-162.000	0.000
28	0	0	0	0	0	0	0.000	162.000	0.000
29	0	0	0	0	0	0	0.000	135.700	0.000
30	0	0	0	0	0	0	0.000	0.000	0.000
31	0	0	0	0	0	0	0.000	-135.700	0.000
32	0	0	0	0	0	0	0.000	-162.000	0.000
33	0	0	0	0	0	0	1218.000	162.000	0.000
34	0	0	0	0	0	0	1218.000	135.700	0.000
35	0	0	0	0	0	0	1218.000	0.000	0.000
36	0	0	0	0	0	0	1218.000	-135.700	0.000
37	0	0	0	0	0	0	1218.000	-162.000	0.000
38	0	0	0	0	0	1	-2058.000	0.000	-23.400
39	0	0	0	0	0	1	1830.000	0.000	-23.400
40	0	0	0	0	0	0	-1218.000	135.700	-200.000
41	0	0	0	0	0	0	-1218.000	0.000	-200.000
42	0	0	0	0	0	0	-1218.000	-135.700	-200.000
43	0	0	0	0	0	0	-1218.000	135.700	-218.400
44	0	0	0	0	0	0	-1218.000	0.000	-218.400
45	0	0	0	0	0	0	-1218.000	-135.700	-218.400
46	0	0	0	0	0	0	-1218.000	135.700	-266.500
47	0	0	0	0	0	0	-1218.000	0.000	-266.500
48	0	0	0	0	0	0	-1218.000	-135.700	-266.500
49	0	0	0	0	0	0	-1218.000	135.700	-282.500
50	0	0	0	0	0	0	-1218.000	0.000	-282.500
51	0	0	0	0	0	0	-1218.000	-135.700	-282.500
52	0	0	0	0	0	1	-1218.000	135.700	-318.500
53	0	0	0	0	0	1	-1218.000	0.000	-318.500
54	0	0	0	0	0	1	-1218.000	-135.700	-318.500
55	0	0	0	0	0	0	0.000	135.700	-100.000
56	0	0	0	0	0	0	0.000	0.000	-100.000
57	0	0	0	0	0	0	0.000	-135.700	-100.000
58	0	0	0	0	0	0	0.000	135.700	-218.400
59	0	0	0	0	0	0	0.000	0.000	-218.400
60	0	0	0	0	0	0	0.000	-135.700	-218.400
61	0	0	0	0	0	0	0.000	135.700	-266.600
62	0	0	0	0	0	0	0.000	0.000	-266.600
63	0	0	0	0	0	0	0.000	-135.700	-266.600
64	0	0	0	0	0	0	0.000	135.700	-282.600
65	0	0	0	0	0	0	0.000	0.000	-282.600
66	0	0	0	0	0	0	0.000	-135.700	-282.600
67	0	0	0	0	0	0	0.000	135.700	-318.600
68	0	0	0	0	0	0	0.000	0.000	-318.600
69	0	0	0	0	0	0	0.000	-135.700	-318.600
70	0	0	0	0	0	0	1218.000	135.700	-100.000
71	0	0	0	0	0	0	1218.000	0.000	-100.000
72	0	0	0	0	0	0	1218.000	-135.700	-100.000

73	0	0	0	0	0	0	1218.000	135.700	-190.000
74	0	0	0	0	0	0	1218.000	0.000	-190.000
75	0	0	0	0	0	0	1218.000	-135.700	-190.000
76	0	0	0	0	0	0	1218.000	135.700	-237.700
77	0	0	0	0	0	0	1218.000	0.000	-237.700
78	0	0	0	0	0	0	1218.000	-135.700	-237.700
79	0	0	0	0	0	0	1218.000	135.700	-252.500
80	0	0	0	0	0	0	1218.000	0.000	-252.500
81	0	0	0	0	0	0	1218.000	-135.700	-252.500
82	0	0	0	0	0	0	1218.000	135.700	-288.500
83	0	0	0	0	0	0	1218.000	0.000	-288.500
84	0	0	0	0	0	0	1218.000	-135.700	-288.500
85	1	1	1	1	1	1	-2058.000	200.000	0.000
86	1	1	1	1	1	1	-1219.000	200.000	0.000
87	1	1	1	1	1	1	-0.750	200.000	0.000
88	1	1	1	1	1	1	1217.000	200.000	0.000
89	1	1	1	1	1	1	1830.000	200.000	0.000
90	1	1	1	1	1	1	1830.000	-200.000	0.000
91	1	1	1	1	1	1	-1218.000	200.000	0.000
92	1	1	1	1	1	1	0.000	200.000	0.000
93	1	1	1	1	1	1	1218.000	200.000	0.000
94	1	1	1	1	1	1	-1218.000	180.000	-318.500
95	1	1	1	1	1	1	-1210.000	135.700	-318.500
96	1	1	1	1	1	1	-1210.000	0.000	-318.500
97	1	1	1	1	1	1	-1210.000	-135.700	-318.500
98	1	1	1	1	1	1	0.000	180.000	-318.500
99	1	1	1	1	1	1	8.000	135.700	-318.500
100	1	1	1	1	1	1	8.000	0.000	-318.500
101	1	1	1	1	1	1	8.000	-135.700	-318.500
102	1	1	1	1	1	1	1218.000	180.000	-288.500
103	1	1	1	1	1	1	1224.000	135.700	-288.500
104	1	1	1	1	1	1	1224.000	0.000	-288.500
105	1	1	1	1	1	1	1224.000	-135.700	-288.500
106	1	1	1	1	1	1	-2058.000	10.000	-23.400
107	1	1	1	1	1	1	-2050.000	0.000	-23.400
108	1	1	1	1	1	1	1830.000	10.000	-23.400
109	1	1	1	1	1	1	1838.000	0.000	-23.400
110	0	0	0	0	0	0	-1218.000	135.700	-52.000
111	0	0	0	0	0	0	-1218.000	0.000	-52.000
112	0	0	0	0	0	0	-1218.000	-135.700	-52.000
113	0	0	0	0	0	0	0.000	135.700	-52.000
114	0	0	0	0	0	0	0.000	0.000	-52.000
115	0	0	0	0	0	0	0.000	-135.700	-52.000
116	0	0	0	0	0	0	1218.000	135.700	-52.000
117	0	0	0	0	0	0	1218.000	0.000	-52.000
118	0	0	0	0	0	0	1218.000	-135.700	-52.000

lequation number of nodal degrees of freedom....

node number	x	y	z	xx	yy	zz	node number	x	y	z	xx	yy	zz
1	1	2	3	4	5	6	2	7	8	9	10	11	12
3	13	14	15	16	17	18	4	19	20	21	22	23	24
5	25	26	27	28	29	30	6	31	32	33	34	35	36
7	37	38	39	40	41	42	8	43	44	45	46	47	48
9	49	50	51	52	53	54	10	55	56	57	58	59	60
11	61	62	63	64	65	66	12	67	68	69	70	71	72
13	73	74	75	76	77	78	14	79	80	81	82	83	84
15	85	86	87	88	89	90	16	91	92	93	94	95	96
17	97	98	99	100	101	102	18	103	104	105	106	107	108
19	109	110	111	112	113	114	20	115	116	117	118	119	120
21	121	122	123	124	125	126	22	127	128	129	130	131	132
23	133	134	135	136	137	138	24	139	140	141	142	143	144
25	145	146	147	148	149	150	26	151	152	153	154	155	156
27	157	158	159	160	161	162	28	163	164	165	166	167	168
29	169	170	171	172	173	174	30	175	176	177	178	179	180
31	181	182	183	184	185	186	32	187	188	189	190	191	192
33	193	194	195	196	197	198	34	199	200	201	202	203	204
35	205	206	207	208	209	210	36	211	212	213	214	215	216
37	217	218	219	220	221	222	38	223	224	225	226	227	0

39	228	229	230	231	232	0	40	233	234	235	236	237	238
41	239	240	241	242	243	244	42	245	246	247	248	249	250
43	251	252	253	254	255	256	44	257	258	259	260	261	262
45	263	264	265	266	267	268	46	269	270	271	272	273	274
47	275	276	277	278	279	280	48	281	282	283	284	285	286
49	287	288	289	290	291	292	50	293	294	295	296	297	298
51	299	300	301	302	303	304	52	305	306	307	308	309	0
53	310	311	312	313	314	0	54	315	316	317	318	319	0
55	320	321	322	323	324	325	56	326	327	328	329	330	331
57	332	333	334	335	336	337	58	338	339	340	341	342	343
59	344	345	346	347	348	349	60	350	351	352	353	354	355
61	356	357	358	359	360	361	62	362	363	364	365	366	367
63	368	369	370	371	372	373	64	374	375	376	377	378	379
65	380	381	382	383	384	385	66	386	387	388	389	390	391
67	392	393	394	395	396	397	68	398	399	400	401	402	403
69	404	405	406	407	408	409	70	410	411	412	413	414	415
71	416	417	418	419	420	421	72	422	423	424	425	426	427
73	428	429	430	431	432	433	74	434	435	436	437	438	439
75	440	441	442	443	444	445	76	446	447	448	449	450	451
77	452	453	454	455	456	457	78	458	459	460	461	462	463
79	464	465	466	467	468	469	80	470	471	472	473	474	475
81	476	477	478	479	480	481	82	482	483	484	485	486	487
83	488	489	490	491	492	493	84	494	495	496	497	498	499
85	0	0	0	0	0	0	86	0	0	0	0	0	0
87	0	0	0	0	0	0	88	0	0	0	0	0	0
89	0	0	0	0	0	0	90	0	0	0	0	0	0
91	0	0	0	0	0	0	92	0	0	0	0	0	0
93	0	0	0	0	0	0	94	0	0	0	0	0	0
95	0	0	0	0	0	0	96	0	0	0	0	0	0
97	0	0	0	0	0	0	98	0	0	0	0	0	0
99	0	0	0	0	0	0	100	0	0	0	0	0	0
101	0	0	0	0	0	0	102	0	0	0	0	0	0
103	0	0	0	0	0	0	104	0	0	0	0	0	0
105	0	0	0	0	0	0	106	0	0	0	0	0	0
107	0	0	0	0	0	0	108	0	0	0	0	0	0
109	0	0	0	0	0	0	110	500	501	502	503	504	505
111	506	507	508	509	510	511	112	512	513	514	515	516	517
113	518	519	520	521	522	523	114	524	525	526	527	528	529
115	530	531	532	533	534	535	116	536	537	538	539	540	541
117	542	543	544	545	546	547	118	548	549	550	551	552	553

1.....three dimensional beam elements

```

number of beams                = 84
number of geometric property sets= 6
number of fixed end force sets = 0
number of materials             = 3
number of beam n/l property sets = 15
material properties....

```

material number	young's modulus	poisson's ratio	mass density
1	1000000.	0.18000	0.00000
2	3604.	0.18000	0.00000
3	360400.	0.18000	0.00000

beam geometric properties....

element type	area x	area y	area z	inertia x	inertia y	inertia z
1	1018.000	855.300	855.300	164900.000	82450.000	82450.000
2	7134.000	7134.000	7134.000	110100.000	4257000.000	*****

3	1872.000	1872.000	1872.00011140000.000*****
4	1872.000	1872.000	1872.00012070000.000*****
5	1872.000	1872.000	1872.00010720000.000*****
6	1018.000	1018.000	1018.000 164900.000 20000.000 20000.000

element load multipliers.....

	a	b	c	d
x-dir	0.000000E+00	0.000000E+00	0.000000E+00	0.000000E+00
y-dir	0.000000E+00	0.000000E+00	0.000000E+00	0.000000E+00
z-dir	-0.386400E+03	0.000000E+00	0.000000E+00	0.000000E+00

1

beam element nonlinear parameters

npar	axial		moment		axial		yield		
	no	pu	mu/y	mu/z	tu	a0	a1	a2	a3
b0	b1	b2	b3						
1	0.111E+04	0.158E+05	0.133E+05	0.101E+00	1.000	-7.881	-10.240	-1.356	
1.000	-7.881	-10.240	-1.356						
2	0.111E+04	0.169E+05	0.143E+05	0.101E+00	1.000	-7.880	-10.240	-1.360	
1.000	-7.880	-10.240	-1.360						
3	0.111E+04	0.149E+05	0.126E+05	0.101E+00	1.000	-7.880	-10.240	-1.360	
1.000	-7.880	-10.240	-1.360						
4	0.611E+04	0.967E+04	0.967E+04	0.160E+00	1.000	-8.461	-13.350	-3.888	
1.000	-8.461	-13.350	-3.888						
5	0.611E+04	0.967E+04	0.967E+04	0.160E+00	1.000	-8.461	-13.350	-3.888	
1.000	-8.461	-13.350	-3.888						
6	0.611E+04	0.967E+04	0.967E+04	0.160E+00	1.000	-8.461	-13.350	-3.888	
1.000	-8.461	-13.350	-3.888						
7	0.611E+04	0.967E+04	0.967E+04	0.160E+00	1.000	-8.461	-13.350	-3.888	
1.000	-8.461	-13.350	-3.888						
8	0.611E+04	0.967E+04	0.967E+04	0.160E+00	1.000	-8.461	-13.350	-3.888	
1.000	-8.461	-13.350	-3.888						
9	0.611E+04	0.967E+04	0.967E+04	0.160E+00	1.000	-8.461	-13.350	-3.888	
1.000	-8.461	-13.350	-3.888						
10	0.611E+04	0.122E+05	0.122E+05	0.161E+00	1.000	-6.336	-9.664	-2.328	
1.000	-6.336	-9.664	-2.328						
11	0.611E+04	0.122E+05	0.122E+05	0.161E+00	1.000	-6.336	-9.664	-2.328	
1.000	-6.336	-9.664	-2.328						
12	0.611E+04	0.122E+05	0.122E+05	0.161E+00	1.000	-6.336	-9.664	-2.328	
1.000	-6.336	-9.664	-2.328						
13	0.611E+04	0.122E+05	0.122E+05	0.161E+00	1.000	-6.336	-9.664	-2.328	
1.000	-6.336	-9.664	-2.328						
14	0.611E+04	0.122E+05	0.122E+05	0.161E+00	1.000	-6.336	-9.664	-2.328	
1.000	-6.336	-9.664	-2.328						
15	0.611E+04	0.122E+05	0.122E+05	0.161E+00	1.000	-6.336	-9.664	-2.328	
1.000	-6.336	-9.664	-2.328						

npar	cri. curv. damage	cri. curv. coeffi. at j end	max. curv.	max. damage	coeffi. at i end	cri. curv.	max. curv.	max.
1	0.500E+02	0.500E+02	0.900E+02	0.800E+00	0.500E+02	0.900E+02		
0.600E+00								
2	0.500E+02	0.500E+02	0.900E+02	0.800E+00	0.500E+02	0.900E+02		
0.800E+00								
3	0.500E+02	0.500E+02	0.900E+02	0.800E+00	0.500E+02	0.900E+02		
0.800E+00								
4	0.363E-01	0.363E-01	0.261E+00	0.820E+00	0.363E-01	0.261E+00		
0.820E+00								
5	0.363E-01	0.363E-01	0.261E+00	0.770E+00	0.363E-01	0.261E+00		
0.770E+00								
6	0.363E-01	0.363E-01	0.261E+00	0.770E+00	0.363E-01	0.261E+00		
0.770E+00								
7	0.363E-01	0.363E-01	0.261E+00	0.730E+00	0.363E-01	0.261E+00		
0.730E+00								
8	0.363E-01	0.363E-01	0.261E+00	0.830E+00	0.363E-01	0.261E+00		
0.830E+00								

```

 9      0.363E-01  0.261E+00      0.790E+00      0.363E-01  0.261E+00
0.790E+00
10      0.363E-01  0.261E+00      0.820E+00      0.363E-01  0.261E+00
0.820E+00
11      0.363E-01  0.261E+00      0.770E+00      0.363E-01  0.261E+00
0.770E+00
12      0.363E-01  0.261E+00      0.770E+00      0.363E-01  0.261E+00
0.770E+00
13      0.363E-01  0.261E+00      0.770E+00      0.363E-01  0.261E+00
0.770E+00
14      0.363E-01  0.261E+00      0.830E+00      0.363E-01  0.261E+00
0.830E+00
15      0.363E-01  0.261E+00      0.790E+00      0.363E-01  0.261E+00
0.790E+00
lbeam element data.....

```

lbeam no	nodes			matl geom		elem loads				end codes		l/nl
	i	j	k	no	no	a	b	c	d	i	j	ind
1	2	3	85	3	2	0	0	0	0	0	0	0
2	3	4	85	3	2	0	0	0	0	0	0	0
3	4	5	85	3	2	0	0	0	0	0	0	0
4	5	6	85	3	2	0	0	0	0	0	0	0
5	7	8	85	3	2	0	0	0	0	0	0	0
6	8	9	85	3	2	0	0	0	0	0	0	0
7	9	10	85	3	2	0	0	0	0	0	0	0
8	10	11	85	3	2	0	0	0	0	0	0	0
9	12	13	85	3	2	0	0	0	0	0	0	0
10	13	14	85	3	2	0	0	0	0	0	0	0
11	14	15	85	3	2	0	0	0	0	0	0	0
12	15	16	85	3	2	0	0	0	0	0	0	0
13	17	18	85	3	2	0	0	0	0	0	0	0
14	18	19	85	3	2	0	0	0	0	0	0	0
15	19	20	85	3	2	0	0	0	0	0	0	0
16	20	21	85	3	2	0	0	0	0	0	0	0
17	23	24	2	3	3	0	0	0	0	0	0	0
18	24	25	2	3	3	0	0	0	0	0	0	0
19	25	26	2	3	3	0	0	0	0	0	0	0
20	26	27	2	3	3	0	0	0	0	0	0	0
21	28	29	2	3	4	0	0	0	0	0	0	0
22	29	30	2	3	4	0	0	0	0	0	0	0
23	30	31	2	3	4	0	0	0	0	0	0	0
24	31	32	2	3	4	0	0	0	0	0	0	0
25	33	34	2	3	5	0	0	0	0	0	0	0
26	34	35	2	3	5	0	0	0	0	0	0	0
27	35	36	2	3	5	0	0	0	0	0	0	0
28	36	37	2	3	5	0	0	0	0	0	0	0
29	1	38	3	1	1	0	0	0	0	0	0	0
30	49	52	55	1	1	0	0	0	0	0	0	0
31	50	53	56	1	1	0	0	0	0	0	0	0
32	51	54	57	1	1	0	0	0	0	0	0	0
33	64	67	69	1	1	0	0	0	0	0	0	0
34	65	68	71	1	1	0	0	0	0	0	0	0
35	66	69	72	1	1	0	0	0	0	0	0	0
36	79	82	67	1	1	0	0	0	0	0	0	0
37	80	83	65	1	1	0	0	0	0	0	0	0
38	81	84	66	1	1	0	0	0	0	0	0	0
39	22	39	35	1	1	0	0	0	0	0	0	0
40	24	110	55	1	1	0	0	0	0	0	0	0
41	25	111	30	1	1	0	0	0	0	0	0	0
42	26	112	31	1	1	0	0	0	0	0	0	0
43	40	43	29	2	6	0	0	0	0	0	0	0
44	41	44	30	2	6	0	0	0	0	0	0	0
45	42	45	31	2	6	0	0	0	0	0	0	0
46	43	46	29	2	6	0	0	0	0	0	0	5
47	44	47	30	2	6	0	0	0	0	0	0	4
48	45	48	31	2	6	0	0	0	0	0	0	5
49	46	49	29	2	6	0	0	0	0	0	0	0
50	47	50	30	2	6	0	0	0	0	0	0	0
51	48	51	31	2	6	0	0	0	0	0	0	0
52	29	113	24	1	1	0	0	0	0	0	0	0
53	30	114	25	1	1	0	0	0	0	0	0	0

54	31	115	26	1	1	0	0	0	0	0	0	0
55	55	58	40	2	6	0	0	0	0	0	0	0
56	56	59	41	2	6	0	0	0	0	0	0	0
57	57	60	42	2	6	0	0	0	0	0	0	0
58	58	61	40	2	6	0	0	0	0	0	0	7
59	59	62	25	2	6	0	0	0	0	0	0	6
60	60	63	26	2	6	0	0	0	0	0	0	7
61	61	64	24	2	6	0	0	0	0	0	0	0
62	62	65	25	2	6	0	0	0	0	0	0	0
63	63	66	26	2	6	0	0	0	0	0	0	0
64	34	116	29	1	1	0	0	0	0	0	0	0
65	35	117	30	1	1	0	0	0	0	0	0	0
66	36	118	31	1	1	0	0	0	0	0	0	0
67	70	73	29	2	6	0	0	0	0	0	0	0
68	71	74	30	2	6	0	0	0	0	0	0	0
69	72	75	31	2	6	0	0	0	0	0	0	0
70	73	76	29	2	6	0	0	0	0	0	0	9
71	74	77	30	2	6	0	0	0	0	0	0	8
72	75	78	31	2	6	0	0	0	0	0	0	9
73	76	79	29	2	6	0	0	0	0	0	0	0
74	77	80	30	2	6	0	0	0	0	0	0	0
75	78	81	31	2	6	0	0	0	0	0	0	0
76	110	40	55	2	6	0	0	0	0	0	0	11
77	111	41	30	2	6	0	0	0	0	0	0	10
78	112	42	31	2	6	0	0	0	0	0	0	11
79	113	55	24	2	6	0	0	0	0	0	0	13
80	114	56	25	2	6	0	0	0	0	0	0	12
81	115	57	26	2	6	0	0	0	0	0	0	13
82	116	70	29	2	6	0	0	0	0	0	0	15
83	117	71	30	2	6	0	0	0	0	0	0	14
84	118	72	31	2	6	0	0	0	0	0	0	15

1.....boundary elements

number of elements = 11

number of stiffness sets = 5

number of n/l par. sets = 0

lset no	stiffnesses of boundary springs					
	r1	r2	r3	m1	m2	m3
1	0.836E+03	0.111E+03	0.253E+05	0.100E+08	0.100E+08	0.175E+07
2	0.712E+04	0.712E+04	0.305E+05	0.575E+06	0.932E+06	0.129E+06
3	0.747E+04	0.747E+04	0.318E+05	0.728E+06	0.102E+07	0.140E+06
4	0.674E+04	0.674E+04	0.290E+05	0.441E+06	0.859E+06	0.117E+06
5	0.836E+03	0.111E+03	0.253E+05	0.100E+08	0.100E+08	0.175E+07

lele. no	nodes		matl k	nind no	
	i	j,			
1	38	107	106	1	0
2	52	95	94	2	0
3	53	96	94	2	0
4	54	97	94	2	0
5	67	99	98	3	0
6	68	100	98	3	0
7	69	101	98	3	0
8	82	103	102	4	0
9	83	104	102	4	0
10	84	105	102	4	0
11	39	109	108	5	0

1.....expansion joint elements

number of elements = 11

number of stiffness sets = 2

number of n/l par. sets = 3

lset no	stiffnesses of expansion springs					
	r1	r2	r3	m1	m2	m3

```

1 0.100E+01 0.100E+01 0.100E+01 0.100E+01 0.100E+01 0.100E+01
2 0.124E+03 0.124E+03 0.100E+08 0.124E+03 0.100E+08 0.100E+08
lnonlinear parameters of expansion joint elements....

```

npar no.	friction coeff.	friction stiffness	seat gap	tie gap	tie stiff	tie yield force	impact spring
1	0.200E-01	0.100E+01	0.000E+00	0.000E+00	0.000E+00	0.000E+00	0.100E+01
2	0.000E+00	0.100E+01	0.150E+01	0.000E+00	0.000E+00	0.000E+00	0.221E+05
3	0.200E-01	0.100E+01	0.150E+01	0.000E+00	0.000E+00	0.000E+00	0.221E+05

joint tie bars.....

npar no.	number of ties	tie positions relative to joint center					
		1	2	3	4	5	6
1	0	0.000	0.000	0.000	0.000	0.000	0.000
2	0	0.000	0.000	0.000	0.000	0.000	0.000
3	0	0.000	0.000	0.000	0.000	0.000	0.000

expansion joint element data.....

elem no.	node i	node j	node k	joint l	joint code	joint sign	spring set no	n/l ind	joint width	skew angle	joint stiffness
1	1	2	85	25	545535	1	2	3	324.000	0.000	0.200E+08
2	6	25	86	30	545535	-1	2	1	324.000	0.000	0.200E+08
3	25	7	91	30	545535	1	2	1	324.000	0.000	0.200E+08
4	11	30	87	35	545535	-1	2	1	324.000	0.000	0.200E+08
5	30	12	92	35	545535	1	2	1	324.000	0.000	0.200E+08
6	16	35	88	22	545535	-1	2	1	324.000	0.000	0.200E+08
7	35	17	93	22	545535	1	2	1	324.000	0.000	0.200E+08
8	22	21	90	35	545535	1	2	3	324.000	0.000	0.200E+08
9	6	7	86	30	545535	1	1	2	324.000	0.000	0.100E+01
10	11	12	87	35	545535	1	1	2	324.000	0.000	0.100E+01
11	16	17	88	22	545535	1	1	2	324.000	0.000	0.100E+01

total number of nonlinear elements = 29

element type of l/nl indicator.....

element number	ind type	element number	ind type	element number	ind type	element number	ind type	element number	ind type
1	-2	2	-2	3	-2	4	-2	5	-2
6	-2	7	-2	8	-2	9	-2	10	-2
11	-2	12	-2	13	-2	14	-2	15	-2
16	-2	17	-2	18	-2	19	-2	20	-2
21	-2	22	-2	23	-2	24	-2	25	-2
26	-2	27	-2	28	-2	29	-2	30	-2
31	-2	32	-2	33	-2	34	-2	35	-2
36	-2	37	-2	38	-2	39	-2	40	-2
41	-2	42	-2	43	-2	44	-2	45	-2
46	2	47	2	48	2	49	-2	50	-2
51	-2	52	-2	53	-2	54	-2	55	-2
56	-2	57	-2	58	2	59	2	60	2
61	-2	62	-2	63	-2	64	-2	65	-2
66	-2	67	-2	68	-2	69	-2	70	2
71	2	72	2	73	-2	74	-2	75	-2
76	2	77	2	78	2	79	2	80	2
81	2	82	2	83	2	84	2	85	-4
86	-4	87	-4	88	-4	89	-4	90	-4
91	-4	92	-4	93	-4	94	-4	95	-4
96	5	97	5	98	5	99	5	100	5
101	5	102	5	103	5	104	5	105	5

system setup information...

total number of equations = 553

band width = 367

element load multiplier for static analysis.....

structure load case	element load multiplier			
	a	b	c	d
1	1.000	0.000	0.000	0.000

lprint of static displacements.....

node no.	node, type	x	y	z	xx	yy	
1		-2.737E-06	-1.614E-07	-1.010E-02	6.566E-09	-5.126E-09	-
8.593E-12							
2		-1.158E-05	-1.614E-07	-1.011E-02	6.566E-09	2.534E-05	-
3.964E-09							
3		-1.158E-05	-9.820E-07	-1.518E-02	7.374E-09	2.236E-05	-
3.964E-09							
4		-1.158E-05	-1.803E-06	-1.917E-02	8.183E-09	1.582E-05	-
3.964E-09							
5		-1.158E-05	-2.623E-06	-2.173E-02	8.991E-09	9.271E-06	-
3.964E-09							
6		-1.158E-05	-3.444E-06	-2.321E-02	9.799E-09	6.297E-06	-
3.964E-09							
7		-3.008E-05	-3.444E-06	-2.322E-02	9.799E-09	3.306E-05	-
1.796E-08							
8		-3.008E-05	-9.111E-06	-3.261E-02	6.264E-09	2.298E-05	-
1.796E-08							
9		-3.008E-05	-1.436E-05	-3.654E-02	2.987E-09	2.871E-06	-
1.796E-08							
10		-3.008E-05	-1.983E-05	-3.408E-02	-4.246E-10	-1.793E-05	-
1.796E-08							
11		-3.008E-05	-2.530E-05	-2.666E-02	-3.836E-09	-2.739E-05	-
1.796E-08							
12		-2.987E-05	-2.530E-05	-2.666E-02	-3.837E-09	2.425E-05	
1.896E-08							
13		-2.987E-05	-1.953E-05	-3.312E-02	-2.580E-09	1.479E-05	
1.896E-08							
14		-2.987E-05	-1.376E-05	-3.462E-02	-1.324E-09	-6.015E-06	
1.896E-08							
15		-2.987E-05	-8.213E-06	-2.978E-02	-1.169E-10	-2.612E-05	
1.896E-08							
16		-2.987E-05	-2.232E-06	-1.939E-02	1.185E-09	-3.620E-05	
1.896E-08							
17		-1.128E-05	-2.232E-06	-1.938E-02	1.185E-09	-1.675E-05	
4.067E-09							
18		-1.127E-05	-1.626E-06	-1.685E-02	1.104E-09	-1.786E-05	
4.067E-09							
19		-1.127E-05	-1.020E-06	-1.402E-02	1.023E-09	-2.030E-05	
4.067E-09							
20		-1.127E-05	-4.140E-07	-1.080E-02	9.426E-10	-2.274E-05	
4.067E-09							

21	-1.127E-05	1.919E-07	-7.281E-03	8.619E-10	-2.385E-05	
4.067E-09						
22	-2.665E-06	1.919E-07	-7.271E-03	8.618E-10	-4.991E-09	
8.816E-12						
23	-1.904E-05	-3.444E-06	-2.309E-02	1.872E-08	-8.343E-08	-
7.633E-09						
24	-1.924E-05	-3.444E-06	-2.309E-02	1.872E-08	-8.343E-08	-
7.633E-09						
25	-2.027E-05	-3.444E-06	-2.320E-02	9.800E-09	-8.344E-08	-
7.633E-09						
26	-2.131E-05	-3.444E-06	-2.310E-02	8.751E-10	-8.344E-08	-
7.633E-09						
27	-2.151E-05	-3.444E-06	-2.310E-02	8.773E-10	-8.344E-08	-
7.633E-09						
28	-3.981E-05	-2.530E-05	-2.653E-02	6.139E-09	1.368E-06	-
4.014E-10						
29	-3.983E-05	-2.530E-05	-2.653E-02	6.141E-09	1.368E-06	-
4.014E-10						
30	-3.988E-05	-2.530E-05	-2.665E-02	-3.837E-09	1.368E-06	-
4.014E-10						
31	-3.993E-05	-2.530E-05	-2.652E-02	-1.381E-08	1.368E-06	-
4.015E-10						
32	-3.994E-05	-2.530E-05	-2.652E-02	-1.381E-08	1.368E-06	-
4.015E-10						
33	-2.144E-05	-2.232E-06	-1.928E-02	9.511E-09	-8.797E-08	
1.008E-08						
34	-2.117E-05	-2.232E-06	-1.928E-02	9.513E-09	-8.797E-08	
1.008E-08						
35	-1.981E-05	-2.232E-06	-1.937E-02	1.185E-09	-8.797E-08	
1.008E-08						
36	-1.844E-05	-2.232E-06	-1.928E-02	-7.143E-09	-8.797E-08	
1.008E-08						
37	-1.817E-05	-2.232E-06	-1.928E-02	-7.141E-09	-8.797E-08	
1.008E-08						
38	-2.617E-06	-7.996E-09	-1.010E-02	6.547E-09	-5.118E-09	
0.000E+00						
39	-2.548E-06	2.120E-07	-7.267E-03	8.593E-10	-4.984E-09	
0.000E+00						
40	-4.496E-06	-5.862E-07	-1.364E-02	7.634E-09	-5.380E-08	-
2.732E-09						
41	-5.031E-06	-1.206E-06	-1.370E-02	1.193E-08	-5.893E-08	-
2.732E-09						
42	-5.565E-06	-1.824E-06	-1.364E-02	1.620E-08	-6.407E-08	-
2.732E-09						
43	-3.552E-06	-4.554E-07	-1.243E-02	6.617E-09	-4.875E-08	-
2.124E-09						
44	-3.991E-06	-9.902E-07	-1.248E-02	1.151E-08	-5.385E-08	-
2.124E-09						
45	-4.431E-06	-1.523E-06	-1.243E-02	1.639E-08	-5.895E-08	-
2.124E-09						
46	-1.549E-06	-1.947E-07	-9.223E-03	4.335E-09	-3.411E-08	-
5.334E-10						
47	-1.757E-06	-4.743E-07	-9.263E-03	9.723E-09	-3.842E-08	-
5.334E-10						
48	-1.965E-06	-7.528E-07	-9.224E-03	1.509E-08	-4.274E-08	-
5.334E-10						
49	-1.045E-06	-1.307E-07	-8.145E-03	3.697E-09	-2.878E-08	-
4.290E-12						
50	-1.187E-06	-3.248E-07	-8.180E-03	8.899E-09	-3.261E-08	-
4.290E-12						
51	-1.329E-06	-5.182E-07	-8.146E-03	1.408E-08	-3.644E-08	-
4.290E-12						
52	-9.045E-09	2.385E-09	-8.136E-03	3.696E-09	-2.877E-08	
0.000E+00						
53	-1.347E-08	-4.502E-09	-8.172E-03	8.897E-09	-3.259E-08	
0.000E+00						
54	-1.790E-08	-1.136E-08	-8.137E-03	1.408E-08	-3.642E-08	
0.000E+00						
55	-1.749E-04	-2.745E-05	-2.298E-02	-1.010E-07	1.286E-06	-
3.522E-10						

56		-1.751E-04	-2.505E-05	-2.309E-02	2.094E-08	1.290E-06	-
4.804E-10							
57		-1.750E-04	-2.542E-05	-2.298E-02	3.548E-08	1.285E-06	-
5.042E-10							
58		-3.054E-04	-4.793E-05	-1.404E-02	-2.057E-07	8.644E-07	-
2.316E-10							
59		-3.064E-04	-2.058E-05	-1.411E-02	4.559E-08	8.722E-07	-
6.745E-10							
60		-3.054E-04	-1.719E-05	-1.404E-02	8.598E-08	8.638E-07	-
7.565E-10							
61		-3.410E-04	-5.750E-05	-1.031E-02	-1.836E-07	6.043E-07	-
1.826E-10							
62		-3.424E-04	-1.845E-05	-1.035E-02	4.080E-08	6.108E-07	-
7.535E-10							
63		-3.411E-04	-1.316E-05	-1.031E-02	7.761E-08	6.038E-07	-
8.592E-10							
64		-3.500E-04	-6.033E-05	-9.056E-03	-1.680E-07	5.066E-07	-
1.663E-10							
65		-3.514E-04	-1.782E-05	-9.096E-03	3.731E-08	5.123E-07	-
7.798E-10							
66		-3.500E-04	-1.197E-05	-9.056E-03	7.114E-08	5.062E-07	-
8.933E-10							
67		-3.682E-04	-6.638E-05	-9.046E-03	-1.679E-07	5.064E-07	-
1.661E-10							
68		-3.698E-04	-1.648E-05	-9.086E-03	3.730E-08	5.121E-07	-
7.800E-10							
69		-3.682E-04	-9.405E-06	-9.046E-03	7.112E-08	5.060E-07	-
8.935E-10							
70		-1.239E-05	-1.296E-06	-1.658E-02	8.823E-09	-8.638E-08	
9.868E-09							
71		-1.113E-05	-1.974E-06	-1.665E-02	6.558E-09	-8.211E-08	
9.868E-09							
72		-9.875E-06	-2.652E-06	-1.658E-02	4.298E-09	-7.783E-08	
9.868E-09							
73		-5.255E-06	-5.788E-07	-1.138E-02	6.993E-09	-6.866E-08	
9.483E-09							
74		-4.580E-06	-1.111E-06	-1.143E-02	1.141E-08	-6.113E-08	
9.483E-09							
75		-3.906E-06	-1.643E-06	-1.138E-02	1.583E-08	-5.360E-08	
9.483E-09							
76		-2.363E-06	-2.741E-07	-8.544E-03	5.743E-09	-5.148E-08	
9.278E-09							
77		-2.038E-06	-5.615E-07	-8.583E-03	1.124E-08	-4.473E-08	
9.278E-09							
78		-1.712E-06	-8.485E-07	-8.544E-03	1.673E-08	-3.798E-08	
9.278E-09							
79		-1.647E-06	-1.922E-07	-7.653E-03	5.315E-09	-4.505E-08	
9.215E-09							
80		-1.417E-06	-3.976E-07	-7.688E-03	1.080E-08	-3.890E-08	
9.215E-09							
81		-1.188E-06	-6.028E-07	-7.653E-03	1.627E-08	-3.275E-08	
9.215E-09							
82		-2.531E-08	-9.066E-10	-7.645E-03	5.314E-09	-4.503E-08	
9.214E-09							
83		-1.715E-08	-8.945E-09	-7.680E-03	1.080E-08	-3.888E-08	
9.214E-09							
84		-8.987E-09	-1.697E-08	-7.646E-03	1.627E-08	-3.273E-08	
9.214E-09							
85	fixed	0.000E+00	0.000E+00	0.000E+00	0.000E+00	0.000E+00	
0.000E+00							
86	fixed	0.000E+00	0.000E+00	0.000E+00	0.000E+00	0.000E+00	
0.000E+00							
87	fixed	0.000E+00	0.000E+00	0.000E+00	0.000E+00	0.000E+00	
0.000E+00							
88	fixed	0.000E+00	0.000E+00	0.000E+00	0.000E+00	0.000E+00	
0.000E+00							
89	fixed	0.000E+00	0.000E+00	0.000E+00	0.000E+00	0.000E+00	
0.000E+00							
90	fixed	0.000E+00	0.000E+00	0.000E+00	0.000E+00	0.000E+00	
0.000E+00							

91	fixed	0.000E+00	0.000E+00	0.000E+00	0.000E+00	0.000E+00	0.000E+00
0.000E+00							
92	fixed	0.000E+00	0.000E+00	0.000E+00	0.000E+00	0.000E+00	0.000E+00
0.000E+00							
93	fixed	0.000E+00	0.000E+00	0.000E+00	0.000E+00	0.000E+00	0.000E+00
0.000E+00							
94	fixed	0.000E+00	0.000E+00	0.000E+00	0.000E+00	0.000E+00	0.000E+00
0.000E+00							
95	fixed	0.000E+00	0.000E+00	0.000E+00	0.000E+00	0.000E+00	0.000E+00
0.000E+00							
96	fixed	0.000E+00	0.000E+00	0.000E+00	0.000E+00	0.000E+00	0.000E+00
0.000E+00							
97	fixed	0.000E+00	0.000E+00	0.000E+00	0.000E+00	0.000E+00	0.000E+00
0.000E+00							
98	fixed	0.000E+00	0.000E+00	0.000E+00	0.000E+00	0.000E+00	0.000E+00
0.000E+00							
99	fixed	0.000E+00	0.000E+00	0.000E+00	0.000E+00	0.000E+00	0.000E+00
0.000E+00							
100	fixed	0.000E+00	0.000E+00	0.000E+00	0.000E+00	0.000E+00	0.000E+00
0.000E+00							
101	fixed	0.000E+00	0.000E+00	0.000E+00	0.000E+00	0.000E+00	0.000E+00
0.000E+00							
102	fixed	0.000E+00	0.000E+00	0.000E+00	0.000E+00	0.000E+00	0.000E+00
0.000E+00							
103	fixed	0.000E+00	0.000E+00	0.000E+00	0.000E+00	0.000E+00	0.000E+00
0.000E+00							
104	fixed	0.000E+00	0.000E+00	0.000E+00	0.000E+00	0.000E+00	0.000E+00
0.000E+00							
105	fixed	0.000E+00	0.000E+00	0.000E+00	0.000E+00	0.000E+00	0.000E+00
0.000E+00							
106	fixed	0.000E+00	0.000E+00	0.000E+00	0.000E+00	0.000E+00	0.000E+00
0.000E+00							
107	fixed	0.000E+00	0.000E+00	0.000E+00	0.000E+00	0.000E+00	0.000E+00
0.000E+00							
108	fixed	0.000E+00	0.000E+00	0.000E+00	0.000E+00	0.000E+00	0.000E+00
0.000E+00							
109	fixed	0.000E+00	0.000E+00	0.000E+00	0.000E+00	0.000E+00	0.000E+00
0.000E+00							
110		-1.490E-05	-2.470E-06	-2.308E-02	1.871E-08	-8.343E-08	-
7.626E-09							
111		-1.593E-05	-2.935E-06	-2.319E-02	9.766E-09	-8.343E-08	-
7.626E-09							
112		-1.697E-05	-3.398E-06	-2.309E-02	8.644E-10	-8.344E-08	-
7.626E-09							
113		-1.110E-04	-2.499E-05	-2.651E-02	5.961E-09	1.368E-06	-
4.010E-10							
114		-1.110E-04	-2.550E-05	-2.663E-02	-3.812E-09	1.368E-06	-
4.017E-10							
115		-1.111E-04	-2.602E-05	-2.651E-02	-1.375E-08	1.368E-06	-
4.019E-10							
116		-1.660E-05	-1.737E-06	-1.927E-02	9.516E-09	-8.798E-08	
1.007E-08							
117		-1.523E-05	-2.170E-06	-1.936E-02	1.195E-09	-8.797E-08	
1.007E-08							
118		-1.386E-05	-2.603E-06	-1.927E-02	-7.115E-09	-8.796E-08	
1.007E-08							

1 static stress output.....

0straight beam forces and moments

0beam load	axial	shear	shear	torsion	bending	bending	
no.	no.	r1	r2	r3	m1	m2	m3
1	1	2.184E-03	4.833E-07	2.556E+02	-6.566E-02	-4.671E-02	2.552E-02
		-2.184E-03	-4.833E-07	-1.278E+02	6.566E-02	-3.969E+04	-2.553E-02
2	1	2.194E-03	3.947E-07	1.278E+02	-6.566E-02	3.969E+04	2.541E-02
		-2.194E-03	-3.947E-07	-1.196E-03	6.566E-02	-5.292E+04	-2.535E-02
3	1	2.188E-03	1.210E-06	9.803E-04	-6.566E-02	5.292E+04	2.515E-02
		-2.188E-03	-1.210E-06	1.278E+02	6.566E-02	-3.969E+04	-2.506E-02

4	1	2.197E-03 -2.197E-03	2.436E-06 -2.436E-06	-1.278E+02 2.556E+02	-6.566E-02 6.566E-02	3.969E+04 -1.062E-01	2.485E-02 -2.444E-02
5	1	2.474E-03 -2.474E-03	1.511E-04 -1.511E-04	3.757E+02 -1.809E+02	1.884E-01 -1.884E-01	2.537E-01 -8.781E+04	6.824E-02 -2.025E-02
6	1	2.439E-03 -2.439E-03	1.499E-04 -1.499E-04	1.809E+02 -3.076E-01	1.884E-01 -1.884E-01	8.781E+04 -1.143E+05	2.061E-02 2.319E-02
7	1	2.426E-03 -2.426E-03	1.598E-04 -1.598E-04	3.070E-01 1.877E+02	1.884E-01 -1.884E-01	1.143E+05 -8.578E+04	-2.248E-02 7.037E-02
8	1	2.427E-03 -2.427E-03	1.510E-04 -1.510E-04	-1.877E+02 3.757E+02	1.884E-01 -1.884E-01	8.578E+04 -3.618E-02	-7.032E-02 1.159E-01
9	1	-2.474E-03 2.474E-03	-1.477E-04 1.477E-04	3.757E+02 -1.877E+02	-6.937E-02 6.937E-02	-1.601E-01 -8.578E+04	-1.276E-01 8.154E-02
10	1	-2.474E-03 2.474E-03	-1.581E-04 1.581E-04	1.877E+02 3.073E-01	-6.937E-02 6.937E-02	8.578E+04 -1.143E+05	-8.184E-02 3.305E-02
11	1	-2.518E-03 2.518E-03	-1.525E-04 1.525E-04	-3.062E-01 1.809E+02	-6.937E-02 6.937E-02	1.143E+05 -8.781E+04	-3.425E-02 -9.980E-03
12	1	-2.523E-03 2.523E-03	-1.535E-04 1.535E-04	-1.809E+02 3.757E+02	-6.937E-02 6.937E-02	8.781E+04 -2.017E-01	1.029E-02 -5.853E-02
13	1	-2.135E-03 2.135E-03	2.365E-05 -2.365E-05	1.840E+02 -9.201E+01	9.115E-03 -9.115E-03	-3.148E-01 -2.056E+04	3.984E-02 -3.640E-02
14	1	-2.134E-03 2.134E-03	2.326E-05 -2.326E-05	9.200E+01 6.482E-04	9.115E-03 -9.115E-03	2.056E+04 -2.742E+04	3.639E-02 -3.306E-02
15	1	-2.132E-03 2.132E-03	2.267E-05 -2.267E-05	1.364E-03 9.200E+01	9.115E-03 -9.115E-03	2.742E+04 -2.056E+04	3.305E-02 -2.974E-02
16	1	-2.130E-03 2.130E-03	2.309E-05 -2.309E-05	-9.200E+01 1.840E+02	9.115E-03 -9.115E-03	2.056E+04 -7.667E-02	2.976E-02 -2.642E-02
17	1	3.635E-06 -3.635E-06	-1.275E-05 1.275E-05	-7.639E-03 -4.258E+00	2.190E-05 -2.190E-05	5.403E-03 -5.617E+01	2.409E-04 1.835E-04
18	1	4.244E-06 -4.244E-06	-6.496E-05 6.496E-05	-2.234E+02 2.014E+02	-6.649E-03 6.649E-03	5.592E+01 2.876E+04	-1.150E-02 1.172E-03
19	1	1.090E-04 -1.090E-04	1.357E-04 -1.357E-04	2.014E+02 -2.234E+02	-6.560E-03 6.560E-03	-2.876E+04 -5.590E+01	3.464E-02 -1.703E-02
20	1	1.874E-05 -1.874E-05	1.702E-05 -1.702E-05	-4.243E+00 -6.595E-03	-1.584E-04 1.584E-04	5.589E+01 -8.241E-02	1.374E-02 -1.338E-02
21	1	-7.278E-06 7.278E-06	-3.713E-06 3.713E-06	1.791E-02 -4.268E+00	-3.290E-03 3.290E-03	-3.416E-01 -5.612E+01	-3.452E-04 8.884E-05
22	1	1.116E-03 -1.116E-03	1.605E-03 -1.605E-03	-2.633E+02 2.413E+02	4.334E-03 -4.334E-03	5.633E+01 3.418E+04	-1.810E-04 2.172E-01
23	1	6.260E-04 -6.260E-04	-1.646E-03 1.646E-03	2.413E+02 -2.633E+02	1.972E-03 -1.972E-03	-3.418E+04 -5.583E+01	-2.283E-01 5.586E-03
24	1	-6.697E-05 6.697E-05	-7.537E-05 7.537E-05	-4.257E+00 -2.391E-02	-1.064E-02 1.064E-02	5.669E+01 -7.054E-01	-2.562E-03 2.151E-03
25	1	3.203E-07 -3.203E-07	-1.231E-05 1.231E-05	-1.466E-03 -4.264E+00	2.125E-04 -2.125E-04	1.217E-01 -5.623E+01	-1.185E-03 -5.085E-03
26	1	-2.030E-05 2.030E-05	-1.772E-04 1.772E-04	-1.995E+02 1.775E+02	1.030E-02 -1.030E-02	5.622E+01 2.552E+04	1.802E-03 -2.527E-02
27	1	1.150E-04 -1.150E-04	7.345E-05 -7.345E-05	1.775E+02 -1.995E+02	1.033E-02 -1.033E-02	-2.552E+04 -5.669E+01	6.844E-03 3.853E-03

28	1	9.843E-06 -9.843E-06	2.954E-06 -2.954E-06	-4.242E+00 -8.178E-03	-5.268E-04 5.268E-04	5.614E+01 -4.340E-01	9.246E-03 -1.557E-02
29	1	2.556E+02 -2.556E+02	-2.189E-03 2.189E-03	4.319E-07 -4.319E-07	2.566E-02 -2.566E-02	6.553E-02 -6.554E-02	-2.759E-05 -5.121E-02
30	1	2.479E+02 -2.479E+02	-6.447E-05 6.447E-05	-1.700E-05 1.700E-05	8.327E-03 -8.327E-03	2.739E-03 -2.124E-03	2.453E-02 -2.680E-02
31	1	2.490E+02 -2.490E+02	-9.627E-05 9.627E-05	3.229E-05 -3.229E-05	8.327E-03 -8.327E-03	3.963E-03 -5.114E-03	2.694E-02 -3.036E-02
32	1	2.479E+02 -2.479E+02	-1.271E-04 1.271E-04	8.078E-05 -8.078E-05	8.327E-03 -8.327E-03	5.198E-03 -8.085E-03	2.940E-02 -3.394E-02
33	1	2.879E+02 -2.879E+02	-1.185E-03 1.185E-03	-1.792E-03 1.792E-03	2.564E-04 -2.564E-04	-4.568E-01 5.141E-01	8.032E-02 -1.222E-01
34	1	2.892E+02 -2.892E+02	1.693E-03 -1.693E-03	2.495E-04 -2.495E-04	-4.130E-04 4.130E-04	1.791E-02 -2.711E-02	-4.583E-01 5.206E-01
35	1	2.879E+02 -2.879E+02	1.718E-03 -1.718E-03	5.130E-04 -5.130E-04	-5.367E-04 5.367E-04	3.320E-02 -5.180E-02	-4.527E-01 5.171E-01
36	1	2.214E+02 -2.214E+02	1.709E-04 -1.709E-04	-6.002E-06 6.002E-06	-1.079E-03 1.079E-03	-2.131E-03 2.343E-03	-3.257E-02 3.871E-02
37	1	2.224E+02 -2.224E+02	1.152E-04 -1.152E-04	-6.054E-05 6.054E-05	-1.078E-03 1.078E-03	-2.596E-03 4.764E-03	-2.929E-02 3.339E-02
38	1	2.214E+02 -2.214E+02	6.035E-05 -6.035E-05	-1.145E-04 1.145E-04	-1.079E-03 1.079E-03	-3.070E-03 7.176E-03	-2.597E-02 2.812E-02
39	1	1.840E+02 -1.840E+02	2.133E-03 -2.133E-03	2.350E-05 -2.350E-05	-2.633E-02 2.633E-02	-9.102E-03 8.553E-03	3.314E-06 4.982E-02
40	1	2.276E+02 -2.276E+02	-6.766E-05 6.766E-05	-1.226E-05 1.226E-05	8.346E-03 -8.346E-03	2.128E-02 -2.067E-02	6.003E-03 -9.569E-03
41	1	2.287E+02 -2.287E+02	-1.057E-04 1.057E-04	3.267E-05 -3.267E-05	8.368E-03 -8.368E-03	5.197E-02 -5.367E-02	-3.068E-04 -4.799E-03
42	1	2.277E+02 -2.277E+02	-1.416E-04 1.416E-04	8.717E-05 -8.717E-05	8.345E-03 -8.345E-03	1.476E-02 -1.923E-02	-6.995E-03 -2.906E-04
43	1	2.406E+02 -2.423E+02	-6.451E-05 6.451E-05	-1.697E-05 1.697E-05	8.327E-03 -8.327E-03	4.139E-03 -3.827E-03	1.920E-02 -2.039E-02
44	1	2.417E+02 -2.433E+02	-9.601E-05 9.601E-05	3.208E-05 -3.208E-05	8.327E-03 -8.327E-03	1.322E-03 -1.912E-03	1.904E-02 -2.081E-02
45	1	2.407E+02 -2.423E+02	-1.276E-04 1.276E-04	8.093E-05 -8.093E-05	8.327E-03 -8.327E-03	-1.483E-03 -6.609E-06	1.888E-02 -2.122E-02
46	1	2.423E+02 -2.465E+02	-6.450E-05 6.451E-05	-1.697E-05 1.697E-05	8.327E-03 -8.327E-03	3.827E-03 -3.011E-03	2.039E-02 -2.349E-02
47	1	2.433E+02 -2.476E+02	-9.604E-05 9.605E-05	3.208E-05 -3.208E-05	8.327E-03 -8.327E-03	1.912E-03 -3.456E-03	2.081E-02 -2.543E-02
48	1	2.423E+02 -2.465E+02	-1.276E-04 1.276E-04	8.093E-05 -8.093E-05	8.327E-03 -8.327E-03	6.546E-06 -3.899E-03	2.122E-02 -2.736E-02
49	1	2.465E+02 -2.479E+02	-6.451E-05 6.451E-05	-1.697E-05 1.697E-05	8.327E-03 -8.327E-03	3.011E-03 -2.739E-03	2.349E-02 -2.452E-02
50	1	2.476E+02 -2.490E+02	-9.605E-05 9.605E-05	3.208E-05 -3.208E-05	8.327E-03 -8.327E-03	3.456E-03 -3.969E-03	2.543E-02 -2.696E-02
51	1	2.465E+02	-1.276E-04	8.092E-05	8.327E-03	3.899E-03	2.736E-02

		-2.479E+02	1.276E-04	-8.092E-05	-8.327E-03	-5.194E-03	-2.940E-02
52	1	2.676E+02	-1.618E-03	1.180E-03	4.282E-04	-3.153E-01	3.402E-03
		-2.676E+02	1.618E-03	-1.180E-03	-4.282E-04	2.541E-01	-8.682E-02
53	1	2.688E+02	-1.613E-03	-2.581E-04	-3.438E-04	4.623E-02	-6.726E-03
		-2.688E+02	1.613E-03	2.581E-04	3.438E-04	-3.280E-02	-7.821E-02
54	1	2.675E+02	-1.579E-03	-5.112E-04	-5.575E-04	1.125E-01	4.745E-03
		-2.675E+02	1.579E-03	5.112E-04	5.575E-04	-8.583E-02	-8.682E-02
55	1	2.718E+02	-1.590E-03	1.163E-03	2.564E-04	-1.326E-01	1.624E-01
		-2.822E+02	1.590E-03	-1.163E-03	-2.564E-04	-5.072E-03	-3.506E-01
56	1	2.731E+02	-1.640E-03	-2.663E-04	-4.129E-04	3.077E-02	1.573E-01
		-2.835E+02	1.640E-03	2.663E-04	4.129E-04	7.518E-04	-3.514E-01
57	1	2.718E+02	-1.586E-03	-5.191E-04	-5.365E-04	6.147E-02	1.628E-01
		-2.822E+02	1.586E-03	5.191E-04	5.365E-04	-7.481E-06	-3.506E-01
58	1	2.822E+02	-1.590E-03	1.163E-03	2.564E-04	5.071E-03	3.506E-01
		-2.865E+02	1.590E-03	-1.163E-03	-2.564E-04	-6.114E-02	-4.272E-01
59	1	2.835E+02	-1.639E-03	-2.662E-04	-4.129E-04	-7.520E-04	3.514E-01
		-2.877E+02	1.639E-03	2.662E-04	4.129E-04	1.359E-02	-4.304E-01
60	1	2.822E+02	-1.586E-03	-5.191E-04	-5.365E-04	7.438E-06	3.506E-01
		-2.865E+02	1.586E-03	5.191E-04	5.365E-04	2.501E-02	-4.270E-01
61	1	2.865E+02	-1.591E-03	1.164E-03	2.564E-04	6.114E-02	4.272E-01
		-2.879E+02	1.591E-03	-1.164E-03	-2.564E-04	-7.975E-02	-4.527E-01
62	1	2.877E+02	-1.640E-03	-2.663E-04	-4.129E-04	-1.358E-02	4.304E-01
		-2.892E+02	1.640E-03	2.663E-04	4.129E-04	1.784E-02	-4.567E-01
63	1	2.865E+02	-1.586E-03	-5.192E-04	-5.365E-04	-2.501E-02	4.270E-01
		-2.879E+02	1.586E-03	5.192E-04	5.365E-04	3.332E-02	-4.524E-01
64	1	2.037E+02	1.670E-04	-1.414E-05	-1.068E-03	4.013E-03	1.045E-02
		-2.037E+02	-1.670E-04	1.414E-05	1.068E-03	-3.264E-03	-1.783E-03
65	1	2.047E+02	1.174E-04	-5.759E-05	-1.077E-03	1.746E-02	1.194E-04
		-2.047E+02	-1.174E-04	5.759E-05	1.077E-03	-1.448E-02	5.942E-03
66	1	2.037E+02	6.803E-05	-1.294E-04	-1.060E-03	4.886E-02	-1.043E-02
		-2.037E+02	-6.803E-05	1.294E-04	1.060E-03	-4.212E-02	1.370E-02
67	1	2.080E+02	1.709E-04	-6.153E-06	-1.080E-03	-1.189E-03	-6.502E-03
		-2.159E+02	-1.709E-04	6.153E-06	1.080E-03	1.742E-03	2.188E-02
68	1	2.090E+02	1.159E-04	-6.035E-05	-1.080E-03	6.605E-03	-1.159E-02
		-2.169E+02	-1.159E-04	6.035E-05	1.080E-03	-1.174E-03	2.202E-02
69	1	2.080E+02	6.086E-05	-1.145E-04	-1.080E-03	1.439E-02	-1.667E-02
		-2.159E+02	-6.086E-05	1.145E-04	1.080E-03	-4.086E-03	2.215E-02
70	1	2.159E+02	1.709E-04	-6.153E-06	-1.080E-03	-1.742E-03	-2.188E-02
		-2.201E+02	-1.709E-04	6.153E-06	1.080E-03	2.036E-03	3.004E-02
71	1	2.169E+02	1.159E-04	-6.035E-05	-1.080E-03	1.174E-03	-2.202E-02
		-2.211E+02	-1.158E-04	6.035E-05	1.080E-03	1.705E-03	2.754E-02
72	1	2.159E+02	6.086E-05	-1.145E-04	-1.080E-03	4.086E-03	-2.215E-02
		-2.201E+02	-6.081E-05	1.145E-04	1.080E-03	1.375E-03	2.505E-02
73	1	2.201E+02	1.709E-04	-6.155E-06	-1.080E-03	-2.036E-03	-3.004E-02
		-2.214E+02	-1.709E-04	6.155E-06	1.080E-03	2.127E-03	3.257E-02
74	1	2.211E+02	1.159E-04	-6.036E-05	-1.080E-03	-1.705E-03	-2.754E-02
		-2.224E+02	-1.159E-04	6.036E-05	1.080E-03	2.598E-03	2.926E-02

75	1	2.201E+02	6.082E-05	-1.145E-04	-1.080E-03	-1.375E-03	-2.505E-02
		-2.214E+02	-6.082E-05	1.145E-04	1.080E-03	3.069E-03	2.595E-02
76	1	2.276E+02	-6.449E-05	-1.697E-05	8.327E-03	6.650E-03	9.658E-03
		-2.406E+02	6.449E-05	1.697E-05	-8.327E-03	-4.139E-03	-1.920E-02
77	1	2.287E+02	-9.604E-05	3.208E-05	8.327E-03	-3.427E-03	4.826E-03
		-2.417E+02	9.604E-05	-3.208E-05	-8.327E-03	-1.322E-03	-1.904E-02
78	1	2.276E+02	-1.276E-04	8.093E-05	8.327E-03	-1.346E-02	-6.247E-06
		-2.407E+02	1.276E-04	-8.093E-05	-8.327E-03	1.482E-03	-1.888E-02
79	1	2.676E+02	-1.590E-03	1.163E-03	2.564E-04	-1.885E-01	8.607E-02
		-2.718E+02	1.590E-03	-1.163E-03	-2.564E-04	1.326E-01	-1.624E-01
80	1	2.688E+02	-1.640E-03	-2.662E-04	-4.129E-04	4.355E-02	7.856E-02
		-2.731E+02	1.640E-03	2.662E-04	4.129E-04	-3.077E-02	-1.573E-01
81	1	2.676E+02	-1.586E-03	-5.191E-04	-5.365E-04	8.639E-02	8.663E-02
		-2.718E+02	1.586E-03	5.191E-04	5.365E-04	-6.147E-02	-1.628E-01
82	1	2.037E+02	1.709E-04	-6.153E-06	-1.080E-03	-8.933E-04	1.702E-03
		-2.080E+02	-1.709E-04	6.153E-06	1.080E-03	1.189E-03	6.502E-03
83	1	2.048E+02	1.159E-04	-6.035E-05	-1.080E-03	9.502E-03	-6.024E-03
		-2.090E+02	-1.159E-04	6.035E-05	1.080E-03	-6.605E-03	1.159E-02
84	1	2.037E+02	6.086E-05	-1.145E-04	-1.080E-03	1.989E-02	-1.375E-02
		-2.080E+02	-6.086E-05	1.145E-04	1.080E-03	-1.439E-02	1.667E-02

1 static stress output.....

0boundary spring forces and moments

0 bd. load		axial	shear	shear	torsion	bending	bending
no	no	r1	r2	r3	m1	m2	m3
1	1	-2.189E-03	-8.884E-07	-2.556E+02	6.547E-02	-5.118E-02	0.000E+00
2	1	-6.440E-05	1.698E-05	-2.479E+02	2.124E-03	-2.681E-02	0.000E+00
3	1	-9.593E-05	-3.205E-05	-2.490E+02	5.112E-03	-3.038E-02	0.000E+00
4	1	-1.275E-04	-8.088E-05	-2.479E+02	8.089E-03	-3.395E-02	0.000E+00
5	1	-3.597E+00	-6.486E-01	-2.879E+02	-1.222E-01	5.140E-01	1.109E-04
6	1	-3.613E+00	-1.609E-01	-2.891E+02	2.714E-02	5.198E-01	-2.151E-04
7	1	-3.597E+00	-9.169E-02	-2.879E+02	5.175E-02	5.136E-01	-2.730E-04
8	1	-1.705E-04	-6.107E-06	-2.214E+02	2.343E-03	-3.868E-02	1.079E-03
9	1	-1.155E-04	-6.026E-05	-2.224E+02	4.760E-03	-3.339E-02	1.079E-03
10	1	-6.053E-05	-1.143E-04	-2.214E+02	7.174E-03	-2.811E-02	1.079E-03
11	1	-2.131E-03	2.356E-05	-1.840E+02	8.593E-03	-4.984E-02	0.000E+00

1 static stress output.....

0expansion joint forces and moments

0 jt. load		axial	shear	shear	axial	bending	shear
no.	no.	r1	r2	r3	r4	r5	r6
1	1	1.172E-03	7.348E-07	1.278E+02	1.014E-03	0.000E+00	1.278E+02
		-1.172E-03	-7.348E-07	-1.278E+02	-1.014E-03	0.000E+00	-1.278E+02
2	1	1.148E-03	5.928E-06	-1.278E+02	1.001E-03	0.000E+00	-1.278E+02
		-1.148E-03	-5.928E-06	1.278E+02	-1.001E-03	0.000E+00	1.278E+02
3	1	1.418E-03	1.529E-04	1.878E+02	1.005E-03	0.000E+00	1.878E+02
		-1.418E-03	-1.529E-04	-1.878E+02	-1.005E-03	0.000E+00	-1.878E+02
4	1	8.600E-04	5.937E-05	-1.878E+02	1.563E-03	0.000E+00	-1.878E+02
		-8.600E-04	-5.937E-05	1.878E+02	-1.563E-03	0.000E+00	1.878E+02
5	1	-1.625E-03	-1.472E-04	1.879E+02	-8.498E-04	0.000E+00	1.879E+02
		1.625E-03	1.472E-04	-1.879E+02	8.498E-04	0.000E+00	-1.879E+02
6	1	-1.066E-03	-1.536E-04	-1.879E+02	-1.421E-03	0.000E+00	-1.878E+02
		1.066E-03	1.536E-04	1.879E+02	1.421E-03	0.000E+00	1.878E+02

7	1	-9.340E-04	2.176E-05	9.199E+01	-1.175E-03	0.000E+00	9.199E+01
		9.340E-04	-2.176E-05	-9.199E+01	1.175E-03	0.000E+00	-9.199E+01
8	1	-1.145E-03	2.267E-05	9.201E+01	-9.829E-04	0.000E+00	9.200E+01
		1.145E-03	-2.267E-05	-9.201E+01	9.829E-04	0.000E+00	-9.200E+01
9	1	2.076E-05	7.958E-12	6.004E-06	1.623E-05	0.000E+00	6.003E-06
		-2.076E-05	-7.958E-12	-6.004E-06	-1.623E-05	0.000E+00	-6.003E-06
10	1	-6.190E-06	-3.638E-12	2.471E-09	5.771E-06	0.000E+00	1.254E-09
		6.190E-06	3.638E-12	-2.471E-09	-5.771E-06	0.000E+00	-1.254E-09
11	1	-1.618E-05	-6.594E-12	-9.585E-06	-2.100E-05	0.000E+00	-9.585E-06
		1.618E-05	6.594E-12	9.585E-06	2.100E-05	0.000E+00	9.585E-06

ldynamic load input control data.....

time increment dt (sec) = 0.010
total number of time steps = 9205
output interval = 20
number of time functions = 3

step-by-step dynamic analysis control data.....

integration indicator = 0
damping factor alpha = 5.692E-01
damping factor beta = 4.392E-03
lsubdivision of time increment control data

number of subdivision = 20
relative tolerance of subdivision = 0.5000000E-01
lequilibrium iteration control data

maximum number of iteration = 200
type of iteration = 1
relative tolerance to use iteration = 0.1000000E-01
relative tolerance for convergence = 0.5000000E-02
lground motion input key.....

	direction		
	x	y	z
function number...	1	2	3
scale factor.....	1.000	1.000	1.000
ltime history no. 1.....	eru		

number of data point = 9200
scaling factor = 386.4000

time increment of data (sec)= 0.010000

zero correction = 0.0000

1	-3.910	-1.946	0.316	1.479	0.928	-0.686
-2.087	-2.498					
2	-2.069	-1.470	-1.339	-2.046	-3.473	-4.842
-5.061	-3.742					
3	-1.833	-0.874	-1.403	-2.366	-2.255	-0.703
1.308	2.601					
4	2.867	2.526	2.039	1.651	1.618	2.140
2.952	3.217					
5	2.212	0.119	-1.966	-2.968	-2.739	-2.089
-1.919	-2.356					
6	-2.689	-2.192	-0.936	0.232	0.543	0.026
-0.644	-0.921					
7	-0.840	-0.788	-1.009	-1.442	-1.843	-1.929
-1.527	-0.849					
8	-0.533	-1.157	-2.517	-3.636	-3.649	-2.647
-1.428	-0.520					
9	0.270	1.228	1.983	1.691	0.012	-2.364
-4.239	-4.937					

***** File Cut Here *****

ldisplacement components for which
output time history is required....

node	displacement components					
1	1	2	3	4	5	6
2	1	2	3	4	5	6
21	1	2	3	4	5	6
22	1	2	3	4	5	6
28	1	2	3	4	5	6
29	1	2	3	4	5	6
30	1	2	3	4	5	6
31	1	2	3	4	5	6
32	1	2	3	4	5	6
52	1	2	3	4	5	6
52	6	fixed dof...no output				
53	1	2	3	4	5	6
53	6	fixed dof...no output				
54	1	2	3	4	5	6
54	6	fixed dof...no output				
56	1	2	3	4	5	6
59	1	2	3	4	5	6
62	1	2	3	4	5	6
65	1	2	3	4	5	6
67	1	2	3	4	5	6
68	1	2	3	4	5	6
69	1	2	3	4	5	6
82	1	2	3	4	5	6
83	1	2	3	4	5	6
84	1	2	3	4	5	6
110	1	2	3	4	5	6
111	1	2	3	4	5	6
112	1	2	3	4	5	6
113	1	2	3	4	5	6
114	1	2	3	4	5	6
115	1	2	3	4	5	6
116	1	2	3	4	5	6
117	1	2	3	4	5	6
118	1	2	3	4	5	6

output type.... 4
plot spacing... 0
lelement stress components for which
output time history is required....

element	desired stress components					
---------	---------------------------	--	--	--	--	--

type no.

2	46	1	2	3	4	5	6	7	8	9	10	11	12
2	47	1	2	3	4	5	6	7	8	9	10	11	12
2	48	1	2	3	4	5	6	7	8	9	10	11	12
2	58	1	2	3	4	5	6	7	8	9	10	11	12
2	59	1	2	3	4	5	6	7	8	9	10	11	12
2	60	1	2	3	4	5	6	7	8	9	10	11	12
2	70	1	2	3	4	5	6	7	8	9	10	11	12
2	71	1	2	3	4	5	6	7	8	9	10	11	12
2	72	1	2	3	4	5	6	7	8	9	10	11	12
2	76	1	2	3	4	5	6	7	8	9	10	11	12
2	77	1	2	3	4	5	6	7	8	9	10	11	12
2	78	1	2	3	4	5	6	7	8	9	10	11	12
2	79	1	2	3	4	5	6	7	8	9	10	11	12
2	80	1	2	3	4	5	6	7	8	9	10	11	12
2	81	1	2	3	4	5	6	7	8	9	10	11	12
2	82	1	2	3	4	5	6	7	8	9	10	11	12
2	83	1	2	3	4	5	6	7	8	9	10	11	12
2	84	1	2	3	4	5	6	7	8	9	10	11	12
4	1	1	2	3	4	5	6	7	8	9	10	11	12
4	11	1	2	3	4	5	6	7	8	9	10	11	12
5	1	1	2	3	4	5	6	7	8	9	10	11	12
5	2	1	2	3	4	5	6	7	8	9	10	11	12
5	3	1	2	3	4	5	6	7	8	9	10	11	12
5	4	1	2	3	4	5	6	7	8	9	10	11	12
5	5	1	2	3	4	5	6	7	8	9	10	11	12
5	6	1	2	3	4	5	6	7	8	9	10	11	12
5	7	1	2	3	4	5	6	7	8	9	10	11	12
5	8	1	2	3	4	5	6	7	8	9	10	11	12
5	9	1	2	3	4	5	6	7	8	9	10	11	12
5	10	1	2	3	4	5	6	7	8	9	10	11	12
5	11	1	2	3	4	5	6	7	8	9	10	11	12

Appendix C

Additional Output from Study

C.1 Introduction

This appendix presents the additional plots and tables for the analysis results from Chapter 5. The plots and tables are from the analyses of Bridges 5/518 and 5/826 using the unmodified Peru earthquake, unmodified Chile earthquake, Mexico City 475-year and 950-year earthquakes, Olympia 475-year and 950-year earthquakes, and the Kobe 475-year and 950-year earthquakes.

C.2 Bridge 5/518; Unmodified Peru

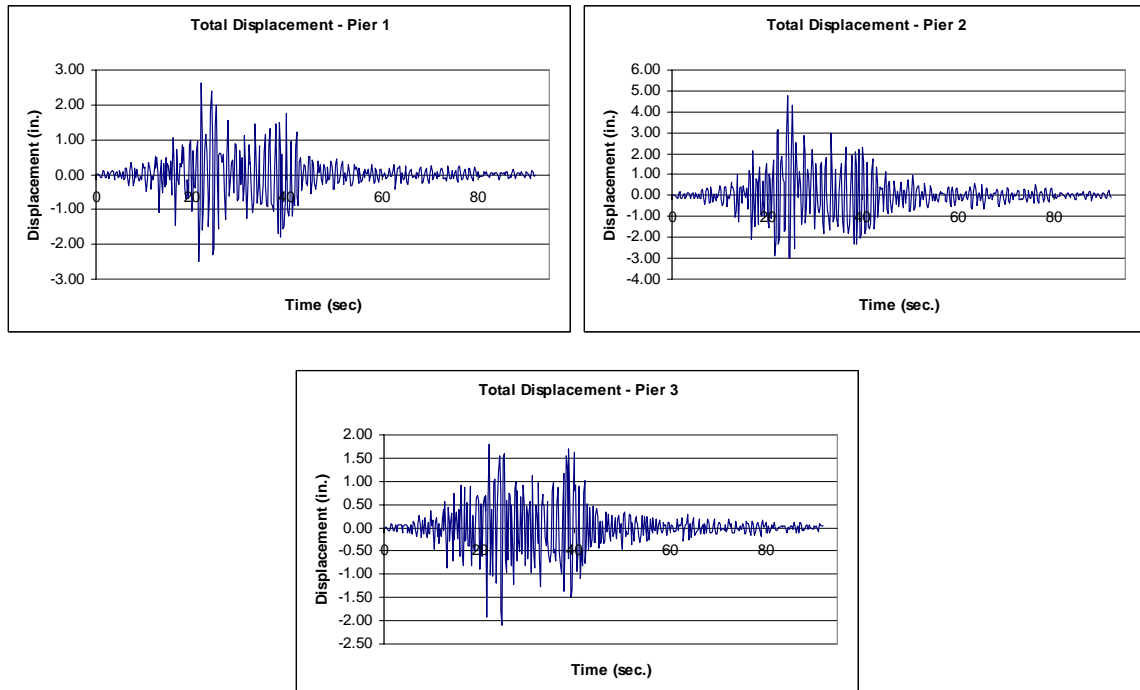


Figure C.2-1 Total Displacement at Piers

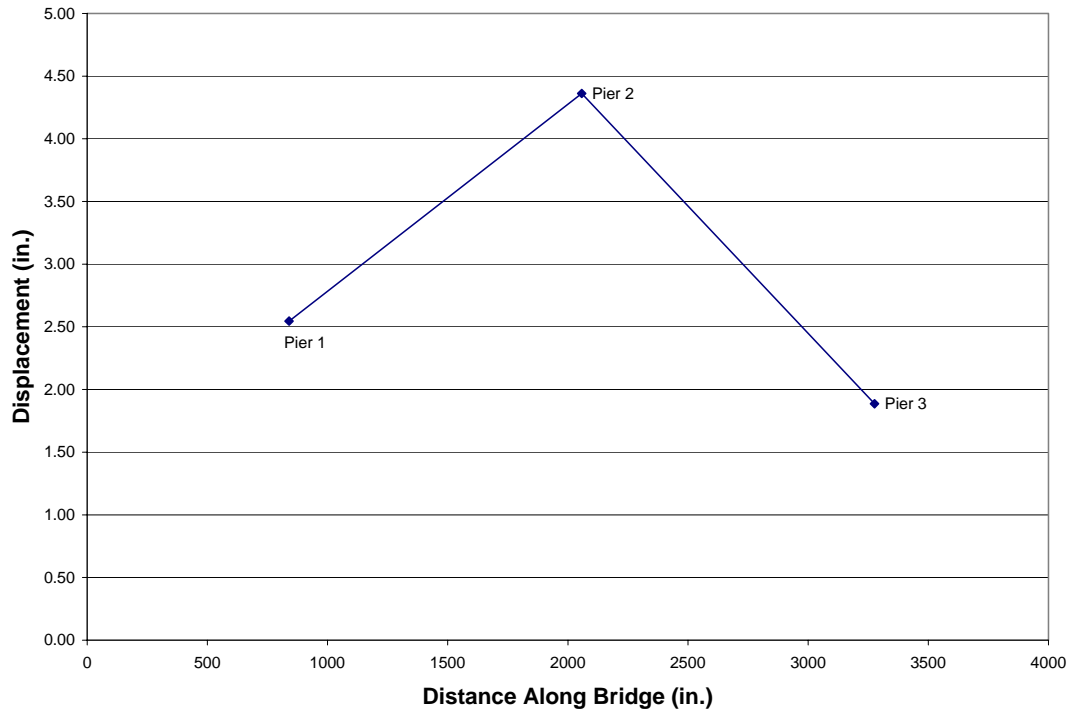


Figure C.2-2 Transverse Displacement Envelope of Bridge Deck

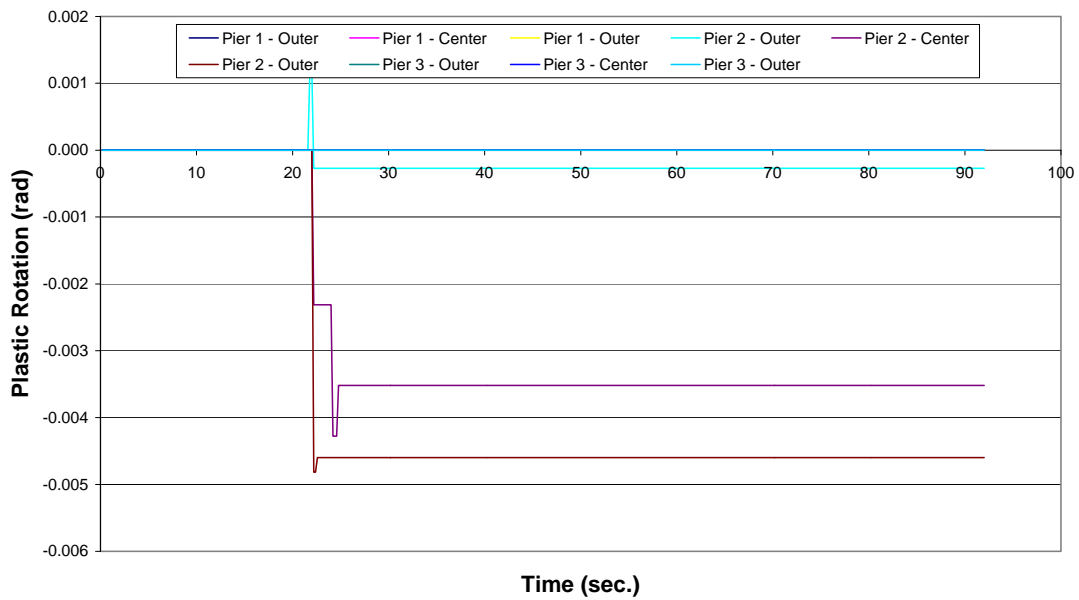


Figure C.2-3 Plastic Rotations at the Top of the Columns

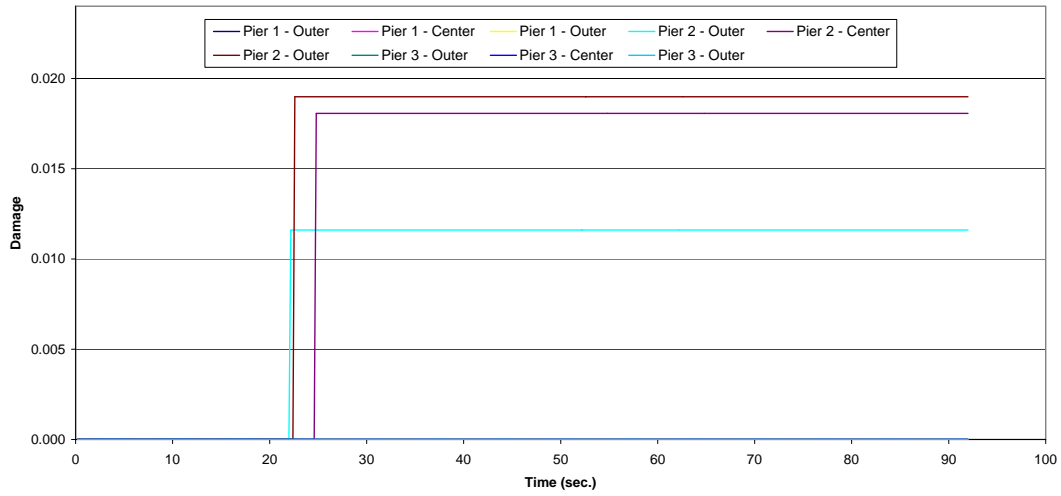


Figure C.2-4 Damage at the Top of the Columns

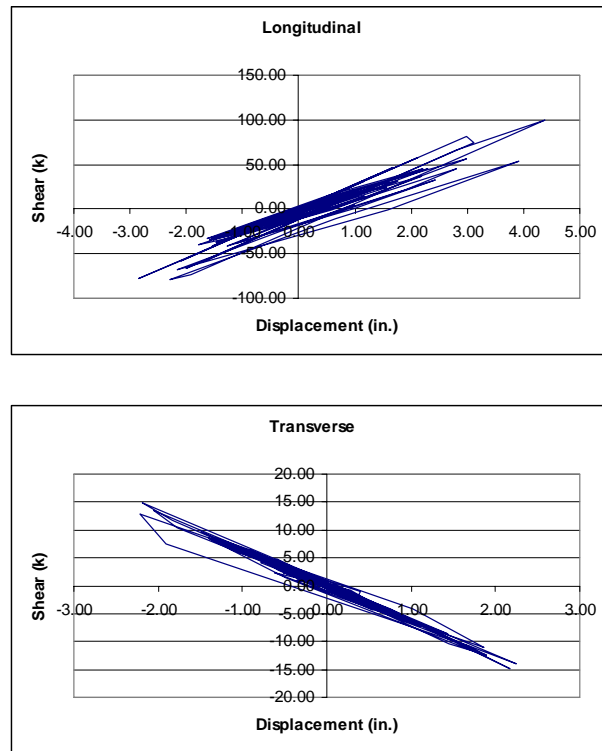


Figure C.2-5 Hysteresis Plots for the Center Column of Pier 2

Table C.2-1 Maximum Moment (kip-in) at the Top and Bottoms of Columns

Pier No.	Column	Moment	
		Top	Bottom
1	1	10519.4	3159.5
	2	10512.3	3204.5
	3	10547.5	3423.7
2	1	14389.2	7106.0
	2	14465.0	7073.4
	3	13960.1	6868.1
3	1	9191.0	3216.3
	2	9131.2	3062.8
	3	9161.7	3117.8

Table C.2-2 Maximum Shear (kips) in the Columns

Pier No.	Column	Shear			
		Top	Demand/ Capacity	Bottom	Demand/ Capacity
1	1	62.41	0.29	64.54	0.30
	2	62.00	0.29	64.17	0.30
	3	61.90	0.29	64.07	0.30
2	1	95.68	0.45	96.20	0.45
	2	93.72	0.44	100.80	0.47
	3	85.80	0.40	82.15	0.38
3	1	54.98	0.26	58.27	0.27
	2	54.87	0.26	58.12	0.27
	3	55.50	0.26	58.75	0.27

Table C.2-3 Maximum Shear (kips) at the Abutments

Abutment	Shear			
	Longitudinal	Demand/ Capacity	Transverse	Demand/ Capacity
West	294	0.09	1030	0.71
East	299	0.09	751	0.52

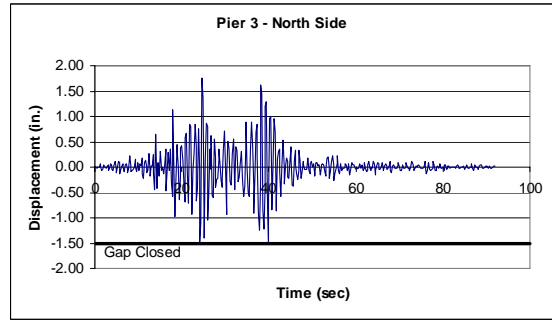
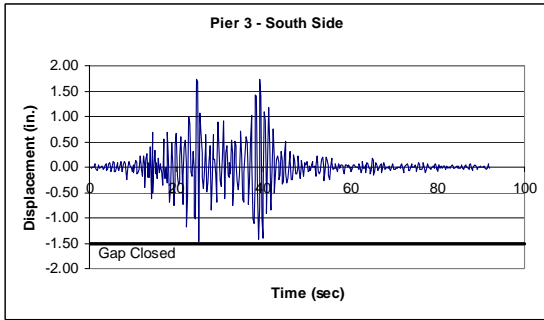
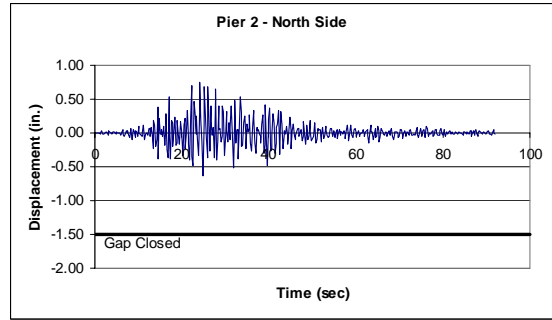
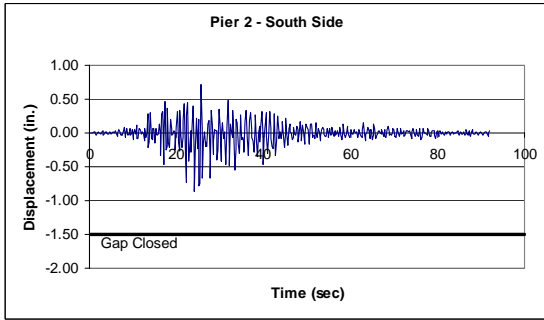
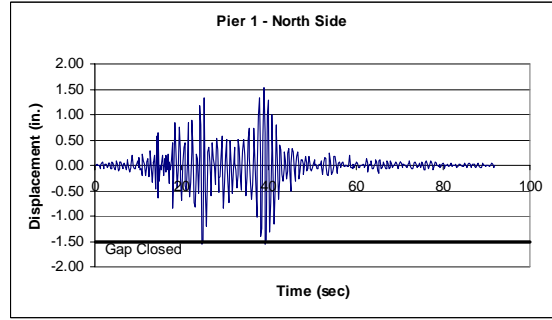
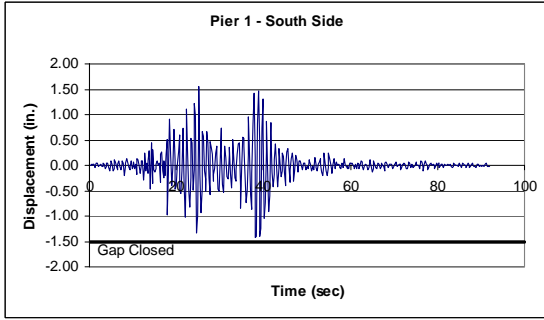
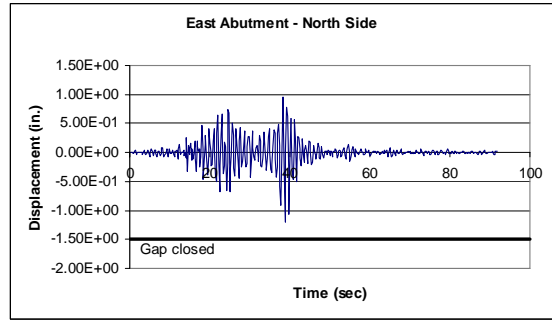
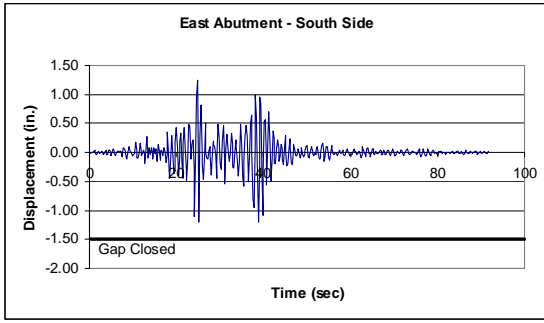
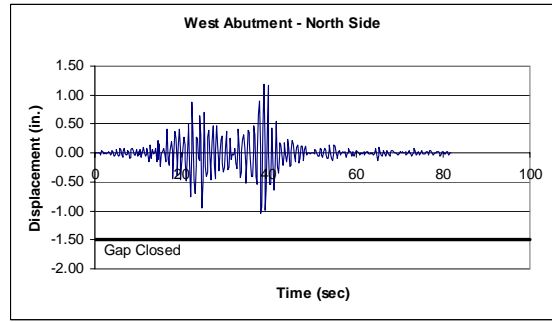
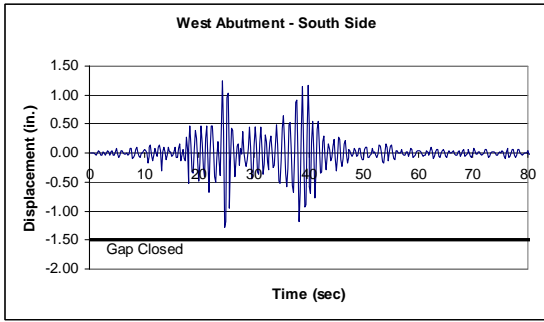


Figure C.2-6 Longitudinal Displacement of Expansion Joints

C.3 Bridge 5/518; Unmodified Chile Earthquake

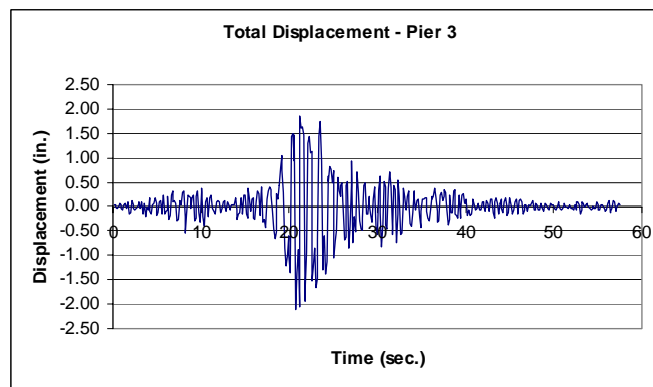
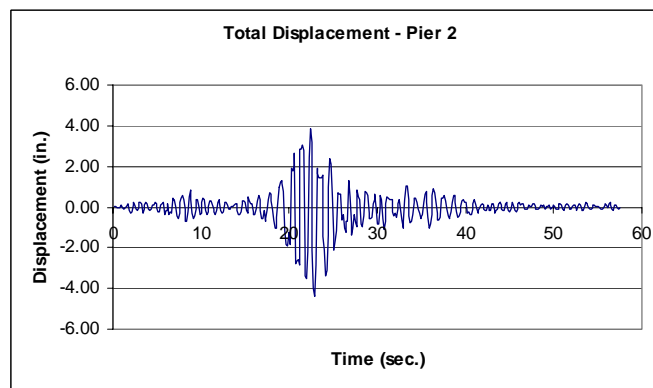
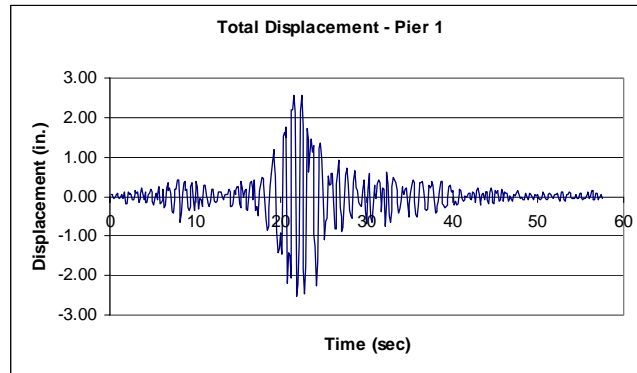


Figure C.3-1 Total Displacement at Piers

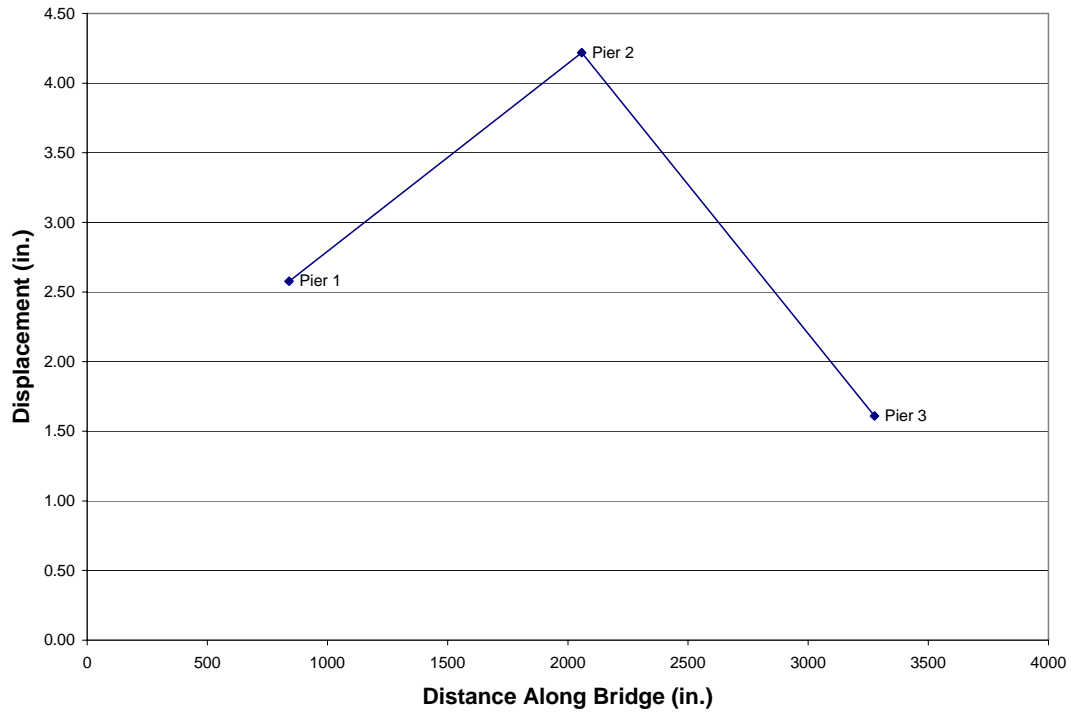


Figure C.3-2 Transverse Displacement Envelope of Bridge Deck

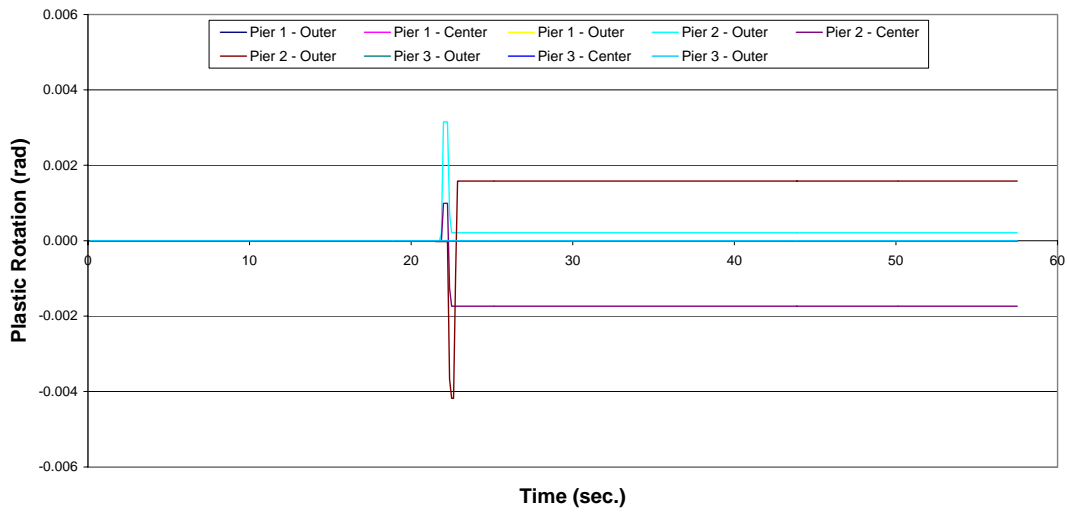


Figure C.3-3 Plastic Rotations at the Top of the Columns

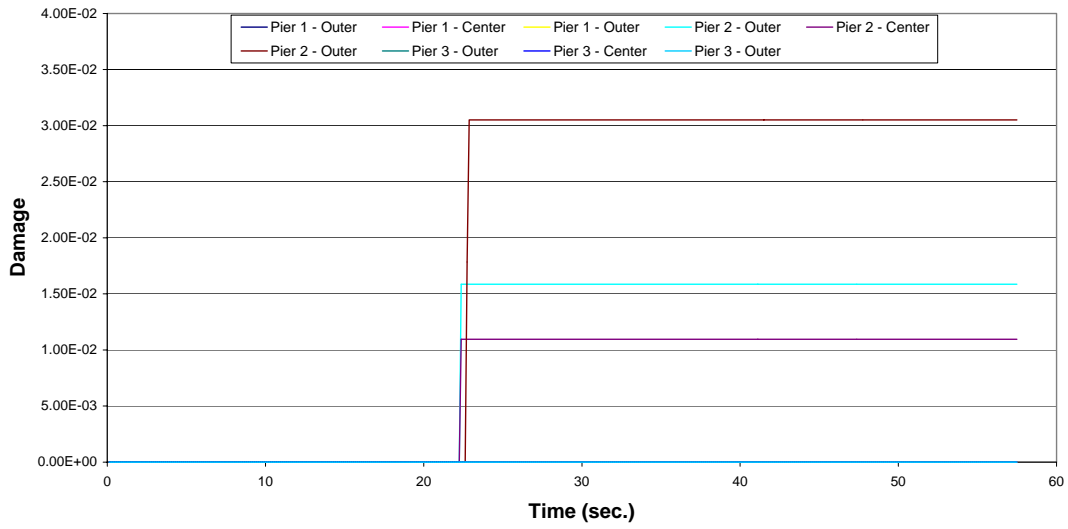


Figure C.3-4 Damage at the Top of the Columns

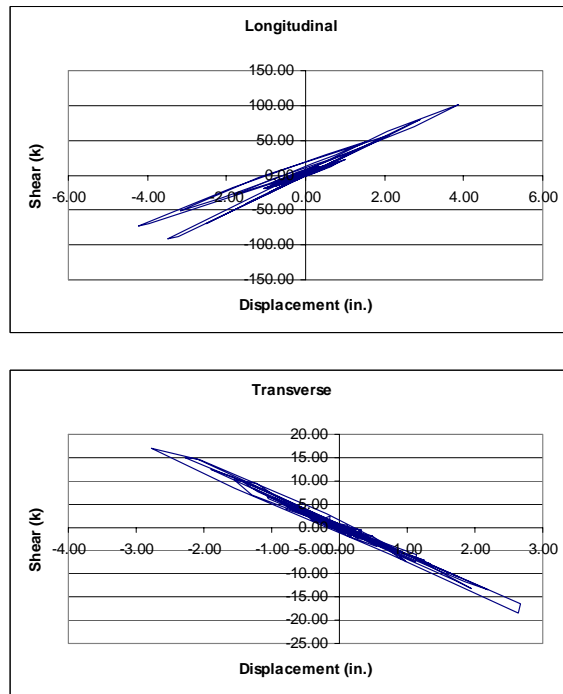


Figure C.3-5 Hysteresis Plots for the Center Column of Pier 2

Table C.3-1 Maximum Moment (kip-in) at the Top and Bottoms of Columns

Pier No.	Column	Moment	
		Top	Bottom
1	1	10709.8	3499.0
	2	10680.0	3477.1
	3	10708.1	3539.3
2	1	17021.9	6283.2
	2	14860.1	6333.3
	3	16472.1	6548.2
3	1	7816.8	3712.5
	2	7793.1	3704.5
	3	7787.7	3745.9

Table C.3-2 Maximum Shear (kips) in the Columns

Pier No.	Column	Shear			
		Top	Demand/ Capacity	Bottom	Demand/ Capacity
1	1	63.25	0.30	64.78	0.30
	2	63.07	0.30	64.54	0.30
	3	63.29	0.30	64.72	0.30
2	1	91.48	0.43	111.31	0.52
	2	86.78	0.41	101.00	0.47
	3	103.12	0.49	113.00	0.53
3	1	46.71	0.22	49.78	0.23
	2	46.72	0.22	49.98	0.23
	3	47.09	0.22	50.35	0.23

Table C.3-3 Maximum Shear (kips) at the Abutments

Abutment	Shear			
	Longitudina I	Demand/ Capacity	Transverse	Demand/ Capacity
West	433	0.13	114	0.08
East	489	0.15	133	0.09

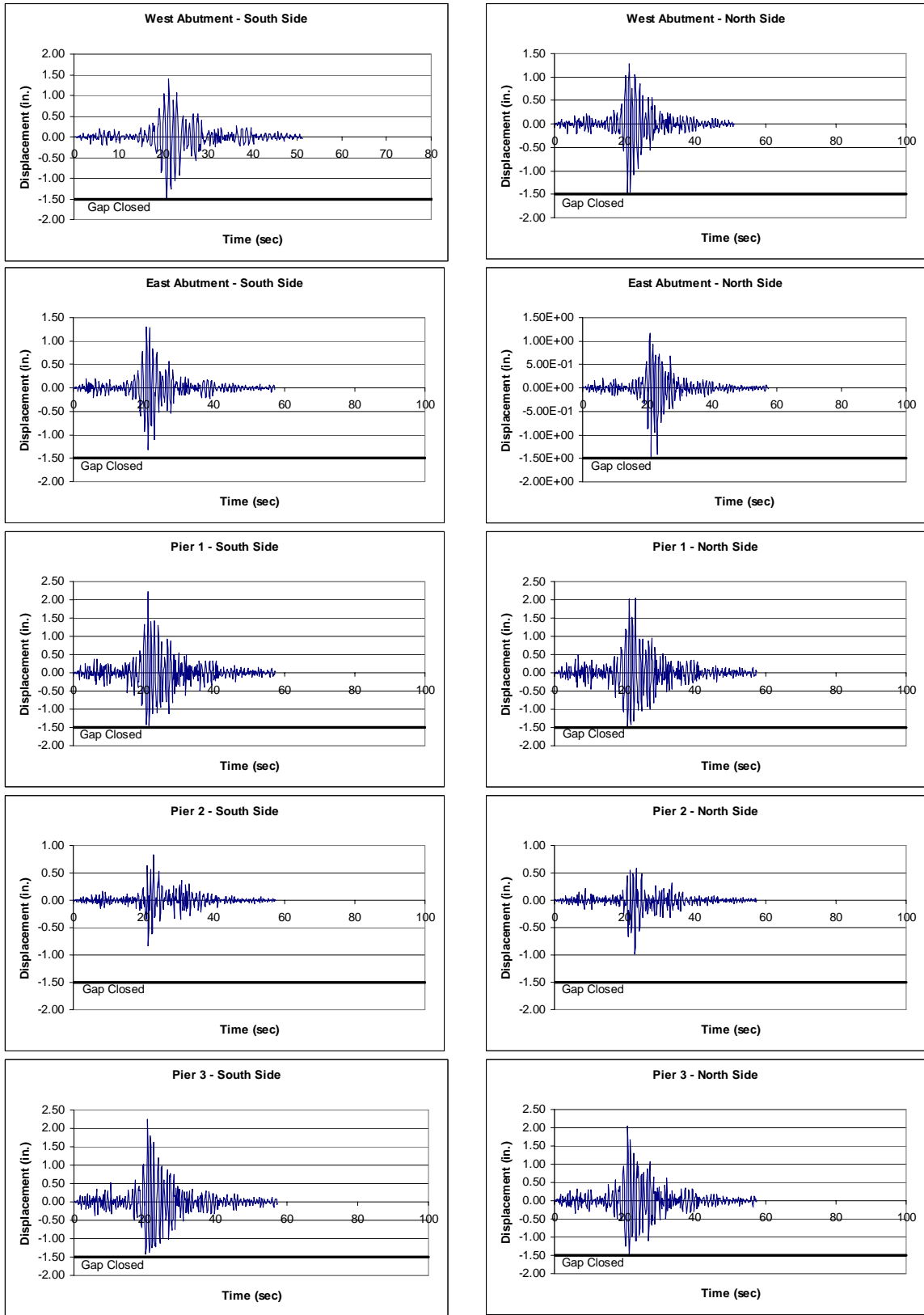


Figure C.3-6 Longitudinal displacement of Expansion Joints

C.4 Bridge 5/518; Mexico City 475-Year Earthquake

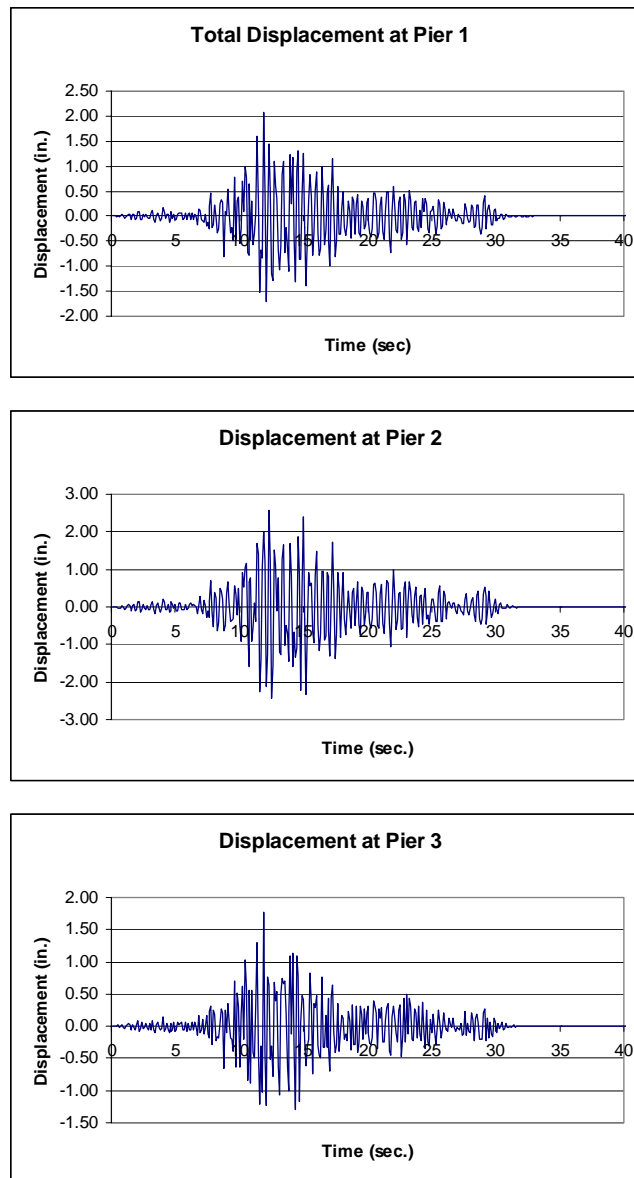


Figure C.4-1 Total Displacement at Piers

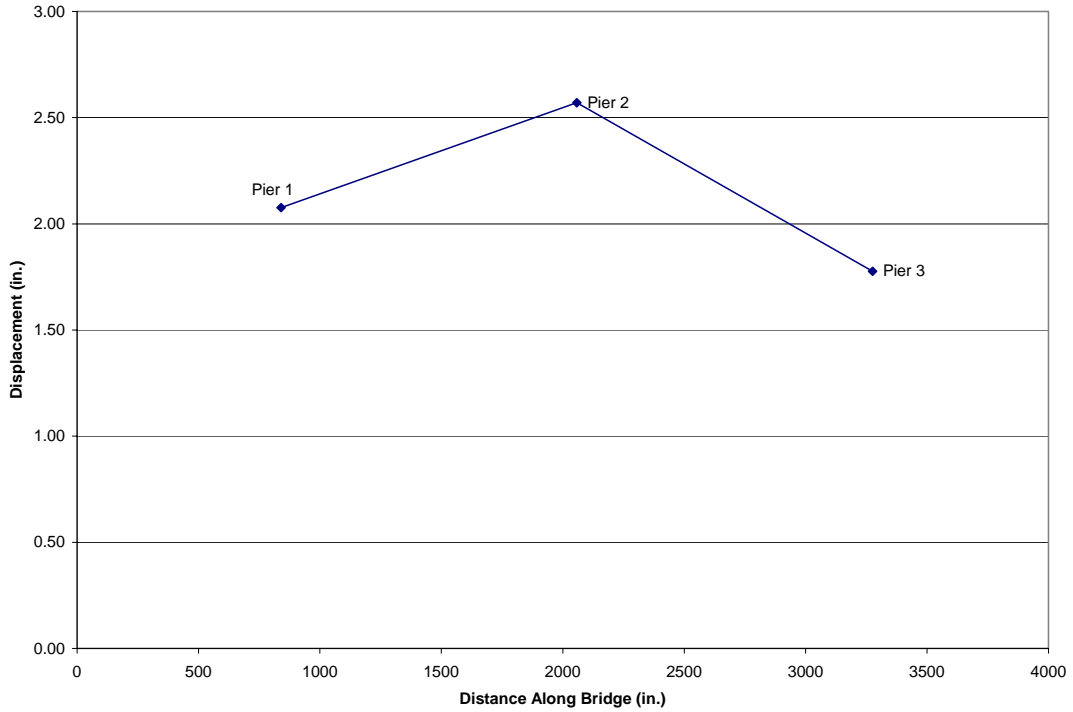


Figure C.4-2 Transverse Displacement Envelope of Bridge Deck

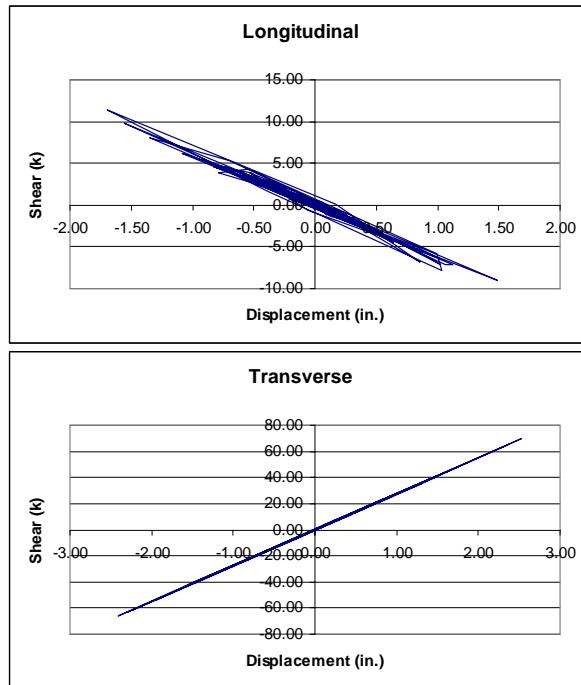


Figure C.4-3 Hysteresis Plots for the Center Column of Pier 2

Table C.4-1 Maximum Moment (kip-in) at the Top and Bottoms of Columns

Pier No.	Column	Moment	
		Top	Bottom
1	1	7979.1	2431.1
	2	7956.4	2499.3
	3	7952.8	2577.5
2	1	10950.3	3846.7
	2	10950.7	3827.2
	3	10954.8	3809.5
3	1	7988.6	2281.9
	2	7985.0	2121.0
	3	8026.4	1983.2

Table C.4-2 Maximum Shear (kips) in the Columns

Pier No.	Column	Shear			
		Top	Demand/ Capacity	Bottom	Demand/ Capacity
1	1	46.78	0.27	48.74	0.28
	2	46.93	0.27	48.88	0.28
	3	47.23	0.27	49.19	0.28
2	1	66.74	0.39	69.59	0.41
	2	66.65	0.39	69.53	0.41
	3	66.59	0.39	69.48	0.41
3	1	48.42	0.28	51.85	0.30
	2	47.82	0.28	51.25	0.30
	3	47.57	0.28	51.05	0.30

Table C.4-3 Maximum Shear (kips) at the Abutments

Abutment	Shear			
	Longitudina l	Demand/ Capacity	Transverse	Demand/ Capacity
West	219	0.06	50.6	0.03
East	171	0.05	66.1	0.03

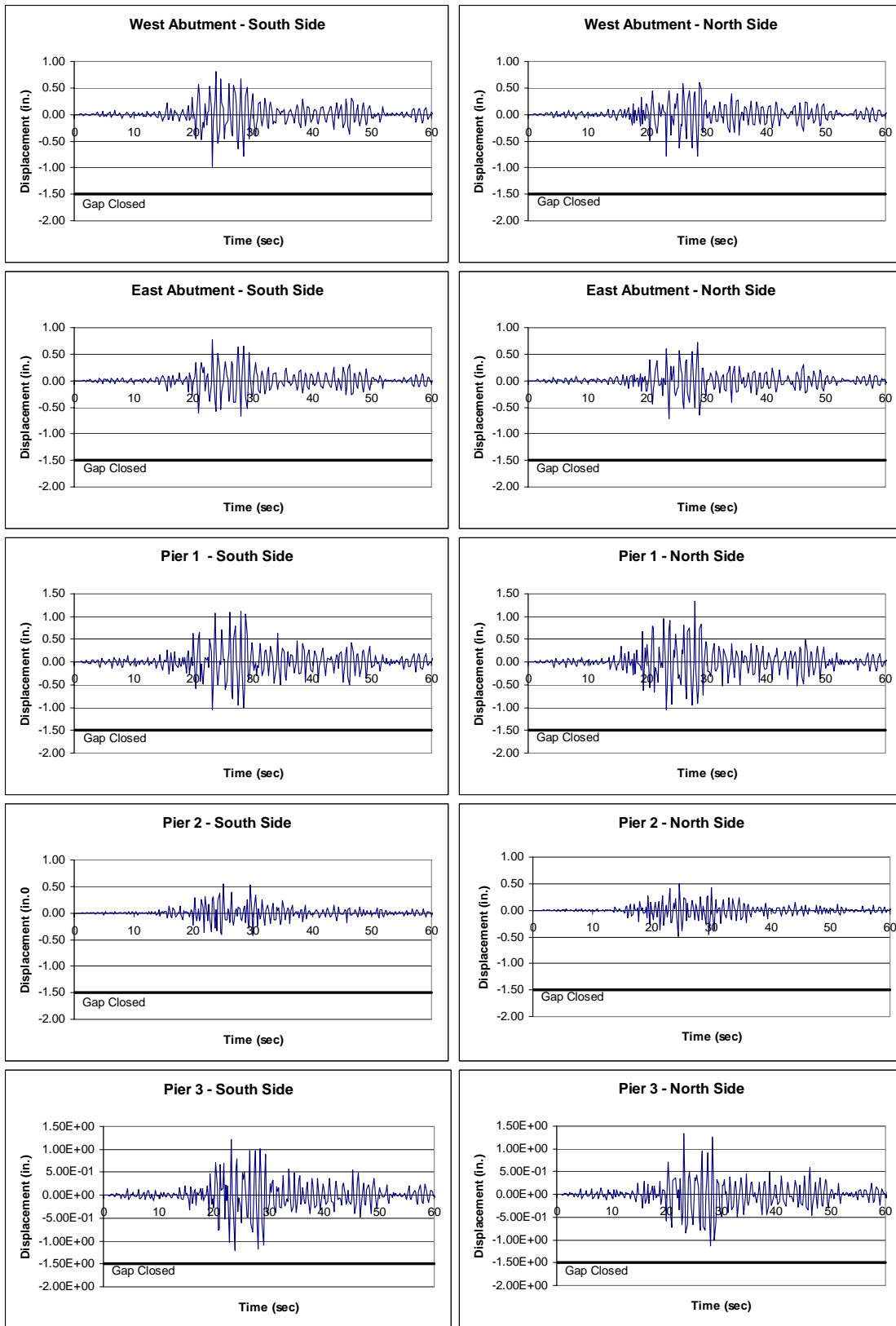


Figure C.4-4 Longitudinal Displacement of Expansion Joints

C.5 Bridge 5/518; Mexico City 950-Year Earthquake

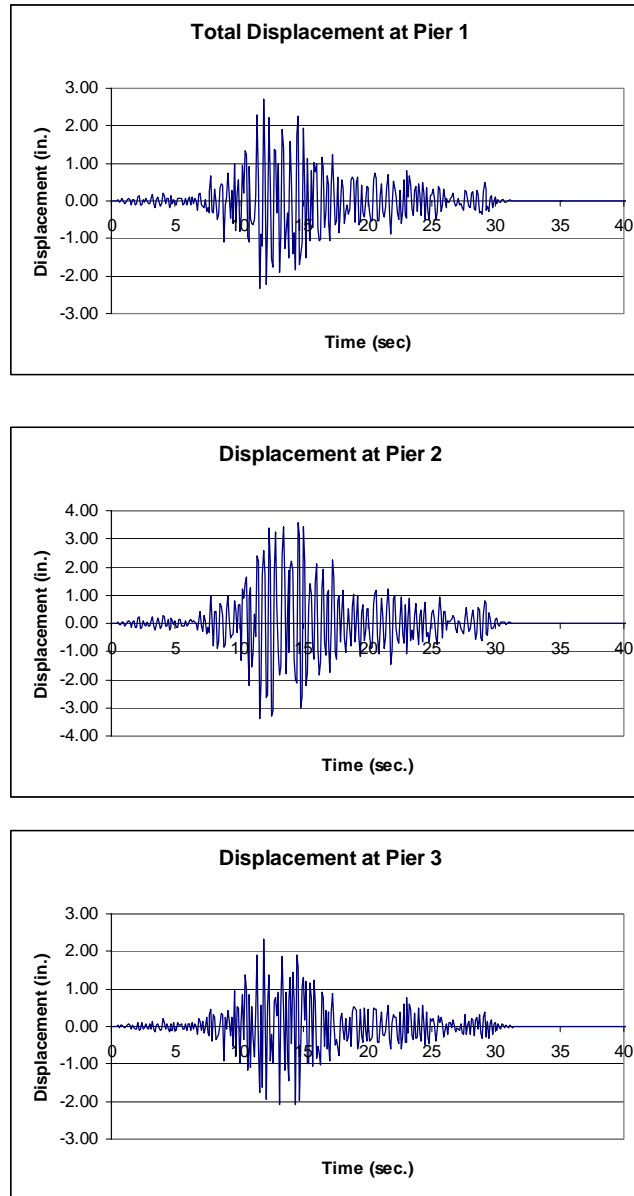


Figure C.5-1 Total Displacement at Piers

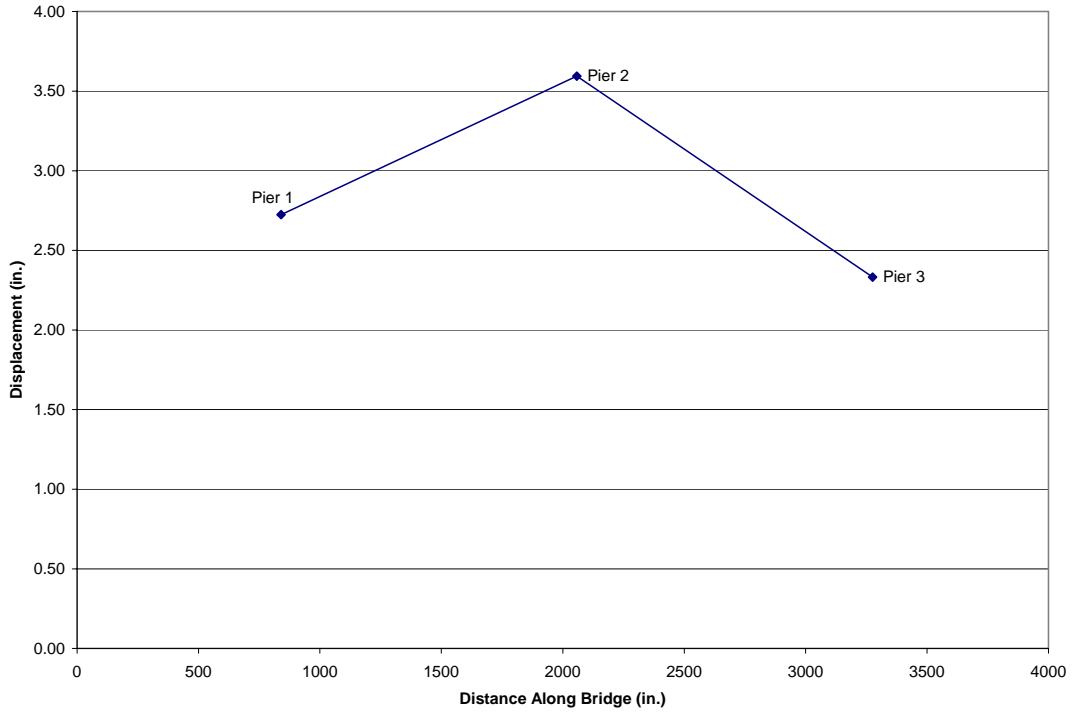


Figure C.5-2 Transverse Displacement Envelope of the Bridge Deck

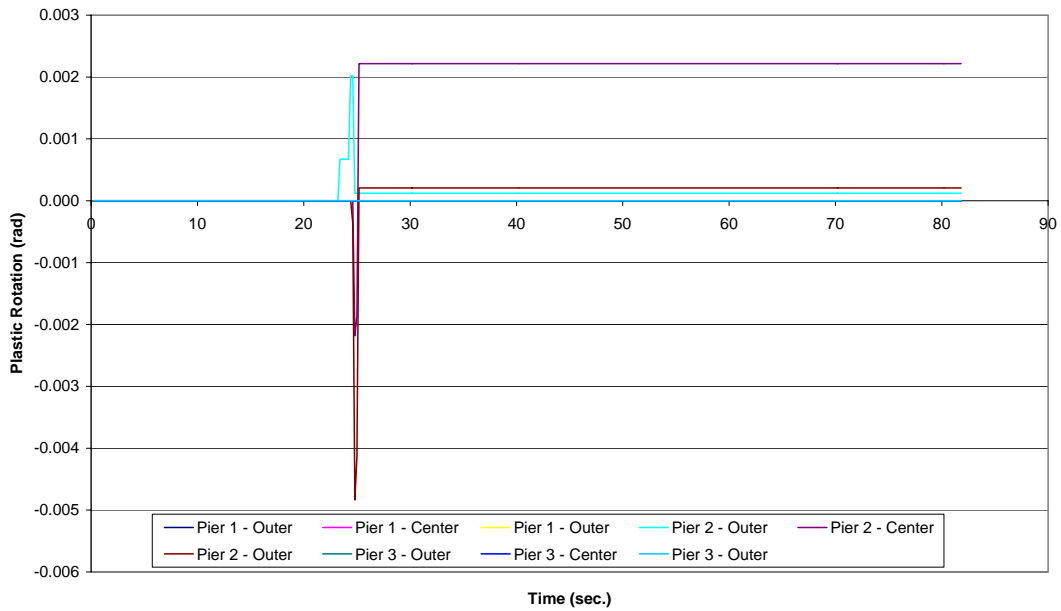


Figure C.5-3 Plastic Rotation at the Top of the Columns

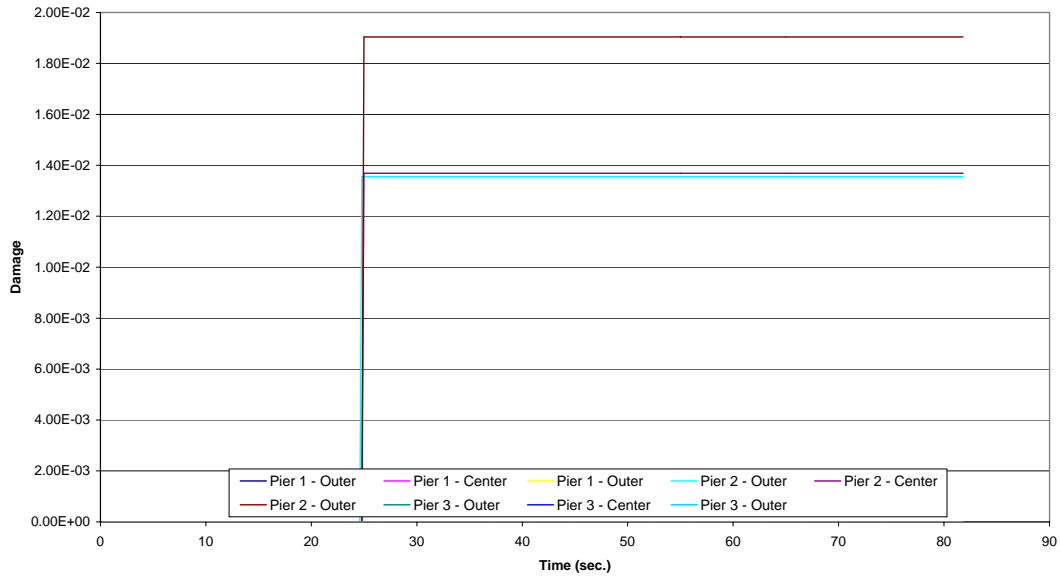


Figure C.5-4 Damage at the Top of the Columns

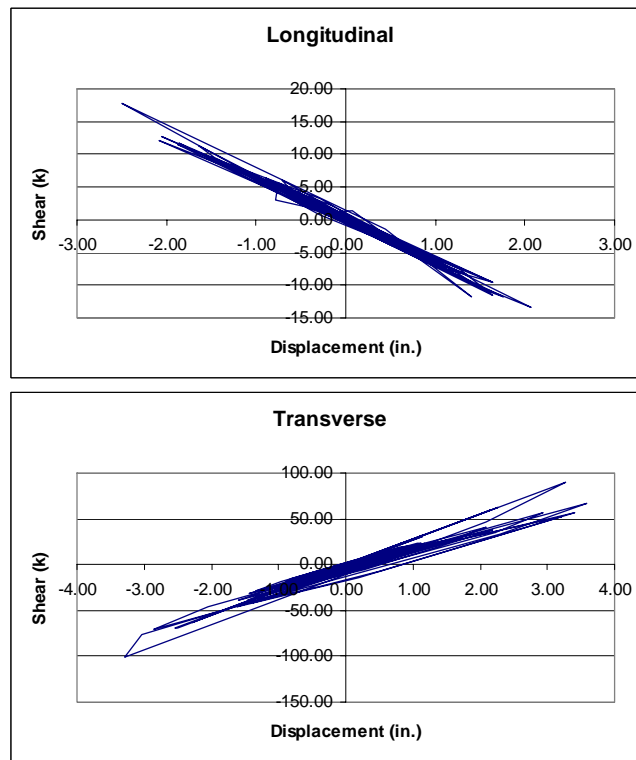


Figure C.5-5 Hysteresis Plots for the Center Column of Pier 2

Table C.5-1 Maximum Moment (kip-in) at the Top and Bottoms of Columns

Pier No.	Column	Moment	
		Top	Bottom
1	1	10389.2	3261.5
	2	10366.8	3409.8
	3	10360.0	3559.9
2	1	16210.1	5408.6
	2	1524.0	5364.3
	3	17094.3	5321.4
3	1	10388.6	3270.8
	2	10387.6	2991.2
	3	10450.8	3093.3

Table C.5-2 Maximum Shear (kips) in the Columns

Pier No.	Column	Shear			
		Top	Demand/ Capacity	Bottom	Demand/ Capacity
1	1	60.79	0.35	63.85	0.37
	2	61.01	0.35	64.02	0.37
	3	61.32	0.35	64.30	0.37
2	1	96.19	0.56	99.86	0.58
	2	86.77	0.51	100.90	0.59
	3	95.70	0.56	110.26	0.65
3	1	63.16	0.37	67.54	0.39
	2	62.30	0.36	66.72	0.39
	3	61.97	0.36	66.42	0.39

Table C.5-3 Maximum Shear (kips) at the Abutments

Abutment	Shear			
	Longitudina I	Demand/ Capacity	Transverse	Demand/ Capacity
West	344	0.10	98.3	0.67
East	289	0.86	124	0.85

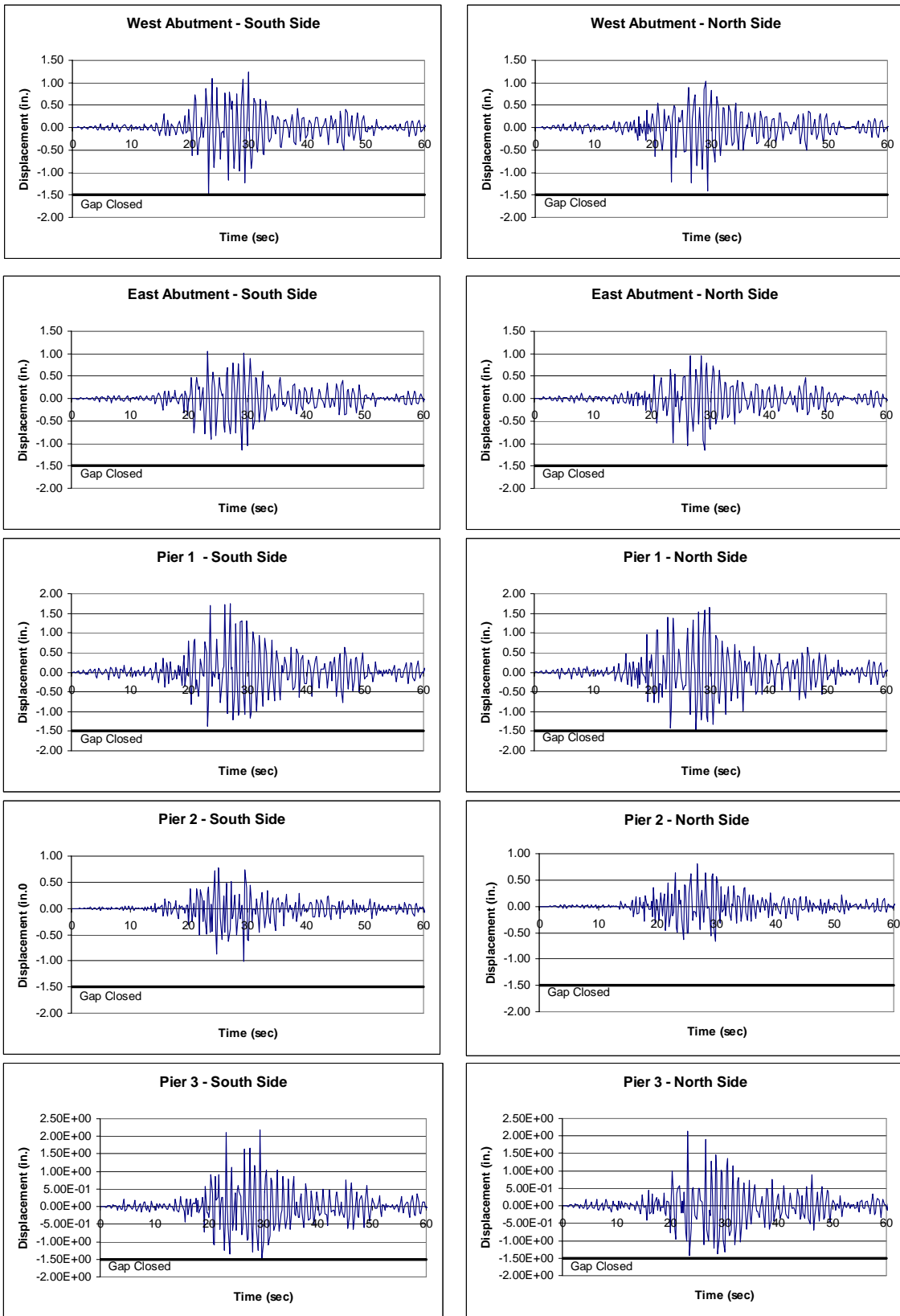


Figure C.5-6 Longitudinal Displacement of Expansion Joints

C.6 Bridge 5/518; Olympia 475-Year Earthquake

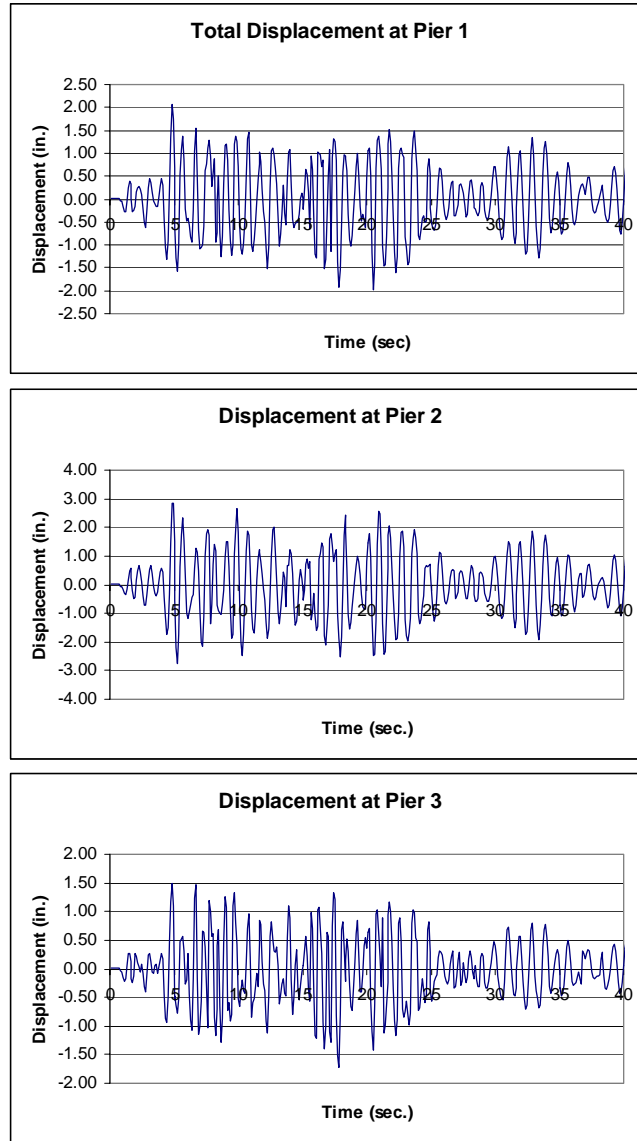


Figure C.6-1 Total Displacement at Piers

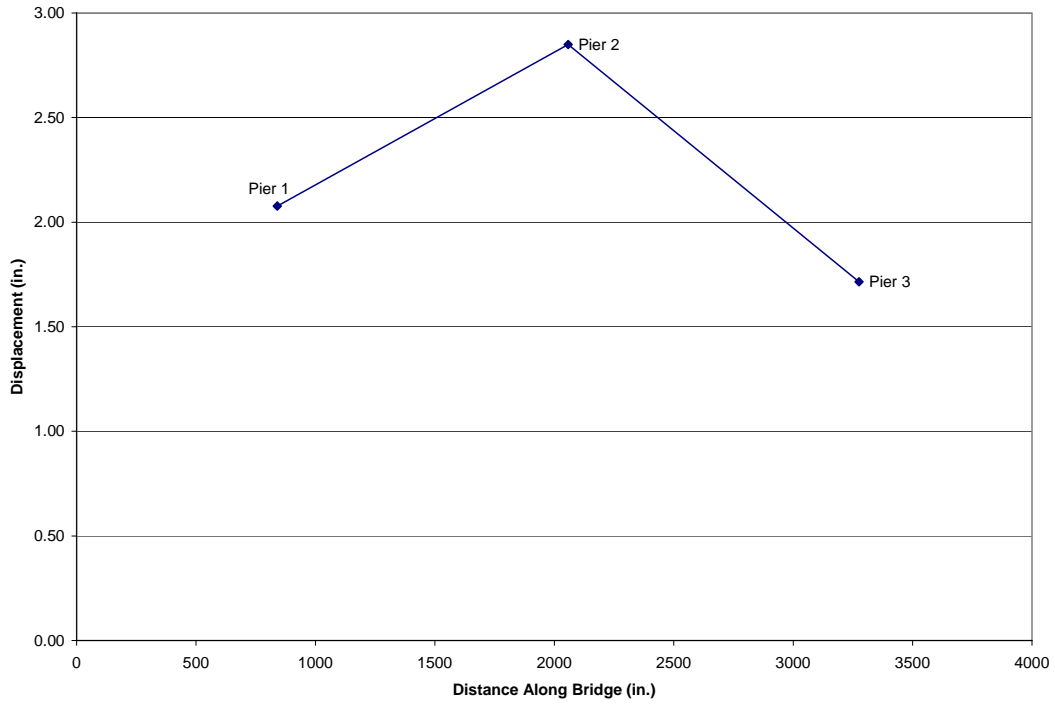


Figure C.6-2 Transverse Displacement Envelope of Bridge Deck

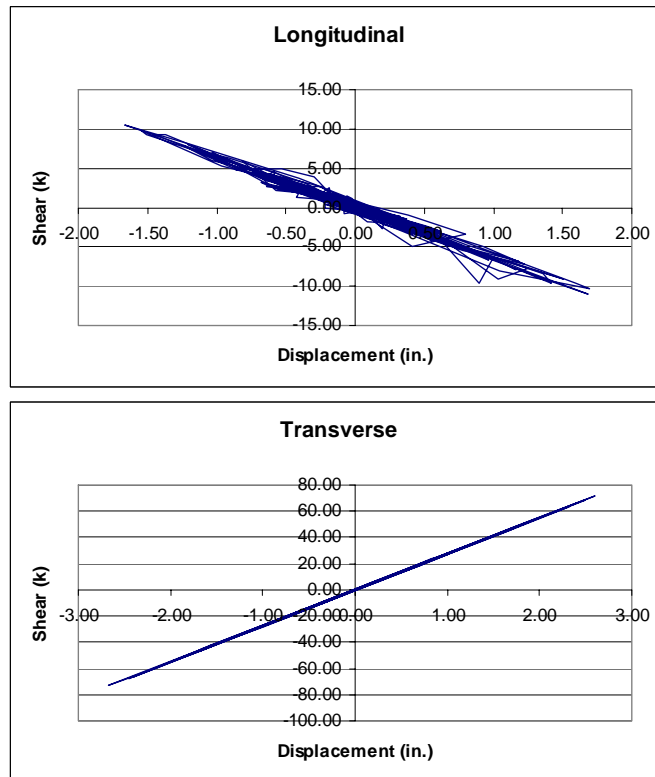


Figure C.6-3 Hysteresis Plots for the Center Column of Pier 2

Table C.6-1 Maximum Moment (kip-in) at the Top and Bottoms of Columns

Pier No.	Column	Moment	
		Top	Bottom
1	1	8217.7	2519.7
	2	8205.2	2639.6
	3	8224.8	2770.7
2	1	11560.0	4365.2
	2	11562.0	4329.3
	3	11567.2	4292.7
3	1	8269.6	2192.3
	2	8240.1	2221.1
	3	8262.9	2285.2

Table C.6-2 Maximum Shear (kips) in the Columns

Pier No.	Column	Shear			
		Top	Demand/ Capacity	Bottom	Demand/ Capacity
1	1	48.82	0.28	49.58	0.29
	2	48.62	0.28	49.36	0.29
	3	48.66	0.28	49.42	0.29
2	1	70.54	0.41	73.34	0.43
	2	70.46	0.41	73.26	0.43
	3	70.42	0.41	73.20	0.43
3	1	49.50	0.29	52.69	0.31
	2	49.31	0.29	52.46	0.31
	3	49.55	0.29	52.66	0.31

Table C.6-3 Maximum Shear (kips) at the Abutments

Abutment	Shear			
	Longitudina I	Demand/ Capacity	Transverse	Demand/ Capacity
West	231	0.07	80.3	0.06
East	188	0.06	89.6	0.06

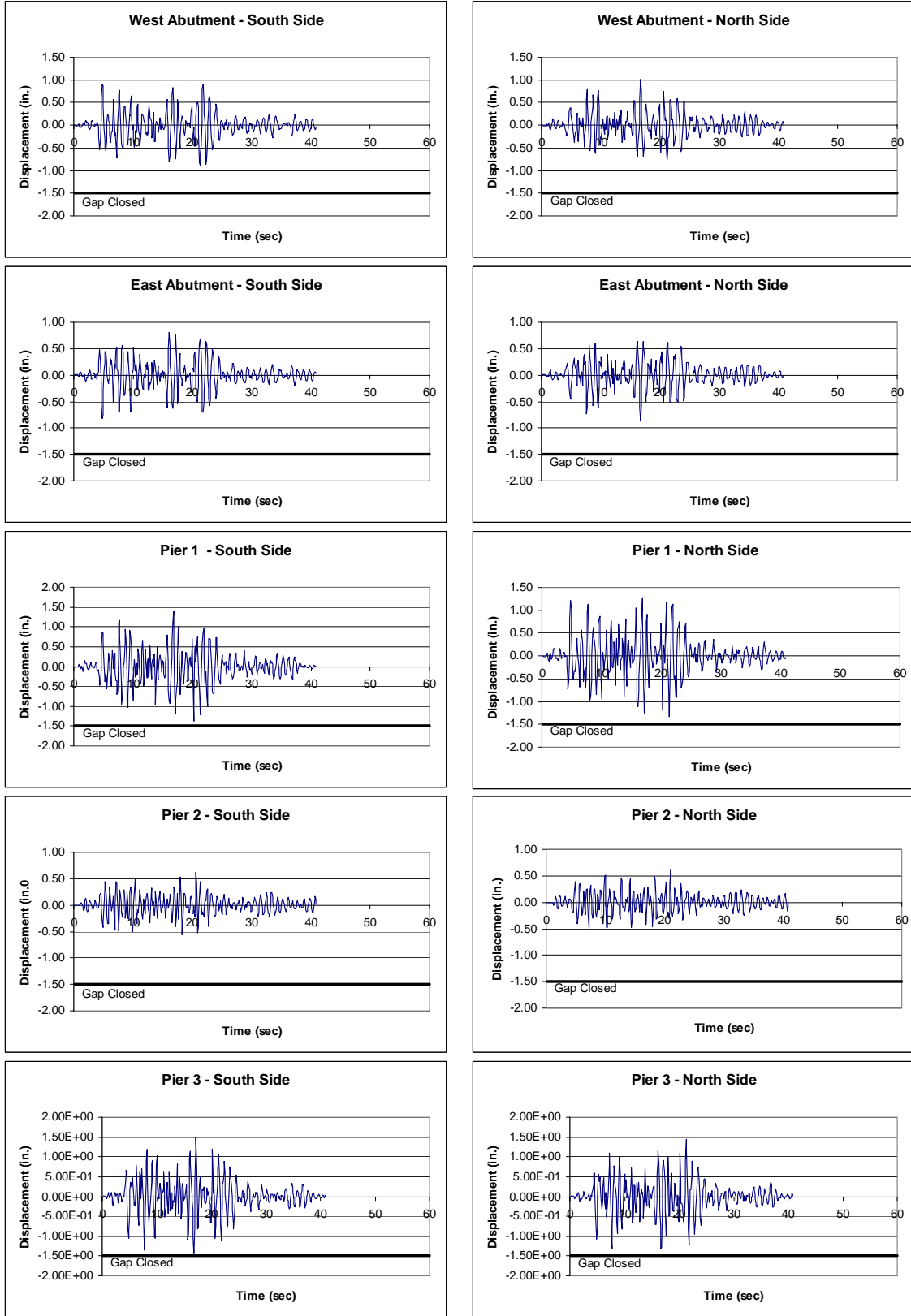


Figure C.6-4 Longitudinal Displacement of Expansion Joints

C.7 Bridge 5/518; Olympia 950-Year Earthquake

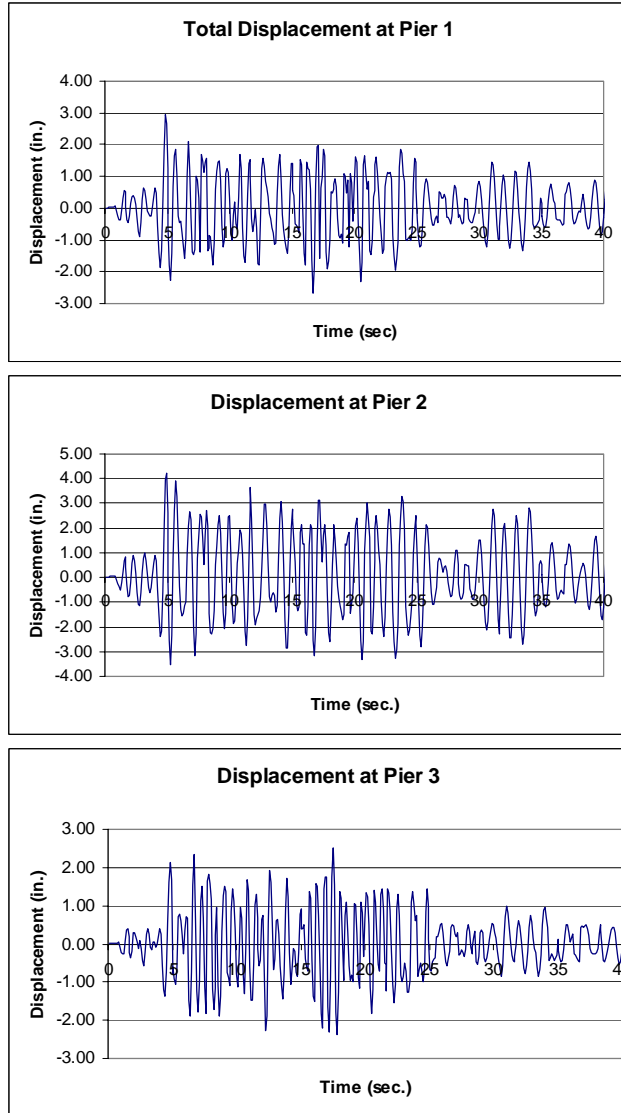


Figure C.7-1 Total Displacement at Piers

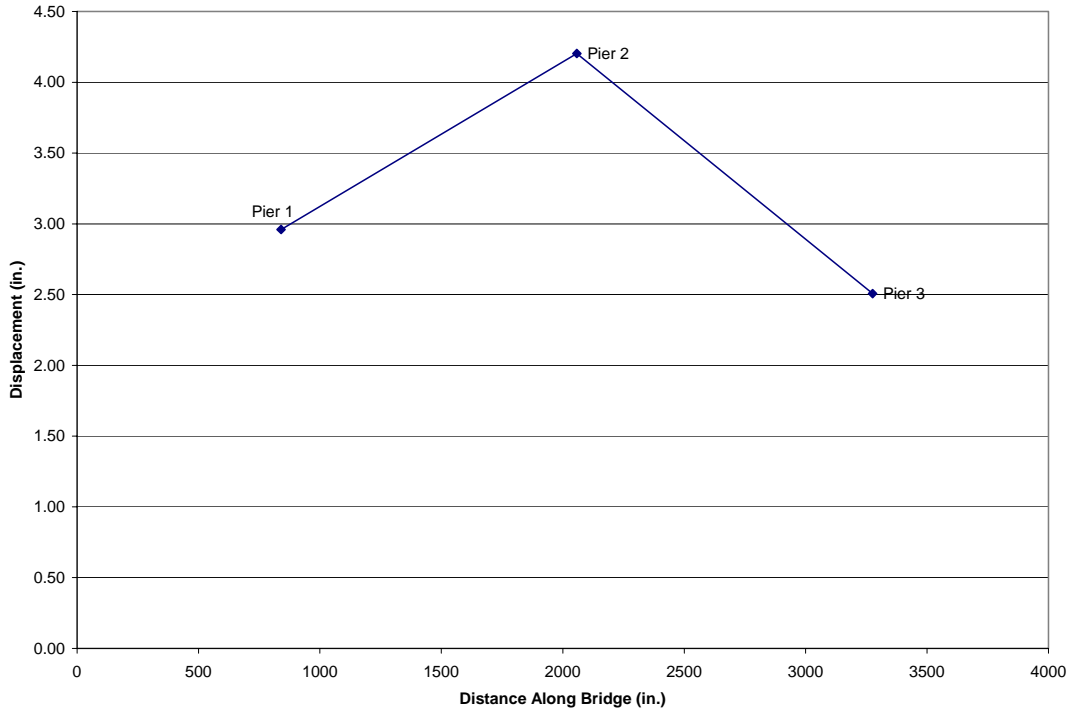


Figure C.7-2 Transverse Displacement Envelope of Bridge Deck

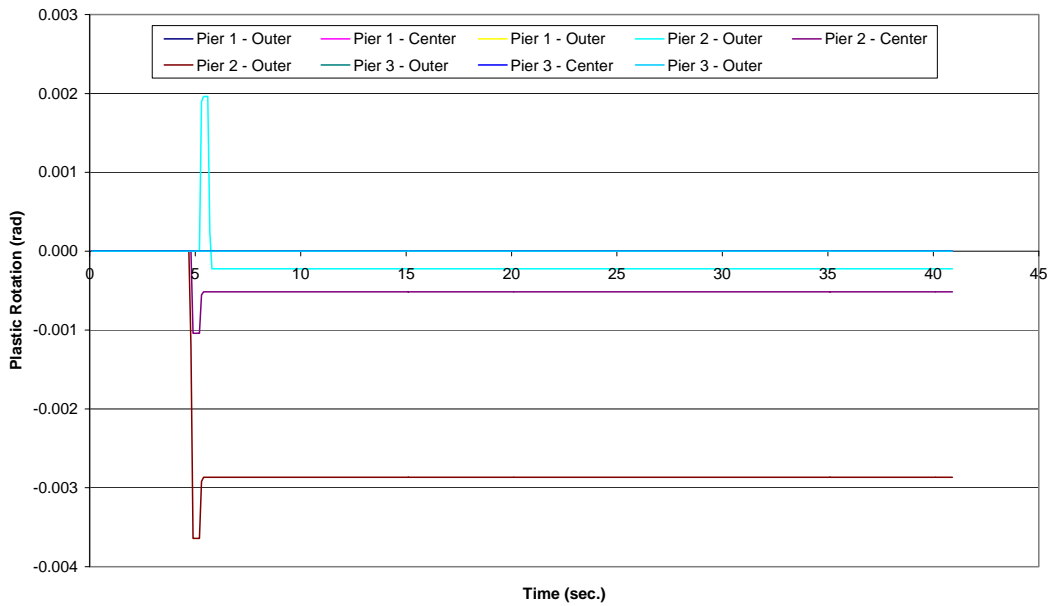


Figure C.7-3 Plastic Rotations at the Top of the Columns

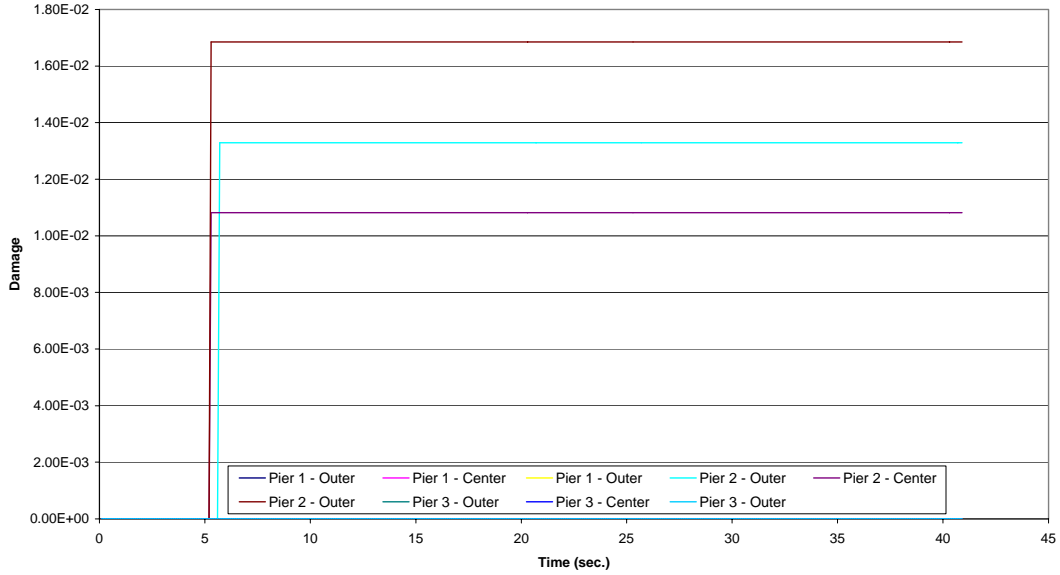


Figure C.7-4 Damage at the Top of the Columns

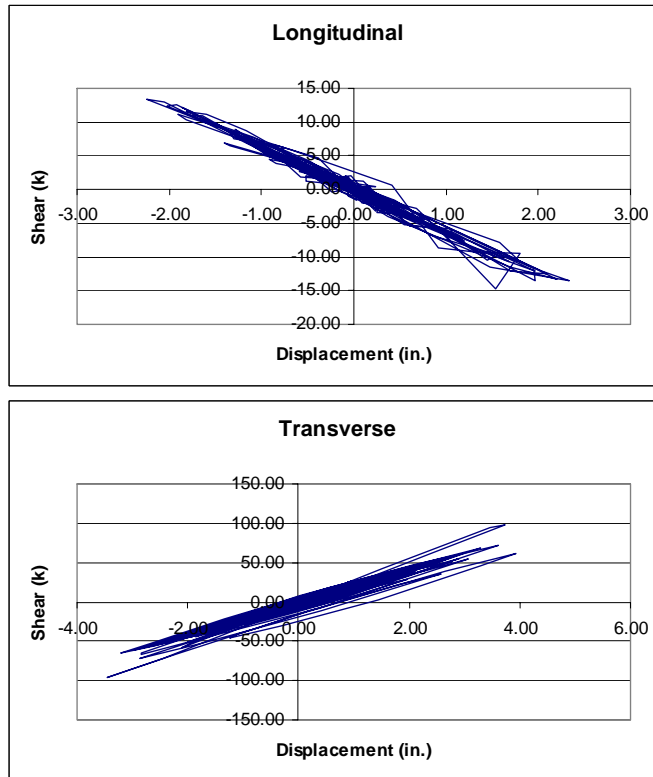


Figure C.7-5 Hysteresis Plots for the Center Column of Pier 2

Table C.7-1 Maximum Moment (kip-in) at the Top and Bottoms of Columns

Pier No.	Column	Moment	
		Top	Bottom
1	1	10726.2	3856.1
	2	10677.7	3773.5
	3	10673.8	3927.8
2	1	16700.5	6425.6
	2	15162.3	6345.1
	3	17222.9	6247.0
3	1	11360.1	3353.4
	2	11340.0	3378.4
	3	11357.0	3404.4

Table C.7-2 Maximum Shear (kips) in the Columns

Pier No.	Column	Shear			
		Top	Demand/ Capacity	Bottom	Demand/ Capacity
1	1	63.29	0.37	64.49	0.38
	2	63.75	0.37	64.95	0.38
	3	64.53	0.37	65.78	0.38
2	1	98.64	0.57	108.80	0.64
	2	93.82	0.55	98.48	0.57
	3	94.71	0.56	106.43	0.62
3	1	67.07	0.39	73.17	0.42
	2	66.88	0.39	72.90	0.42
	3	66.95	0.39	72.97	0.42

Table C.7-3 Maximum Shear (kips) at the Abutments

Abutment	Shear			
	Longitudina I	Demand/ Capacity	Transverse	Demand/ Capacity
West	449	0.13	148	0.10
East	337	0.10	195	0.13

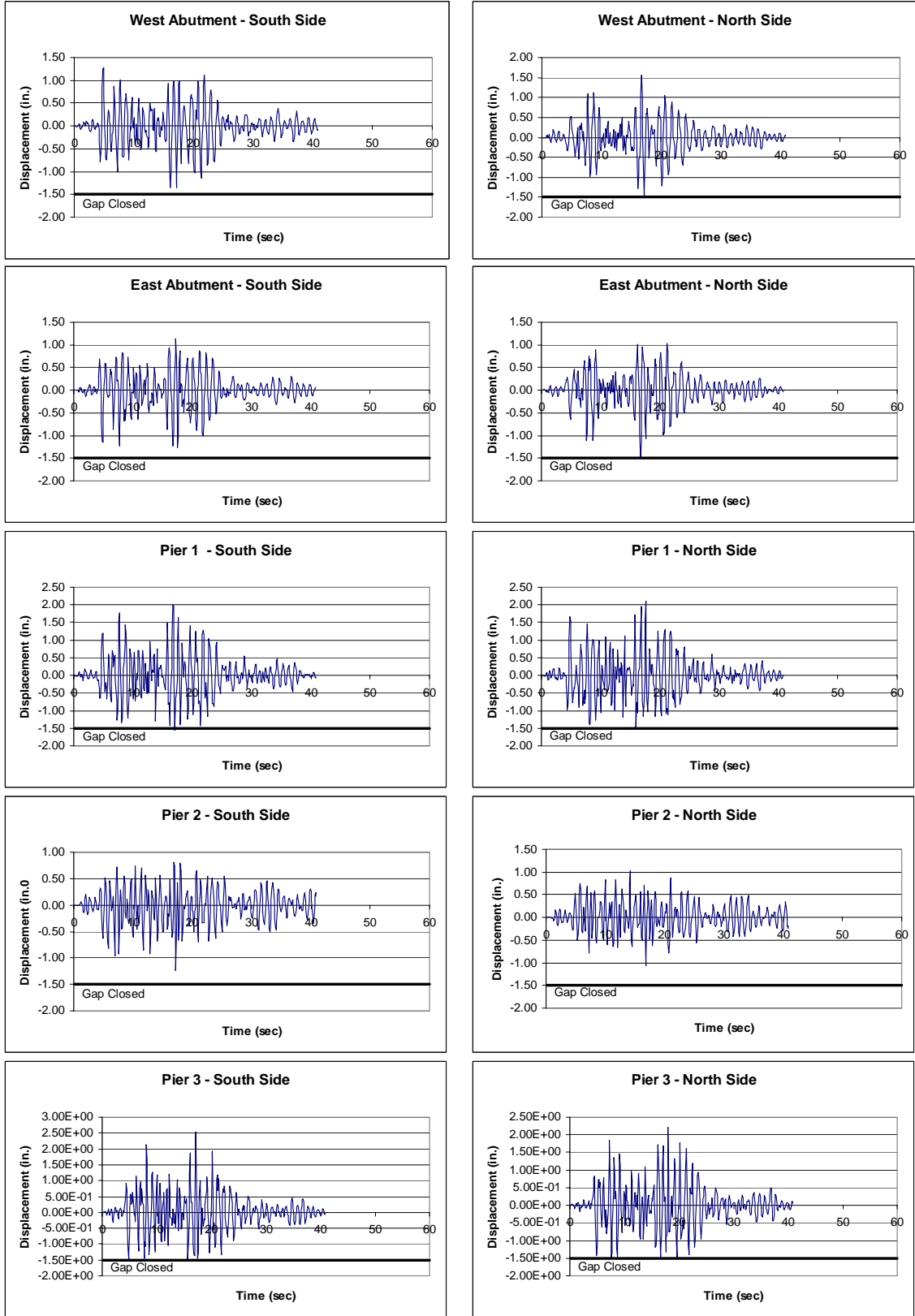


Figure C.7-6 Longitudinal Displacement of Expansion Joints

C.8 Bridge 5/518; Kobe 475-Year Earthquake

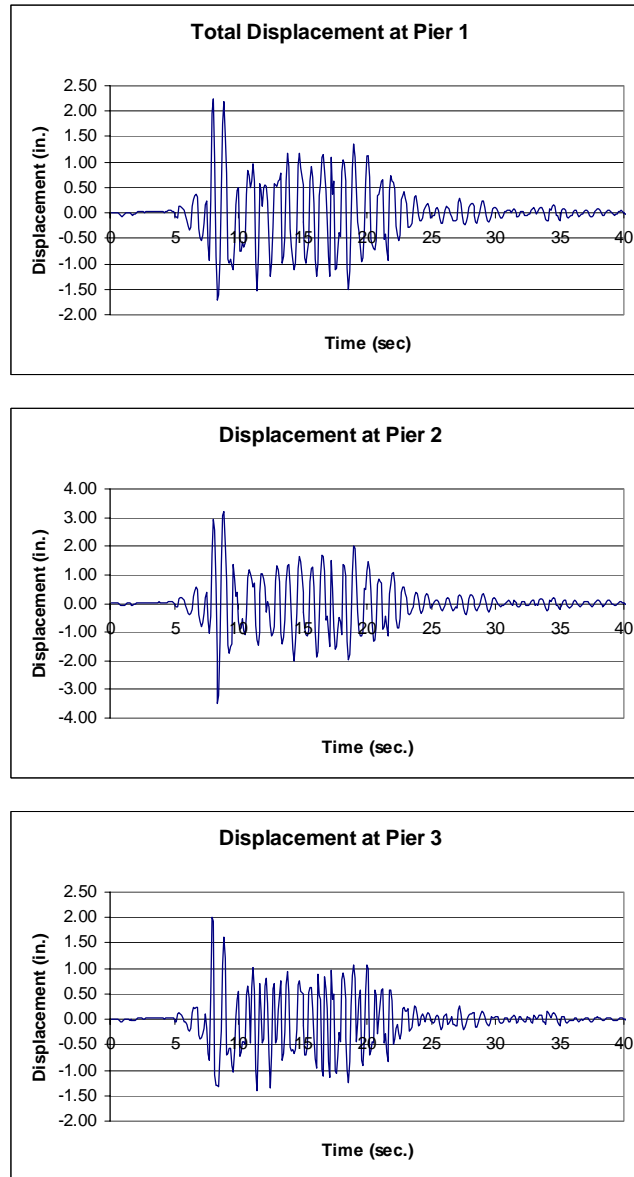


Figure C.8-1 Total Displacement at Piers

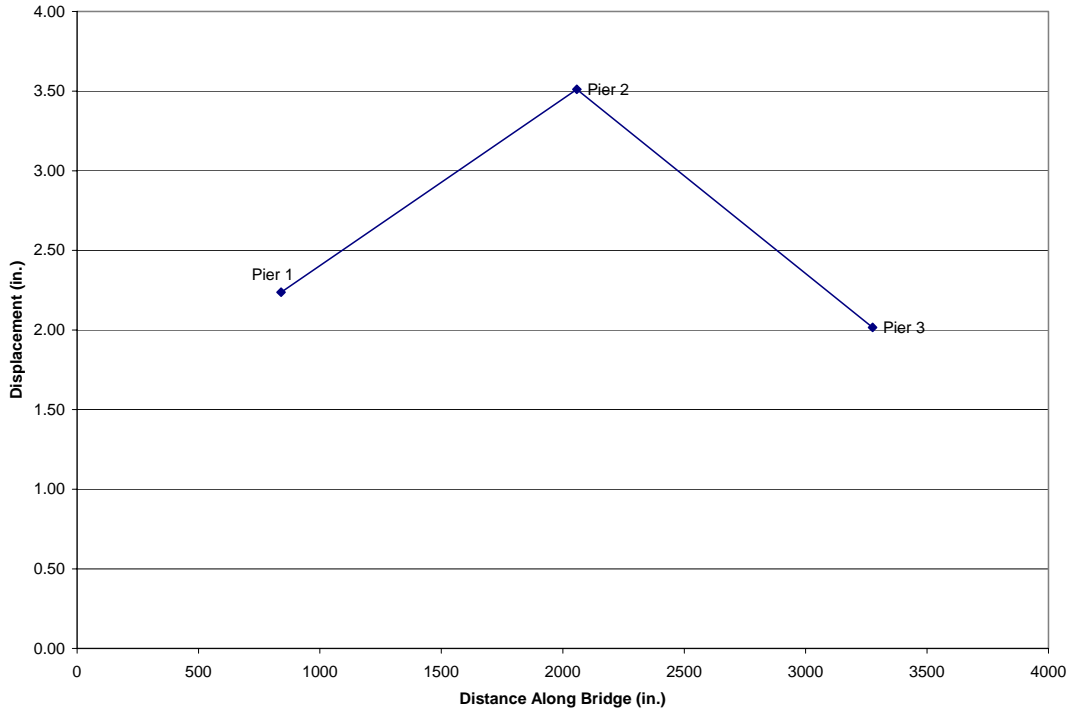


Figure C.8-2 Transverse Displacement Envelope of Bridge Deck

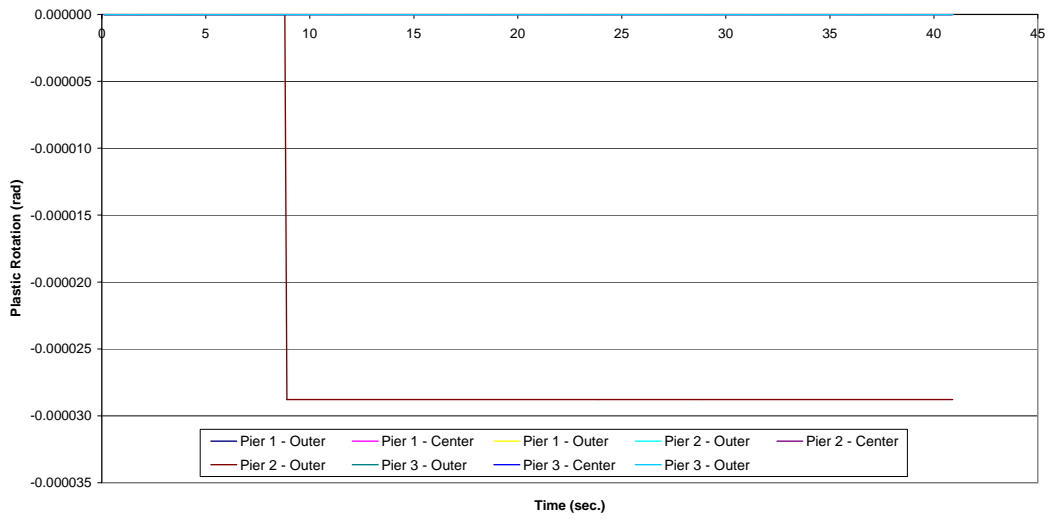


Figure C.8-3 Plastic Rotation at the Top of the Columns

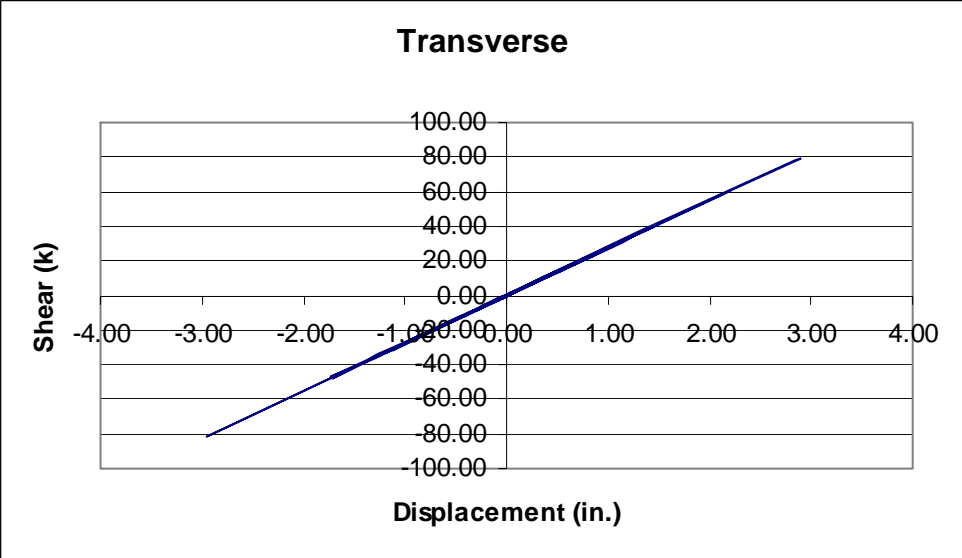
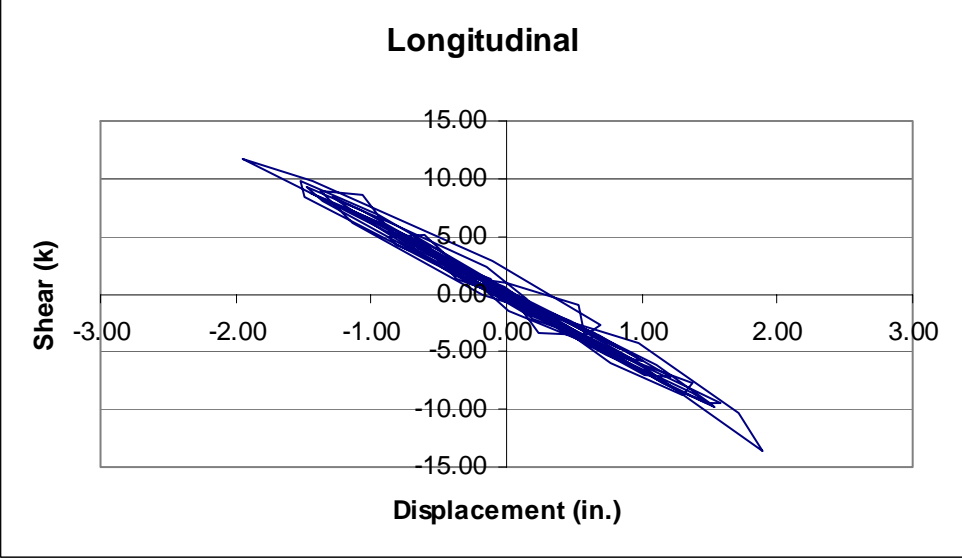


Figure C.8-4 Hysteresis Plots for the Center Column of Pier 2

Table C.8-1 Maximum Moment (kip-in) at the Top and Bottoms of Columns

Pier No.	Column	Moment	
		Top	Bottom
1	1	8169.4	3247.1
	2	8168.5	3112.6
	3	8218.5	2981.1
2	1	12710.9	5323.9
	2	12700.7	5377.4
	3	12693.9	5428.6
3	1	8487.1	2442.8
	2	8463.9	2681.4
	3	8456.1	2923.6

Table C.8-2 Maximum Shear (kips) in the Columns

Pier No.	Column	Shear			
		Top	Demand/ Capacity	Bottom	Demand/ Capacity
1	1	49.05	0.29	50.77	0.30
	2	48.37	0.29	50.08	0.30
	3	48.04	0.29	49.77	0.30
2	1	76.81	0.45	82.93	0.48
	2	76.81	0.45	83.17	0.48
	3	76.90	0.45	83.41	0.48
3	1	50.62	0.30	54.27	0.32
	2	50.91	0.30	54.57	0.32
	3	51.32	0.30	54.98	0.32

Table C.8-3 Maximum Shear (kips) at the Abutments

Abutment	Shear			
	Longitudinal	Demand/ Capacity	Transverse	Demand/ Capacity
West	326	0.10	739	0.51
East	240	0.07	776	0.53

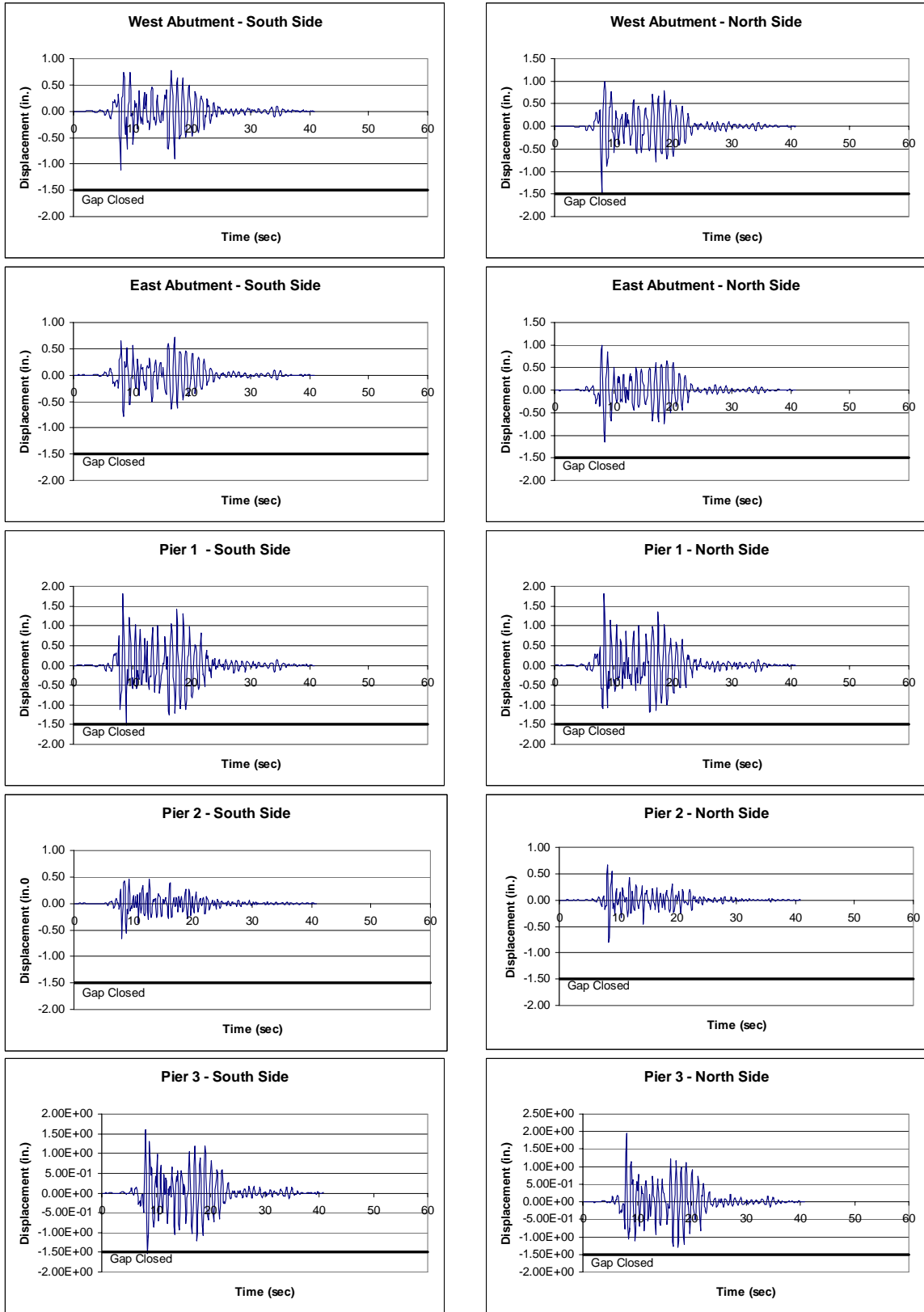


Figure C.8-5 Longitudinal Displacement of Expansion Joints

C.9 Bridge 5/518; Kobe 950-Year Earthquake

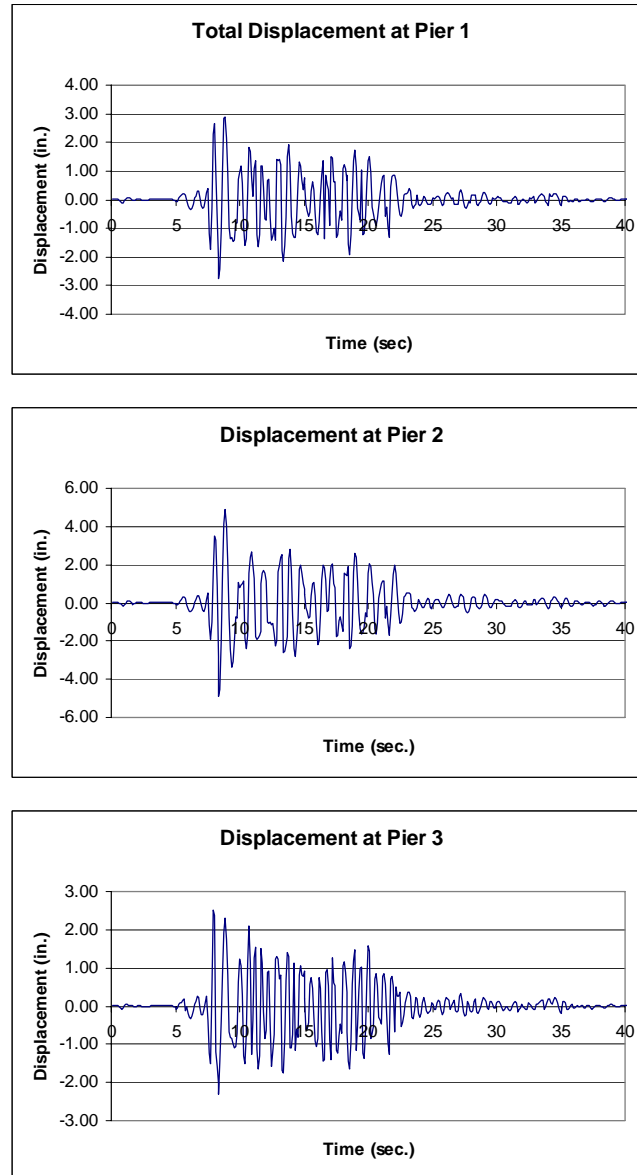


Figure C.9-1 Total Displacement at Piers

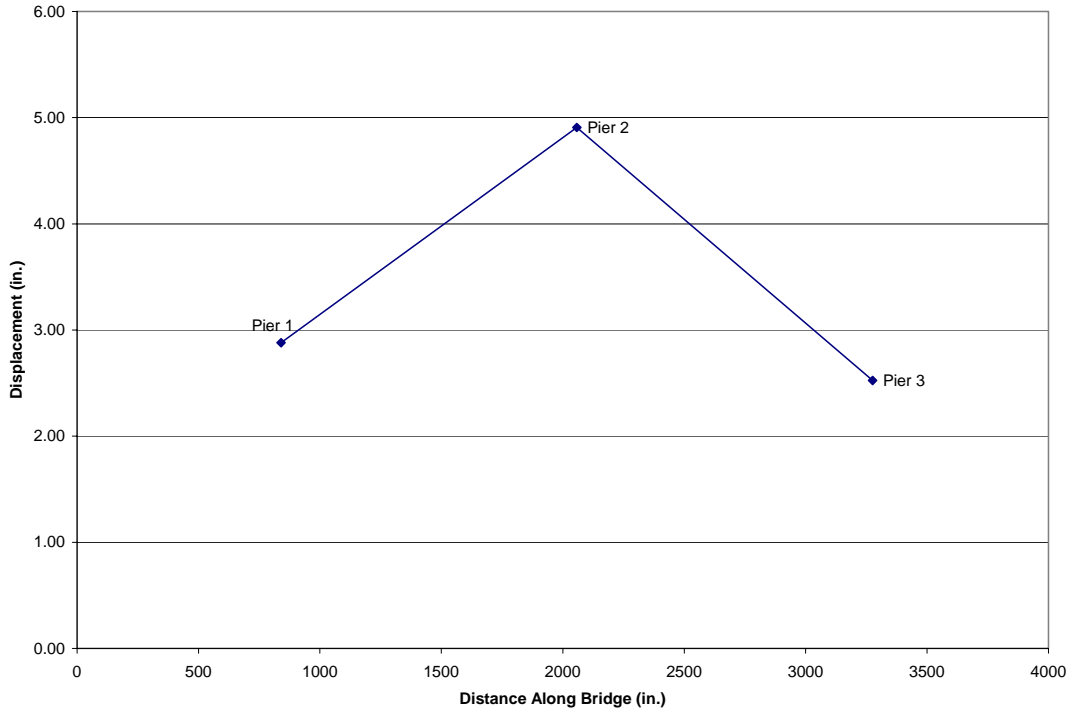


Figure C.9-2 Transverse Displacement Envelope of Bridge Deck

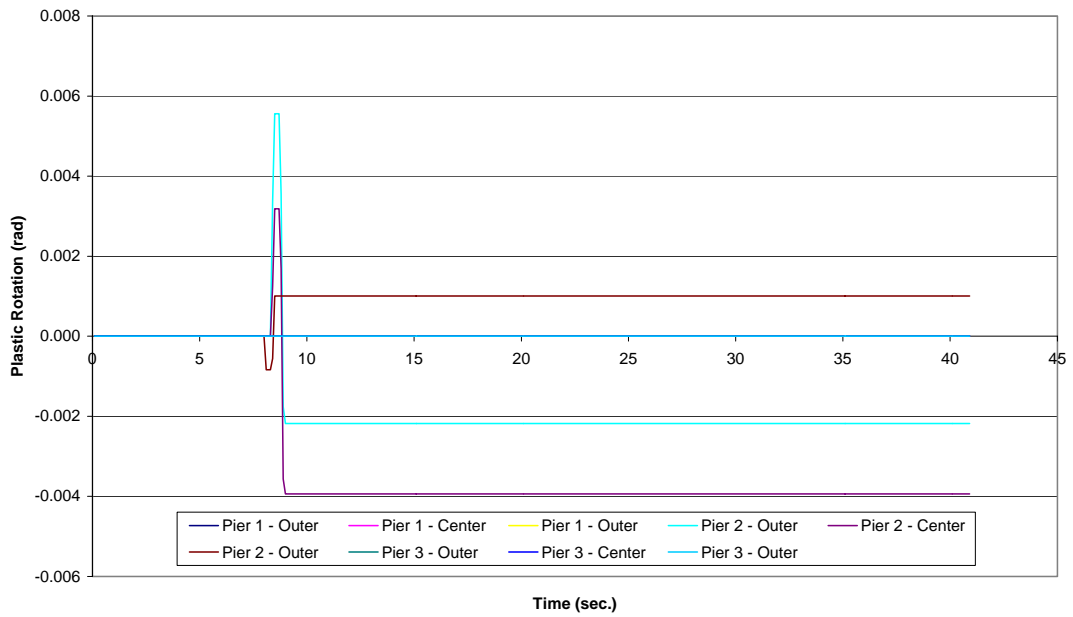


Figure C.9-3 Plastic Rotations at the Top of the Columns

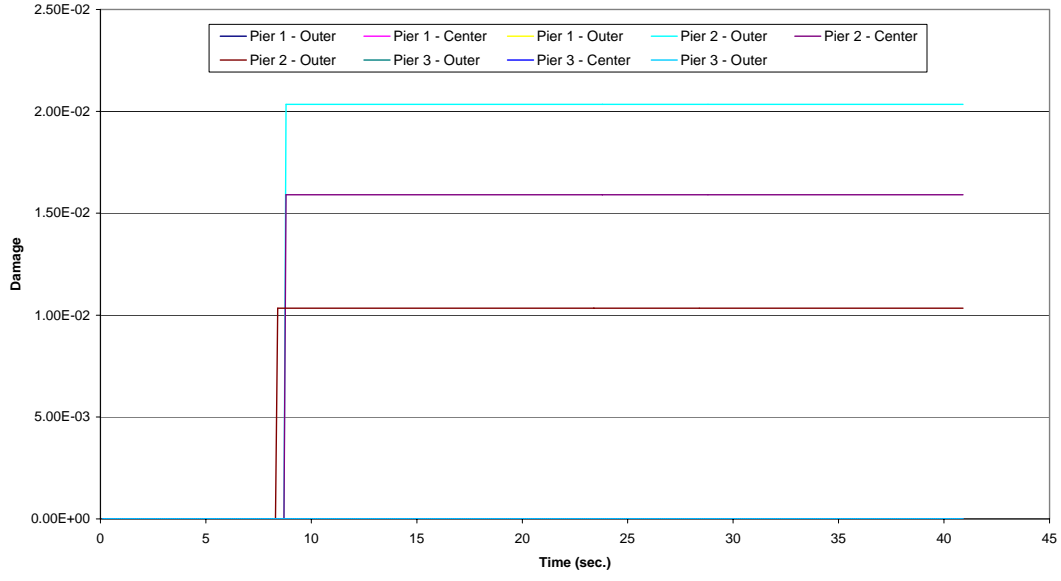


Figure C.9-4 Damage at the Top of the Columns

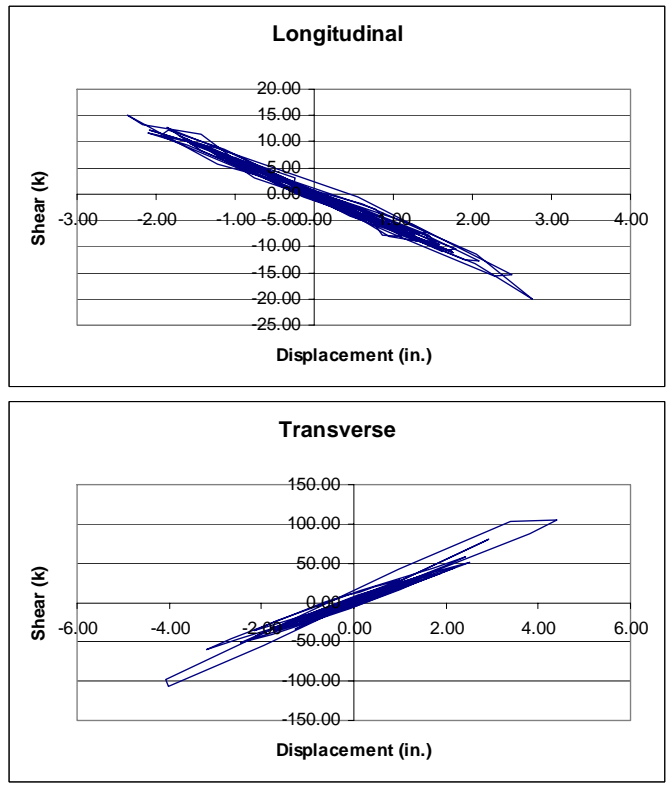


Figure C.9-5 Hysteresis Plots for the Center Column of Pier 2

Table C.9-1 Maximum Moment (kip-in) at the Top and Bottoms of Columns

Pier No.	Column	Moment	
		Top	Bottom
1	1	9645.5	4229.4
	2	9658.6	3866.9
	3	9725.1	3626.6
2	1	17010.4	7378.3
	2	15087.3	7447.5
	3	17160.5	7511.7
3	1	11433.6	3571.8
	2	11414.8	3956.6
	3	11410.2	4341.6

Table C.9-2 Maximum Shear (kips) in the Columns

Pier No.	Column	Shear			
		Top	Demand/ Capacity	Bottom	Demand/ Capacity
1	1	58.58	0.34	60.32	0.35
	2	57.61	0.34	59.46	0.35
	3	57.04	0.34	58.88	0.35
2	1	103.64	0.61	114.64	0.67
	2	94.64	0.55	108.66	0.63
	3	112.12	0.65	117.54	0.69
3	1	68.12	0.40	72.94	0.43
	2	68.31	0.40	73.21	0.43
	3	68.61	0.40	73.55	0.43

Table C.9-3 Maximum Shear (kips) at the Abutments

Abutment	Shear			
	Longitudina I	Demand/ Capacity	Transverse	Demand/ Capacity
West	563	0.17	156	0.11
East	673	0.20	121	0.08

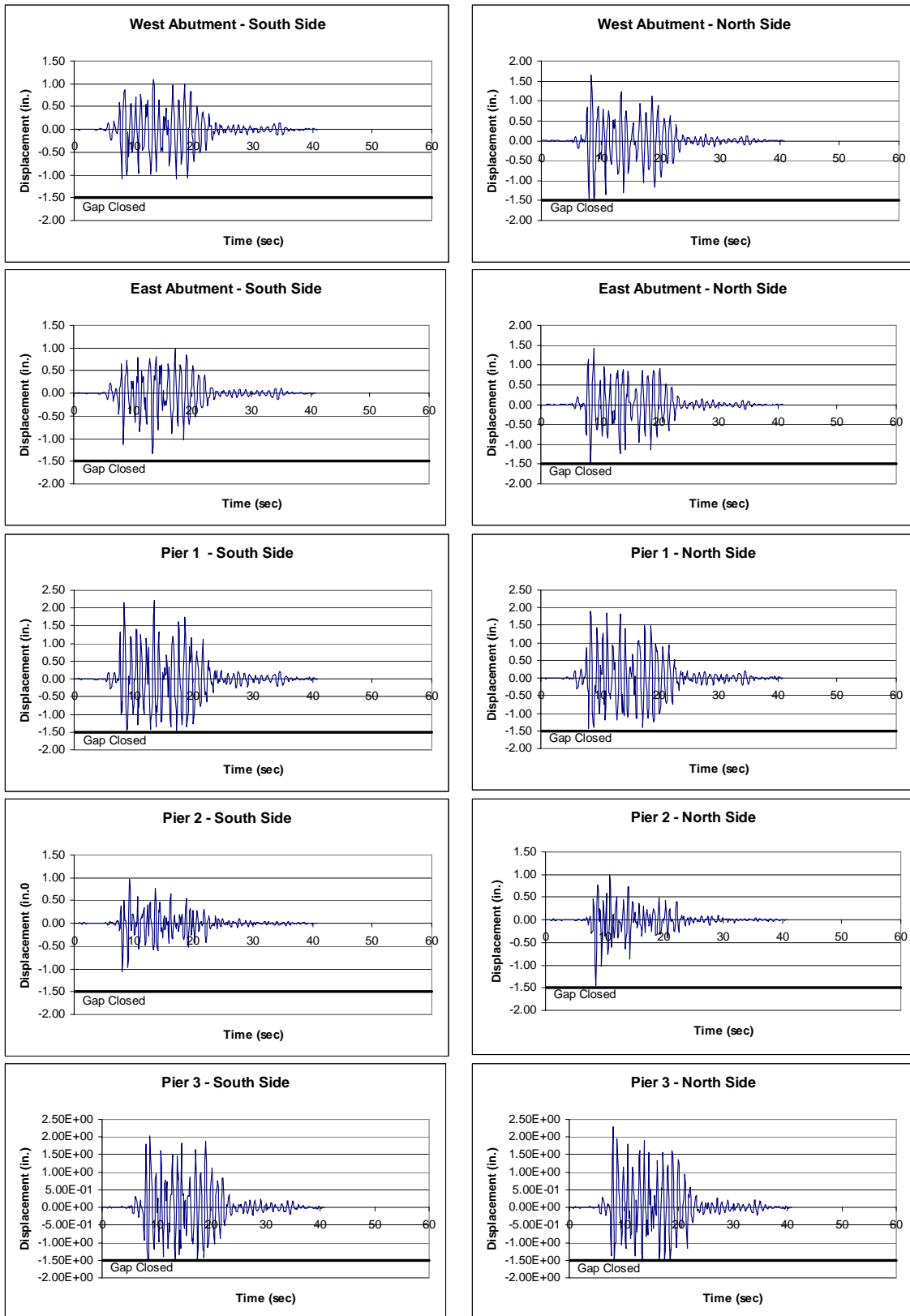


Figure C.9-6 Longitudinal Displacement of the Expansion joints

C.10 Bridge 5/826; Unmodified Peru Earthquake

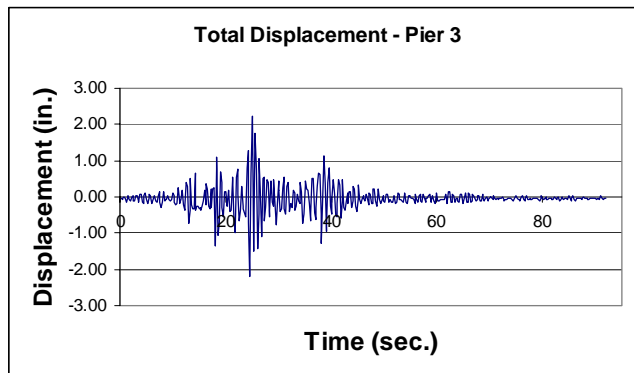
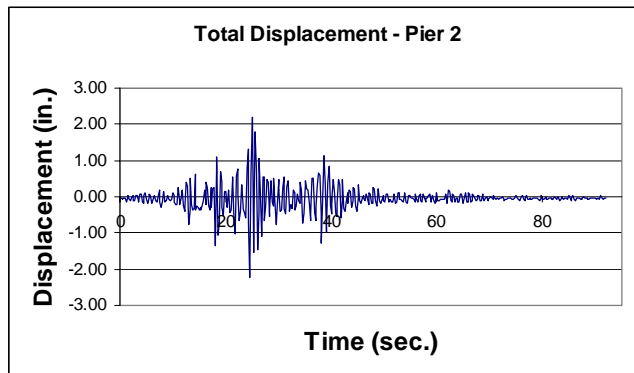
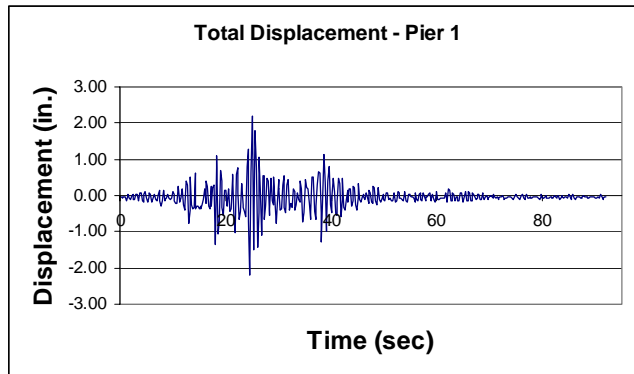


Figure C.10-1 Total Displacement at Piers

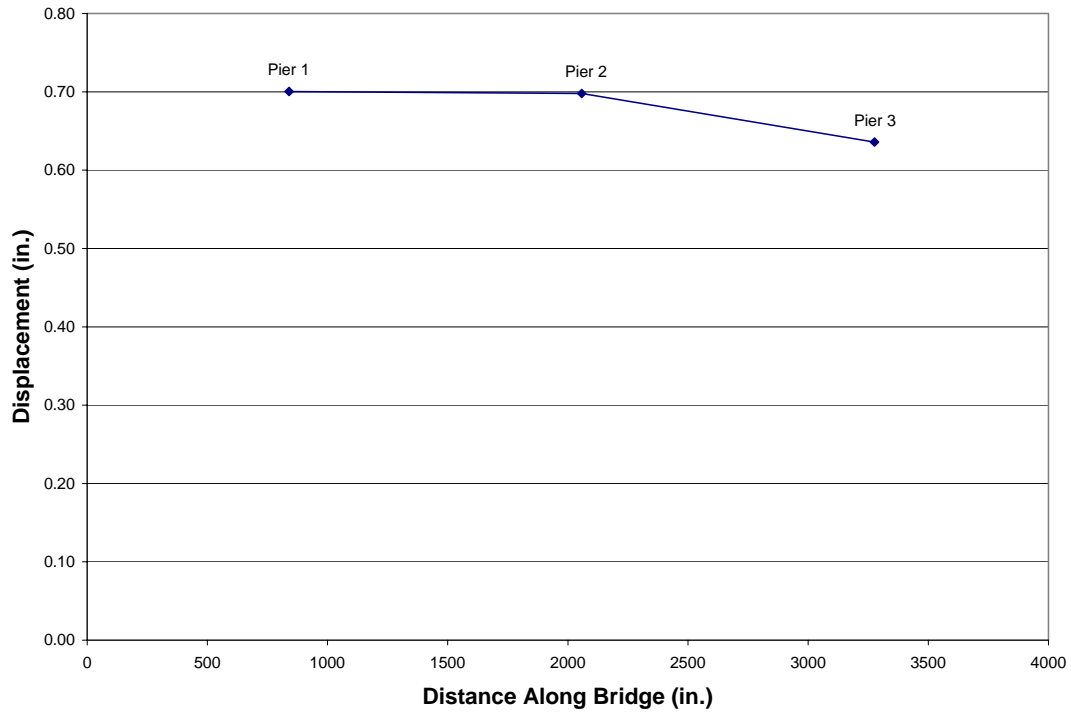


Figure C.10-2 Transverse Displacement Envelope of the Bridge Deck

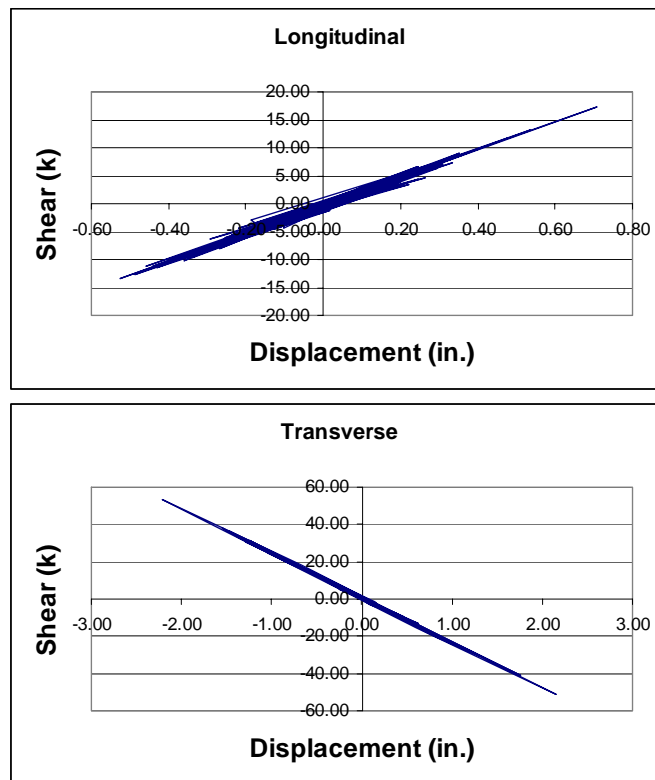


Figure C.10-3 Hysteresis Plots for the Center Column of Pier 2

Table C.10-1 Maximum Moment (kip-in) at the Top and Bottoms of Columns

Pier No.	Column	Moment	
		Top	Bottom
1	1	10808.4	9116.9
	2	10798.8	9118.2
	3	10732.1	9089.4
2	1	8759.4	7795.6
	2	8722.7	7773.5
	3	8646.8	7731.9
3	1	9873.5	8437.8
	2	9835.7	8410.6
	3	9753.8	8360.8

Table C.10-2 Maximum Shear (kips) in the Columns

Pier No.	Column	Shear			
		Top	Demand/ Capacity	Bottom	Demand/ Capacity
1	1	69.66	0.33	74.83	0.35
	2	69.57	0.33	74.80	0.35
	3	69.20	0.33	74.47	0.35
2	1	49.33	0.23	55.31	0.26
	2	49.13	0.23	55.11	0.26
	3	48.75	0.23	54.72	0.26
3	1	60.59	0.28	66.06	0.31
	2	60.30	0.28	65.82	0.31
	3	59.87	0.28	65.37	0.31

Table C.10-3 Maximum Shear (kips) at the Abutments

Abutment	Shear			
	Longitudina I	Demand/ Capacity	Transverse	Demand/ Capacity
West	686	0.13	748	0.14
East	806	0.16	713	0.13

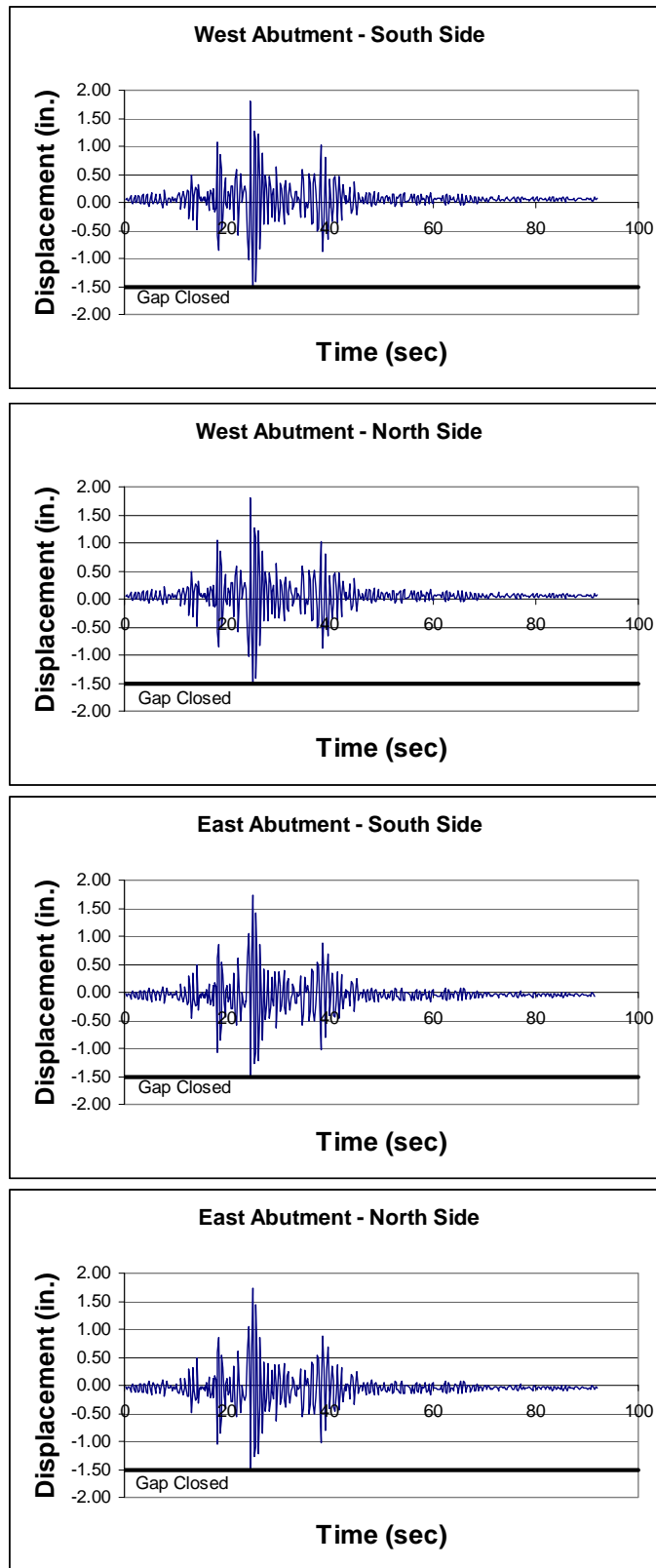


Figure C.10-4 Longitudinal Displacement of the Expansion Joints

C.11 Bridge 5/826; Unmodified Chile Earthquake

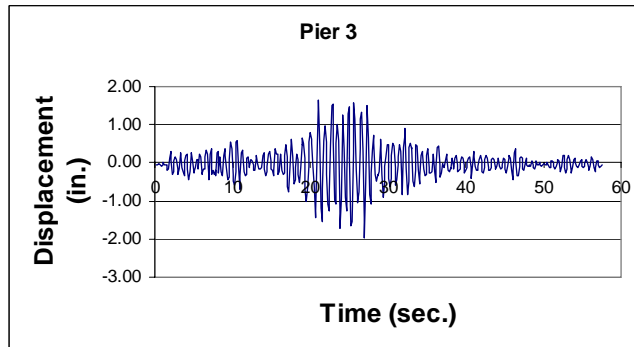
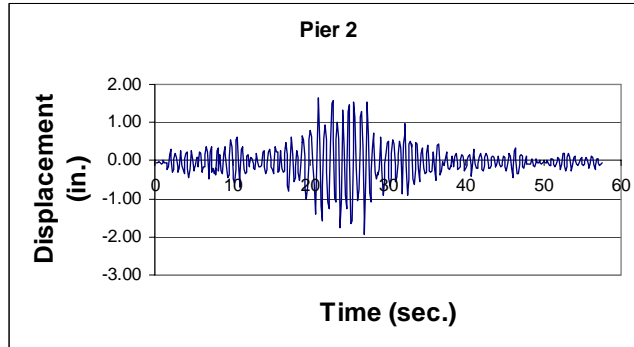
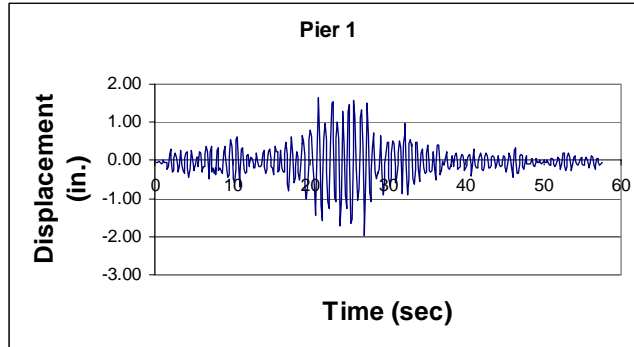


Figure C.11-1 Total Displacement at Piers

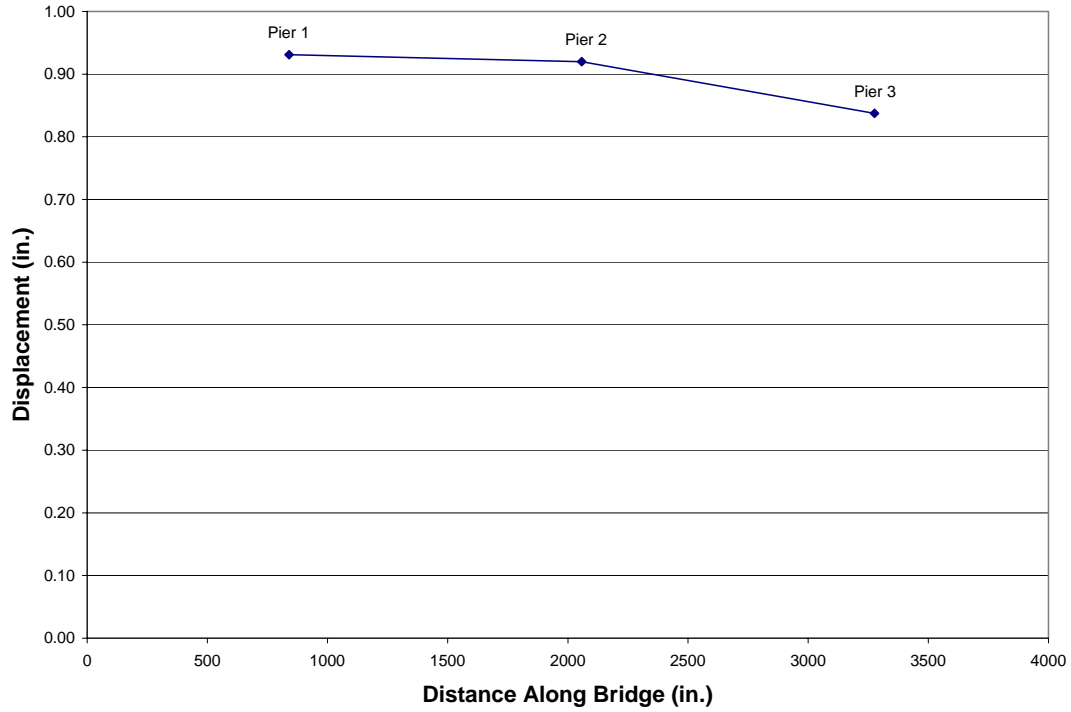


Figure C.11-2 Transverse Displacement Envelope of the Bridge Deck

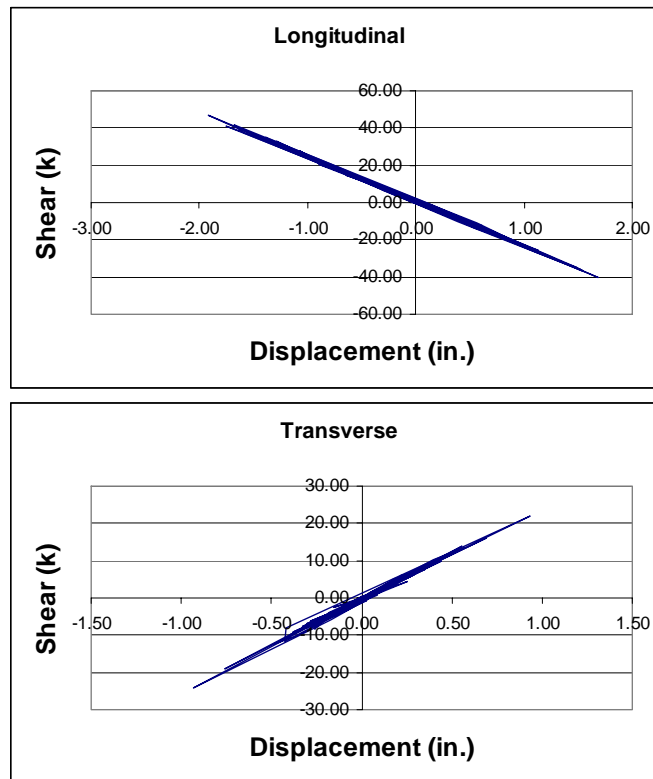


Figure C.11-3 Hysteresis Plots for the Center Column of Pier 2

Table C.11-1 Maximum Moment (kip-in) at the Top and Bottoms of Columns

Pier No.	Column	Moment	
		Top	Bottom
1	1	9340.5	7851.9
	2	9314.2	7838.6
	3	9240.3	7802.5
2	1	7571.3	6693.63
	2	7520.0	6670.6
	3	7443.3	6632.7
3	1	8510.7	7243.9
	2	8487.7	7237.6
	3	8434.3	7212.6

Table C.11-2 Maximum Shear (kips) in the Columns

Pier No.	Column	Shear			
		Top	Demand/ Capacity	Bottom	Demand/ Capacity
1	1	60.50	0.35	64.50	0.38
	2	60.44	0.35	64.35	0.38
	3	60.00	0.35	63.94	0.38
2	1	43.17	0.25	47.64	0.28
	2	42.89	0.25	47.41	0.28
	3	42.49	0.25	47.06	0.28
3	1	52.62	0.31	56.82	0.33
	2	52.50	0.31	56.73	0.33
	3	52.25	0.31	56.46	0.33

Table C.11-3 Maximum Shear (kips) at the Abutments

Abutment	Shear			
	Longitudina I	Demand/ Capacity	Transverse	Demand/ Capacity
West	373	0.07	998	0.18
East	484	0.09	939	0.17

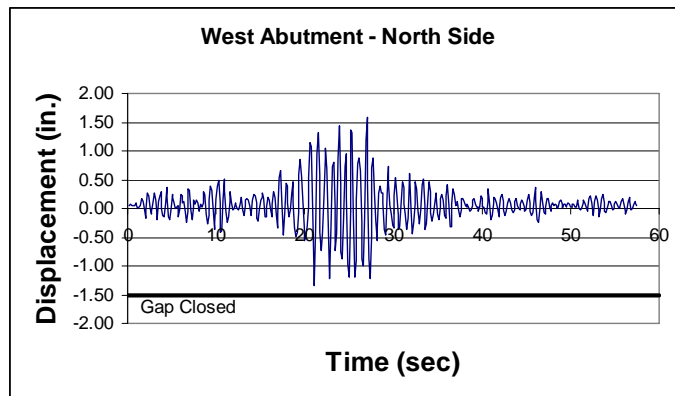
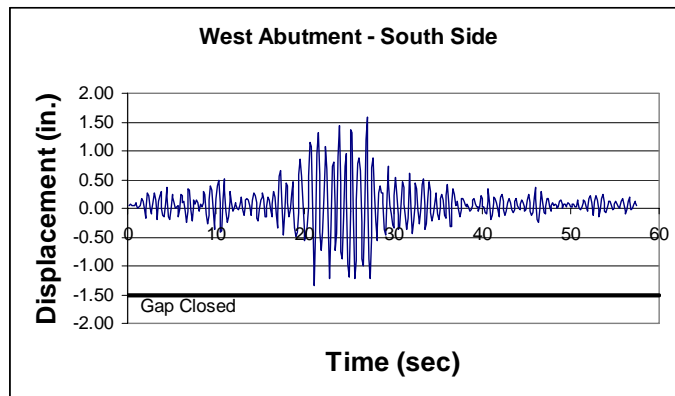
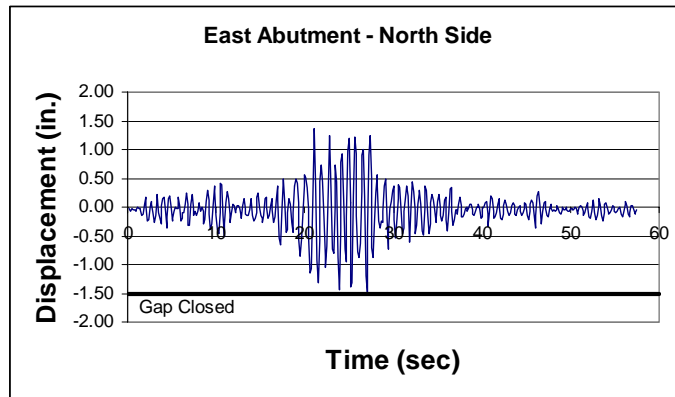
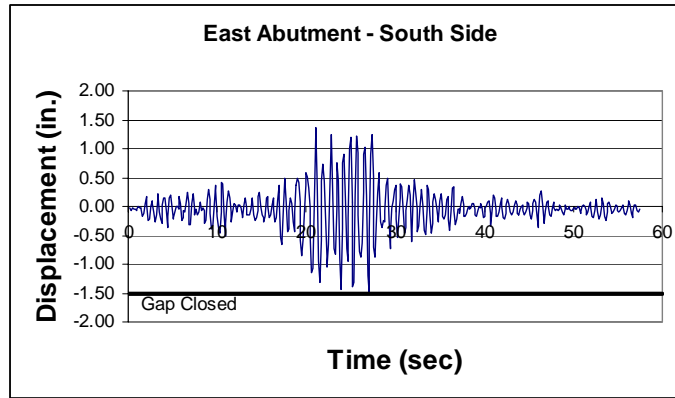


Figure C.11-4 Longitudinal Displacement of Expansion Joints

C.12 Bridge 5/826; Mexico City 475-Year Earthquake

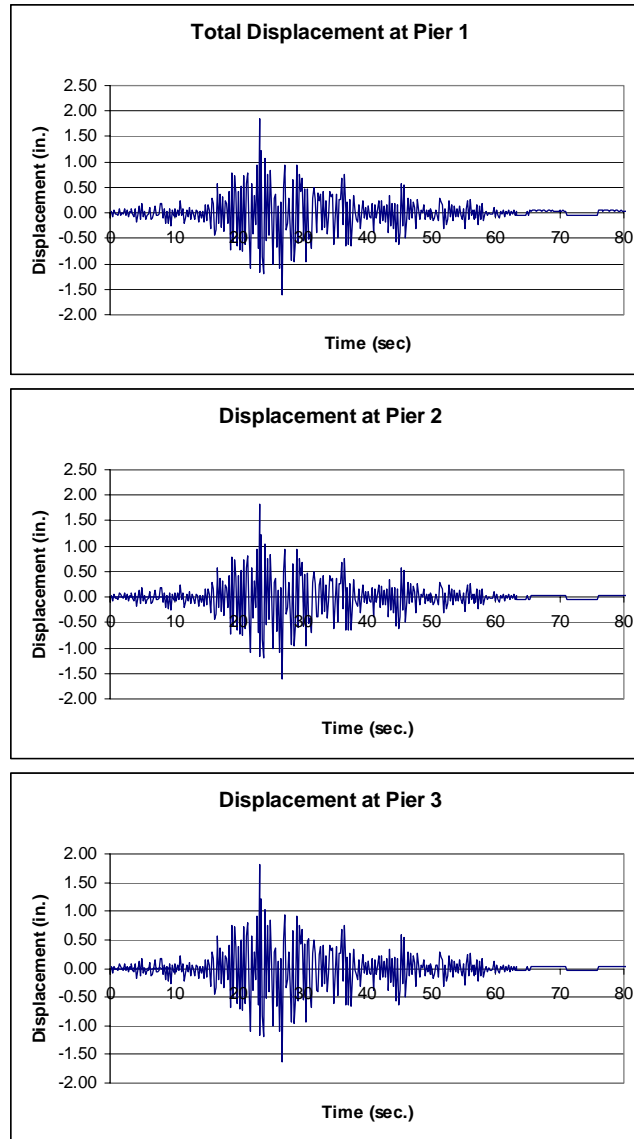


Figure C.12-1 Total Displacement at Piers

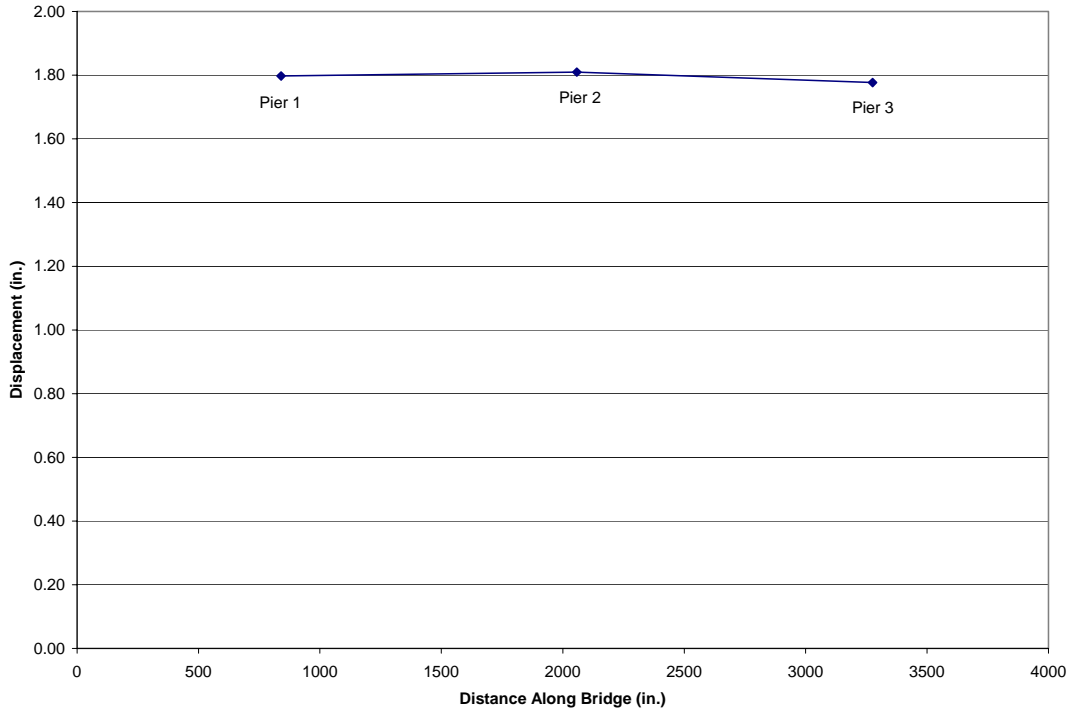


Figure C.12-2 Transverse Displacement Envelope of the Bridge Deck

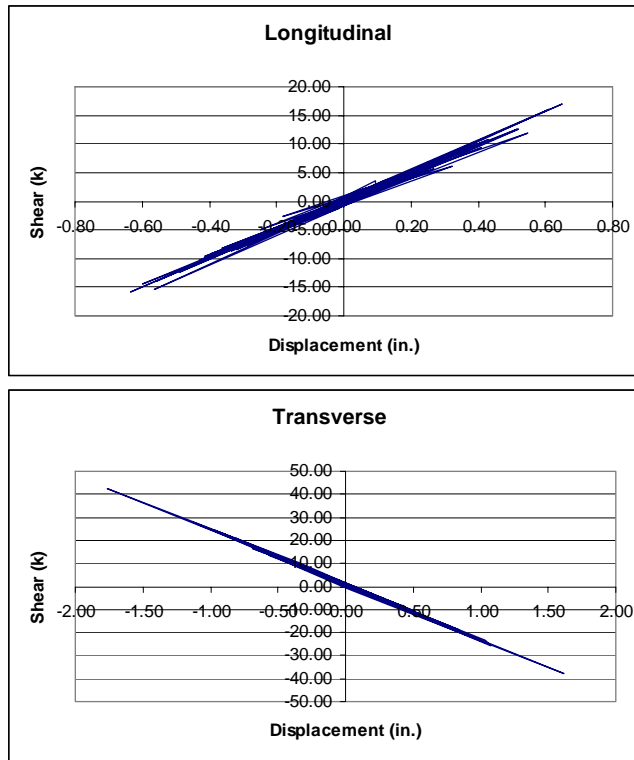


Figure C.12-3 Hysteresis Plots for the Center Column of Pier 2

Table C.12-1 Maximum Moment (kip-in) at the Top and Bottoms of Columns

Pier No.	Column	Moment	
		Top	Bottom
1	1	8901.4	7452.1
	2	8856.9	7432.1
	3	8777.7	7395.3
2	1	7210.7	6353.5
	2	7147.4	6324.9
	3	7069.4	6289.1
3	1	8035.5	6805.5
	2	8013.9	6808.2
	3	7974.2	6799.9

Table C.12-2 Maximum Shear (kips) in the Columns

Pier No.	Column	Shear			
		Top	Demand/ Capacity	Bottom	Demand/ Capacity
1	1	57.49	0.34	60.76	0.35
	2	57.32	0.34	60.50	0.35
	3	56.83	0.34	60.06	0.35
2	1	40.92	0.24	44.52	0.26
	2	40.65	0.24	44.22	0.26
	3	40.25	0.24	43.83	0.26
3	1	49.62	0.29	52.79	0.31
	2	49.51	0.29	52.74	0.31
	3	49.31	0.29	52.57	0.31

Table C.12-3 Maximum Shear (kips) at the Abutments

Abutment	Shear			
	Longitudina I	Demand/ Capacity	Transverse	Demand/ Capacity
West	367	0.07	688	0.13
East	377	0.72	656	0.12

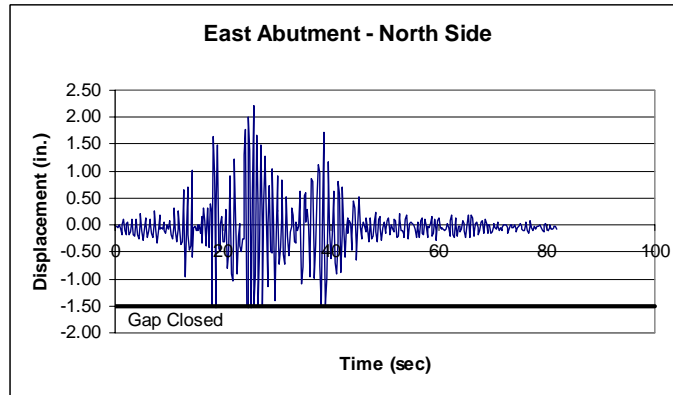
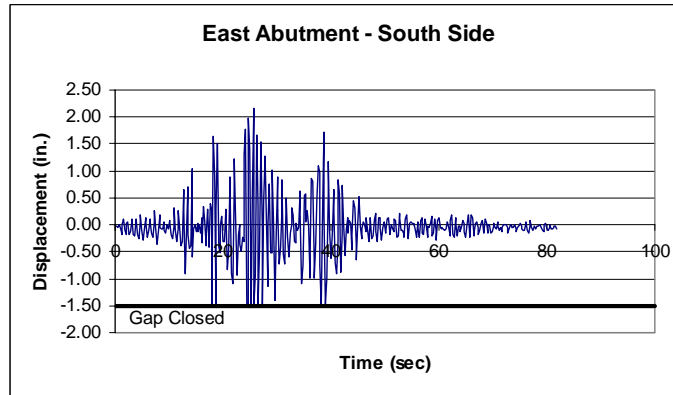
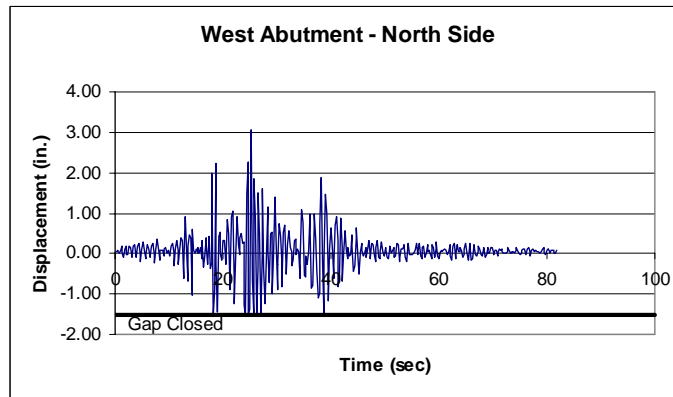
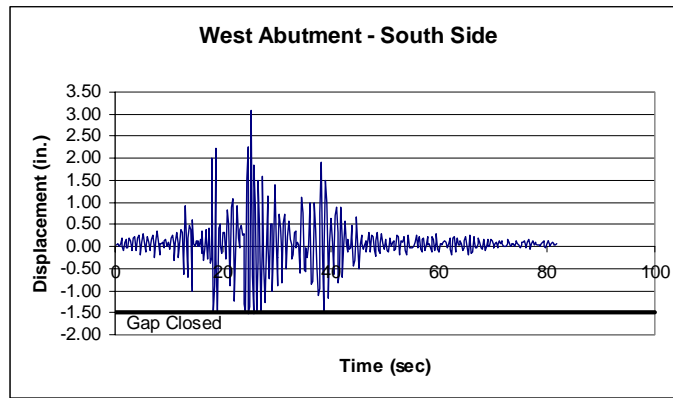


Figure C.12-4 Longitudinal Displacement of Expansion Joints

C.13 Bridge 5/826; Mexico City 950-Year Earthquake

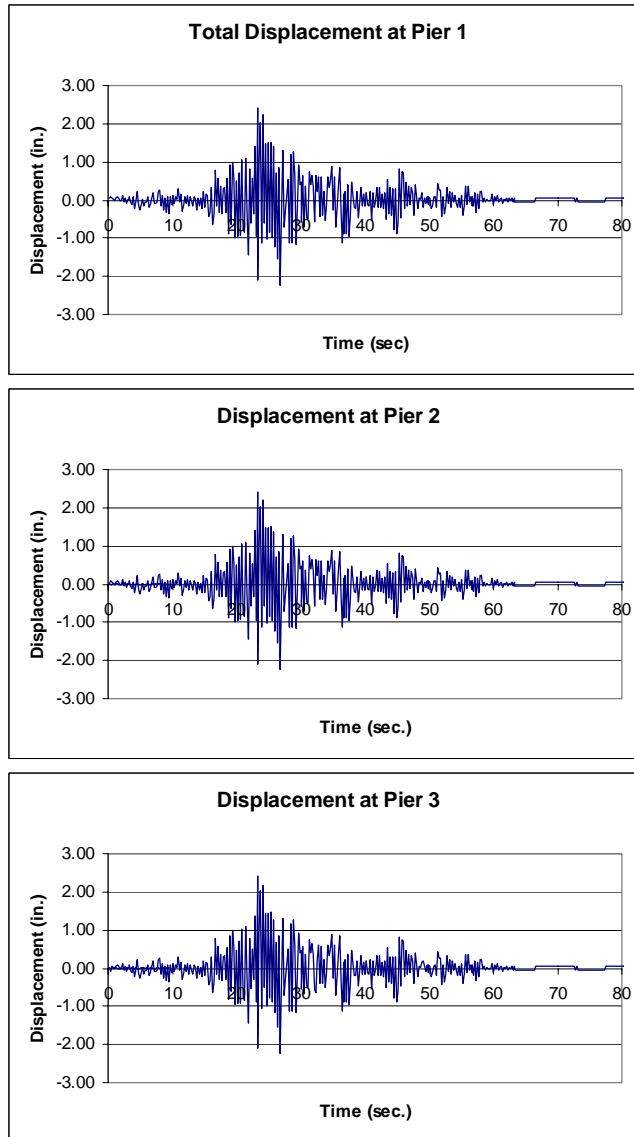


Figure C.13-1 Total Displacement at Piers

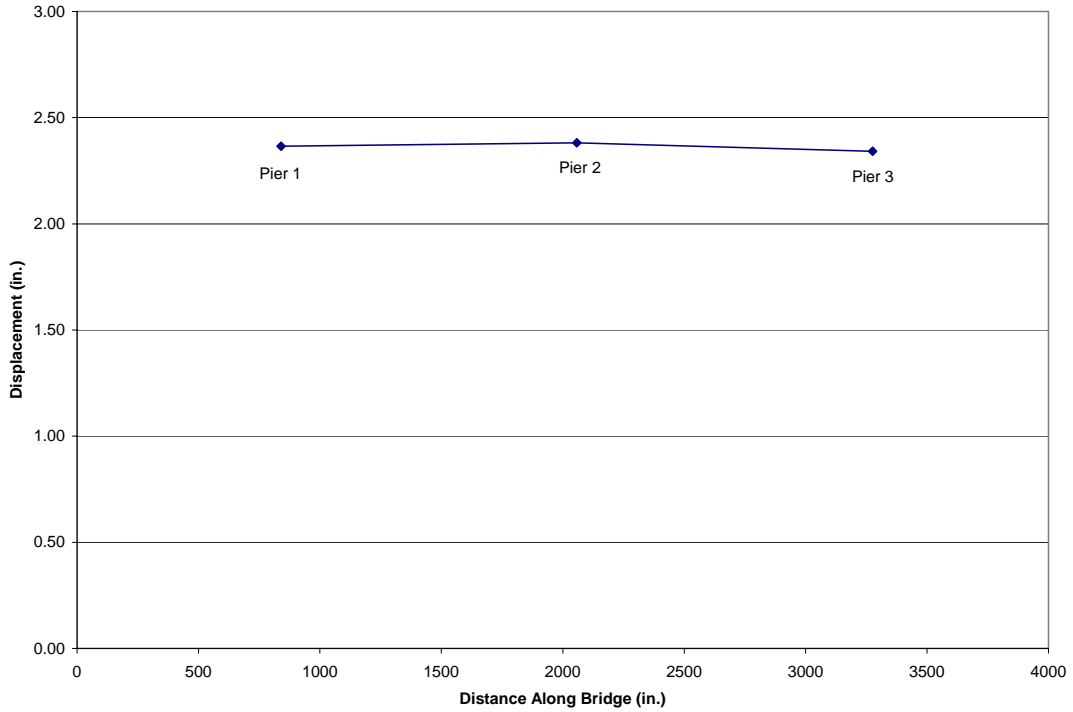


Figure C.13-2 Transverse Displacement Envelope of the Bridge Deck

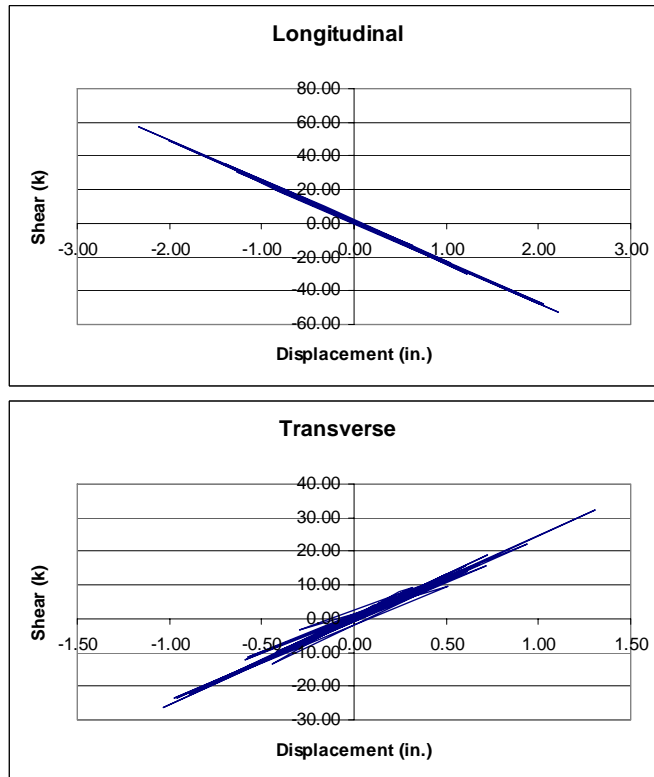


Figure C.13-3 Hysteresis Plots for the Center Column of Pier 2

Table C.13-1 Maximum Moment (kip-in) at the Top and Bottoms of Columns

Pier No.	Column	Moment	
		Top	Bottom
1	1	11589.3	9789.0
	2	11542.8	9770.0
	3	11459.8	9731.1
2	1	9369.3	8358.8
	2	9307.6	8332.8
	3	9229.8	8296.9
3	1	1047.1	8969.5
	2	10467.6	8977.8
	3	10422.7	8972.5

Table C.13-2 Maximum Shear (kips) in the Columns

Pier No.	Column	Shear			
		Top	Demand/ Capacity	Bottom	Demand/ Capacity
1	1	74.17	0.43	80.65	0.47
	2	74.04	0.43	80.41	0.47
	3	73.55	0.43	79.97	0.47
2	1	52.41	0.31	59.67	0.35
	2	52.08	0.31	59.38	0.35
	3	51.74	0.31	58.99	0.35
3	1	63.98	0.37	70.57	0.41
	2	63.88	0.37	70.56	0.41
	3	63.60	0.37	70.42	0.41

Table C.13-3 Maximum Shear (kips) at the Abutments

Abutment	Shear			
	Longitudinal	Demand/ Capacity	Transverse	Demand/ Capacity
West	748	0.14	1400	0.26
East	952	0.18	1290	0.24

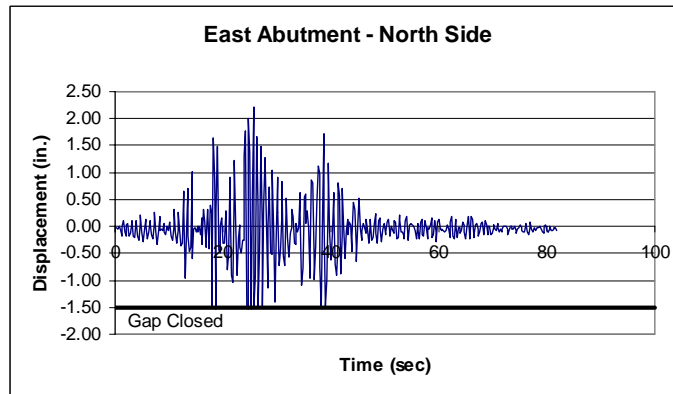
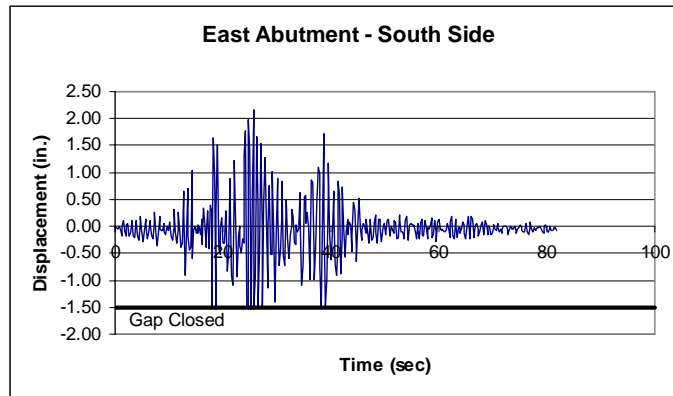
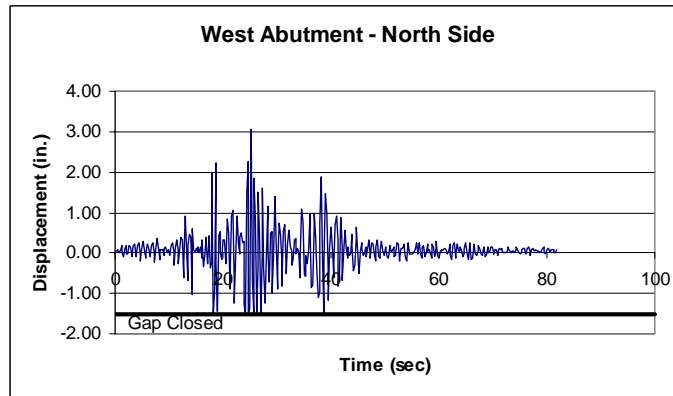
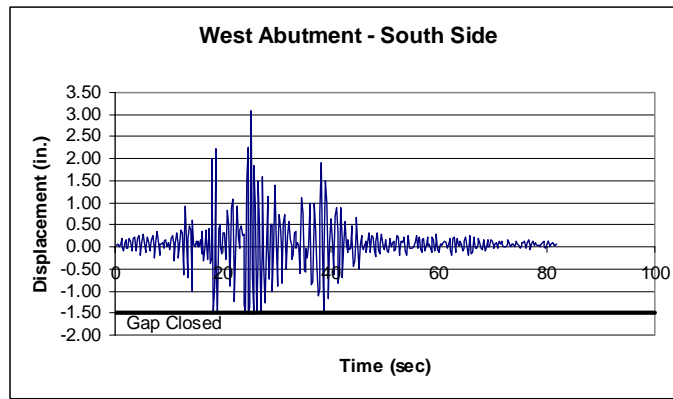


Figure C.13-4 Longitudinal Displacement of Expansion Joints

C.14 Bridge 5/826; Olympia 475-Year Earthquake

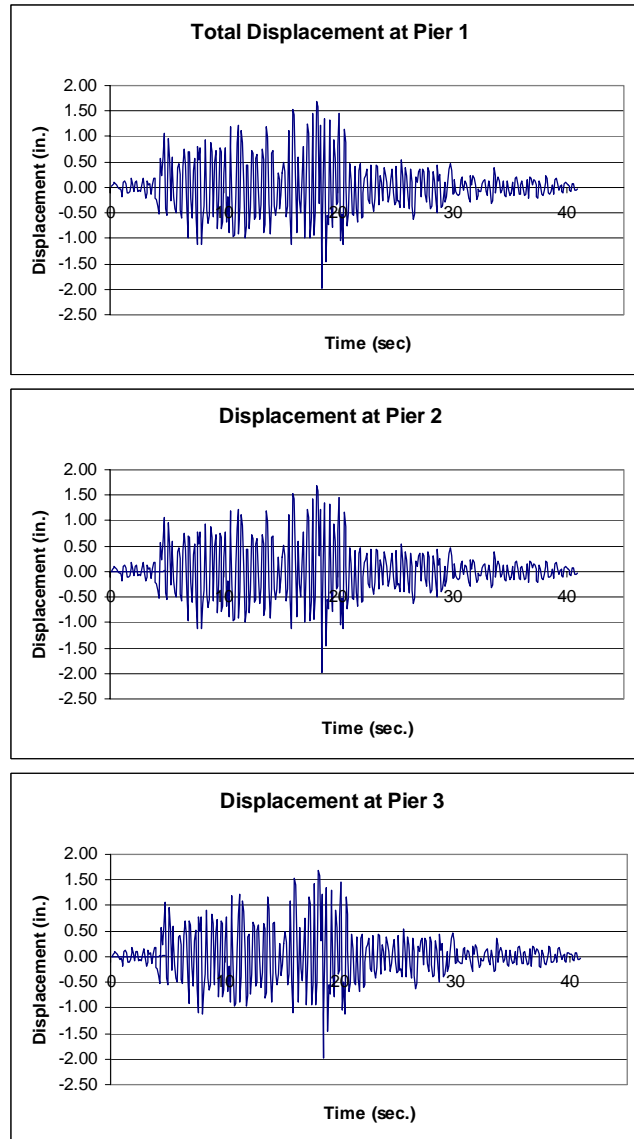


Figure C.14-1 Total Displacement at Piers

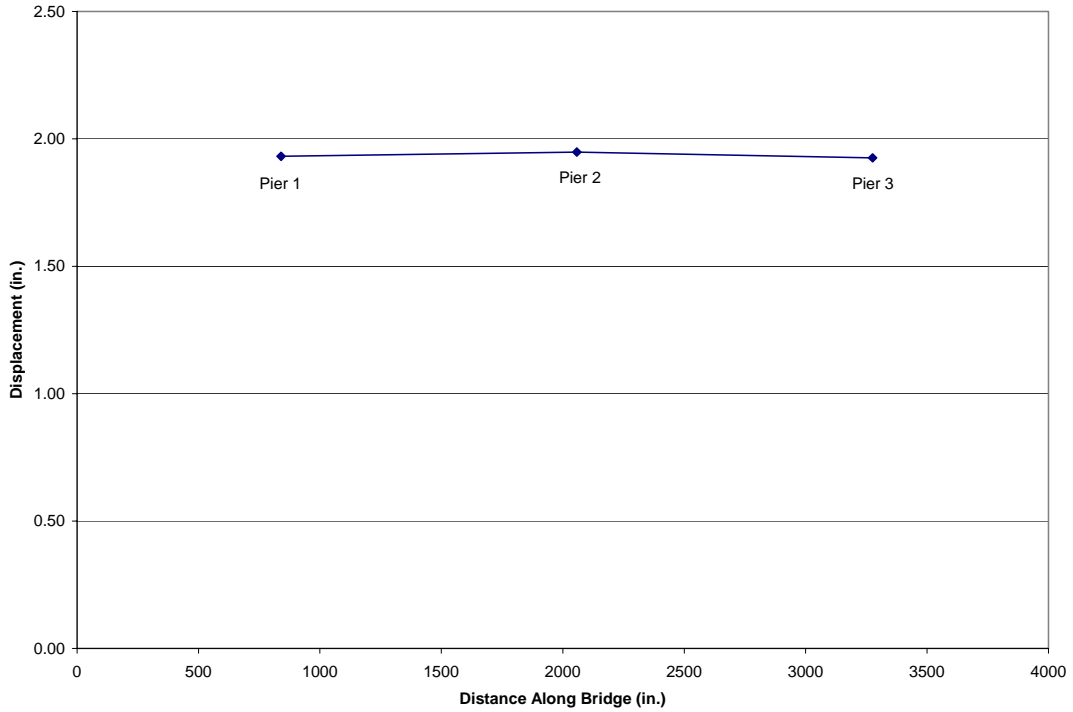


Figure C.14-2 Transverse Displacement Envelope of Bridge Deck

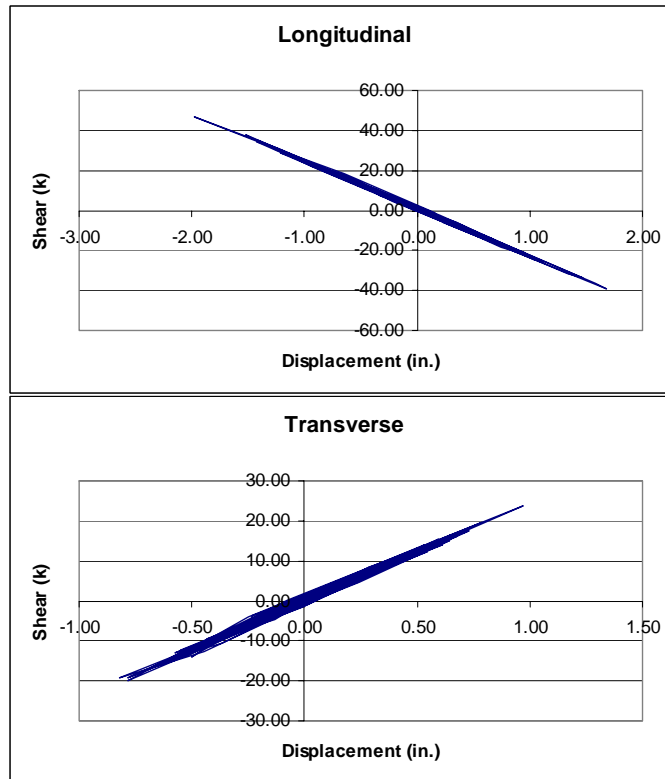


Figure C.14-3 Hysteresis Plots for the Center Column of Pier 2

Table C.14-1 Maximum Moment (kip-in) at the Top and Bottoms of Columns

Pier No.	Column	Moment	
		Top	Bottom
1	1	9608.9	8021.6
	2	9585.9	8015.2
	3	9517.3	7984.8
2	1	7792.6	6820.7
	2	7748.8	6799.6
	3	7678.0	6763.8
3	1	8772.1	7407.9
	2	8748.0	7397.5
	3	8694.3	7369.1

Table C.14-2 Maximum Shear (kips) in the Columns

Pier No.	Column	Shear			
		Top	Demand/ Capacity	Bottom	Demand/ Capacity
1	1	62.57	0.36	64.91	0.38
	2	62.36	0.36	64.79	0.38
	3	61.94	0.36	64.45	0.38
2	1	44.61	0.26	47.24	0.28
	2	44.36	0.26	47.03	0.28
	3	44.03	0.26	46.69	0.28
3	1	54.43	0.32	56.96	0.33
	2	54.29	0.32	56.86	0.33
	3	54.07	0.32	56.56	0.33

Table C.14-3 Maximum Shear (kips) at the Abutments

Abutment	Shear			
	Longitudina I	Demand/ Capacity	Transverse	Demand/ Capacity
West	365	0.07	1030	0.19
East	542	0.10	974	0.18

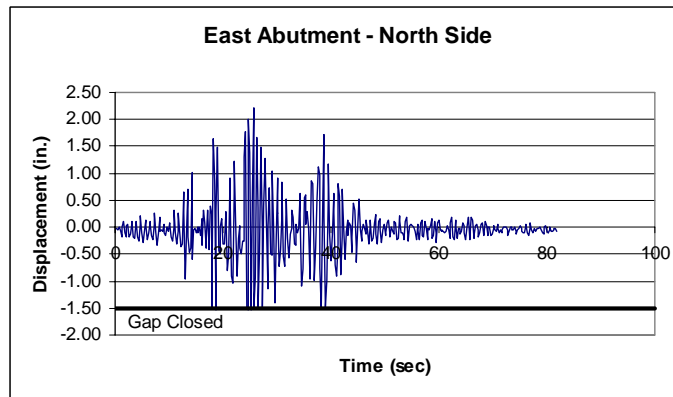
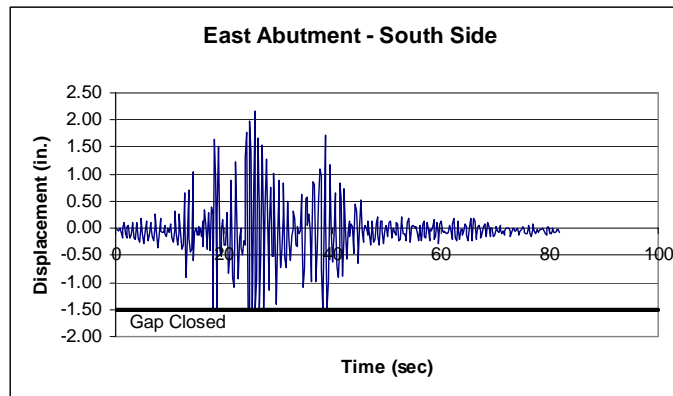
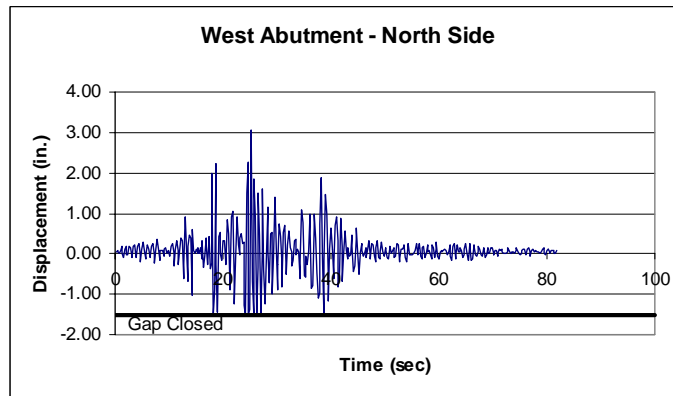
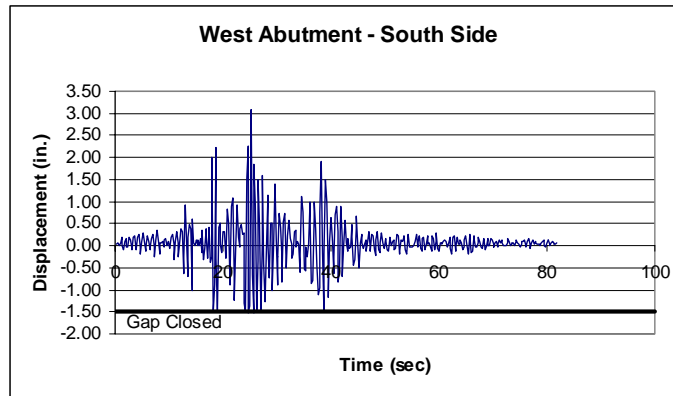


Figure C.14-4 Longitudinal Displacement of Expansion Joints

C.15 Bridge 5/826; Olympia 950-Year Earthquake

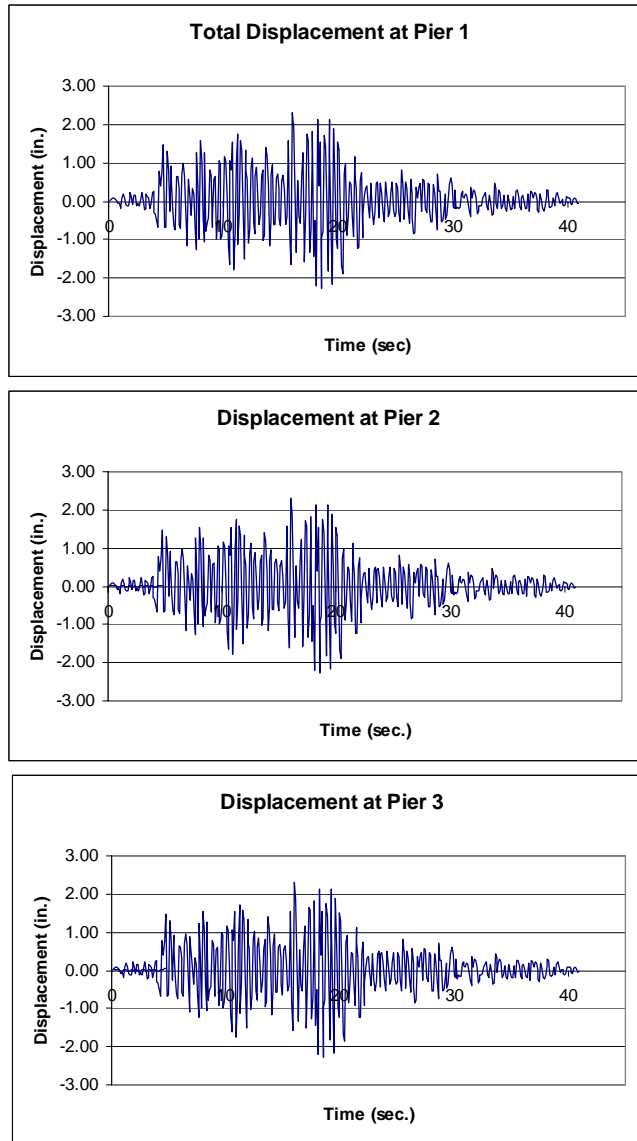


Figure C.15-1 Total Displacement at Piers

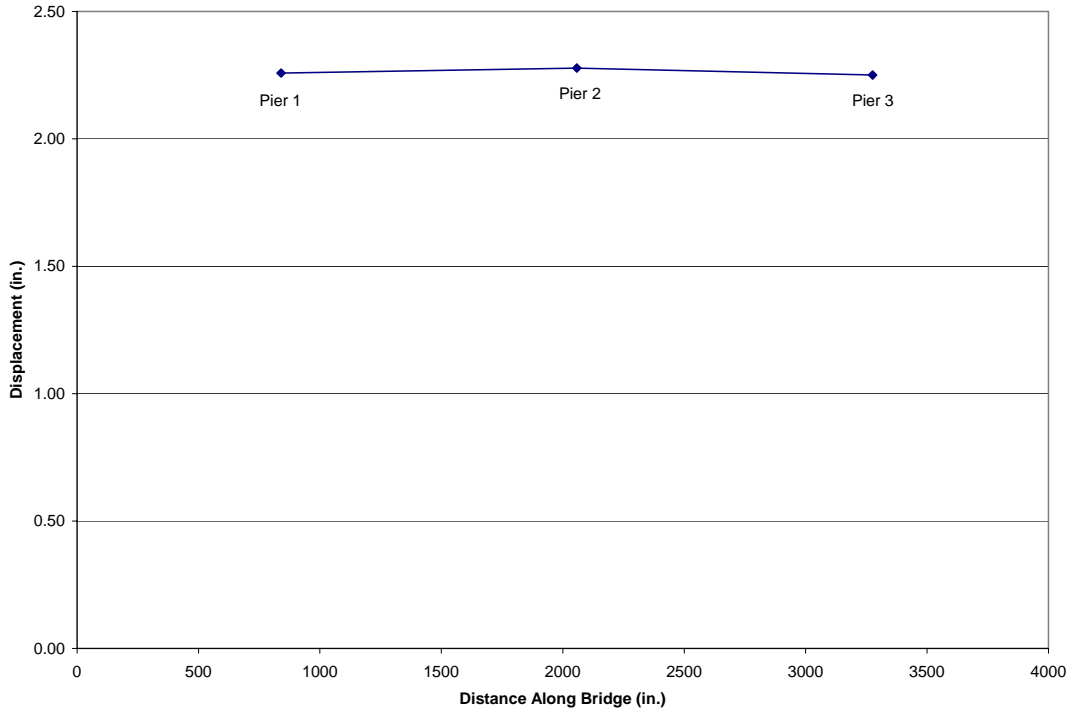


Figure C.15-2 Transverse Displacement Envelope of Bridge Deck

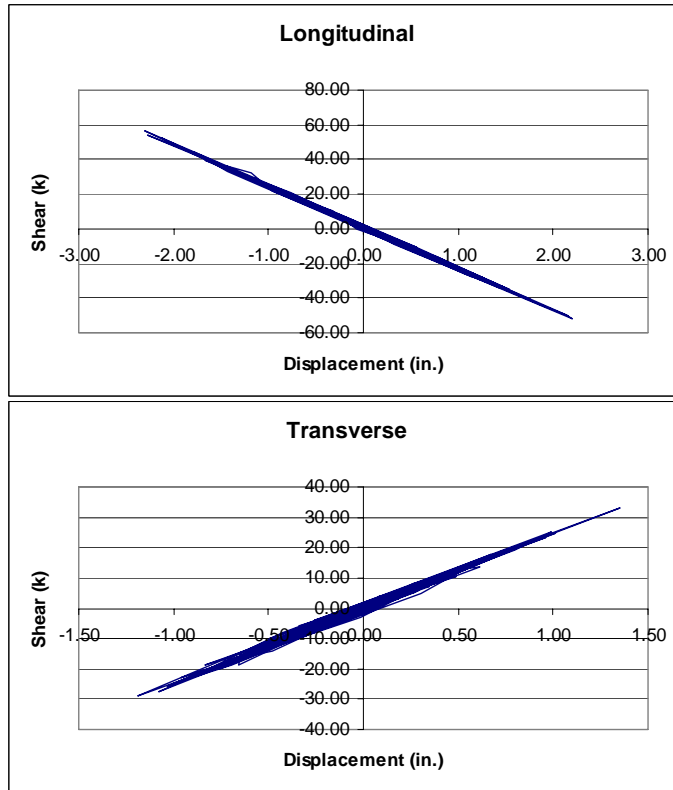


Figure C.15-3 Hysteresis Plots for the Center Column of Pier 2

Table C.15-1 Maximum Moment (kip-in) at the Top and Bottoms of Columns

Pier No.	Column	Moment	
		Top	Bottom
1	1	11142.0	9396.5
	2	11119.2	9384.5
	3	11045.8	9346.9
2	1	9022.9	8005.4
	2	8976.9	7983.5
	3	8906.4	7943.8
3	1	10167.1	8669.7
	2	10143.9	8665.8
	3	10100.8	8641.3

Table C.15-2 Maximum Shear (kips) in the Columns

Pier No.	Column	Shear			
		Top	Demand/ Capacity	Bottom	Demand/ Capacity
1	1	71.73	0.42	77.01	0.45
	2	71.64	0.42	76.86	0.45
	3	71.23	0.42	76.46	0.45
2	1	50.74	0.30	56.70	0.33
	2	50.56	0.30	56.47	0.33
	3	50.37	0.30	56.07	0.33
3	1	62.32	0.36	67.76	0.39
	2	62.21	0.36	67.69	0.39
	3	62.14	0.36	67.42	0.39

Table C.15-3 Maximum Shear (kips) at the Abutments

Abutment	Shear			
	Longitudina I	Demand/ Capacity	Transverse	Demand/ Capacity
West	701	0.14	1450	0.27
East	871	0.17	1340	0.25

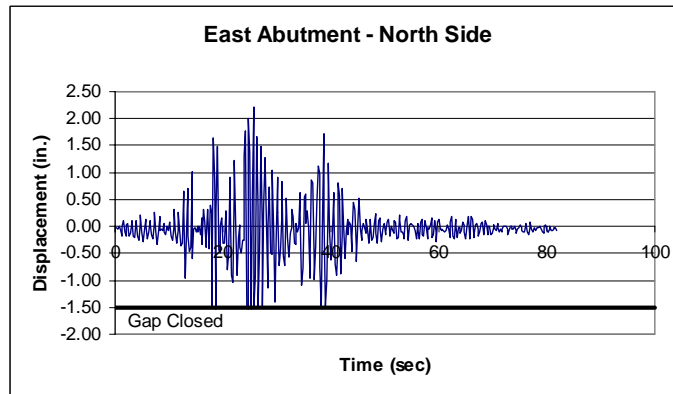
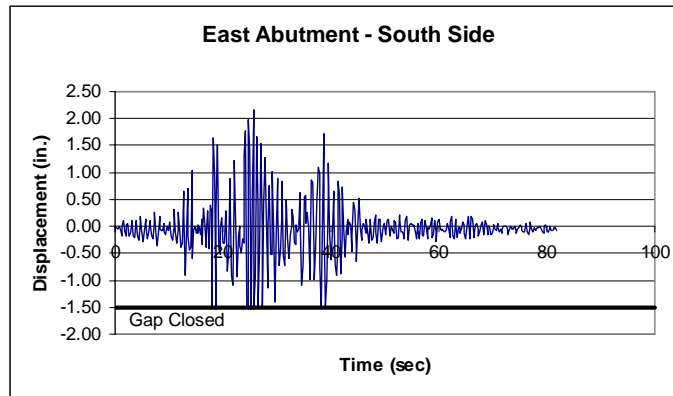
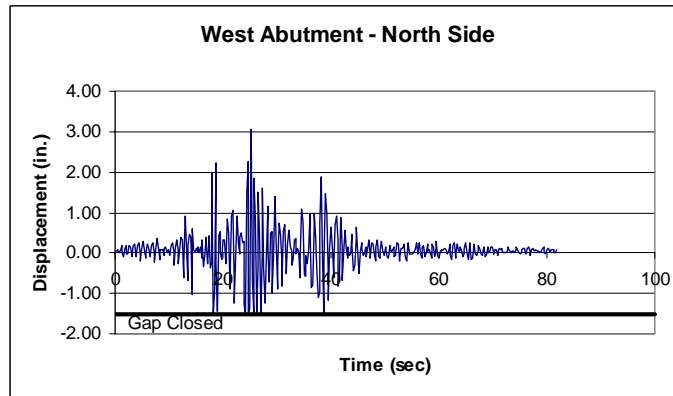
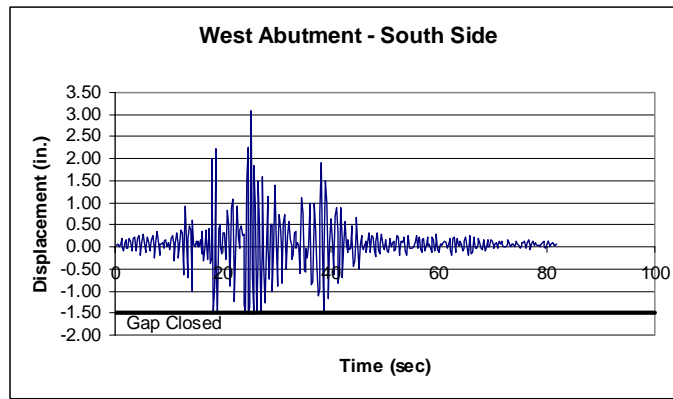


Figure C.15-4 Longitudinal Displacement of Expansion Joints

C.16 Bridge 5/826; Kobe 475-Year Earthquake

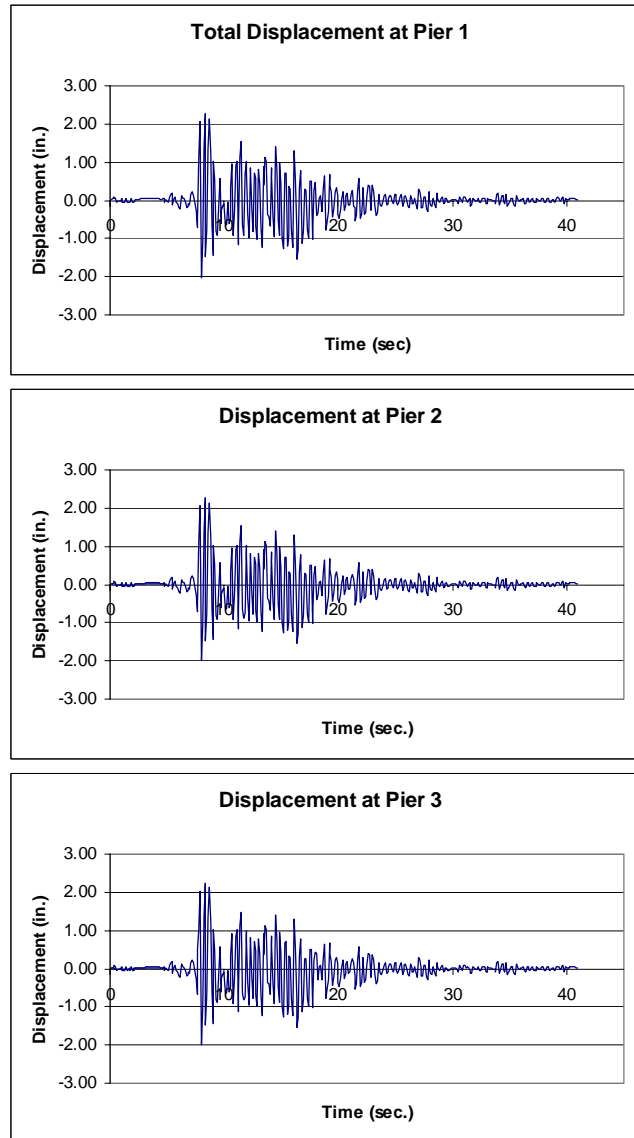


Figure C.16-1 Total Displacement at Piers

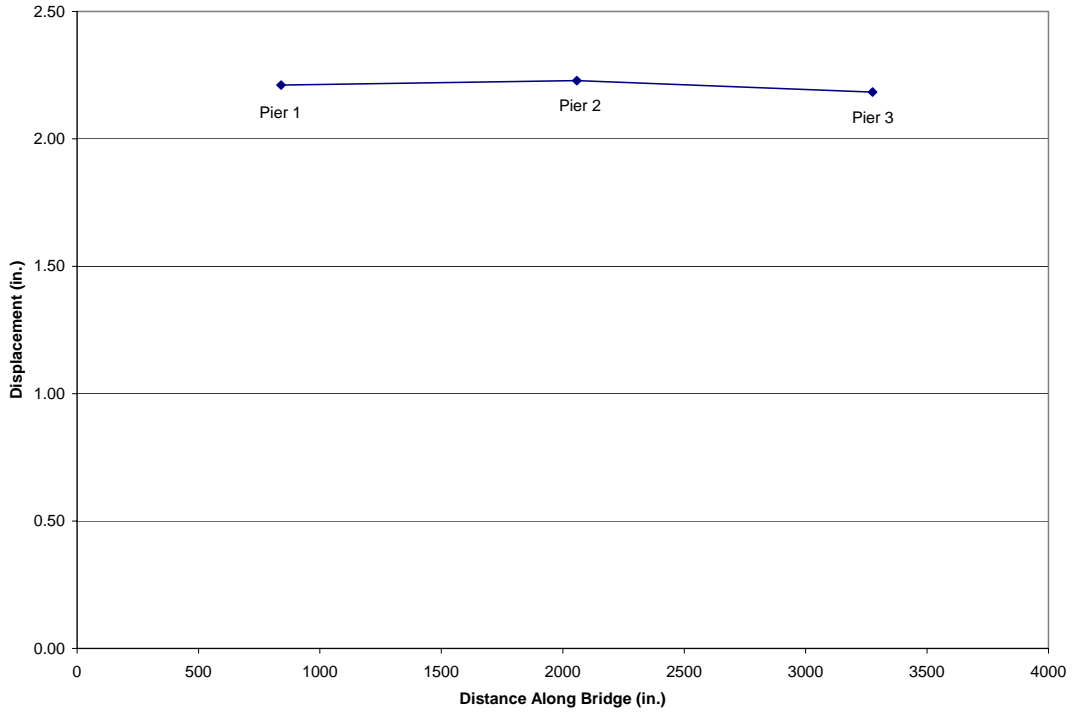


Figure C.16-2 Transverse Displacement Envelope of Bridge Deck

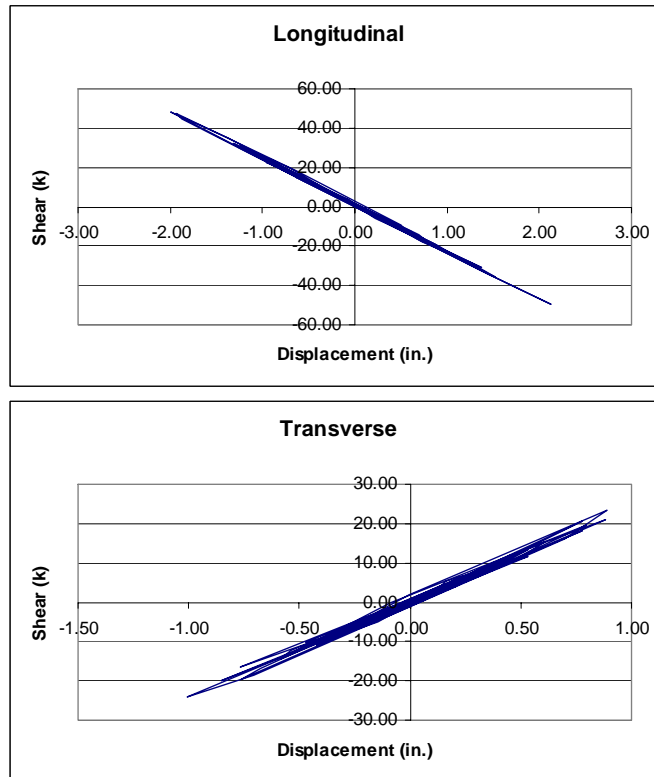


Figure C.16-3 Hysteresis Plots for the Center Column of Pier 2

Table C.16-1 Maximum Moment (kip-in) at the Top and Bottoms of Columns

Pier No.	Column	Moment	
		Top	Bottom
1	1	10307.3	8776.4
	2	10342.1	8794.6
	3	10335.3	8789.2
2	1	8399.8	7546.6
	2	8417.7	7544.7
	3	8398.1	7526.2
3	1	9497.6	8145.1
	2	9487.1	8114.7
	3	9424.9	8062.2

Table C.16-2 Maximum Shear (kips) in the Columns

Pier No.	Column	Shear			
		Top	Demand/ Capacity	Bottom	Demand/ Capacity
1	1	66.26	0.39	71.47	0.42
	2	66.39	0.39	71.69	0.42
	3	66.39	0.39	71.65	0.42
2	1	47.02	0.27	52.98	0.31
	2	47.07	0.27	53.03	0.31
	3	46.89	0.27	52.90	0.31
3	1	57.94	0.34	63.41	0.37
	2	57.91	0.34	63.23	0.37
	3	57.51	0.34	62.82	0.37

Table C.16-3 Maximum Shear (kips) at the Abutments

Abutment	Shear			
	Longitudina I	Demand/ Capacity	Transverse	Demand/ Capacity
West	648	0.13	1060	0.19
East	566	0.11	1010	0.19

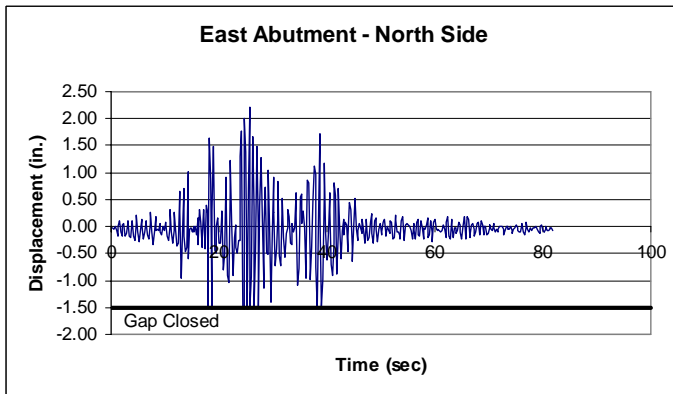
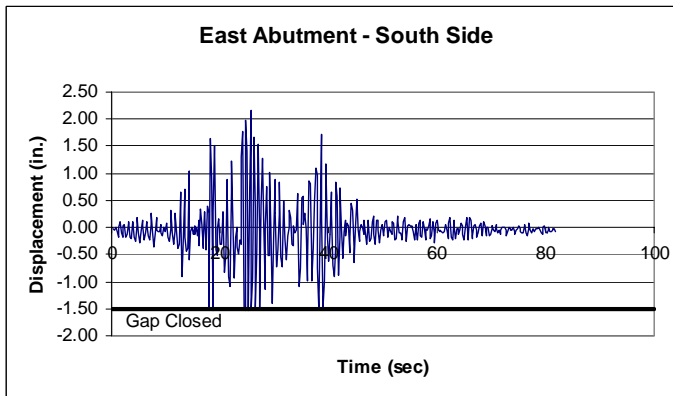
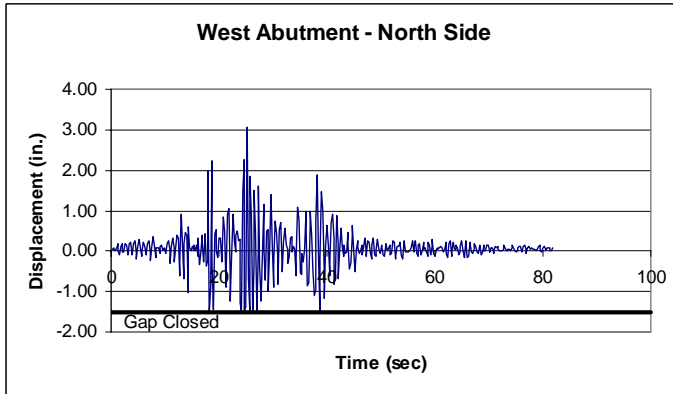
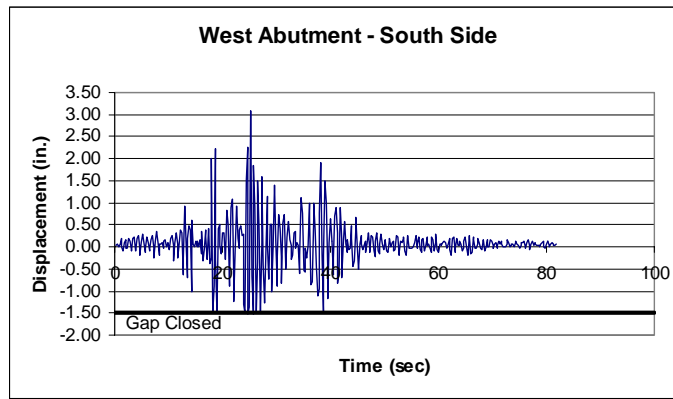


Figure C.16-4 Longitudinal Displacement of Expansion Joints

C.17 Bridge 5/826; Kobe 950-Year Earthquake

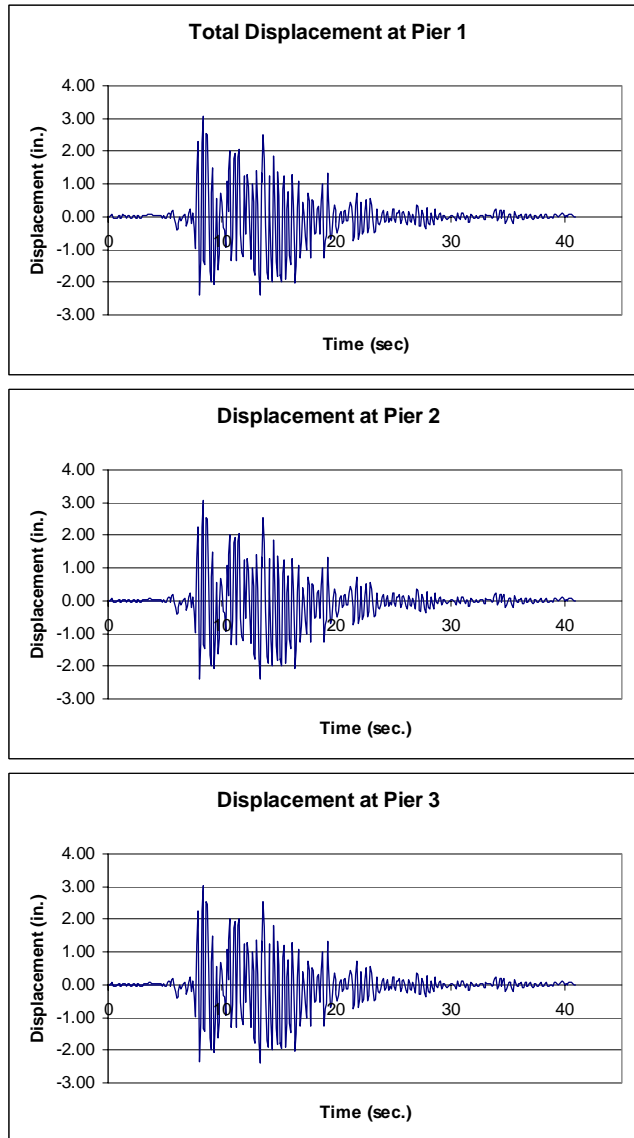


Figure C.17-1 Total Displacement at Piers

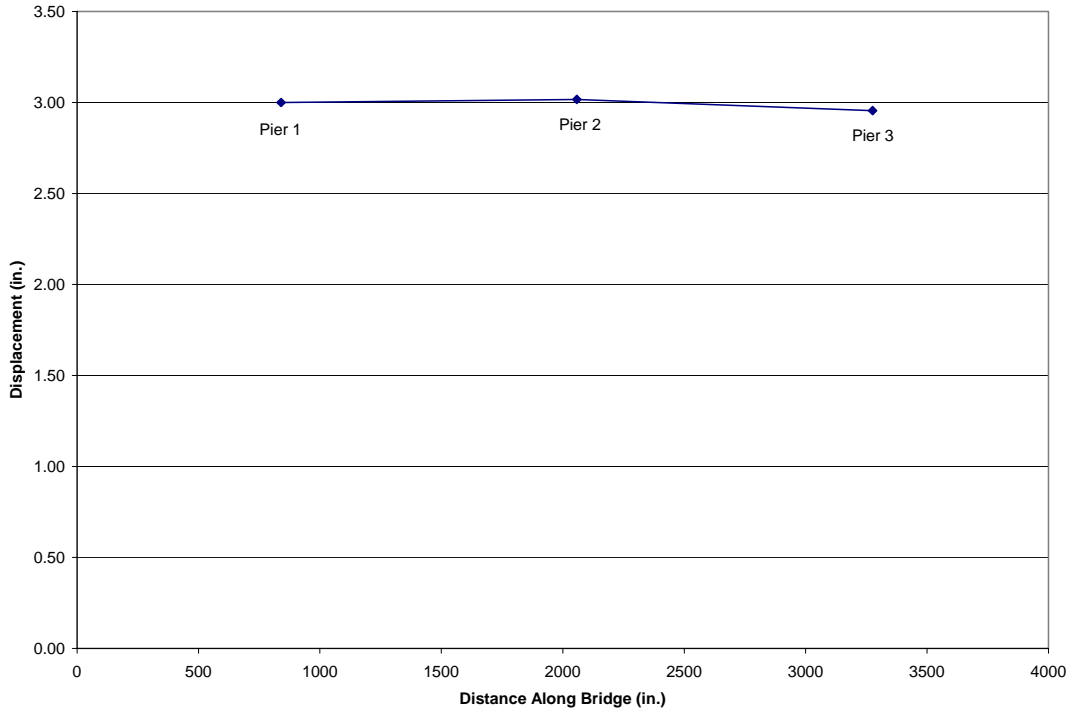


Figure C.17-2 Transverse Displacement Envelope of Bridge Deck

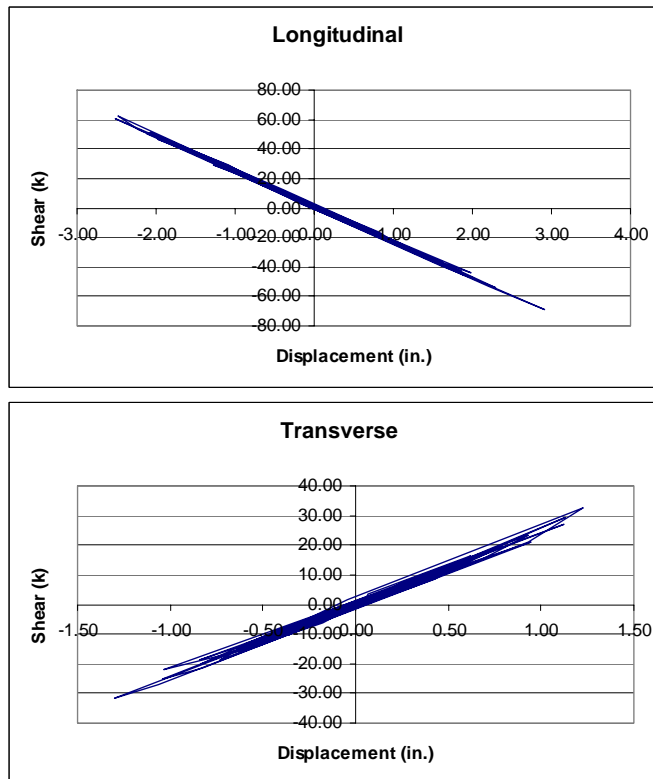


Figure C.17-3 Hysteresis Plots for the Center Column of Pier 2

Table C.17-1 Maximum Moment (kip-in) at the Top and Bottoms of Columns

Pier No.	Column	Moment	
		Top	Bottom
1	1	14042.6	11980.5
	2	14075.8	11990.5
	3	14037.9	11973.4
2	1	11392.0	10264.3
	2	11407.2	10250.3
	3	11375.6	10213.6
3	1	12887.1	11085.0
	2	12858.0	11026.3
	3	12778.7	10951.4

Table C.17-2 Maximum Shear (kips) in the Columns

Pier No.	Column	Shear			
		Top	Demand/ Capacity	Bottom	Demand/ Capacity
1	1	89.41	0.52	97.59	0.57
	2	89.55	0.52	97.75	0.57
	3	89.18	0.52	97.57	0.57
2	1	62.58	0.36	71.96	0.42
	2	62.73	0.36	71.94	0.42
	3	62.66	0.36	71.70	0.42
3	1	77.81	0.45	86.26	0.50
	2	77.73	0.45	85.89	0.50
	3	77.46	0.45	85.24	0.50

Table C.17-3 Maximum Shear (kips) at the Abutments

Abutment	Shear			
	Longitudina I	Demand/ Capacity	Transverse	Demand/ Capacity
West	1440	0.28	1420	0.26
East	1140	0.22	1260	0.23

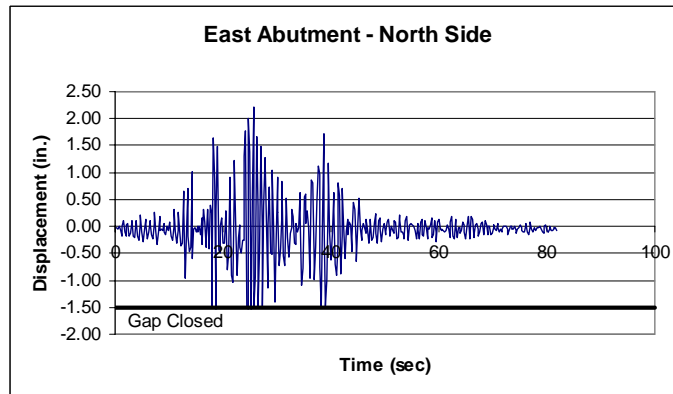
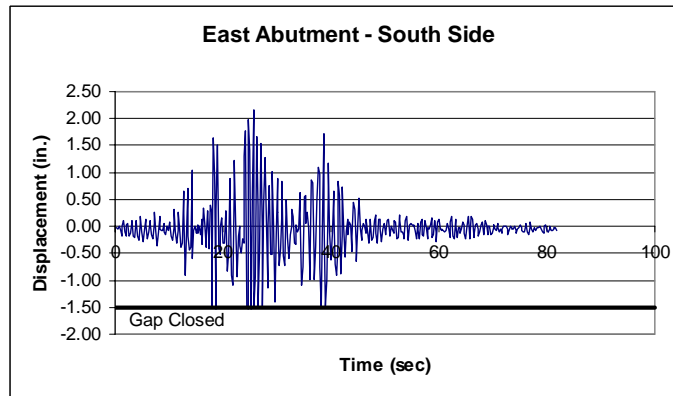
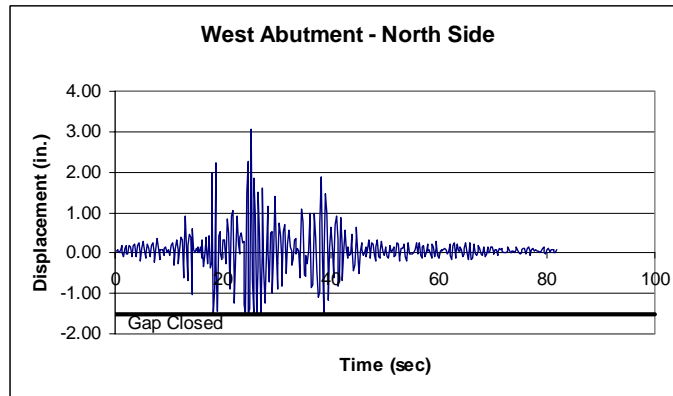
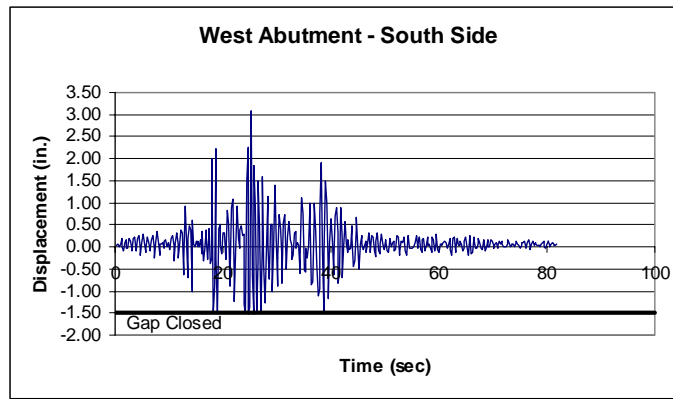


Figure C.17-4 Longitudinal Displacement of Expansion Joints

Appendix D

Additional Output from Soil-Structure Study

D.1 Introduction

This appendix presents the additional plots and tables for the analysis results from Chapter 6. The plots and tables are from the analyses of Bridges 5/518 and 5/826 using the study protocol as defined in the chapter.

D.2 Run No. 1

The additional plots for the response of Bridge 5/518, with fixed columns and rollers at the abutments in both directions, to the modified Peru earthquake are presented here.

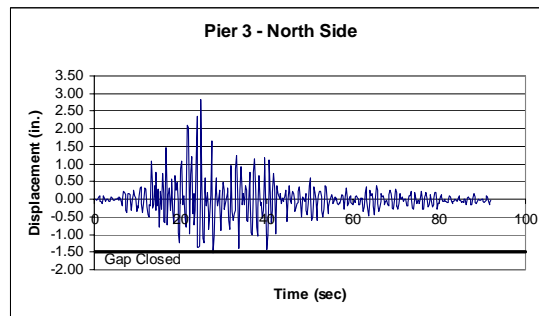
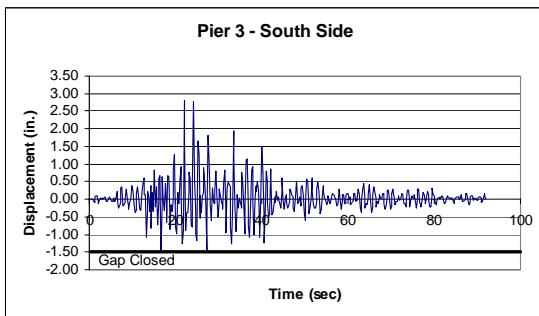
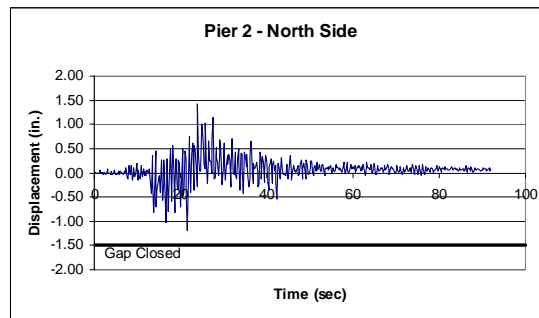
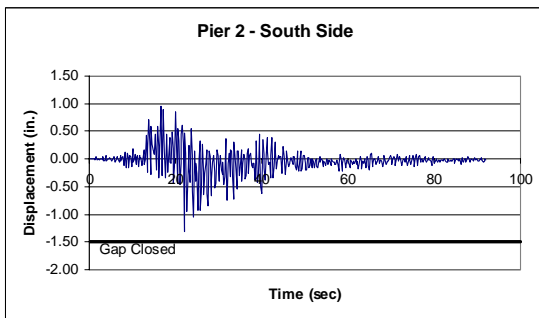
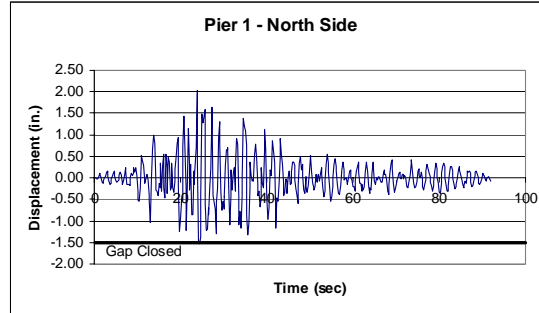
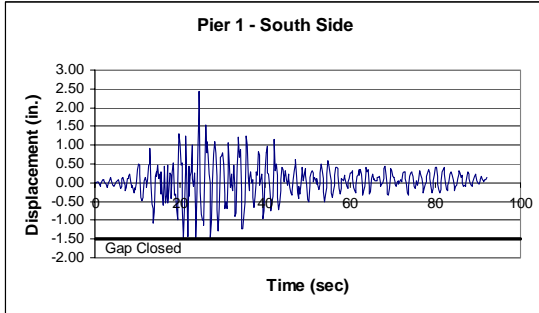


Figure D.2-1 Longitudinal Displacement of Expansion Joints

D.3 Run No. 2

The plots and tables for the response of Bridge 5/518, with fixed columns and rollers at the abutments in the longitudinal direction only, to the modified Peru earthquake are presented here.

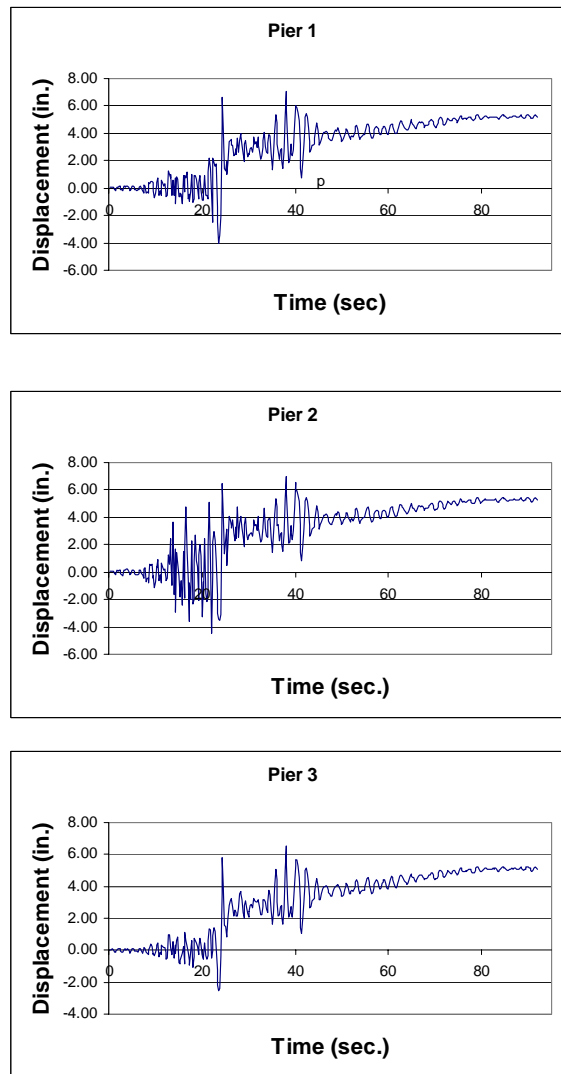


Figure D.3-1 Total Relative Displacement at Piers

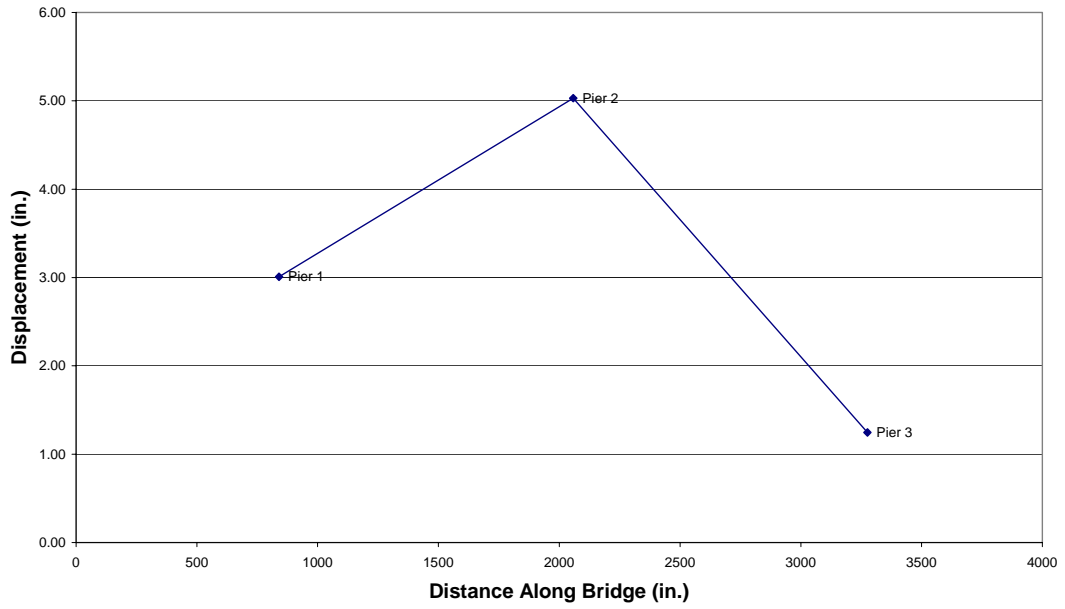


Figure D.3-2 Transverse Displacement Envelope of Bridge Deck

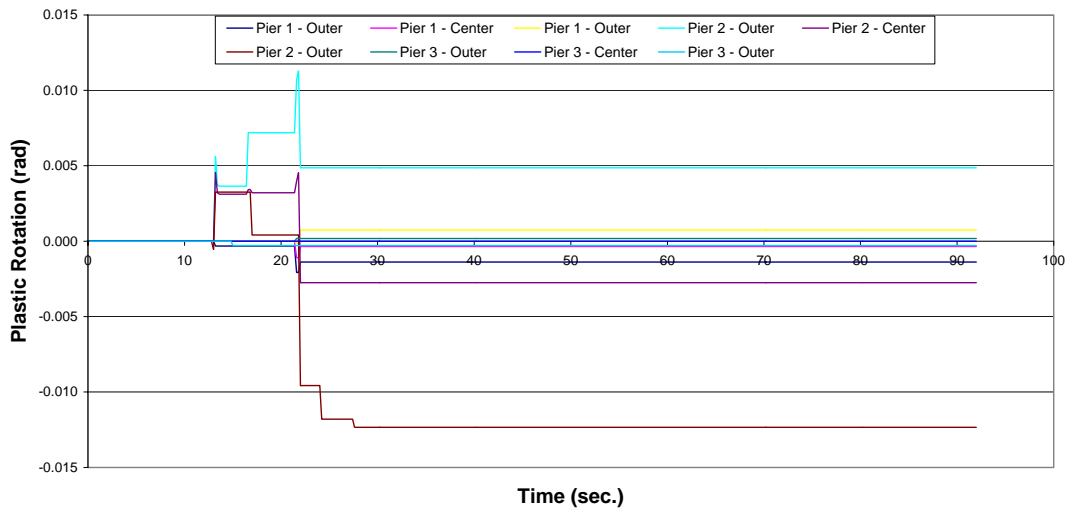


Figure D.3-3 Plastic Rotations at the Top of the Columns

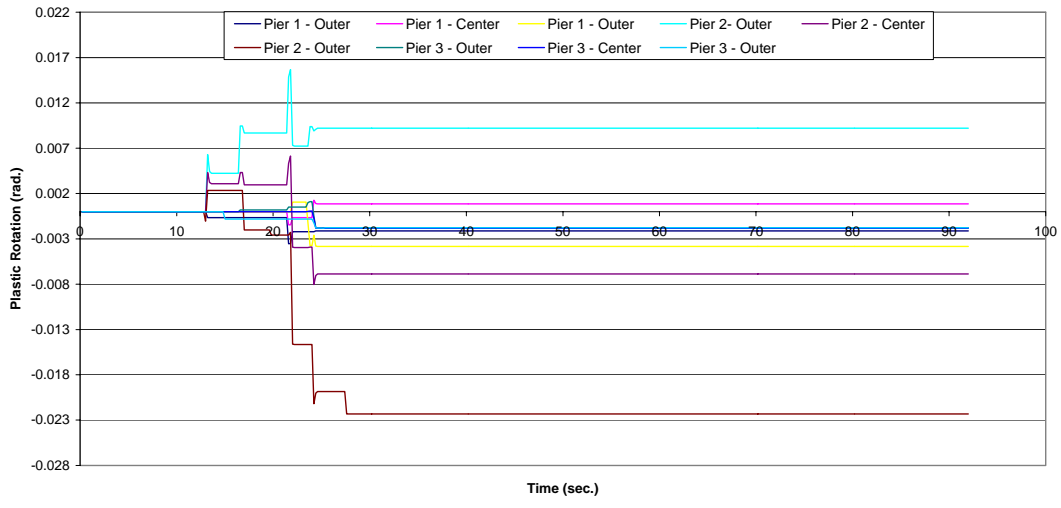


Figure D.3-4 Plastic Rotations at the Bottom of the Columns

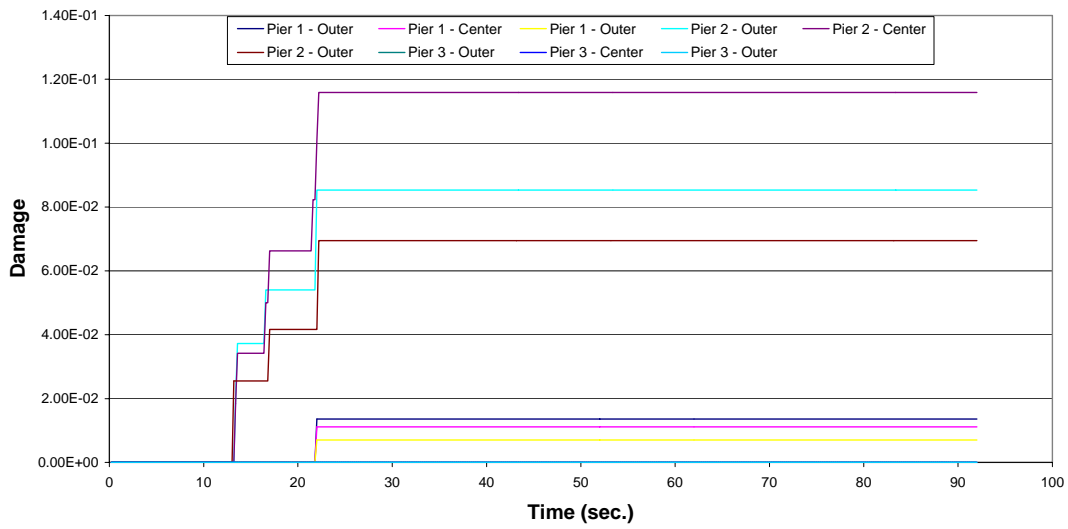


Figure D.3-5 Damage at Top of Columns

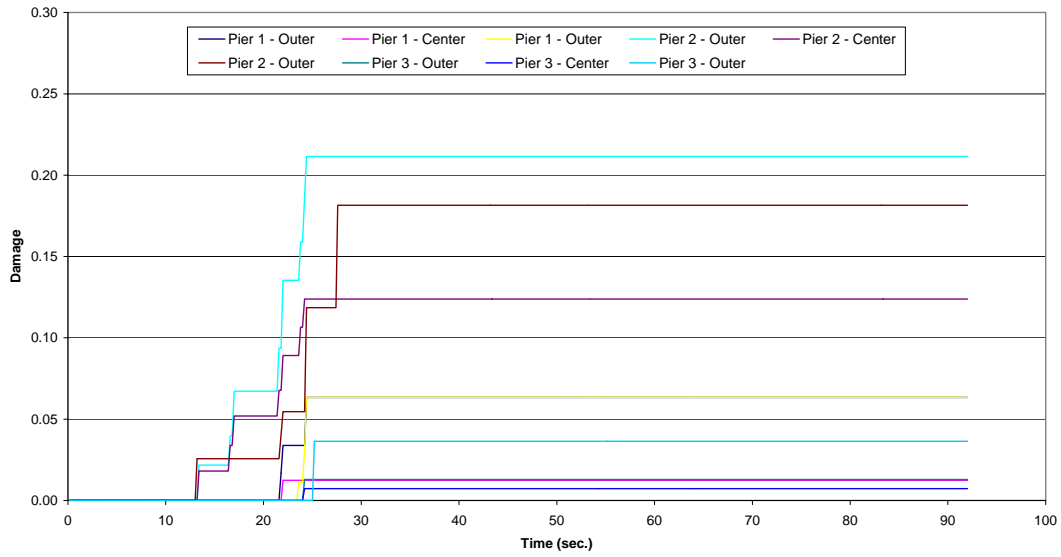


Figure D.3-6 Damage at Bottom of Columns

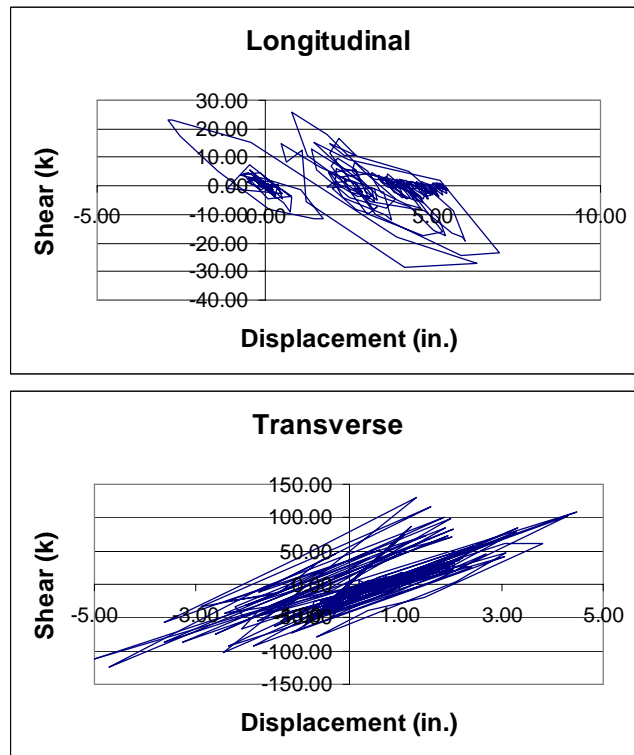


Figure D.3-7 Hysteresis Plots for the Center Column of Pier 2

Table D.3-1 Maximum Moment (kip-in) at the Top and Bottoms of Columns

Pier No.	Column	Moment	
		Top	Bottom
1	1	16863.4	15141.5
	2	14210.9	12833.6
	3	15898.9	13902.0
2	1	17331.3	15428.1
	2	15571.6	13631.0
	3	16042.1	15174.5
3	1	13502.4	12802.9
	2	12900.0	12601.9
	3	12768.4	12560.4

Table D.3-2 Maximum Shear (kips) in the Columns

Pier No.	Column	Shear			
		Top	Demand/ Capacity	Bottom	Demand/ Capacity
1	1	150.07	0.87	146.15	0.85
	2	123.91	0.72	127.61	0.74
	3	137.33	0.80	139.15	0.81
2	1	142.14	0.83	145.12	0.85
	2	124.80	0.73	129.90	0.76
	3	140.22	0.82	142.04	0.83
3	1	133.32	0.78	140.42	0.82
	2	126.00	0.74	133.10	0.78
	3	131.54	0.77	135.40	0.79

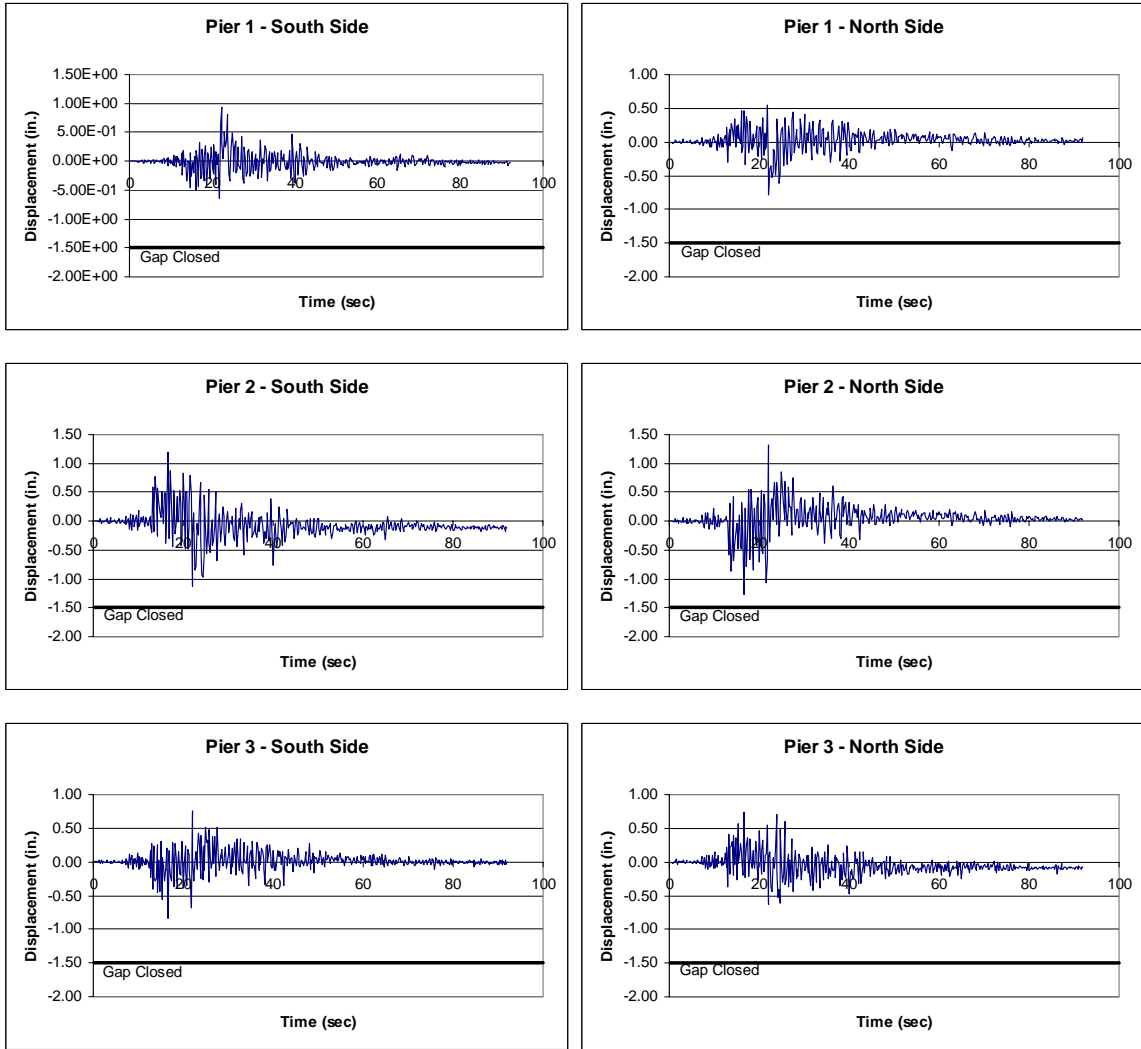


Figure D.3-8 Longitudinal Displacement of Expansion Joints

D.4 Run No. 3

The plots and tables for the response of Bridge 5/518, with the soil spring stiffness of the columns left unchanged and the soil spring stiffness of the abutments increased by a factor of ten, to the modified Peru earthquake are presented here.

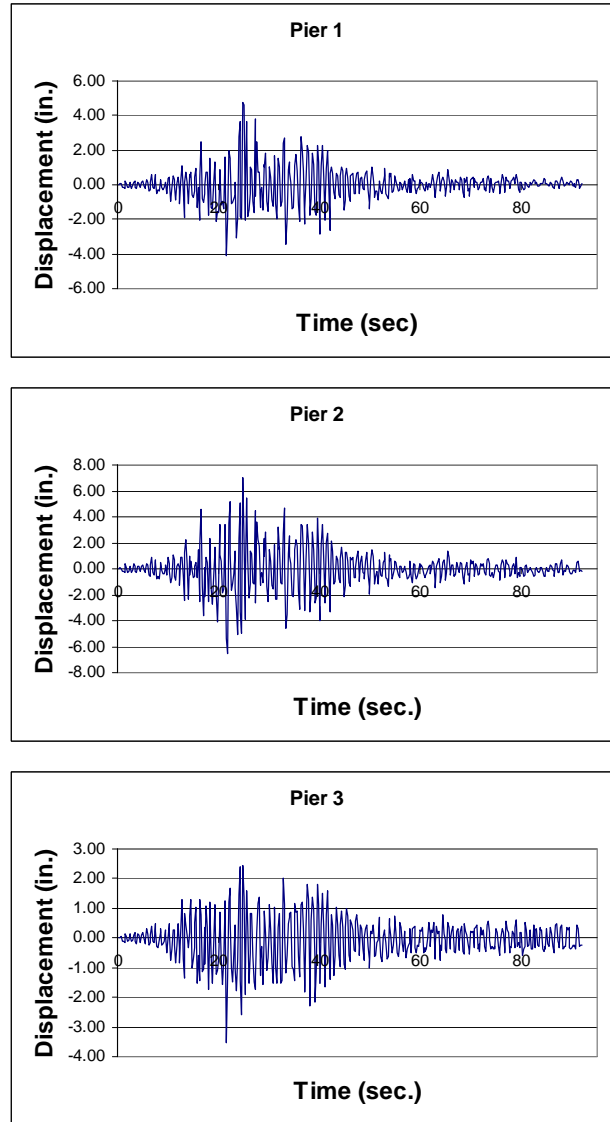


Figure D.4-1 Total Relative Displacement at Piers

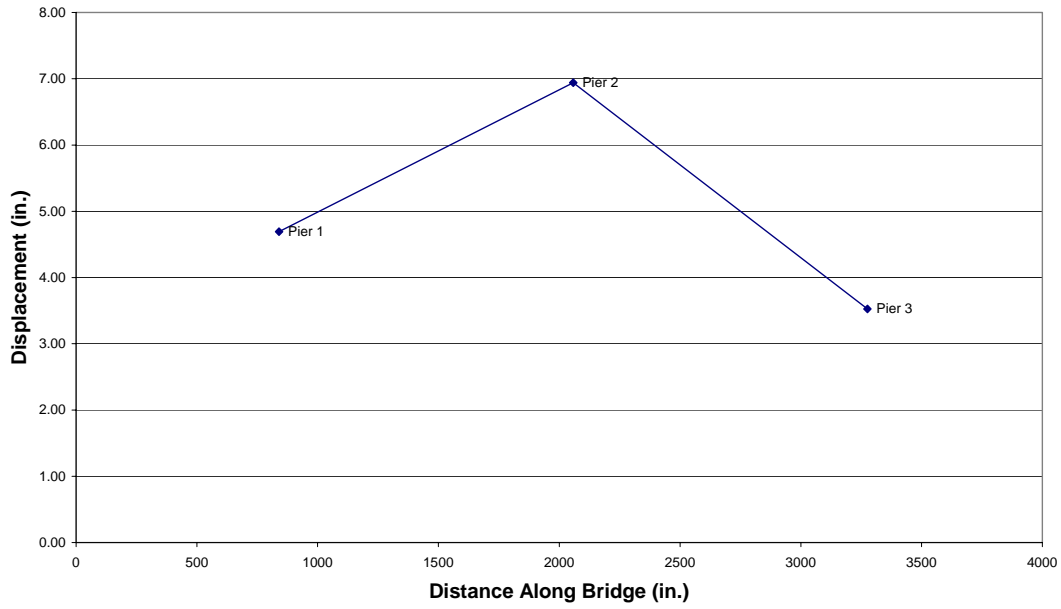


Figure D.4-2 Transverse Displacement Envelope of Bridge Deck

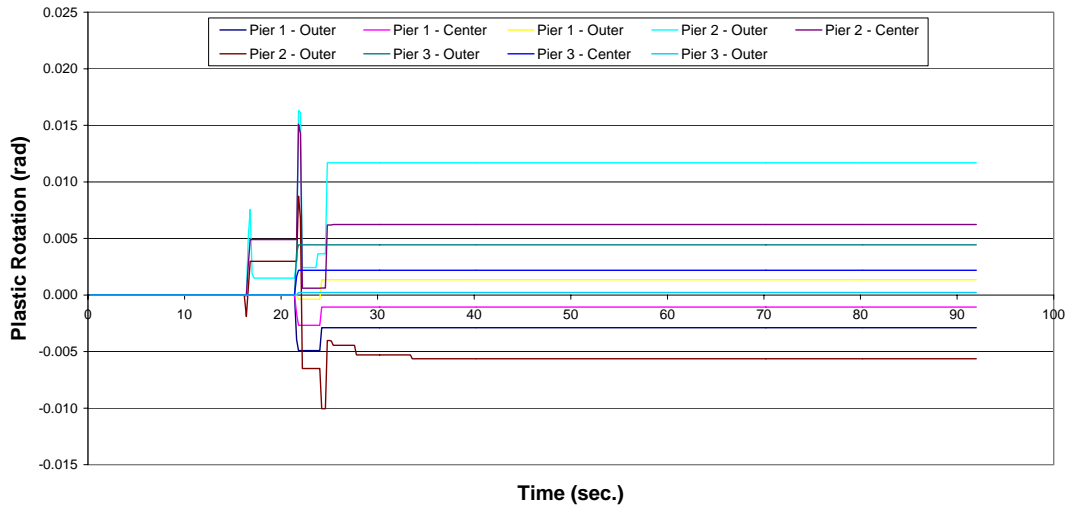


Figure D.4-3 Plastic Rotations at Top of Columns

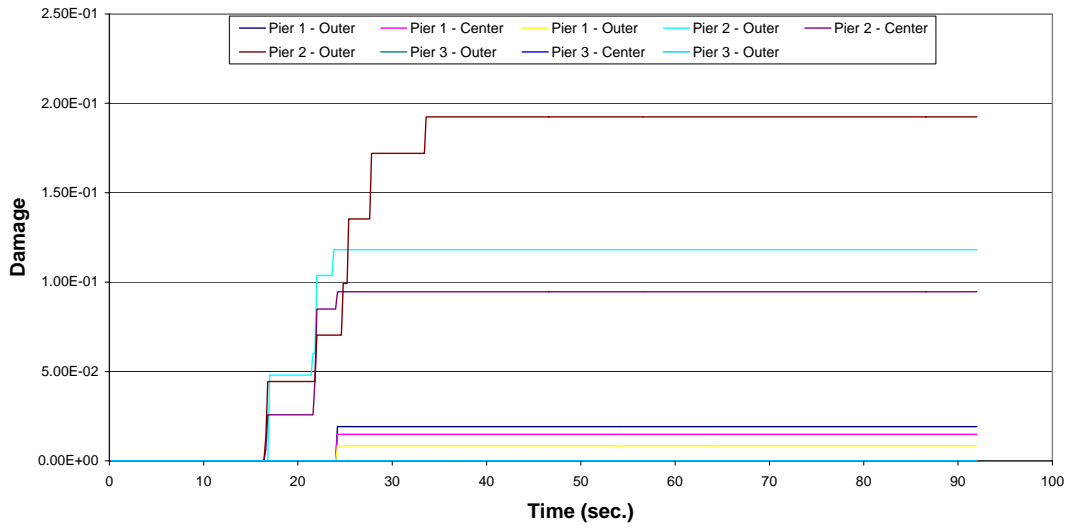


Figure D.4-4 Damage at Top of Columns

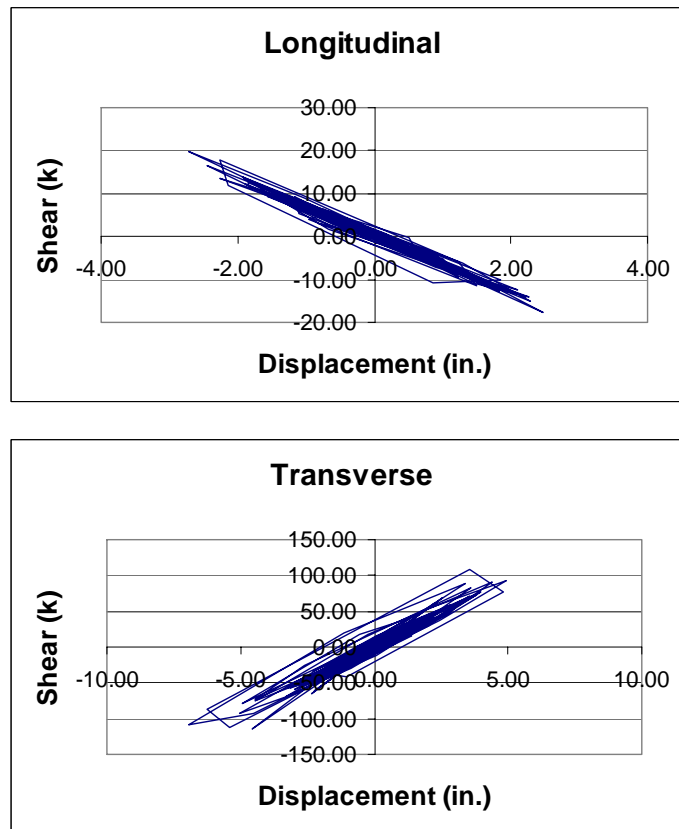


Figure D.4-5 Hysteresis Plots for the Center Column of Pier 2

Table D.4-1 Maximum Moment (kip-in) at the Top and Bottoms of Columns

Pier No.	Column	Moment	
		Top	Bottom
1	1	16042.4	5696.6
	2	15260.2	5593.5
	3	16910.9	5508.9
2	1	16112.2	9330.2
	2	15971.5	10043.9
	3	18191.3	10083.9
3	1	16154.7	4329.3
	2	14891.2	4048.3
	3	17124.7	3829.4

Table D.4-2 Maximum Shear (kips) in the Columns

Pier No.	Column	Shear			
		Top	Demand/ Capacity	Bottom	Demand/ Capacity
1	1	91.42	0.54	94.81	0.56
	2	90.54	0.53	95.95	0.56
	3	99.57	0.58	103.39	0.61
2	1	103.45	0.60	118.63	0.69
	2	110.22	0.64	113.83	0.66
	3	119.07	0.69	124.30	0.73
3	1	91.16	0.53	98.35	0.57
	2	75.81	0.44	100.93	0.59
	3	101.77	0.59	109.68	0.64

Table D.4-3 Maximum Shear (kips) at the Abutments

Abutment	Shear			
	Longitudina l	Demand/ Capacity	Transverse	Demand/ Capacity
West	1230	0.36	205	0.14
East	1280	0.38	318	0.22

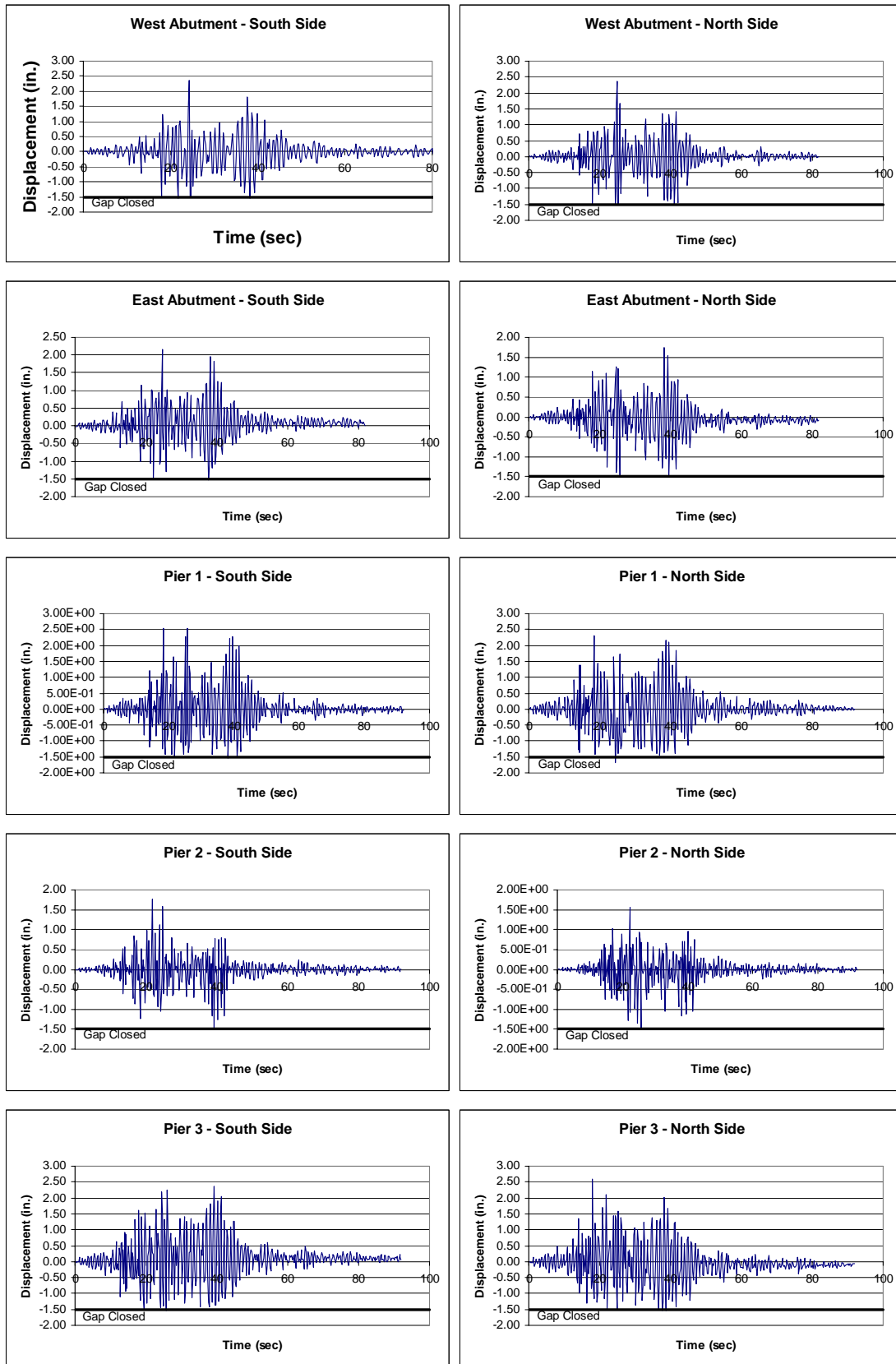


Figure D.4-6 Longitudinal Displacement of Expansion Joints

D.5 Run No. 4

The plots and tables for the response of Bridge 5/518, with the soil spring stiffness of the columns left unchanged and rollers at the abutments in the longitudinal direction only, to the modified Peru earthquake are presented here.

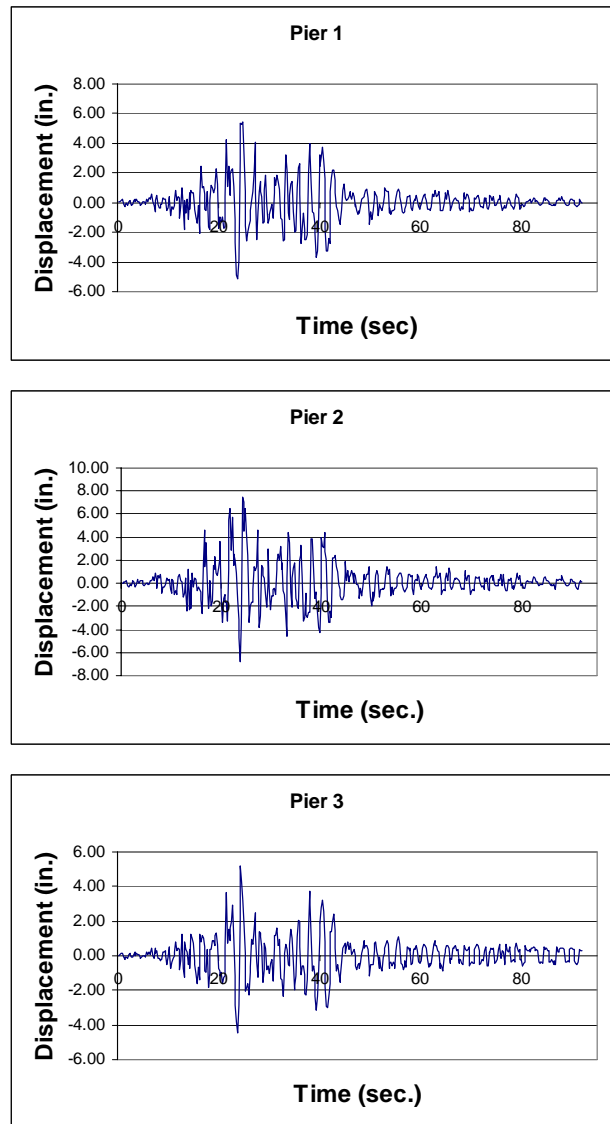


Figure D.5-1 Total Relative Displacement at Piers

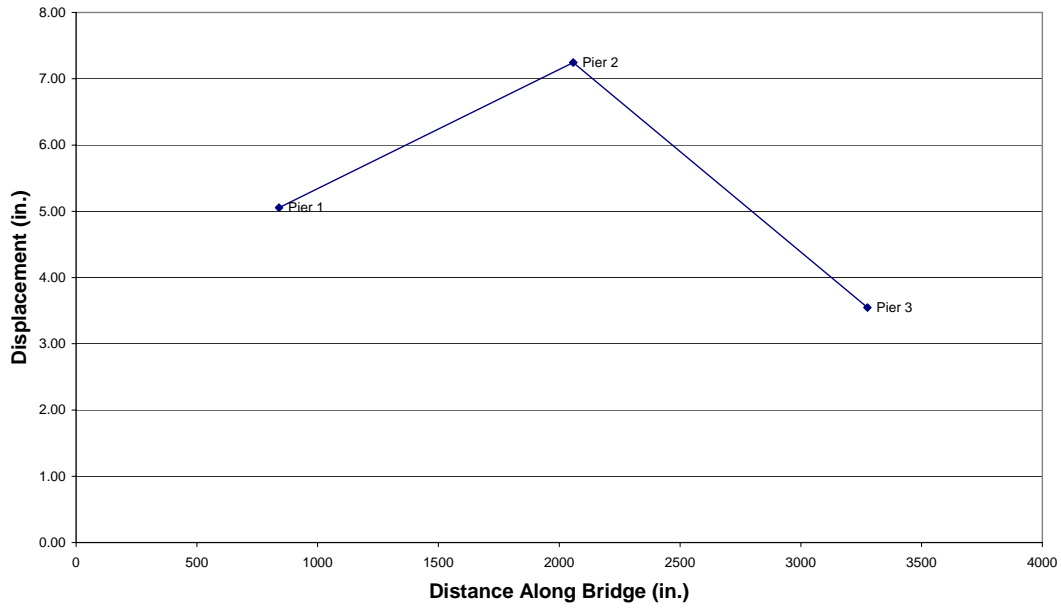


Figure D.5-2 Transverse Displacement Envelope of Bridge Deck

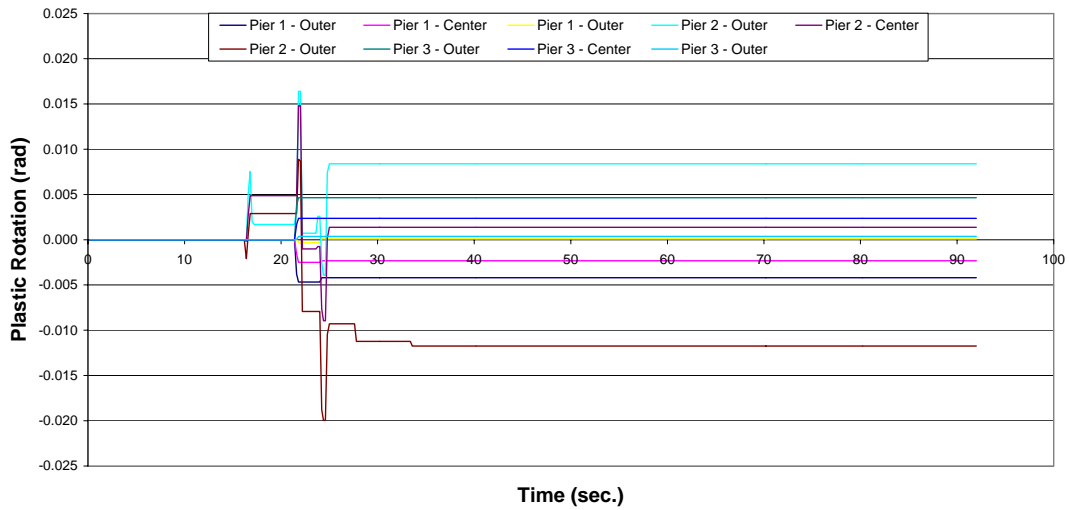


Figure D.5-3 Plastic Rotations at Top of Columns

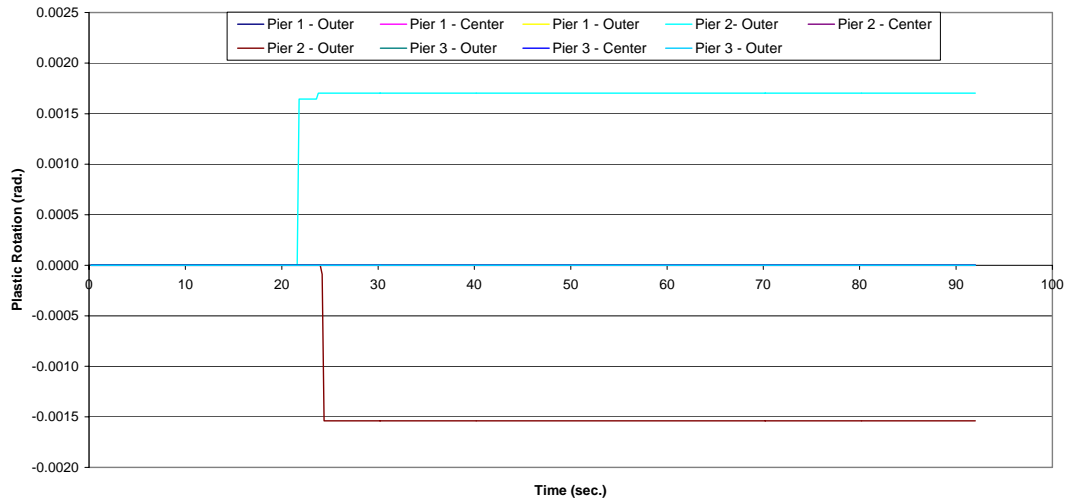


Figure D.5-4 Plastic Rotations at Bottom of Column

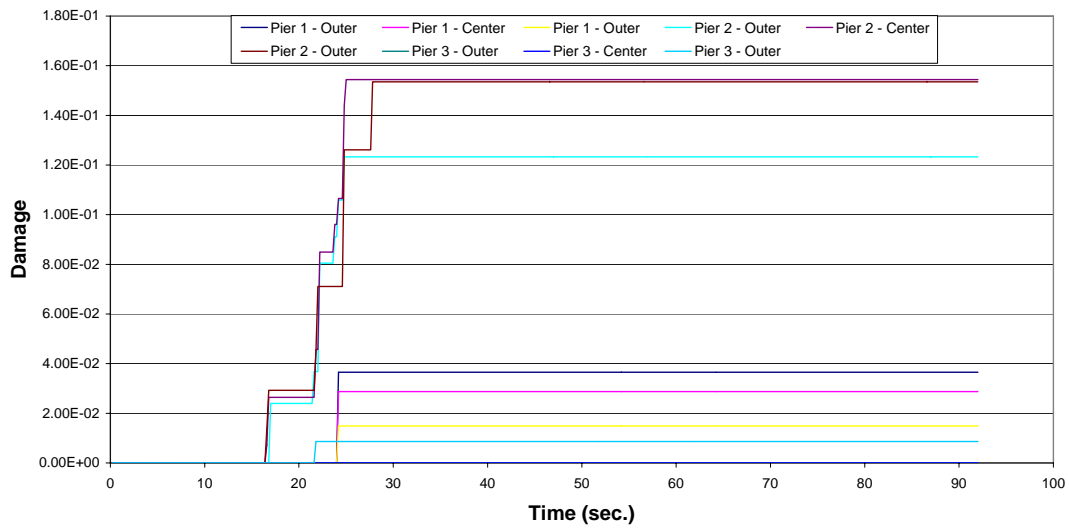


Figure D.5-5 Damage at Top of Columns

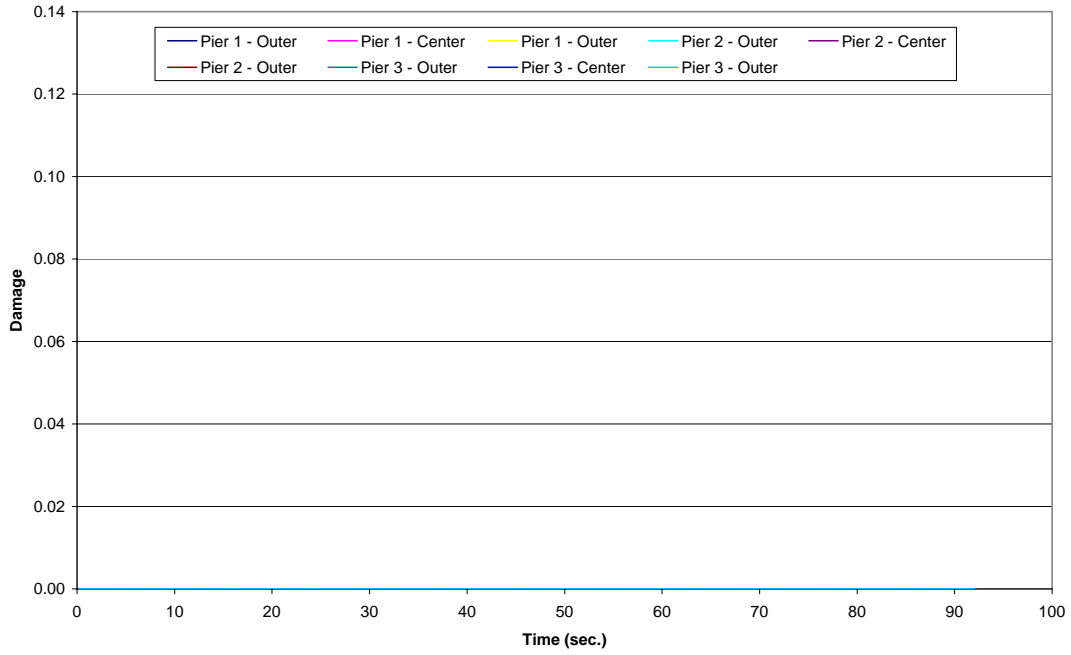


Figure D.5-6 Damage at Bottom of Columns

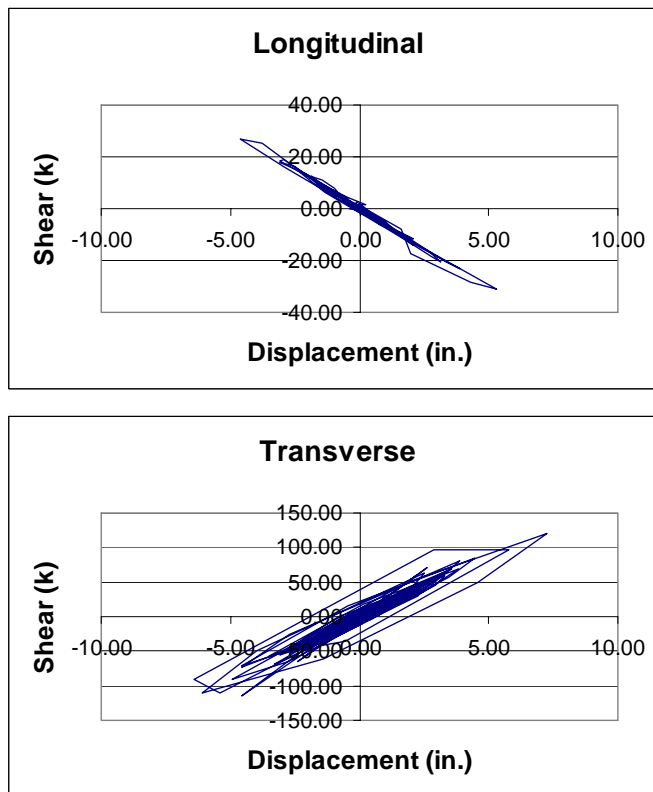


Figure D.5-7 Hysteresis Plots for the Center Column of Pier 2

Table D.5-1 Maximum Moment (kip-in) at the Top and Bottoms of Columns

Pier No.	Column	Moment	
		Top	Bottom
1	1	15349.9	8232.6
	2	15252.1	8649.9
	3	16854.0	8971.5
2	1	16532.7	11411.3
	2	15950.7	10945.7
	3	18180.9	10487.5
3	1	12447.8	9650.6
	2	14890.4	9164.0
	3	17085.9	8709.7

Table D.5-2 Maximum Shear (kips) in the Columns

Pier No.	Column	Shear			
		Top	Demand/ Capacity	Bottom	Demand/ Capacity
1	1	84.17	0.49	86.85	0.51
	2	90.76	0.53	95.87	0.56
	3	98.63	0.58	102.36	0.60
2	1	114.43	0.67	133.94	0.78
	2	104.74	0.61	120.94	0.70
	3	115.55	0.67	124.44	0.73
3	1	79.17	0.46	89.71	0.52
	2	74.11	0.44	101.53	0.59
	3	101.20	0.59	111.71	0.65

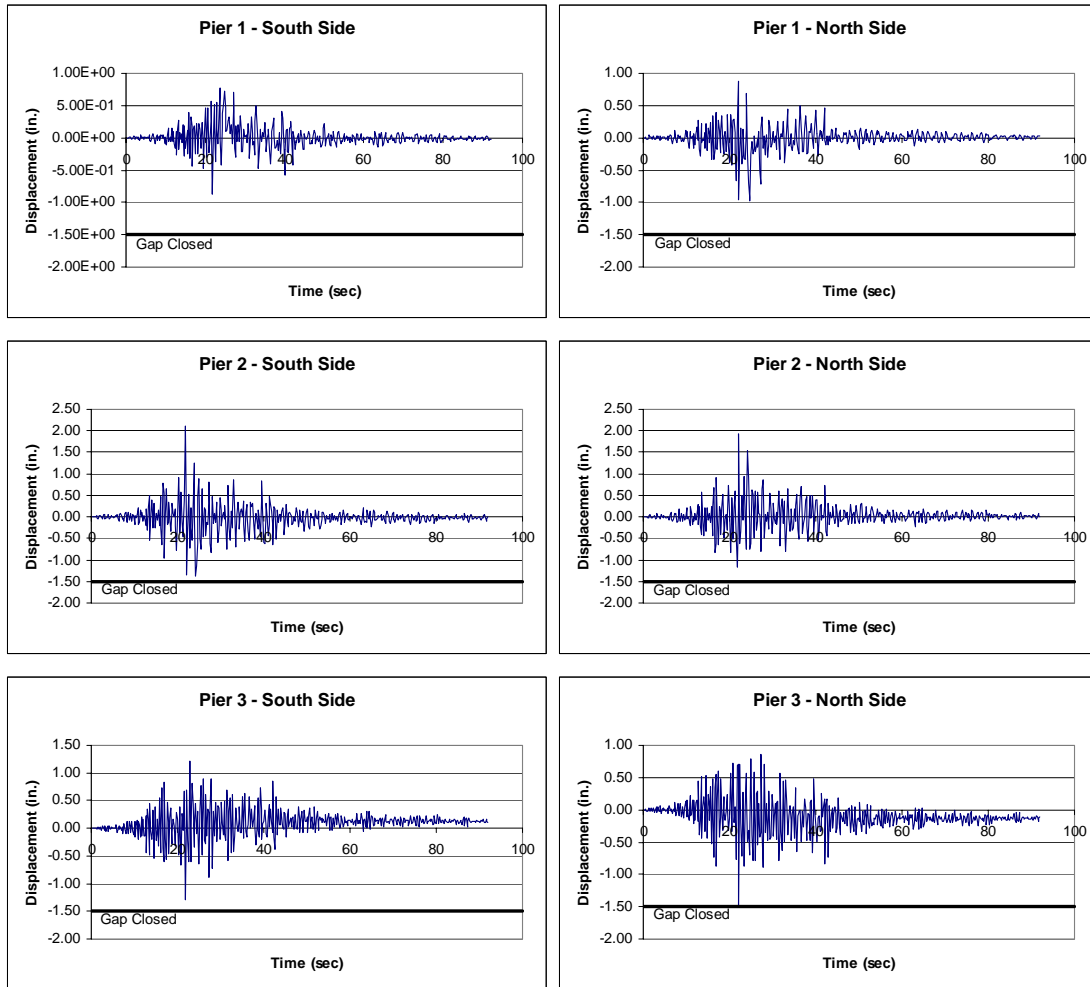


Figure D.5-8 Longitudinal Displacement of Expansion Joints

D.6 Run No. 5

The plots and tables for the response of Bridge 5/518, with the soil spring stiffness of the columns decreased by a factor of ten and the soil spring stiffness at the abutments was left unchanged, to the modified Peru earthquake are presented here.

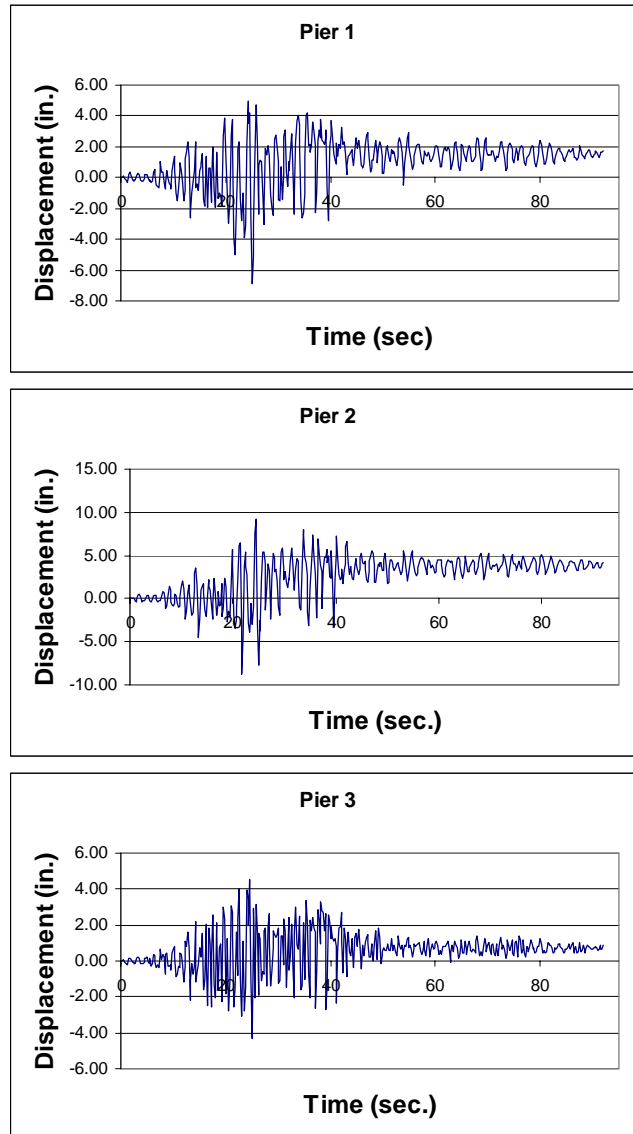


Figure D.6-1 Total Relative Displacement at Piers

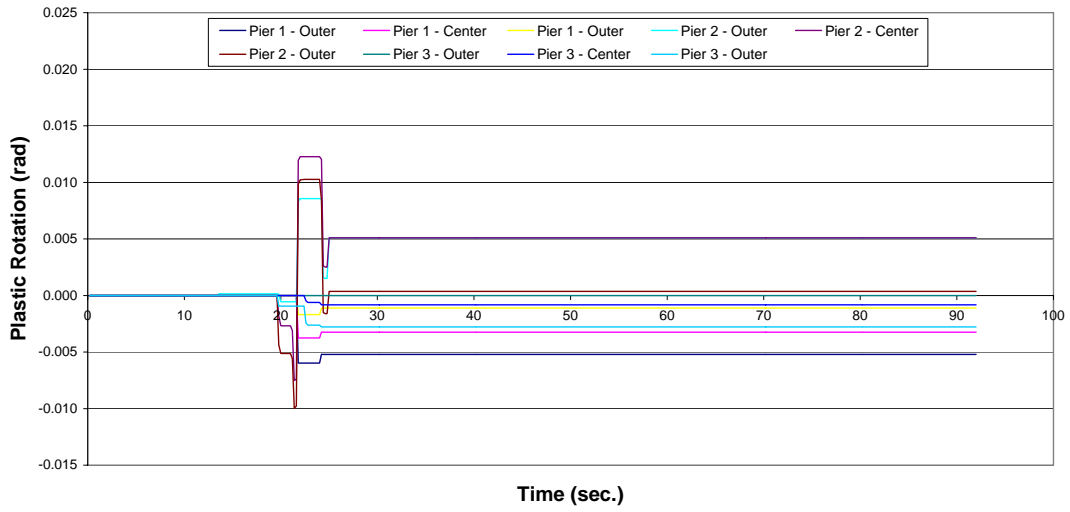


Figure D.6-2 Plastic Rotations at the Top of the Columns

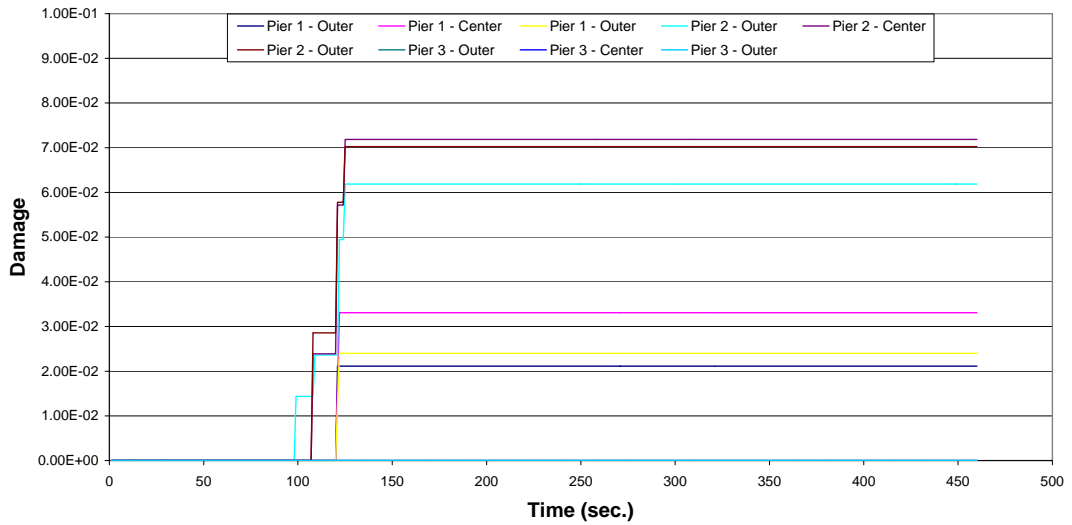


Figure D.6-3 Damage at Top of Columns

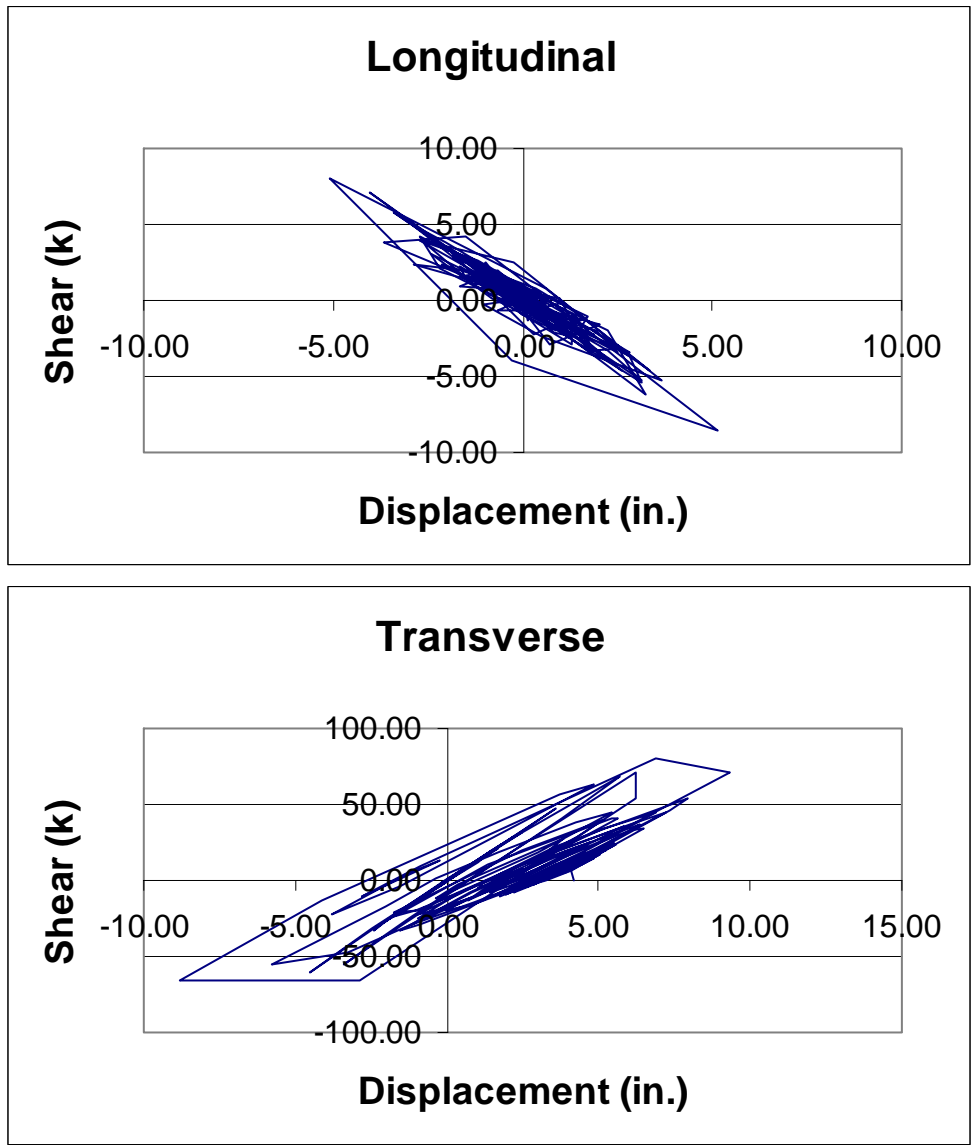


Figure D.6-4 Hysteresis Plots for the Center Column of Pier 2

Table D.6-1 Maximum Moment (kip-in) at the Top and Bottoms of Columns

Pier No.	Column	Moment	
		Top	Bottom
1	1	16011.9	2058.4
	2	14190.2	1738.2
	3	13901.1	1491.7
2	1	17341.8	1992.4
	2	15580.0	2116.2
	3	16507.9	2415.2
3	1	15541.3	2642.5
	2	14980.7	2531.5
	3	13550.5	2747.5

Table D.6-2 Maximum Shear (kips) in the Columns

Pier No.	Column	Shear			
		Top	Demand/ Capacity	Bottom	Demand/ Capacity
1	1	66.53	0.39	62.50	0.36
	2	59.72	0.35	56.00	0.33
	3	58.01	0.34	58.29	0.34
2	1	70.80	0.41	78.55	0.46
	2	104.23	0.61	80.88	0.47
	3	68.30	0.40	77.86	0.45
3	1	67.32	0.39	72.08	0.42
	2	62.25	0.36	69.79	0.41
	3	57.49	0.34	62.36	0.36

Table D.6-3 Maximum Shear (kips) at the Abutments

Abutment	Shear			
	Longitudina l	Demand/ Capacity	Transverse	Demand/ Capacity
West	2180	0.65	189	0.04
East	2170	0.64	207	0.06

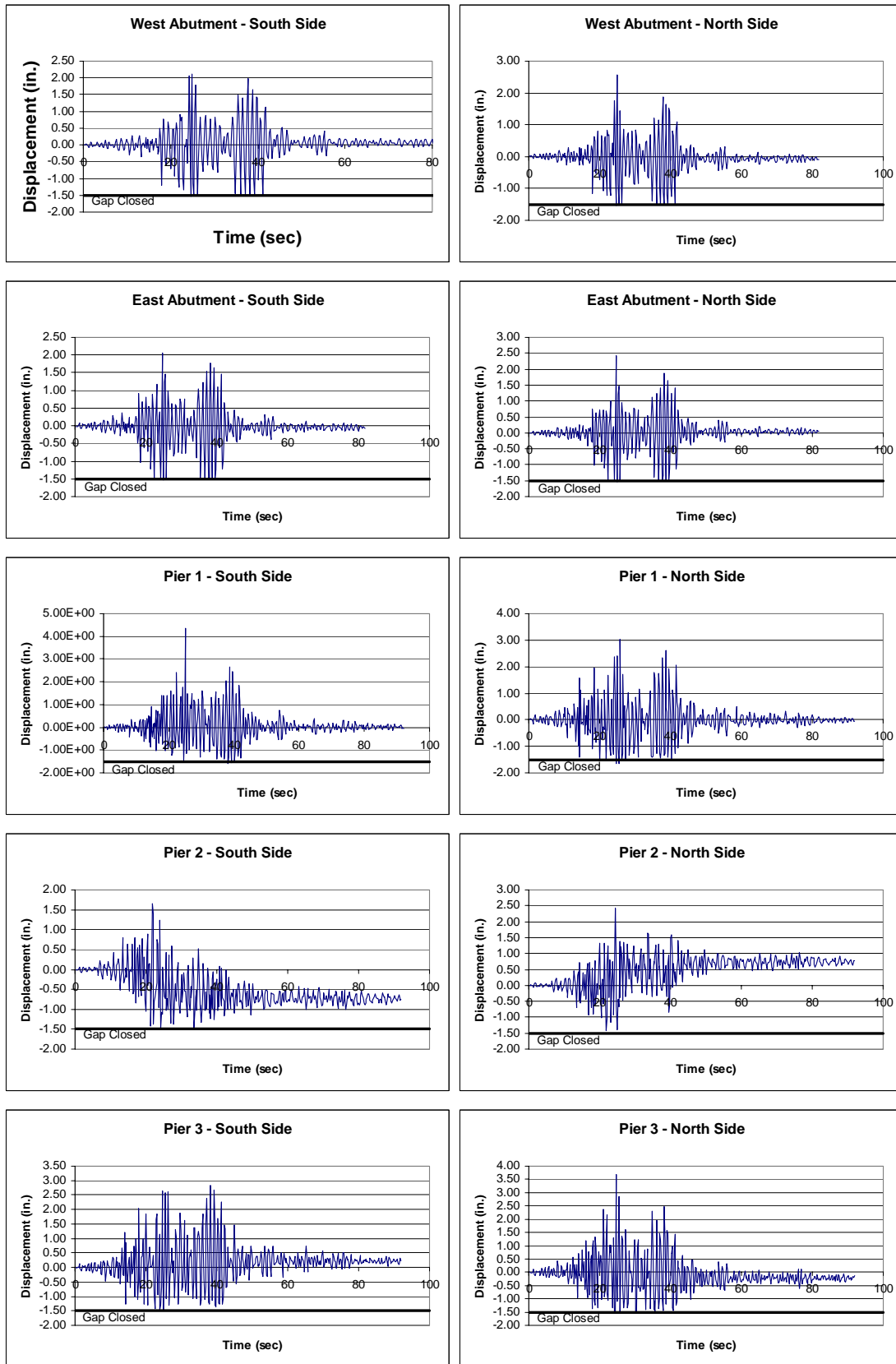


Figure D.6-5 Longitudinal Displacement of Expansion Joints

D.7 Run No. 6

The plots and tables for the response of Bridge 5/518, with columns fixed at their bases and the soil spring stiffness at the abutments was left unchanged, to the modified Peru earthquake are presented here.

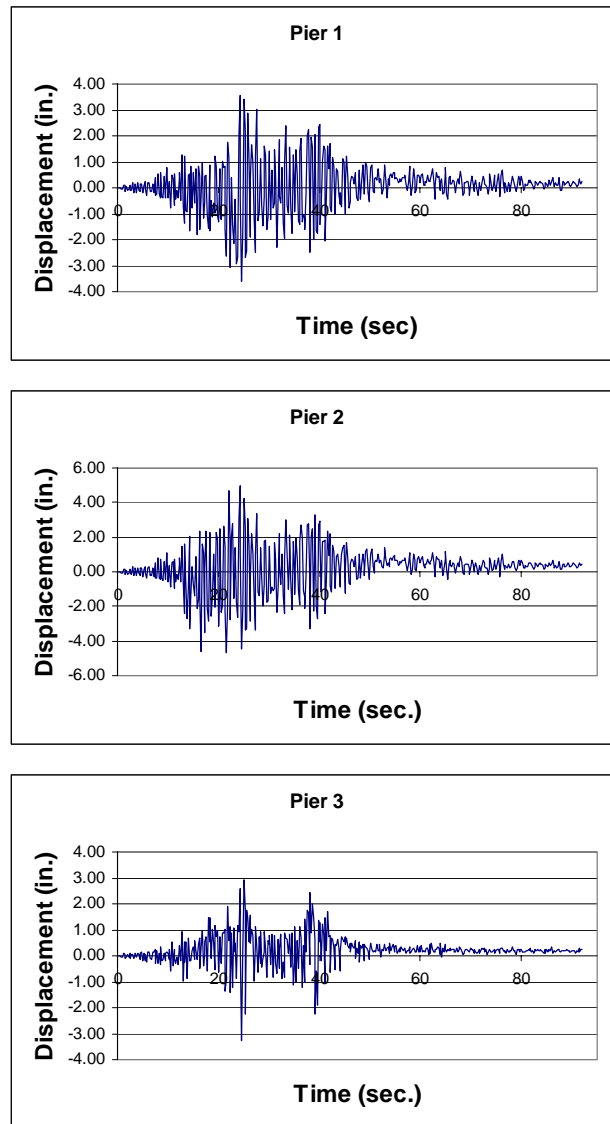


Figure D.7-1 Total Relative Displacement at Piers

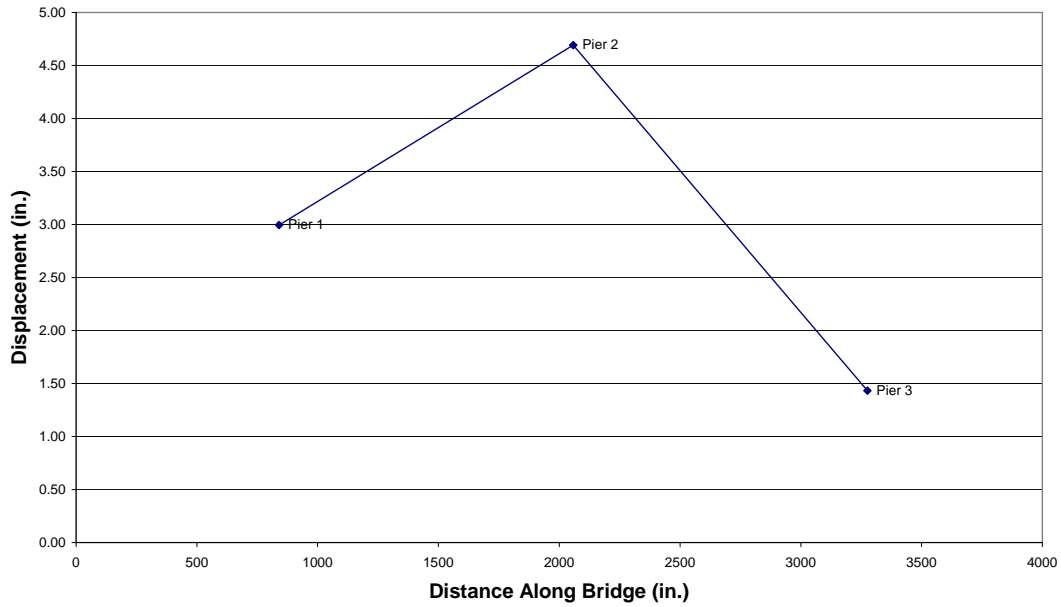


Figure D.7-2 Transverse Displacement Envelope of Bridge Deck

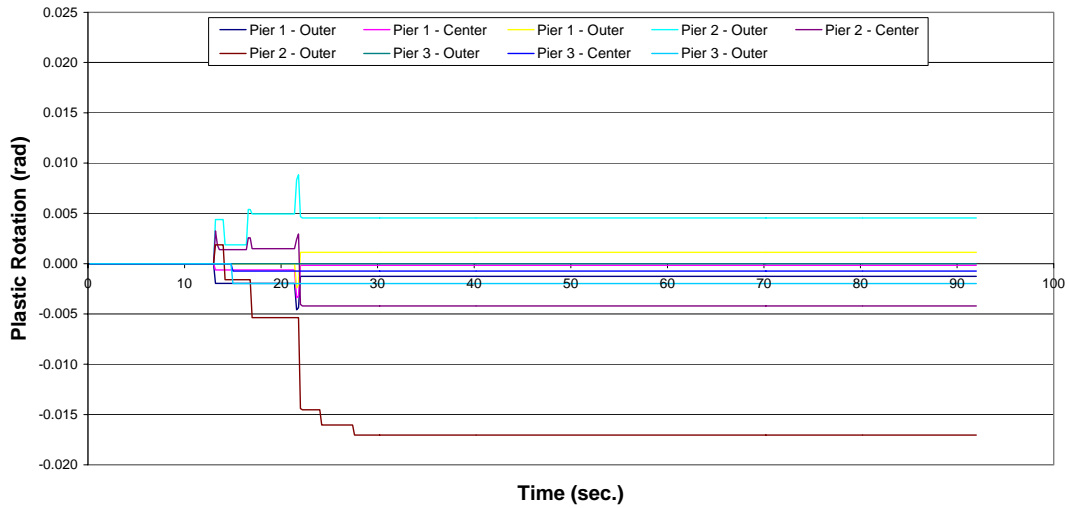


Figure D.7-3 Plastic Rotations at the Top of Columns

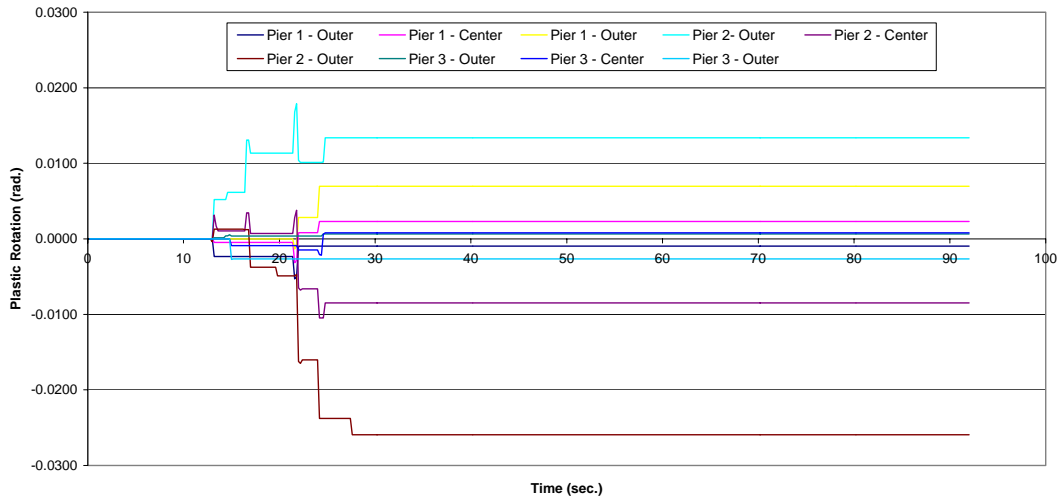


Figure D.7-4 Plastic Rotations at the Bottom of Columns

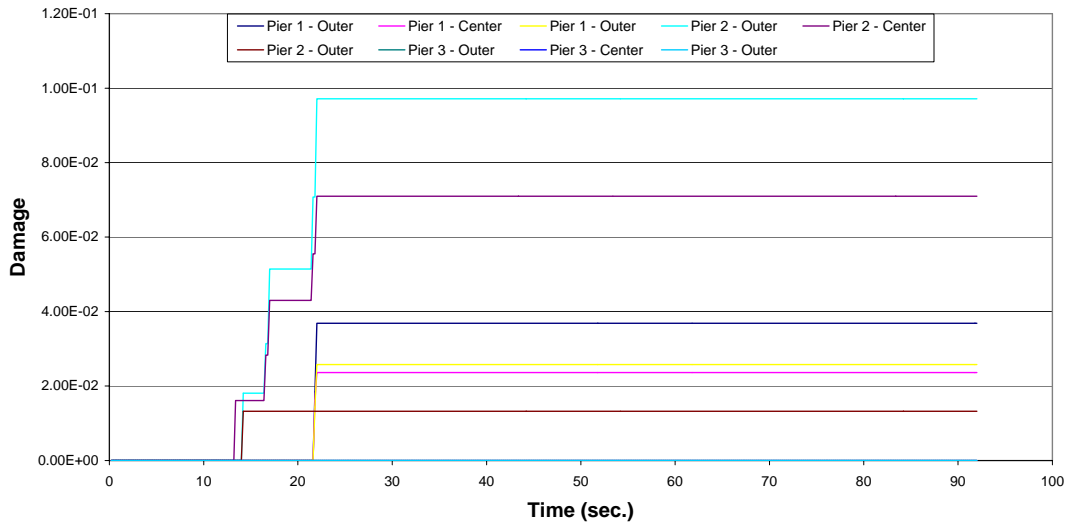


Figure D.7-5 Damage at Top of Columns

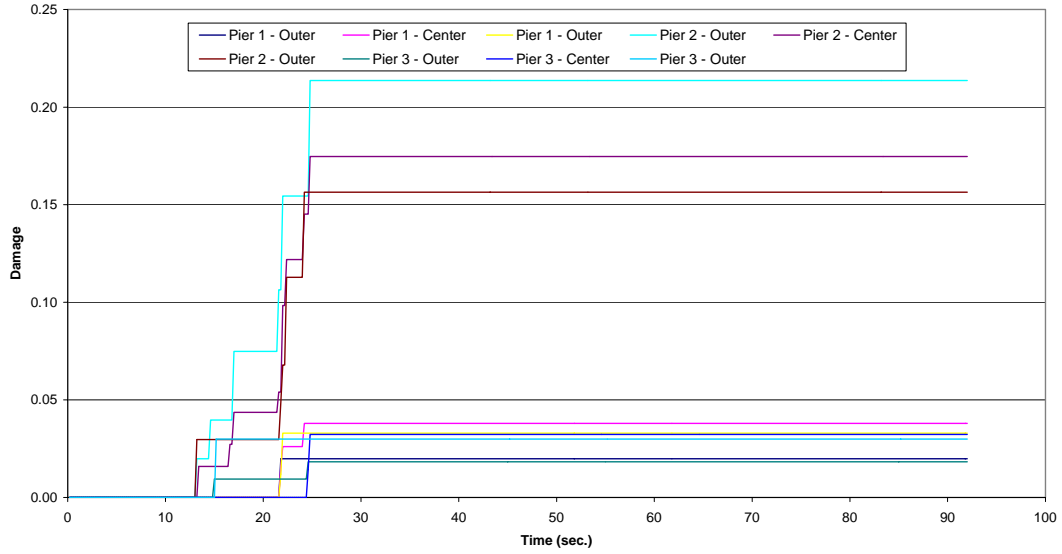


Figure D.7-6 Damage at Bottom of Columns

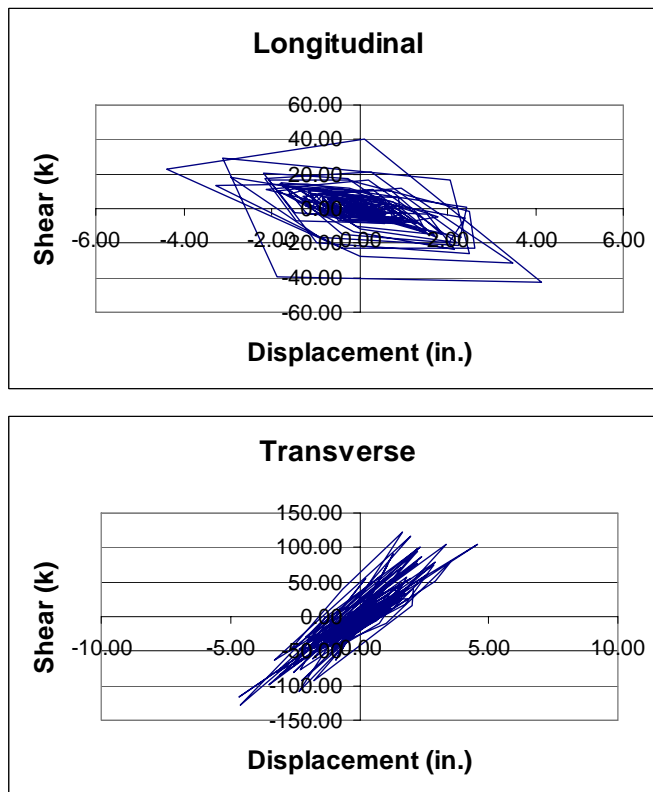


Figure D.7-7 Hysteresis Plots for the Center Column of Pier 2

Table D.7-1 Maximum Moment (kip-in) at the Top and Bottoms of Columns

Pier No.	Column	Moment	
		Top	Bottom
1	1	17314.9	15444.9
	2	14807.4	12875.2
	3	17008.7	15428.4
2	1	16913.0	12974.3
	2	15570.1	13613.2
	3	16522.9	14880.2
3	1	12514.7	10307.9
	2	12995.7	12666.6
	3	11754.0	10316.8

Table D.7-2 Maximum Shear (kips) in the Columns

Pier No.	Column	Shear			
		Top	Demand/ Capacity	Bottom	Demand/ Capacity
1	1	151.19	0.88	132.10	0.77
	2	127.67	0.74	127.61	0.74
	3	150.75	0.88	152.49	0.89
2	1	126.31	0.83	127.13	0.86
	2	125.81	0.74	128.56	0.74
	3	139.62	0.81	144.34	0.84
3	1	107.34	0.62	104.50	0.61
	2	130.09	0.76	135.82	0.79
	3	103.87	0.61	104.66	0.61

Table D.7-3 Maximum Shear (kips) at the Abutments

Abutment	Shear			
	Longitudina l	Demand/ Capacity	Transverse	Demand/ Capacity
West	1800	0.53	202	0.14
East	1740	0.52	147	0.10

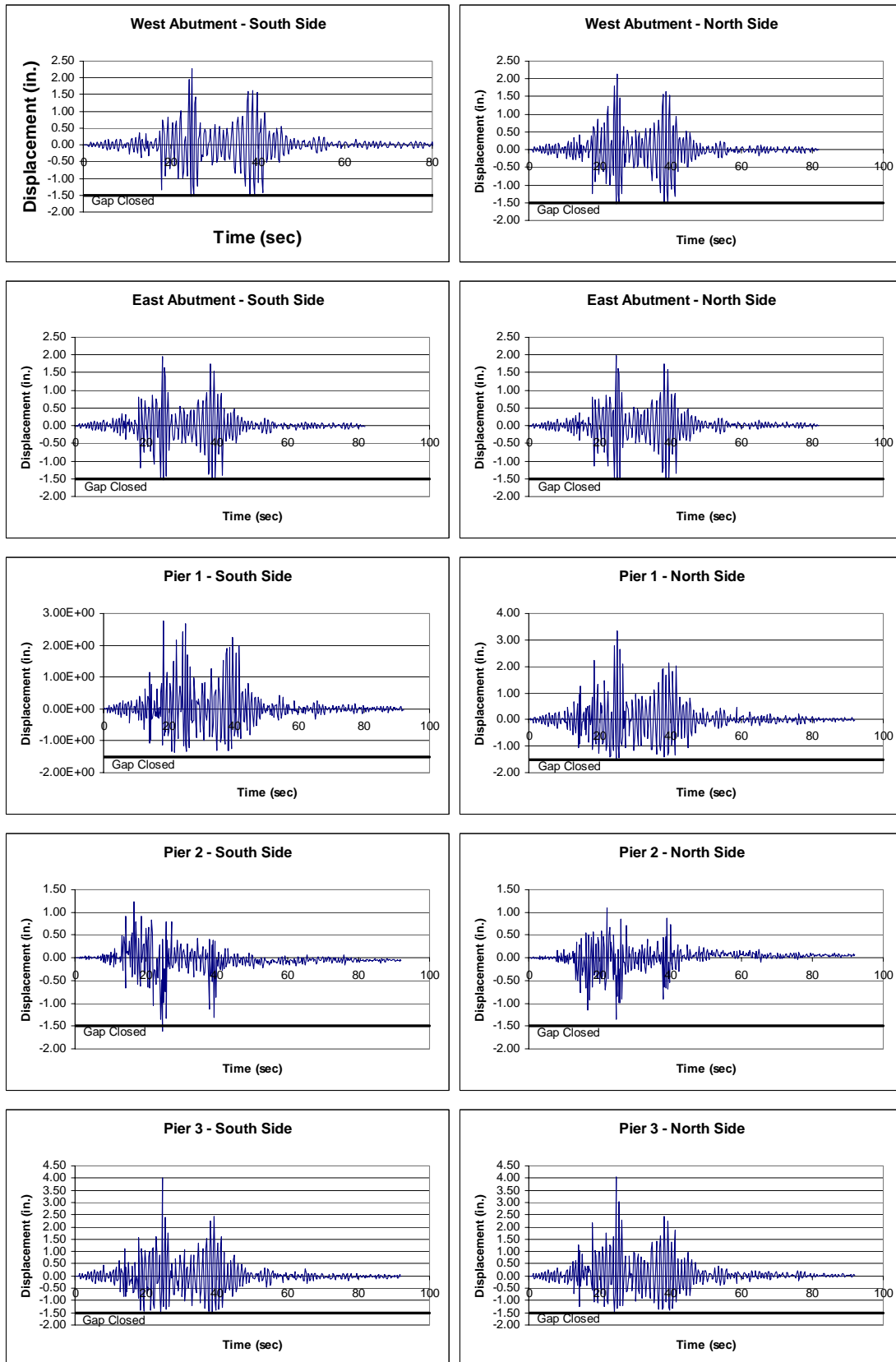


Figure D.7-8 Longitudinal Displacement of Expansion Joints

D.8 Run No. 7

The plots and tables for the response of Bridge 5/518, with columns fixed at their bases and the abutments have a roller in the expansion joint in the both directions, to the modified Chile earthquake are presented here.

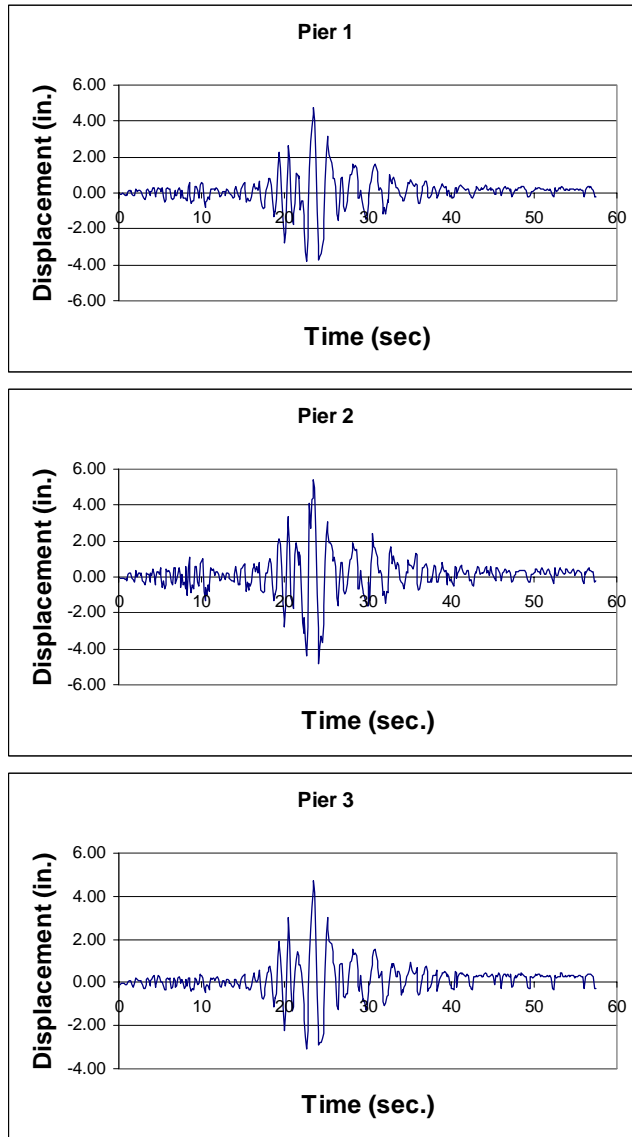


Figure D.8-1 Total Relative Displacement at Piers

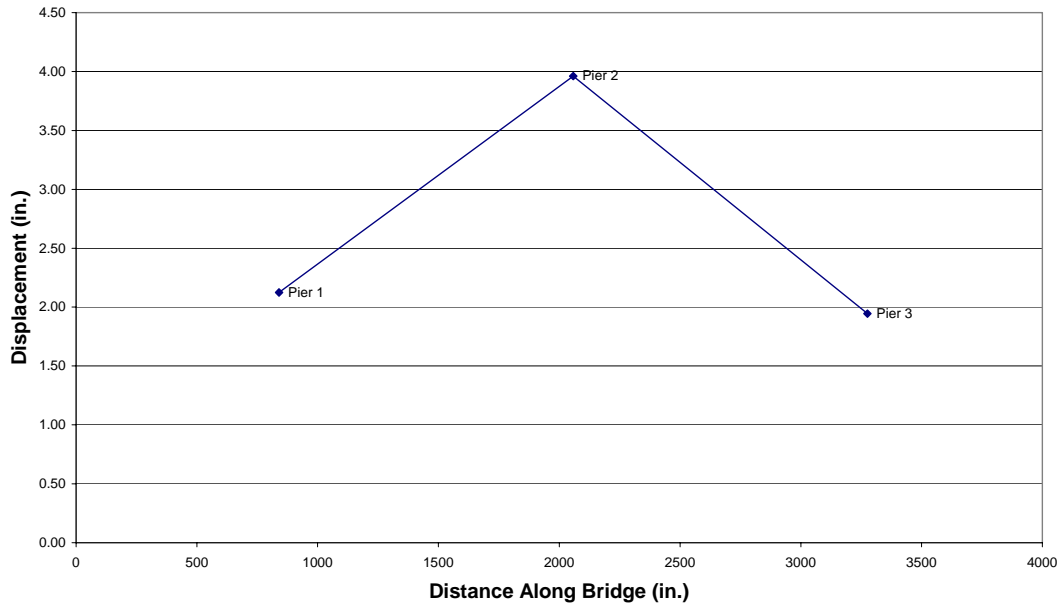


Figure D.8-2 Transverse Displacement Envelope of Bridge Deck

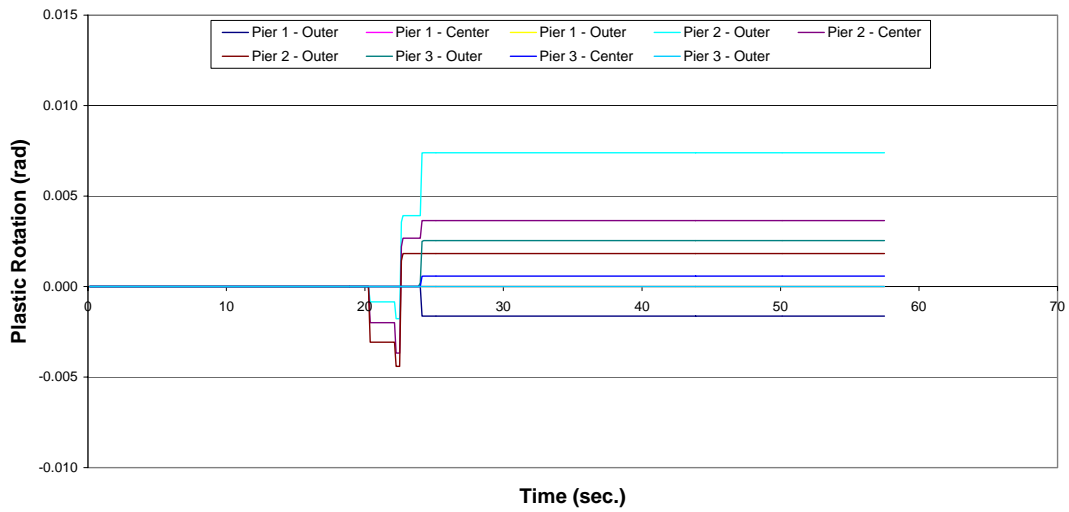


Figure D.8-3 Plastic Rotations at the Top of the Columns

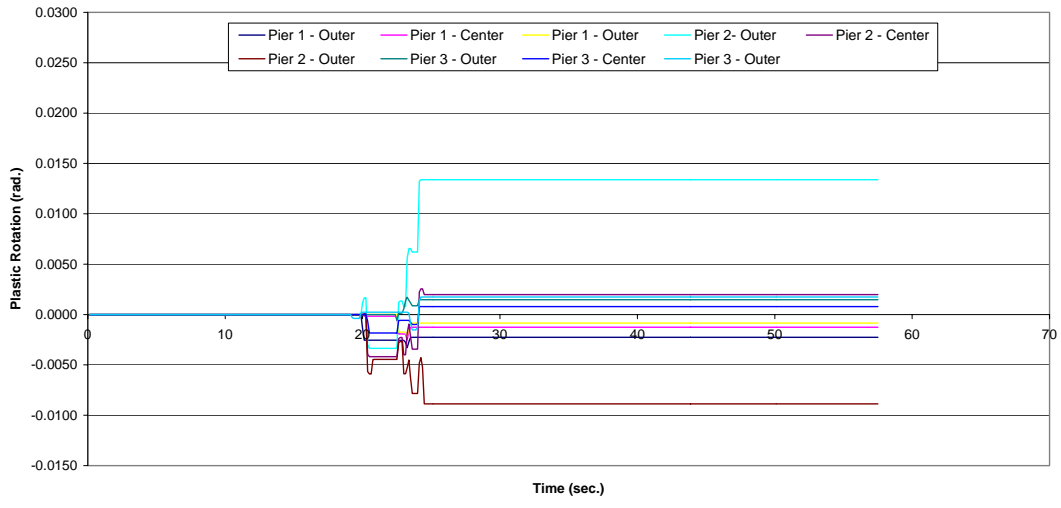


Figure D.8-4 Plastic Rotations at the Bottom of the Columns

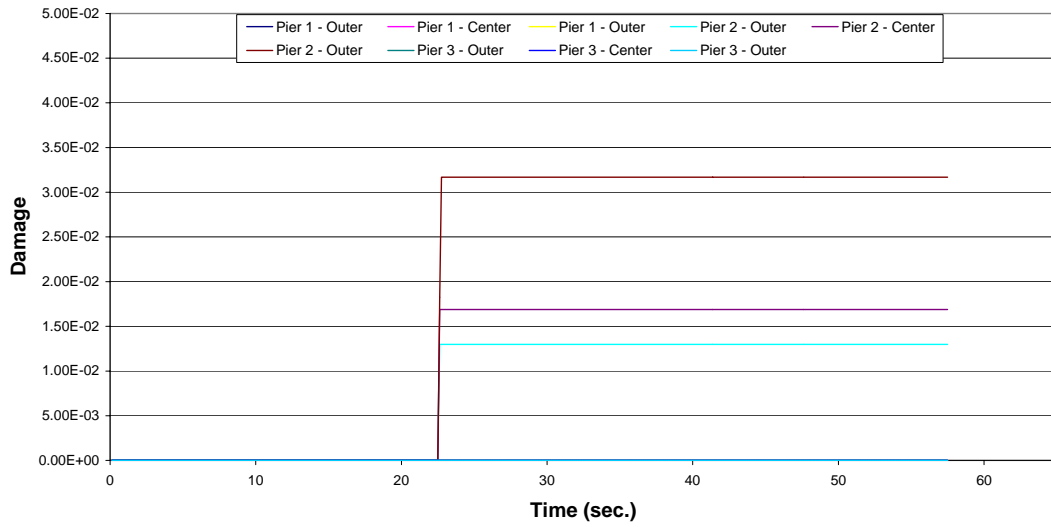


Figure D.8-5 Damage at the Top of Columns

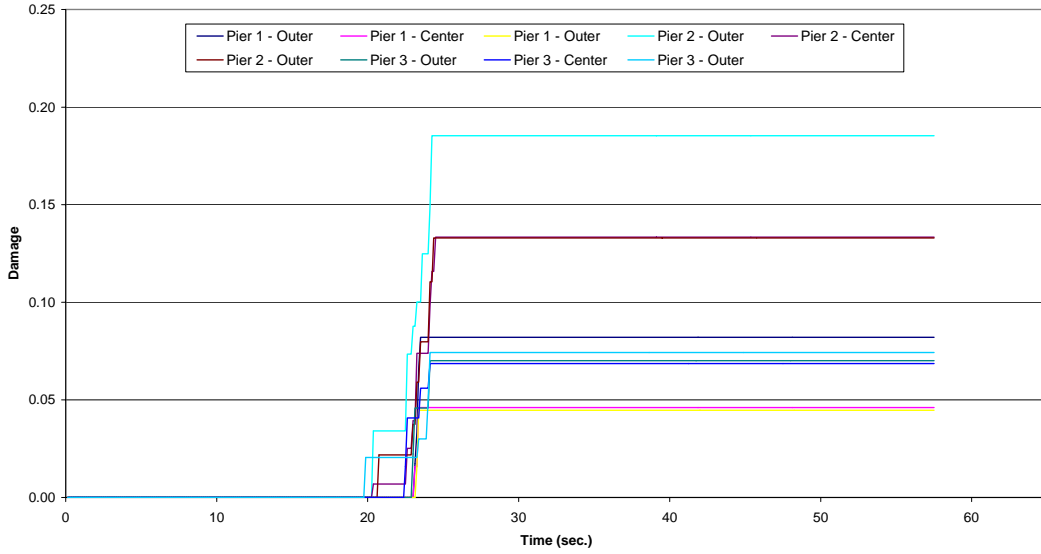


Figure D.8-6 Damage at Bottom of Columns

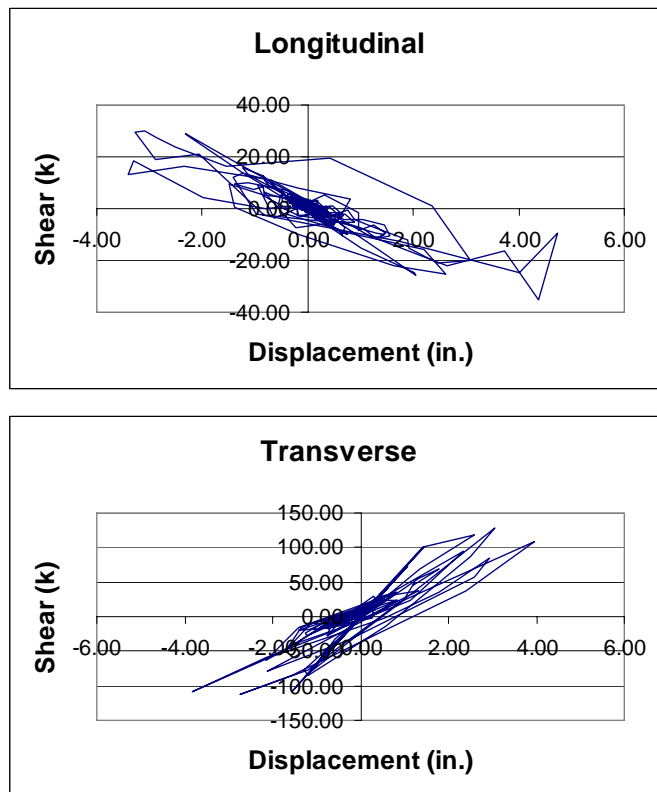


Figure D.8-7 Hysteresis Plots of the Center Column at Pier 2

Table D.8-1 Maximum Moment (kip-in) at the Top and Bottoms of Columns

Pier No.	Column	Moment	
		Top	Bottom
1	1	11507.7	12562.3
	2	13125.7	13116.2
	3	13744.4	14563.7
2	1	17515.0	15137.3
	2	15731.3	13460.2
	3	16928.8	14919.8
3	1	12659.2	13763.8
	2	15195.5	13475.6
	3	15919.2	14278.3

Table D.8-2 Maximum Shear (kips) in the Columns

Pier No.	Column	Shear			
		Top	Demand/ Capacity	Bottom	Demand/ Capacity
1	1	96.78	0.56	95.84	0.56
	2	109.87	0.64	109.54	0.64
	3	111.63	0.65	112.05	0.66
2	1	145.91	0.85	139.74	0.81
	2	125.19	0.73	128.60	0.75
	3	142.26	0.83	136.65	0.80
3	1	119.25	0.69	121.48	0.71
	2	128.40	0.75	129.81	0.76
	3	148.06	0.86	137.49	0.80

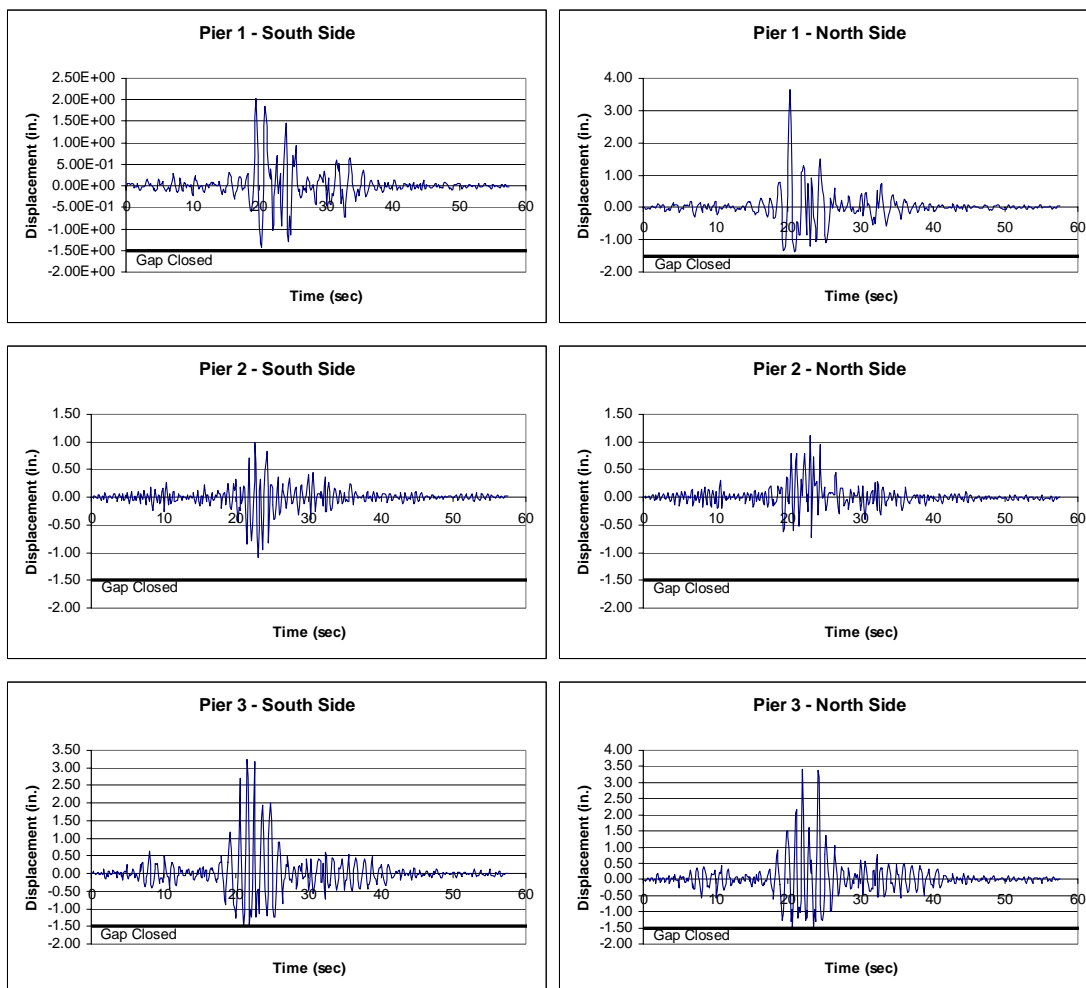


Figure D.8-8 Longitudinal Displacement of Expansion Joints

D.9 Run No. 8

The plots and tables for the response of Bridge 5/826, with columns fixed at their bases and the abutments have a roller in the longitudinal direction only, to the modified Peru earthquake are presented here.

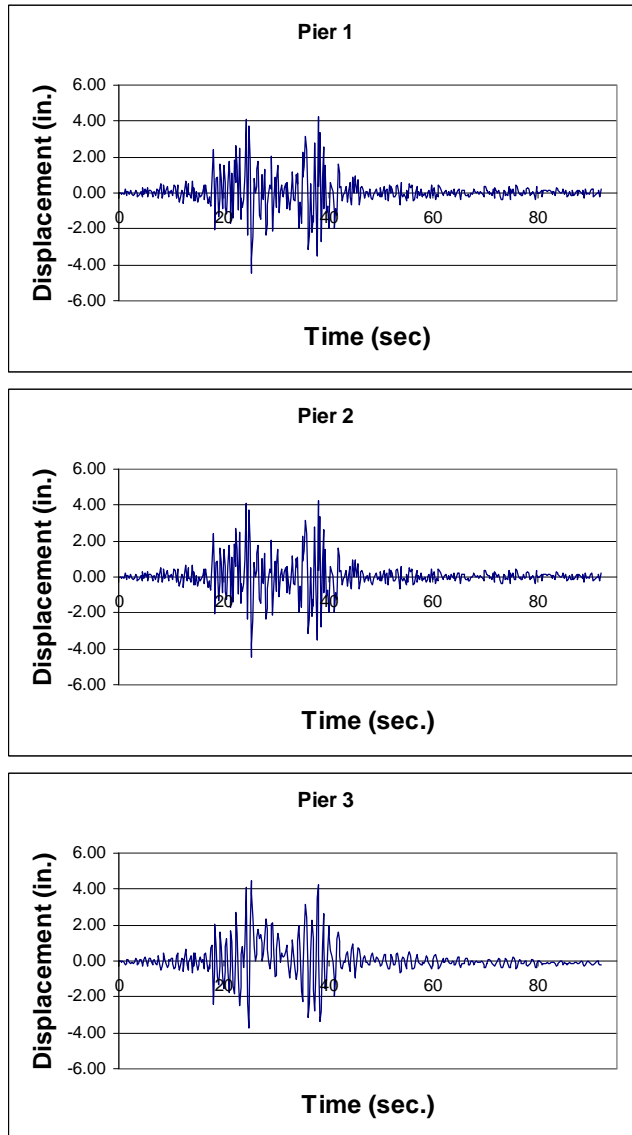


Figure D.9-1 Total Relative Displacement at Piers

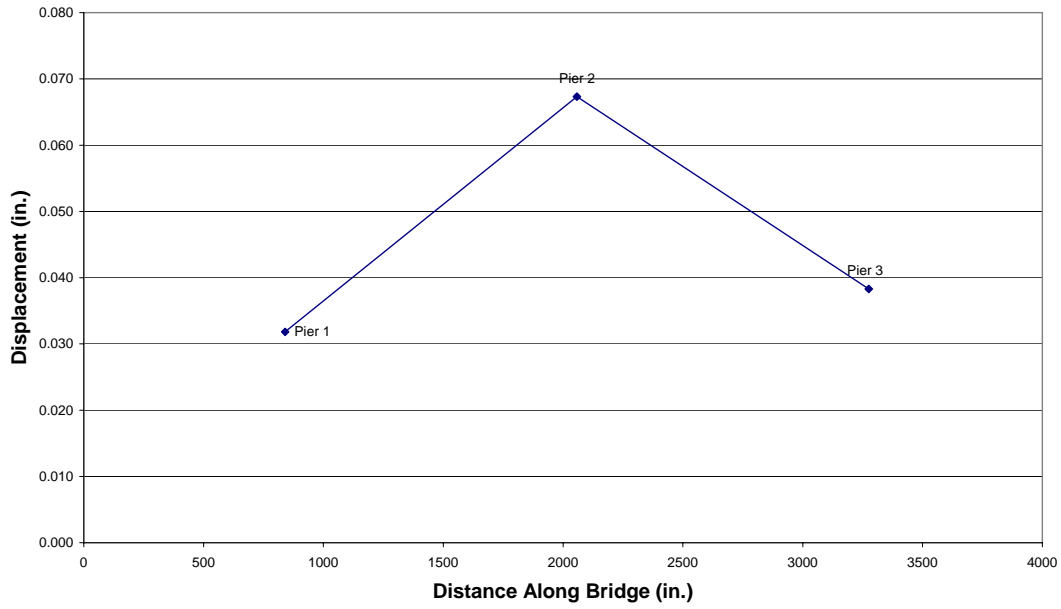


Figure D.9-2 Transverse Displacement Envelope of Bridge Deck

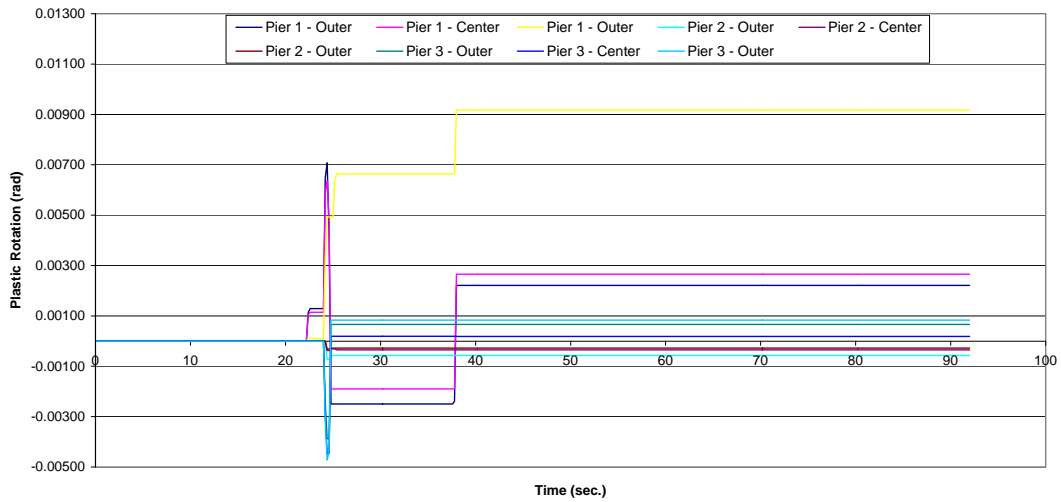


Figure D.9-3 Plastic Rotations at the Top of the Columns

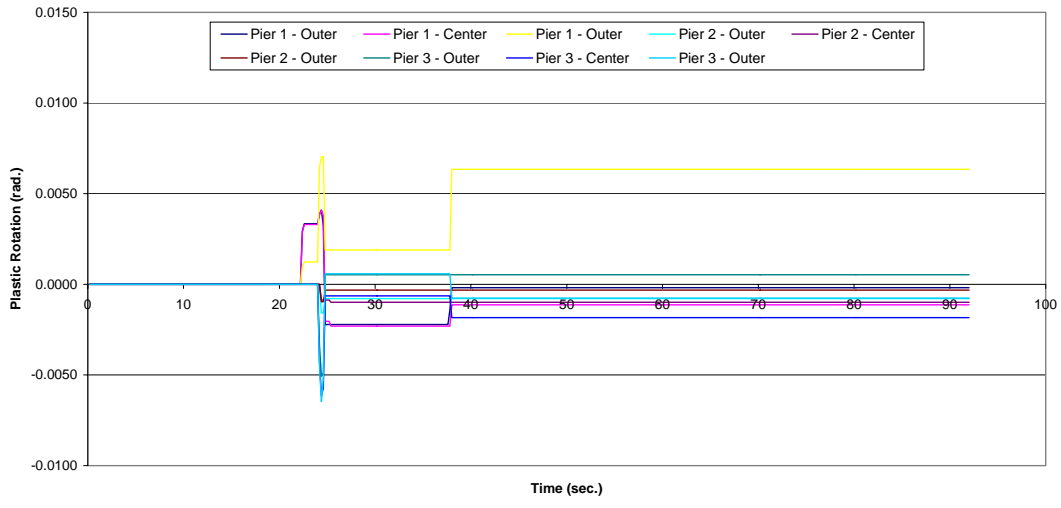


Figure D.9-4 Plastic Rotations at the Bottom of the Columns

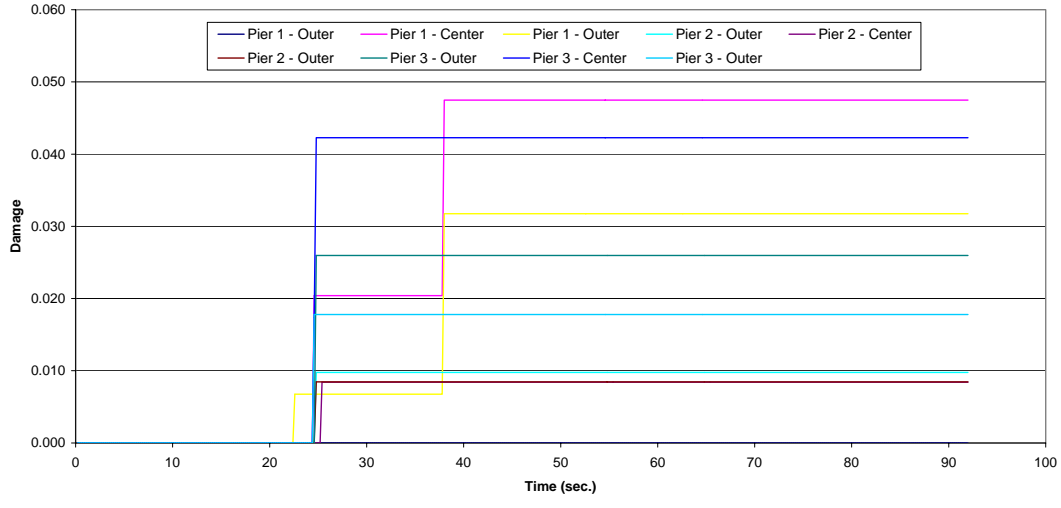


Figure D.9-5 Damage at the Top of Columns

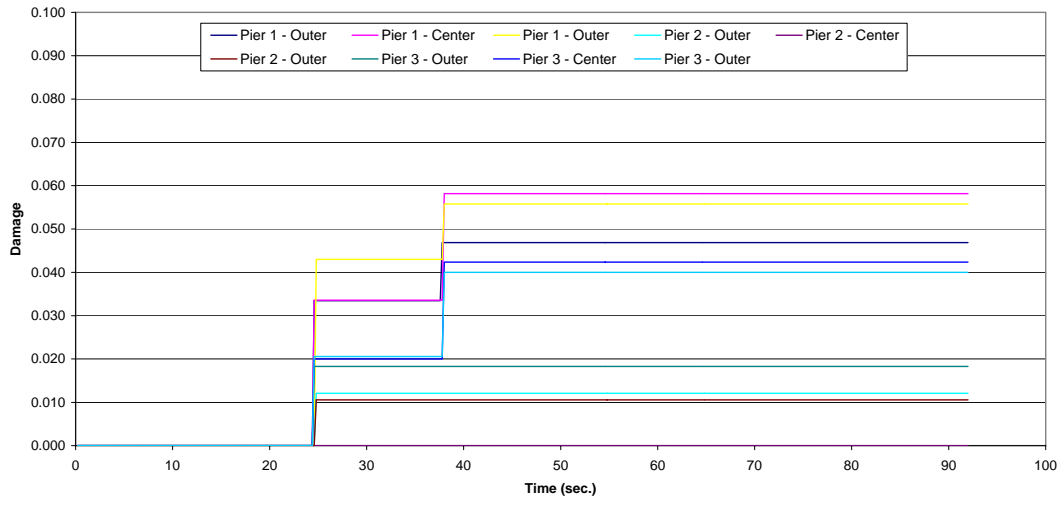


Figure D.9-6 Damage at the Bottom of Columns

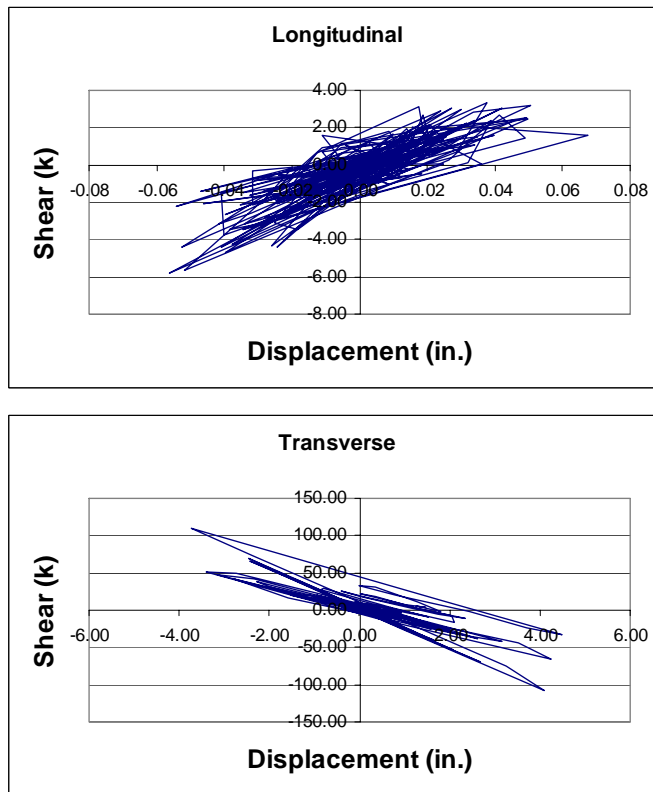


Figure D.9-7 Hysteresis Plots for the Center Column of Pier 2

Table D.9-1 Maximum Moment (kip-in) at the Top and Bottoms of Columns

Pier No.	Column	Moment	
		Top	Bottom
1	1	23141.4	22540.4
	2	24870.0	23590.1
	3	15600.4	20300.5
2	1	17660.2	16440.2
	2	17760.0	16360.0
	3	16940.2	15980.5
3	1	19400.2	17750.0
	2	20280.0	19010.0
	3	19100.2	17690.3

Table D.9-2 Maximum Shear (kips) in the Columns

Pier No.	Column	Shear			
		Top	Demand/ Capacity	Bottom	Demand/ Capacity
1	1	174.01	1.01	176.70	1.03
	2	182.20	1.06	184.70	1.07
	3	136.60	0.80	139.10	0.81
2	1	114.20	0.67	116.80	0.68
	2	110.50	0.64	109.30	0.64
	3	109.50	0.64	112.31	0.65
3	1	131.51	0.77	134.40	0.78
	2	142.40	0.83	145.40	0.85
	3	134.90	0.79	137.50	0.80

D.10 Run No. 9

The plots and tables for the response of Bridge 5/826, with columns fixed at their bases and the abutments have rollers in both directions, to the modified Peru earthquake are presented here.

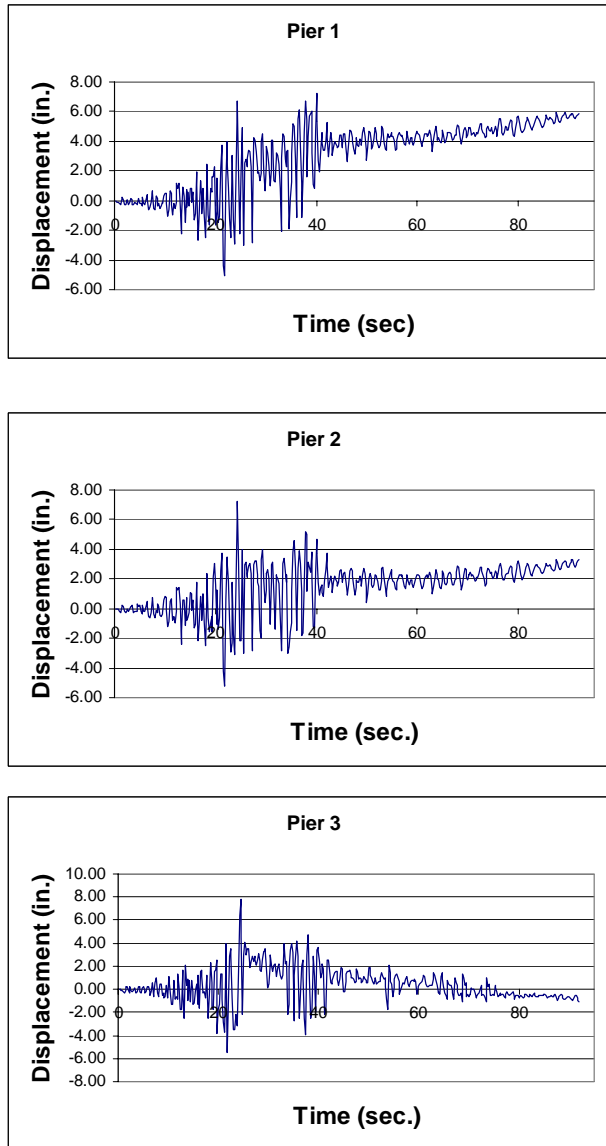


Figure D.10-1 Total Relative Displacement at Piers

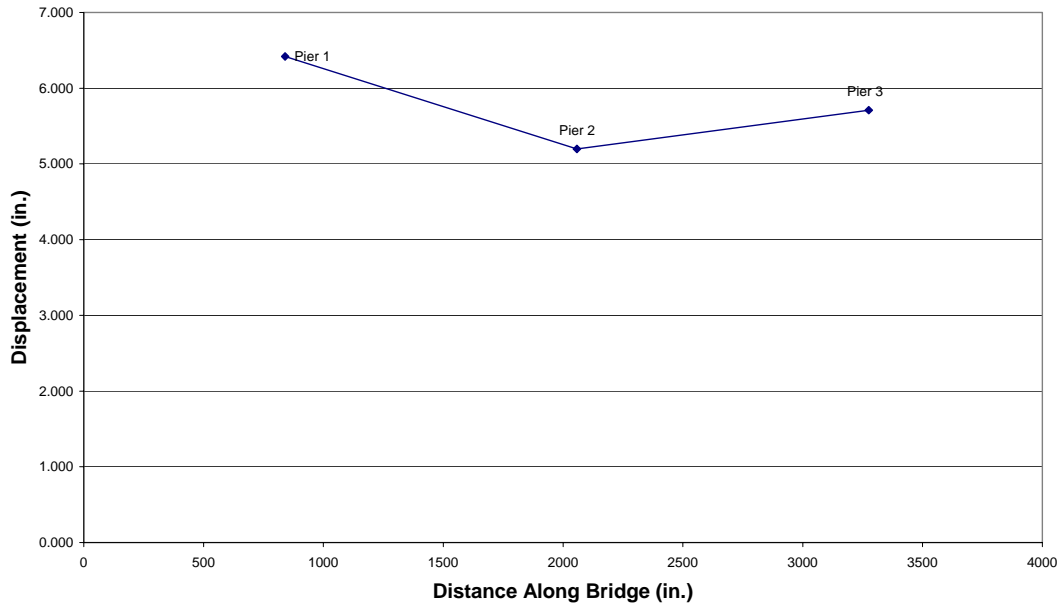


Figure D.10-2 Transverse Displacement Envelope of Bridge Deck

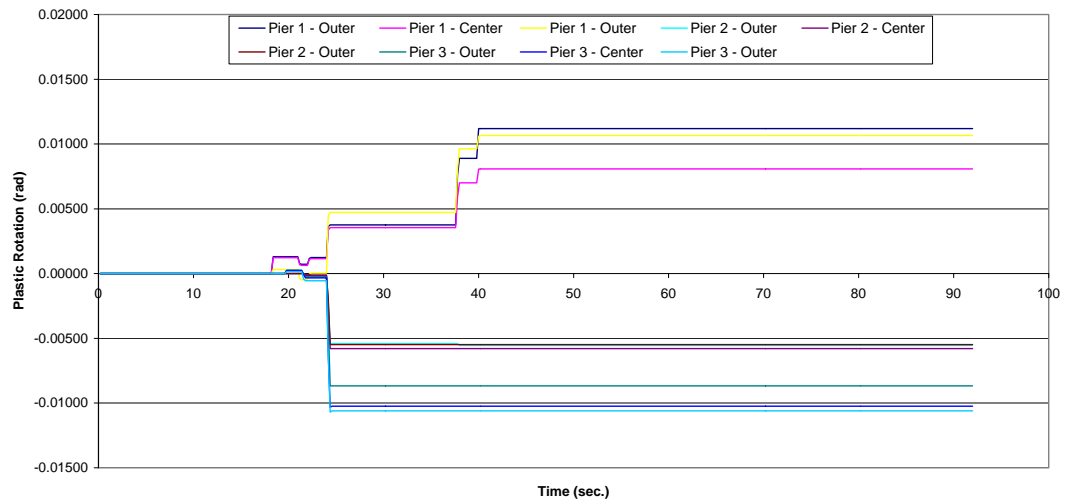


Figure D.10-3 Plastic Rotations at the Top of the Columns

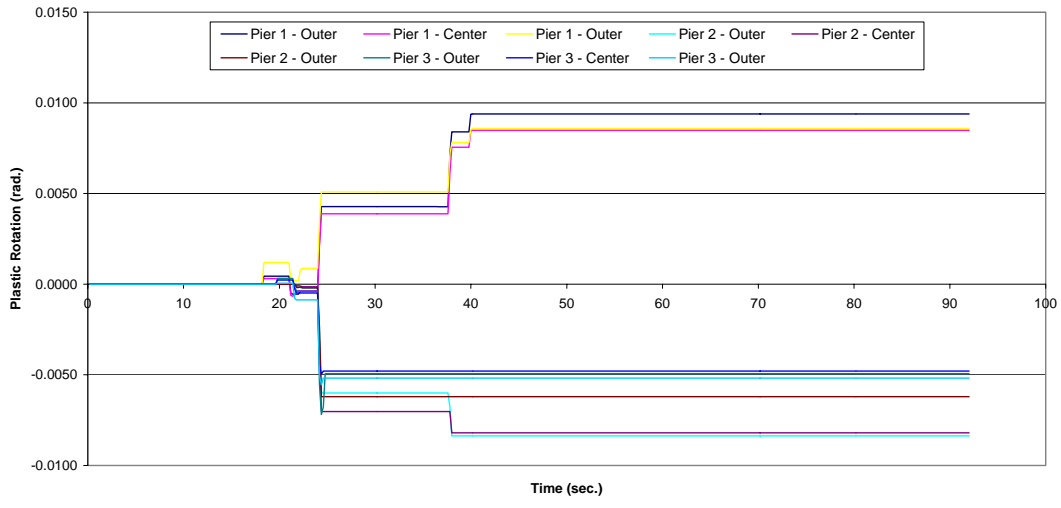


Figure D.10-4 Plastic Rotations at the Bottom of the Columns

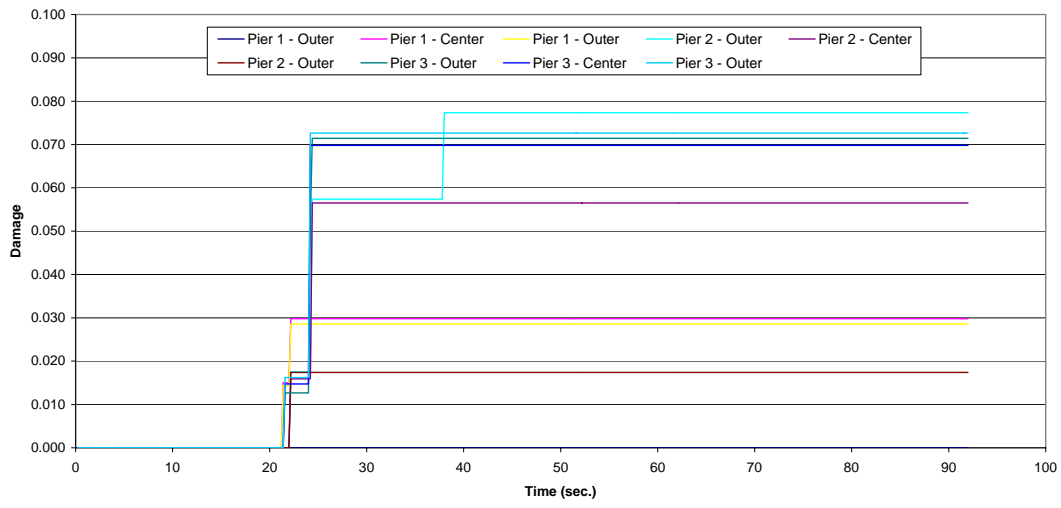


Figure D.10-5 Damage at the Top of Columns

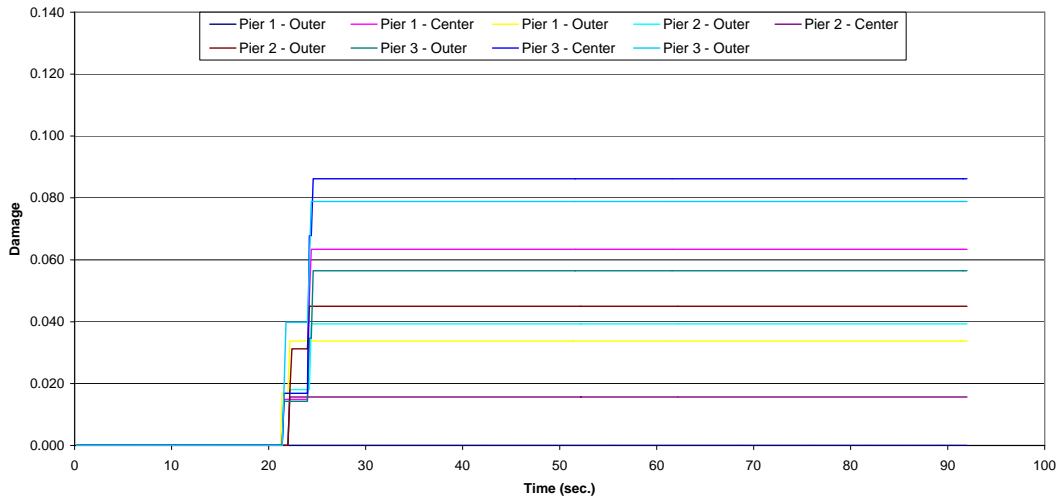


Figure D.10-6 Damage at the Bottom of Columns

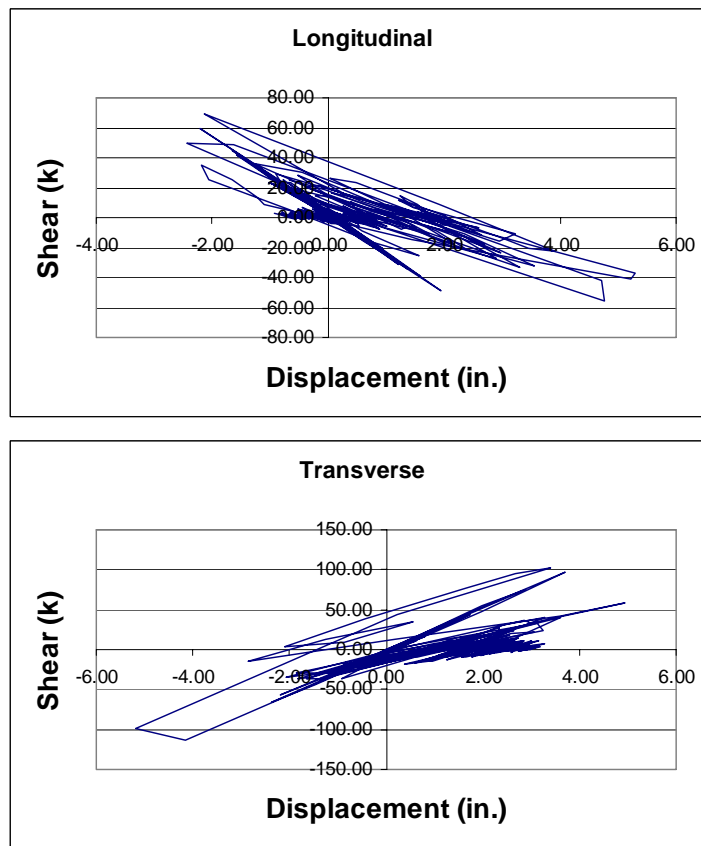


Figure D.10-7 Hysteresis Plots for the Center Column of Pier 2

Table D.10-1 Maximum Moment (kip-in) at the Top and Bottoms of Columns

Pier No.	Column	Moment	
		Top	Bottom
1	1	20539.9	21518.4
	2	17080.9	24003.2
	3	17666.6	15897.3
2	1	17931.8	17027.0
	2	18206.4	17040.5
	3	17982.5	17015.3
3	1	19191.0	17827.9
	2	21043.8	19849.2
	3	20245.1	18649.9

Table D.10-2 Maximum Shear (kips) in the Columns

Pier No.	Column	Shear			
		Top	Demand/ Capacity	Bottom	Demand/ Capacity
1	1	157.78	0.92	161.43	0.94
	2	152.20	0.89	151.76	0.88
	3	124.24	0.72	123.38	0.72
2	1	110.20	0.64	114.82	0.67
	2	110.47	0.64	115.09	0.67
	3	110.26	0.64	114.97	0.67
3	1	133.11	0.78	133.10	0.78
	2	149.75	0.88	149.73	0.88
	3	142.10	0.84	142.16	0.84

D.11 Run No. 10

The plots and tables for the response of Bridge 5/518, with columns fixed at their bases and the abutments have rollers in both directions, to the Olympia 950-year are presented here.

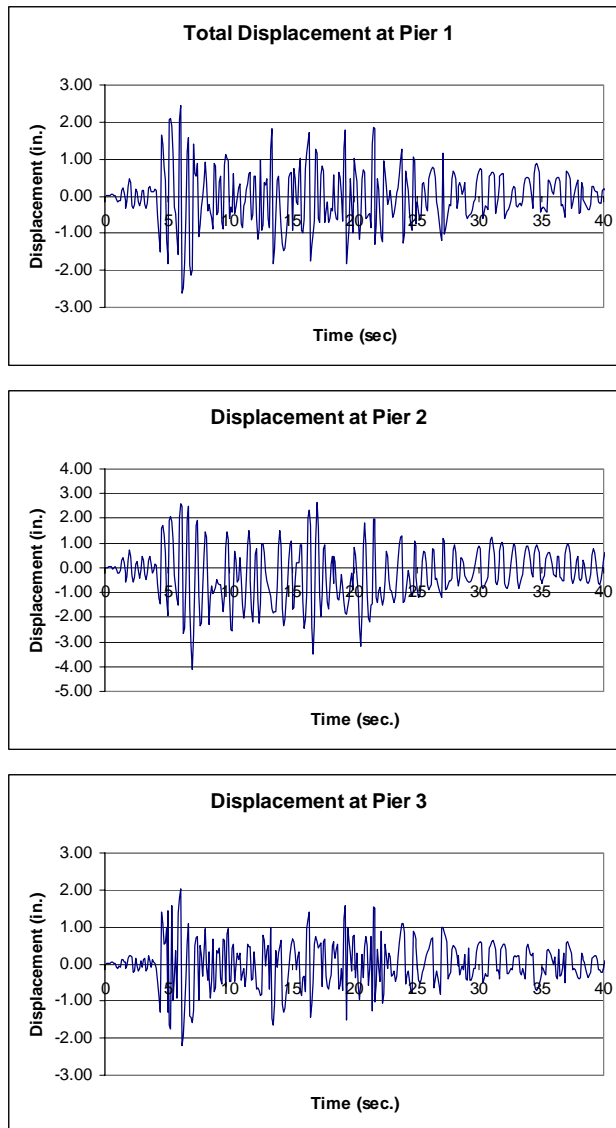


Figure D.11-1 Total Relative Displacement at Piers

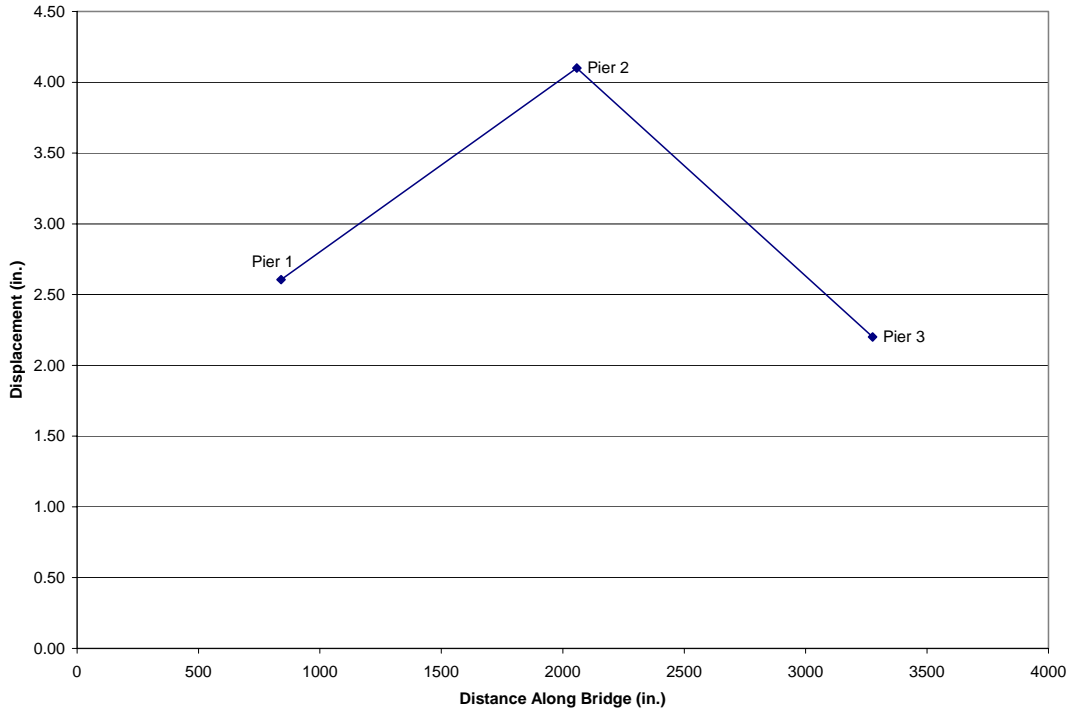


Figure D.11-2 Transverse Displacement Envelope of Bridge Deck

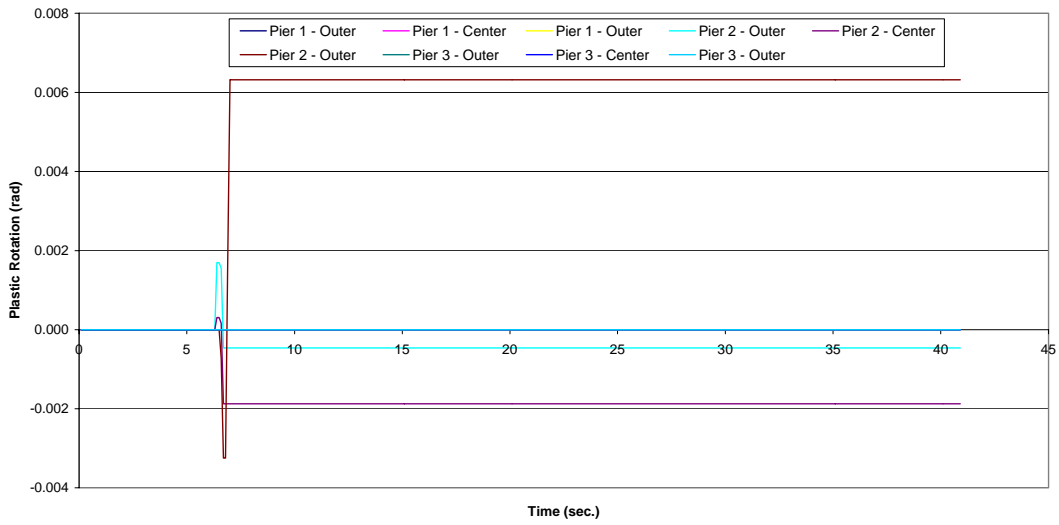


Figure D.11-3 Plastic Rotations at the Top of the Columns

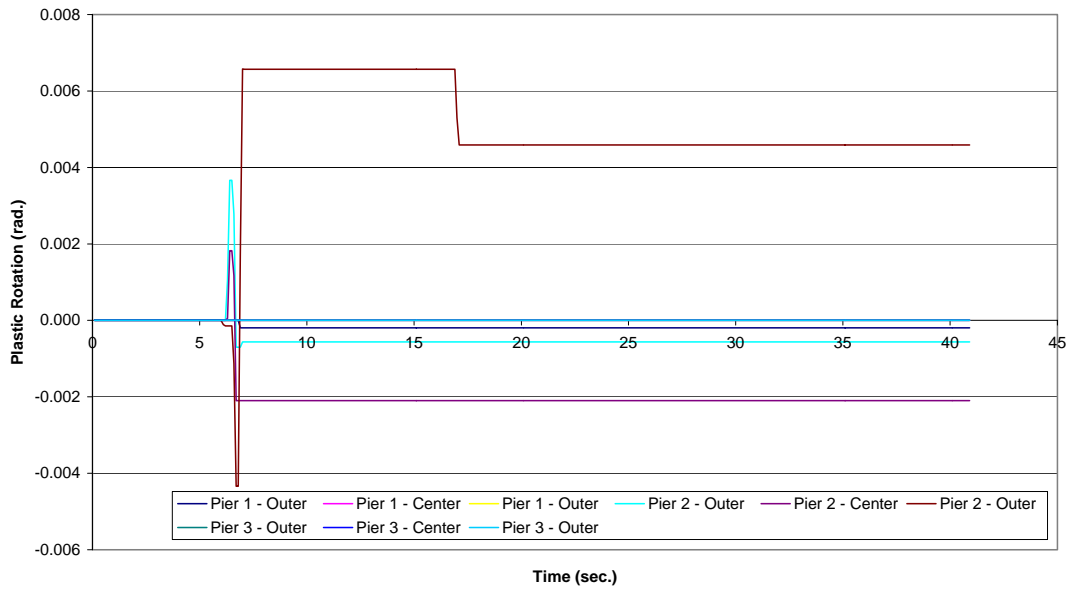


Figure D.11-4 Plastic Rotations at the Bottom of the Columns

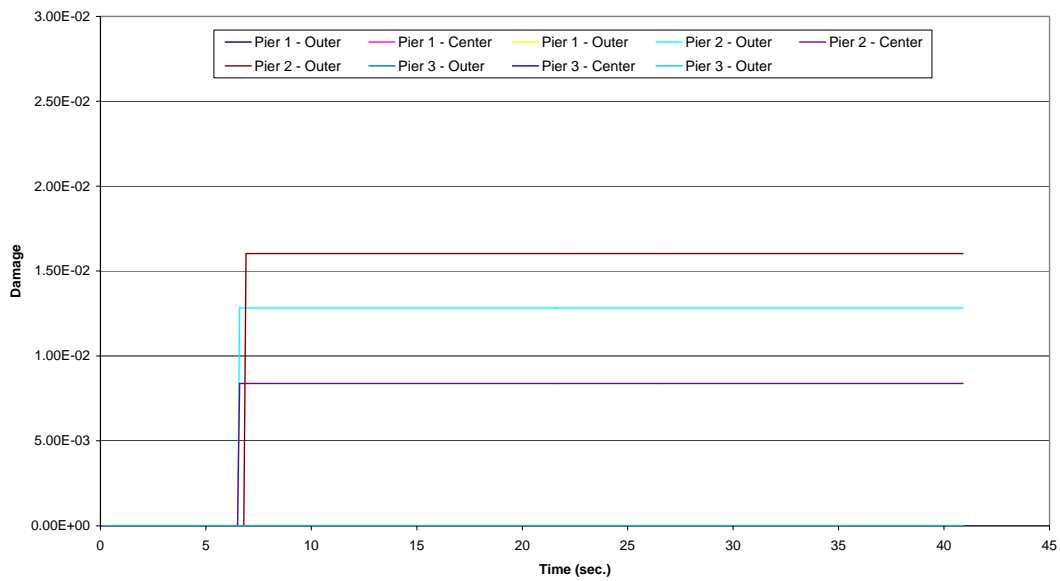


Figure D.11-5 Damage at the Top of the Columns

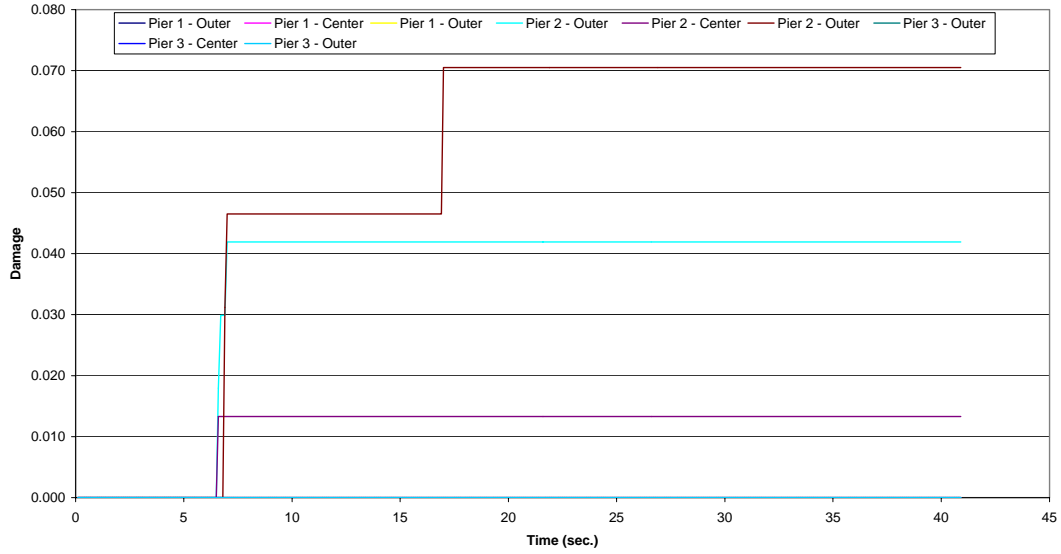


Figure D.11-6 Damage at the Bottom of Columns

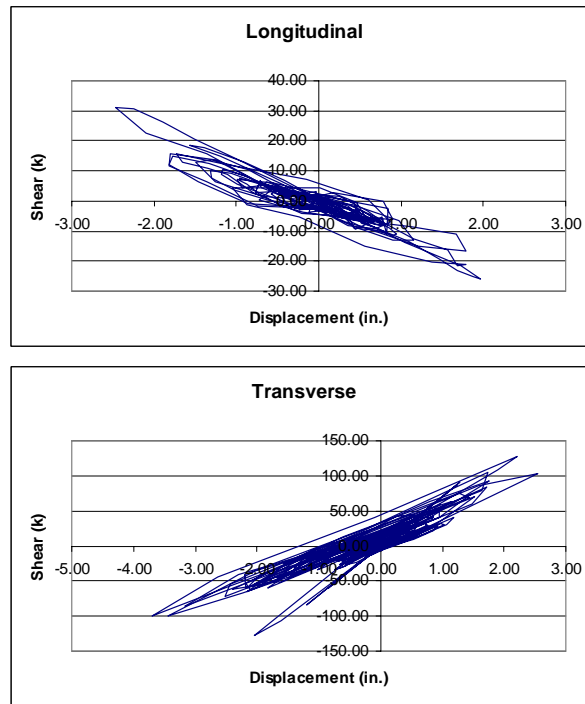


Figure D.11-7 Hysteresis Plots for the Center Column of Pier 2

Table D.11-1 Maximum Moment (kip-in) at the Top and Bottoms of Columns

Pier No.	Column	Moment	
		Top	Bottom
1	1	9255.9	10898.7
	2	9304.1	10896.6
	3	9557.1	10895.1
2	1	1710.22	15765.8
	2	15388.2	13282.3
	3	17314.9	15027.6
3	1	9808.1	10520.7
	2	9799.2	10125.1
	3	9826.9	9731.8

Table D.11-2 Maximum Shear (kips) in the Columns

Pier No.	Column	Shear			
		Top	Demand/ Capacity	Bottom	Demand/ Capacity
1	1	85.83	0.50	89.88	0.52
	2	83.54	0.49	87.51	0.51
	3	81.83	0.48	84.73	0.49
2	1	147.83	0.86	149.33	0.87
	2	127.69	0.74	128.92	0.75
	3	142.73	0.83	149.21	0.87
3	1	96.67	0.56	100.67	0.59
	2	96.34	0.56	100.41	0.59
	3	96.38	0.56	100.48	0.59

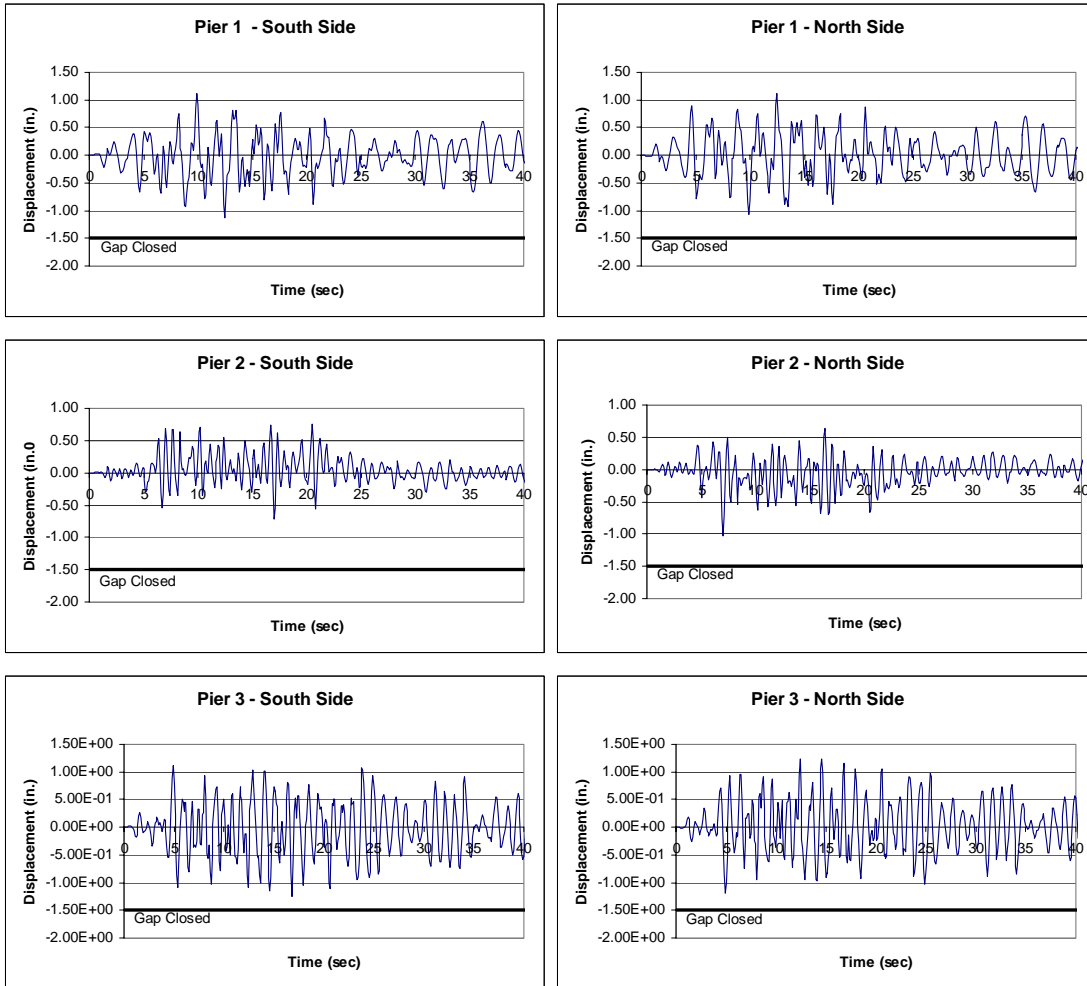


Figure D.11-8 Longitudinal Displacement of Expansion Joints

D.12 Run No. 11

The plots and tables for the response of Bridge 5/518, with columns fixed at their bases and the abutments have rollers in both directions, to the Kobe 950-year are presented here.

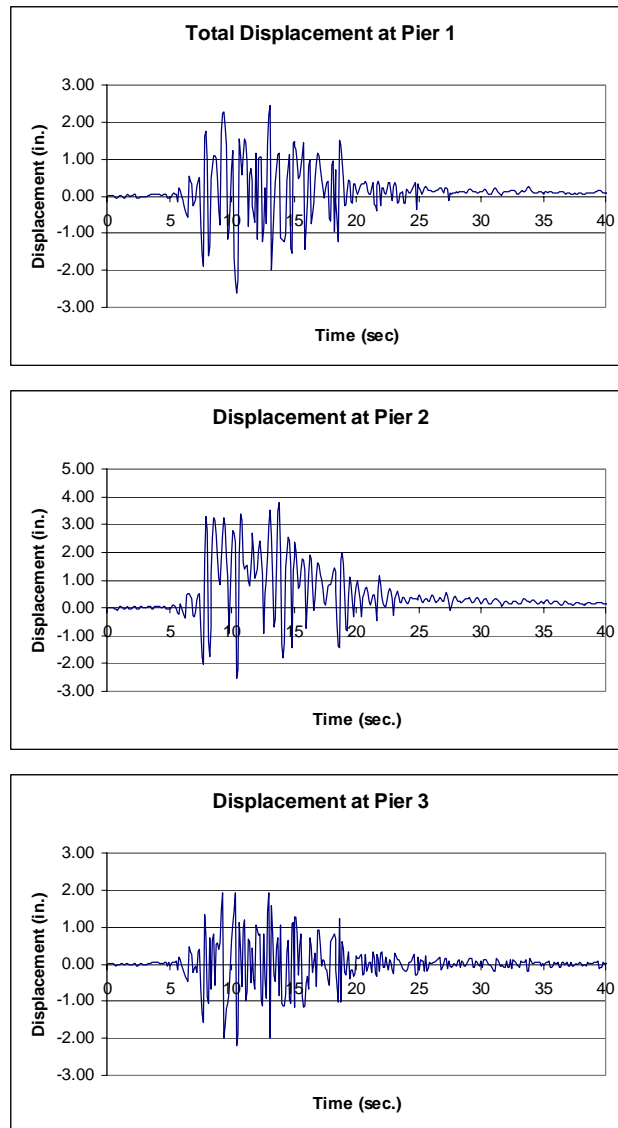


Figure D.12-1 Total Relative Displacement at Piers

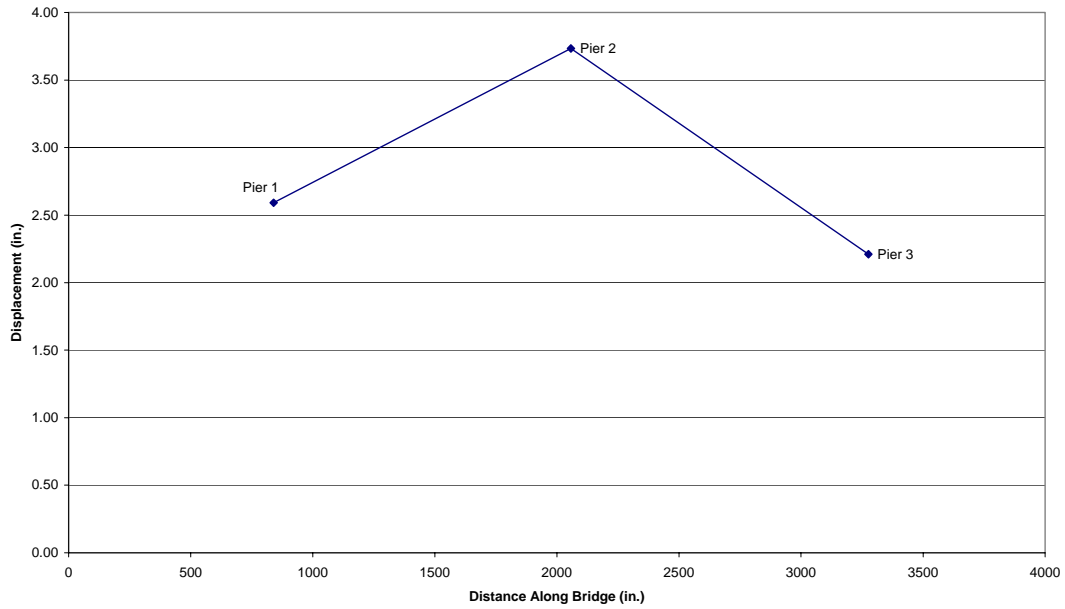


Figure D.12-2 Transverse Displacement Envelope of Bridge Deck

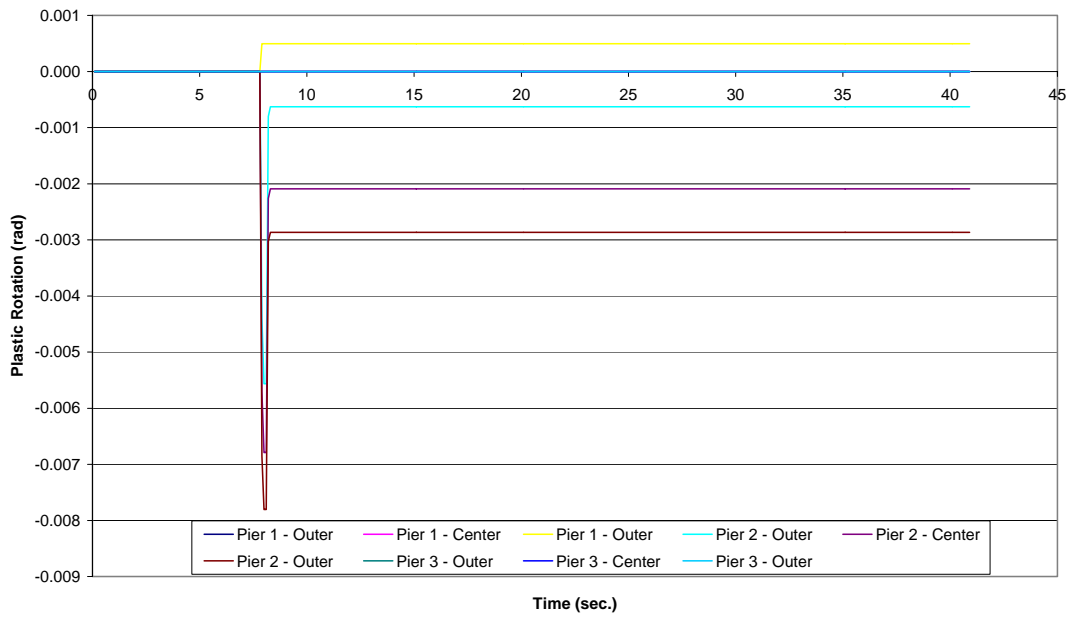


Figure D.12-3 Plastic Rotations at the Top of the Columns

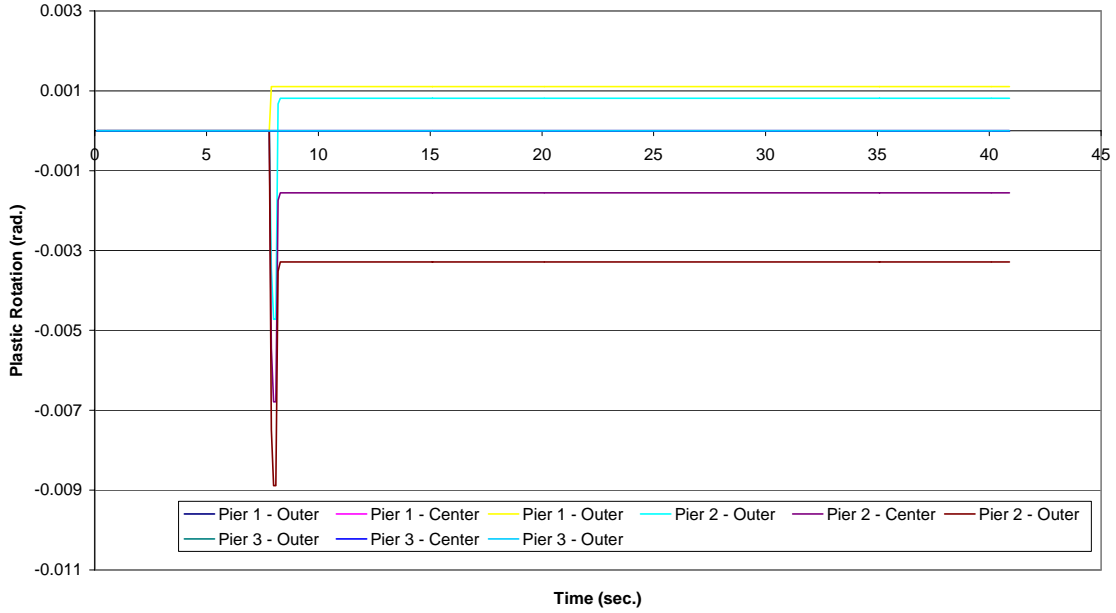


Figure D.12-4 Plastic Rotations at the Bottom of the Columns

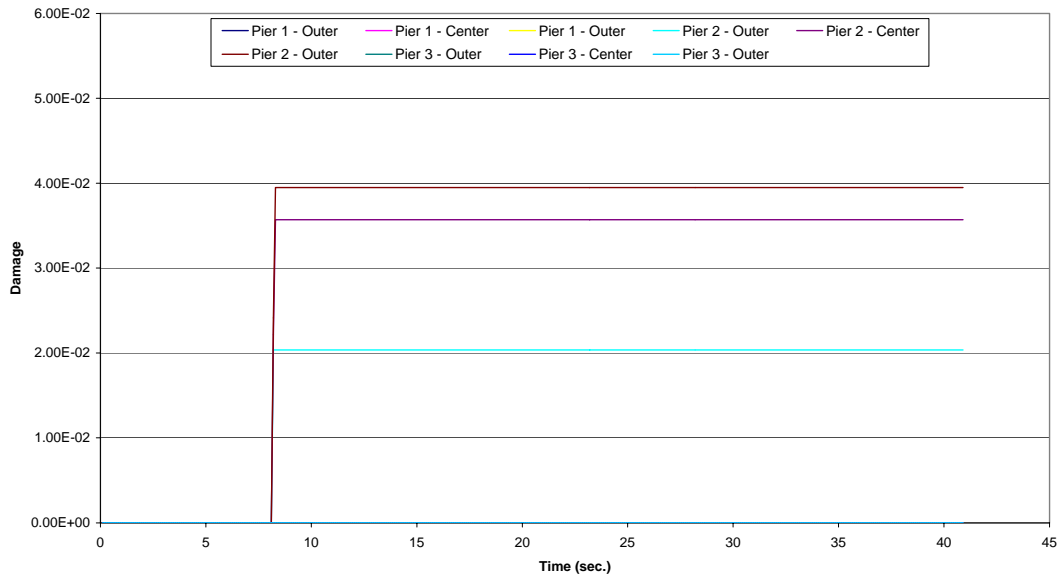


Figure D.12-5 Damage at the Top of the Columns

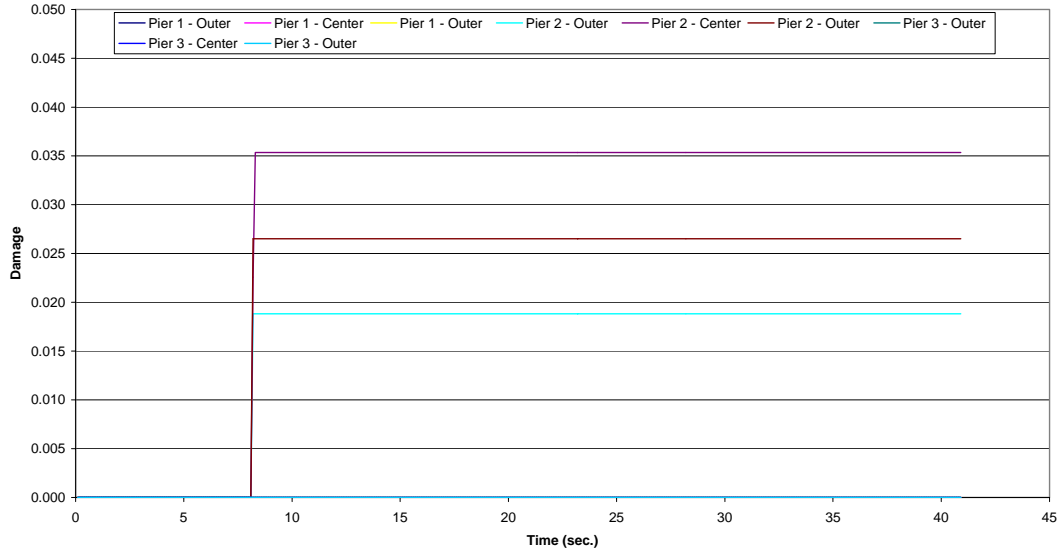


Figure D.12-6 Damage at the Bottom of Columns

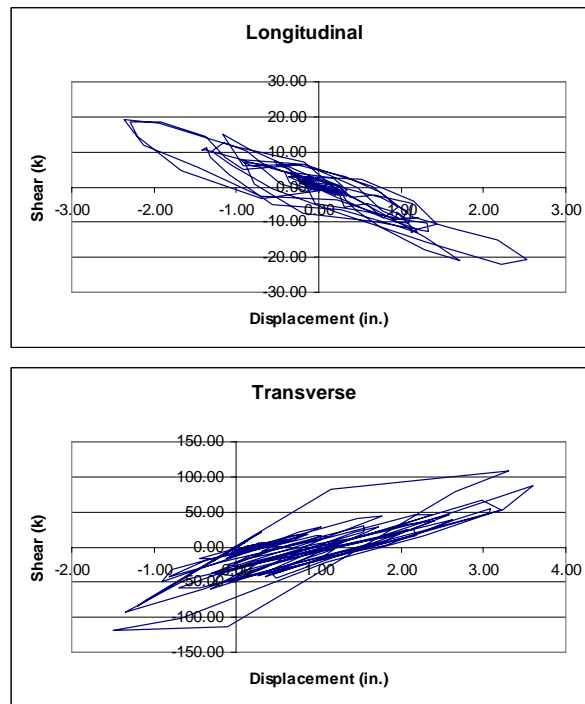


Figure D.12-7 Hysteresis Plots for the Center Column of Pier 2

Table D.12-1 Maximum Moment (kip-in) at the Top and Bottoms of Columns

Pier No.	Column	Moment	
		Top	Bottom
1	1	11948.9	13856.3
	2	11974.2	13760.1
	3	10605.2	12412.0
2	1	16058.63	17981.3
	2	13360.4	15380.0
	3	15189.9	17138.2
3	1	10055.8	7680.1
	2	10155.5	7679.5
	3	11231.2	8047.3

Table D.12-2 Maximum Shear (kips) in the Columns

Pier No.	Column	Shear			
		Top	Demand/ Capacity	Bottom	Demand/ Capacity
1	1	119.99	0.70	120.70	0.70
	2	119.66	0.70	120.36	0.70
	3	106.11	0.62	105.72	0.62
2	1	125.94	0.73	135.42	0.80
	2	114.45	0.67	119.45	0.69
	3	139.57	0.82	142.97	0.83
3	1	82.06	0.48	86.25	0.50
	2	76.13	0.44	80.92	0.47
	3	76.11	0.44	78.67	0.46

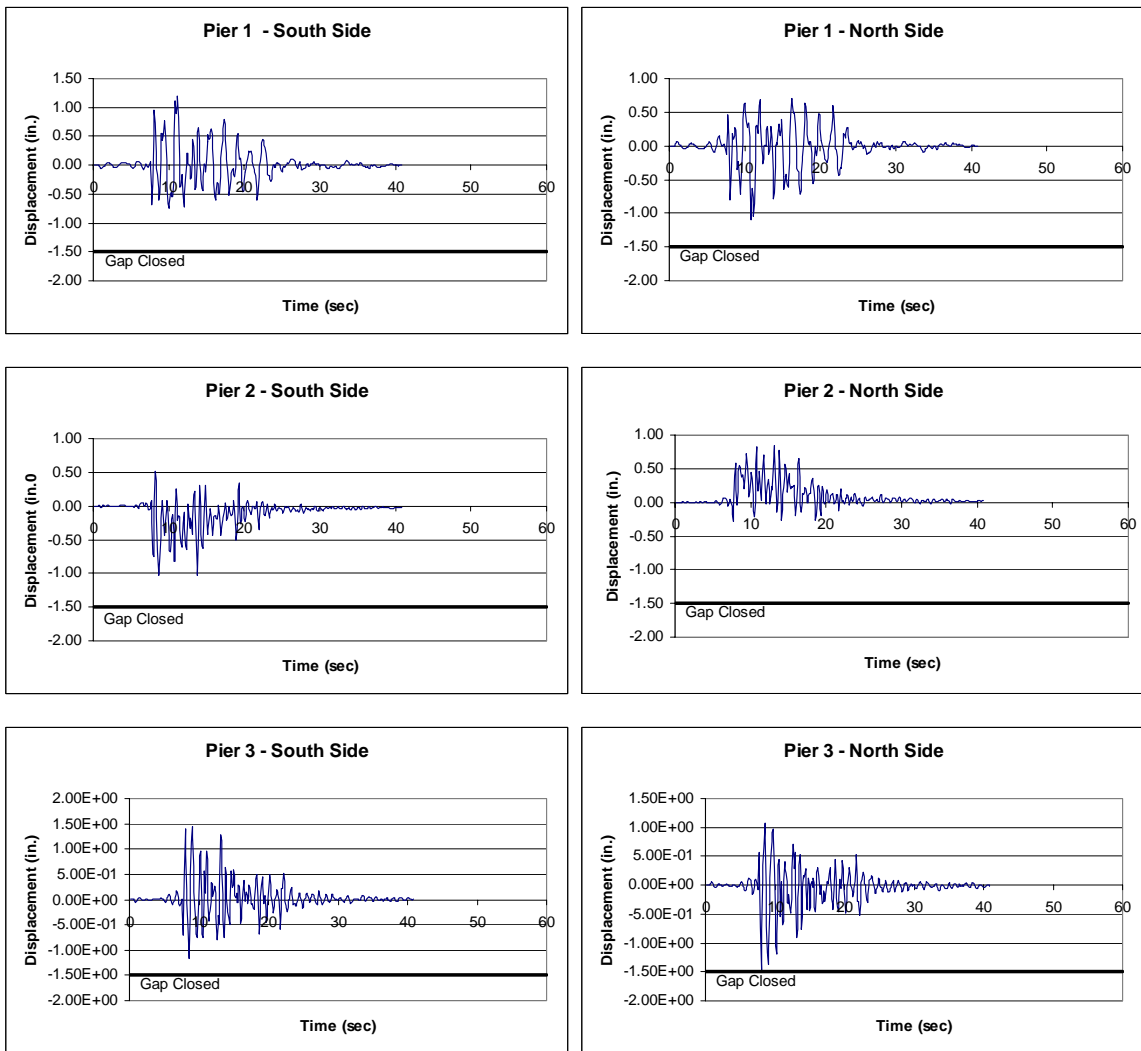


Figure D.12-8 Longitudinal Displacement of Expansion Joints

D.13 Run No. 12

The plots and tables for the response of Bridge 5/826, with columns fixed at their bases and the abutments have rollers in both directions, to the Olympia 950-year are presented here.

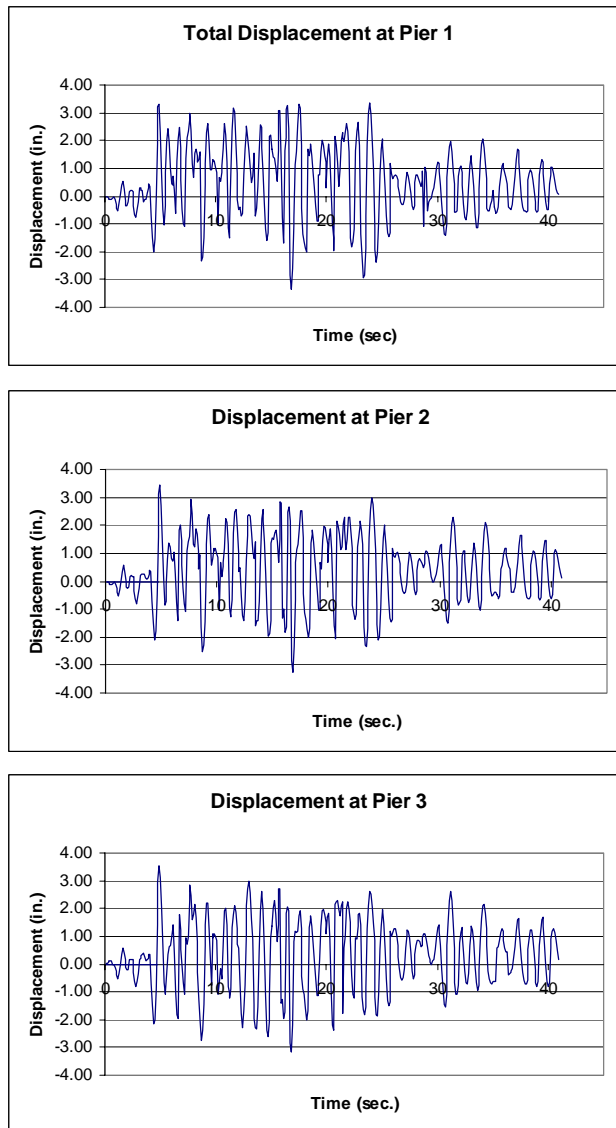


Figure D.13-1 Total Relative Displacement at Piers

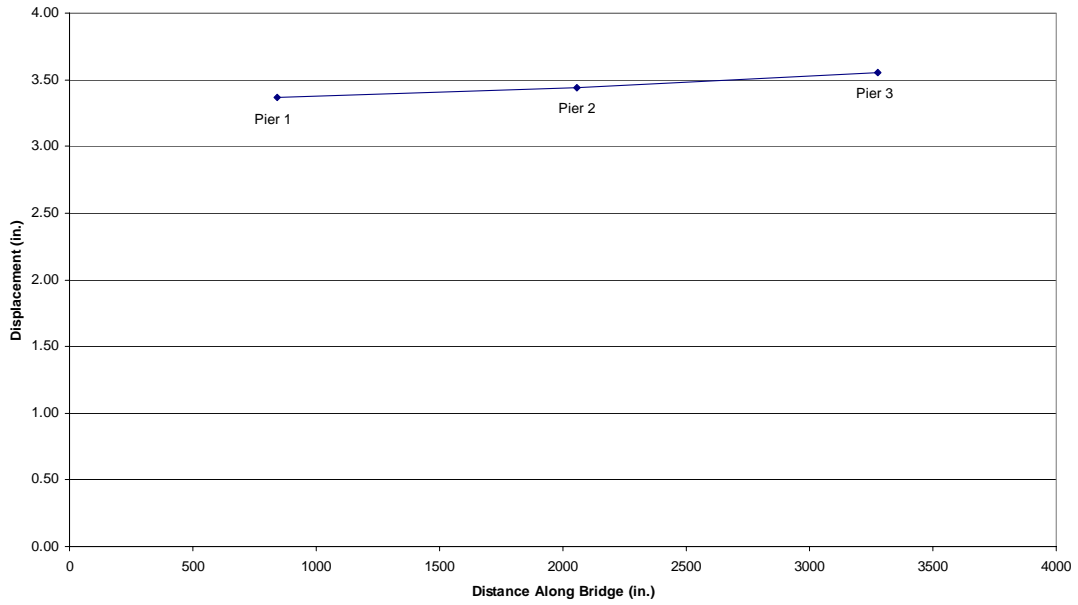


Figure D.13-2 Transverse Displacement Envelope of Bridge Deck

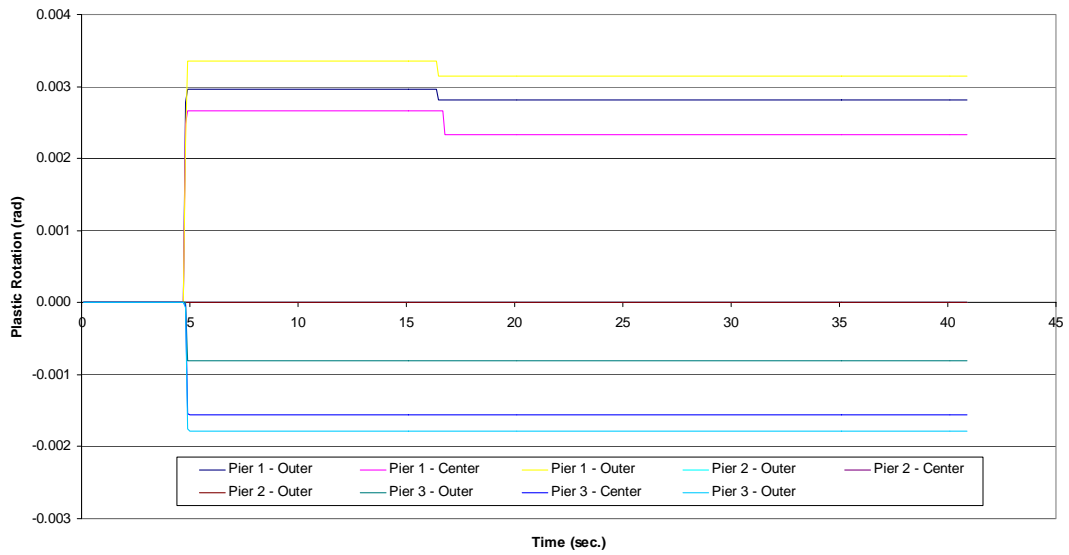


Figure D.13-3 Plastic Rotations at the Top of the Columns

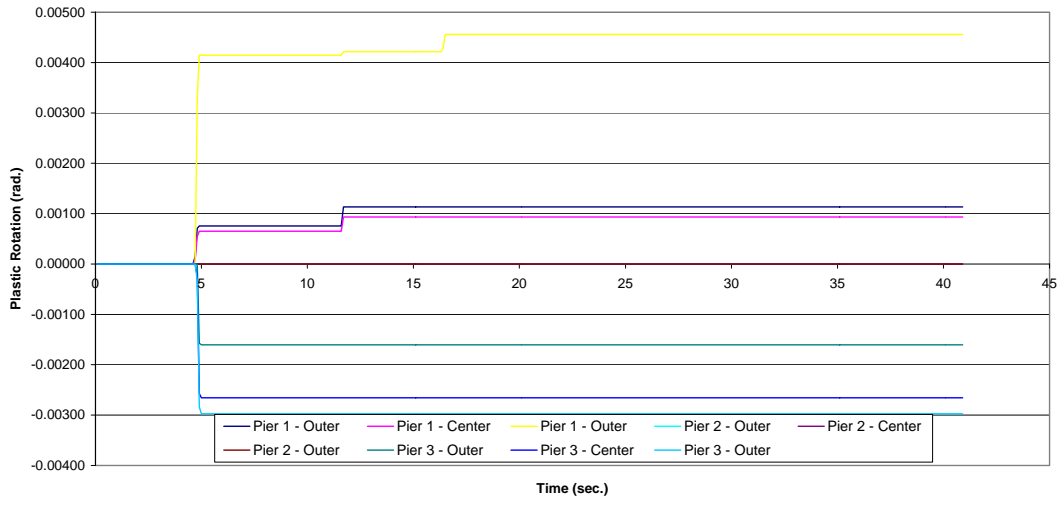


Figure D.13-4 Plastic Rotations at the Bottom of the Columns

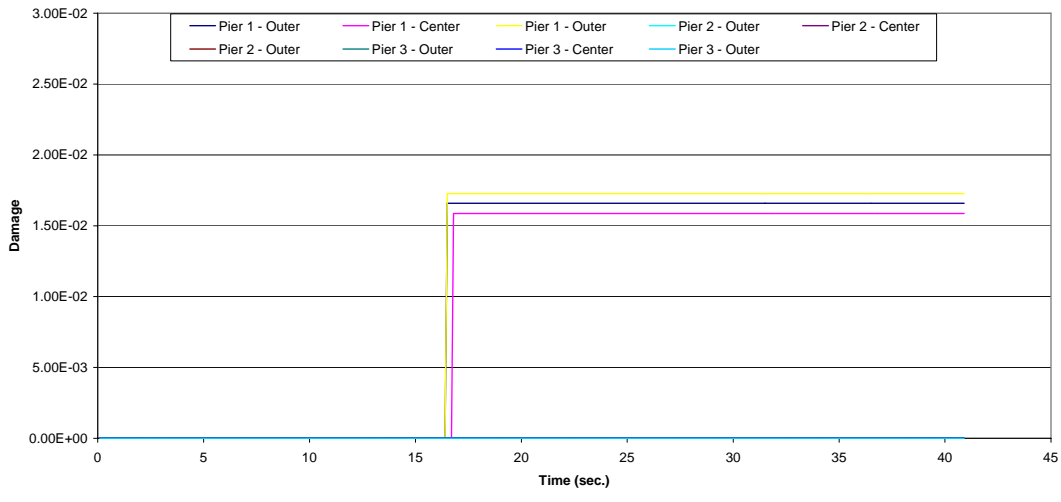


Figure D.13-5 Damage at the Top of the Columns

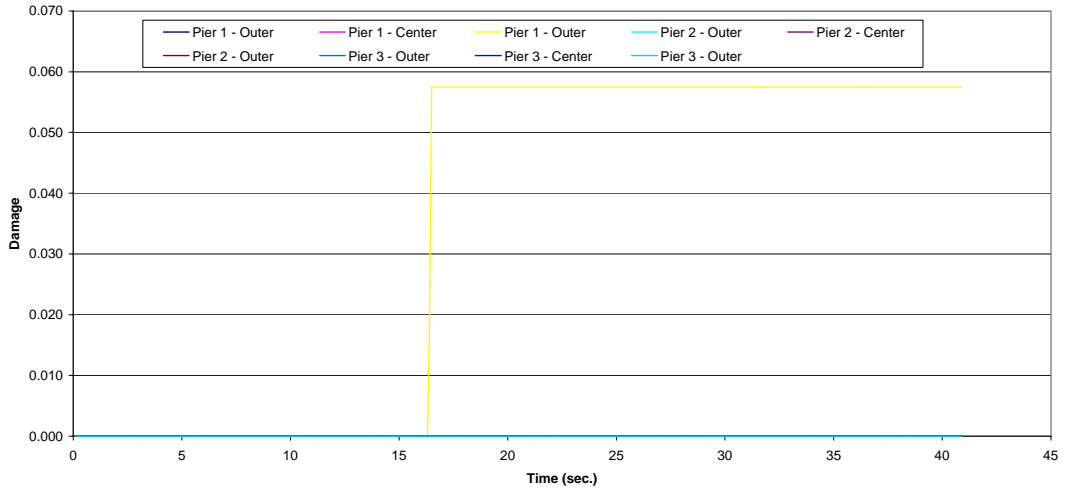


Figure D.13-6 Damage at the Bottom of Columns

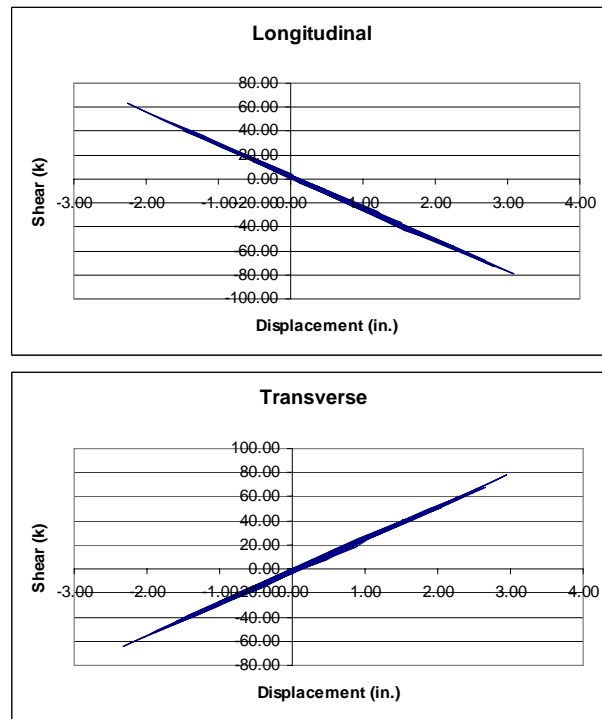


Figure D.13-7 Hysteresis Plots for the Center Column of Pier 2

Table D.13-1 Maximum Moment (kip-in) at the Top and Bottoms of Columns

Pier No.	Column	Moment	
		Top	Bottom
1	1	20215.6	18714.3
	2	20063.7	18326.6
	3	18411.9	17770.8
2	1	13917.8	13164.3
	2	14050.8	13279.9
	3	14125.4	13367.8
3	1	14701.4	13399.6
	2	15838.2	15537.2
	3	16984.8	16651.1

Table D.13-2 Maximum Shear (kips) in the Columns

Pier No.	Column	Shear			
		Top	Demand/ Capacity	Bottom	Demand/ Capacity
1	1	141.08	0.82	143.34	0.84
	2	139.13	0.81	141.32	0.82
	3	131.10	0.76	133.18	0.78
2	1	85.61	0.50	88.33	0.51
	2	86.52	0.50	89.15	0.52
	3	86.98	0.50	89.67	0.52
3	1	95.79	0.56	97.81	0.57
	2	108.98	0.64	110.38	0.64
	3	117.01	0.68	118.27	0.69

D.14 Run No. 13

The plots and tables for the response of Bridge 5/826, with columns fixed at their bases and the abutments have rollers in both directions, to the Kobe 950-year are presented here.

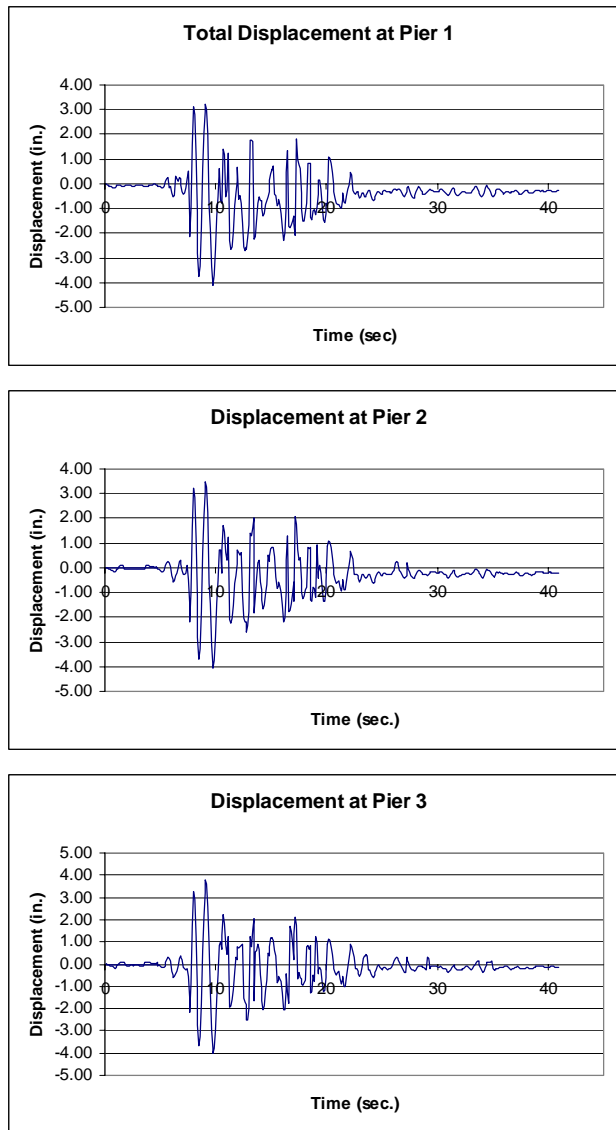


Figure D.14-1 Total Relative Displacement at Piers

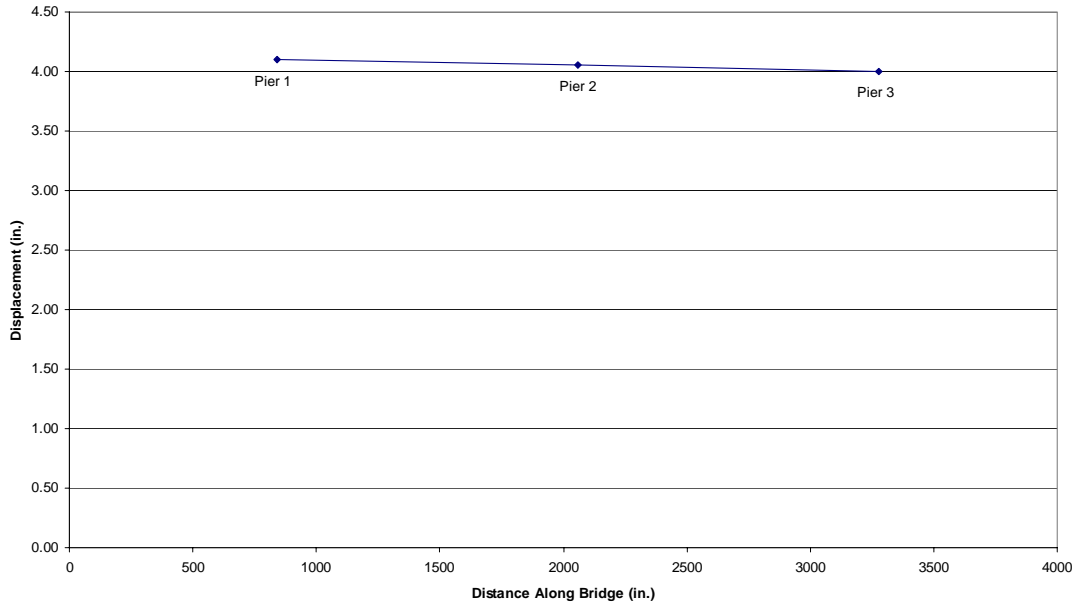


Figure D.14-2 Transverse Displacement Envelope of Bridge Deck

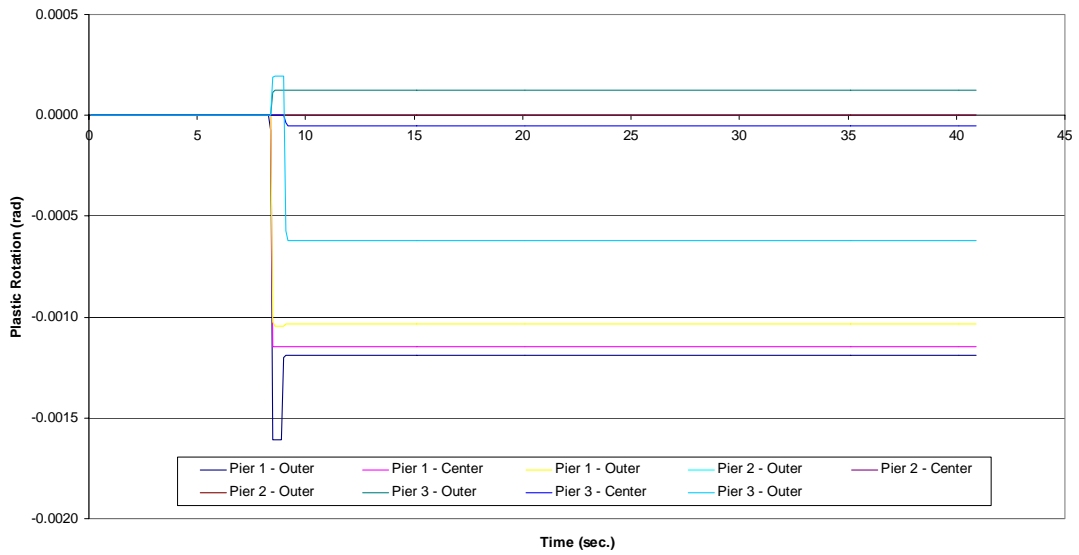


Figure D.14-3 Plastic Rotations at the Top of the Columns

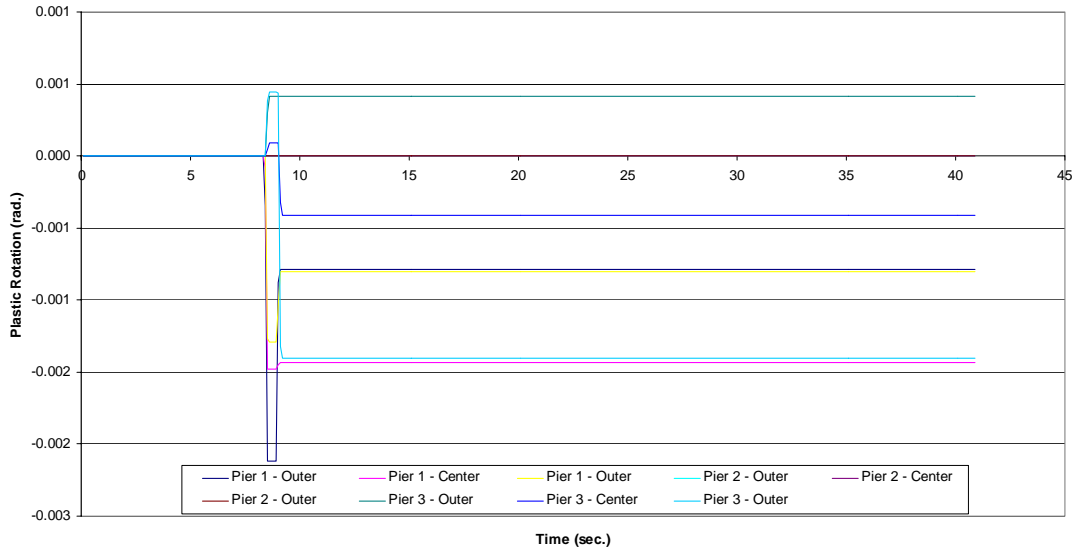


Figure D.14-4 Plastic Rotations at the Bottom of the Columns

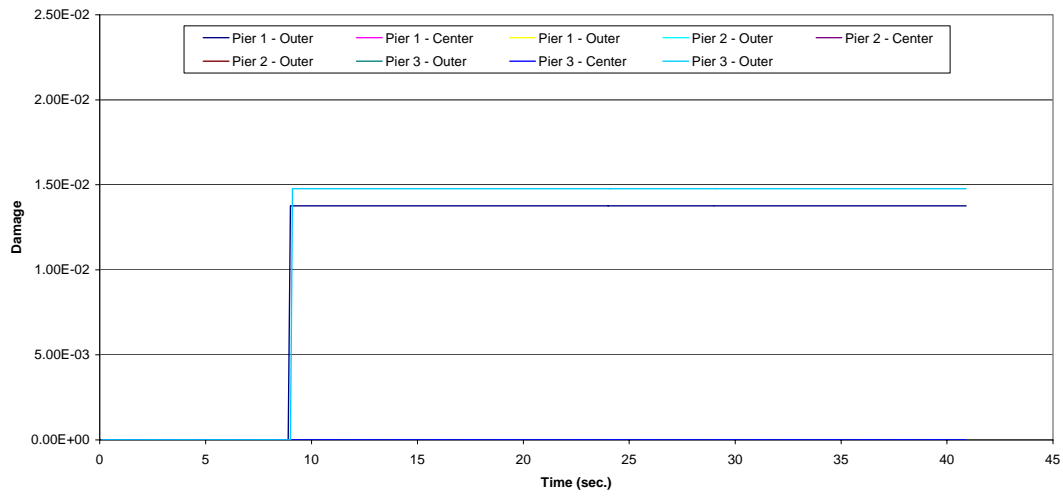


Figure D.14-5 Damage at the Top of the Columns

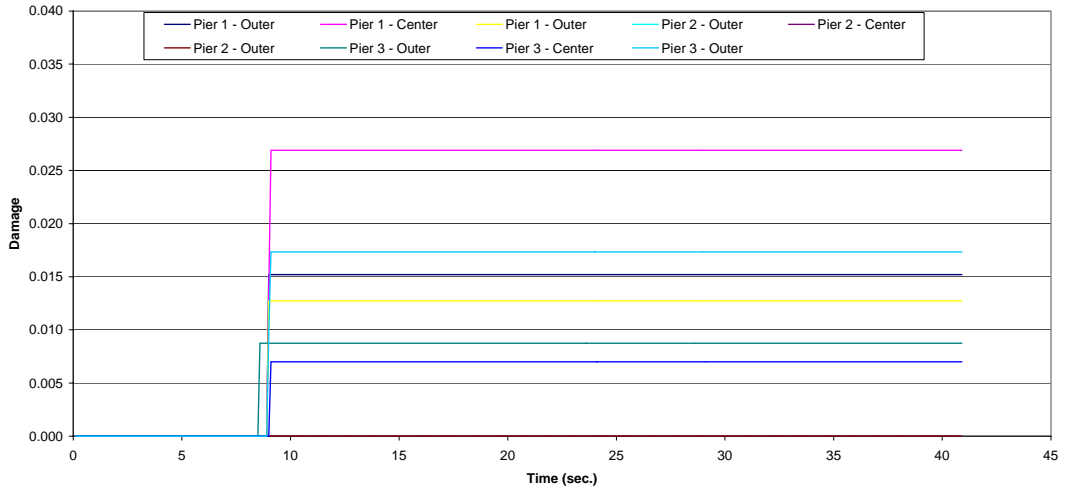


Figure D.14-6 Damage at the Bottom of Columns

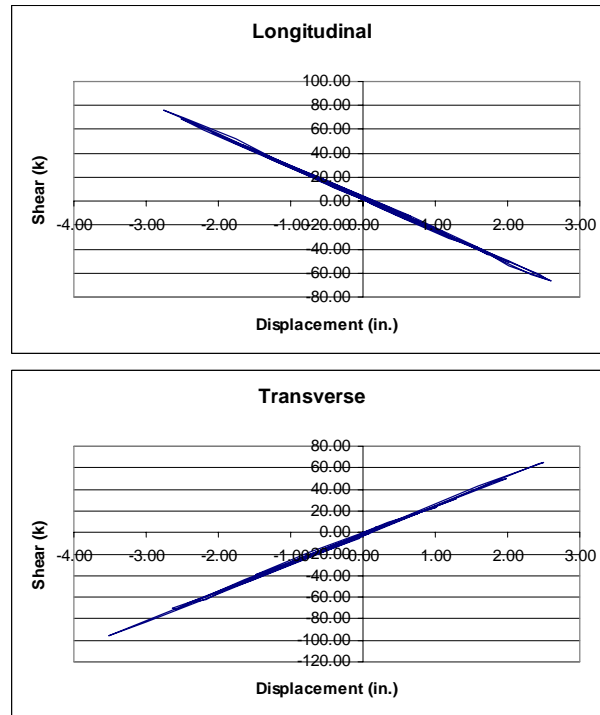


Figure D.14-7 Hysteresis Plots for the Center Column of Pier 2

Table D.14-1 Maximum Moment (kip-in) at the Top and Bottoms of Columns

Pier No.	Column	Moment	
		Top	Bottom
1	1	19100.7	17679.5
	2	19731.0	18388.7
	3	18952.8	17313.2
2	1	17034.7	16125.8
	2	17156.8	16194.7
	3	17207.6	16221.1
3	1	17595.4	16048.6
	2	18436.9	16921.4
	3	17469.7	16046.9

Table D.14-2 Maximum Shear (kips) in the Columns

Pier No.	Column	Shear			
		Top	Demand/ Capacity	Bottom	Demand/ Capacity
1	1	134.03	0.78	135.98	0.79
	2	137.57	0.81	143.71	0.84
	3	131.40	0.77	133.83	0.78
2	1	105.68	0.62	108.87	0.64
	2	106.30	0.62	109.49	0.64
	3	106.61	0.62	109.76	0.64
3	1	114.93	0.67	113.24	0.66
	2	121.56	0.71	125.21	0.73
	3	114.58	0.67	113.83	0.67